Metal-free Approaches towards the Construction of Heterocycles

By

SHYAMAL KANTI BERA

CHEM11201704025

National Institute of Science Education and Research Bhubaneswar,
Odisha – 752050

A thesis submitted to the
Board of Studies in Chemical Sciences
In partial fulfillment of requirements
for the Degree of

DOCTOR OF PHILOSOPHY

of

HOMI BHABHA NATIONAL INSTITUTE

July, 2022

Homi Bhabha National Institute[1]

Recommendations of the Viva Voce Committee

As members of the Viva Voce Committee, we certify that we have read the dissertation prepared by **Shyamal Kanti Bera** entitled **"Metal-free Approaches towards the Construction of Heterocycles"** and recommend that it may be accepted as fulfilling the thesis requirement for the award of Degree of Doctor of Philosophy.

Chairman – Prof. A. Srinivasan		**Date:** 21.10.22
Guide/Convener- Dr. Prasenjit Mal	Prasenjit Mal	**Date:** 21/10/22
Examiner- Dr. Sandip Murarka	Sandip Murarka	**Date:** 27/10/2022
Member 1- Dr. Sudip Barman	Sudip Barman	**Date:** 21/10/22
Member 2- Dr. Subhadip Ghosh	Subhadip	**Date:** 21/10/2022
Member 3- Dr. Shantanu Pal	Shantanu Pal.	**Date:** 21/10/22

Final approval and acceptance of this thesis is contingent upon the candidate's submission of the final copies of the thesis to HBNI.

I/We hereby certify that I/we have read this thesis prepared under my/our direction and recommend that it may be accepted as fulfilling the thesis requirement.

Date: 21.10.2022

Place: NISER, Bhubaneswar

Prasenjit Mal

(Dr. Prasenjit Mal)

Guide

[1] This page is to be included only for final submission after successful completion of viva voce.

~ 2 ~

STATEMENT BY AUTHOR

This dissertation has been submitted in partial fulfillment of requirements for an advanced degree at Homi Bhabha National Institute (HBNI) and is deposited in the library to be made available to borrowers under the rules of the HBNI.

Brief quotations from this dissertation are allowable without special permission, provided that accurate acknowledgement of source is made. Requests for permission for extended quotation from or reproduction of this manuscript in whole or in part may be granted by the Competent Authority of HBNI when in his or her judgment the proposed use of the material is in the interests of scholarship. In all other instances, however, permission must be obtained from the author.

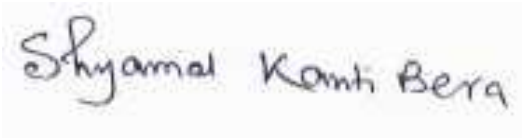

Shyamal Kanti Bera

DECLARATION

I, hereby declare that the investigation presented in the thesis has been carried out by me. The work is original and has not been submitted earlier as a whole or in part for a degree / diploma at this or any other Institution / University.

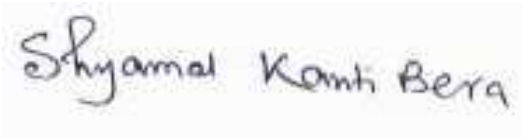

Shyamal Kanti Bera

List of Publications arising from the thesis: (# Pertaining to The Thesis)

Journal Published

1. **#Bera, S. K†.;** Alam, M. T†.; Mal, P., C–N Coupling via Antiaromatic Endocyclic Nitrenium Ions. *J. Org. Chem.* **2019,** *84*, 12009-12020.

2. **#Bera, S. K†.;** Boruah, P. J†.; Parida, S. S.; Paul, A. K.; Mal, P., A Photochemical Intramolecular C–N Coupling Toward the Synthesis of Benzimidazole-Fused Phenanthridines. *J. Org. Chem.* **2021,** *86* (14), 9587-9602.

3. **#Bera, S. K.;** Mal, P., Mechanochemical-Cascaded C–N Cross-Coupling and Halogenation Using N-Bromo- and N-Chlorosuccinimide as Bifunctional Reagents. *J. Org. Chem.* **2021,** *86* (20), 14144-14159.

4. **#Bera, S. K.**; Mal, P., Regiodivergent C–N Coupling of Quinazolinones Controlled by the Dipole Moments of Tautomers. *Org. Lett.* **2022,** *24* (17), 3144-3148.

5. **Bera, S. K**.; Bose, A.; Mal, P., C-H Functionalization by Weak Interactions (Wiley Publishers, Book chapter, accepted).

6. **Bera, S. K†**.; Bhanja, R†.; Mal, P., DDQ in mechanochemical C–N coupling reactions. *Beilstein J. Org. Chem.* **2022,** *18*, 639-646.

7. **#Bera, S. K.;** Maharana, R. R.; Samanta, K.; Mal, P., CBr_4 catalyzed activation of *α,β*-unsaturated ketones. *Org. Biomol. Chem.* **2022,** *20* (35), 7085-7091.

Manuscript Communicated

8. Boruah, P. J[†].; **Bera, S. K**[†].; Mukherjee, S.; Mal, P.; Paul, A. K., Role of Singlet and Triplet Excited States and Non-Adiabatic Coupling in Electronically Controlled Photochemical Intramolecular C-N Coupling Reaction (*manuscript submitted*).
9. **Bera, S. K**.; Bhanja, R.; Mal, P., Photoinduced Carbon-Carbon and Carbon-Heteroatom Bond Formation Reactions under Catalyst-Free Conditions (*manuscript submitted*).

Manuscript under preparation:

10. **Bera, S. K**.; Bhanja, R.; Mal, P., Regioselective oxidative C-N coupling under photochemical condition. (*manuscript under preparation*).
11. **Bera, S. K**.; Shau, C. C.; Mal, P., Synthesis of benzimidazole-fused phenanthridines using iodine(I) reagent. (*manuscript under preparation*).

CONFERENCE AND PRESENTATIONS

1. **Poster Presentation:** International Conference on ‘‘Emerging Trends in Catalysis &Synthesis’’ (IC-ETCS – 2020) (March 11-12th, 2020) Indian Institute of Technology Kharagpur.
2. **Poster Presentation:** First Virtual JNOST Conference (JNOST-16) (October 31 –November 1, 2020) Indian Institute of Science, Bangalore, India.
3. **Poster Presentation:** International E-Conference on Advances in Chemical Research 2021 (ACR-2021) (19th - 20th April 2021) Department of Chemistry, GITAM Institute of Science, Visakhapatnam.

4. **Poster Presentation:** International e-Conference on Developments in Chemical, Biological and Environmental Sciences (DCBES-2021) (28th - 30th June 2021) GITAM School of Science, Hyderabad.
5. **Poster Presentation:** MedChem 2021 (Emerging Infectious Diseases & Therapeutics Strategies) (December 1-3, 2021) Department of Chemistry, Indian Institute of Technology, Madras.
6. **Poster Presentation:** International Conference on Main-group Molecules to Materials-II (MMM-II) (December 13-15, 2021) NISER Bhubaneswar.
7. **Poster Presentation:** Research and Industrial Conclave Integration 2022 (20th – 22th January 2022) Indian Institute of Technology Guwahati, India.

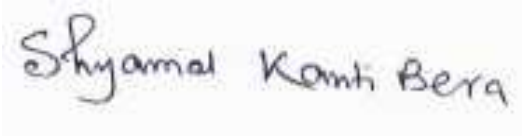

Shyamal Kanti Bera

Dedicated
To
My Parents

ACKNOWLEDGEMENTS

First and foremost, praise the almighty for the shower of blessing throughout this delightful journey of my research and lead me to accomplish the goal successfully. It's high time to express my heartfelt gratitude to many people who influenced and contributed in numerous ways to this expedition.

First of all, a profound sense of gratitude binds me to my guide, Dr. Prasenjit Mal. His constant support, timely motivation, wise guidance, and prompt suggestions have been the torch-bearer of my research career. My sincere thanks go to Prof. T. K. Chandrashekar, founder Director, NISER, and Prof. Sudhakar Panda, Director, NISER, for providing nice institutional infrastructure. I want to thank DST-INSPIRE for the financial support.

It gives me immense pleasure to thank my doctoral committee members Prof. A. Srinivasan, Dr. Sudip Barman, Dr. Subhadip Ghosh, and Dr. Shantanu Pal for their cooperation during my research. I wish to extend my warmest thanks to all other faculty members and staff for providing a healthy research atmosphere. I am also grateful to, Dr. C. Gunanathan, Dr. N. K. Sharma, Prof. A. Srinivasan Dr. Moloy Sarkar, Dr. Prasenjit Mal and Dr. U. Lourderaj who taught me through my course-work, which helped to strengthen my knowledge. I am highly obliged to Dr. Pathik Maji, my MSc. guide for his worth suggestions and direction. I wish to express my indebtedness to Dr. Alakesh Bisai (IISER Kolkata, West Bengal) for laying the foundation of my research journey with his valuable guidance. I would like to take the opportunity to thank Palash J. Boruah, Dr. Amit K. Paul, Rajat R. Maharana, and Dr. Kousik Samanta for extending their kind collaboration to my work.

My deep respect to my elder brother Dr. Kamal Kanti Bera for his kind assistance that lifted my spirit up and inspired me to overcome the obstacles in this path.

A journey can be momentous only with the right companions. I am fortunate enough to get surrounded by such loving seniors, juniors and friends both inside and outside lab. These five years of mixed emotions in this lab always give me sense of a home away from home. My warmest regards to my lab mates Dr. Debdeep Maiti, Dr. Saikat Maity, Dr. Anima Bose, Dr. Khokan Choudhuri, Dr. Toufique Alam, Dr. Ankita Bal, Dr. Amarchand Parida, Dr. Arkalekha Mandal, Dr. Monojit Das, Dr. Milan Pramanik, Dr. Anupam Manna for their valuable time to share my research problem to personal dilemma every time I need. I owe my warmest thanks to all my present and past lab members Sudip Sau, Ashis Mathuri, Tarun Kumar Dinda, Rosalin Bhanja, Buddhadev Pal, Shraddha and Keshab, Prabhu, Sunil, Himangshu, Vrittik, Keshav, Abhishek, Chandan, and Uday for their constant encouragement and cheerful company. It's wonderful to work and share the lab with you all. I thank to all my NISER friends, especially Dr. Subhayan Chakraborty, Dr. Shreenibasa Sa, Dr. Narayan Chandra Jana, Akshay Kumar, and Shyam K. Banjare for spending time over some fruitful discussions during this journey. Thanks to all my friends outside NISER for always being there for me.

Last but not the least, no words of thanks can sum up the gratitude that I owe to my beloved parents (Mr. Mihir Kanti Bera and Mrs. Anima Bera) for their tons of love, care, support and encouragement. Gratitude to all my family members who witnessed every step of this way and supported me in all aspects.

Above all, thank you everyone for your unconditional love ……...

...Shyamal Kanti Bera

CONTENTS

SUMMARY

Chemists are constantly striving to develop an efficient and convenient synthetic route so that molecular building blocks can be made by reducing the multiple-step in the reaction conditions, using new synthons, improving atom and step economies, etc. Although transition metal-catalyzed reactions are potent tools for synthesizing heterocycles which have severe limitations such as the use of toxic reagents, expensive methods, harsh conditions, several problematic side reactions, etc. In search of a waste-free and cost-effective way to synthesize C-N and C-O bonds, metal-free approaches are becoming highly popular. In this regard, metal-free strategies have become an efficient and cost-effective method for constructing carbon-heteroatom bonds due to the avoidance of expensive metal, additives, and harsh reaction conditions. This thesis is based on the synthesis of various heterocycles under the metal-free and mild reaction conditions. Initially, we have demonstrated the PIFA mediated oxidative C-N cross-coupling reaction to synthesize benzimidazole-fused phenanthridines via the antiaromatic endocyclic nitrenium ion. Next, we have shown the catalyst-free photochemical intramolecular C−N coupling reaction toward the synthesis of benzimidazole-fused phenanthridines. In continuation, we report the PIFA-assisted regiodivergent synthesis of phenanthridine-fused quinazolinones, where the regioselectivity of the products was controlled by the dipole moments of the tautomers. It was observed that the tautomer having a high dipole moment led to the corresponding regioisomers in a solvent having a high dielectric constant. We have also discussed, the N-halosuccinamide mediated synthesis of phenanthridinones and their derivatives under solvent-free and mild reaction conditions. Additionally, halogen bond catalysis for C-N and C-O bond formation was explored to synthesize flavanones and aza-flavanones. Furthermore, the theoretical studies also supported the catalytic activity of the CBr_4 reagent in the reaction mechanism.

LIST OF SCHEMES

LIST OF FIGURES

LIST OF TABLES

List of Abbreviations Used

Å	Angstrom
Ar	Aryl/Aromatic
Ac	Acetyl
br	Broad
BHT	Butylated hydroxy toluene
ºC	Degree Celcius
Calcd	Calculated
cm	Centimeter
d	Doublet, Days
DBU	1,8-Diazabicyclo-(5.4.0)-undec-7-ene
DCE	1,2-Dichloroethane
DCM	Dichloromethane
dd	Doublet of a Doublet
Dil	Dilute
DMF	*N*,*N*-Dimethyl formamide
DMAc	Dimethyl acetamide
DMPO	5,5-Dimethyl-1-pyrroline N-oxide
DMSO	Dimethyl sulfoxide
DTBP	Di-tert-butyl peroxide
DFT	Density Functional Theory
Equiv	Equivalent
ESI-TOF	Electrospray ionization time-of-flight
Et	Ethyl
EtOAC	Ethyl acetate
EtOH	Ethyl alcohol
g	Grams
h	Hours
HFIP	1,1,1,3,3,3-Hexafluoro-2-propanol
HRMS	High-Resolution Mass Spectrometry

H_2O	Water
Hz	Hertz
IR	Infrared
$K_2S_2O_8$	Potasium persulfate
NIS	*N*-iodosuccinimide
NCS	*N*-chlorosuccinimide
NBS	*N*-bromosuccinimide
PIDA	Phenyliodine diacetate
PIFA	Phenyliodo(bistrifluoroacetate)
CBr_4	Carbon tetrabromide
MeCN	Acetonitrile
mp	Melting point
Me	Methyl
^tBu	*Tert*-butyl
Min	Minutes
mL	Milliliter
mmol	Millimole
mol	Mole
M	Molar
m	Multiplet
MS	Mass Spectra, Molecular Sieves
M/Z	Mass to charge ratio
nm	Nanometer
NMR	Nuclear Magnetic Resonance
[O]	Oxidation
O_2	Oxygen
OTf	Trifluromethanesulfonate
Py	Pyridine
Ph	Phenyl
rt	Room Temperature
s	Singlet, Seconds

t	*Tert*
TBHP	Tert-Butylhydroperoxide
TBAI	Tetrabutylammonium iodide
TEMPO	(2,2,6,6-Tetramethylpiperidin-1-yl)oxyl
TEC	Thiol-ene-click
TFE	2,2,2-Trifluoroethanol
THF	Tetrahydrofuran
TLC	Thin layer chromatography
TMS	Trimethylsilyl
Ts	*p*-Toluenesulfonyl
XB	Halogen bond
XRD	X-Ray diffraction
TFA	Trifluoroacetic acid

CHAPTER 1

Introduction: Overview of Iodine Reagents and Halogen Bonded Catalysts with Their Applications

1.1 ABSTRACT

This chapter is mainly based on a brief introduction to iodine reagents and halogen bond catalysts as well as some photoinduced chemical reactions. It is classified into three-part: (1) historical background of various iodine reagents and their application for the C-N bond formation reactions, (2) photoinduced C-N cross-coupling reactions under the catalyst-free conditions, (3) halogen bond assisted various C-H bond functionalization reactions. Finally, this chapter highlights the goal of the current thesis for the formation of C-N and C-O bonds.

1.2 INTRODUCTION

Iodine(I) is a fifth-row element (group 17) in the p-block, having an atomic number of 53 and electronic configuration [Kr]$d^{10}s^2p^5$. So, from the electronic configuration, the favored oxidation state of iodine is -1. In molecular iodine, the oxidation state is zero (0), whereas, in covalent iodo compounds like iodoarene, the oxidation state is one. The iodine atom can construct poly-coordinated multivalent compounds with lower electronegative atoms (such as oxygen, sulfur, and nitrogen atom) due to its high polarisability.

In 1811, French scientist Bernard Courtois found iodine in seaweed ashes, and J. L. Gay Lussac named it in 1813. The name comes from the Greek word "iodes," which signifies purple or violet. The generation of thyroid hormone requires iodine, a vital trace element in the human body. Thyroxin, a hormone that regulates metabolism, is produced by the thyroid gland. Thyroid enlargement can be caused by iodine insufficiency. Iodized salt is the most cost-effective way to minimize iodine deficiency (IDD) because the body does not generate it. It is the heaviest non-radioactive element in the periodic table that is classified as a non-metal.

On the other hand, the non-covalent electrostatic interaction between the positive -holes of the halogen atom and a Lewis base of another entity is known as halogen bonding interaction. Again, the orbital interactions in halogen bond[1] signifies that the electron transfer takes place from the nonbonding orbital of the nucleophilic region to the antibonding orbital of the halogen atom ($n \rightarrow \sigma^*$) without sharing of an electron. The strength of the halogen bond (XB) depends on the electronic properties of the halogen bond accepter atom (such as -O, -S), as well as the polarizability of the XB donor atom (I > Br > Cl >> F). The strength of XB[2] lies in the range of 10 - 200 $kJmol^{-1}$.

1.3. IODINE REAGENTS AND THEIR APPLICATION IN THE FORMATION OF C-N BONDS

Iodine has to have a favored oxidation state of -1, although it can also have oxidation states ranging from -1 to +VII. Hypervalent compounds contain main group elements with more than eight electrons in their valance shell. In this thesis, N-iodosuccinamide as iodine(I) reagent and PIFA as iodine(III) reagent are being used to construct the C-N bond. As a result, we will solely discuss oxidative C-N cross-coupling reactions involving iodine(I) and iodine(III) reagents in this chapter.

1.3.1 C-N coupling reactions using iodine(I) reagent

Iodine centre having +1 oxidation state behaves as electrophilic iodine sources in organic bond formation reactions. Due to various compelling features like environmentally benign, economic, metal-free and non- toxicity, these reagents are important for many organic transformations. N-iodosuccinimide (NIS) is one of the commonly used monovalent iodine reagent in several organic synthesis. It is readily soluble in MeCN, THF and dioxane but insoluble in ether and CCl_4. Since last decade, NIS has been frequently applied as a

replacement for metal catalyst in synthetic chemistry. C(sp^2-H) amidation via C-N bond formation reaction to construct various N- heterocycles are reported using NIS reagent.

1.3.1.1 Synthesis of indolo[1,2-a]quinazolinones using NIS as an oxidant

G. Sekar and co-workers reported the *N*-iodosuccinimide (NIS) mediated direct oxidative C-N cross-coupling reaction for the synthesis of indolo[1,2-a]quinazolinones (Scheme 1.1)[4]. A wide range of indolo[1,2-a]quinazolinones were synthesized using 1 equiv of NIS in DCE solvent at 80 ^oC. Various electron-withdrawing groups and electron-donating groups were well tolerated under the additive free and base free conditions.

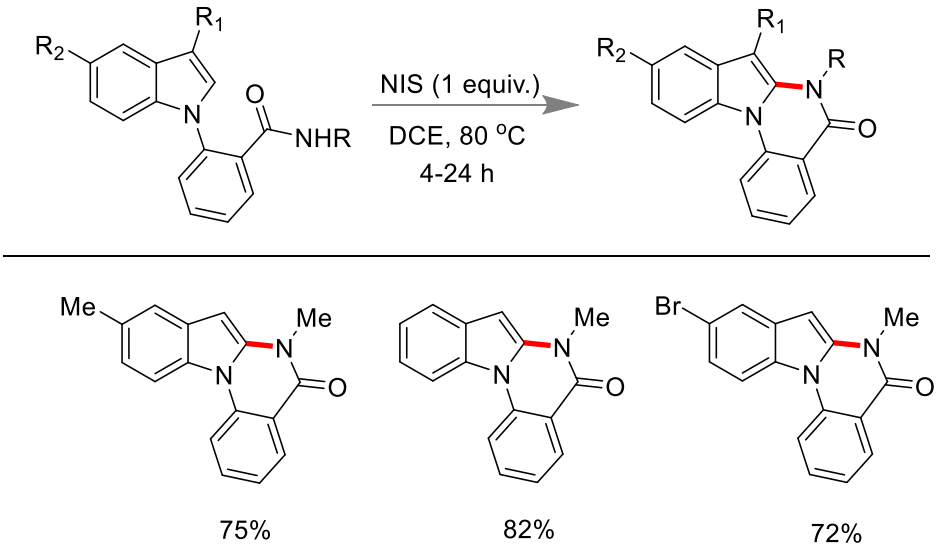

Scheme 1.1. Synthesis of indolo[1,2-a]quinazolinones using NIS as an oxidant.

1.3.1.2 NIS mediated synthesis of indoles

NIS-mediated intramolecular C-N cross-coupling reaction towards the synthesis of Indole derivatives was achieved in DCE solvent at room temperature conditions (Scheme 1.2).[5] A range of indoles with diverse functional groups have been synthesized in good to excellent yields without use of any other additives or catalysts.

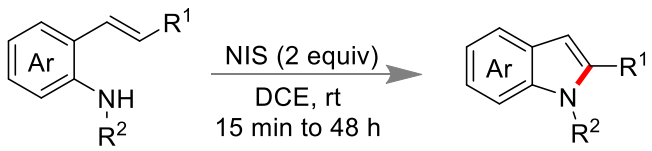

Scheme 1.2. NIS mediated synthesis of indoles.

1.3.1.3 Synthesis of *N*-substituted benzimidazoles

Mal and co-workers also demonstrated an efficient and convenient method for synthesizing 1,2-disubstituted benzimidazoles under mild reaction conditions. (Scheme 1.3).[6] The reaction was successful when NIS has been used in a trifluoroethanol solvent without the addition of any base or additives. This operationally simple and environmentally friendly strategy delivers a wide range of 1,2-disubstituted benzimidazoles from the easily available starting materials.

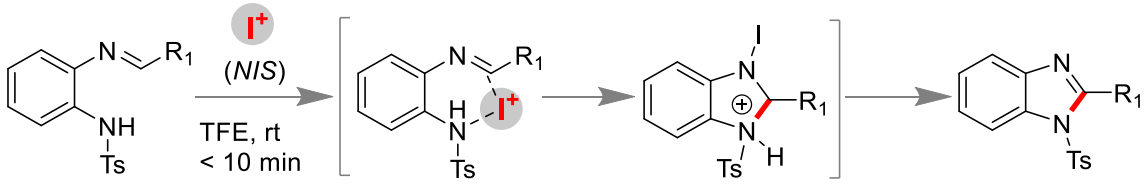

Scheme 1.3. Synthesis of *N*-substituted benzimidazoles

1.3.1.4 Synthesis of spiro[4,5]trienyl acetates using NIS

In this context, the synthesis of spiro[4,5]trienyl acetates has been demonstrated in the presence of AcOH and NIS (N-iodosuccimide) at room temperature conditions (Scheme1.4).[7] The reaction proceeded through the intramolecular ipso-iodocyclization which deliver the library of spiro cyclized products with good yields.

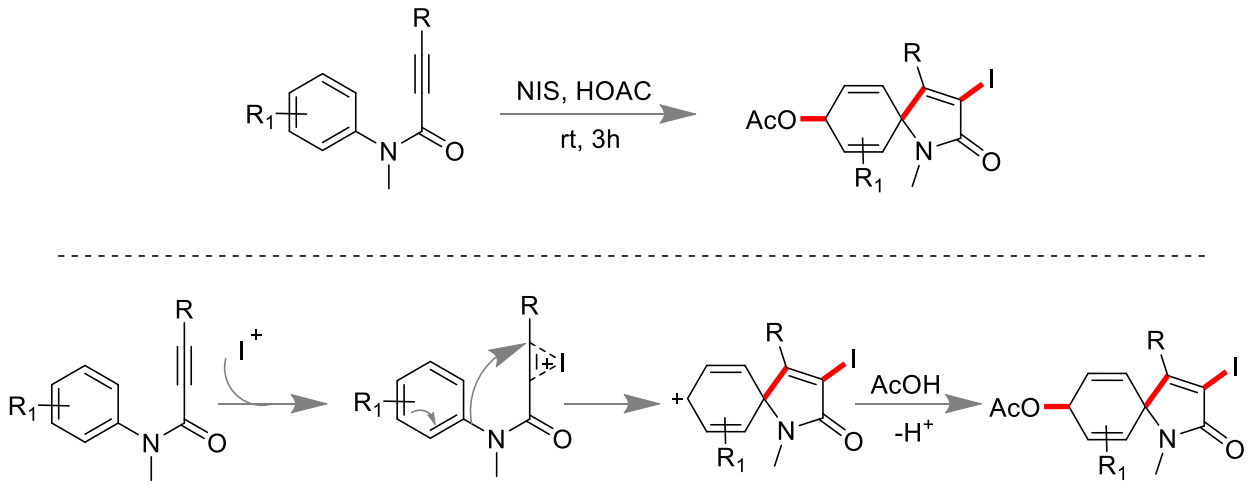

Scheme 1.4. NIS mediated ipso-iodocyclization for the synthesis of spiro[4,5]trienyl acetates.

1.3.2 HYPER VALENT IODINE ASSISTED C-N BOND FORMATION

A hypervalent compound (also known as an expanded octet) has one or more main group elements with valence shell containing more than eight electrons. Iodine can be generated into three forms of hypervalent iodine compounds: (i) trivalent iodine compounds (λ^3-iodanes), which have 10 electrons in their valance shell (i.e., PIDA, PIFA, IBD and IDB), (ii) pentavalent iodine compounds (λ^5-iodanes), which have 12 electrons in their valance shell (i.e., IBX and DMP), and (iii) heptavalent iodine compounds (λ^7-iodanes), which have 14 electrons in their valance shell of iodine (i.e., $NaIO_4$, HIO_4 and IF_7 etc). Some of the iodine(III) reagents are shown in figure 1.1. The most popular approach for synthesizing hypervalent organoiodine(III) compounds uses readily accessible and affordable iodoarene precursors in combination with an appropriate oxidant. It is also possible to synthesize the various iodine(III) reagent from PIDA via the ligand exchange or by using the different type of oxidizing reagents. The metal-free strategies have become an efficient and cost-effective method for constructing carbon-heteroatom bonds due to the avoidance of expensive metal, additives, and harsh reaction conditions. The combination of amines or amides with the iodine(III) reagent to generate the nitrenium ion intermediate under the mild reaction condition. In modern literature, it is accepted that contribution of d orbital for the formation

of hypervalent compounds is not essential and the best way to describe hypervalent bonding is through a description of the molecular orbital that includes a three-center-four-electron bond (3c–4e bond).

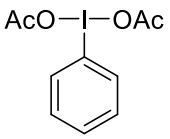

(Diacetoxyiodo)benzene
PIDA

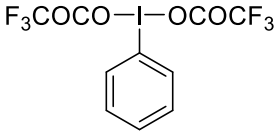

[Bis(trifluoroacetoxy)iodo] benzene
PIFA

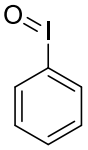

Iodosylbenzene
IDB

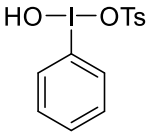

Hydroxy(4-methylphenyl sulfonyloxy)iodo]benzene
Köser's reagent

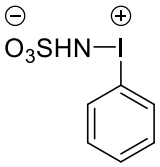

(Phenyliodonio)sulfamate
(PISA)

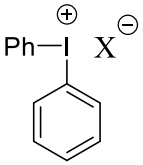

Aryliodonium salts
(X = OTf , PF_6, Br)

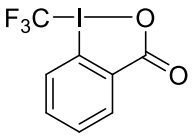

Tögni's reagent

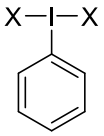

X= F, Cl, Br, N_3
(Dihaloiodo) arenes

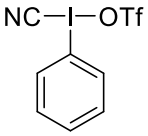

Stang's reagent

Figure 1.1 Various iodine(III) reagents.

One bonding electron pair is delocalized to the two ligands in the 3c–4e bond of a hypervalent molecule, resulting in a charge distribution of –0.5 on each ligand and +1.0 on the central atom. The highly polarised three-center-four-electron (3c-4e) bond, in which the central atom carries a positive charge and two monovalent ligands share the corresponding negative charge, is the key component of these compounds (shown in figure 1.2).

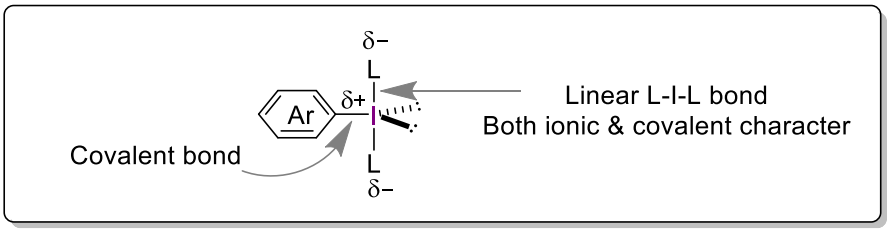

Figure 1.2 Geometry of iodine(III) reagents.

Iodine(III) mediated the formation of nitrenium ion and applications

Generally, three steps are involved in the generation of nitrenium ions. First, it undergoes the ligand exchange followed by the reductive elimination and ligand coupling (Scheme1.5). Nucleophilic attack of amine center to electron-deficient iodine(III) center to generate the *trans*- hypervalent 12-I-4 square-planar species via the associative pathway. Next, it forms *cis* 12-I-4 square-planar intermediate species through the isomerization pathway. Further, it undergoes the reductive elimination pathway, where elimination of iodobenzene or other reduced iodine species takes place to form the nitrenium ion. Finally, the nucleophilic attack of arene on the intermediate nitrenum ion results in the formation of the C-N bond. In many reactions involving hypervalent iodine reagents, reductive elimination is a common mechanism that results in the formal umpolung of the nucleophile's reactivity, Nu: to Nu+.

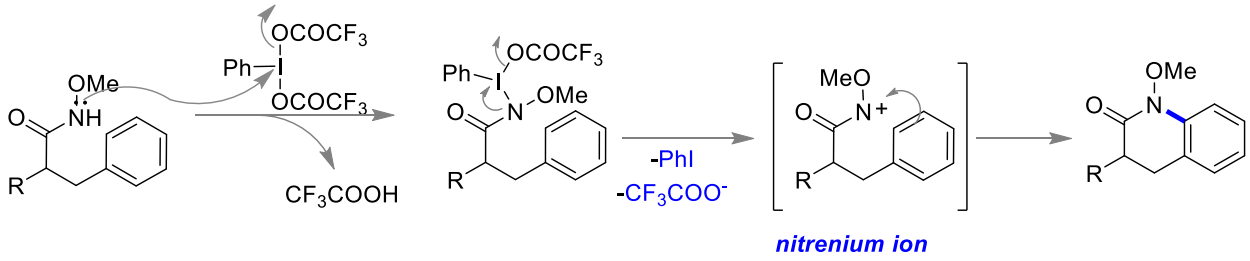

Scheme 1.5. Iodine(III) mediated the formation of nitrenium ion.

The formation of nitrenium ion intermediates is the key step for synthesis of various heterocycles. Figure 1.3 depicts the C-C, C-N, C-O, and N-N bond formation reaction those are used to synthesise several heterocycles using nitrenium ions as intermediates.

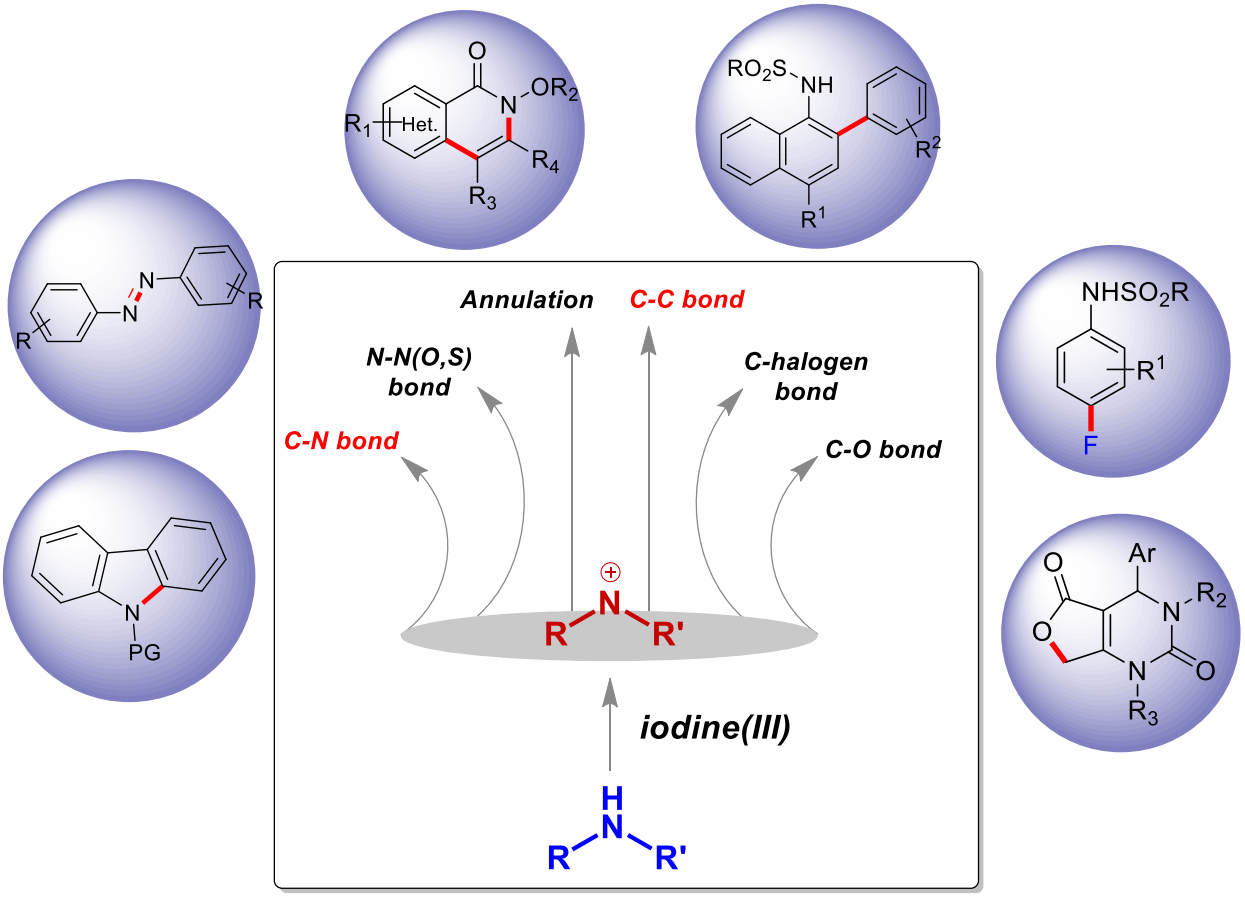

Figure 1.3. Synthetic application of nitrenium ions.

1.3.2.1. PIDA assisted the synthesis of benzodiazepines

In 2014, Zhao and co-workers reported PIDA-mediated synthesis of 1,4-benzodiazepines using acetonitrile as a solvent at room temperature (Scheme 1.6)[8]. The formation of the *N*-acyl nitrenium ion intermediate was the key step in this intramolecular cyclization reaction. However, the cyclized product was not formed when the OMe group (at the R3 position) was replaced by the -Me group. This result confirms that the -OMe group plays an important role in the stabilization of nitrenium ions.

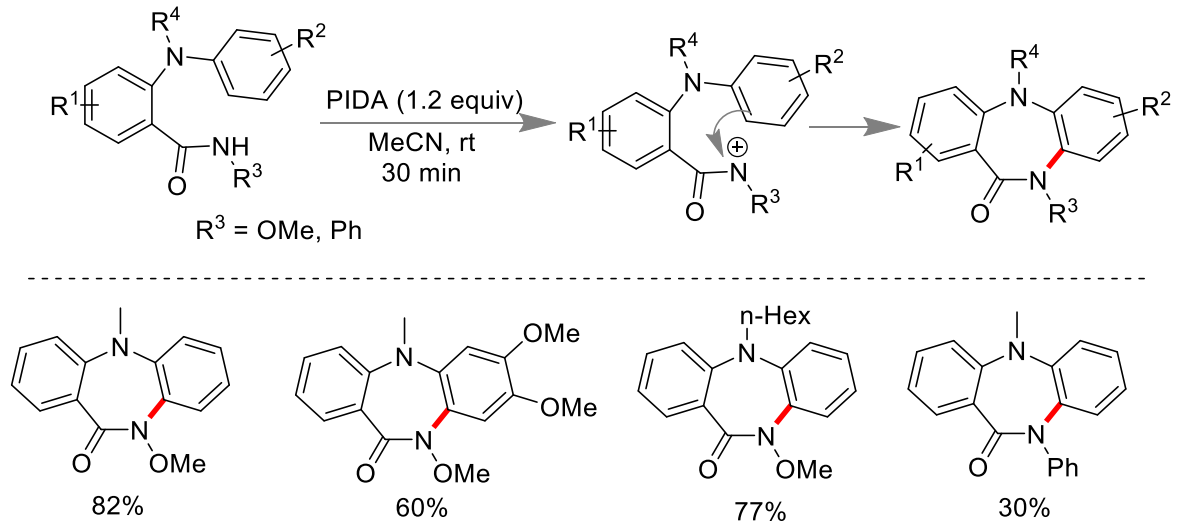

Scheme 1.6. PIDA assisted the synthesis of benzodiazepines.

1.3.2.2 PIFA mediated intramolcular C-N coupling reaction

Litina and co-workers demonstrated the phenyliodine bis trifluoroacetate (PIFA) mediated intramolecular C-N bond formation for the synthesis of indenodiazepinones (Scheme 1.7)[9] at room temperature. The cyclized product was formed as a result of the nucleophilic attack of the aryl ring on the intermediate nitrenium ion.

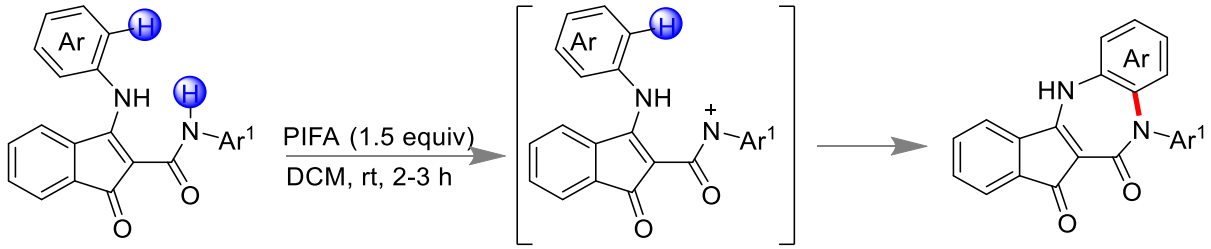

Scheme 1.7. PIFA mediated intramolcular C-N coupling reaction.

1.3.2.3 PIFA mediated synthesis of 1H-indazoles

By treating with the phenyliodine bis trifluoroacetate (PIFA) and arylhydrazones could lead to the formation of nitrenium ion intermediate, followed by nucleophilic attack of arene to produce the 1H-indazoles (Scheme 1.8).[10] A wide range of 1H-indazole derivatives was synthesized under the metal-free and mild reaction conditions.

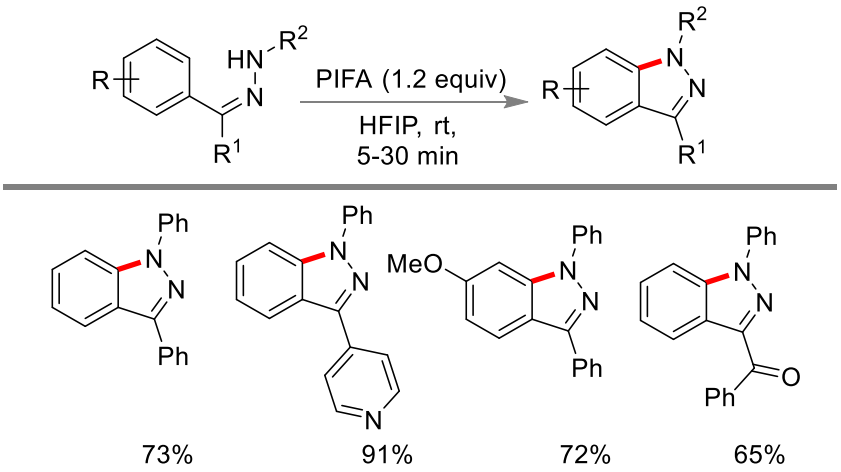

Scheme 1.8. Zhang's approach for the construction of 1H-indazoles.

1.3.2.4 Indazoles synthesis using organocatalytic condition

Tanimori and co-workers devolved a metal free approach for the synthesis of N-aryl-substituted 1H-indazoles using 10 mol% iodo arene as a catalyst and 1.5 equiv oxone as oxidant in TFA solvent (Scheme 1.9).[11]

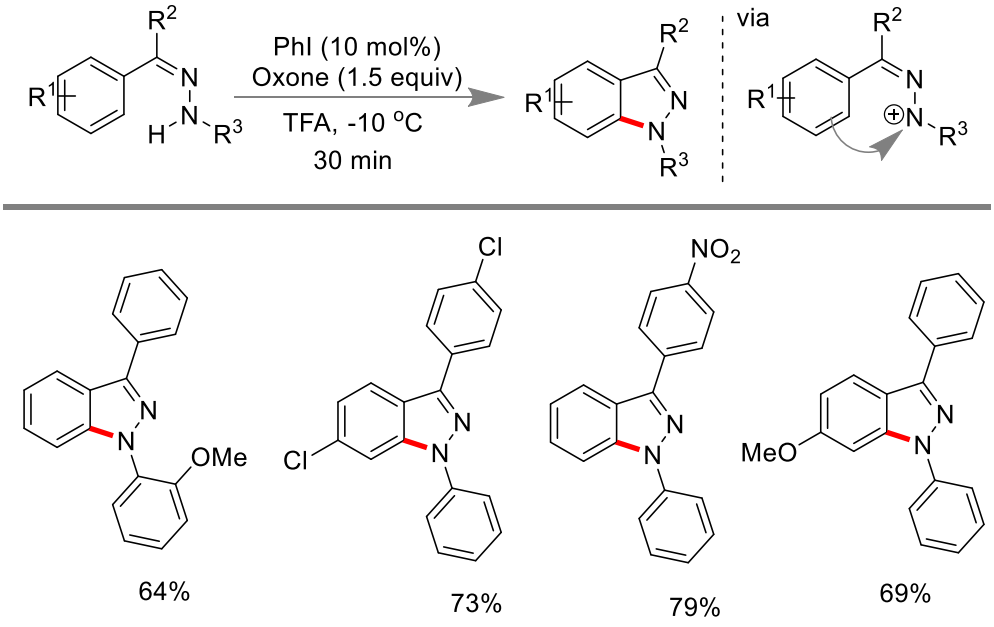

Scheme 1.9. Indazoles synthesis using organocatalytic condition.

The combination of PhI and oxone produces the iodine(III), which deliver the nitrenium intermediate. Next nitrenium intermediate undergoes intramolecular cyclization reaction to form the indazole products.

1.3.2.5 Synthesis of 2-aminobenzimidazole derivatives

Iodine(III) assisted divergent synthesis of guanidines was reported toward the synthesis of 2-aminobenzimidazoles and acetoxyl-substituted 2-aminobenimidazoles (Scheme 1.10),[12] where the C–H amination or acetoxylation process was controlled by the type and amount of iodine(III) reagent. Due to the presence of one more free NH-group, $PhI(OAc)_2$ could be subsequently reacted with to produce an acetoxylation product through the nucleophilic attack of the acetate ion, which was produced from $PhI(OAc)_2$. Notably, only oxidative C-N bond synthesis was observed when $PhI(OCOCF_3)_2$ oxidant was used in excess, without any trifluoroacetoxy group incorporation.

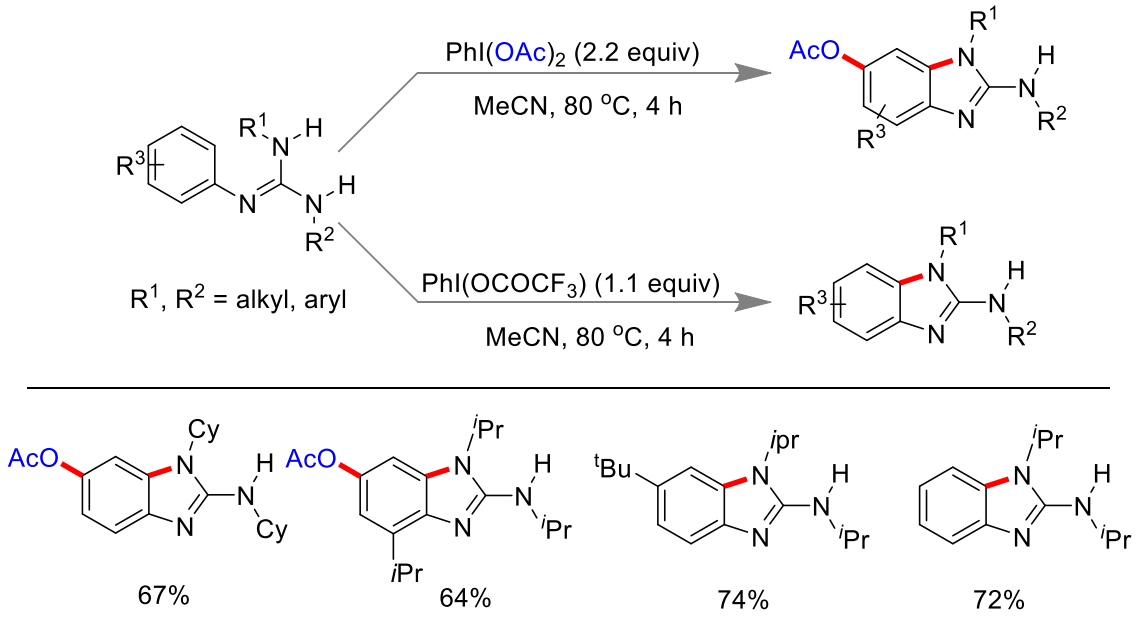

Scheme 1.10. Synthesis of 2-aminobenzimidazole derivatives.

1.3.2.6 PIDA mediated synthesis of benzimidazoles

Similarly, Mal co-workers also synthesized the 1,2-disubstituted benzimidazole with help of 1.1 equivalent of PIDA as an oxidant and TFE as a solvent (Scheme 1.11).[13] The reaction goes via the formation of nitrenium ion intermediate. A series of benzimidazole derivatives

were synthesized under the metal-free and mild reaction conditions. ICP-OES experiments were used to investigate if PIDA may contain any Pd-impurities at ppm levels. This experiment suggests that PIDA does not have any metal impurities.

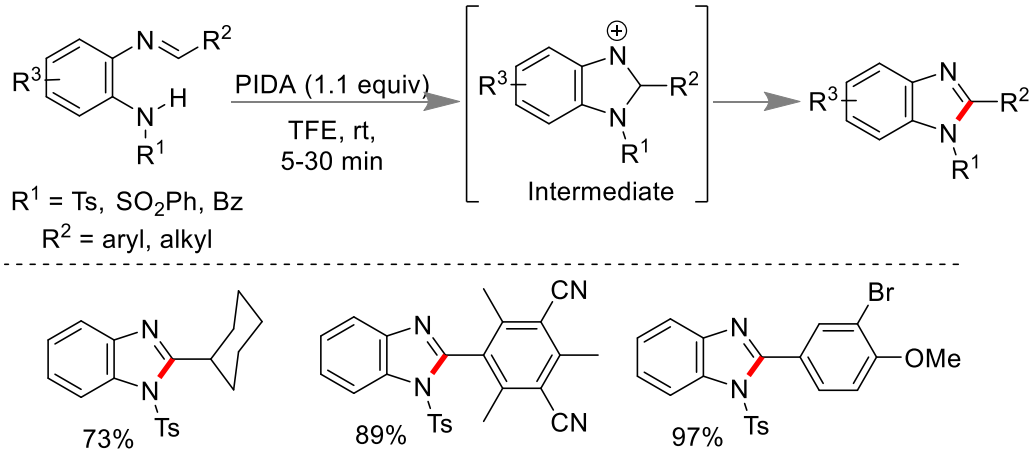

Scheme 1.11. PIDA mediated synthesis of benzimidazoles.

1.3.2.7 Synthesis of benzimidazolinones using PIDA reagent

Fu and co-workers reported an intramolecular oxidative C-H amination utilizing PIDA as an oxidant and Cs_2CO_3 as an additive in HFIP solvent to produce benzimidazol-2-ones under the catalyst and ligand-free conditions (Scheme 1.12).[14]

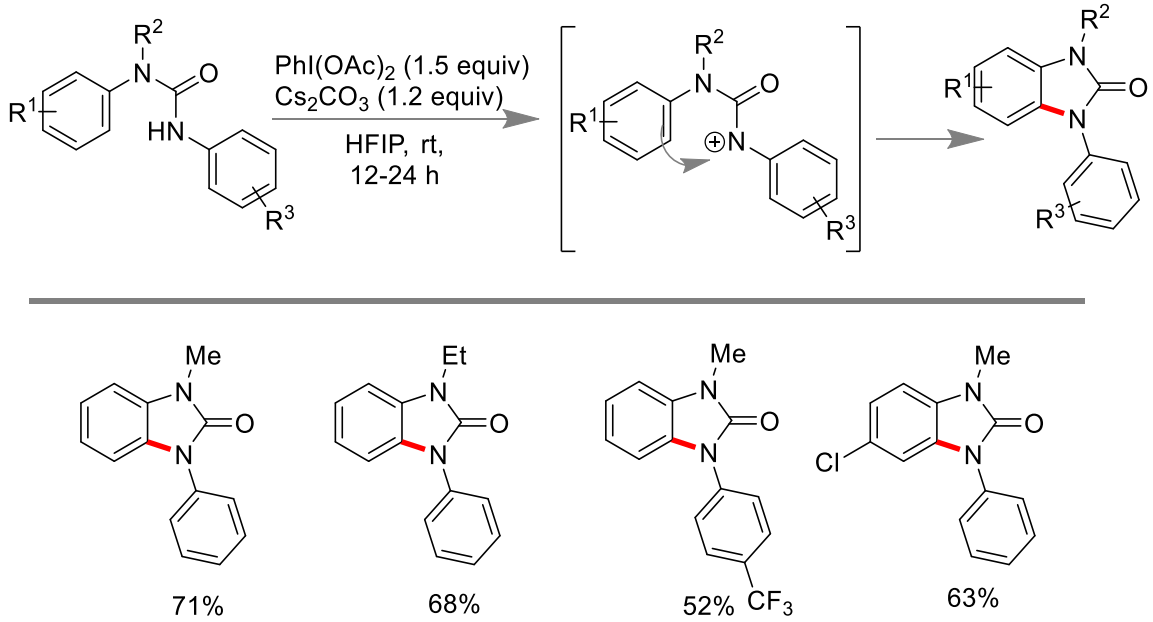

Scheme 1.12. Fu's approach for the synthesis of benzimidazolinones.

The key intermediate for this cyclization reaction is the formation of the niternium ion from N, N-diarylurea and PIDA. The substrate having various functional groups was smoothly converted to the corresponding product with moderate to good yields.

1.3.2.8 Synthesis of lactams and spiro-fused lactams

Kikugawa and co-workers reported the PIFA mediated C-N cross-coupling reaction for the synthesis of lactams and spiro-fused lactams via the intramolecular electrophilic substitution reaction (Scheme 1.13).[15] The key intermediate for this cyclization reaction was the formation of nitrenium ion from N-acylaminophthalimides and PIFA in a TFA or HFIP solvent.

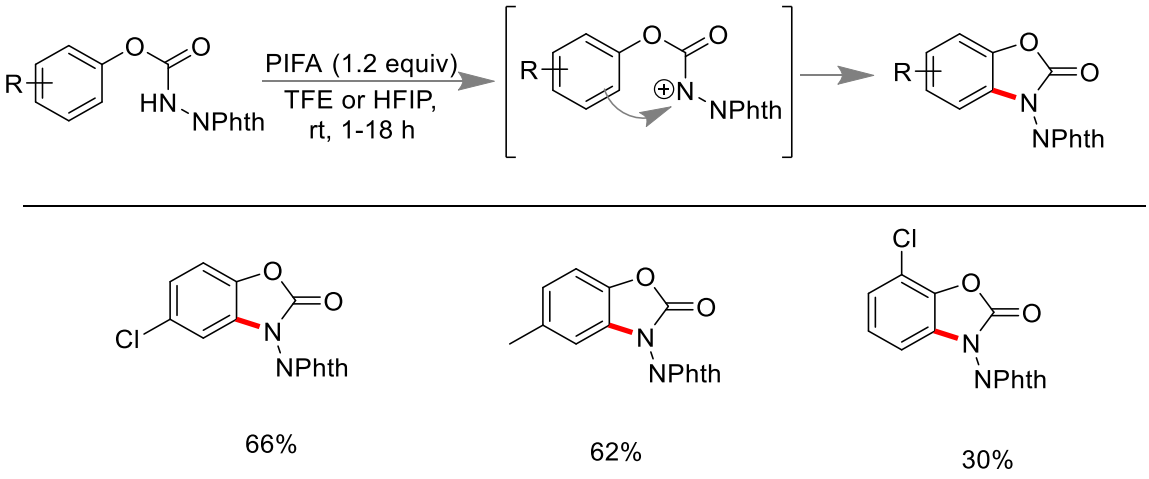

Scheme 1.13. Synthesis of lactams and spiro-fused lactams.

1.3.2.9 PIDA mediated synthesis carbazoles

In 2018, Mal and co-workers developed an efficient strategy for the synthesis of carbazoles using 1.2 equiv of PIDA in TFE solvent at room temperature conditions (Scheme 1.14).[16] The formation of nitrenium ions as intermediates in the reaction leads to the nucleophilic attack from nearby arenes, followed by the breaking of the C-C bond to produce the N-arylation product. It was found that, compared to ^{i}Pr group cleavage, the ^{t}Bu group cleavage produced larger yields of carbazoles product.

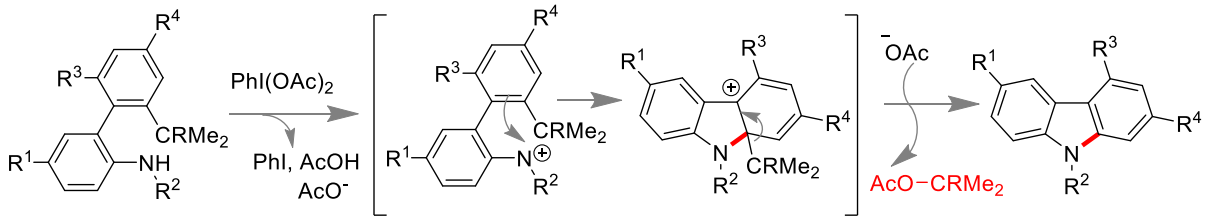

Scheme 1.14. C-C bond functionalization for the synthesis carbazoles.

The same group have reported the intermolecular C-C and C-N cross-coupling reaction towards the synthesis of carbazole derivatives using 2.5 equivalent of $PhI(OAc)_2$ in HFIP: DCM (1:1) solvent at room temperature conditions (Scheme 1.15).[17] Initially, C-arylated intermediated was formed when 1 equiv of PIDA interacts with sulfonanilides to produce nitrenium, which is then transformed to carbenium ion. The second equivalent of PIDA reacts with C-arylated intermediates to generate the nitrenium ion which then undergoes intramolecular cyclization followed by the methyl group migration to deliver the substituted carbazole derivatives with good yields.

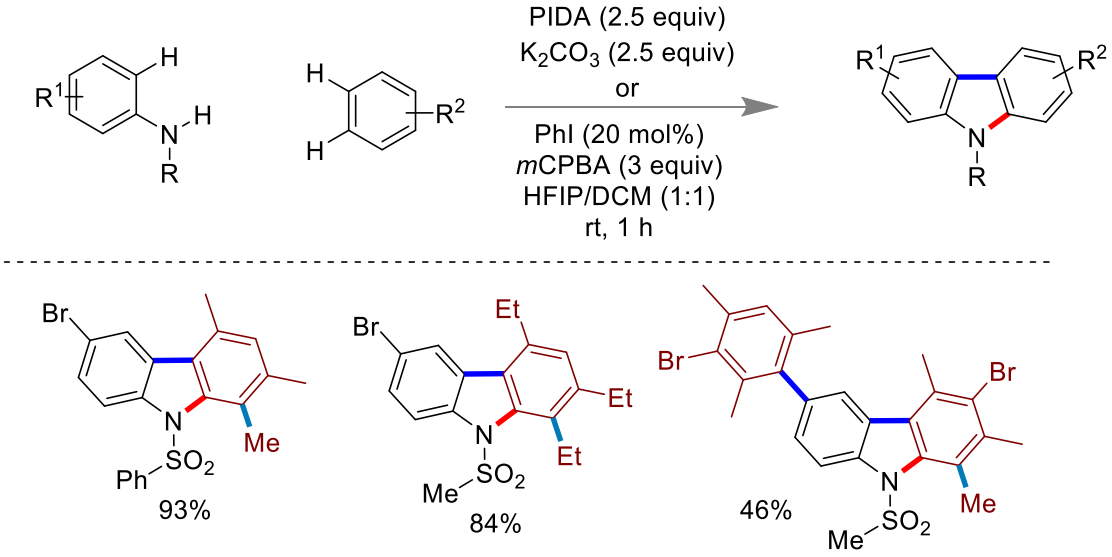

Scheme 1.15. Synthesis of carbazoles via the dehygrogenative annulation pathway.

1.3.2.10 Synthesis of isoquinolones using iodine(III)

Antonchick group developed the intermolecular annulation of alkynes and benzamide derivatives towards the contraction of isoquinolones using iodobenzene and peracetic acid combination (Scheme 1.16).[18] The use of unsymmetrical alkynes also afforded the annulated product with high regioselectively. This regioselective annulation reaction also delivers a library of isoquinolones via the cascaded C-C and C-N bond formation.

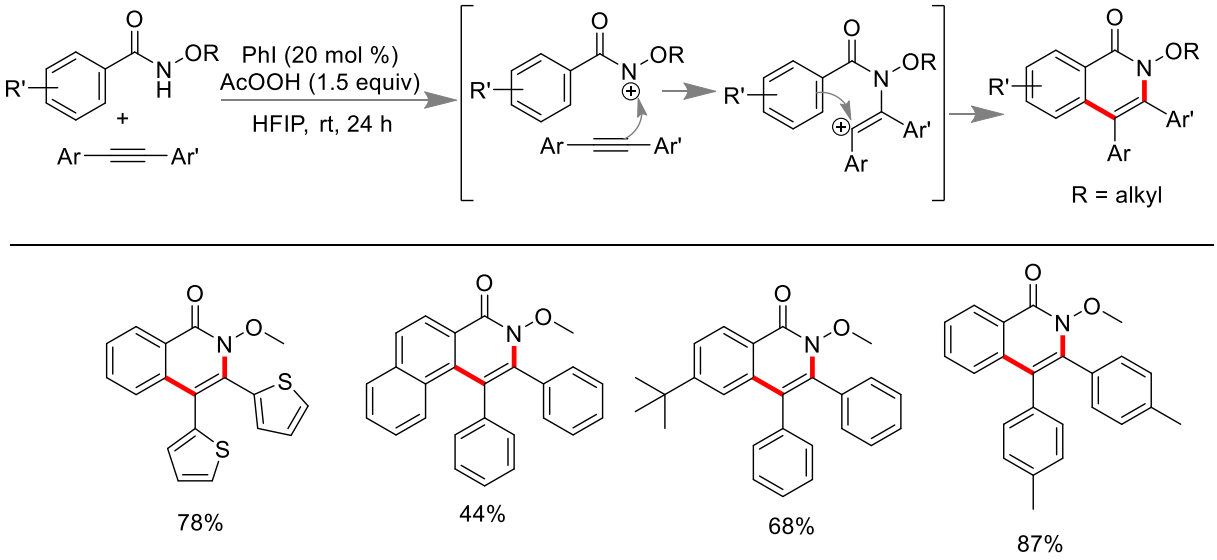

Scheme 1.16. Synthesis of isoquinolones via cascaded C-C and C-N bond formation.

1.3.2.11 Synthesis of bisindoles using PIDA

Chang and co-workers investigated the PIDA-mediated intramolecular diamination of olefins for the synthesis of bisindoles (Scheme 1.17).[19] In the presence of a halide additive, PIDA promotes the development of hypohalite. The electrophilic addition of olefin was then used to generate a halonium intermediate, which was then followed by a two-step S_N^2 reaction to produce the bisindoles product.

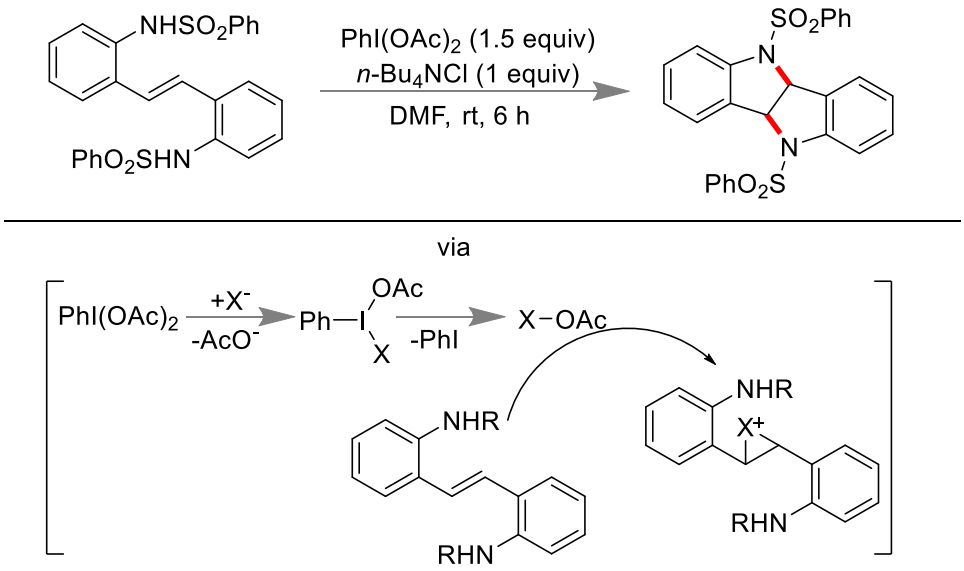

Scheme 1.17. Synthesis of bisindoles using PIDA.

1.4 PHOTOINDUCED C-N CROSS-COUPLING REACTIONS UNDER THE CATALYST-FREE CONDITION

Photochemical conversion is renowned as an eco-friendly and efficient method in organic synthesis due to the avoidance of any metal-based reagent, photocatalyst, or external oxidant, harsh reaction conditions, and less purification of by-products. Furthermore, it is a well-known green synthetic approach that offers a novel synthetic area, where the reaction is performed without adding any reagent except light. Generally, the photoreactions take place either in the presence of sensitizers or the substrate must include chromophores. Here, we will discuss the photo-induced C-N cross-coupling reaction under photo catalyst and metal-free conditions.

1.4.1 Photochemical synthesis of benzimidazole-fused phenanthridines

In 2021, Mal and co-workers investigated the photochemical dehydrogenative C-N coupling towards the synthesis of benzo[4,5]imidazo[1,2-f]phenanthridine using 350 nm light source (Scheme 1.18).[20] The N-H…π interaction assisted the cyclization reaction at lower energy compared to the corresponding absorption maxima. Imidazolyl-type radical was formed via

the homolytic cleavage of N-H bond, followed by ε-hydrogen abstraction to produce 1,6-diradical. Further radical-radical coupling delivered the benzo[4,5]imidazo[1,2-f]phenanthridine.

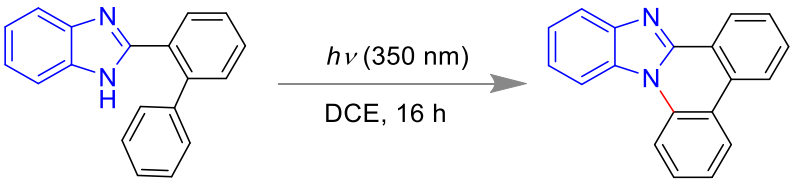

Scheme. 1.18. Photoinduced intramolecular C–N coupling reaction for the synthesis of benzimidazole-fused phenanthridines.

1.4.2 Intramolecular C-N coupling under photochemical condition

In 2020, Kaszynski and co-workers developed an intramolecular photocyclization reaction of 8-aryloxy benzo [*e*] [1,2,4] triazines upon irradiation of halogen lamp (300 W) in CH_2Cl_2 solvent. (Scheme. 1.19).[21]

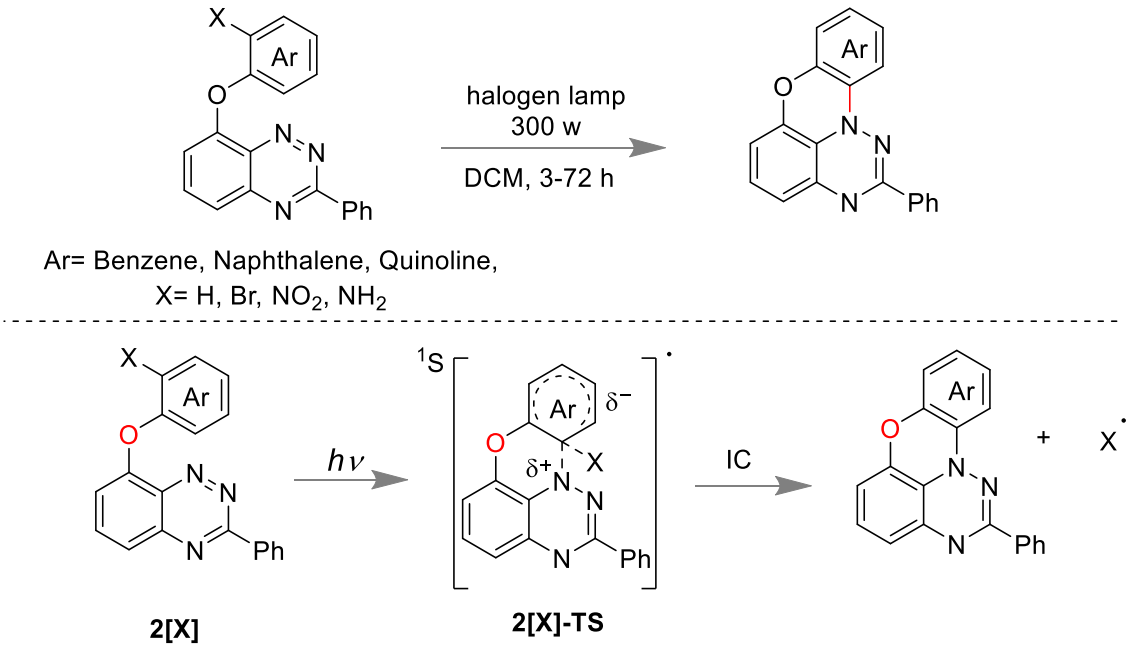

Scheme. 1.19. Intramolecular C-N coupling under photochemical condition.

The reaction goes via the formation of stable polycyclic [1,2,4] triazinyl radical, which was also supported by a number of control experiments (XRD, electrochemical and EPR, UV-

vis). The high regioselectivity of this photocyclization reaction was further demonstrated by DFT experiments.

1.4.3 Photoinduced [3+2] cycloaddition reactions

Schnarr and co-workers developed a benzyne-based [3+2] cycloaddition reaction under the photochemical condition (λ = 365 nm) and without added any reagent (Scheme 1.20).[22] The use of polar protic solvent, shorter reaction time, radially available starting materials, and room temperature conditions are the reaction's unique features. In addition to this, various functional groups also well tolerated using 365 nm of light source.

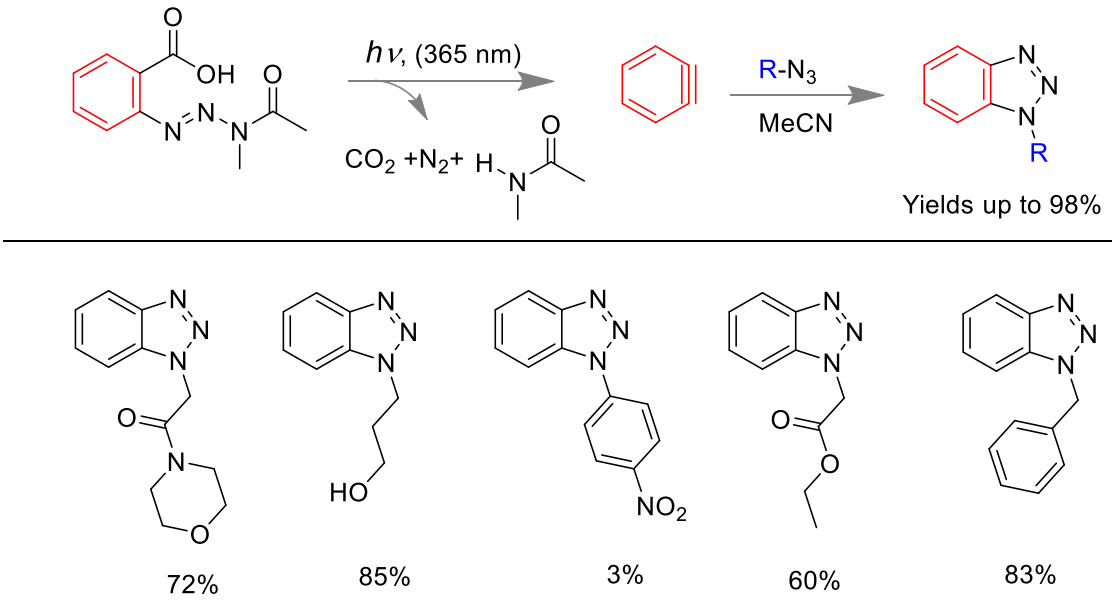

Scheme. 1.20. Photoinduced [3+2] cycloaddition reactions.

1.4.4 Visible-light-promoted dehydrogenative cross-coupling reaction

In 2016, Xia and co-workers invented a visible light-mediated cross-dehydrogenative coupling (CDC) reaction between cyclic anilines and phenols using $K_2S_2O_8$ as an oxidant in CH_3CN solvent (Scheme. 1.21).[23] This photocatalyst and metal-free approach afforded a wide range of substrate scopes with good yield and regioselectivity. A radical-induced process was proposed by several control experiments and the formation of the TEMPO adduct.

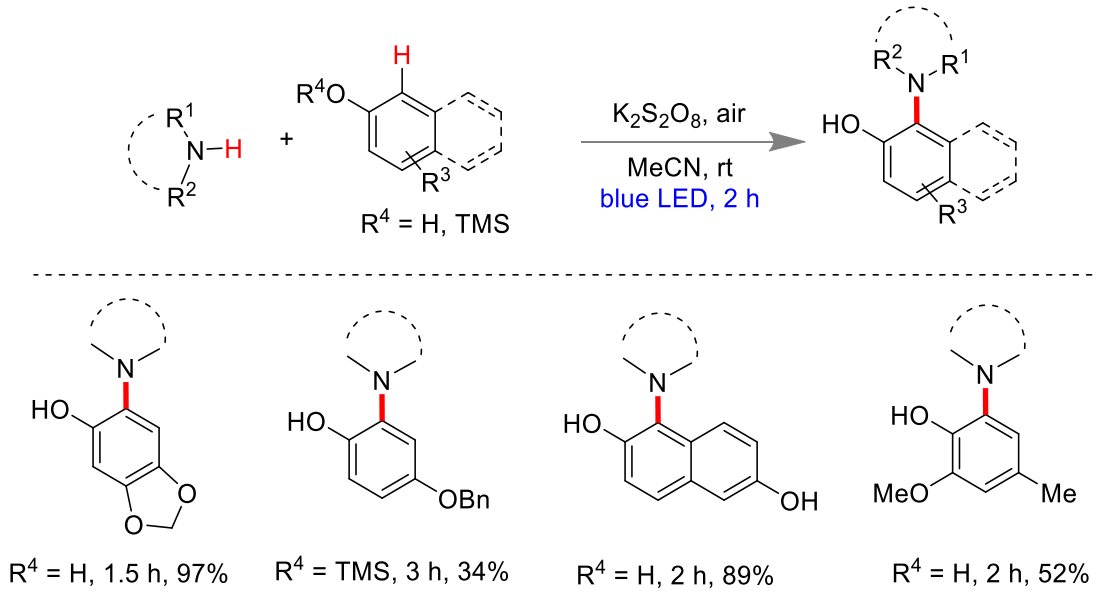

Scheme. 1.21. Visible-light-promoted dehydrogenative cross-coupling reaction.

1.5 HALOGEN BOND CATALYST IN ORGANIC SYNTHESIS

Non-covalent interaction has been well explored in the field of supramolecular chemistry,[24] anion recognition,[25] medicinal chemistry, chemical biology,[26] organic synthesis,[27] catalysis,[28] etc. This interaction facilitates the organic reaction by activating functional groups or stabilizing reaction intermediates. The XB catalysis has been widely used in halogen abstraction reactions,[29] and the activation of aldehydes, ketone, imines, and heteroarenes. According to the literature, the formation of XB co-crystals is often preferred in a more polar solvent over a less polar solvent.[30] In organic systems, noncovalent interactions play a significant role in controlling product selectivity, which mimics a biological phenomenon.[31] Use of noncovalent interactions like H-bonding,[32] sulfur-oxygen (S…O),[33] hydrophobic effect,[34] charge-transfer,[35] halogen bonding,[36] cation-π,[37] anion-π,[38] etc., which have utilities in organic synthesis is emerging at a fast pace.[39] The noncovalent interactions mediated C-H functionalization can offer a robust and sustainable strategy in modern organic synthesis.[39a]

1.5.1. Halogen bond assisted various C-H bond functionalization reactions

1.5.1.1 Benzyl C-H bond functionalization

In 2016, Xi and coworkers demonstrated halogen bonding interaction assisted benzyl C-H bond functionalization for the synthesis of 2H-indazoles (Scheme 1.22).[40] Simple reaction conditions, excellent efficiency, and use of less expensive molecular iodine instead of expensive transition metal catalysts could make the process more environmentally friendly. Both the electron-donating as well as electron-withdrawing substrates were well suited under the standard reaction condition. Several control experiments and mechanistic studies using far-infrared, EPR, NMR confirmed the halogen bonding interaction between I_2 and the nitrogen center of the azo group. This reaction is assisted by the weak N-I interaction, which brings the ortho-methylene group near to the I_2.

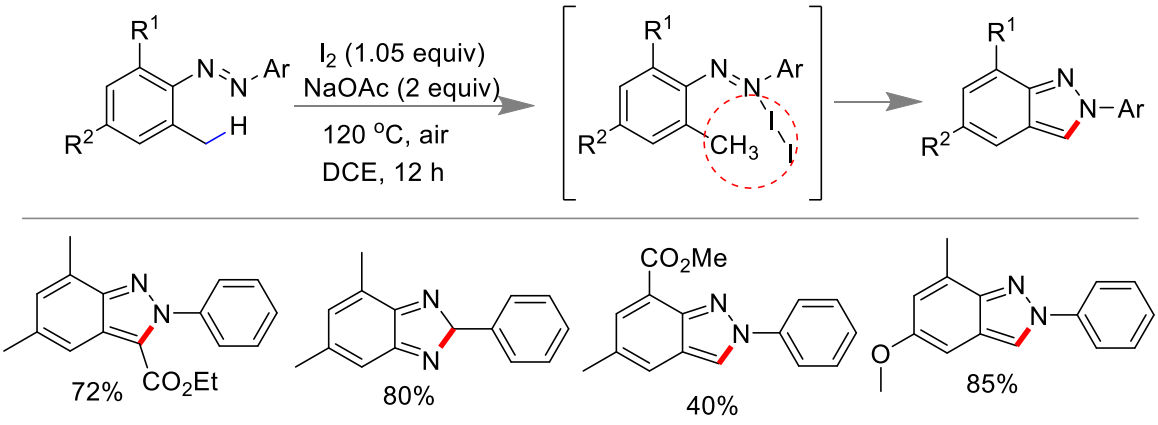

Scheme. 1.22. XB-assisted benzyl C–H functionalization toward the synthesis of 2H-indazoles.[40]

1.5.1.2 Aromatic C-H functionalization

In 2019, aromatic C-H bond iodination of heterocyclic rings had been developed with the help of halogen bonding interaction between molecular iodine and nitrogen center of the heterocyclic ring under room temperature conditions (Scheme 1.23).[41] In this method, the

mono-iodo product of several heterocyclic compounds like quinolones, isoquinolines, 7-azaindoles, 8-aminoquinolines was synthesized as a single regioisomer with good to moderate yields by the use of semi stoichiometric amount of I_2 and *tert*-butylhydroperoxide (TBHP) as an oxidant. The halogen bonding interaction was established via spectroscopic analysis, control experiments, and DFT calculations, which was responsible for lowering the activation energy in electron transfer radical mechanisms.

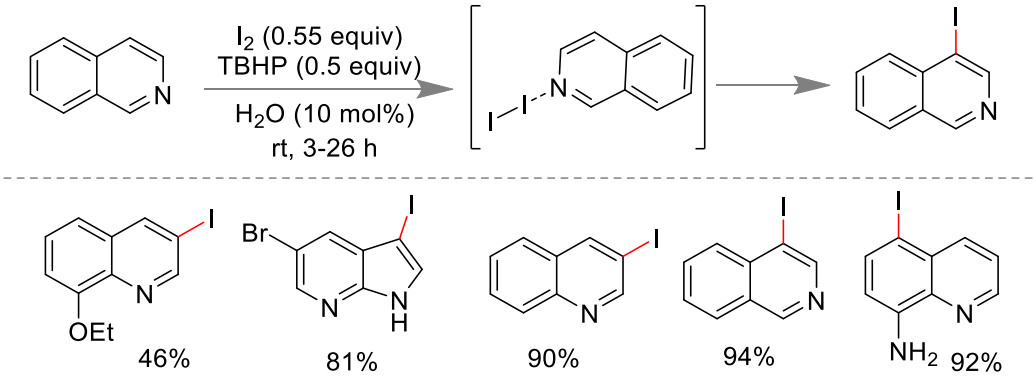

Scheme. 1.23. XB-assisted iodination of heteroarenes at room temperature.[41]

1.5.1.3 Halogen bond assisted C-S bond formation

XB-assisted C-H functionalization of heteroarenes was achieved to synthesize thioether under visible-light (Scheme 1.24).[42] This reaction involves the iodination of heteroarenes followed by the C-S coupling reactions. The halogen bonded intermediate was proposed between the iodoarene and the thiolate anions, which promoted the electron transfer process to afford the thioethers. The photoexcitation on the halogen bonded complex helped in the electron transfer process at room temperature to generate the radical anion of iodo-isoquinoline. At that point, removal of iodide ions from the radical anion produces isoquinoline radical, which reacts with thiolate anion to produce thioether via electron transfer process. A series of thioether derivatives were synthesized with the help of various heteroarenes, as well as aromatic and aliphatic thiols.

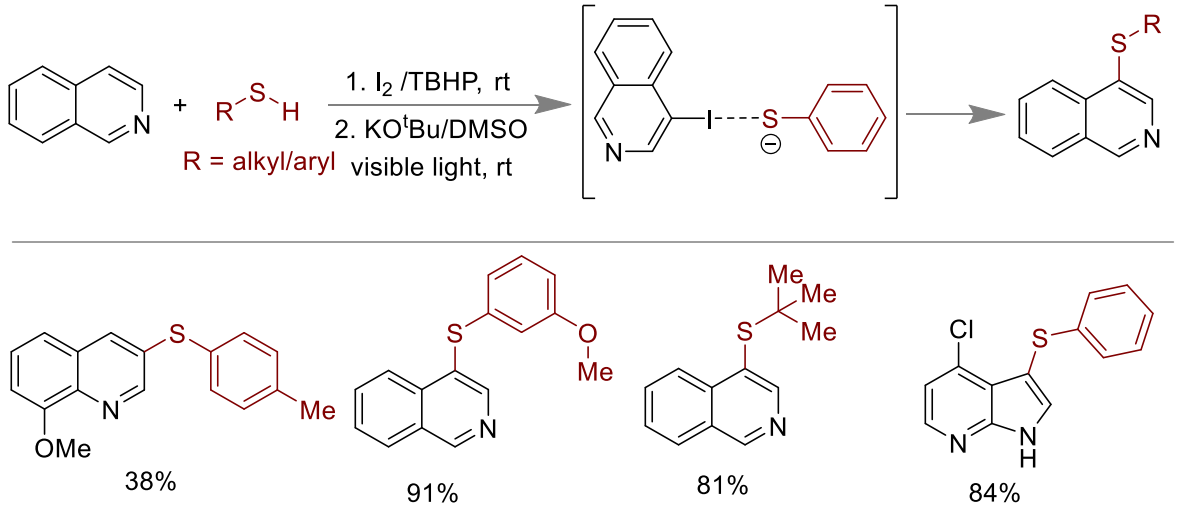

Scheme. 1.24. XB-assisted synthesis of heteroaryl thioethers.[42]

1.5.1.4 $C_{(sp3)}$-H bond functionalization

Halogen bonded iodonium ions generated from Lewis base and halogen(I) reagent are the stable and versatile reagents used in various organic transformations. Few examples are Hofmann–Loffler reaction[43] and the oxidative alkene functionalization[44] assisted by the carboxylate-coordinated iodonium ions, and DMSO-coordinated iodonium ions.

The *α*-hydroxy ketones (Scheme 1.25)[45] were synthesized from the benzylic secondary alcohols *via* selective oxidation of secondary alcohol to ketone, and simultaneously α-$C_{(sp3)}$-H bond of the newly formed carbonyl group was converted to the secondary hydroxyl group without any over oxidation. A catalytic amount of iodine in the presence of iodine(V) reagent generated the DMSO-coordinated iodonium ions, which were investigated by the spectroscopic evidence.

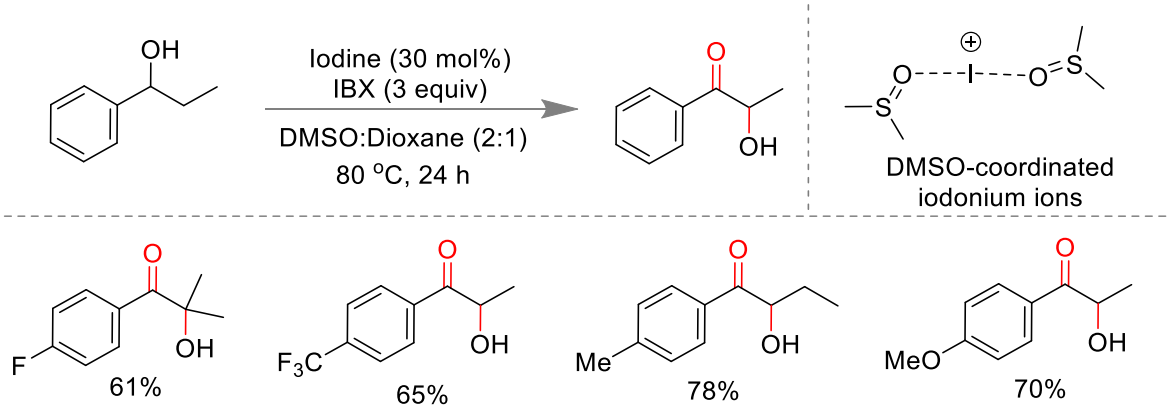

Scheme. 1.25. Synthesis of *α*-hydroxy ketones using halogen bonded iodonium ion catalyst.[45]

1.5.1.5 $C_{(sp2)}$-H bond functionalization

Neutral bidentate triazole derivatives were widely used as anion receptors.[46] In this context, Huber and coworkers demonstrated a new synthetic strategy for halide abstraction reaction using a bidentate triazolium-based halogen bond activator (Scheme 1.26).[47] The C-Br bond of benzhydryl bromide was activated in the presence of the stoichiometric amount of XB-catalyst, to generate the benzhydryl cation. Further, the nucleophilic attack of 1,3,5-trimethoxybenzene to benzhydryl cation produces ((2,4,6-trimethoxyphenyl)methylene)dibenzene product.

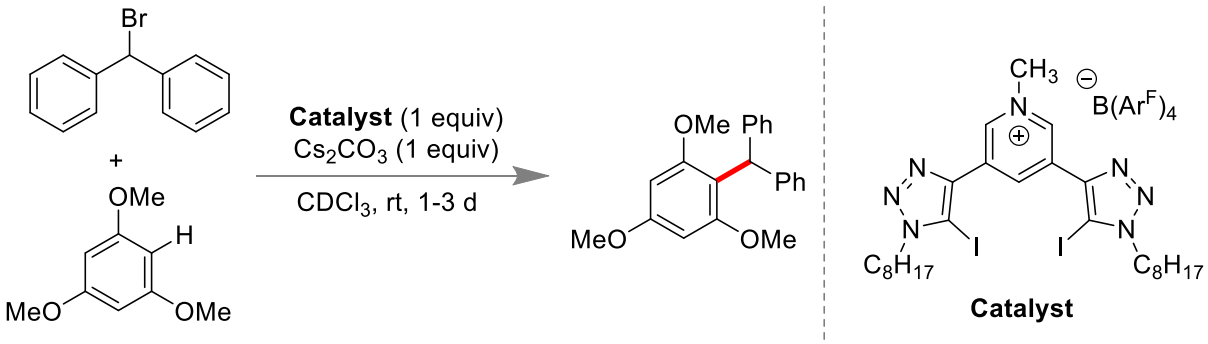

Scheme. 1.26. Friedel–Crafts alkylation by charge-assisted halogen bond donors.[47]

Furthermore, 1.0 equiv Cs_2CO_3 was used to rule out any hidden acid catalysis for this transformation. Again, the halide binding ability of counter anion was found to be in the

order of ($B(Ar^F)_4^-$ > NTf_2^- > OTf^-) and the planar bis(iodotriazolyl)pyridinium moiety delocalized the positive charge.

Legros and co-workers reported an easily recyclable and recoverable halogen bonded fluorous organocatalyst ($DABCO{\cdot}(C_8F_{17}I)_2$) mediated Morita-Baylis-Hillman reaction (Scheme 1.27).[48] This supramolecular catalyst was synthesized by the simple addition of DABCO (mp 156 ^oC) and $C_8F_{17}I$ (mp 25 ^oC) in DCM. The catalyst was precipitated out as a solid (mp 93 ^oC) and isolated by filtration. Benzaldehydes having different functional groups and heterocyclic moiety was reacted smoothly with methyl vinyl ketone and acrylonitrile with good yields.

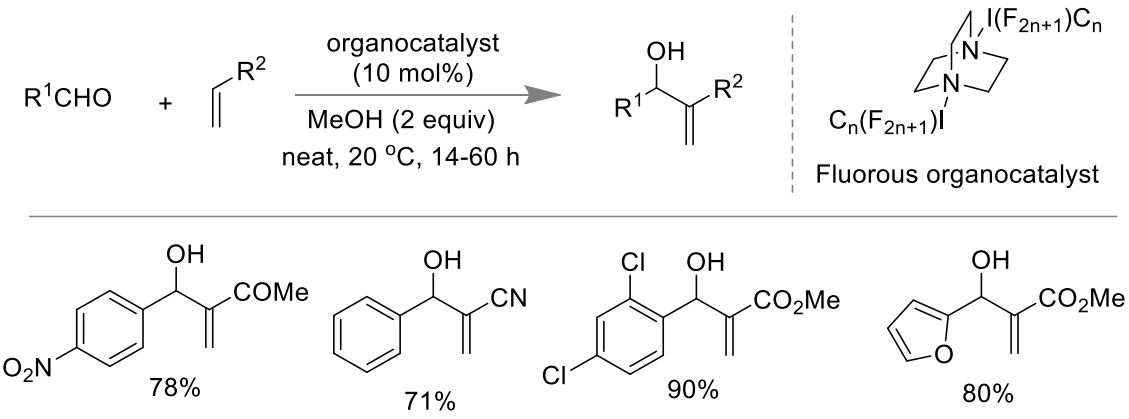

Scheme.1.27. Halogen-bonded fluorous organocatalyst mediated Morita-Baylis–Hillman reaction.[48]

1.5.2. Activation of carbonyl compound

In 2014, Huber and co-workers developed a synthetic procedure for a Diels-Alder reaction using imidazolinium-based halogen-bond donor organocatalyst (Scheme 1.28).[49] The neutral compound, such as ketone was activated by the dicationic halogen-bond donor catalyst. The electrophilic iodine center helped for the activation process as well as non-coordinating counter ions of halogen-bond donor's catalyst played a crucial role in the prototypical Diels-

Alder reaction. Furthermore, the theoretical study also revealed that the bidentate coordination between the halogen bond donor and ketone decreases the activation barrier significantly compared to the uncatalyzed Diels-Alder reaction.

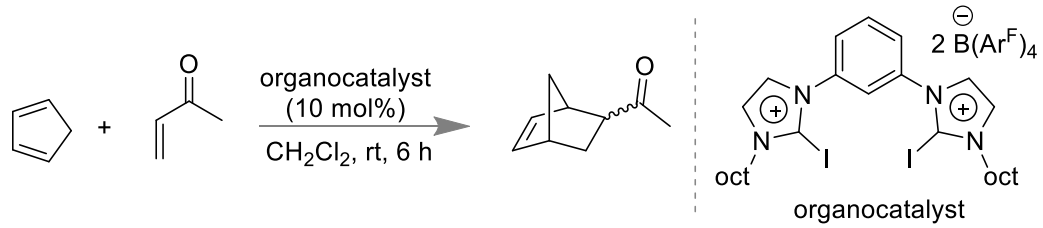

Scheme.1.28. Halogen bond assisted activation of a carbonyl compound for Diels-Alder reaction.[49]

Takemoto and co-workers investigated the iodo-imidazolium-based halogen bond donor catalyst assisted activation of iodonium ylides for the alkylation reaction of silyl enol ethers and 3-substituted oxindoles (Scheme 1.29).[50]

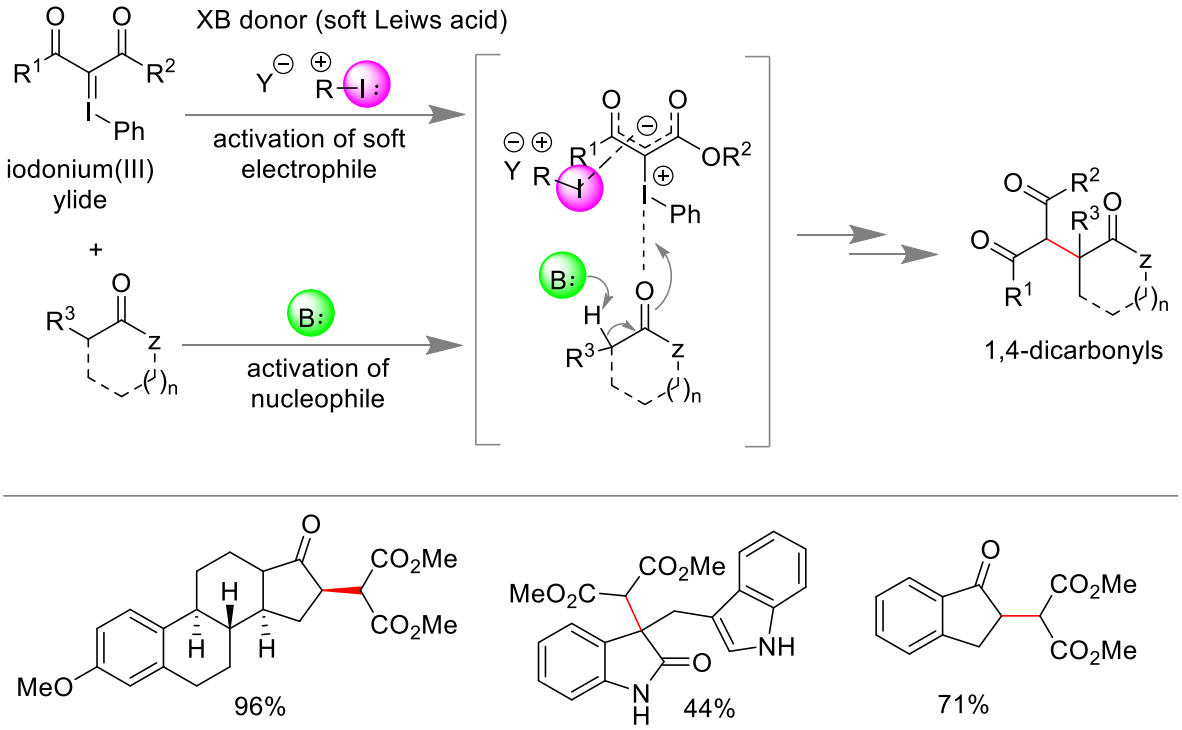

Scheme.1.29. Halogen bond promoted electrophilic activation of iodonium ylides.[50]

Various functional groups and different heterocyclic scaffolds were also well-tolerated, and a series of 1,4-dicarbonyl compounds were synthesized with good to excellent yields. A systematic study suggested that the XB donor catalyst activated iodonium(III) ylide, and then the nucleophilic attack of silyl enol ether to the activated ylide took place. Further rearrangements afforded the 1,4-dicarbonyl compounds. Again, the use of THF solvent suppressed the decomposition of the iodonium ylides *via* the coordination of solvent and iodine(III) center.

Sekar and co-workers demonstrate the halogen bonding assisted the construction of *α,β*-unsaturated ketones *via* the activation of an aldehyde group (Scheme 1.30).[51] Many functional groups, acid, and base-sensitive groups were found to be compatible under solvent-free conditions, which could compete with the traditional Cannizaro reaction. Initially, the aldehyde group was activated by CBr_4; further, it reacted with an enolized ketone to form the aldol product. Finally, the elimination of water molecules took place, which was assisted by the weak interaction of CBr_4 with the hydroxyl group to generate the chalcone derivatives, and CBr_4 was also regenerated. However, the existence of halogen bonds was established by UV-visible as well as IR spectroscopy.

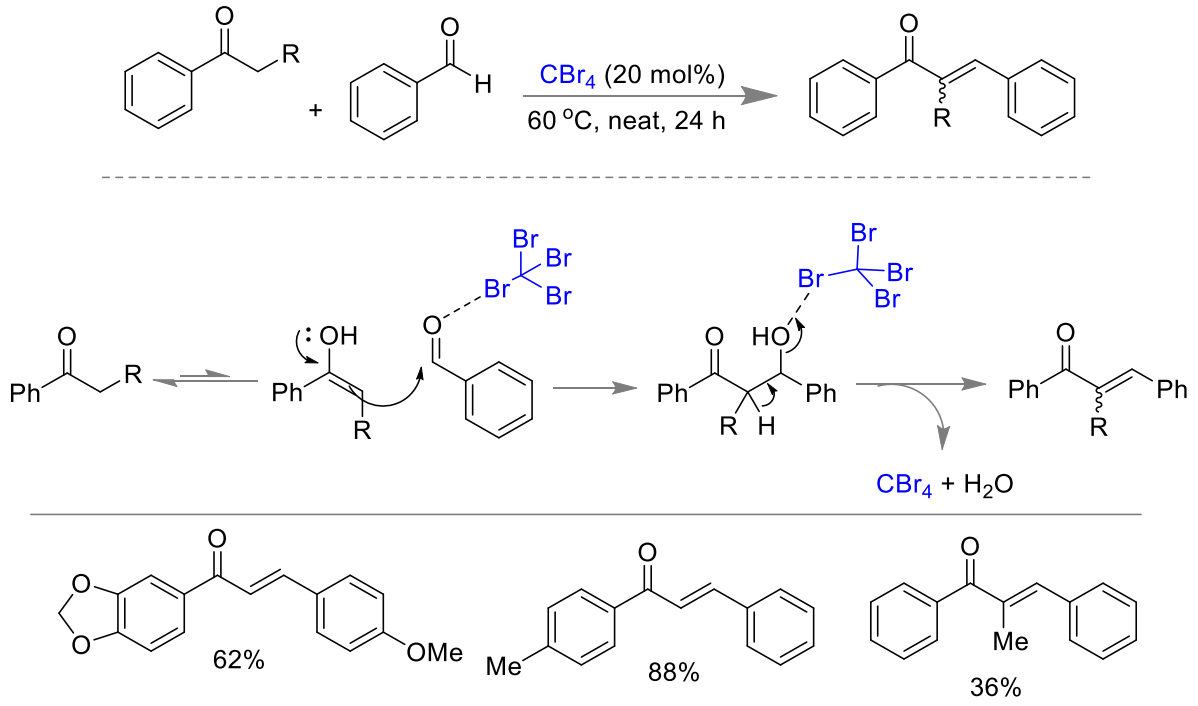

Scheme.1.30. Activation of aldehyde toward the synthesis of chalcone derivatives.[51]

1.5.3. Activation of conjugated ketones

In addition to the carbonyl group activation by halogen bond donor catalysts, it is also possible to activate the conjugated ketones to form the Michael addition product. Banik and coworkers reported the catalytic iodine-mediated conjugated addition of indoles and imidazoles with α,β-unsaturated ketones under the solvent-free condition.[52] Similarly, Huber and coworkers investigated the activation of *α,β*-unsaturated ketones using the (benz)imidazolium-based halogen bond donors catalysts (Scheme 1.31).[53] Again, the use of two iodobenzimidazolium scaffolds increases the rate of the Michael addition reaction by 50 times compared to the similar compounds having -bromo or -chloro substitution in the place of iodine atom. In the same way, Breugst also reported the monodentate halogen-bond donors catalyzed a Michael addition reaction between the indole and *trans*-crotonophenone (Scheme 1.31).[54]

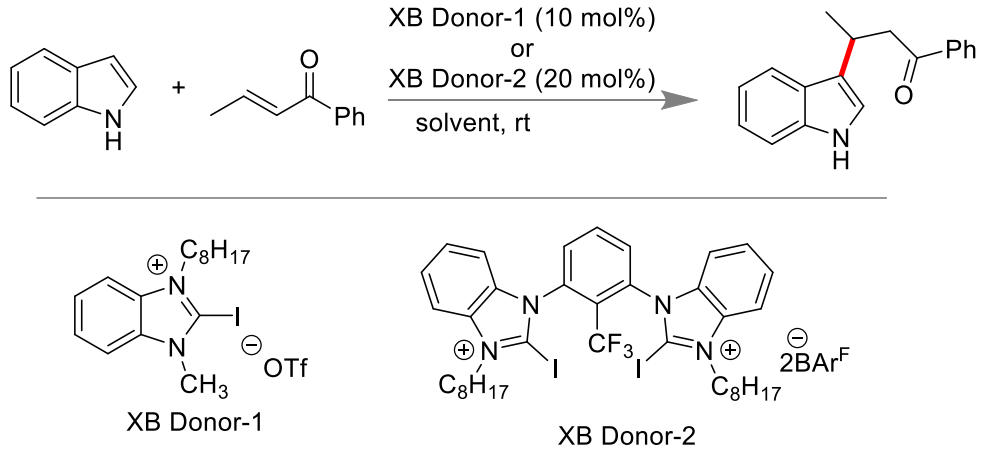

Scheme.1.31. XB induced Michael addition reaction.[53-54]

Wong and Tan also reported the XB-assisted conjugated addition of thiophenes to enones and enals to synthesize alkylated thiophenes, where 2-iodoimidazolinium triflate salt acted as an XB donor catalyst (Scheme 1.32).[55] Experimental and theoretical studies supported the formation of XB interaction between the bidentate halogen bond catalysts and carbonyl oxygen, which was the driving force for the reaction. A series of alkylated thiophenes were synthesized with good to excellent yields.

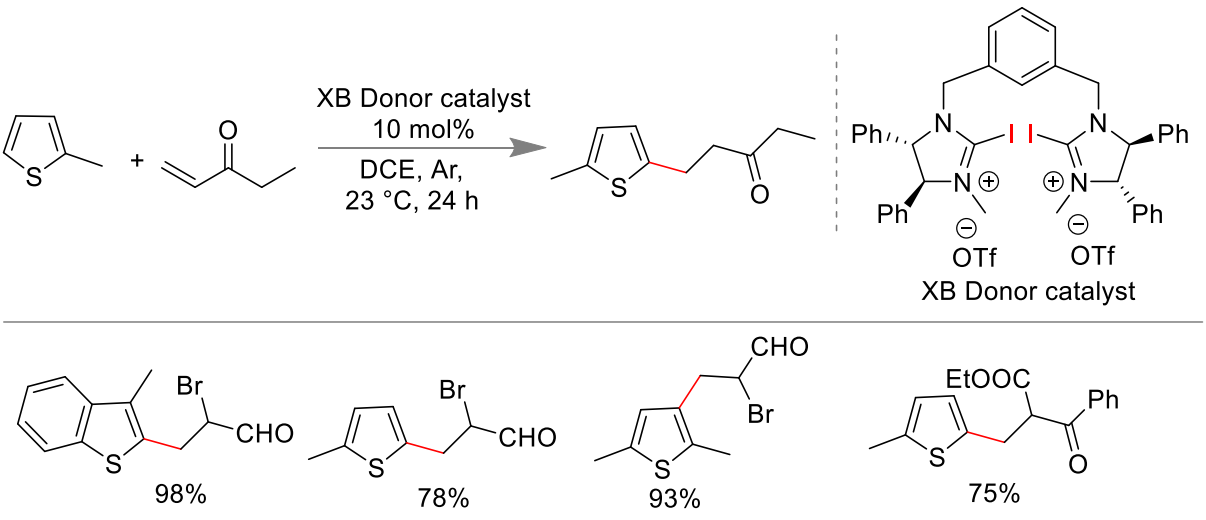

Scheme.1.32. Synthesis of alkylated thiophenes using 2-iodoimidazolinium-based catalyst.[55]

1.5.4. Heterobenzylic C-H bond functionalization

Furthermore, halogen bond controlled selective oxidation of heterobenzylic C-H bond produces ketone and ester, where the selectivity was controlled depending on the nucleophilic partner present in the reaction medium (Scheme 1.33).[56] DMSO as a solvent afforded the ketones *via* Kornblum oxidation; otherwise, carboxylic acids could be converted to the corresponding esters.

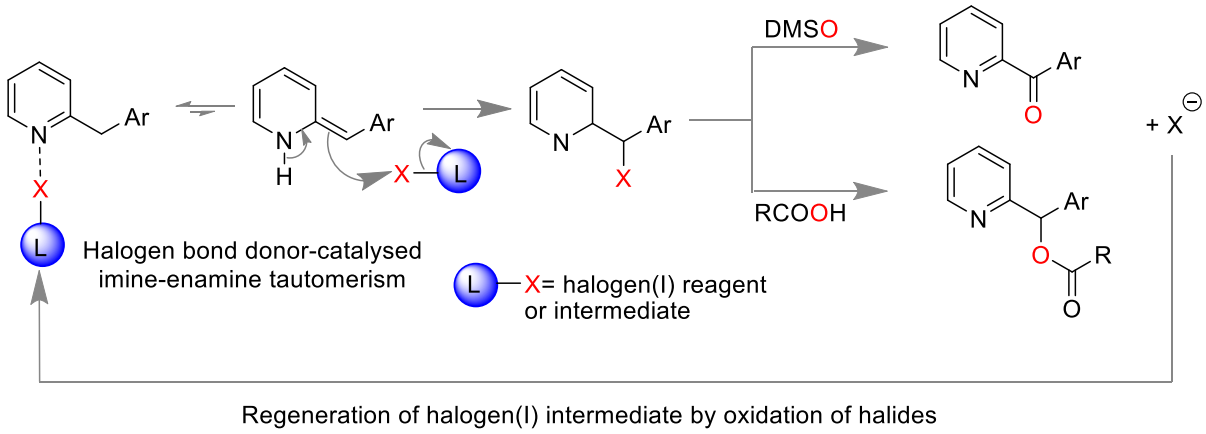

Scheme.1.33. Halogen(I) species-catalyzed selective heterobenzylic oxidation with oxygenated solvents.[56]

A catalytic amount of NBS with DMSO led to the formation of ketones (Scheme 1.34),[56] whereas acetylated product was formed using a catalytic amount of iodine and TBHP in acetic acid solvent (Scheme 1.35).[56] Several controlled experiments and DFT studies revealed that NBS formed a halogen bonded complex with heteroarene. The key intermediate for the generation of heterobenzylic radicals is that halogen bonded complex, followed by aerobic

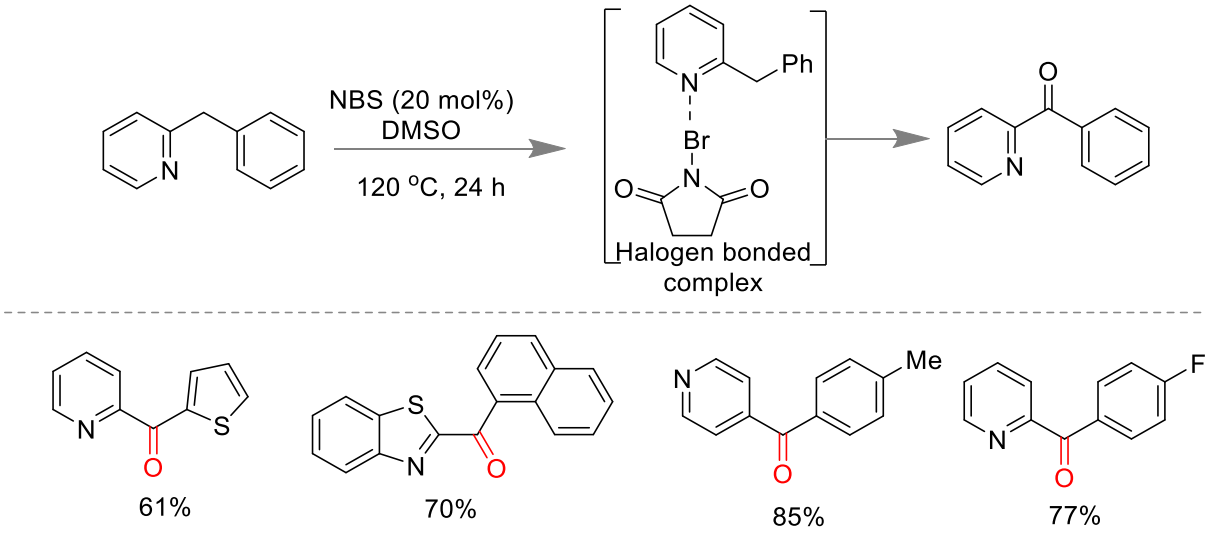

Scheme.1.34. Halogen(I) catalysts for the oxidation of aryl(heteroaryl)methanes to ketones.[56]

oxygenation to generate the ketone as a product. The isotope-labeling experiment suggested that a Kornblum-type oxidation occurred between the molecular oxygen and the DMSO solvent. Various substituted benzylpyridines and arenes having different electron-donating as well as electron-withdrawing group also afforded the heterobenzyl ketones in high yields.

In acetic acid solvent, the addition of tert-butyl hydroperoxide and a catalytic quantity of iodine generates the acetoxylated product. The generation of acetyl hypoiodite as an intermediate has indeed been confirmed by Time-Dependent Density Functional Theory (TD–DFT), GC-MS, and UV/Visible spectroscopy. Unlike previously thought, the isotope labeling study demonstrates that solvents containing a nucleophilic oxygen atom operate as a source of oxygen.

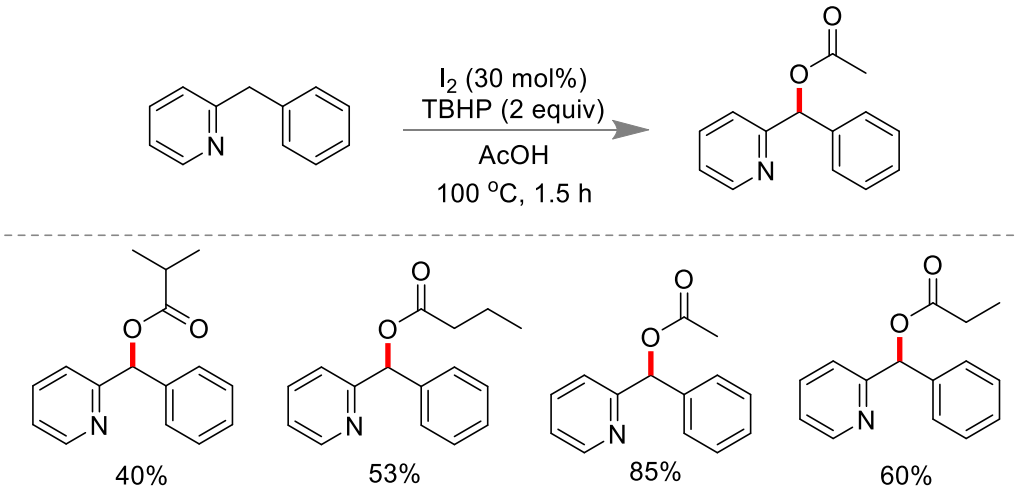

Scheme.1.35. Halogen(I) compounds acted as catalysts for the oxidation of aryl(heteroaryl)methanes to the ketones or esters.[56]

1.6. CONCLUSION & OBJECTIVE

In summary, we have demonstrated various sustainable strategies for the construction of C-N bonds using various iodine reagents and photocatalyst-free conditions. In addition to this, halogen bond catalyst assisted various C-H funtionaliazation reactions are also included in this chapter. The objectives of the current thesis are represented in a visual format below.

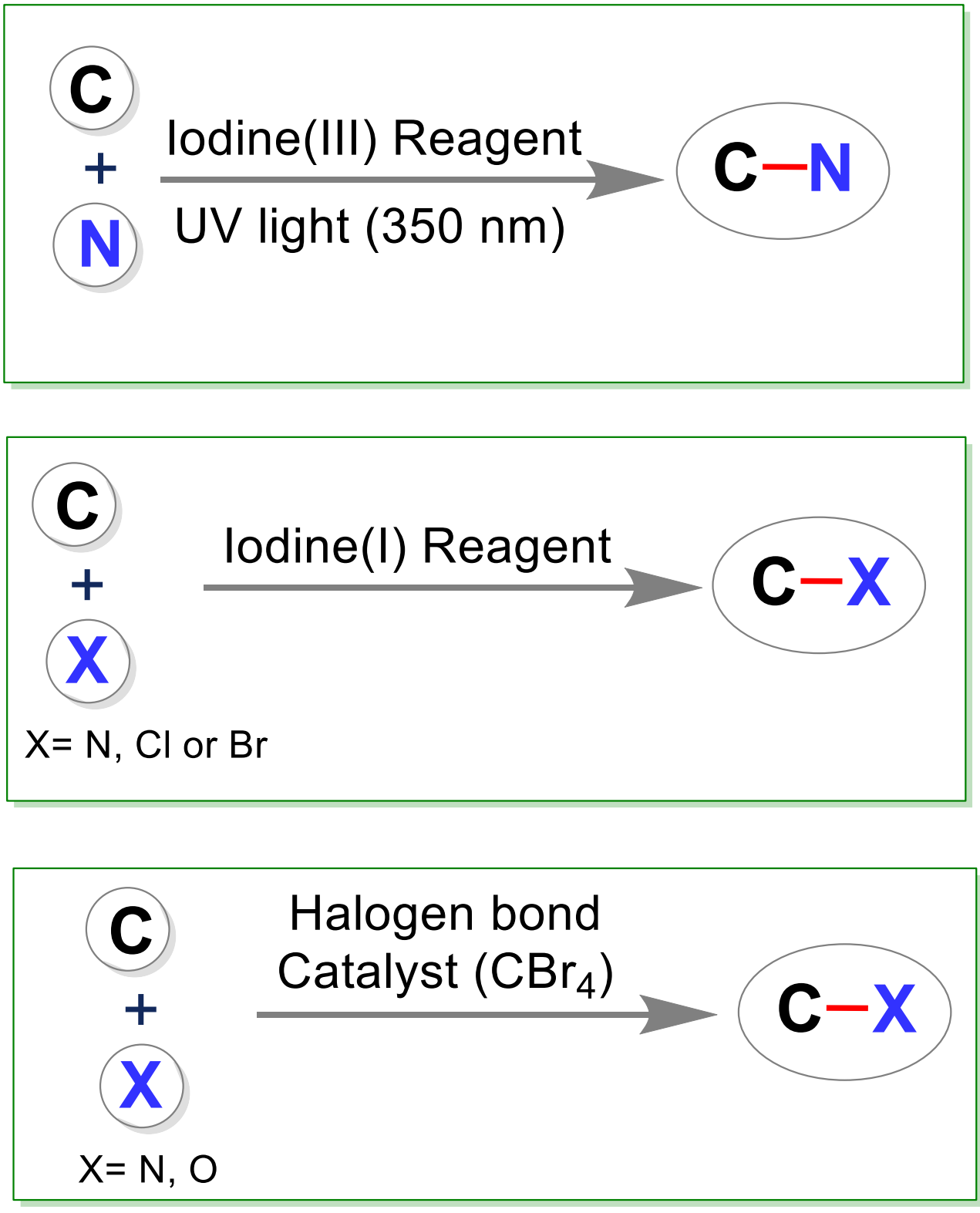

Figure 1.4. Strategies for the intramolecular C-N, C-O, C-Cl and C-Br bond formation reactions under the metal free and mild reaction.

1.7. REFERENCES

1. Cavallo, G.; Metrangolo, P.; Milani, R.; Pilati, T.; Priimagi, A.; Resnati, G.; Terraneo, G., *Chem. Rev.* **2016,** *116* (4), 2478-2601.

2. Metrangolo, P.; Meyer, F.; Pilati, T.; Resnati, G.; Terraneo, G., *Angew. Chem. Int. Ed. Engl.* **2008,** *47* (33), 6114-27.

3. Akiba, K. In Chemistry of Hypervalent Compounds; Akiba, K., Ed.; VCH Publishers: New York, 1999; Chapter 1, pp. 1-8.

4. Badigenchala, S.; Sekar, G., *J. Org. Chem.* **2017,** *82* (14), 7657-7665.

5. Li, Y.-L.; Li, J.; Ma, A.-L.; Huang, Y.-N.; Deng, J., *J. Org. Chem.* **2015,** *80* (8), 3841-3851.

6. Alam, M. T.; Maiti, S.; Mal, P., *Eur. J. Org. Chem.* **2018,** (30), 4178-4186.

7. Tang, B.-X.; Tang, D.-J.; Tang, S.; Yu, Q.-F.; Zhang, Y.-H.; Liang, Y.; Zhong, P.; Li, J.-H., *Org. Lett.* **2008,** *10* (6), 1063-1066.

8. Li, X.; Yang, L.; Zhang, X.; Zhang-Negrerie, D.; Du, Y.; Zhao, K., *J. Org. Chem.* **2014,** *79* (3), 955-962.

9. Malamidou-Xenikaki, E.; Spyroudis, S.; Tsanakopoulou, M.; Hadjipavlou-Litina, D., *J. Org. Chem.* **2009,** *74* (19), 7315-7321.

10. Zhang, Z.; Huang, Y.; Huang, G.; Zhang, G.; Liu, Q., *J. Heterocycl. Chem.* **2017,** *54* (4), 2426-2433.

11. Kashiwa, M.; Sonoda, M.; Tanimori, S., *Eur. J. Org. Chem.* **2014,** (22), 4720-4723.

12. Chi, Y.; Zhang, W.-X.; Xi, Z., *Org. Lett.* **2014,** *16* (24), 6274-6277.

13. Maiti, S.; Mal, P., *Adv. Synth. Catal.* **2015,** *357* (7), 1416-1424.

14. Yu, J.; Gao, C.; Song, Z.; Yang, H.; Fu, H., *Eur. J. Org. Chem.* **2015,** (26), 5869-5875.

15. Kikugawa, Y.; Nagashima, A.; Sakamoto, T.; Miyazawa, E.; Shiiya, M., *J. Org. Chem.* **2003,** *68* (17), 6739-6744.

16. Maiti, S.; Bose, A.; Mal, P., *J. Org. Chem.* **2018,** *83* (15), 8127-8138.

17. Maiti, S.; Achar, T. K.; Mal, P., *Org. Lett.* **2017,** *19* (8), 2006-2009.

18. Manna, S.; Antonchick, A. P., *Angew. Chem. Int. Ed.* **2014,** *53* (28), 7324-7327.

19. Kim, H. J.; Cho, S. H.; Chang, S., *Org. Lett.* **2012,** *14* (6), 1424-1427.

20. Bera, S. K.; Boruah, P. J.; Parida, S. S.; Paul, A. K.; Mal, P., *J. Org. Chem.* **2021,** *86* (14), 9587-9602.

21. Bartos, P.; Young, V. G.; Kaszyński, P., *Org. Lett.* **2020,** *22* (10), 3835-3840.

22. Gann, A. W.; Amoroso, J. W.; Einck, V. J.; Rice, W. P.; Chambers, J. J.; Schnarr, N. A., *Org. Lett.* **2014,** *16* (7), 2003-5.

23. Zhao, Y.; Huang, B.; Yang, C.; Xia, W., *Org. Lett.* **2016,** *18* (14), 3326-3329.

24. Gilday, L. C.; Robinson, S. W.; Barendt, T. A.; Langton, M. J.; Mullaney, B. R.; Beer, P. D., *Chem. Rev.* **2015,** *115* (15), 7118-7195.

25. Brown, A.; Beer, P. D., *Chem. Commun.* **2016,** *52* (56), 8645-8658.

26. Wilcken, R.; Zimmermann, M. O.; Lange, A.; Joerger, A. C.; Boeckler, F. M., *J. Med. Chem.* **2013,** *56* (4), 1363-1388.

27. Sun, X.; Wang, W.; Li, Y.; Ma, J.; Yu, S., *Org. Lett.* **2016,** *18* (18), 4638-41.

28. (a) Bulfield, D.; Huber, S. M., *Chem. Eur. J.* **2016,** *22* (41), 14434-14450; (b) Sutar, R. L.; Huber, S. M., *ACS Catal.* **2019,** *9* (10), 9622-9639.

29. Jungbauer, S. H.; Huber, S. M., *J. Am. Chem. Soc.* **2015,** *137* (37), 12110-20.

30. Robertson, C. C.; Wright, J. S.; Carrington, E. J.; Perutz, R. N.; Hunter, C. A.; Brammer, L., *Chem. Sci.* **2017,** *8* (8), 5392-5398.

31. Riley, K. E.; Hobza, P., *WIREs Comput. Mol. Sci.* **2011,** *1* (1), 3-17.

32. Pramanik, M.; Choudhuri, K.; Chakraborty, S.; Ghosh, A.; Mal, P., *Chem. Commun.* **2020,** *56* (20), 2991-2994.

33. Pramanik, M.; Mathuri, A.; Mal, P., *Chem. Commun.* **2021,** *57* (46), 5698-5701.

34. Raynal, M.; Ballester, P.; Vidal-Ferran, A.; van Leeuwen, P. W. N. M., *Chem. Soc. Rev.* **2014,** *43* (5), 1660-1733.

35. Achar, T. K.; Mal, P., *Adv. Synth. Catal.* **2015,** *357* (18), 3977-3985.

36. (a) Politzer, P.; Murray, J. S.; Clark, T., *PCCP* **2013,** *15* (27), 11178-11189; (b) Turunen, L.; Erdélyi, M., *Chem. Soc. Rev.* **2020,** *49* (9), 2688-2700; (c) Zhu, Z.; Xu, Z.; Zhu, W., *J Chem Inf Model* **2020,** *60* (6), 2683-2696.

37. Dougherty, D. A., *Acc. Chem. Res.* **2013,** *46* (4), 885-893.

38. (a) Breugst, M.; von der Heiden, D.; Schmauck, J., *Synthesis* **2017,** *49* (15), 3224-3236; (b) Giese, M.; Albrecht, M.; Rissanen, K., *Chem. Rev.* **2015,** *115* (16), 8867-8895.

39. (a) Choudhuri, K.; Pramanik, M.; Mal, P., *J. Org. Chem.* **2020,** *85* (19), 11997-12011; (b) Kennedy, C. R.; Lin, S.; Jacobsen, E. N., *Angew. Chem. Int. Ed.* **2016,** *55* (41), 12596–12624; (c) Mahadevi, A. S.; Sastry, G. N., *Chem. Rev.* **2016,** *116* (5), 2775-2825.

40. Yi, X.; Jiao, L.; Xi, C., *Org. Biomol. Chem.* **2016,** *14* (41), 9912-9918.

41. Kazi, I.; Guha, S.; Sekar, G., *J. Org. Chem.* **2019,** *84* (11), 6642-6654.

42. Nandy, A.; Kazi, I.; Guha, S.; Sekar, G., *J. Org. Chem.* **2021,** *86* (3), 2570-2581.

43. Martínez, C.; Muñiz, K., *Angew. Chem. Int. Ed.* **2015,** *54* (28), 8287-91.

44. Ashikari, Y.; Shimizu, A.; Nokami, T.; Yoshida, J., *J. Am. Chem. Soc.* **2013,** *135* (43), 16070-3.

45. Guha, S.; Kazi, I.; Mukherjee, P.; Sekar, G., *Chem. Commun.* **2017,** *53* (79), 10942-10945.

46. (a) Tepper, R.; Schulze, B.; Bellstedt, P.; Heidler, J.; Görls, H.; Jäger, M.; Schubert, U. S., *Chem. Commun.* **2017,** *53* (14), 2260-2263; (b) Tepper, R.; Schulze, B.; Jäger, M.; Friebe, C.; Scharf, D. H.; Görls, H.; Schubert, U. S., *J. Org. Chem.* **2015,** *80* (6), 3139-3150.

47. Dreger, A.; Engelage, E.; Mallick, B.; Beer, P. D.; Huber, S. M., *Chem. Commun.* **2018,** *54* (32), 4013-4016.

48. Dordonne, S.; Crousse, B.; Bonnet-Delpon, D.; Legros, J., *Chem. Commun.* **2011,** *47* (20), 5855-7.

49. Jungbauer, S. H.; Walter, S. M.; Schindler, S.; Rout, L.; Kniep, F.; Huber, S. M., *Chem. Commun.* **2014,** *50* (47), 6281-4.

50. Saito, M.; Kobayashi, Y.; Tsuzuki, S.; Takemoto, Y., *Angew. Chem. Int. Ed.* **2017,** *56* (26), 7653-7657.

51. Kazi, I.; Guha, S.; Sekar, G., *Org. Lett.* **2017,** *19* (5), 1244-1247.

52. Banik, B. K.; Fernandez, M.; Alvarez, C., *Tetrahedron Lett.* **2005,** *46* (14), 2479-2482.

53. Gliese, J.-P.; Jungbauer, S. H.; Huber, S. M., *Chem. Commun.* **2017,** *53* (88), 12052-12055.

54. Breugst, M.; von der Heiden, D.; Detmar, E.; Kuchta, R., *Synlett* **2017,** *29* (10), 1307-1313.

55. Ge, Y. C.; Yang, H.; Heusler, A.; Chua, Z.; Wong, M. W.; Tan, C. H., *Chem. Asian J.* **2019,** *14* (15), 2656-2661.

56. Guha, S.; Sekar, G., *Chem. Eur. J.* **2018,** *24* (53), 14171-14182.

CHAPTER 2

Iodine(III) Reagent in Intramolecular C-N Cross-coupling Reactions

2.1 ABSTRACT

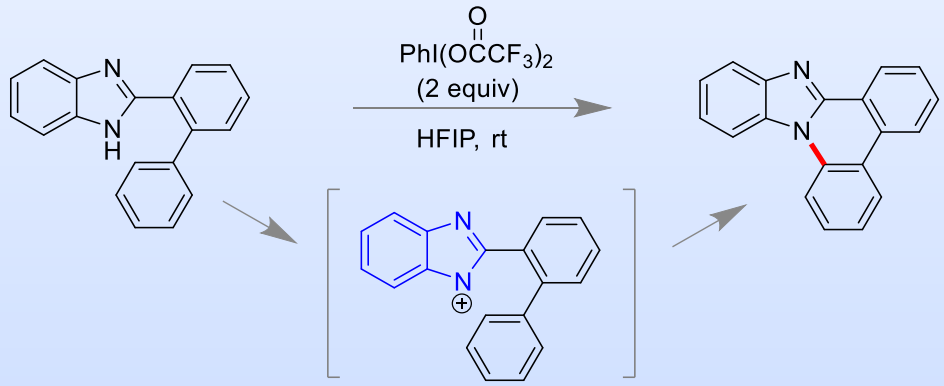

antiaromatic and endocyclic nitrenium ion

Herein, we report a C-N coupling reaction *via* antiaromatic endocyclic nitrenium ion. The nitrenium ion intermediate was generated by the combination of iodine(III) reagent $PhI(OCOCF_3)_2$ and N-H center of benzimidazole units at ambient laboratory conditions. Metal-free synthesis of benzimidazole-fused phenanthridine derivatives was achieved in good to excellent yields. During the synthesis we have avoided the use of any expensive catalyst (mainly metal-based), harsh conditions and the reactions were performed using PIFA as a sole reagent. Additionally, ambient conditions, commercial viability of iodide reagent, made the methodology more synthetically attractive towards the construction of heterocyclic. This metal-free approach offers a wide range of substrates with good to excellent yield under mild reaction conditions.

2.2 INTRODUCTION

The nitrenium ion chemistry rose to prominence among synthetic chemists since beginning.[1] The combinations of amine or amine derivatives with hypervalent iodine(III) reagents[2] generally produce nitrenium ion.[3] The divalent nitrogen-containing species with six

electrons in its valence shell with positive charge on nitrogen is recognized as nitrenium ion (Figure 2.1a).[4] Nitrenium ions are isoelectronic with carbene family having two non-bonding electrons. Nitrenium ion is considered as one of the most important synthetic intermediates in innumerable chemical transformations.[5] Depending on the nature and stability of nitrenium ion, many oxidative transformations are reported for the preparation of functional molecules of interests using exocyclic nitrenium ions.[6] Due to the electron spin orientation nitrenium ions exist in two different forms *i.e.*, singlet state and triplet state (Figure 2.1a).[7] In Figure 2.1b, generation of nitrenium ion is shown from the mixtures of amine or amide with iodine(III) reagents. In general, nitrenium ion is electrophilic and highly reactive intermediate with the formula of RR'N^+.[8]

The Hückel aromatic and antiaromatic systems consist of [4n + 2] or [4n] delocalized circuits electrons, respectively and display ring currents around their perimeters.[9] The antiaromatic compounds are highly reactive and unstable. Therefore the existence of antiaromatic compounds are often found in porphyrinoid systems[10] or in large ring macrocycles.[11]

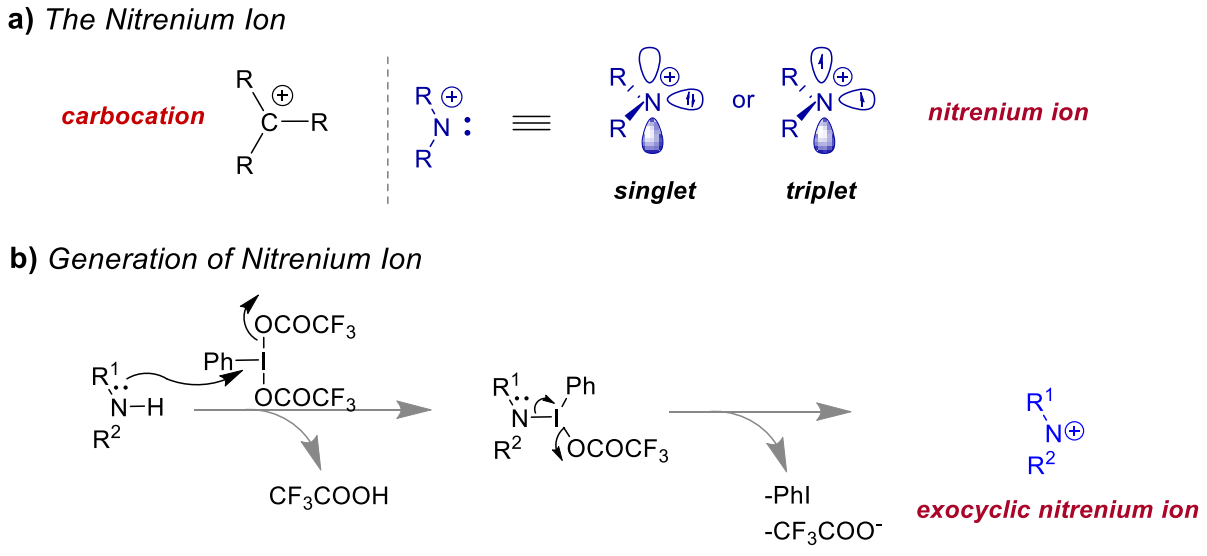

Figure 2. 1 a) The nitrenium ion. b) Generation of nitrenium ion.

However, in case of small molecules the antiaromaticity is demonstrated in acene systems having1,4-diazapentalene core.[12] The mixture of iodine(III) reagent $PhI(OCOCF_3)_2$ (PIFA) and N-H center of benzimidazole scaffold produced endocyclic nitrenium ion which has 4nπ system and is considered to be antiaromatic. The antiaromatic transition state is possibly stabilized *via* resonance. Interestingly, limited reports are available in which endocyclic and antiaromatic nitrenium ions are directly used for synthesis.[8b] Falvey and co-workers demonstrated the existence of endocyclic and antiaromatic nitrenium ions through spectroscopic investigations and theoretical calculations.[8b, 13] The term endocyclic was documented to demonstrate that nitrenium ions having cationic nitrogen contained inside a ring and possesses antiaromatic character (Scheme 2.1.a).[13]

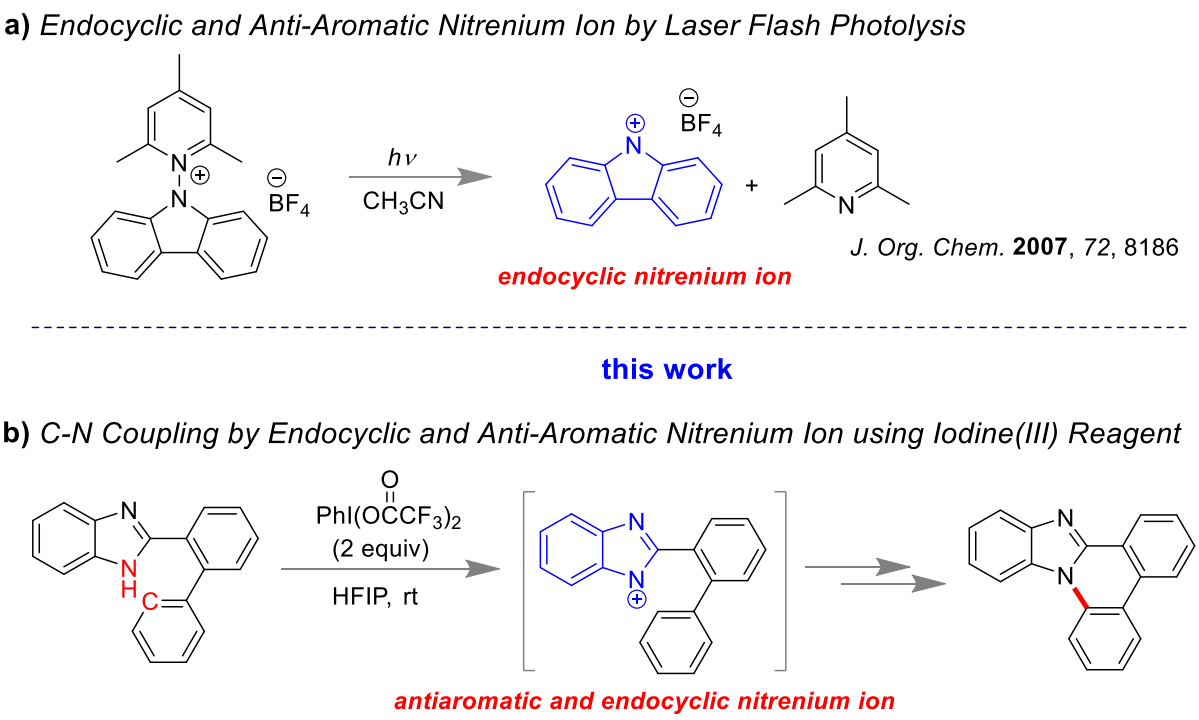

Scheme 2.1. a) Using laser flash photolysis Falvey and co-workers reported the generation and detection of endocyclic and antiaromatic nitrenium ion.[13] b) Our current work on the C-N coupling reaction based on the generation of endocyclic and antiaromatic nitrenium ion using iodine(III) reagent PIFA.

Herein, we report the synthesis of phenanthridine derivatives *via* C-N coupling reaction. And, demonstrated the use of antiaromatic and endocyclic nitrenium ions as the intermediate which were directly generated from benzimidazole system using iodine(III) reagent $PhI(OCOCF_3)_2$ (PIFA) (Scheme 2.1.b).

2.3 RESULTS AND DISCUSSION

Nitrogen-containing fused heteroaromatic compounds having phenanthridine moiety are ubiquitous in many pharmaceuticals and natural products.[14] Owing to extensive π-conjugation, these type of compounds are utilized as organic semiconductors and luminescent materials.[15] For example, 1,2-disubstituted (hetero)aryl-fused benzimidazoles acts as an electron-transporting and emission functional units.[16] Due to the planarity of the system, phenanthridine moiety shows the ability to bind with human telomere derived g-quadruplexes.[17] Considerable efforts have been paid for developing the methods for synthetic transformations of (hetero)aryl-fused phenanthridines using metal catalyst.[18a, 15, 18b] Moreover, this type of methodology suffers from disadvantages like metal contamination in products, reusability of metal catalyst, requirements of multistep paths, etc.[19] We anticipate that our current N-H/C-H arylation method (Scheme 2.1.b) using PIFA in 1,1,1,3,3,3-hexafluoro-2-propanol (HFIP) for the preparation of benzimidazole-fused phenanthridines can be considered as the easiest approach known in literature.

Towards optimization of the reaction condition, compound 2-([1,1'-biphenyl]-2-yl)-5,6-dichloro-1H-benzo[d]imidazole (**1e**) was chosen as a model substrate (Table 2.1). When **1e** was treated with 2.0 equiv of PIFA in dichloromethane, the product **2e** was isolated in 57% yield after 20 h of stirring at room temperature (entry 1). However, using polar protic solvent such as ethanol (EtOH) and methanol (MeOH), trace amount of product formation was

observed. However, in water no product was obtained (entry 10). When the reaction was carried out in solvents DCE (1,2-dichloroethane), TFE (2,2,2-trifluoroethanol), CH_3CN (acetonitrile) and DMF, yield of the products were found to be poor. Contrastingly, in non-polar solvents like benzene and toluene, 70% and 40% yield of final products were obtained, respectively. In this reaction, HFIP was found to be the best among the solvents examined (entry 7). The reaction did not proceed in absence of any oxidant (entry 16). Upon lowering the equivalence of PIFA, inferior results were obtained (entries 17-18). Attempts to the use of $PhI(OAc)_2$ (PIDA) instead of PIFA did not make any appreciable change in yield (entry 19). The oxidizing ability of PIDA is much less than that of PIFA. In case of PIDA, under the standard condition 44% yield of final products were obtained and 52% of the starting material was recovered. Use of molecular iodine was also found to be unsuccessful (entry 20). Finally, the most appropriate condition was recognized when the reaction was performed using PIFA (2.0 equiv) in HFIP. Under this optimized condition, the final product 11,12-dichlorobenzo[4,5]imidazo[1,2-f]phenanthridine (**2e**) was isolated in near quantitative (98%) yield within 20 h at room temperature (entry 7). In addition, using PhIO the product **2e** was obtained in 48% yield (entry 21).

Table 2.1 Condition Optimization.[a]

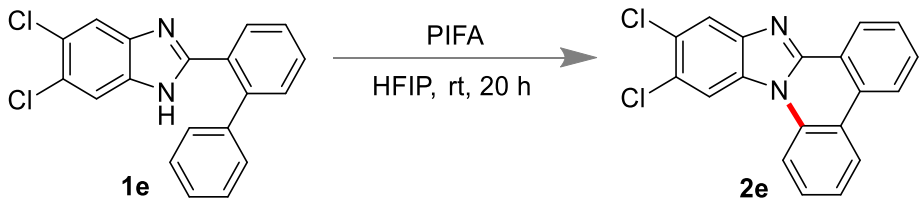

Entry	Reagent (equiv)	Solvent	Yield (%)[b]
1	PIFA (2)	DCM	57
2	PIFA (2)	DCE	28
3	PIFA (2)	CH_3CN	38
4	PIFA (2)	Benzene	70

5	PIFA (2)	Toluene	40
6	PIFA (2)	TFE	25
7	**PIFA (2)**	**HFIP**	**98**
8	PIFA (2)	DMSO	60
9	PIFA (2)	DMF	35
10	PIFA (2)	H_2O	-[c]
11	PIFA (2)	EtOH	07
12	PIFA (2)	MeOH	06
13	PIFA (2)	Acetone	05
14	PIFA (2)	EtOAc	09
15	PIFA (2)	HFIP:DCM (1:1)	60
16	-[d]	HFIP	-[c]
17	PIFA (1)	HFIP	67
18	PIFA (1.5)	HFIP	80
19	PIDA (2)	HFIP	44
20	I_2 (2)	HFIP	-[c]
21	PhIO (2)	HFIP	48

[a]Reaction conditions: 0.176 mmol of **1e** and 0.353 mmol of PIFA (2 equiv) in 1.0 mL HFIP at room temperature for 20 h. [b]Yield of isolated product after purification through silica-gel column chromatography. [c]No reaction. [d]Without any reagent.

Under standard conditions, the substrate scope was explored for the synthesis of highly substituted fused heterocycles *via* C-N bond formation reaction. Symmetrically substituted or disubstituted benzimidazoles having various neutral, electron rich and electron poor functional groups could be efficiently converted into benzimidazole-fused phenanthridine derivatives (Figure 2.2). Benzimidazoles bearing ethyl, fluoro, acetyl groups of the 2-aryl moiety afforded **2b**, **2c** and **2d** with 96%, 95% and 94%, respectively. Similarly, the unsubstituted aryl skeleton at the 2-position of benzimidazole produced **2a** with 91% yield of

product. Again the substitutions in 2-aryl moiety by electron withdrawing (fluoro, chloro, acetyl, trifluoromethyl), as well as electron donating groups (such as ethyl, ^{t}butyl) of the 5,6-dichloro benzimidazoles, could be successfully converted to corresponding products (**2f- 2k**) in good to excellent yields. However, 5,6-dimethyl benzimidazoles with a variety of substituents (ethyl, ^{t}butyl, fluoro, chloro and acetyl) at the 2-aryl group also afforded the respective product (**2m-2q)** in good yields. The unsubstituted aryl group at 2-position of 5,6-dichloro and 5,6-dimethyl benzimidazoles gave **2e** and **2I** with 98% and 96% yield, respectively. The incorporation of the electron withdrawing fluoro group in the meta-position of the 2-aryl moiety of 5,6-dichloro and 5,6-dimethyl benzimidazoles correspondingly provided **2r** and **2s** with 95% and 94% yield, respectively. Overall, electron deficient functional group containing substrates took longer time than that of electron rich substrates. Notably, substrate **1e** was prepared by the reaction of commercially available *o*-phenylene diamines and formylbiphenyl derivatives in presence of dimethyl formamide (DMF) as a solvent at 80 ^{o}C.

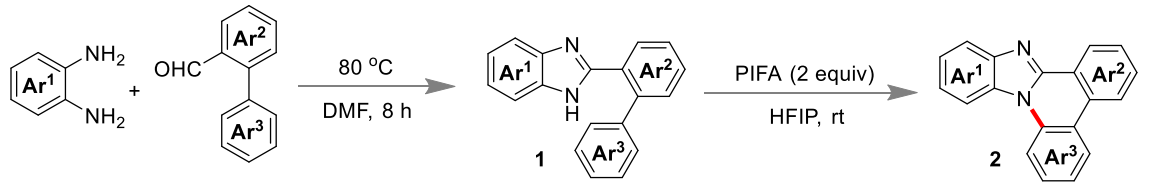

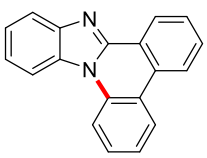

2a, 91%, 28 h

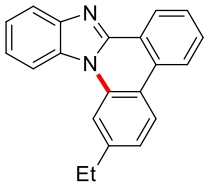

2b, 96%, 22 h

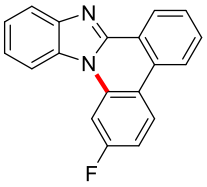

2c, 95%, 24 h

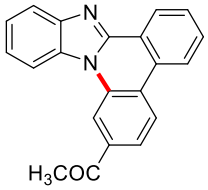

2d, 94%, 48 h

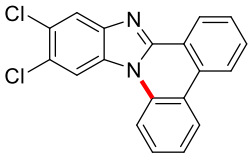

2e, 98%, 20 h

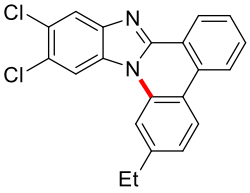

2f, 93%, 19 h

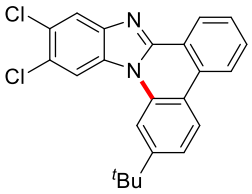

2g, 94%, 20 h

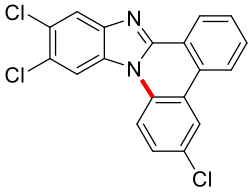

2h, 92%, 42 h

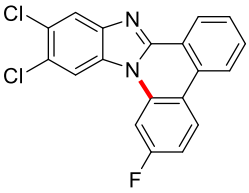

2i, 94 %, 42 h

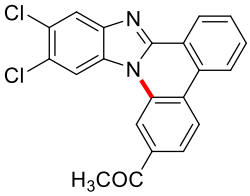

2j, 93%, 36 h

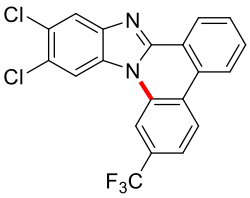

2k, 92%, 24 h

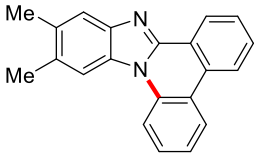

2l, 96%, 19 h

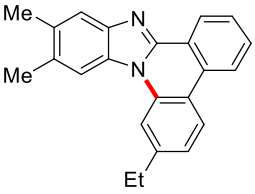

2m, 94%, 21 h

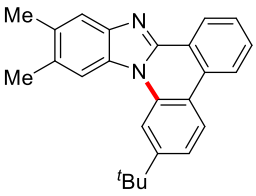

2n, 82%, 22 h

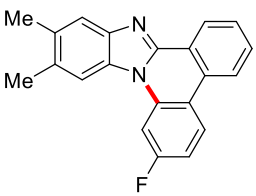

2o, 92%, 24 h

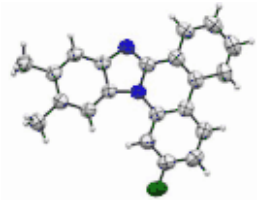

CCDC 1910734

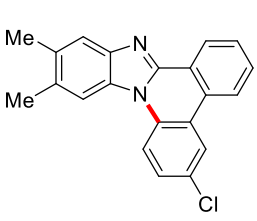

2p, 89%, 22 h

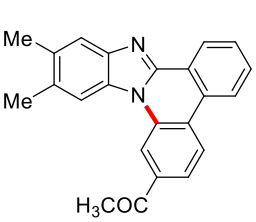

2q, 82%, 28 h

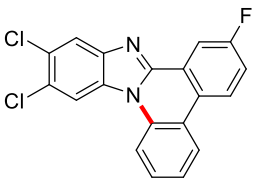

2r, 95%, 23 h

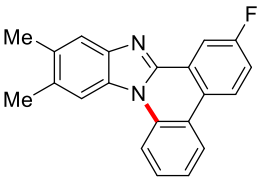

2s, 94%, 22 h

Figure 2.2 Functional-group tolerance in synthesis of benzimidazole-fused phenanthridines.

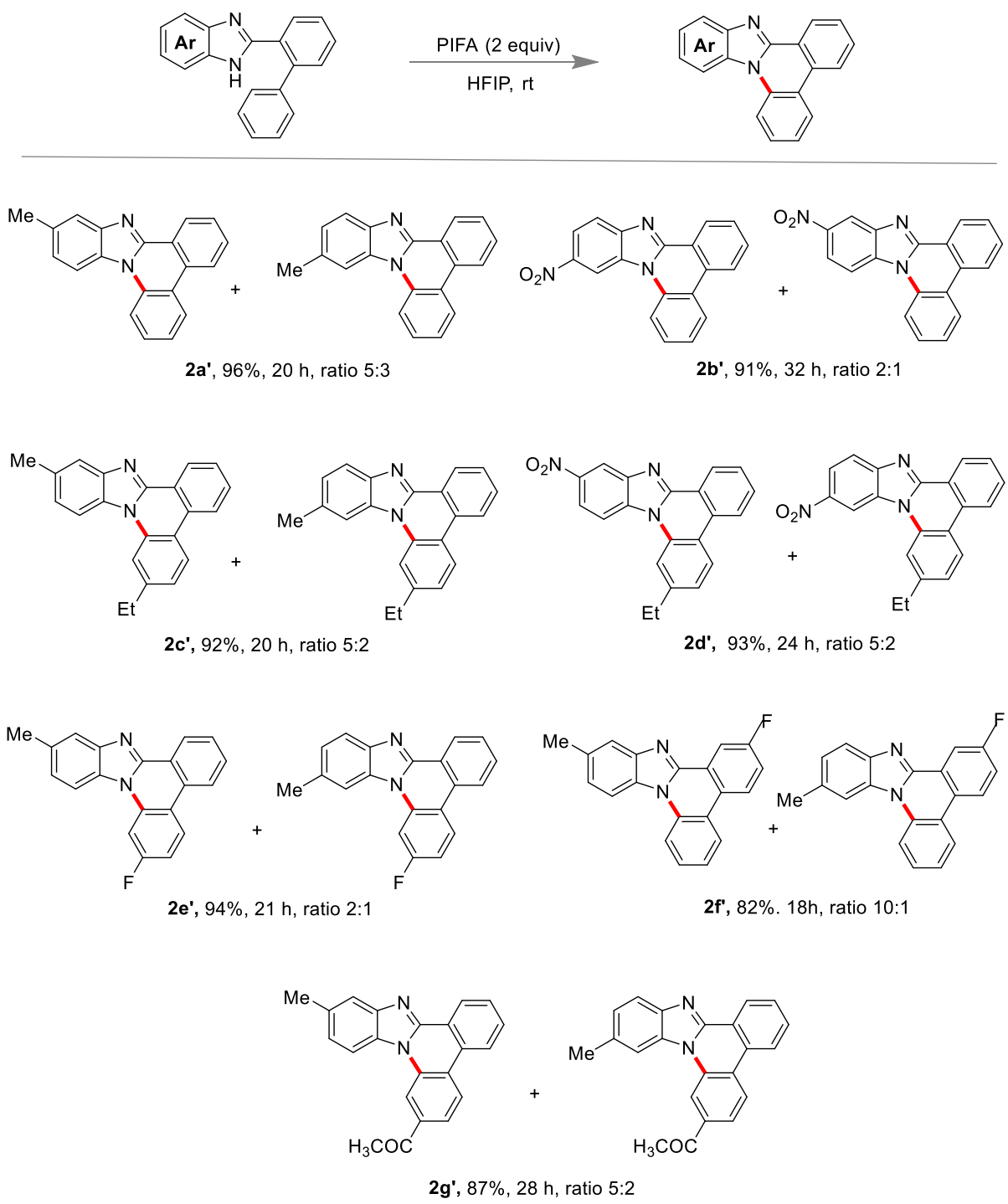

Figure 2.3 Inseparable mixture of regioisomers.

The substrates scope for this methodology was further extended to unsymmetrically substituted or mono substituted benzimidazoles, which furnished the mixture of regioisomers

under standard reaction condition (Figure 2.3). Thus, for the mono substituted benzimidazoles, there are two possibilities for the formation of products. One is 11-substituted and another is 12-substituted (hetero)aryl-fused phenanthridines. The aryl group at 2-position of 3-methyl and 3-nitro benzimidazoles led to 5:3 and 2:1 mixture of regioisomers **2a'** and **2b'** with 96% and 91% yield, respectively. Similarly, 3-methyl and 3-nitro benzimidazoles bearing ethyl group in the 2-aryl moiety also afforded 5:2 mixture of regioisomers **2c'** and **2d'** with excellent yield of products. Nevertheless, the electron withdrawing fluoro group in the *meta*-position of 2-aryl moiety of 3-methyl benzimidazole gave 10:1 mixture of regioisomers **2f'**. Again, 3-methyl benzimidazoles bearing fluoro and acetyl group in the 2-aryl moiety also produced 2:1 and 5:2 mixture of regioisomers **2e'** and **2g'** with 94% and 87% yield of products.

To establish the mechanism of the reaction, control experiments were performed which are shown in (Figure 2.4). In presence of TEMPO[6a] at standard condition, reaction proceeded smoothly and giving 98% of the product as isolated (based on recovery yield, Figure 2.4a). This fact clearly indicates that radical pathway for the reaction was not operative. For the generation of nitrenium ion the presence of N-H group in the benzimidazole core was one of the essential criteria. After the removal of N-H bond in presence of iodine(III) reagent the antiaromatic transition state was created. This hypothesis was further proved when N-Me substituted benzimidazole moiety (**2ab**) was found to be unreactive under standard condition (Figure 2.4b).

Based on control experiments and literature precedence[20] a plausible mechanism is proposed in Figure 2.4c. Initially, substrate **1a** was reacted with PIFA to form eminium ion intermediate **3**, [21] which could undergo proton abstraction by trifluoroacetate ion and

followed by elimination of trifluoroacetic acid and iodobenzene to produce nitrenium ion intermediate **4.** Following, the nitrenium ion **4** underwent C-N bond formation *via* cyclization to form the Wheland intermediate **5** or **6**.[22] Finally, the product **2a** was formed after elimination of one hydrogen by trifluoroacetate anion. Trifluoroacetic acid is generated in the reaction mixture as a by-product, which can also protonate the N-H proton that's why higher concentration (2 equiv) of oxidant PIFA was required for the conversion.

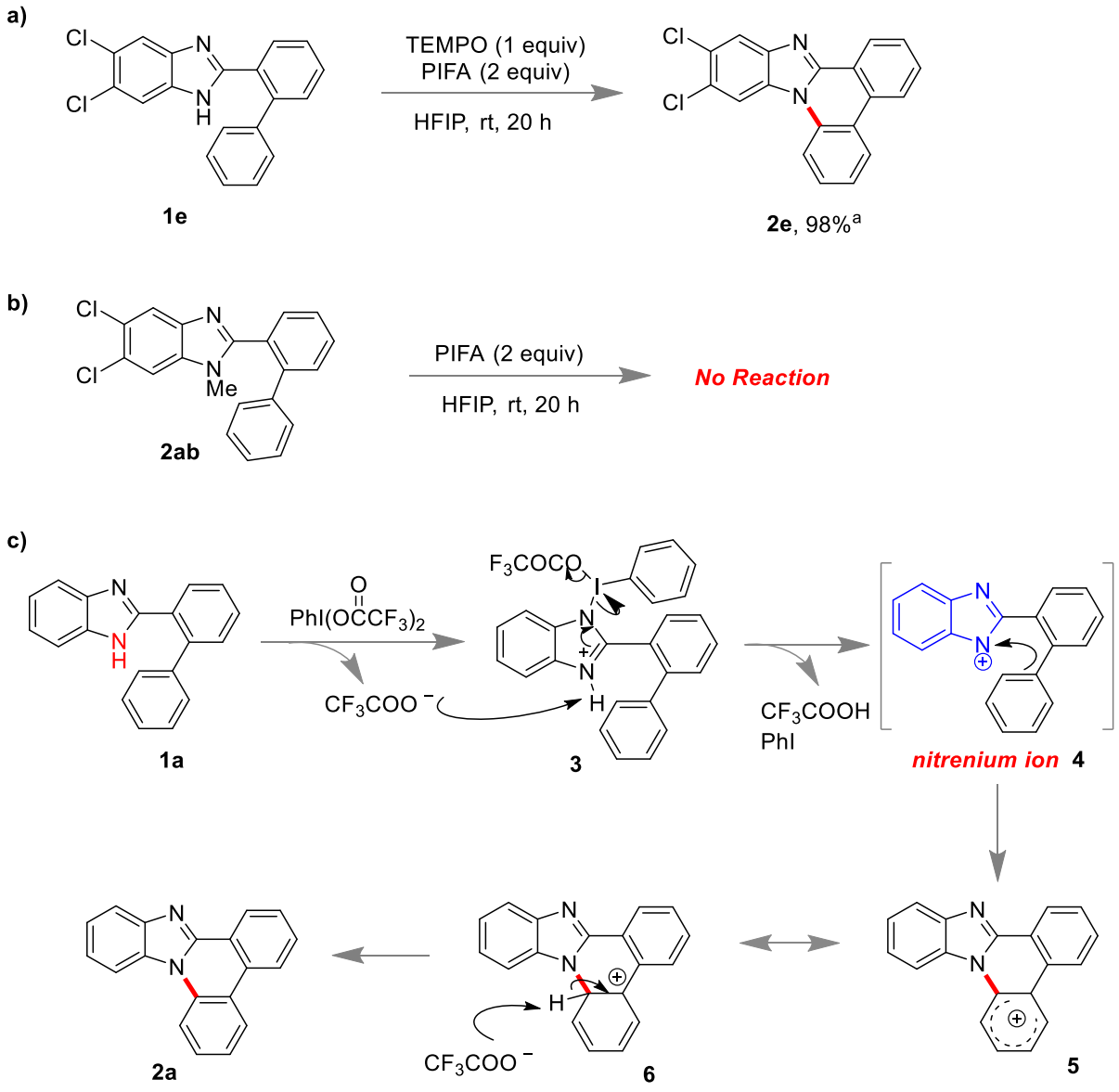

Figure 2.4 a) and b) Control experiments. c) Plausible mechanism.

Towards exploring the synthetic utility of the method, we have carried out the same transformation using PhI (iodobenzene, 1.0 equiv)-*m*CPBA (1.5 equiv) in HFIP as the organocatalytic condition[23] and the product **2e** was isolated in 94% (based on recovered starting materials, Figure 2.5a). It is established in literature that PhIO is the reactive intermediate from PhI-mCPBA combination,[23] however, HFIP stabilizes the iodinium intermediates.[24] Furthermore, the efficiency of the method was verified by scaling up the reaction up to ~4.0 mmol of substrate **1c** (gram scale, Figure 2.5b). Under optimized condition when the reaction was performed with 2-(4'-fluoro-[1,1'-biphenyl]-2-yl)-1H-benzo[d]imidazole **1c**, fluorobenzo[4,5]imidazo[1,2-f]phenanthridine **2c** was isolated in 96% of yield after 20 h of reaction time.

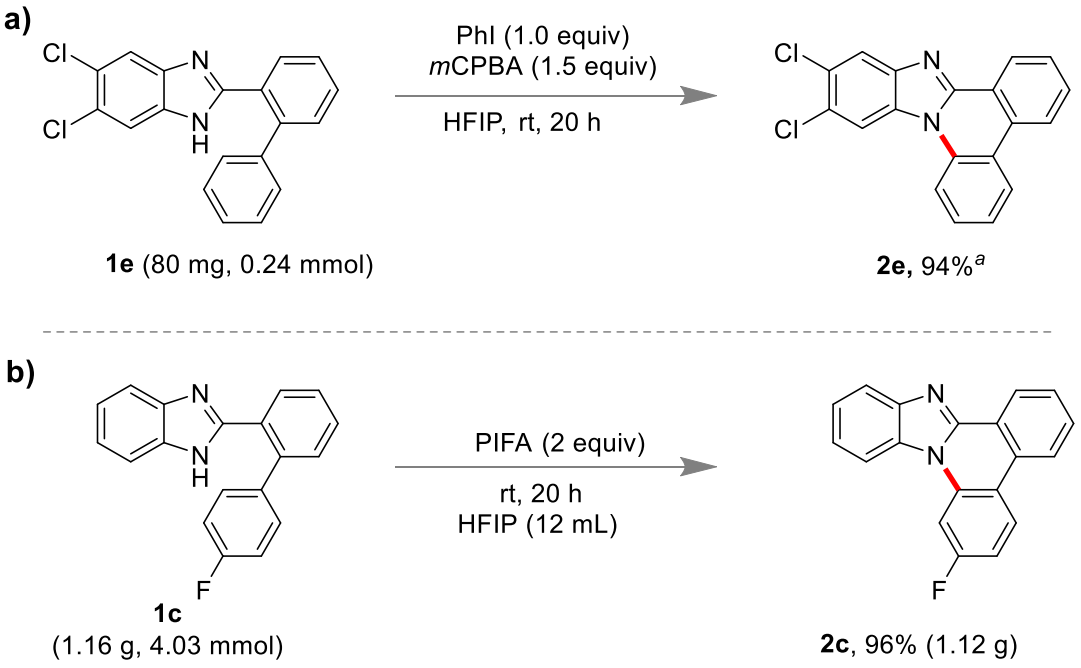

Figure 2.5 a) Synthesis of benzimidazole-fused phenanthridines in organocatalytic condition. b) Gram scale synthesis of 2-fluorobenzo[4,5]imidazo[1,2-f]phenanthridine (**2c**). [a]Based on recovered starting material.

Due to extended π-conjugation nitrogen-containing fused heteroaromatic compounds become potential fluorophores and shown to have strong luminescence behavior. For selected benzimidazole-fused phenanthridines (**2f, 2d, 2o, 2r, 2a**) absorption and emission properties are shown in Figure 2.6. For the acetyl containing benzimidazole-fused phenanthridine **2d**, high bathochromically shifted emission behavior was observed.

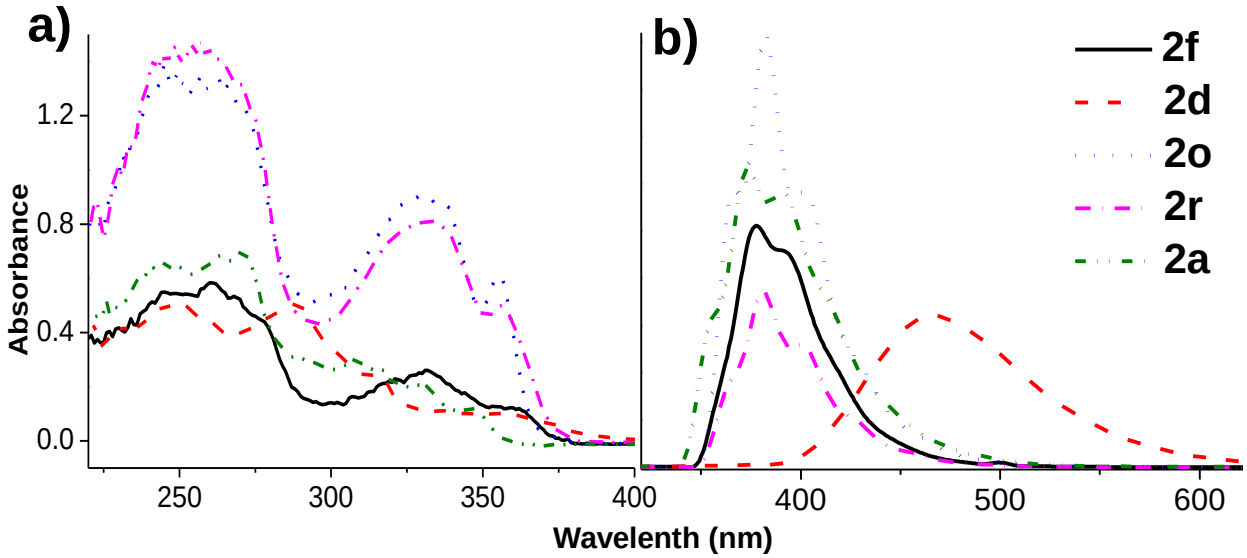

Figure 2.6. a) Absorption and b) emission spectra for selected compounds. Concentration: 3 × 10^{-5} M in dichloromethane.

2.4 CONCLUSION

In summary, we have shown here that direct C-N coupling reaction could be done *via* antiaromatic endocyclic nitrenium ion and subsequently synthesis of fused heterocycles like benzimidazole-fused phenanthridines were achieved under metal free condition. During the synthesis we have avoided the use of any expensive catalyst (mainly metal based), harsh condition and the reactions were performed using PIFA as a sole reagent. Additionally,

ambient condition, commercial viability of iodide reagent, made the methodology more synthetically attractive towards construction of heterocycles. We anticipate that this approach can provide direct access to various heteroaromatic compounds which might be useful in the synthesis of complex structural motifs.

2.5 EXPERIMENTAL SECTION

General Information. Commercially available reagents and solvents were used as received. Column chromatographic purifications of the compounds were performed using silica gel (mesh 230–400) and hexane – ethyl acetate solvent mixtures. NMR spectra were recorded on a 400 MHz or 700 MHz instrument at 25 °C. The chemical shift values are reported in parts per million (ppm) with respect to residual trichloromethane (7.26 ppm for ^{1}H and 77.16 ppm for ^{13}C). The peak patterns are designated as follows: s: singlet; d: doublet; t: triplet; q: quartet; m: multiplet; dd: doublet of doublets; td: triplet of doublets; br s: broad singlet. The coupling constants (J) are reported in hertz (Hz). High-resolution mass spectra (HR-MS) were recorded on an ESI-TOF (time of flight) mass spectrometer. Infrared spectral data are reported in wave number (cm-1). FT-IR spectra were recorded after making thin layer of the compounds on the surface of NaCl crystal using dichloromethane. Melting points of the compounds were determined using a digital melting point apparatus and uncorrected.

Representative Procedure for Preparation of 2-([1,1'-biphenyl]-2-yl)-5,6-dichloro-1H-benzo[d]imidazole 1e.[25] A solution of [1,1'-biphenyl]-2-carbaldehyde (500 mg, 2.82 mmol) and the appropriate *o*-phenylenediamine (2.82 mmol) in DMF (5 mL) was heated at 80 °C. The reaction mixture was allowed to stir for 8 h and resulting solution was brought to room temperature and then extracted with ethyl acetate (EtOAc). The organic layer washed with brine, dried over anhydrous Na_2SO_4 and concentrated under reduced pressure. The crude

product was purified by silica gel column chromatography with *n*-Hexane-EtOAc. The compound **1e** was obtained as white solid. (914 mg, 95% yield), R_f = 0.45 (hexane/ethyl acetate 4:1).

Representative Procedure for Preparation of 11,12-Dichlorobenzo[4,5]imidazo[1,2-f]phenanthridine (2e). To a stirred solution of 2-([1,1'-Biphenyl]-2-yl)-5,6-dichloro-1H-benzo[d]imidazole **1e** (60 mg, 0.176 mmol), in 1,1,1,3,3,3-hexafluoro-2-propanol (HFIP) (2.0 mL), PIFA (152 mg, 0.35 mmol) was added slowly at room temperature. The reaction mixture was allowed to stir until completion. Progress of reaction was monitored by TLC using ethyl acetate and hexane as eluent. After the completion of reaction (20 h) resulting solution was evaporated to dryness. The crude residue was purified on silica gel column chromatography (20% EtOAc in hexane) to get the pure product 11, 12-dichlorobenzo[4,5]imidazo[1,2-f]phenanthridine **2e** (59 mg, yield 98%).

X-ray crystallography analysis

Procedure for preparing the crystal of 2-fluoro-11,12-dimethylbenzo[4,5]imidazo[1,2-f]phenanthridine (2o). In a 10 mL round bottom flask 20 mg of 2-fluoro-11,12-dimethylbenzo[4,5]imidazo[1,2-f]phenanthridine (**2o**) was dissolved by using ethyl acetate and hexane mixture = 1:1 (6 mL). After that the solution was allowed for slow evaporation to obtain good quality of crystal of compound **2o**.

Crystal measurement:

The crystals data were collected with Bruker SMART D8 goniometer equipped with an APEX CCD detector and with an INCOATEC micro source (Cu-Kα radiation, λ = 0.71073 Å). SAINT+[26] and SADABS[27] were used to integrate the intensities and to correct the absorption respectively The structure was resolved by direct methods and refined on F^2 with

SHELXL-97.[28] ORTEP Drawing of the compound **2o** shows ellipsoid contour at the 50% probability level.

Crystallographic data

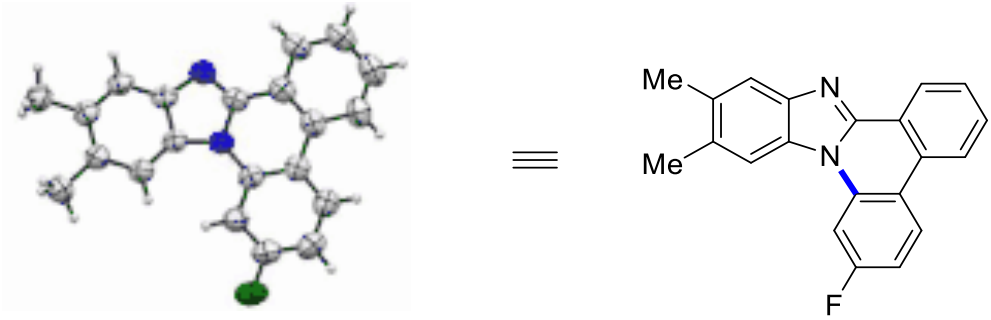

Figure 2.7. Crystal structure of **2o** (50% ellipsoid probability).

Table 2.2. Crystal data and structure refinement for **2o.**

CCDC No.	**1910734**
Chemical Formula	$C_{21}H_{15}FN_2$
Formula Weight	314.35
Crystal system	triclinic
Space group	$P2_1/c$
Unit cell dimensions	a=8.5984(3) Å α = 90°.
	b=17.4730(5) Å β = 110°.
	c=10.8764(4) Å γ = 90°.
Volume	1530.72(10) Å3
Z	4
Density (calculated)	1.364 g/cm3
Crystal size	0.2, 0.18, 0.18
Final R indice [I>2sigma(I)]	R_1 = 0.0638, wR_2 = 0.1703
R indices (all data)	R_1 = 0.0666, wR_2 = 0.1738

Characterisation Data

2-([1,1'-Biphenyl]-2-yl)-1H-benzo[d]imidazole (1a). R_f = 0.70 (hexane/ethyl acetate 7:3); white solid; yield 71% (440 mg); mp 214−216 °C (lit.[29] mp 212-213 °C); ^{1}H NMR (700 MHz, DMSO-d_6) δ 12.08 (s, 1H), 7.72 (d, *J* = 7.7 Hz, 1H), 7.61 (t, *J* = 7.0 Hz, 1H), 7.59 – 7.55 (m, 1H), 7.53 (t, *J* = 8.4 Hz, 2H), 7.35 – 7.31 (m, 1H), 7.25 (d, *J* = 7.7 Hz, 3H), 7.19 (d, *J* = 6.3 Hz, 2H), 7.16 – 7.11 (m, 2H); ^{13}C{^{1}H} NMR (175 MHz, DMSO-d_6) δ 152.1, 143.5, 141.0, 140.2, 134.5, 131.1, 130.5, 130.2, 129.9, 128.8, 128.1, 127.4, 127.1, 122.1, 121.2, 118.9, 111.3; IR (KBr) $\tilde{\nu}$ = 3431, 3061, 2981, 2929, 2882, 2733, 1469, 1446, 1432, 1275 cm^{-1}; HR-MS (ESI-TOF) m/z calcd for $C_{19}H_{15}N_2$ $[M + H]^+$ 271.1230, found 271.1247.

2-(4'-Ethyl-[1,1'-biphenyl]-2-yl)-1H-benzo[d]imidazole (1b). R_f = 0.45 (hexane/ethyl acetate 4:1); white solid; yield 72% (138 mg); mp 230 °C; ^{1}H NMR (700 MHz, DMSO-d_6) δ 12.07 (s, 1H), 7.68 (d, *J* = 7.0 Hz, 1H), 7.62 – 7.56 (m, 2H), 7.50 (t, *J* = 7.0 Hz, 2H), 7.35 – 7.32 (m, 1H), 7.15 – 7.12 (m, 2H), 7.11-7.08 (m, 4H), 2.55 (q, *J* = 7.7 Hz, 2H), 1.13 (t, *J* = 7.7 Hz, 3H); ^{13}C{^{1}H} NMR (175 MHz, DMSO-d_6) δ 152.3, 143.5, 142.5, 140.9, 137.5, 134.5, 131.2, 130.5, 130.1, 129.9, 128.7, 127.6, 127.1, 122.1, 121.2, 118.9, 111.3, 27.7, 15.3; IR (KBr) $\tilde{\nu}$ = 3425, 3058, 2969, 2924, 2857, 1450, 1410, 1282, 1098 cm^{-1}; HR-MS (ESI-TOF) m/z calcd for $C_{21}H_{19}N_2$ $[M + H]^+$ 299.1543, found 299.1530.

2-(4'-Fluoro-[1,1'-biphenyl]-2-yl)-1H-benzo[d]imidazole (1c). R_f = 0.60 (hexane/ethyl acetate 7:3); white solid; yield 97% (387 mg); mp 254 °C; ^{1}H NMR (700 MHz, DMSO-d_6) δ 12.14 (s, 1H), 7.73 (d, *J* = 7.0 Hz, 1H), 7.60 (t, *J* = 7.7, Hz, 1H), 7.49 – 7.58 (m, 3H), 7.36 (s, 1H), 7.21-7.19 (m, 2H), 7.14 (d, *J* = 4.2 Hz, 2H), 7.09 (t, *J* = 8.4 Hz, 2H); ^{13}C{^{1}H} NMR (175 MHz, DMSO-d_6) δ 161.9 (d, $^1J_{C,F}$ = 243.9 Hz), 152.3, 143.9, 140.4, 137.0 (d, $^4J_{C,F}$ =

3.1 Hz), 135.0, 131.5, 131.2 (d, $^{3}J_{C,\,F}$ = 8.2 Hz), 131.0, 130.6, 130.4, 128.0, 122.6, 121.8, 119.3, 115.4 (d, $^{2}J_{C,\,F}$ = 21.4 Hz), 111.8; IR (KBr) $\tilde{\nu}$ = 3440, 3060, 2922, 1445, 1423, 1279, 1227, 1163 cm^{-1}; HR-MS (ESI-TOF) m/z calcd for $C_{19}H_{14}FN_2$ $[M + H]^+$ 289.1136, found 289.1149.

1-(2'-(1H-Benzo[d]imidazol-2-yl)-[1,1'-biphenyl]-4-yl)ethan-1-one (1d). R_f = 0.50 (hexane/ethyl acetate 7:3); white solid; yield 72% (311 mg); mp 276 °C; ^{1}H NMR (700 MHz, DMSO-d_6) δ 12.26 (s, 1H), 7.84 (d, *J* = 8.4 Hz, 2H), 7.77 (dd, *J* = 7.7, 0.7 Hz, 1H), 7.65 (td, *J* = 7.7, 1.4 Hz, 1H), 7.59 (td, *J* = 7.7, 1.4 Hz, 1H), 7.56 (d, *J* = 7.7 Hz, 2H), 7.36 (d, *J* = 7.0 Hz, 1H), 7.33 (d, *J* = 8.4 Hz, 2H), 7.11 – 7.16 (m, 2H), 2.53 (s, 3H); $^{13}C\{^{1}H\}$ NMR (175 MHz, DMSO-d_6) δ 197.6, 151.7, 145.1, 143.5, 139.9, 135.3, 134.6, 131.2, 130.6, 130.2, 130.0, 129.2, 128.1, 128.1, 122.3, 121.4, 118.9, 111.4, 26.7; IR (KBr) $\tilde{\nu}$ = 3418, 2924, 2847, 1678, 1651, 1381, 1269, 1098 cm^{-1}; HR-MS (ESI-TOF) m/z calcd for $C_{21}H_{17}N_2O$ $[M + H]^+$: 313.1335, found 313.1325.

2-([1,1'-Biphenyl]-2-yl)-5,6-dichloro-1H-benzo[d]imidazole (1e). R_f = 0.45 (hexane/ethyl acetate 4:1); white solid; yield 95% (914 mg); mp 249-251 °C; ^{1}H NMR (700 MHz, DMSO-d_6) δ 12.47 (s, 1H), 7.85 (s, 1H), 7.72 (d, *J* = 7.0 Hz, 1H), 7.66 – 7.63 (m, 1H), 7.59 (s, 1H), 7.55 (t, *J* = 7.0 Hz, 2H), 7.26 (d, *J* = 7.0 Hz, 3H), 7.14 – 7.17 (m, 2H); $^{13}C\{^{1}H\}$ NMR (175 MHz, DMSO-d_6) δ 154.8, 143.1, 141.1, 139.8, 134.0, 131.0, 130.6, 130.4, 129.2, 128.7, 128.3, 127.5, 127.3, 124.5, 123.9, 120.0, 112.7 ; IR (KBr) $\tilde{\nu}$ = 3095, 2922, 2842, 2364, 2337, 1448, 1428, 1388, 1296, 1101 cm^{-1}; HR-MS (ESI-TOF) m/z calcd for $C_{19}H_{13}Cl_2N_2$ $[M + H]^+$ 339.0450, found 339.0463.

5,6-Dichloro-2-(4'-ethyl-[1,1'-biphenyl]-2-yl)-1H-benzo[d]imidazole (1f). R_f = 0.60 (hexane/ethyl acetate 4:1); white solid; yield 97% (307 mg); mp 285 °C; ^{1}H NMR (700 MHz, DMSO-d_6) δ 12.46 (s, 1H), 7.87 (s, 1H), 7.69 (d, *J* = 7.7 Hz, 1H), 7.64 – 7.61 (m, 1H), 7.60 (s, 1H), 7.52 (t, *J* = 7.7 Hz, 2H), 7.07 – 7.12 (m, 4H), 2.55 (q, *J* = 7.7 Hz, 2H), 1.14 (t, *J* = 7.7 Hz, 3H); ^{13}C{^{1}H} NMR (175 MHz, DMSO-d_6) δ 154.9, 143.1, 142.7, 140.9, 137.1, 134.0, 131.1, 130.5, 130.4, 129.1, 128.6, 127.7, 127.2, 124.5, 123.9, 120.0, 112.7, 27.7, 15.3; IR (KBr) $\tilde{\nu}$ = 3420, 2966, 2929, 1445, 1428, 1386, 1296, 1096 cm^{-1}; HR-MS (ESI-TOF) m/z calcd for $C_{21}H_{17}Cl_2N_2$ $[M + H]^+$ 367.0763, found 367.0764.

2-(4'-(Tert-butyl)-[1,1'-biphenyl]-2-yl)-5,6-dichloro-1H-benzo[d]imidazole (1g). R_f = 0.45 (hexane/ethyl acetate 4:1); white solid; yield 79% (315 mg); mp 215 °C; ^{1}H NMR (700 MHz, DMSO-d_6) δ 12.49 (s, 1H), 7.87 (s, 1H), 7.68 (d, *J* = 7.7 Hz, 1H), 7.63 – 7.58 (m, 2H), 7.54 – 7.50 (m, 2H), 7.28 (d, *J* = 8.4 Hz, 2H), 7.11 (d, *J* = 7.7 Hz, 2H), 1.23 (s, 9H); ^{13}C{^{1}H} NMR (175 MHz, DMSO-d_6) δ 155.0, 149.6, 143.2, 140.8, 136.9, 134.1, 131.2, 130.7, 130.4, 129.1, 128.4, 127.3, 125.1, 124.5, 124.0, 120.1, 112.7, 34.3, 31.1; IR (KBr) $\tilde{\nu}$ = 3417, 2969, 1650, 1445, 1383, 1097 cm^{-1}; HR-MS (ESI-TOF) m/z calcd for $C_{23}H_{20}Cl_2N_2$ $[M + H]^+$ 395.1076, found 395.1084.

5,6-Dichloro-2-(3'-chloro-[1,1'-biphenyl]-2-yl)-1H-benzo[d]imidazole (1h). R_f = 0.60 (hexane/ethyl acetate 4:1); pale yellow solid; yield 96% (205 mg); mp 226 °C; ^{1}H NMR (700 MHz, DMSO-d_6) δ 12.60 (s, 1H), 7.86 (s, 1H), 7.76 (d, *J* = 7.0 Hz, 1H), 7.67 – 7.62 (m, 2H), 7.60 – 7.55 (m, 2H), 7.32 (dd, *J* = 8.4, 1.4 Hz, 1H), 7.29 (s, 1H), 7.24 (t, *J* = 7.7 Hz, 1H), 7.00 (d, *J* = 7.7 Hz, 1H); ^{13}C{^{1}H} NMR (175 MHz, DMSO-d_6) δ 154.4, 143.1, 142.0, 139.6, 134.1, 132.9, 131.1, 130.7, 130.6, 130.0, 129.2, 128.6, 128.2, 127.6, 127.2, 124.7, 124.1,

120.1, 112.8; IR (KBr) $\tilde{\nu}$ = 3418, 3065, 2924, 2857, 1594, 1382, 1296, 1096 cm^{-1}; HR-MS (ESI-TOF) m/z calcd for $C_{19}H_{12}Cl_3N_2$ $[M + H]^+$ 373.0061, found 373.0048.

5,6-Dichloro-2-(4'-fluoro-[1,1'-biphenyl]-2-yl)-1H-benzo[d]imidazole (1i). R_f = 0.40 (hexane/ethyl acetate 4:1); white solid; yield 93% (280 mg); mp 224 °C; ^1H NMR (400 MHz, DMSO-d_6) δ 12.53 (brs, 1H), 7.73 (d, *J* = 7.2 Hz, 3H), 7.67 – 7.59 (m, 2H), 7.54 (dd, *J* = 12.4, 7.2 Hz, 3H), 7.21 – 7.15 (m, 3H), 7.12 – 7.05 (m, 3H); $^{13}C\{^1H\}$ NMR (100 MHz, DMSO-d_6) δ 161.6 (d, $^1J_{C,F}$ = 244.3 Hz), 154.6 (×2), 142.9, 140.0, 136.2 (d, $^4J_{C,F}$ = 3.2 Hz), 134.1, 131.0, 130.8 (d, $^3J_{C,F}$ = 8.3 Hz), 130.6, 130.4, 129.2, 127.7, 124.3, 120.0, 115.1 (d, $^2J_{C,F}$ = 21.5 Hz), 112.7; IR (KBr) $\tilde{\nu}$ = 3437, 2947, 2855, 1522, 1485, 1455, 1425, 1396, 1304, 1222, 1158, 1106 cm^{-1}; HR-MS (ESI-TOF) m/z calcd for $C_{19}H_{12}Cl_2FN_2$ $[M + H]^+$ 357.0356, found 357.0372.

1-(2'-(5,6-Dichloro-1H-benzo[d]imidazol-2-yl)-[1,1'-biphenyl]-4-yl)ethan-1-one (1j). R_f = 0.40 (hexane/ethyl acetate 4:1); white solid; yield 92% (296 mg); mp 285 °C; ^1H NMR (700 MHz, DMSO-d_6) δ 12.63 (s, 1H), 7.85 (d, *J* = 8.4 Hz, 3H), 7.77 (d, *J* = 7.0 Hz, 1H), 7.70 – 7.65 (m, 1H), 7.64 – 7.55 (m, 3H), 7.30 (d, *J* = 8.4 Hz, 2H), 2.53 (s, 3H); $^{13}C\{^1H\}$ NMR (175 MHz, DMSO-d_6) δ 197.6, 154.4, 144.7, 143.1, 140.1, 135.4, 134.1, 131.1, 130.7, 130.5, 129.2, 129.1, 128.3, 128.1, 124.7, 124.1, 120.1, 112.8, 26.7; IR (KBr) $\tilde{\nu}$ = 3417, 2924, 2855, 1685, 1653, 1443, 1262, 1096 cm^{-1}; HR-MS (ESI-TOF): m/z calcd for $C_{21}H_{15}Cl_2N_2O$ $[M + H]^+$: 381.0556, found: 381.0570.

5,6-Dichloro-2-(4'-(trifluoromethyl)-[1,1'-biphenyl]-2-yl)-1H-benzo[d]imidazole (1k). R_f = 0.40 (hexane/ethyl acetate 4:1); white solid; yield 93% (320 mg); mp 286 °C; ^1H NMR (400 MHz, DMSO-d_6) δ 12.66 (s, 1H), 7.84 (s, 1H), 7.79 (d, *J* = 7.6 Hz, 1H), 7.71 – 7.67 (m,

1H), 7.66 – 7.60 (m, 4H), 7.59 (d, *J* = 7.6 Hz, 1H), 7.38 (d, *J* = 8.0 Hz, 2H); $^{13}C\{^{1}H\}$ NMR (100 MHz, DMSO-d_6) δ 154.2, 144.2, 143.1, 139.6, 134.0, 131.1, 130.8, 130.5, 129.6, 129.2, 128.4, 127.8, 127.4, 125.6, 125.0 (q, $^{3}J_{C,F}$ = 3.9 Hz), 124.7, 124.1, 120.1, 112.8; IR (KBr) $\tilde{\nu}$ = 3440, 2922, 2850, 1653, 1324, 1128, 1078 cm^{-1}; HR-MS (ESI-TOF): m/z calcd for $C_{20}H_{12}N_2Cl_2F_3$ $[M + H]^+$: 407.0324, found: 407.0324.

2-([1,1'-Biphenyl]-2-yl)-5,6-dimethyl-1H-benzo[d]imidazole (1l). R_f = 0.40 (hexane/ethyl acetate 4:1); orange-red solid; yield 98% (538 mg); mp 248-250 °C; ^{1}H NMR (700 MHz, DMSO-d_6) δ 11.81 (s, 1H), 7.68 (dd, *J* = 7.7, 1.4 Hz, 1H), 7.62 – 7.57 (m, 1H), 7.51 (t, *J* = 7.0 Hz, 2H), 7.31 (s, 1H), 7.24 (d, *J* = 7.0 Hz, 3H), 7.18 – 7.14 (m, 2H), 7.08 (s, 1H), 2.27 (s, 6H); $^{13}C\{^{1}H\}$ NMR (175 MHz, DMSO-d_6) δ 151.1, 142.2, 140.9, 140.2, 133.1, 131.0, 130.6, 130.5, 130.4, 129.7, 129.4, 128.7, 128.1, 127.3, 127.0, 118.9, 111.30, 19.9 (×2); IR (KBr) $\tilde{\nu}$ = 3445, 3057, 2974, 2921, 2696, 1455, 1431, 1402, 1311, 1267, 1165, 1108 cm^{-1}; HR-MS (ESI-TOF) m/z calcd for $C_{21}H_{19}N_2$ $[M + H]^+$ 299.1543, found 299.1548.

2-(4'-Ethyl-[1,1'-biphenyl]-2-yl)-5,6-dimethyl-1H-benzo[d]imidazole (1m). R_f = 0.50 (hexane/ethyl acetate 4:1); white solid; yield 88% (306 mg); mp 218-220 °C; ^{1}H NMR (700 MHz, DMSO-d_6) δ 11.80 (s, 1H), 7.65 (d, *J* = 7.0 Hz, 1H), 7.57 (t, *J* = 7.7 Hz, 1H), 7.48 (t, *J* = 7.7 Hz, 2H), 7.33 (s, 1H), 7.08 (s, 5H), 2.55 (q, *J* = 7.0 Hz, 2H), 2.27 (s, 6H), 1.14 (t, *J* = 7.7 Hz, 3H); $^{13}C\{^{1}H\}$ NMR (175 MHz, DMSO-d_6) δ 151.3, 142.4, 142.2, 140.8, 137.5, 133.1, 131.1, 130.5, 130.4, 130.4, 129.6, 129.4, 128.6, 127.5, 127.0, 118.9, 111.3, 27.7, 19.9 (×2), 15.3; IR (KBr) $\tilde{\nu}$ = 3438, 2964, 2925, 1633, 1455, 1407, 1312, 1264 cm^{-1}; HR-MS (ESI-TOF) m/z calcd for $C_{23}H_{23}N_2$ $[M + H]^+$ 327.1856, found 327.1861.

2-(4'-(Tert-butyl)-[1,1'-biphenyl]-2-yl)-5,6-dimethyl-1H-benzo[d]imidazole (1n). R_f = 0.40 (hexane/ethyl acetate 4:1); white solid; yield 82% (320 mg); mp 205 °C. ^{1}H NMR (700 MHz, DMSO-d_6) δ 11.87 (s, 1H), 7.62 (d, *J* = 7.5 Hz, 1H), 7.57 (dd, *J* = 10.8, 4.2 Hz, 1H), 7.48 (dd, *J* = 15.6, 7.8 Hz, 2H), 7.32 (s, 1H), 7.26 (d, *J* = 8.4 Hz, 2H), 7.12 (d, *J* = 8.4 Hz, 2H), 7.08 (s, 1H), 2.27 (s, 6H), 1.22 (s, 9H). ^{13}C{^{1}H} NMR (175 MHz, DMSO-d_6) δ 151.4, 149.4, 142.2, 140.6, 137.3, 133.2, 131.3, 130.7, 130.6, 130.3, 129.7, 129.5, 128.5, 127.1, 125.0, 118.9, 111.3, 34.2, 31.1, 20.0 (×2); IR (KBr) $\tilde{\nu}$ = 3439, 2962, 2924, 2860, 1457, 1405, 1316, 1269, 1111, 1002 cm^{-1}; HR-MS (ESI-TOF) m/z calcd for $C_{25}H_{27}N_2$ $[M + H]^+$ 356.2202, found 356.2214.

2-(4'-Fluoro-[1,1'-biphenyl]-2-yl)-5,6-dimethyl-1H-benzo[d]imidazole (1o). R_f = 0.40 (hexane/ethyl acetate 4:1); white solid; yield 96% (337 mg); mp 230 °C; ^{1}H NMR (700 MHz, DMSO-d_6) δ 11.85 (s, 1H), 7.71 – 7.67 (m, 1H), 7.58 (td, *J* = 7.7, 1.4 Hz, 1H), 7.53 – 7.47 (m, 2H), 7.32 (s, 1H), 7.18 (dd, *J* = 8.4, 5.6 Hz, 2H), 7.08 (dd, *J* = 16.8, 7.7 Hz, 3H), 2.27 (s, 6H); ^{13}C{^{1}H} NMR (175 MHz, DMSO-d_6) δ 161.4 (d, $^1J_{C,F}$ = 243.7 Hz), 150.9, 142.2, 139.8, 136.6, 133.1, 131.0, 130.8, 130.7, 130.4, 130.4, 129.7, 129.5, 127.5, 119.0, 114.9 (d, $^2J_{C,F}$ = 21.4 Hz), 111.3, 20.0, 19.9 (×2); IR (KBr) $\tilde{\nu}$ = 3048, 2971, 2921, 2857, 2689, 1514, 1462, 1405, 1316, 1227, 1160 cm^{-1}; HR-MS (ESI-TOF) m/z calcd for $C_{21}H_{18}FN_2$ $[M + H]^+$ 317.1448, found 317.1422.

2-(3'-Chloro-[1,1'-biphenyl]-2-yl)-5,6-dimethyl-1H-benzo[d]imidazole (1p). R_f = 0.40 (hexane/ethyl acetate 4:1); white solid; yield 93% (340 mg); mp 232 °C; ^{1}H NMR (700 MHz, DMSO-d_6) δ 11.95 (s, 1H), 7.72 (dd, *J* = 7.7, 1.4 Hz, 1H), 7.60 (td, *J* = 7.7, 1.4 Hz, 1H), 7.56 – 7.49 (m, 2H), 7.34 – 7.25 (m, 3H), 7.22 (t, *J* = 8.4 Hz, 2H), 7.00 (d, *J* = 7.7 Hz, 1H), 2.27 (s, 6H); ^{13}C{^{1}H} NMR (175 MHz, DMSO-d_6) δ 150.6, 142.5, 142.2, 139.3, 133.0, 132.7,

131.0, 130.5, 130.4, 129.8, 129.7, 128.7, 128.6, 128.1, 128.0, 127.5, 126.9, 118.9, 111.4, 20.0 (×2); IR (KBr) $\tilde{\nu}$ = 3440, 3058, 2969, 2917, 2867, 1601, 1457, 1408, 1319, 1262, 1081 cm^{-1}; HR-MS (ESI-TOF) m/z calcd for $C_{21}H_{18}ClN_2$ $[M + H]^+$ 333.1153, found 333.1164.

1-(2'-(5,6-Dimethyl-1H-benzo[d]imidazol-2-yl)-[1,1'-biphenyl]-4-yl)ethan-1-one (1q). R_f = 0.40 (hexane/ethyl acetate 7:3); white solid; yield 73% (272 mg); mp 278 °C; ^1H NMR (700 MHz, DMSO-d_6) δ 12.00 (s, 1H), 7.82 (d, *J* = 8.4 Hz, 2H), 7.72 (d, *J* = 7.0 Hz, 1H), 7.62 (td, *J* = 7.7, 1.4 Hz, 1H), 7.57 (dd, *J* = 7.7, 1.4 Hz, 1H), 7.54 (d, *J* = 7.7 Hz, 1H), 7.29 (d, *J* = 8.4 Hz, 3H), 7.10 (s, 1H), 2.52 (s, 3H), 2.26 (s, 6H); $^{13}C\{^1H\}$ NMR (175 MHz, DMSO-d_6) δ 197.6, 150.8, 145.2, 142.2, 139.9, 135.2, 133.1, 131.1, 130.8, 130.5, 130.4, 129.8, 129.6, 129.1, 128.1, 128.0, 119.0, 111.4, 26.7, 19.9 (×2); IR (KBr) $\tilde{\nu}$ = 3440, 2966, 2924, 2862, 2681, 1681, 1651, 1605, 1403, 1353, 1267, 1009 cm^{-1}; HR-MS (ESI-TOF) m/z calcd for $C_{23}H_{21}N_2O$ $[M + H]^+$ 341.1648, found 341.1660.

5,6-Dichloro-2-(4-fluoro-[1,1'-biphenyl]-2-yl)-1H-benzo[d]imidazole (1r). R_f = 0.50 (hexane/ethyl acetate 4:1); white solid; yield 84% (255 mg); mp 258-260 °C; ^1H NMR (700 MHz, DMSO-d_6) δ 12.57 (s, 1H), 7.86 (s, 1H), 7.62 (s, 1H), 7.60 – 7.55 (m, 2H), 7.49 (td, *J* = 8.4, 2.8 Hz, 1H), 7.28 – 7.23 (m, 3H), 7.14 (dd, *J* = 6.4, 2.8 Hz, 2H). $^{13}C\{^1H\}$ NMR (175 MHz, DMSO-d_6) δ 161.1 (d, $^1J_{C,F}$ = 245.5 Hz), 153.4, 142.9, 138.9, 137.6 (d, $^4J_{C,F}$ = 3.0 Hz), 133.9, 132.8 (d, $^3J_{C,F}$ = 8.2 Hz), 131.0 (d, $^3J_{C,F}$ = 8.3 Hz), 128.8, 128.3, 127.3, 124.9, 124.2, 120.2, 117.6 (d, $^2J_{C,F}$ = 23.0 Hz), 117.3 (d, $^2J_{C,F}$ = 21.0 Hz), 112.8; IR (KBr) $\tilde{\nu}$ = 3417, 2927, 2845, 1655, 1477, 1448, 1383, 1200, 1093 cm^{-1}; HR-MS (ESI-TOF) m/z calcd for $C_{19}H_{12}Cl_2FN_2$ $[M + H]^+$ 357.0356, found 357.0368.

2-(4-Fluoro-[1,1'-biphenyl]-2-yl)-5,6-dimethyl-1H-benzo[d]imidazole (1s). R_f = 0.60 (hexane/ethyl acetate 4:1); white solid; yield 91% (320 mg); mp 220-222 °C; ^{1}H NMR (400 MHz, DMSO-d_6) δ 11.90 (s, 1H), 7.57 – 7.49 (m, 2H), 7.43 (td, *J* = 8.4, 2.8 Hz, 1H), 7.32 (s, 1H), 7.24 – 7.21 (m, 3H), 7.16 – 7.04 (m, 3H), 2.26 (s, 6H). ^{13}C{^{1}H} NMR (100 MHz, DMSO-d_6) δ 161.1 (d, $^1J_{C,F}$ = 245.2 Hz), 149.8, 142.0, 139.3, 137.5 (d, $^4J_{C,F}$ = 3.1 Hz), 133.1, 132.7 (d, $^3J_{C,F}$ = 8.3 Hz), 132.3 (d, $^3J_{C,F}$ = 8.3 Hz), 131.1, 129.8, 128.8, 128.2, 127.2, 119.1, 117.4 (d, $^2J_{C,F}$ = 22.6 Hz), 116.6 (d, $^2J_{C,F}$ = 20.9 Hz), 111.5, 19.98 (×2); IR (KBr) $\tilde{\nu}$ = 3438, 2969, 2919, 2857, 1610, 1586, 1460, 1417, 1314, 1200, 1006 cm^{-1}; HR-MS (ESI-TOF) m/z calcd for $C_{21}H_{18}FN_2$ $[M + H]^+$ 317.1449, found 317.1451.

Mixture of 2-([1,1'-Biphenyl]-2-yl)-5-methyl-1H-benzo[d]imidazole and 2-([1,1'-Biphenyl]-2-yl)-6-methyl-1H-benzo[d]imidazole (1a'). R_f = 0.60 (hexane/ethyl acetate 7:3); inseparable white solid (1:1); yield 85% (590 mg); mp 220-222 °C; ^{1}H NMR (700 MHz, DMSO-d_6) δ 11.97 (s, 1H), 11.92 (s, 1H), 7.69 (d, *J* = 7.0 Hz, 2H), 7.62 – 7.56 (m, 2H), 7.52 (t, *J* = 7.0 Hz, 4H), 7.43 (s, 1H), 7.34 (s, 1H), 7.21 – 7.25 (m, 6H), 7.18 (dd, *J* = 7.0, 1.4 Hz, 5H), 7.10 (s, 1H), 6.95 (d, *J* = 8.4 Hz, 2H), 2.37 (s, 6H); ^{13}C{^{1}H} NMR (175 MHz, DMSO-d_6) δ 152.0, 151.6, 144.8, 141.6, 140.9, 140.2, 134.8, 132.6, 131.4, 131.1, 130.5, 130.3, 130.1, 129.8, 128.8, 128.1, 127.4, 127.1, 123.5, 122.8, 118.5, 118.4, 111.0, 110.8, 21.3; IR (KBr) $\tilde{\nu}$ = 3440, 3057, 2922, 2867, 2664, 2362, 2337, 1455, 1434, 1403, 1311, 1289, 1232, 1148 cm^{-1}; HR-MS (ESI-TOF) m/z calcd for $C_{20}H_{17}N_2$ $[M + H]^+$ 285.1386, found 285.1361.

2-([1,1'-Biphenyl]-2-yl)-5-nitro-1H-benzo[d]imidazole (1b'). R_f = 0.40 (hexane/ethyl acetate 4:1); white solid; yield 81% (332 mg); mp 234-236 °C; ^{1}H NMR (400 MHz, DMSO-d_6) δ 12.84 (s, 1H), 8.41 (s, 1H), 8.07 (dd, *J* = 8.8, 2.0 Hz, 1H), 7.78 (d, *J* = 7.2 Hz, 1H), 7.68 (t, *J* = 7.6 Hz, 1H), 7.58 (t, *J* = 7.2 Hz, 3H), 7.32 – 7.23 (m, 3H), 7.22 – 7.14 (m, 2H);

$^{13}C\{^{1}H\}$ NMR (175 MHz, DMSO-d_6) δ 156.8, 142.6, 141.2, 139.7, 131.1, 130.7(×2), 129.0, 128.8(×2), 128.3(×2), 127.6, 127.4, 117.7, 114.9, 111.9; IR (KBr) $\tilde{\nu}$ = 3418, 3063, 2922, 2850, 2714, 1636, 1519, 1477, 1430, 1338, 1286, 1068 cm^{-1}; HR-MS (ESI-TOF) m/z calcd for $C_{19}H_{14}N_3O_2$ $[M + H]^+$ 316.1081, found 316.1052.

Mixture of 2-(4'-Ethyl-[1,1'-biphenyl]-2-yl)-5-methyl-1H-benzo[d]imidazole and 2-(4'-Ethyl-[1,1'-biphenyl]-2-yl)-6-methyl-1H-benzo[d]imidazole (1c'). R_f = 0.45 (hexane/ethyl acetate 4:1); Inseparable white solid (1:1.2); yield 92% (355 mg); mp 222 °C; ^{1}H NMR (700 MHz, DMSO-d_6) δ 11.96 (s, 1H), 11.92 (s, 1H), 7.66 (d, *J* = 7.7 Hz, 2.2H), 7.61 – 7.56 (m, 2.2H), 7.51 – 7.47 (m 4.8H), 7.44 (d, *J* = 8.4 Hz, 1.2H), 7.35 (s, 1H), 7.21 (d, *J* = 7.7 Hz, 1H), 7.11 – 7.07 (m 9.6H), 6.95 (d, *J* = 8.4 Hz, 2.2H), 2.55 (q, *J* = 7.7 Hz, 4.4H), 2.37 (s, 6.6H), 1.13 (t, *J* = 7.7 Hz, 6.6H); $^{13}C\{^{1}H\}$ NMR (175 MHz, DMSO-d_6) δ 152.2, 151.7, 143.8, 142.5, 141.6, 140.8, 137.5, 134.8, 132.6, 131.3, 131.1, 130.4, 130.3, 130.1, 129.8, 128.7, 127.6, 127.1, 123.5, 122.7, 118.6, 118.4, 111.0, 110.8, 27.7, 21.3, 15.3; IR (KBr) $\tilde{\nu}$ = 3430, 3057, 2964, 2921, 2872, 2662, 1633, 1446, 1407, 1314, 1282, 1267, 1150, 1054, 1007 cm^{-1}; HR-MS (ESI-TOF) m/z calcd for $C_{22}H_{21}N_2$ $[M + H]^+$ 313.1699, found 313.1710.

Mixture of 2-(4'-Ethyl-[1,1'-biphenyl]-2-yl)-5-nitro-1H-benzo[d]imidazole and 2-(4'-Ethyl-[1,1'-biphenyl]-2-yl)-6-nitro-1H-benzo[d]imidazole (1d'). R_f = 0.55 (hexane/ethyl acetate 4:1); Inseparable pale yellow solid(1:1); yield 84% (283 mg); mp 228-230 °C; ^{1}H NMR (700 MHz, DMSO-d_6) δ 12.81 (s, 1H), 8.49 (s, 1H), 8.22 (s, 1H), 8.10 – 8.05 (m, 2H), 7.79 – 7.72 (m, 3H), 7.65 (t, *J* = 7.0 Hz, 2H), 7.56 – 7.53 (m, 5H), 7.11 (s, 8H), 2.55 (q, *J* = 7.7 Hz, 4H), 1.13 (t, *J* = 7.7 Hz, 6H); $^{13}C\{^{1}H\}$ NMR (175 MHz, DMSO-d_6) δ 158.1, 156.9, 148.5, 143.3, 143.1, 143.0, 141.5, 139.7, 137.5, 134.2, 131.6, 131.1, 129.4, 129.2, 128.2, 127.8, 119.5, 118.5, 117.7, 115.5, 112.2, 108.3, 28.1, 15.7 ; IR (KBr) $\tilde{\nu}$ = 3403, 2966, 2929,

2850, 2364, 2342, 1625, 1521, 1476, 1339, 1066 cm^{-1}; HR-MS (ESI-TOF) m/z calcd for $C_{21}H_{18}N_3O_2$ $[M + H]^+$ 344.1394, found 344.1410.

Mixture of 2-(4'-Fluoro-[1,1'-biphenyl]-2-yl)-5-methyl-1H-benzo[d]imidazole and 2-(4'-Fluoro-[1,1'-biphenyl]-2-yl)-6-methyl-1H-benzo[d]imidazole (1e'). R_f = 0.50 (hexane/ethyl acetate 7:3); Inseparable white solid (1:1.2); yield 86% (319 mg); mp 226-228 °C; ^{1}H NMR (700 MHz, DMSO-d_6) δ 12.01 (s, 1H), 11.96 (s, 1H), 7.71 (d, *J* = 7.0 Hz, 2.2H), 7.59 (td, *J* = 7.7, 1.4 Hz, 2.2H), 7.53 (dd, *J* = 7.7, 1.4 Hz, 2.2H), 7.52 – 7.49 (m, 2.2H), 7.43 (s, 1.2H), 7.35 (s, 1H), 7.23 (s, 1H), 7.22 – 7.18 (m, 4.4H), 7.13 (s, 1.2H), 7.09 (t, *J* = 9.1 Hz, 4.4H), 6.96 (d, *J* = 7.0 Hz, 2.2H), 2.38 (s, 6.6H); ^{13}C{^{1}H} NMR (100 MHz, DMSO-d_6) δ 161.5 (d, $^1J_{C,F}$ = 243.9 Hz), 151.8, 151.4, 143.9, 141.6, 139.9, 136.6 (d, $^4J_{C,F}$ = 3.0 Hz), 134.8, 132.6, 131.5, 131.0, 130.8 (d, $^3J_{C,F}$ = 8.2 Hz), 130.5, 130.3, 129.8, 127.5, 123.6, 122.9, 118.7, 118.5, 115.0 (d, $^2J_{C,F}$ = 21.4 Hz), 111.1, 110.9, 21.3; IR (KBr) $\tilde{\nu}$ = 3444, 3057, 2971, 2919, 2855, 2669, 1633, 1605, 1511, 1494, 1446, 1463, 1403, 1309, 1280, 1222, 1158, 1094 cm^{-1}; HR-MS (ESI-TOF) m/z calcd for $C_{20}H_{16}FN_2$ $[M + H]^+$ 303.1292, found 303.1272.

Mixture of 2-(4-Fluoro-[1,1'-biphenyl]-2-yl)-5-methyl-1H-benzo[d]imidazole and 2-(4-Fluoro-[1,1'-biphenyl]-2-yl)-6-methyl-1H-benzo[d]imidazole (1f'). R_f = 0.60 (hexane/ethyl acetate 4:1); Inseparable white solid (1:1.2); yield 85% (154 mg); mp 185 °C; ^{1}H NMR (400 MHz, DMSO-d_6) δ 12.04 (s, 1H), 11.98 (s, 1H), 7.56 – 7.50 (m, 4.8), 7.48 – 7.40 (m, 3.6H), 7.35 (s, 1H), 7.27 – 7.21 (m, 7.2H), 7.18 – 7.09 (m, 5.8H), 6.96 (t, *J* = 7.2 Hz, 2.2H), 2.37 (s, 6.6H); ^{13}C{^{1}H} NMR (100 MHz, DMSO-d_6) δ 161.1 (d, $^1J_{C,F}$ = 245.6 Hz), 150.62, 150.18, 143.7, 141.5, 139.26, 137.5, 134.8, 132.7 (d, $^3J_{C,F}$ = 8.2 Hz), 132.6, 132.1 (d, $^3J_{C,F}$ = 8.9 Hz), 131.8, 130.4, 128.8, 128.2, 127.2, 123.9, 123.0, 118.8, 118.6, 117.5 (d, $^2J_{C,F}$ = 22.5 Hz), 116.7 (d, $^2J_{C,F}$ = 21.2 Hz), 111.2, 111.0, 21.30; IR (KBr) $\tilde{\nu}$ = 3437, 3070, 3023, 2918, 2862,

2778, 1611, 1589, 1509, 1446, 1418, 1284, 1201, 1073 cm^{-1}; HR-MS (ESI-TOF) m/z calcd for $C_{20}H_{16}FN_2$ $[M + H]^+$ 303.1292, found 303.1273.

Mixture of 1-(2'-(5-Methyl-1H-benzo[d]imidazol-2-yl)-[1,1'-biphenyl]-4-yl)ethan-1-one and 1-(2'-(6-Methyl-1H-benzo[d]imidazol-2-yl)-[1,1'-biphenyl]-4-yl)ethan-1-one (1g'). R_f = 0.60 (hexane/ethyl acetate 7:3); Inseparable pale yellow solid (1:1.2); yield 88% (351 mg); mp 265−267 °C; ^{1}H NMR (700 MHz, DMSO-d_6) δ 12.15 (s, 1H), 12.10 (s, 1.2H), 7.82 (d, *J* = 7.7 Hz, 4.4H), 7.74 (d, *J* = 7.7 Hz, 2.2H), 7.63 (td, *J* = 7.7, 1.4 Hz, 2.2H), 7.57 (td, *J* = 7.7, 1.4 Hz, 2.2H), 7.54 (d, *J* = 7.7 Hz, 2.2H), 7.42 (d, *J* = 8.4 Hz, 1.2H), 7.35 – 7.29 (m, 5.6H), 7.23 (d, *J* = 7.7 Hz, 1H), 7.12 (s, 1H), 6.99 – 6.91 (m, 2.2H), 2.52 (s, 6.6H), 2.36 (s, 6.6H); ^{13}C{^{1}H} NMR (175 MHz, DMSO-d_6) δ 197.7, 151.7, 151.2, 145.2, 143.9, 141.7, 139.9, 135.3, 134.9, 132.6, 131.7, 131.2, 130.6, 130.4, 130.3, 130.0, 129.2, 128.2, 128.1, 123.8, 123.0, 118.7, 118.6, 111.2, 111.0, 26.8, 21.4, 21.3; IR (KBr) $\tilde{\nu}$ = 3351, 3060, 2919, 2857, 1682, 1606, 1405, 1361, 1314, 1269, 1185 cm^{-1}; HR-MS (ESI-TOF) m/z calcd for $C_{22}H_{19}N_2O$ $[M + H]^+$ 327.1492, found 327.1475.

Benzo[4,5]imidazo[1,2-f]phenanthridine (2a). R_f = 0.40 (hexane/ethyl acetate 9:1); pale yellow solid; yield 91% (58 mg); mp 144 °C (lit.[18b] mp 144−146 °C); ^{1}H NMR (700 MHz, $CDCl_3$) δ 8.87 (d, *J* = 8.4 Hz, 1H), 8.56 (d, *J* = 7.7 Hz, 1H), 8.47 (d, *J* = 7.0 Hz, 1H), 8.37 (d, *J* = 8.4 Hz, 1H), 8.34 (d, *J* = 7.7 Hz, 1H), 8.06 (d, *J* = 7.7 Hz, 1H), 7.73 (t, *J* = 7.0 Hz, 1H), 7.71 – 7.66 (m, 2H), 7.55 – 7.45 (m, 3H); ^{13}C{^{1}H} NMR (175 MHz, $CDCl_3$) δ 147.7, 144.7, 134.6, 132.0, 130.6, 129.7, 129.3, 128.8, 126.2, 124.6, 124.4, 124.3, 123.6, 123.1, 122.4, 121.9, 120.5, 116.2, 114.1; IR (KBr) $\tilde{\nu}$ = 3351, 2364, 2332, 1532, 1453, 1440, 1373 cm^{-1}; HR-MS (ESI-TOF) m/z calcd for $C_{19}H_{13}N_2$ $[M + H]^+$ 269.1073, found 269.1058.

2-Ethylbenzo[4,5]imidazo[1,2-f]phenanthridine (2b). R_f = 0.55 (hexane/ethyl acetate 4:1); pale yellow solid; yield 96% (57 mg); mp 162 °C; ^{1}H NMR (700 MHz, $CDCl_3$) δ 8.85 (d, *J* = 7.7 Hz, 1H), 8.38 – 8.26 (m, 4H), 8.05 (d, *J* = 7.7 Hz, 1H), 7.71 (t, *J* = 7.0 Hz, 1H), 7.64 (t, *J* = 7.0 Hz, 1H), 7.52 (t, *J* = 7.0 Hz, 1H), 7.48 (t, *J* = 7.7 Hz, 1H), 7.34 (d, *J* = 7.7 Hz, 1H), 2.92 (q, *J* = 7.7 Hz, 2H), 1.42 (t, *J* = 7.7 Hz, 3H); ^{13}C{^{1}H} NMR (175 MHz, $CDCl_3$) δ 147.7, 146.1, 144.3, 134.6, 131.9, 130.7, 129.9, 128.4, 126.2, 124.7, 124.3(×2), 123.0, 122.9, 122.2, 120.3, 119.6, 115.3, 114.2, 29.29, 15.64; IR (KBr) $\tilde{\nu}$ = 3416, 2961, 2923, 2855, 1614, 1537, 1449, 1428, 1665 cm^{-1}; HR-MS (ESI-TOF) m/z calcd for $C_{21}H_{17}N_2$ $[M + H]^+$ 297.1386, found 297.1372.

2-Fluorobenzo[4,5]imidazo[1,2-f]phenanthridine (2c). R_f = 0.55 (hexane/ethyl acetate (4:1); white solid; yield 95% (55 mg); mp 190 °C; ^{1}H NMR (700 MHz, $CDCl_3$) δ 8.77 (d, *J* = 7.7 Hz, 1H), 8.37 – 8.30 (m, 1H), 8.18 (dd, *J* = 12.6, 7.7 Hz, 2H), 8.13 (d, *J* = 9.8 Hz, 1H), 8.01 (d, *J* = 7.7 Hz, 1H), 7.67 (t, *J* = 7.7 Hz, 1H), 7.62 (t, *J* = 7.0 Hz, 1H), 7.51 (t, *J* = 7.7 Hz, 1H), 7.47 (t, *J* = 7.7 Hz, 1H), 7.15 (t, *J* = 7.0 Hz, 1H); ^{13}C{^{1}H} NMR (175 MHz, $CDCl_3$) δ 162.87 (d, $^1J_{C,F}$ = 249.0 Hz), 147.6, 144.6, 135.3 (d, ^4J = 10.6 Hz), 131.7, 130.7, 129.1, 128.5, 126.2, 126.1 (d, $^4J_{C,F}$ = 9.7 Hz), 124.6, 123.3, 122.9, 122.1, 120.6, 118.2, 113.6, 112.1 (d, $^3J_{C,F}$ = 22.0 Hz), 103.32 (d, $^2J_{C,F}$ = 26.9 Hz); IR (KBr) $\tilde{\nu}$ = 3422, 2927, 2857, 1618, 1540, 1450, 1432, 1350, 1169 cm^{-1}; HR-MS (ESI-TOF) m/z calcd for $C_{19}H_{12}FN_2$ $[M + H]^+$ 287.0979, found 287.0971.

1-(Benzo[4,5]imidazo[1,2-f]phenanthridin-2-yl)ethan-1-one (2d). R_f = 0.70 (hexane/ethyl acetate 7:3); white solid; yield 94% (56 mg); mp 222 °C; ^{1}H NMR (700 MHz, $CDCl_3$) δ 8.95 (s, 1H), 8.80 – 8.73 (m, 1H), 8.31 (d, *J* = 8.4 Hz, 1H), 8.27 (d, *J* = 8.4 Hz, 1H), 8.22 – 8.18 (m, 1H), 8.01 (d, *J* = 7.7 Hz, 1H), 7.85 (d, *J* = 7.7 Hz, 1H), 7.67 (dd, *J* = 5.6, 2.8 Hz, 2H),

7.53 (t, *J* = 7.7 Hz, 1H), 7.49 (t, *J* = 7.7 Hz, 1H), 2.71 (s, 3H); $^{13}C\{^{1}H\}$ NMR (100 MHz, $CDCl_3$) δ 196.7, 147.1, 144.2, 136.7, 134.1, 131.7, 130.7, 129.9, 128.4, 126.2, 125.4, 124.7, 124.3, 124.1, 124.0, 123.8, 123.0, 120.5, 115.5, 114.1, 26.9; IR (KBr) $\tilde{\nu}$ = 3439, 3048, 1682, 1620, 1534, 1450, 1427, 1653, 1264 cm^{-1}; HR-MS (ESI-TOF) m/z calcd for $C_{21}H_{15}N_2O$ $[M + H]^+$ 311.1179, found 311.1168.

11,12-Dichlorobenzo[4,5]imidazo[1,2-f]phenanthridine (2e). R_f = 0.55 (hexane/ethyl acetate 4:1); white solid; yield 98% (59 mg); mp 234 °C (lit.[18a] mp 231-232 °C); ^{1}H NMR (700 MHz, $CDCl_3$) δ 8.65 (d, *J* = 7.7 Hz, 1H), 8.36 (d, *J* = 7.7 Hz, 1H), 8.26 (d, *J* = 7.7 Hz, 1H), 8.21 (s, 1H), 8.14 (d, *J* = 8.4 Hz, 1H), 7.93 (s, 1H), 7.71 (t, *J* = 7.0 Hz, 1H), 7.62 (s, 2H), 7.46 (t, *J* = 7.0 Hz, 1H); $^{13}C\{^{1}H\}$ NMR (175 MHz, $CDCl_3$) δ 149.1, 143.9, 133.6, 131.1, 130.7, 129.7, 129.5, 128.9, 128.2, 126.5, 126.3, 125.1, 124.4, 122.8, 122.4, 121.8, 121.1, 115.7, 115.1; IR (KBr) $\tilde{\nu}$ = 3444, 2919, 2852, 1651, 1537, 1438, 1364 cm^{-1}; HR-MS (ESI-TOF) m/z calcd for $C_{19}H_{11}Cl_2N_2$ $[M + H]^+$ 337.0294, found 337.0270.

11,12-Dichloro-2-ethylbenzo[4,5]imidazo[1,2-f]phenanthridine (2f). R_f = 0.60 (hexane/ethyl acetate 4:1); white solid; yield 93% (55.5 mg); mp 241 °C; ^{1}H NMR (700 MHz, $CDCl_3$) δ 8.69 (d, *J* = 7.7 Hz, 1H), 8.29 (d, *J* = 8.4 Hz, 1H), 8.26 (t, *J* = 7.7 Hz, 2H), 7.99 (d, *J* = 11.9 Hz, 2H), 7.71 (t, *J* = 7.7 Hz, 1H), 7.62 (t, *J* = 7.7 Hz, 1H), 7.34 (d, *J* = 8.4 Hz, 1H), 2.90 (q, *J* = 7.7 Hz, 2H), 1.41 (t, *J* = 7.7 Hz, 3H); $^{13}C\{^{1}H\}$ NMR (175 MHz, $CDCl_3$) δ 149.3, 146.4, 143.9, 133.8, 131.1, 130.8, 129.9, 128.5, 128.2, 126.3, 126.3, 125.1, 124.5, 122.4, 122.2, 121.0, 119.5, 115.2, 114.8, 29.3, 15.6; IR (KBr) $\tilde{\nu}$ = 3442, 2969, 2924, 2364, 2335, 1440, 1311, 1116 cm^{-1}; HR-MS (ESI-TOF) m/z calcd for $C_{21}H_{15}Cl_2N_2$ $[M + H]^+$ 365.0607, found 365.0594.

2-(Tert-butyl)-11,12-dichlorobenzo[4,5]imidazo[1,2-f]phenanthridine (2g). R_f = 0.60 (hexane/ethyl acetate 4:1); white solid; yield 94% (56 mg); mp 234 °C; ^{1}H NMR (700 MHz, $CDCl_3$) δ 8.75 (d, J = 7.0 Hz, 1H), 8.39 (t, J = 6.6 Hz, 1H), 8.32 – 8.34 (m, 3H), 8.03 (dd, J = 11.9, 5.6 Hz, 1H), 7.72 – 7.76 (m, 1H), 7.65 (t, J = 7.0 Hz, 1H), 7.62 – 7.58 (m, 1H), 1.54 (s, 9H); ^{13}C{^{1}H} NMR (175 MHz, $CDCl_3$) δ 153.4, 149.5, 144.2, 133.8, 131.2, 130.9, 129.9, 128.6, 128.2, 126.4, 126.3, 124.3, 122.9, 122.7, 122.3, 121.2, 119.4, 115.3, 112.5, 35.6, 31.5; IR (KBr) $\tilde{\nu}$ = 3439, 2959, 2867, 2359, 2339, 1615, 1439 cm^{-1}; HR-MS (ESI-TOF) m/z calcd for $C_{23}H_{19}Cl_2N_2$ $[M + H]^+$ 393.0920, found 393.0932.

3,11,12-Trichlorobenzo[4,5]imidazo[1,2-f]phenanthridine (2h). R_f = 0.70 (hexane/ethyl acetate 4:1); white solid; yield 92% (55 mg); mp 260 °C; ^{1}H NMR (400 MHz, $CDCl_3$ + TFA-D) δ 8.85 (d, *J* = 8.0 Hz, 1H), 8.63 (d, *J* = 1.6 Hz, 1H), 8.61 (s, 1H), 8.54 (t, *J* = 9.2 Hz, 2H), 8.23 (s, 1H), 8.12 (t, *J* = 7.6 Hz, 1H), 7.99 (t, *J* = 7.6 Hz, 1H), 7.90 (dd, *J* = 9.2, 1.6 Hz, 1H); ^{13}C{^{1}H} NMR (175 MHz, $CDCl_3$ + TFA-D) δ 146.5, 138.1, 133.2, 132.7, 130.9, 130.5, 130.3, 130.2, 129.2, 128.9, 128.7, 126.7, 124.4, 123.2, 122.8, 119.5, 119.4, 117.4, 115.4; IR (KBr) $\tilde{\nu}$ = 3439, 2922, 2852, 1651, 1542, 1445, 1368, 1106 cm^{-1}; HR-MS (ESI-TOF) m/z calcd for $C_{19}H_{10}Cl_3N_2$ $[M + H]^+$ 370.9904, found 370.9891.

11,12-Dichloro-2-fluorobenzo[4,5]imidazo[1,2-f]phenanthridine (2i). R_f = 0.60 (hexane/ethyl acetate 4:1); white solid; yield 94% (56 mg); mp 264 °C; ^{1}H NMR (700 MHz, $CDCl_3$: TFA-D 15:1) δ 8.81 (dd, J = 9.1, 5.6 Hz, 1H), 8.74 – 8.68 (m, 2H), 8.65 (d, J = 8.4 Hz, 1H), 8.38 (dd, J = 9.1, 1.4 Hz, 1H), 8.21 – 8.16 (m, 2H), 7.98 (t, J = 7.7 Hz, 1H), 7.72 – 7.68 (m, 1H); ^{13}C{^{1}H} NMR (175 MHz, $CDCl_3$: TFA-D 15:1) δ 163.9 (d, $^1J_{C,F}$ = 255.9 Hz), 144.9, 136.5, 134.8, 132.7, 131.9 (d, $^3J_{C,F}$ = 10.3 Hz), 131.7, 131.0, 130.7, 127.9 (d, $^3J_{C,F}$ = 9.0 Hz), 126.3, 123.6, 119.4 (d, $^4J_{C,F}$ = 2.7 Hz), 117.3 (d, $^2J_{C,F}$ = 22.3 Hz), 115.4, 114.7,

113.7, 112.1, 104.9 (d,[2] $J_{C,F}$ = 27.7 Hz); IR (KBr) $\tilde{\nu}$ = 3053, 2986, 2305, 1621, 1537, 1447, 1345, 1264, 1196, 1113 cm^{-1}; HR-MS (ESI-TOF) m/z calcd for $C_{19}H_{10}Cl_2FN_2$ $[M + H]^+$ 355.0200, found 355.0213.

1-(11,12-Dichlorobenzo[4,5]imidazo[1,2-f]phenanthridin-2-yl)ethan-1-one (2j). R_f = 0.60 (hexane/ethyl acetate 7:3); white solid; yield 93% (55.6 mg); mp 256 °C; ^1H NMR (400 MHz, $CDCl_3$) δ 8.72 (s, 1H), 8.68 (d, *J* = 8.0 Hz, 1H), 8.44 (d, *J* = 8.4 Hz, 1H), 8.30 (d, *J* = 8.0 Hz, 1H), 8.27 (s, 1H), 7.98 (d, *J* = 8.4 Hz, 1H), 7.95 (s, 1H), 7.76 (t, *J* = 7.6 Hz, 1H), 7.70 (t, *J* = 7.6 Hz, 1H), 2.77 (s, 3H); $^{13}C\{^1H\}$ NMR (100 MHz, $CDCl_3$) δ 196.5, 148.8, 143.9, 137.1, 133.6, 131.4, 130.7, 130.1, 128.8, 128.7, 127.2, 126.5, 125.6, 124.8, 124.7, 123.8, 123.2, 121.3, 115.2, 115.1, 26.9; IR (KBr) $\tilde{\nu}$ = 3418, 2919, 1682, 1442, 1353, 1259, 1118 cm^{-1}; HR-MS (ESI-TOF) m/z calcd for $C_{21}H_{13}Cl_2N_2O$ $[M + H]^+$ 379.0399, found 379.0376.

11,12-Dichloro-2-(trifluoromethyl)benzo[4,5]imidazo[1,2-f]phenanthridine (2k). R_f = 0.70 (hexane/ethyl acetate 4:1); white solid; yield 92% (55 mg); mp 275 °C; ^1H NMR (700 MHz, $CDCl_3$) δ 8.73 (d, *J* = 7.7 Hz, 1H), 8.56 (d, *J* = 8.4 Hz, 1H), 8.47 (s, 1H), 8.36 (d, *J* = 8.4 Hz, 1H), 8.23 (s, 1H), 8.00 (s, 1H), 7.85 – 7.76 (m, 2H), 7.74 (t, *J* = 7.7 Hz, 1H); $^{13}C\{^1H\}$ NMR (175 MHz, $CDCl_3$) δ 148.8, 143.8, 133.5, 131.6, 131.3 (q, $^2J_{C,F}$ = 33 Hz), 130.5, 130.3, 129.0, 128.6, 127.4, 126.6 (q, $^1J_{C,F}$ = 273 Hz), 125.3, 124.8, 124.5, 123.4, 122.9, 121.7 (q, $^3J_{C,F}$ = 3.5 Hz), 121.5, 114.9, 112.8 (q, $^3J_{C,F}$ = 3.5 Hz); IR (KBr) $\tilde{\nu}$ = 3422, 2922, 2852, 1620, 1537, 1442, 1302, 1285, 1125, 1112, 1081 cm^{-1}; HR-MS (ESI-TOF) m/z calcd for $C_{20}H_{10}Cl_2F_3N_2$ $[M + H]^+$ 405.0168, found 405.0159.

11,12-Dimethylbenzo[4,5]imidazo[1,2-f]phenanthridine (2l). R_f = 0.60 (hexane/ethyl acetate 4:1); white solid; yield 96% (58 mg); mp 164 °C (lit.[18a] mp 161-162 °C); ^1H NMR

(700 MHz, $CDCl_3$) δ 8.84 (d, *J* = 7.7 Hz, 1H), 8.53 (d, *J* = 8.4 Hz, 1H), 8.47 (d, *J* = 7.7 Hz, 1H), 8.37 (d, *J* = 7.7 Hz, 1H), 8.08 (s, 1H), 7.78 (s, 1H), 7.70 (q, *J* = 7.0 Hz, 2H), 7.66 (t, *J* = 7.0 Hz, 1H), 7.49 (t, *J* = 7.7 Hz, 1H), 2.53 (s, 3H), 2.47 (s, 3H); $^{13}C\{^1H\}$ NMR (175 MHz, $CDCl_3$) δ 146.3, 142.6, 134.1, 132.8, 131.7, 129.9, 129.6, 128.9, 128.6, 128.1, 125.5, 123.7, 123.7, 123.2, 121.8, 121.2, 119.8, 115.5, 113.8, 20.7, 20.0; IR (KBr) $\tilde{\nu}$ = 3202, 2927, 2855, 2359, 1640, 1535, 1439, 1371 cm^{-1}; HR-MS (ESI-TOF) m/z calcd for $C_{21}H_{17}N_2$ $[M + H]^+$ 297.1386, found 297.1359.

2-Ethyl-11,12-dimethylbenzo[4,5]imidazo[1,2-f]phenanthridine (2m). R_f = 0.60 (hexane/ethyl acetate 4:1); white solid; yield 94% (56 mg); mp 186 °C; ^1H NMR (700 MHz, $CDCl_3$) δ 8.82 (d, *J* = 7.7 Hz, 1H), 8.33 (d, *J* = 8.4 Hz, 1H), 8.31 (s, 2H), 8.04 (s, 1H), 7.77 (s, 1H), 7.68 (t, *J* = 7.7 Hz, 1H), 7.62 (t, *J* = 7.7 Hz, 1H), 7.32 (d, *J* = 8.4 Hz, 1H), 2.93 (q, *J* = 7.7 Hz, 2H), 2.53 (s, 3H), 2.46 (s, 3H), 1.43 (t, *J* = 7.7 Hz, 3H); $^{13}C\{^1H\}$ NMR (100 MHz, $CDCl_3$) δ 147.0, 145.9, 142.8, 134.7, 133.4, 132.2, 130.4, 130.3, 129.6, 128.3, 126.1, 124.4, 124.2, 123.1, 122.1, 120.2, 119.5, 115.2, 114.4, 29.3, 21.3, 20.5, 15.6; IR (KBr) $\tilde{\nu}$ = 3404, 2921, 2855, 1686, 1611, 1428 cm^{-1}; HR-MS (ESI-TOF) m/z calcd for $C_{23}H_{21}N_2$ $[M + H]^+$ 325.1699, found 325.1694.

2-(Tert-butyl)-11,12-dimethylbenzo[4,5]imidazo[1,2-f]phenanthridine (2n). R_f = 0.65 (hexane/ethyl acetate 4:1); white solid; yield 82% (49 mg); mp 208 °C; ^1H NMR (700 MHz, $CDCl_3$) δ 8.84 (d, *J* = 8.4 Hz, 1H), 8.58 (s, 1H), 8.40 (d, *J* = 8.4 Hz, 1H), 8.35 (d, *J* = 8.4 Hz, 1H), 8.09 (s, 1H), 7.80 (s, 1H), 7.69 (t, *J* = 7.7 Hz, 1H), 7.64 (t, J = 7.7 Hz, 1H), 7.56 (dd, *J* = 8.4, 1.4 Hz, 1H), 2.55 (s, 3H), 2.48 (s, 3H), 1.54 (s, 9H); $^{13}C\{^1H\}$ NMR (175 MHz, $CDCl_3$) δ 152.9, 147.3, 143.5, 134.7, 133.2, 131.9, 130.5, 130.1, 129.5, 128.3, 126.0, 124.0, 123.6, 122.2, 121.9, 120.5, 119.3, 114.4, 112.9, 35.5, 31.6, 21.5, 20.6; IR (KBr) $\tilde{\nu}$ = 3417, 2960,

2359, 2340, 1615, 1532, 1463, 1428, 1359 cm^{-1}; HR-MS (ESI-TOF) m/z calcd for $C_{25}H_{25}N_2$ $[M + H]^+$ 353.2012, found 353.2025.

2-Fluoro-11,12-dimethylbenzo[4,5]imidazo[1,2-f]phenanthridine (2o). R_f = 0.60 (hexane/ethyl acetate 4:1); white solid; yield 92% (55 mg); mp 208 °C; ^{1}H NMR (700 MHz, $CDCl_3$) δ 8.77 (d, *J* = 7.7 Hz, 1H), 8.37 (dd, *J* = 9.1, 6.3 Hz, 1H), 8.23 (d, *J* = 7.7 Hz, 1H), 8.17 – 8.11 (m, 1H), 7.91 (s, 1H), 7.74 (s, 1H), 7.67 (t, *J* = 7.7 Hz, 1H), 7.62 (t, *J* = 7.7 Hz, 1H), 7.21 – 7.14 (m, 1H), 2.51 (s, 3H), 2.45 (s, 3H); ^{13}C{^{1}H} NMR (175 MHz, $CDCl_3$) δ 162.9 (d, $^1J_{C,F}$ = 248.4 Hz), 147.0, 143.2, 135.5 (d, $^3J_{C,F}$ = 10.6 Hz), 133.7, 132.5, 130.3, 130.2, 128.9, 128.5, 126.0, 126.0, 123.2, 122.1, 120.6 , 118.2, 113.9, 111.8 (d, $^2J_{C,F}$ = 22.1 Hz), 103.2 (d, $^2J_{C,F}$ = 26.8 Hz), 21.2, 20.5; IR (KBr) $\tilde{\nu}$ = 3439, 2922, 2847, 1656, 1651, 1541, 1462, 1434, 1178 cm^{-1}; HR-MS (ESI-TOF) m/z calcd for $C_{21}H_{16}FN_2$ $[M + H]^+$ 315.1292, found 315.1308.

3-Chloro-11,12-dimethylbenzo[4,5]imidazo[1,2-f]phenanthridine (2p). R_f = 0.65 (hexane/ethyl acetate 4:1); white solid; yield 89% (53 mg); mp 210 °C; ^{1}H NMR (700 MHz, $CDCl_3$) δ 8.81 (d, *J* = 7.7 Hz, 1H), 8.41 (d, *J* = 9.1 Hz, 1H), 8.38 (d, *J* = 1.4 Hz, 1H), 8.27 (d, *J* = 7.7 Hz, 1H), 7.96 (s, 1H), 7.76 (s, 1H), 7.73 – 7.66 (m, 2H), 7.61 (dd, *J* = 8.4, 1.4 Hz, 1H), 2.52 (s, 3H), 2.46 (s, 3H); ^{13}C{^{1}H} NMR (175 MHz, $CDCl_3$) δ 146.7, 143.2, 133.6, 133.1, 132.6, 130.4, 130.3, 129.9, 129.4, 129.0, 128.3, 126.1, 124.1, 124.1, 123.4, 122.5, 120.6, 117.3, 114.0, 21.2, 20.6; IR (KBr) $\tilde{\nu}$ = 3417, 2917, 2845, 1534, 1452, 1108, 1024 cm^{-1}; HR-MS (ESI-TOF) m/z calcd for $C_{21}H_{16}ClN_2$ $[M + H]^+$ 331.0997, found 331.1009.

1-(11,12-Dimethylbenzo[4,5]imidazo[1,2-f]phenanthridin-2-yl)ethan-1-one (2q). R_f = 0.70 (hexane/ethyl acetate 7:3); white solid; yield 82% (49 mg); mp 198 °C; ^{1}H NMR (700

MHz, $CDCl_3$) δ 8.88 (s, 1H), 8.75 – 8.69 (m, 1H), 8.32 (d, *J* = 8.4 Hz, 1H), 8.23 – 8.19 (m, 1H), 7.94 (s, 1H), 7.84 (d, *J* = 8.4 Hz, 1H), 7.70 (s, 1H), 7.65 (m, 2H), 2.70 (s, 3H), 2.50 (s, 3H), 2.44 (s, 3H); $^{13}C\{^1H\}$ NMR (175 MHz, $CDCl_3$) δ 196.8, 146.4, 143.0, 136.7, 134.3, 133.7, 132.9, 130.3, 130.2, 129.7, 128.3, 126.0, 125.4, 124.4, 124.2, 123.8, 123.1, 120.5, 115.5, 114.2, 26.8, 21.3, 20.6; IR (KBr) $\tilde{\nu}$ = 2929, 2847, 1685, 1604, 1405, 1274, 1215, 1185, 1106 cm^{-1}; HR-MS (ESI-TOF) m/z calcd for $C_{23}H_{19}N_2O$ $[M + H]^+$ 339.1492, found 339.1518.

11,12-Dichloro-7-fluorobenzo[4,5]imidazo[1,2-f]phenanthridine (2r). R_f = 0.65 (hexane/ethyl acetate 4:1); white solid; yield 95% (57 mg); mp 280 °C; ^1H NMR (400 MHz, $CDCl_3$ + TFA-D 15:1) δ 8.75 (s, 1H), 8.72 – 8.64 (m, 3H), 8.54 (d, *J* = 8.0 Hz, 1H), 8.25 (s, 1H), 8.04 (t, *J* = 8.0 Hz, 1H), 7.92 (t, *J* = 7.6 Hz, 1H), 7.84 (t, *J* = 8.0 Hz, 1H); $^{13}C\{^1H\}$ NMR (100 MHz, $CDCl_3$ + TFA-D 15:1)) δ 163.1 (d, *J* = 256.2 Hz), 143.6, 134.4, 132.3, 131.4 (d, *J* = 16.8 Hz), 130.8, 129.0, 128.4 (d, *J* = 2.6 Hz), 128.0, 126.5 (d, *J* = 8.9 Hz), 125.3, 124.6 (d, *J* = 23.6 Hz), 122.2, 119.1, 117.3, 117.2, 117.1, 113.4, 112.4 (d, *J* = 25.3 Hz), 110.5; IR (KBr) $\tilde{\nu}$ = 2919, 2845, 1537, 1443, 1361, 1331, 1197, 1116, 1083 cm^{-1}; HR-MS (ESI-TOF) m/z calcd for $C_{19}H_9Cl_2FN_2$ $[M + H]^+$ 355.0200, found 355.0196.

7-Fluoro-11,12-dimethylbenzo[4,5]imidazo[1,2-f]phenanthridine (2s). R_f = 0.70 (hexane/ethyl acetate 4:1); white solid; yield 94% (56 mg); mp 215 °C; ^1H NMR (700 MHz, $CDCl_3$) δ 8.48 (d, *J* = 8.4 Hz, 1H), 8.44 (d, *J* = 9.1 Hz, 1H), 8.35 (d, *J* = 8.4 Hz, 1H), 8.31 (dd, *J* = 8.4, 4.9 Hz, 1H), 8.04 (s, 1H), 7.75 (s, 1H), 7.67 (t, *J* = 7.7 Hz, 1H), 7.47 (t, *J* = 7.7 Hz, 1H), 7.39 (t, *J* = 7.0 Hz, 1H), 2.52 (s, 3H), 2.46 (s, 3H); $^{13}C\{^1H\}$ NMR (175 MHz, $CDCl_3$) δ 162.7 (d, $^1J_{C,F}$ = 249.1 Hz), 146.0, 143.1, 134.2, 133.6, 132.7, 130.5, 129.0, 125.8, 125.6 (d, $^3J_{C,F}$ = 9.4 Hz), 124.9 (d, $^3J_{C,F}$ = 8.4 Hz), 124.5, 124.1, 121.2, 120.6, 118.4 (d, $^2J_{C,F}$

= 23.2 Hz), 116.1, 114.3, 111.5 (d, $^{2}J_{C,F}$ = 23.6 Hz), 21.2, 20.6; IR (KBr) $\tilde{\nu}$ = 3417, 2924, 2852, 1509, 1542, 1457, 1433, 1334, 1252, 1210 cm^{-1}; HR-MS (ESI-TOF) m/z calcd for $C_{21}H_{16}FN_2$ $[M + H]^+$ 315.1292, found 315.1292.

Mixture of 11-Methylbenzo[4,5]imidazo[1,2-f]phenanthridine and 12-Methylbenzo[4,5]imidazo[1,2-f]phenanthridine (2a'). R_f = 0.60 (hexane/ethyl acetate 7:3); Inseparable white solid (5:3); yield 96% (57 mg); mp 162 °C; ^{1}H NMR (700 MHz, $CDCl_3$) δ 8.73 (d, *J* = 7.7 Hz, 1.6H), 8.30 – 8.21 (m, 3.2H), 8.17 (d, *J* = 7.7 Hz, 1.6H), 7.98 (d, *J* = 8.4 Hz, 1H), 7.91 (s, 0.6H), 7.85 (d, *J* = 7.7 Hz, 0.6H), 7.74 (s, 1H), 7.63 – 7.56 (m, 3.2H), 7.50 (t, *J* = 7.0 Hz, 1.6H), 7.31 (dd, *J* = 14.0, 7.0 Hz, 1.6H), 7.28 – 7.24 (m, 0.6H), 7.17 (d, *J* = 8.4 Hz, 1H), 2.59 (s, 1.8H), 2.54 (s, 3H). $^{13}C\{^{1}H\}$ NMR (175 MHz, $CDCl_3$) δ 147.2, 146.9, 144.6, 142.4, 134.3, 134.2, 134.0, 132.8, 131.9, 130.2, 130.1, 129.8, 129.3, 129.3, 129.0, 128.9, 128.5, 128.5, 125.9, 125.8, 125.7, 124.4, 124.2, 124.2, 124.0, 123.4, 123.3, 122.2, 122.1, 121.5, 121.4, 119.9, 119.7, 115.8, 115.8, 113.9, 113.4, 22.4, 21.7; IR (KBr) $\tilde{\nu}$ = 3402, 2924, 2852, 2359, 2339, 1539, 1457, 1439, 1376, 1264, 1041 cm^{-1}; HR-MS (ESI-TOF) m/z calcd for $C_{20}H_{15}N_2$ $[M + H]^+$ 283.1230, found 283.1204.

Mixture of 11-Nitrobenzo[4,5]imidazo[1,2-f]phenanthridine and 12-Nitrobenzo[4,5]imidazo[1,2-f]phenanthridine (2b'). R_f = 0.55 (hexane/ethyl acetate 4:1); Inseparable pale yellow solid (2:1); yield 91% (54 mg); mp 256 °C; ^{1}H NMR (400 MHz, $CDCl_3$) δ 9.18 – 9.21 (m, 1H), 8.78 (t, *J* = 8.4 Hz, 2H), 8.45 (t, *J* = 8.8 Hz, 3H), 8.42 – 8.31 (m, 3H), 8.28 (s, 0.5H), 7.96 (d, *J* = 8.8 Hz, 1H), 7.84 – 7.66 (m, 4.5H), 7.61 – 7.52 (m, 1.5H); $^{13}C\{^{1}H\}$ NMR (100 MHz, $CDCl_3$) δ 151.7, 149.1, 143.0, 135.6, 133.7, 133.5, 131.9, 131.7, 130.9, 130.3, 130.0, 129.7, 129.2, 129.2, 126.7, 126.6, 125.7, 124.7, 124.7, 122.6, 122.6, 122.5, 122.0, 120.1, 120.0, 118.1, 116.4, 116.1, 113.8, 110.9; IR (KBr) $\tilde{\nu}$ = 3420,

2924, 2850, 1537, 1460, 1505, 1435, 1348, 1291 cm^{-1}; HR-MS (ESI-TOF) m/z calcd for $C_{19}H_{12}N_3O_2$ $[M + H]^+$ 314.0924, found 314.0925.

Mixture of **2-Ethyl-11-methylbenzo[4,5]imidazo[1,2-f]phenanthridine** and **2-Ethyl-12-methylbenzo[4,5]imidazo[1,2-f]phenanthridine (2c').** R_f = 0.60 (hexane/ethyl acetate 4:1); Inseparable pale yellow solid (5:2); yield 92% (54 mg); mp 175 °C; ^{1}H NMR (700 MHz, $CDCl_3$) δ 8.83 (t, *J* = 8.4 Hz, 1.4H), 8.30 – 8.36 (m, 4.2H), 8.18 (d, *J* = 8.4 Hz, 1H), 8.10 (s, 0.4H), 7.92 (d, *J* = 8.4 Hz, 0.4H), 7.82 (s, 1H), 7.75 – 7.67 (m, 1.4H), 7.64 (t, *J* = 7.0 Hz, 1.4H), 7.34 (d, *J* = 7.7 Hz, 1.8H), 7.28 (d, *J* = 8.4 Hz, 1H), 2.89–2.94 (m, 2.8H), 2.66 (s, 1.2H), 2.58 (s, 3H), 1.42 (t, *J* = 7.7 Hz, 4.2H); ^{13}C{^{1}H} NMR (175 MHz, $CDCl_3$) δ 147.5, 147.2, 146.1, 146.0, 134.7, 134.5, 134.3, 133.0, 132.1, 130.6, 130.5, 129.9, 129.8, 129.7, 128.4, 126.2, 126.1, 125.9, 124.6, 124.6, 124.5, 124.3, 124.3, 123.1, 122.8, 122.2, 120.0, 119.7, 119.6, 119.5, 115.3, 115.2, 114.2, 113.7, 29.3, 22.6, 21.8, 15.7, 15.6; IR (KBr) $\tilde{\nu}$ = 2974, 2922, 2855, 1615, 1590, 1538, 1435, 1362, 1261 cm^{-1}; HR-MS (ESI-TOF) m/z calcd for $C_{22}H_{19}N_2$ $[M + H]^+$ 311.1543, found 311.1540.

Mixture of **2-Ethyl-11-nitrobenzo[4,5]imidazo[1,2-f]phenanthridine** and **2-Ethyl-12-nitrobenzo[4,5]imidazo[1,2-f]phenanthridine (2d').** R_f = 0.50 (hexane/ethyl acetate 4:1); Inseparable Pale yellow solid (5:2); yield 93% (55.5 mg); mp 242 °C; ^{1}H NMR (400 MHz, $CDCl_3$) δ 9.15 (d, *J* = 2.0 Hz, 1H), 8.73 (dd, *J* = 12.0, 8.0 Hz, 1.8H), 8.37 (dd, *J* = 8.8, 2.0 Hz, 1H), 8.33 – 8.27 (m, 2.8H), 8.27 – 8.25 (m, 0.4H), 8.24 (s, 0.4H), 8.19 (s, 1H), 8.16 (s, 0.4H), 7.94 (d, *J* = 9.2 Hz, 1H), 7.80 – 7.71 (m, 1.4H), 7.64 (dd, *J* = 15.2, 8.0 Hz, 1.4H), 7.38 (d, *J* = 8.0 Hz, 1.4H), 3.00 – 2.84 (m, 2.8H), 1.39 – 1.46 (m, 4.2H); ^{13}C{^{1}H} NMR (175 MHz, $CDCl_3$) δ 151.9, 150.7, 149.1, 146.9, 146.5, 144.4, 144.2, 142.8, 135.5, 133.8, 133.7, 131.8, 131.6, 130.9, 130.4, 130.0, 128.7, 128.6, 126.6, 126.5, 125.7, 124.6, 124.6, 122.3, 122.3,

122.2, 120.0, 119.9, 119.8, 119.6, 117.9, 116.3, 115.1, 115.0, 113.8, 110.9, 29.3, 15.6, 15.5; IR (KBr) $\tilde{\nu}$ = 3442, 2966, 2924, 1619, 1594, 1539, 1450, 1430, 1341, 1294, 1086 cm^{-1}; HR-MS (ESI-TOF) m/z calcd for $C_{21}H_{16}N_3O_2$ $[M + H]^+$ 342.1237, found 342.1248.

Mixture of 2-Fluoro-11-methylbenzo[4,5]imidazo[1,2-f]phenanthridine and 2-Fluoro-12-methylbenzo[4,5]imidazo[1,2-f]phenanthridine (2e'). R_f = 0.50 (hexane/ethyl acetate 7:3); Inseparable white solid (2:1); yield 94% (56 mg); mp 165 °C; ^1H NMR (700 MHz, $CDCl_3$) δ 8.81 (t, *J* = 7.7 Hz, 1.5H), 8.45 – 8.36 (m, 1.5H), 8.27 (d, *J* = 7.7 Hz, 1.5H), 8.20 (d, *J* = 9.8 Hz, 0.5H), 8.16 (d, *J* = 9.8 Hz, 1H), 8.08 (d, *J* = 8.4 Hz, 1H), 8.01 (s, 0.5H), 7.91 (d, *J* = 7.7 Hz, 0.5H), 7.81 (s, 1H), 7.67 – 7.73 (m, 1.5H), 7.63 – 7.67 (m, 1.5H), 7.35 (d, *J* = 8.4 Hz, 0.5H), 7.29 (d, *J* = 8.4 Hz, 1H), 7.21 (t, *J* = 7.0 Hz, 1.5H), 2.66 (s, 1.5H), 2.58 (s, 3H); $^{13}C\{^1H\}$ NMR (175 MHz, $CDCl_3$) δ 163.0 (d, $^1J_{C,F}$ = 248.8 Hz), 162.9 (d, $^1J_{C,F}$ = 248.5 Hz), 147.7, 147.3, 144.9, 142.7, 135.5 (d, $^3J_{C,F}$ = 10.5 Hz), 135.4 (d, $^3J_{C,F}$ = 10.3 Hz), 134.6, 133.5, 132.0, 130.6, 130.6, 129.8, 129.1, 129.0, 128.6, 128.6, 126.2 (d, $^3J_{C,F}$ = 6.5 Hz), 126.1 (d, $^3J_{C,F}$ = 8.2 Hz), 124.9, 123.1, 123.0, 122.2, 120.4, 120.1, 118.3 (d, $^4J_{C,F}$ = 3.0 Hz), 118.2 (d, $^4J_{C,F}$ = 2.6 Hz), 113.7, 113.1, 112.0 (d, $^2J_{C,F}$ = 22.1 Hz), 103.4 (d, $^2J_{C,F}$ = 26.9 Hz), 103.3 (d, $^2J_{C,F}$ = 26.8 Hz), 22.5, 21.8; IR (KBr) $\tilde{\nu}$ = 3417, 2922, 2852, 1623, 1534, 1467, 1440, 1384, 1185 cm^{-1}; HR-MS (ESI-TOF) m/z calcd for $C_{20}H_{14}FN_2$ $[M + H]^+$ 301.1136, found 301.1148.

Mixture of **7-Fluoro-11-methylbenzo[4,5]imidazo[1,2-f]phenanthridine** and **7-Fluoro-12-methylbenzo[4,5]imidazo[1,2-f]phenanthridine (2f').** R_f = 0.60 (hexane/ethyl acetate 4:1); Inseparable white solid (10:1); yield 82% (49 mg); mp 170 °C; ^1H NMR (700 MHz, $CDCl_3$) δ 8.41 – 8.45 (m, 2.2H), 8.31 (d, *J* = 7.7 Hz, 1.1H), 8.28 (dd, *J* = 8.4, 5.6 Hz, 1.1H), 8.13 (d, *J* = 8.4 Hz, 1H), 8.06 (s, 1H), 7.88 (d, *J* = 8.4 Hz, 0.1H), 7.78 (s, 1H), 7.63 (t, *J* = 7.7 Hz,

1.1H), 7.44 (t, *J* = 7.7 Hz, 1.1H), 7.41 – 7.36 (m, 1H), 7.33 (d, *J* = 8.4 Hz, 0.1H), 7.27 (s, 1H), 2.64 (s, 0.3H), 2.57 (s, 3H); $^{13}C\{^{1}H\}$ NMR (175 MHz, $CDCl_3$) δ 162.7 (d, $J_{C,F}$ = 249.2 Hz), 146.6, 146.6, 144.8, 142.6, 134.3, 134.0, 133.4, 130.0, 129.1, 129.0, 126.0, 125.9, 125.9, 125.4 (d, $J_{C,F}$ = 9.2 Hz), 124.9, 124.9, 124.8, 124.6, 124.5, 124.1, 121.1, 120.4, 120.1, 118.6 (d, $J_{C,F}$ = 23.1 Hz), 116.1, 116.1, 114.1, 113.6, 111.5 (d, $J_{C,F}$ = 23.5 Hz), 111.5 (d, $J_{C,F}$ = 23.9 Hz), 22.5, 21.8; IR (KBr) $\tilde{\nu}$ = 3417, 2961, 2922, 2850, 2367, 2335, 1626, 1547, 1514, 1480, 1430, 1361, 1339, 1200, 1091 cm^{-1}; HR-MS (ESI-TOF) m/z calcd for $C_{20}H_{14}FN_2$ $[M + H]^+$ 301.1136, found 301.1123.

Mixture of **1-(11-Methylbenzo[4,5]imidazo[1,2-f]phenanthridin-2-yl)ethan-1-one** and **1-(12-Methylbenzo[4,5]imidazo[1,2-f]phenanthridin-2-yl)ethan-1-one (2g').** R_f = 0.50 (hexane/ethyl acetate 7:3); Inseparable pale yellow solid (2.5:1); yield 87% (52 mg); mp 198 °C; ^{1}H NMR (700 MHz, $CDCl_3$) δ 8.89 (s, 0.4H), 8.86 (s, 1H), 8.73 (dd, *J* = 6.3, 3.5 Hz, 1.4H), 8.35 – 8.24 (m, 1.4H), 8.18 (d, *J* = 3.5 Hz, 1.4H), 8.08 (d, *J* = 8.4 Hz, 1H), 7.99 (s, 0.4H), 7.86 (d, *J* = 8.4 Hz, 0.4H), 7.81 (t, *J* = 8.4 Hz, 1.4H), 7.75 (s, 1H), 7.65 (d, *J* = 3.5 Hz, 2.8H), 7.32 (d, *J* = 8.4 Hz, 0.4H), 7.27 (s, 1H), 2.69 (s, 4.2H), 2.64 (s, 1.2H), 2.57 (s, 3H); $^{13}C\{^{1}H\}$ NMR (175 MHz, $CDCl_3$) δ 196.8, 196.8, 147.1, 146.8, 144.7, 142.5, 136.7, 134.5, 134.3, 134.2, 133.7, 132.0, 130.5, 130.4, 129.8, 128.4, 128.3, 126.2, 126.1, 126.1, 125.5, 125.3, 125.2, 124.4, 124.3, 124.2, 124.0, 123.9, 123.0, 120.3, 120.0, 115.5, 115.4, 114.0, 113.5, 26.9, 22.6, 21.8; IR (KBr) $\tilde{\nu}$ = 3403, 2922, 2857, 1682, 1590, 1537, 1434, 1355, 1262 cm^{-1}; HR-MS (ESI-TOF) m/z calcd for $C_{22}H_{17}N_2O$ $[M + H]^+$ 325.1335, found 325.1348.

2.6. REFERENCES

1. Edwards, O. E.; Vocelle, D.; ApSimon, J. W.; Haque, F., *J. Am. Chem. Soc.* **1965,** *87* (3), 678-679.

2. (a) Dohi, T.; Kita, Y., Oxidative C-C Bond Formation (Couplings, Cyclizations, Cyclopropanation, etc.). In *PATAI'S Chemistry of Functional Groups*, Olofsson, B.; Marek, I.; Rappoport, Z., Eds. John Wiley & Sons, Ltd.: 2019; pp 1-84; (b) Elsherbini, M.; Wirth, T., *Chem. Eur. J.* **2018,** *24* (51), 13399-13407; (c) Muñiz, K., *Acc. Chem. Res.* **2018,** *51* (6), 1507-1519; (d) Murarka, S.; Antonchick, A. P., Oxidative Heterocycle Formation Using Hypervalent Iodine(III) Reagents. In *Hypervalent Iodine Chemistry*, Wirth, T., Ed. Springer International: Cham, Switzerland: 2016; pp 75-104; (e) Villo, P.; Olofsson, B., Arylations Promoted by Hypervalent Iodine Reagents. In *PATAI'S Chemistry of Functional Groups*, Olofsson, B.; Marek, I.; Rappoport, Z., Eds. John Wiley & Sons, Ltd.: 2019; pp 1-61; (f) Yoshimura, A.; Zhdankin, V. V., *Chem. Rev.* **2016,** *116* (5), 3328-3435; (g) Yuan, J.; Liu, C.; Lei, A., *Chem. Commun.* **2015,** *51* (8), 1394-1409.

3. (a) Borodkin, G. I.; Shubin, V. G., *Russ. Chem. Rev.* **2008,** *77* (5), 395-419; (b) Maiti, S.; Alam, M. T.; Bal, A.; Mal, P., *Adv. Synth. Catal.* **2019,** *361* (19), 4401-4425.

4. (a) Gassman, P. G., *Acc. Chem. Res.* **1970,** *3* (1), 26-33; (b) Gassman, P. G.; Campbell, G. A.; Frederick, R. C., *J. Am. Chem. Soc.* **1972,** *94* (11), 3884-3891.

5. (a) Bal, A.; Maiti, S.; Mal, P., *J. Org. Chem.* **2018,** *83* (18), 11278-11287; (b) Choudhury, J., *Angew. Chem. Int. Ed.* **2011,** *50* (46), 10772-10774; (c) Maiti, S.; Bose, A.; Mal, P., *J. Org. Chem.* **2018,** *83* (15), 8127-8138; (d) Maiti, S.; Mal, P., *Org. Lett.* **2017,** *19* (9), 2454-2457; (e) Tellitu, I.; Domínguez, E., *Synlett* **2012,** *23* (15), 2165-2175; (f) Wardrop, D. J.; Bowen, E. G., *Org. Lett.* **2011,** *13* (9), 2376-2379.

6. (a) Antonchick, A. P.; Samanta, R.; Kulikov, K.; Lategahn, J., *Angew. Chem. Int. Ed.* **2011,** *50* (37), 8605-8608; (b) Kikugawa, Y.; Nagashima, A.; Sakamoto, T.; Miyazawa, E.; Shiiya, M., *J. Org. Chem.* **2003,** *68* (17), 6739-6744.

7. Falvey, D. E., Electronic Properties of Nitrenium Ions. In *Nitrenes and Nitrenium Ions*, Falvey, D. E.; Gudmundsdottir, A. D., Eds. John Wiley & Sons: Hoboken, 2013; pp 191-216.

8. (a) Chiapperino, D.; McIlroy, S.; Falvey, D. E., *J. Am. Chem. Soc.* **2002,** *124* (14), 3567-3577; (b) Thomas, S. I.; Falvey, D. E., *J. Org. Chem.* **2007,** *72* (13), 4626-4634.

9. Spitler, E. L.; Johnson, C. A.; Haley, M. M., *Chem. Rev.* **2006,** *106* (12), 5344-5386.

10. (a) Fu, X.; Meng, Y.; Li, X.; Stępień, M.; Chmielewski, P. J., *Chem. Commun.* **2018,** *54* (20), 2510-2513; (b) Reddy, B. K.; Basavarajappa, A.; Ambhore, M. D.; Anand, V. G., *Chem. Rev.* **2017,** *117* (4), 3420-3443.

11. Peeks, M. D.; Claridge, T. D. W.; Anderson, H. L., *Nature* **2017,** *541* (7636), 200-203.

12. Qiu, L.; Zhuang, X.; Zhao, N.; Wang, X.; An, Z.; Lan, Z.; Wan, X., *Chem. Commun.* **2014,** *50* (25), 3324-3327.

13. Winter, A. H.; Gibson, H. H.; Falvey, D. E., *J. Org. Chem.* **2007,** *72* (22), 8186-8195.

14. Liu, J.; Zhang, N.; Yue, Y.; Liu, G.; Liu, R.; Zhang, Y.; Zhuo, K., *Eur. J. Org. Chem.* **2013,** (34), 7683-7687.

15. Yan, L.; Zhao, D.; Lan, J.; Cheng, Y.; Guo, Q.; Li, X.; Wu, N.; You, J., *Org. Biomol. Chem.* **2013,** *11* (45), 7966-7977.

16. (a) Almerico, A. M.; Mingoia, F.; Diana, P.; Barraja, P.; Montalbano, A.; Lauria, A.; Loddo, R.; Sanna, L.; Delpiano, D.; Setzu, M. G.; Musiu, C., *Eur. J. Med. Chem.* **2002,** *37* (1), 3-10; (b) Xie, C.; Zhang, Y.; Huang, Z.; Xu, P., *J. Org. Chem.* **2007,** *72* (14), 5431-5434.

17. Castor, K. J.; Liu, Z.; Fakhoury, J.; Hancock, M. A.; Mittermaier, A.; Moitessier, N.; Sleiman, H. F., *Chem. Eur. J.* **2013,** *19* (52), 17836-17845.

18. (a) Chen, C.; Shang, G.; Zhou, J.; Yu, Y.; Li, B.; Peng, J., *Org. Lett.* **2014,** *16* (7), 1872-1875; (b) Zhao, G.; Chen, C.; Yue, Y.; Yu, Y.; Peng, J., *J. Org. Chem.* **2015,** *80* (5), 2827-2834.

19. Sun, C.-L.; Shi, Z.-J., *Chem. Rev.* **2014,** *114* (18), 9219-9280.

20. Reddy Kandimalla, S.; Prathima Parvathaneni, S.; Sabitha, G.; Subba Reddy, B. V., *Eur. J. Org. Chem.* **2019,** (8), 1687-1714.

21. Zheng, Z.; Ma, S.; Tang, L.; Zhang-Negrerie, D.; Du, Y.; Zhao, K., *J. Org. Chem.* **2014,** *79* (10), 4687-4693.

22. (a) Hubig, S. M.; Kochi, J. K., *J. Am. Chem. Soc.* **2000,** *122* (34), 8279-8288; (b) Liang, D.; He, Y.; Liu, L.; Zhu, Q., *Org. Lett.* **2013,** *15* (13), 3476-3479.

23. Dohi, T.; Kita, Y., *Chem. Commun.* **2009,** (16), 2073-2085.

24. (a) Colomer, I.; Batchelor-McAuley, C.; Odell, B.; Donohoe, T. J.; Compton, R. G., *J. Am. Chem. Soc.* **2016,** *138* (28), 8855-8861; (b) Colomer, I.; Chamberlain, A. E. R.; Haughey, M. B.; Donohoe, T. J., *Nat. Rev. Chem.* **2017,** *1*, 0088.

25. Gu, R.; Hameurlaine, A.; Dehaen, W., *J. Org. Chem.* **2007,** *72* (19), 7207-7213.

26. SAINT+, Bruker AXS Inc., Madison, Wisconsin, USA, 1999 (Program for Reduction of Data collected on Bruker CCD Area Detector Diffractometer V. 6.02.)

27. SADABS, Bruker AXS, Madison, Wisconsin, USA, 2004

28. Sheldrick, G., *Acta Crystallogr. Sect. A* **2008,** *64* (1), 112-122.

29. Charton, J.; Girault-Mizzi, S.; Sergheraert, C., *Chem. Pharm. Bull.* **2005,** *53* (5), 492-497.

NMR Spectra

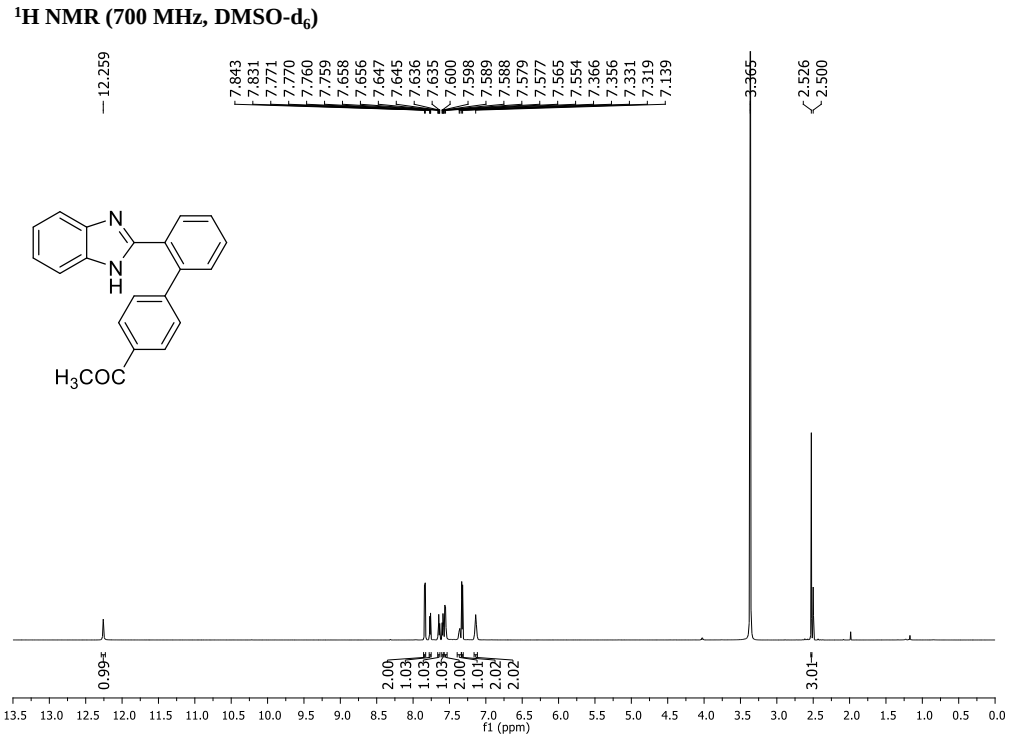

Figure 2.8. ^{1}H NMR spectrum of 1-(2'-(1H-Benzo[d]imidazol-2-yl)-[1,1'-biphenyl]-4-yl)ethan-1-one **(1d).**

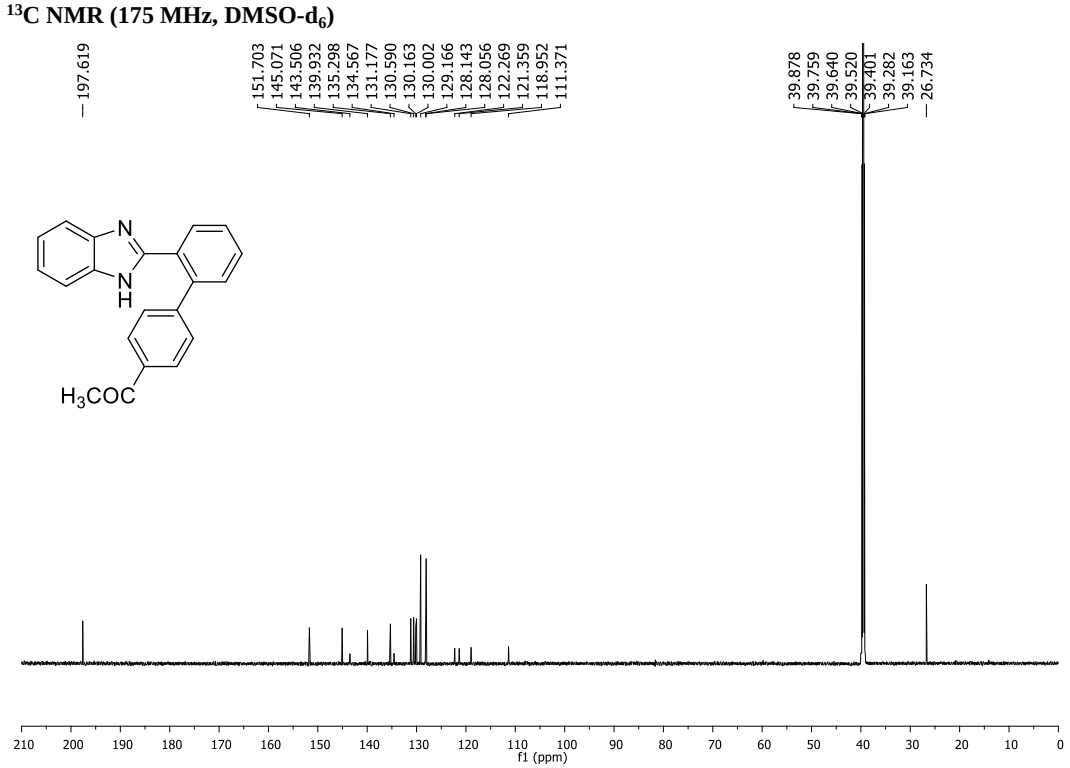

Figure 2.9. ^{13}C NMR spectrum of 1-(2'-(1H-Benzo[d]imidazol-2-yl)-[1,1'-biphenyl]-4-yl)ethan-1-one **(1d).**

^{1}H NMR (700 MHz, DMSO-d_6)

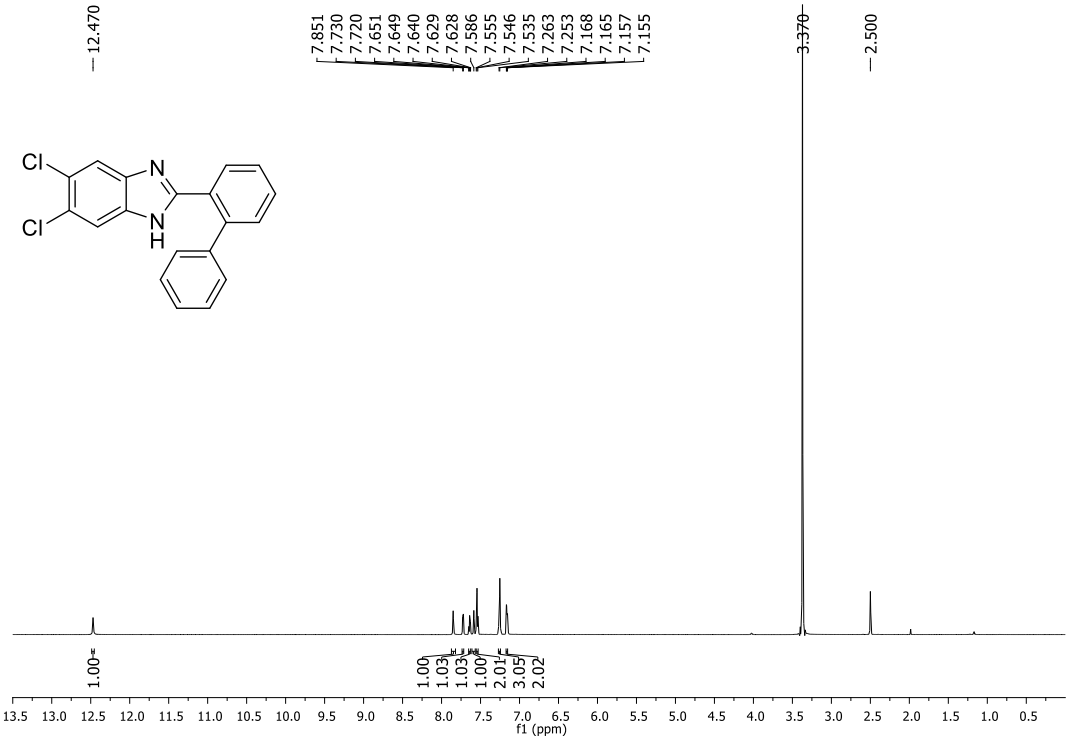

Figure 2.10. ^{1}H NMR spectrum of 2-([1,1'-Biphenyl]-2-yl)-5,6-dichloro-1H-benzo[d]imidazole **(1e)**

^{13}C NMR (175 MHz, DMSO-d_6)

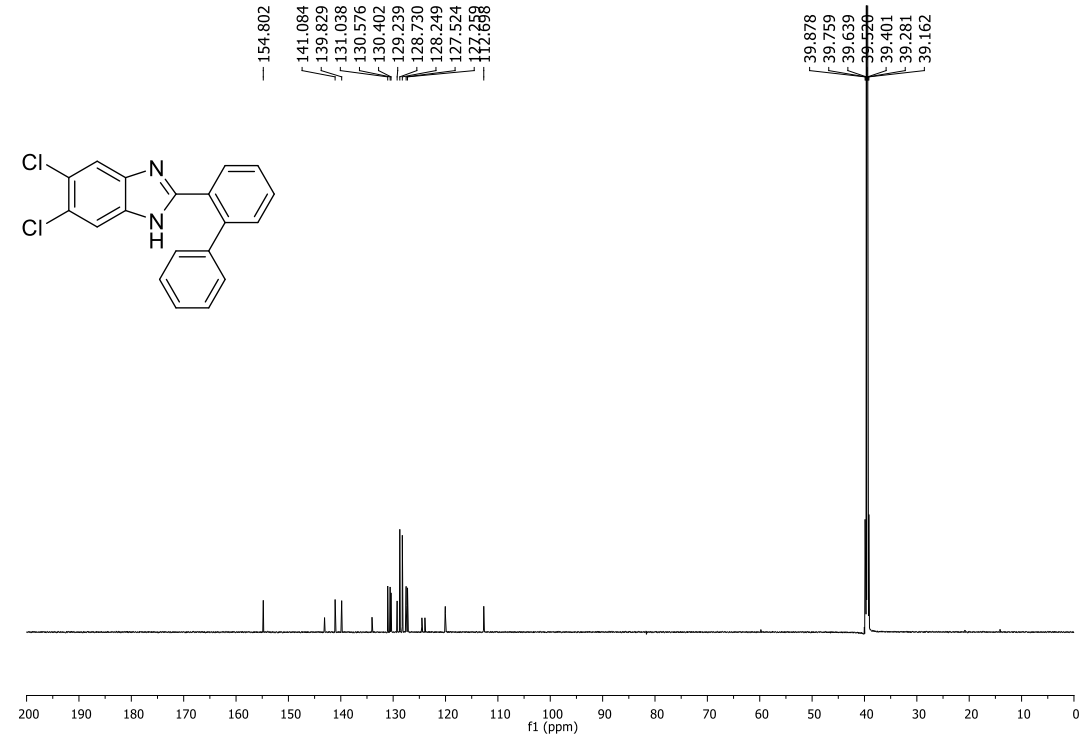

Figure 2.11. ^{13}C NMR spectrum of 2-([1,1'-Biphenyl]-2-yl)-5,6-dichloro-1H-benzo[d]imidazole **(1e).**

^{1}H NMR (700 MHz, DMSO-d_6)

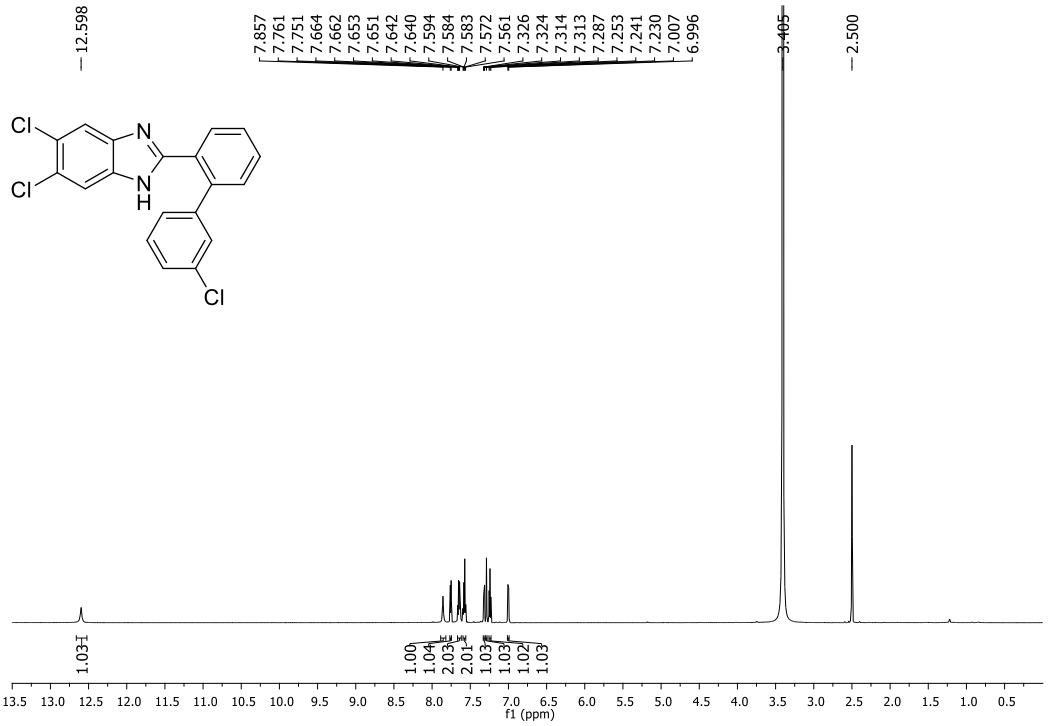

Figure 2.12. ^{1}H NMR spectrum of 5,6-Dichloro-2-(3'-chloro-[1,1'-biphenyl]-2-yl)-1H-benzo[d]imidazole **(1h).**

^{13}C NMR (175 MHz, DMSO-d_6)

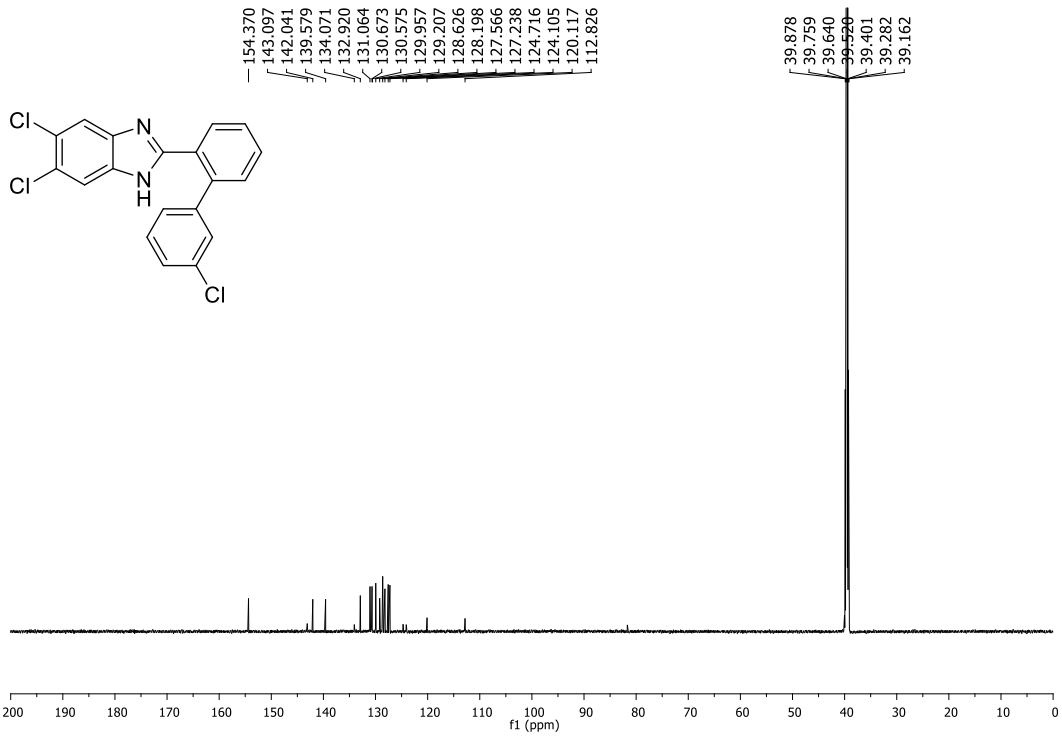

Figure 2.13. ^{13}C NMR spectrum of 5,6-Dichloro-2-(3'-chloro-[1,1'-biphenyl]-2-yl)-1H-benzo[d]imidazole **(1h).**

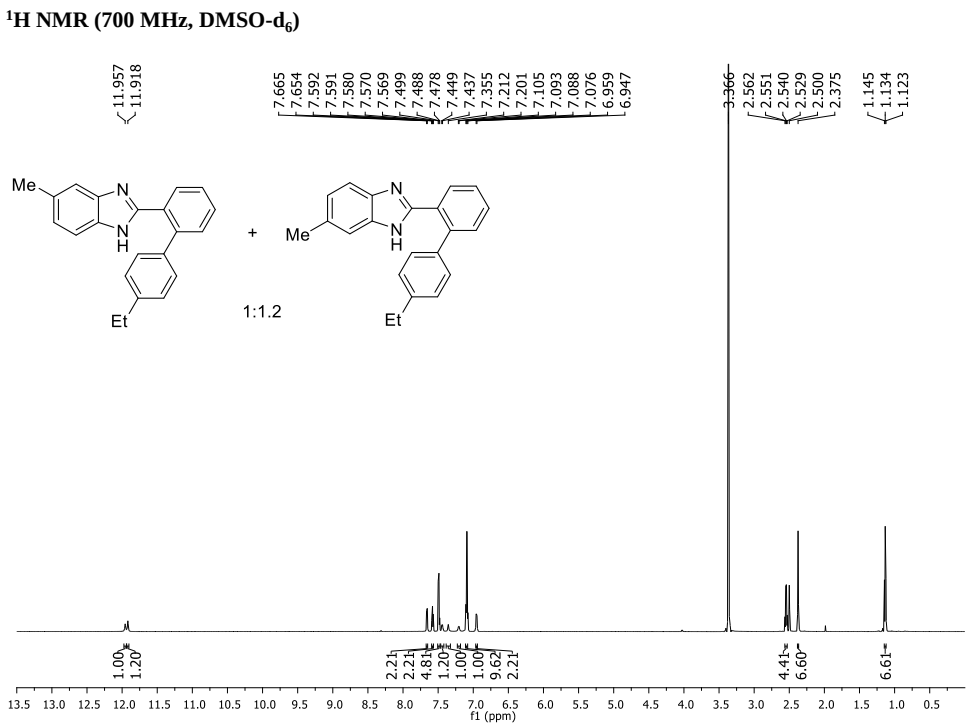

Figure 2.14. ^{1}H NMR spectrum of 2-(4'-Ethyl-[1,1'-biphenyl]-2-yl)-5-methyl-1H-benzo[d]imidazole and 2-(4'-Ethyl-[1,1'-biphenyl]-2-yl)-6-methyl-1H-benzo[d]imidazole **(1c').**

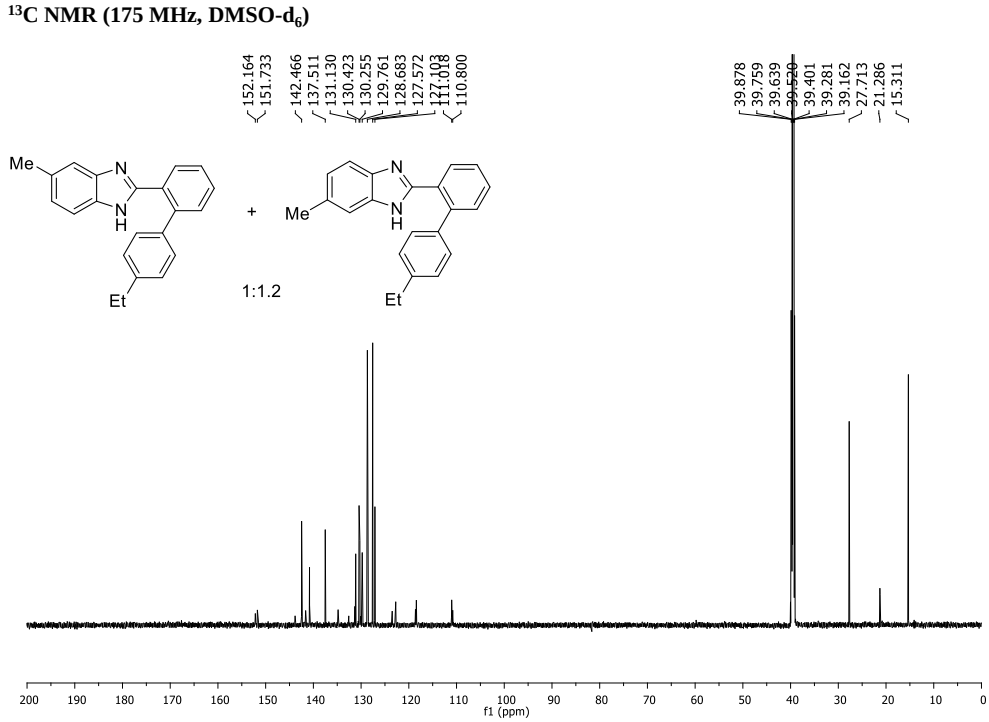

Figure 2.15. ^{13}C NMR spectrum of 2-(4'-Ethyl-[1,1'-biphenyl]-2-yl)-5-methyl-1H-benzo[d]imidazole and 2-(4'-Ethyl-[1,1'-biphenyl]-2-yl)-6-methyl-1H-benzo[d]imidazole **(1c').**

^{1}H NMR (700 MHz, $CDCl_3$)

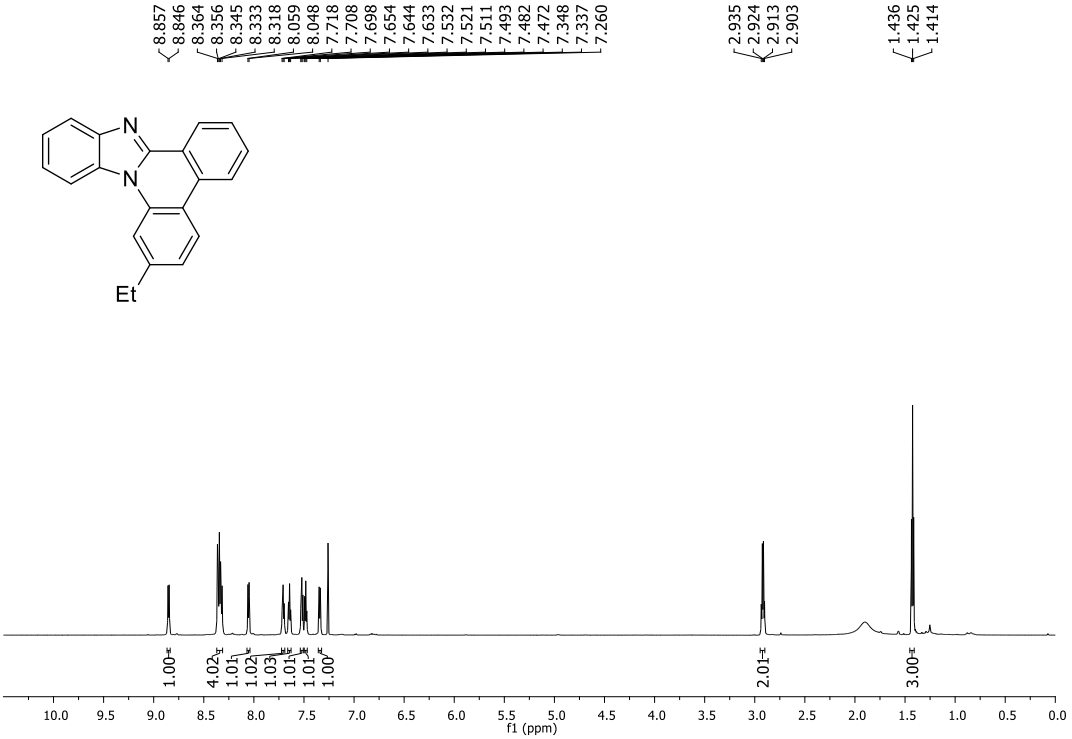

Figure 2.16. ^{1}H NMR spectrum of 2-Ethylbenzo[4,5]imidazo[1,2-f]phenanthridine **(2b).**

^{13}C NMR (175 MHz, $CDCl_3$)

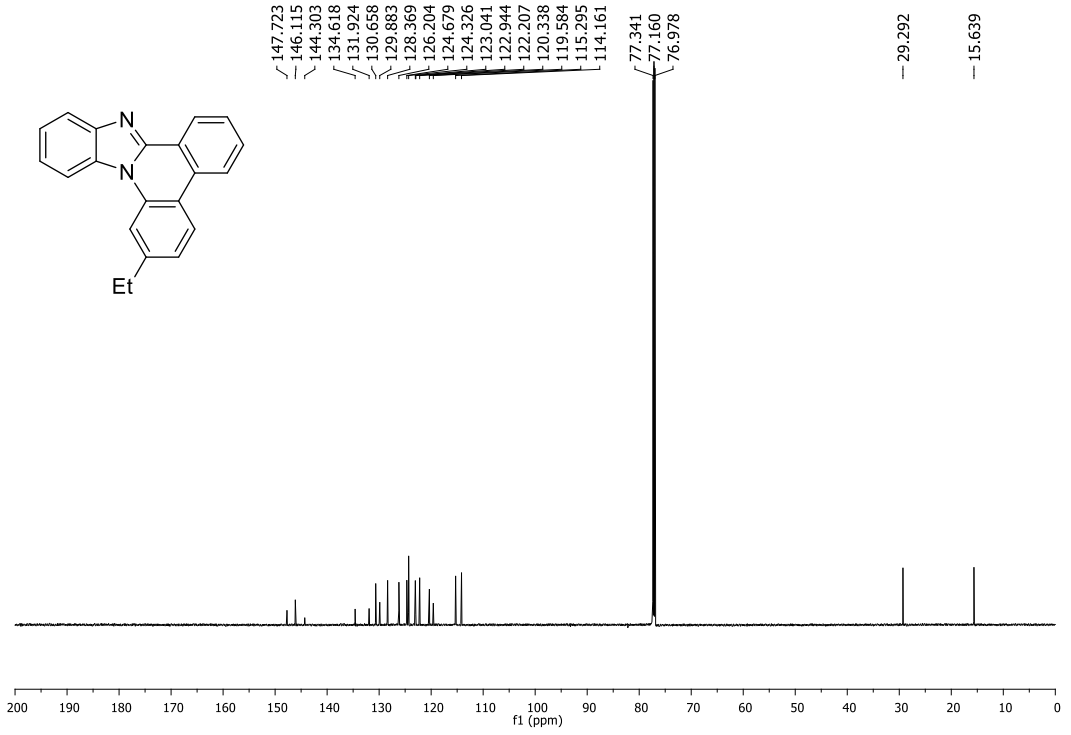

Figure 2.17. ^{13}C NMR spectrum of 2-Ethylbenzo[4,5]imidazo[1,2-f]phenanthridine **(2b).**

^{1}H NMR (700 MHz, $CDCl_3$)

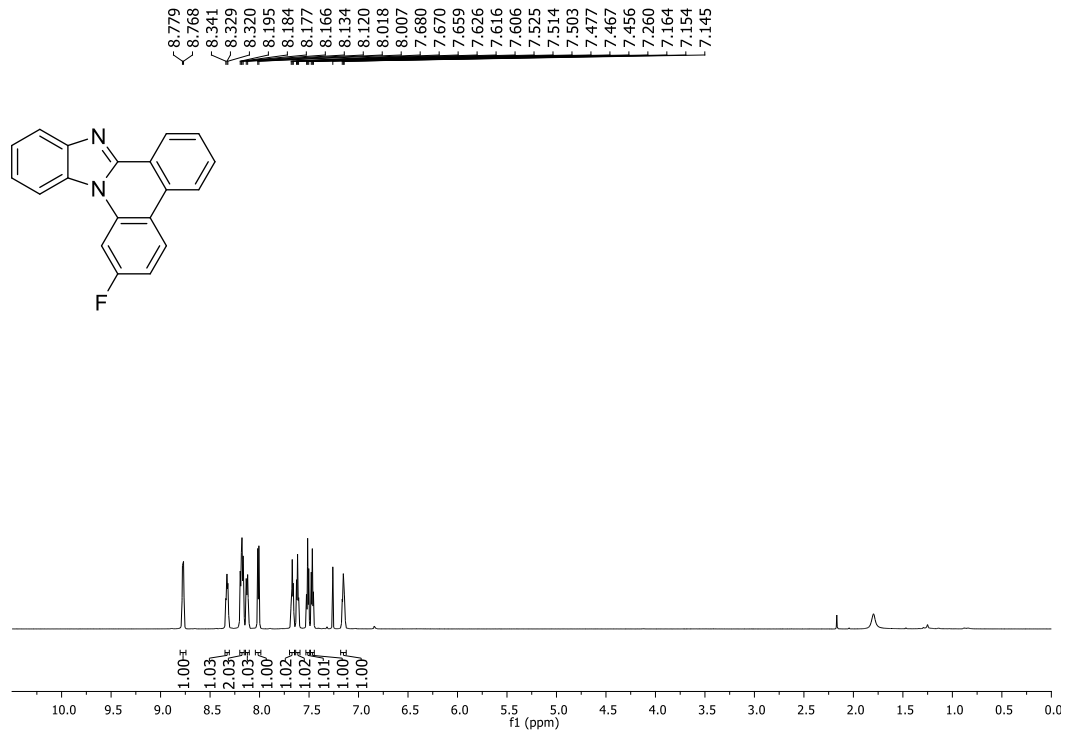

Figure 2.18. ^{1}H NMR spectrum of 2-Fluorobenzo[4,5]imidazo[1,2-f]phenanthridine **(2c).**

^{13}C NMR (175 MHz, $CDCl_3$)

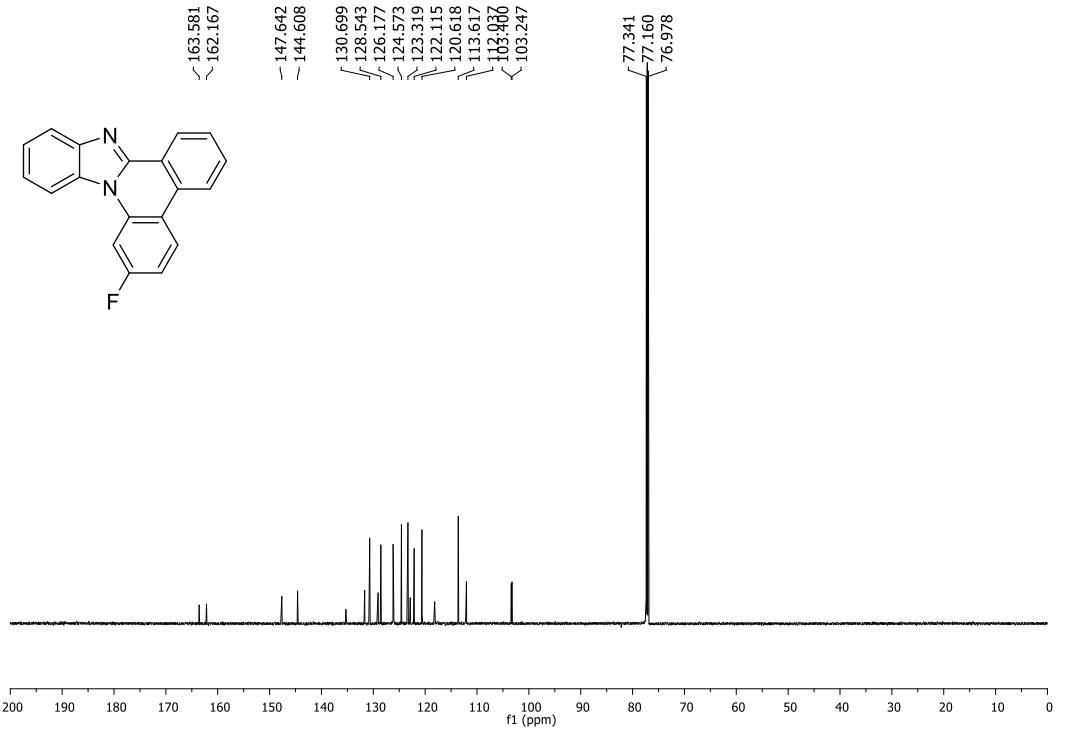

Figure 2.19. ^{13}C NMR spectrum of 2-Fluorobenzo[4,5]imidazo[1,2-f]phenanthridine **(2c).**

^{1}H NMR (700 MHz, $CDCl_3$)

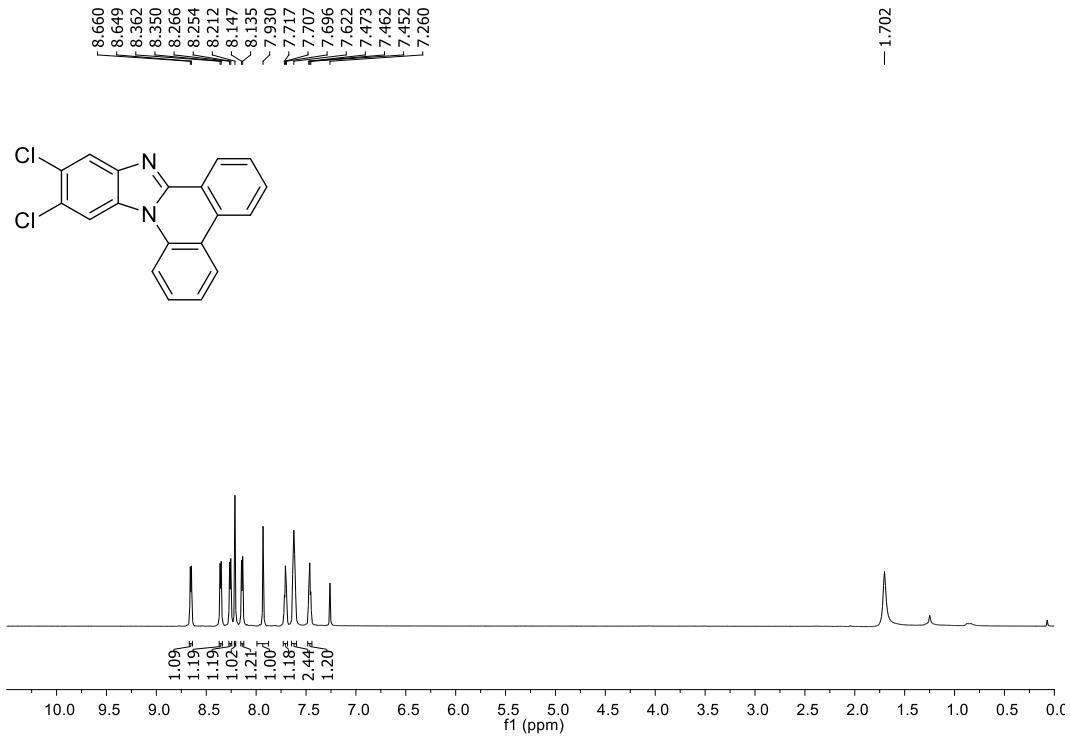

Figure 2.20. ^{1}H NMR spectrum of 11,12-Dichlorobenzo[4,5]imidazo[1,2-f]phenanthridine **(2e).**

^{13}C NMR (175 MHz, $CDCl_3$)

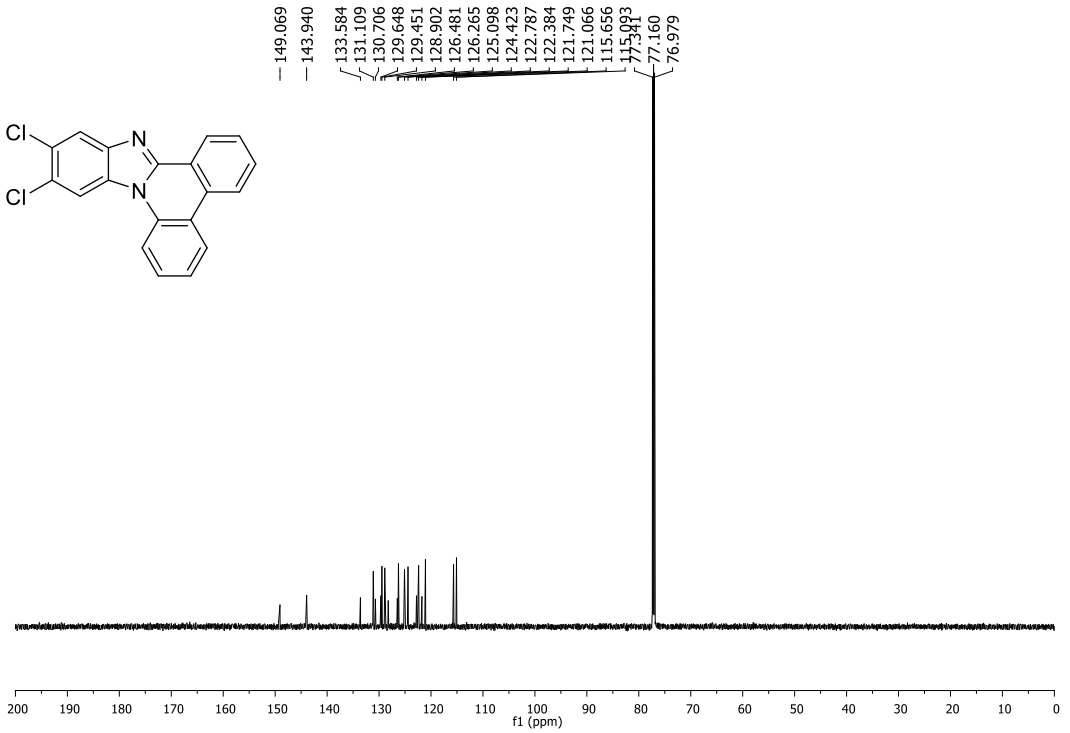

Figure 2.21. ^{13}C NMR spectrum of 11,12-Dichlorobenzo[4,5]imidazo[1,2-f]phenanthridine **(2e)**

^{1}H NMR (400 MHz, $CDCl_3$ + TFA-D)

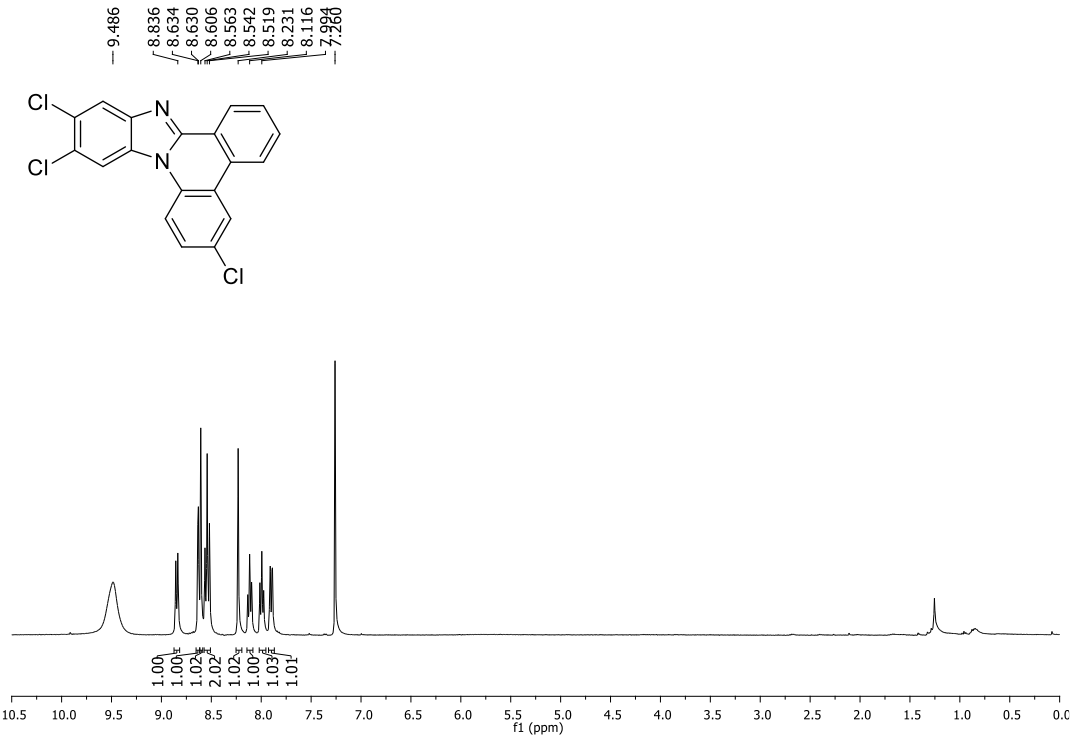

Figure 2.22. ^{1}H NMR spectrum of 3,11,12-Trichlorobenzo[4,5]imidazo[1,2-f]phenanthridine **(2h).**

^{13}C NMR (175 MHz, $CDCl_3$ + TFA-D)

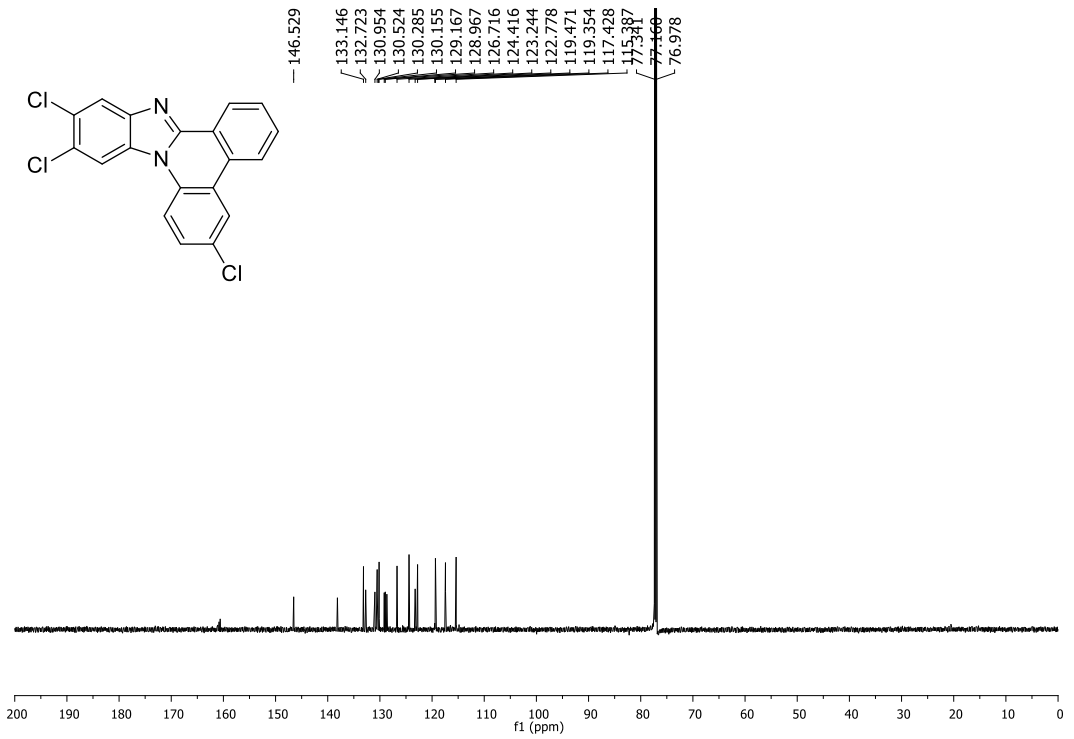

Figure 2.23. ^{13}C NMR spectrum of 3,11,12-Trichlorobenzo[4,5]imidazo[1,2-f]phenanthridine **(2h).**

^{1}H NMR (700 MHz, $CDCl_3$)

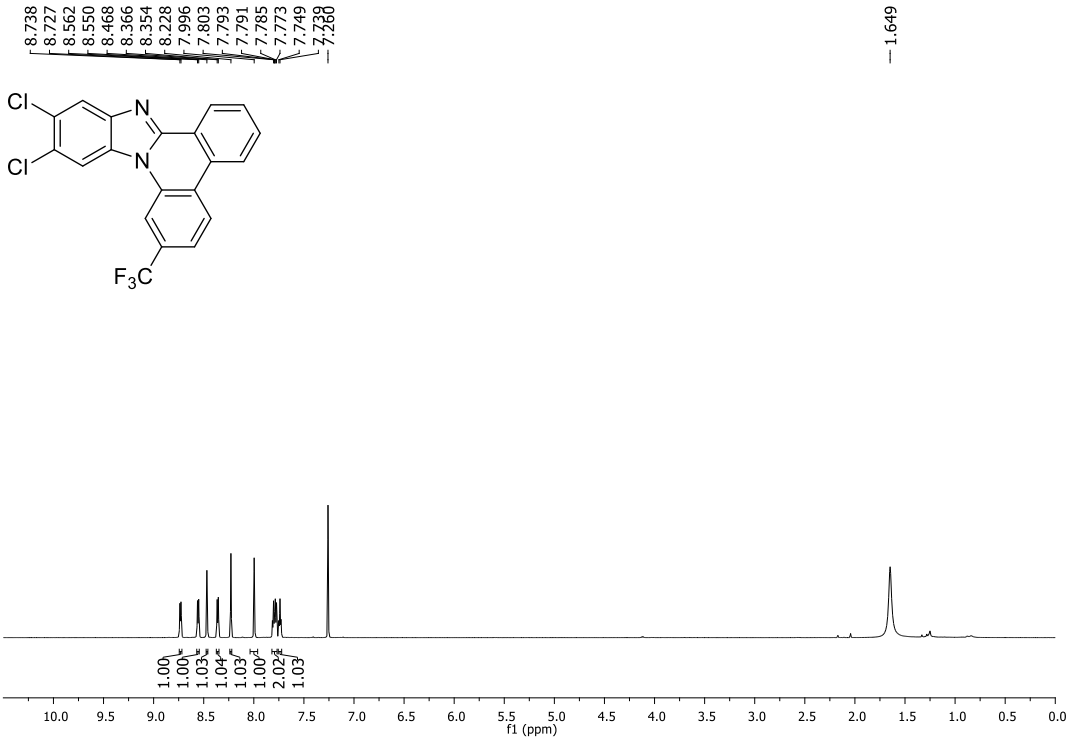

Figure 2.24. ^{1}H NMR spectrum of 11,12-Dichloro-2-(trifluoromethyl)benzo[4,5]imidazo[1,2-f]phenanthridine **(2k).**

^{13}C NMR (175 MHz, $CDCl_3$)

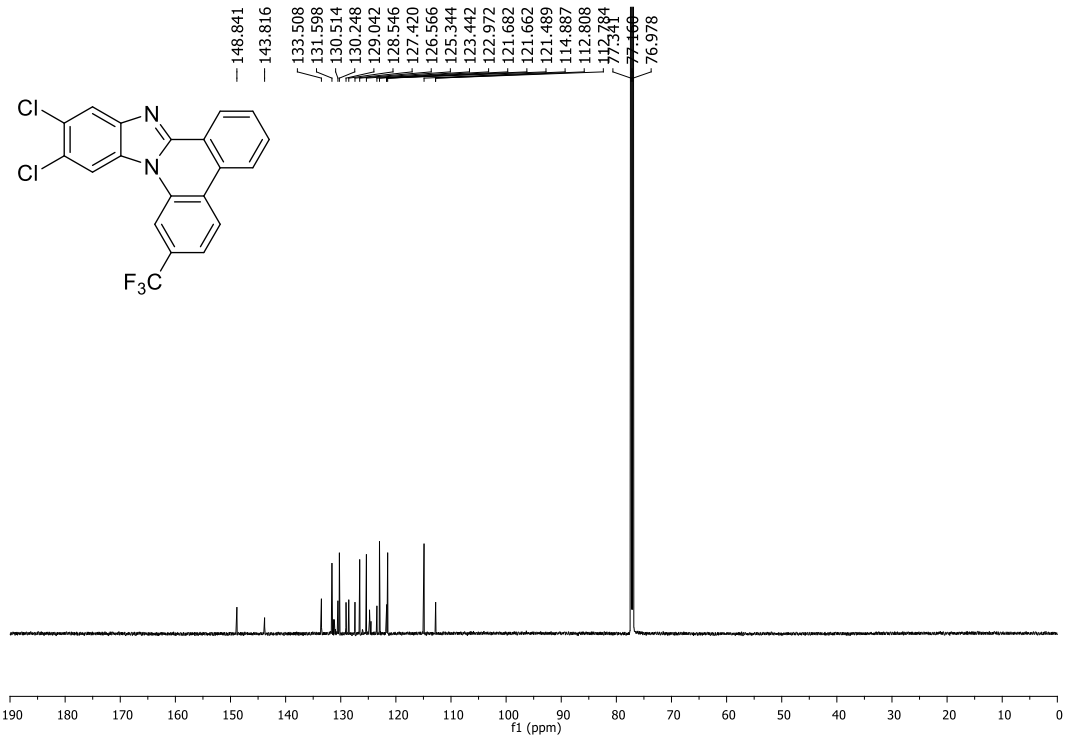

Figure 2.25. ^{13}C NMR spectrum of 11,12-Dichloro-2-(trifluoromethyl)benzo[4,5]imidazo[1,2-f]phenanthridine **(2k).**

^{1}H NMR (700 MHz, $CDCl_3$)

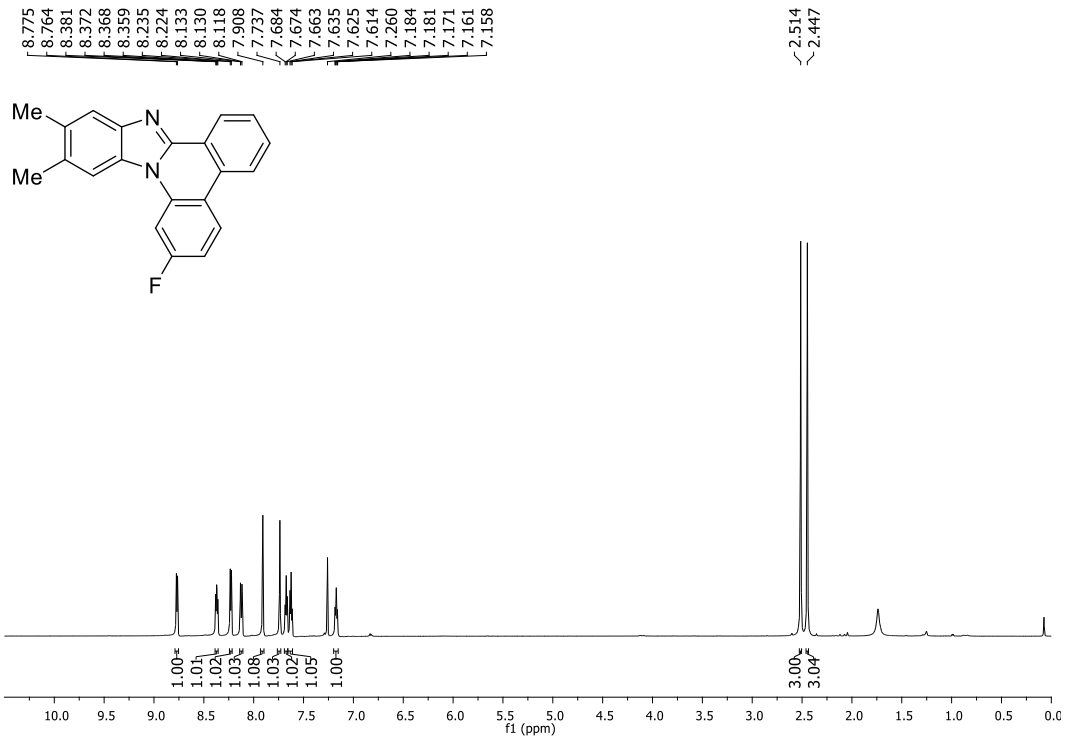

Figure 2.26. ^{1}H NMR spectrum of 2-Fluoro-11,12-dimethylbenzo[4,5]imidazo[1,2-f]phenanthridine **(2o).**

^{13}C NMR (175 MHz, $CDCl_3$)

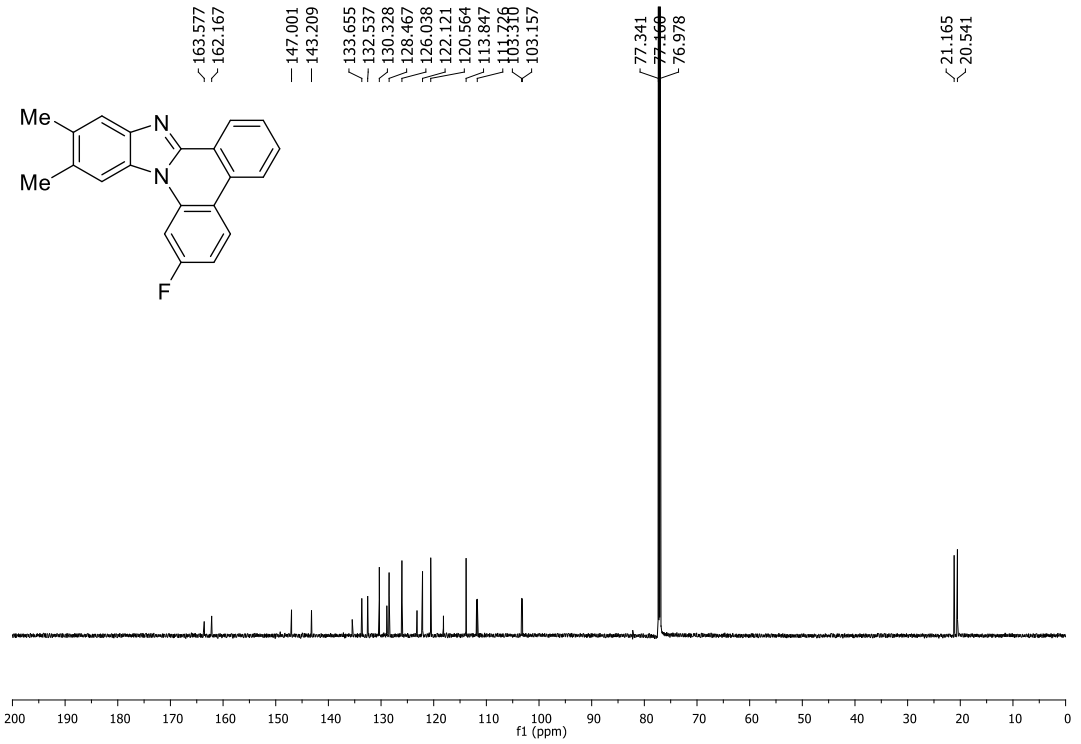

Figure 2.27. ^{13}C NMR spectrum of 2-Fluoro-11,12-dimethylbenzo[4,5]imidazo[1,2-f]phenanthridine **(2o).**

^{1}H NMR (700 MHz, $CDCl_3$)

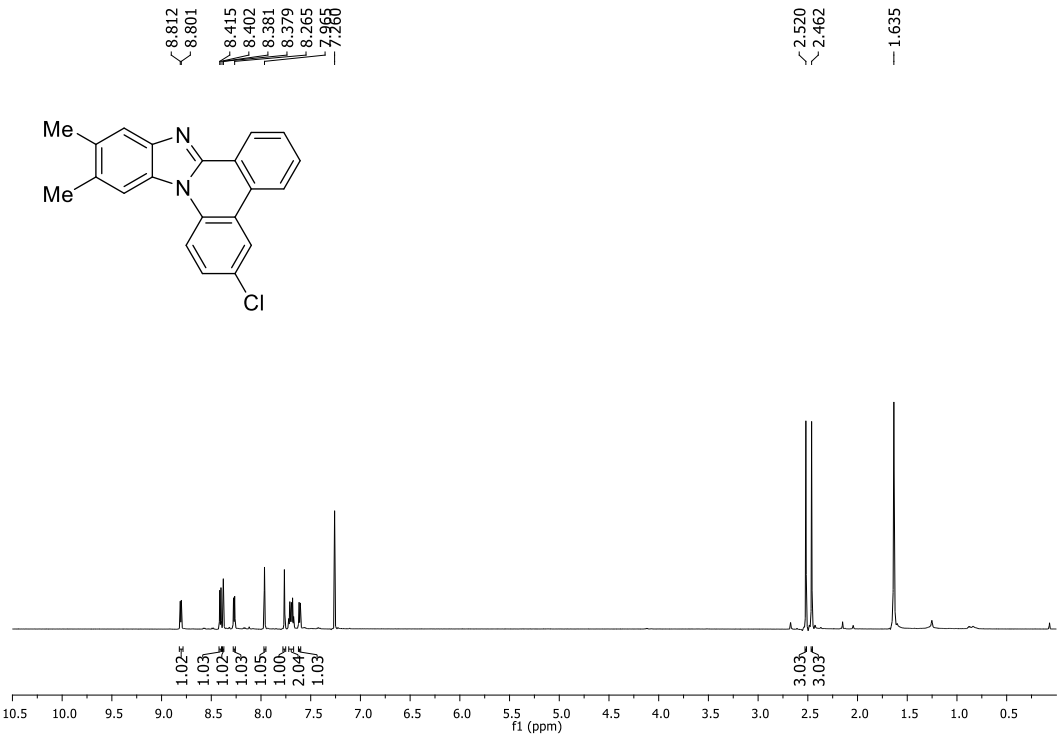

Figure 2.28. ^{1}H NMR spectrum of 3-Chloro-11,12-dimethylbenzo[4,5]imidazo[1,2-f]phenanthridine **(2p).**

^{13}C NMR (175 MHz, $CDCl_3$

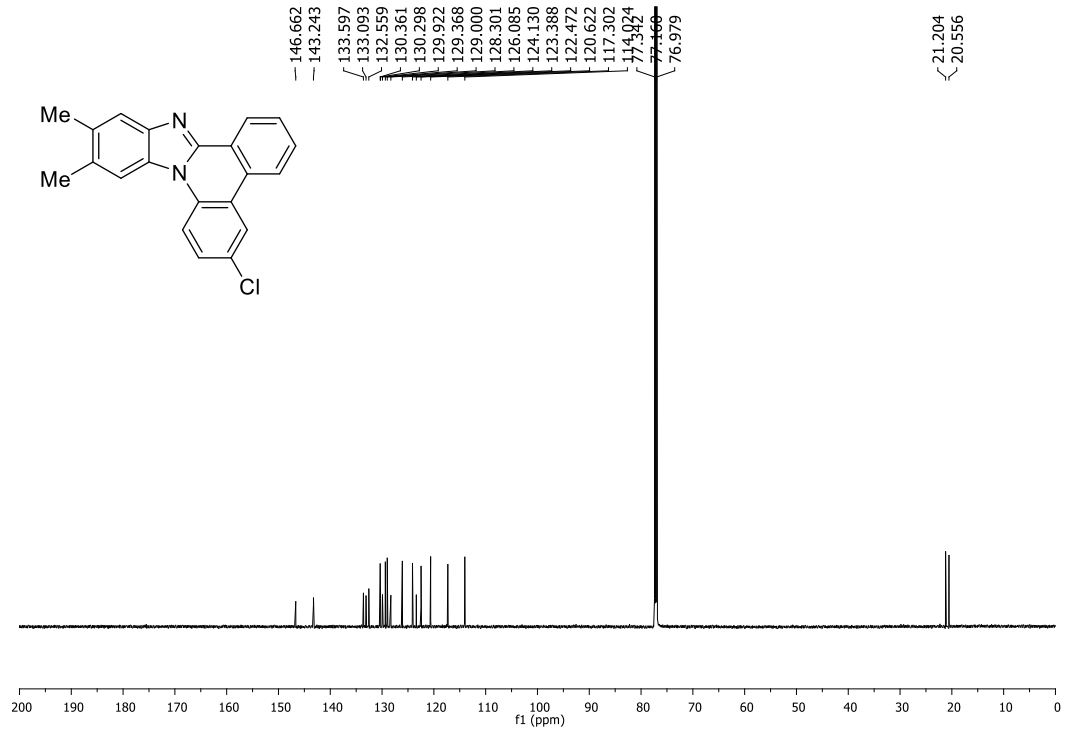

Figure 2.29. ^{13}C NMR spectrum of 3-Chloro-11,12-dimethylbenzo[4,5]imidazo[1,2-f]phenanthridine **(2p).**

^{1}H NMR (700 MHz, $CDCl_3$)

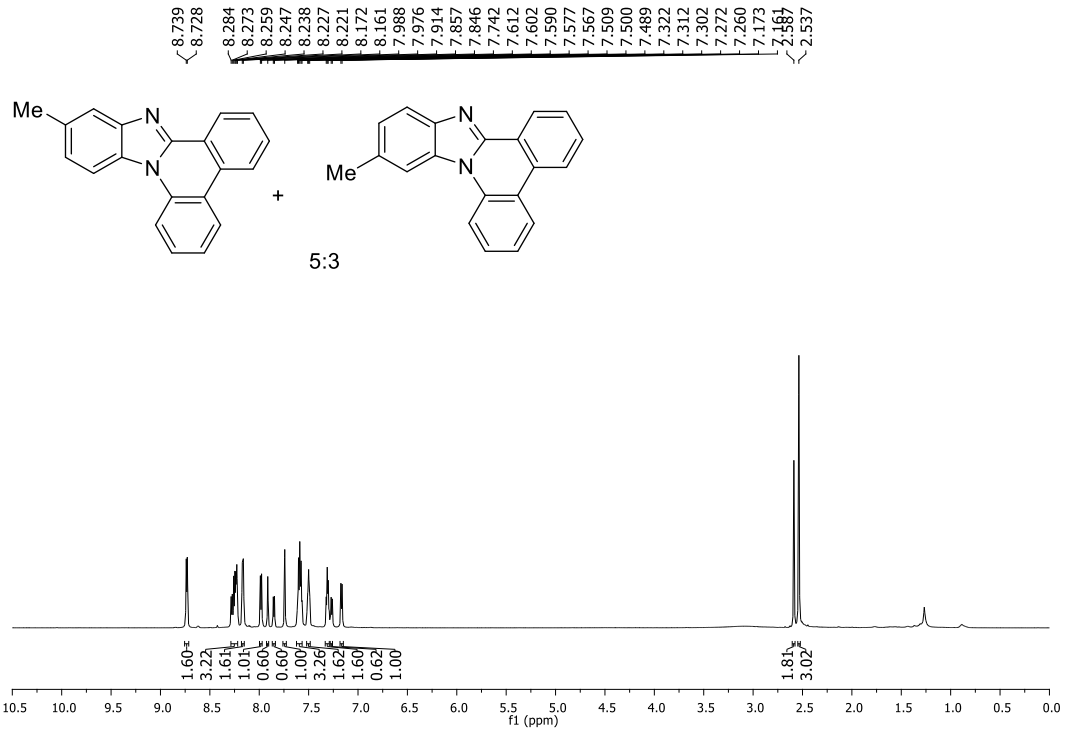

Figure 2.30. ^{1}H NMR spectrum of 11-methylbenzo[4,5]imidazo[1,2-f]phenanthridine and 12-methylbenzo[4,5]imidazo[1,2-f]phenanthridine **(2a').**

^{13}C NMR (175 MHz, $CDCl_3$)

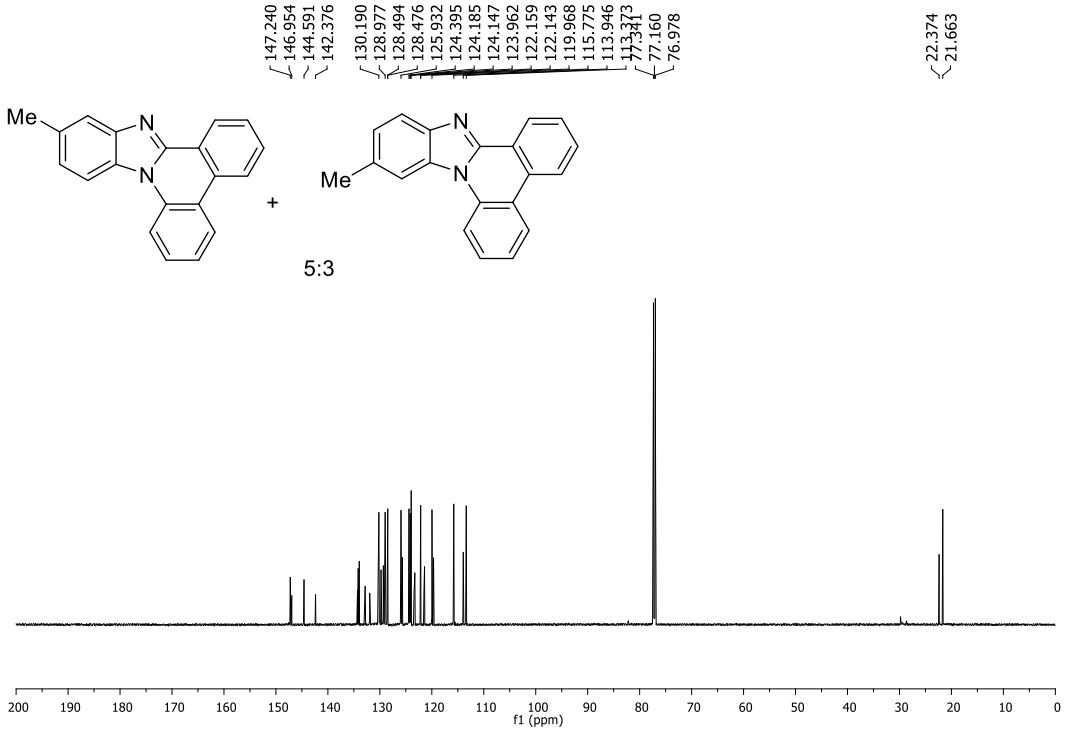

Figure 2.31. ^{13}C NMR spectrum of 11-methylbenzo[4,5]imidazo[1,2-f]phenanthridine and 12-methylbenzo[4,5]imidazo[1,2-f]phenanthridine **(2a').**

^{1}H NMR (400 MHz, $CDCl_3$)

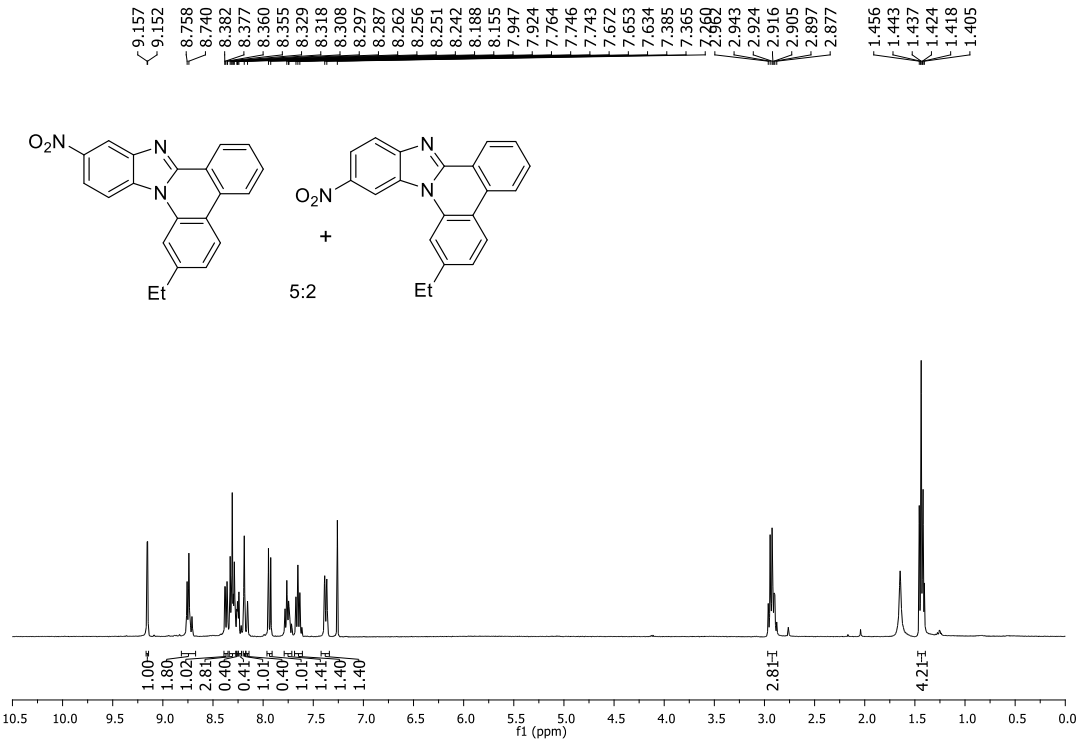

Figure 2.32. ^{1}H NMR spectrum of 2-Ethyl-11-nitrobenzo[4,5]imidazo[1,2-f]phenanthridine and 2-Ethyl-12-nitrobenzo[4,5]imidazo[1,2-f]phenanthridine **(2d').**

^{13}C NMR (175 MHz, $CDCl_3$)

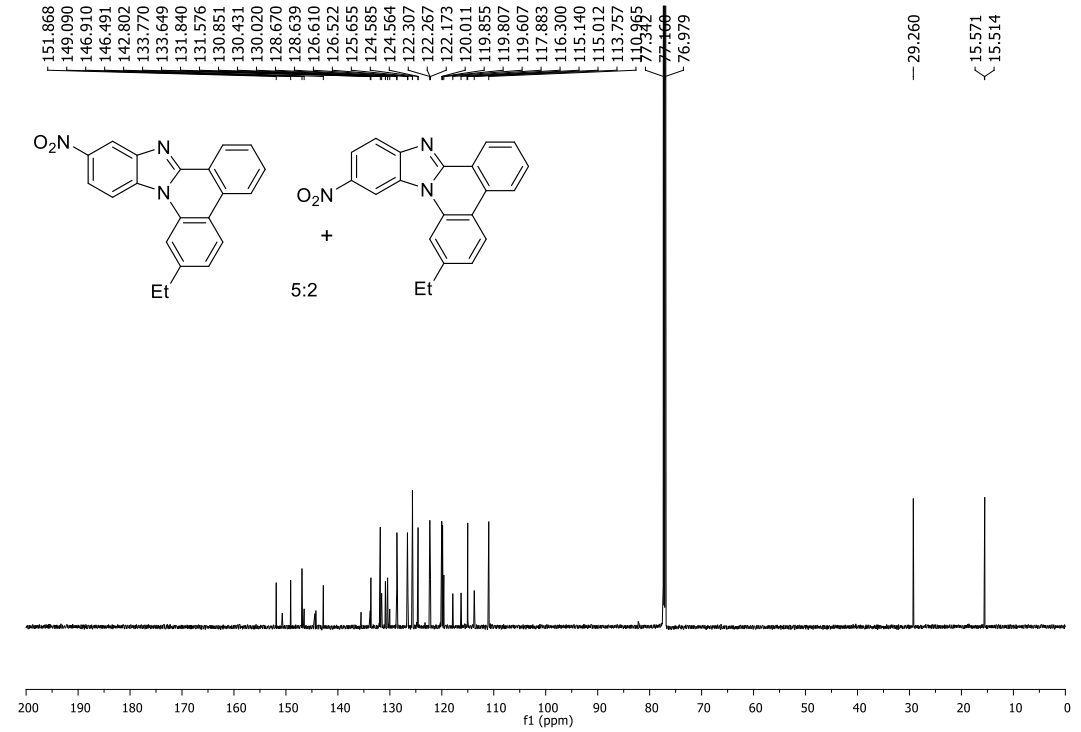

Figure 2.33. ^{13}C NMR spectrum of 2-Ethyl-11-nitrobenzo[4,5]imidazo[1,2-f]phenanthridine and 2-Ethyl-12-nitrobenzo[4,5]imidazo[1,2-f]phenanthridine **(2d').**

CHAPTER 3

Photochemical Intramolecular C-N Coupling toward the Synthesis of Benzimidazole-Fused Phenanthridines

3.1 ABSTRACT

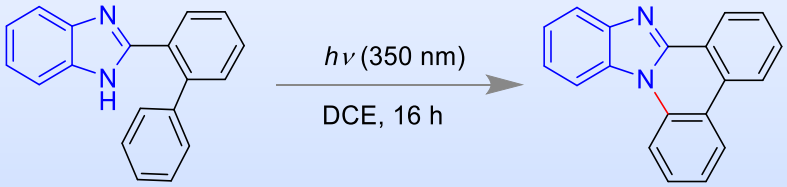

Herein we report a direct photochemical dehydrogenative C-N coupling of unactivated C(sp^2)- H and N(sp^2)-H bonds. The catalysts or additive-free transformation of 2-([1,1′-biphenyl]-2- yl)-1H-benzo[d]imidazole to benzo[4,5]imidazo[1,2-f]phenanthridine was achieved at ~350 nm of irradiation *via* ε-hydrogen abstraction. DFT calculations helped to understand that N- H…π interaction was essential for the reaction to proceed at lower energy than expected.

3.2 INTRODUCTION

The atom- and step-economical synthesis of bioactive molecules, pharmaceuticals, or materials using readily available chemicals is the state of art practice in synthetic organic chemistry.[1] Transition metal-catalyzed reactions in various cross-coupling reactions methodologies have become powerful tools to convert many unreactive C-H and N-H bonds into the corresponding C-C and C-N bonds.[2] For the functionalization of nonreactive C-H bonds using chemical feedstock are the standard practices, however, metal-free approaches are preferable.[3] The dehydrogenative or oxidative cross-coupling reactions between C-H and N-H bonds are challenging but more popular than traditional methodologies because pre-functionalization of the substrates can easily be avoided.[4] Among the metal-free methods, electrochemical[5] and photochemical[6] transformations can be the most convenient because the

reactions can be performed without any added reagents or catalysts, atom-economical and environmentally friendly. The influence of light to affect chemicals has been documented for many years, but still, sufficient understanding has not been attained to place photochemical reactions in the realm of organic synthesis.[7] The photochemical transformations have significantly impacted synthetic chemistry in recent times by the utilization of visible-light photocatalysts.[8] However, traditional photochemical reactions utilize the direct use of light energy with the help of specific chromophores. The photochemical synthesis can be considered as green-synthesis because the reactions can be carried out without the use of any added reagents except light. The photoreactions are carried out either in the presence of sensitizers or the substrates should contain chromophores within the substrate. The photochemical C-C[9] or C-hetero bond formation reactions like borylation of haloarenes,[10] C-P,[11] C-O,[12] C-S,[13] etc. are developed based on the dissociation of carbon-halogen bonds. In photochemistry, few reports have recently appeared in literature based on catalyst-free decarbonylation of *o*-amino benzaldehyde,[14] visible light induced intermolecular amination of phenol,[15] dehydrogenative annulation for the synthesis of polycyclic aromatic heterocycles *via* oxidative electrocyclization,[16] dehydrogenative strategy for the synthesis of aniline with a photoredox- and cobalt-based catalytic system, etc.[17] Also, cross dehydrohalogenative C-N coupling reactions towards intramolecular photocyclization of phenanthro[9,10-d]imidazoles[18] and 8-aryloxy benzo[e][1,2,4]triazines[19] for the construction of *N*-heterocycles was documented. Similarly, intramolecular C-H amination reactions are known for the synthesis of heterocycles *via* electrochemical method.[20] Instead, in traditional photochemistry, no direct dehydrogenative coupling is known.

3.3. RESULTS AND DISCUSSION

In this work, we report a discovery of a direct photochemical dehydrogenative C-N coupling of unactivated C(sp^2)-H and N(sp^2)-H bonds *via* radical-radical coupling at λ_{irr} ~350 nm. The transformation of 2-([1,1′-Biphenyl]-2-yl)-1H-benzo[d]imidazole **1aa** to benzo[4,5]imidazo[1,2-f]phenanthridine **2aa** under direct irradiation ~350 nm is shown in Figure 3.1a. The N-H…π interaction helped the benzimidazole ring of **1aa** for the generation of an *N*-centered (imidazolyl-type) radical[21] *via* the cleavage of N-H bond. Next, ε-hydrogen abstraction, followed by formation of 1,6-diradical (Figure 3.1b) which underwent radical-radical coupling to produce benzo[4,5]imidazo[1,2-f]phenanthridine (Figure 3.1c). To the best of our knowledge, our finding on the direct dehydrogenative C-N coupling of C-H and N-H bonds is unprecedented in photochemistry.

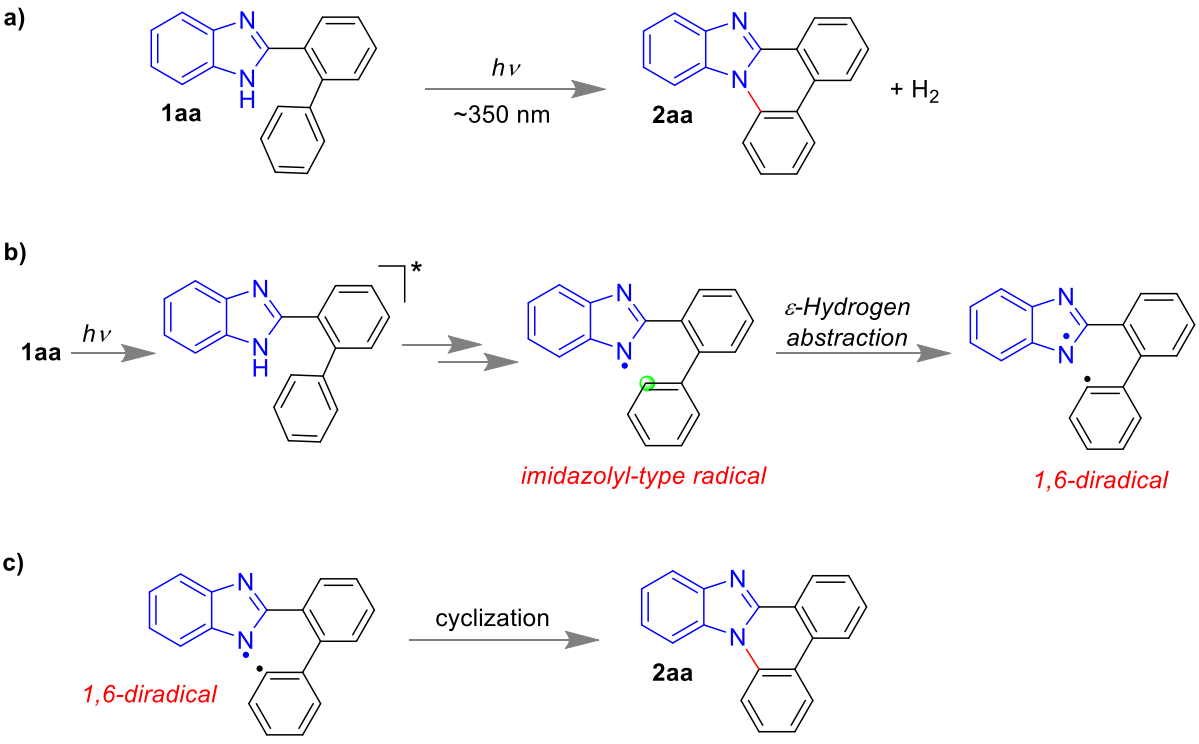

Figure 3.1. a) The photochemical C-N coupling. b) The 1,6-diradical *via* ε-hydrogen abstraction. c) Cyclization reaction.

The standard reaction condition was established using **1aa** as the model substrate, and it was found that the maximum yield (98%) of **2aa** was obtained at λ ~ 350 nm in DCE (dichloroethane) within 16 h (Figure 3.2). The yield was significantly reduced by changing the irradiation wavelength. For example, the yield was 32% at ~ 420 nm and no product was

a)

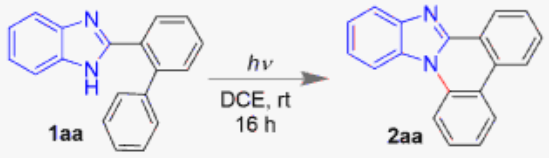

entry	wavelength (nm)	yield (%)
1	254	11
2	300	80
3	**350**	**98**
4	420	32
5	540	00

b)

entry	solvent	yield (%)
1	CH_3CN	86
2	HFIP	85
3	DCM	73
4	DMF	70
5	Toluene	83
6	**DCE**	**98**
7	Ethanol	86
8	Methanol	93
9	1,4- dioxane	10
10	DMSO	26
11	THF	21
12	Acetone	60

c)

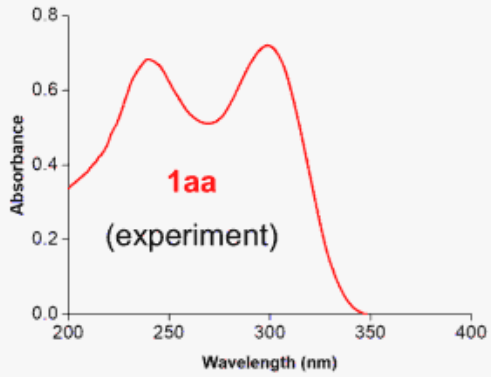

d)

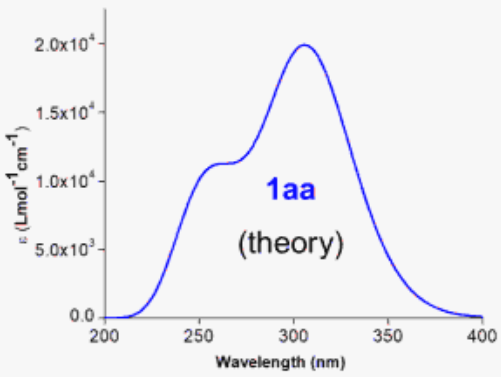

Figure 3.2. a) Optimization of the reaction condition by varying the irradiation wavelength. The reaction was carried out at room temperature in DCE for 16 h. b) Effect of solvents for the conversion of **1aa** to **2aa** at ~ 350 nm. c) UV-vis absorption of **1aa** in DCM. d) UV-vis absorption spectrum of **1aa** obtained from TD-DFT calculations at BYLYP/6-31+G(d,p) level.

obtained at ~ 540 nm. Similarly, amongst the solvents examined DCE was the most effective (Figure 3.2b). The experimentally determined UV-vis absorption spectra of **1aa** in DCM is shown in Figure 3.2c. Time-dependent density functional theory (TD-DFT) calculations were carried out at Becke-3 Lee-Yang-Parr (B3LYP) functional[22] with split valence basis sets, 6-31G(d) and 6-31+G(d,p)[23] to calculate the UV absorption spectra. The result is shown in Figure 3.2d for B3LYP/6-31+G (d, p) level. The λ_{max} was obtained at 308.7 nm and, ~20% of the absorption was observed at ~ 350 nm. However, no absorption at ~ 400 nm and above was detected.

The experiments shown in Figure 3.3 assisted in understanding the mechanism. No product was detected for the compound 2-([1,1'-biphenyl]-2-yl)-1-methyl-1H-benzo[d]imidazole **5ha** under standard condition (Figure 3.3a), which indicated that N-H benzimidazole was one of the essential requirements for the reaction.[24] Next, when **1aa** was treated with radical scavengers like TEMPO or BHT, no cyclized product[25] was identified (Figure 3b), which supported the radical pathway. The EPR experiments (Figure 3.3c) also supported the radical mechanism since a distinct EPR signal was observed when a free-radical spin trapping reagent DMPO (5,5-dimethyl-1-pyrroline-*N*-oxide)[26] was used under the standard condition. Furthermore, the yield of the reaction was unaffected either under argon atmosphere or in the presence of sodium azide,[27] oxygen and DABCO (singlet oxygen scavenger).[28] Therefore, the possibility of oxygen acting as the oxidant for the reaction was ruled out.

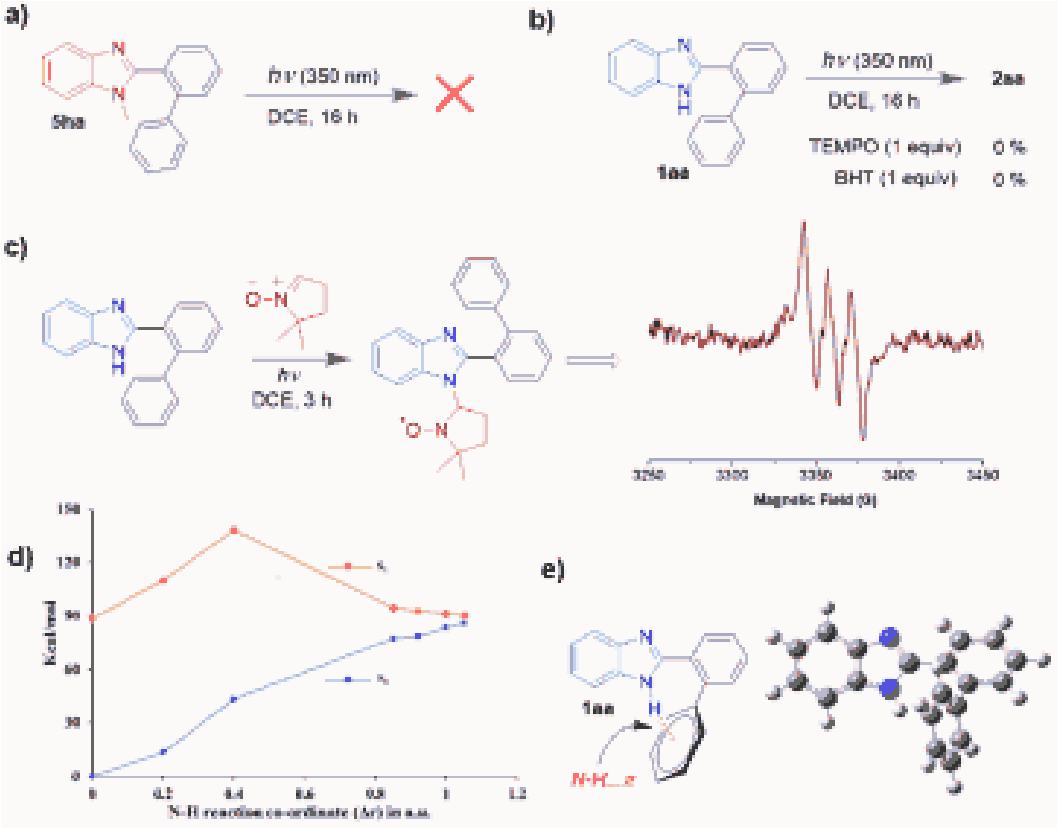

Figure 3.3. a) Reaction of N-Me benzimidazole. b) The experiment with TEMPO and BHT. c) EPR experiment using DMPO and the corresponding spectrum. d) Ground (S_0) and excited state (S_1) energy versus Δr of N-H bond. The calculation was done with CASSCF method using 6-31+G(d,p) basis set. e) Understanding the N-H…π interaction and minimum energy geometry of **1aa**.

The optimized geometry of **1aa** was found to be 3.35 kcal/mol more stable at B3LYP/6-31+ G (d, p) level when N-H is oriented towards the benzene ring compared to the optimized geometry where N-H is oriented away from any benzene ring. The other structural parameters remained the same in both structures. Therefore, this energy of 3.35 kcal/mol might be due to the N-H…π interaction[29] (stabilization, Figure 3.3e). The energy of **2aa** is 9.3 kcal/mol higher than **1aa** and the reaction is endothermic. The ground (S_0) and excited state (S_1) energy versus Δr of N-H bond is shown in Figure 3.3d with a Δr varied from 0 to 1.05 Å. The calculation was done with the complete active space self-consistent field (CASSCF) method

using the 6-31+G(d,p) basis set. The active space was defined by 14 electrons in 12 orbitals. These 14 electrons were assumed to be from π and π* orbitals of benzimidazole moiety, lone pairs of two N atoms and, σ and σ* orbitals of N-H bond of benzimidazole moiety. It can be seen from Figure 3.3d that after the Δ*r* distance of 0.85 Å, the S_1 state starts getting stabilized and finally becomes similar in energy with the S_0 state at a Δ*r* of 1.05 Å. At this point, it can be assumed that the molecule undergoes a homolytic N-H bond cleavage and generates two radicals, and the rest part of the reaction proceeds in the ground state. This study allows one to confirm that when the reactant is irradiated to the LUMO (S_1) state, somehow, the electron was promoted to the σ* orbital of the N-H bond, which resulted in the breaking of N-H bond and the formation of nitrogen and hydrogen radicals. Since the transition was a π-π* one, the promotion of electron to a σ* orbital was only possible if there is a significant coupling between σ* and π* orbitals,[30] which can also be assumed to be true here.

To obtain a better idea about the reaction mechanism, the geometry of **1aa** in the S_1 state was optimized with TDDFT using a 6-31+G(d,p) basis set. The energy was 80.9 kcal/mol higher than the energy of the optimized **1aa** in the S_0 state. This energy corresponds to a wavelength of 353 nm. Since there was ~20% absorption at 350 nm even though the λ_{max} was 308 nm for **1aa** (see Figure 3.2d), the reaction is expected to proceed with a longer wavelength than 308 nm. The optimized geometry of **1aa** in the S_1 state showed a longer N-H distance and a favorable orientation that brought the rings containing N-H and C-H bonds in close proximity. Thus, excitation to S_1 state, the geometrical parameters of **1aa** enhanced the possibility of the radical formation for a dehydrogenative cyclization.

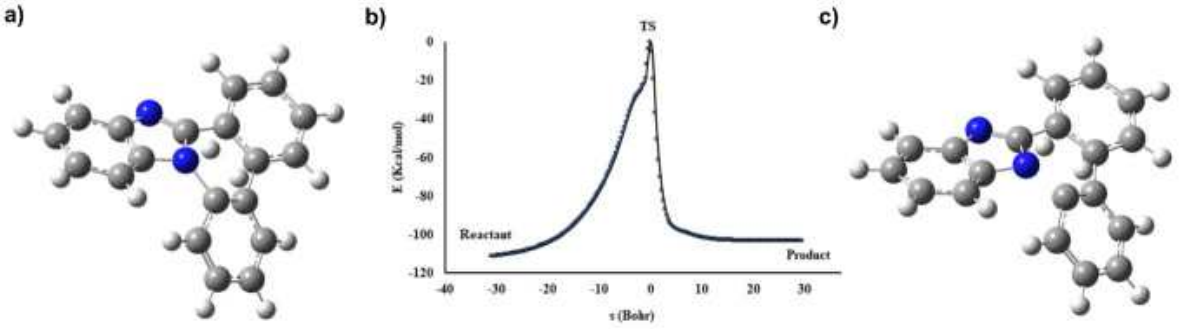

Figure 3.4. a) Optimized geometry of TS at S_1/S_0 state. The calculation was done at B3LYP/6-31+G(d,p) level. b) Reaction path from reactant to product obtained from IRC calculation at S_0 energy state. c) The geometry obtained from IRC scan and next to the TS towards reactant side. It shows that both the N-H and C-H has been broken and a diradical is formed.

The generation of H_2 in the studied photochemical reaction from **1aa** to **2aa** is validated *via* theoretical calculations. The geometry of the transition state (TS) for this reaction is optimized in both S_0 and S_1 states and they converged to the same structure as depicted in Figure 3.4a. The calculation was done at B3LYP/6-31+G(d,p) level and using QST3 option in Gaussian software.[31] The intrinsic reaction coordinate (IRC) scan as shown in Figure 3.4b confirms that the above TS connects the reactant (**1aa**) and product (**2aa**), where in the product side, H_2 is seen to be separated out from **2aa**. While inspecting the geometries along with the IRC scan, the structure next to the TS in the reactant side is given in Figure 3.4c. The geometry clearly illustrates the formation of 1,6-diradical. Thus, from these studies, one can conclude that the reaction proceeds from **1aa** through the formation 1,6-diradical to **2aa** and H_2.

Next, to support the formation of a diradical intermediate, we have further performed a tributyltin hydride experiment. The compound 2-([1,1'-biphenyl]-2-yl)-1H-benzo[d]imidazole **1aa** (0.22 mmol) was dissolved in DCE (1.5 mL) and tributyltin hydride ($^{n}Bu_3SnH$) (1.2 equiv) was added in a 10 mL screw caped quartz tube. Then the reaction mixture was irradiated under ~350 nm at room temperature for 16 h. However, no product formation could be detected.

The heterocyclic core benzimidazole is well recognized in supramolecular chemistry,[32] organic synthesis,[33] medicinal chemistry,[34] materials chemistry,[35] etc. In Figure 3.5, we have established the synthetic utility of this newly identified photochemical reaction. The yield of **2aa** was 98%, however, unsubstituted benzimidazoles having different substitutions like methyl, *tert*-butyl, fluoro, ethyl, methoxy, trifluoromethyl group, etc. at aryl moiety were also efficiently converted to the corresponding products (**2ab – 2ag**). Notably, the reactions were also highly successful with substitutions like methyl, *tert*-butyl, fluoro, ethyl, methoxy, chloro at aryl moiety of dimethyl substituted benzimidazoles (**2bb**, **2bc**, **2bd**, **2be**, **2bf** and **2bh**). The compounds **2ba** and **2bi** were obtained with 94 and 93% yields, respectively. The trifluoromethyl ($-CF_3$) substitution at aryl moiety of dimethyl substituted benzimidazoles gave the desire product **2bg** in 74% yield. To our delight, the biphenyl group of dichloro substituted benzimidazoles was also efficiently converted to the desired product **2ca** with 96% yield. The groups like methyl, *tert*-butyl and ethyl at the aryl ring of dichloro benzimidazole did not have any significant impact in the synthesis of **2cb**, **2cc** and **2ce**. Nevertheless, the fluoro, trifluoromethyl and chloro group containing aryl part gave the products **2cd**, **2cg** and **2ch** with 85, 79 and 87% yield. Similarly, the starting material with fluoro substitution at the *meta*-position of the aryl group was successfully converted to

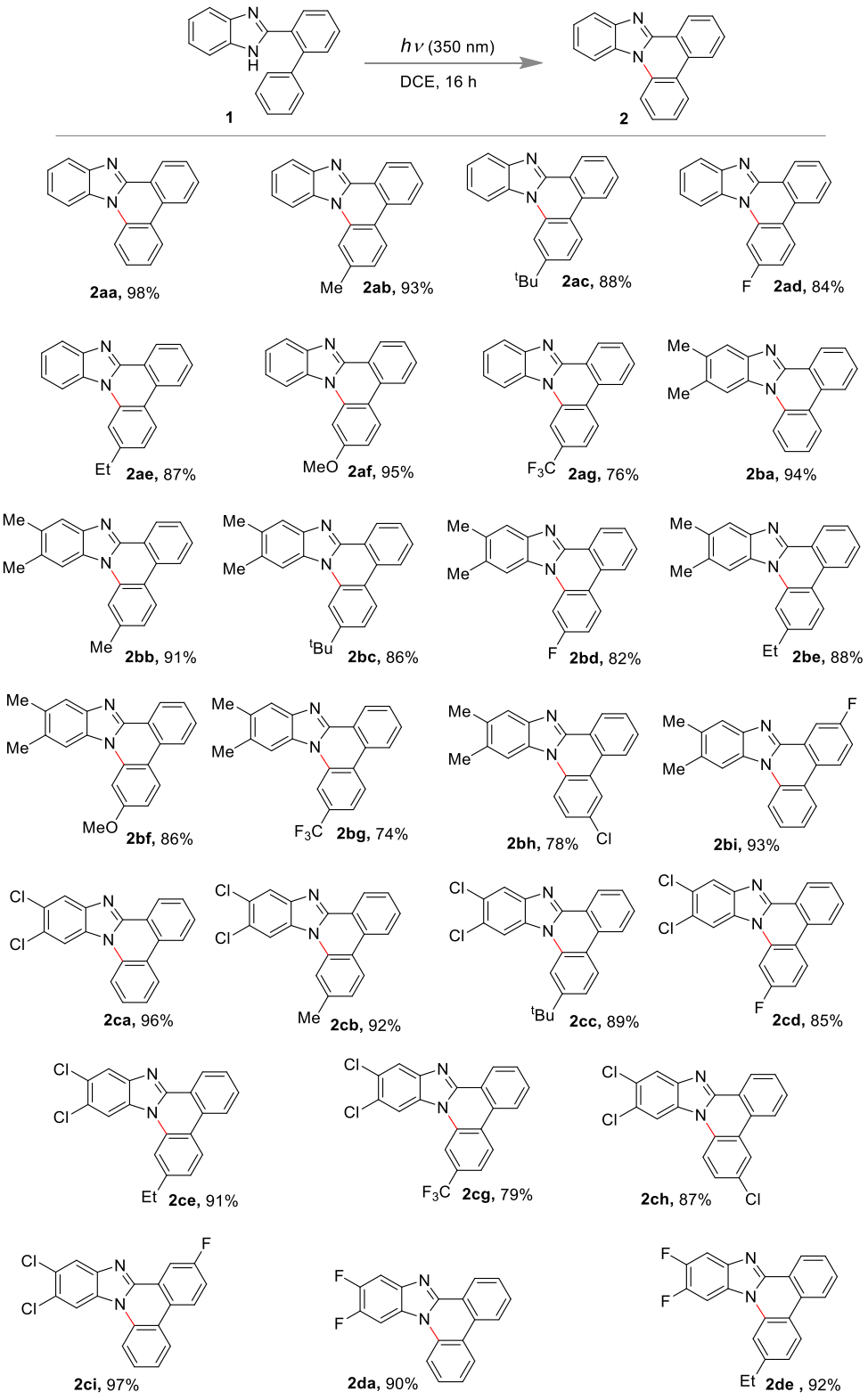

Figure 3.5. The substrate scope of symmetrical -substituted benzimidazole derivatives. Conditions: 0.222 mmol of **1aa** in 1.5 mL of DCE at rt for 16 h.

corresponding product **2ci** with 97% yield. Difluoro benzimidazole having unsubstituted and ethyl group at the aryl skeleton also led to products **2da** and **2de** with 90 and 92% respectively.

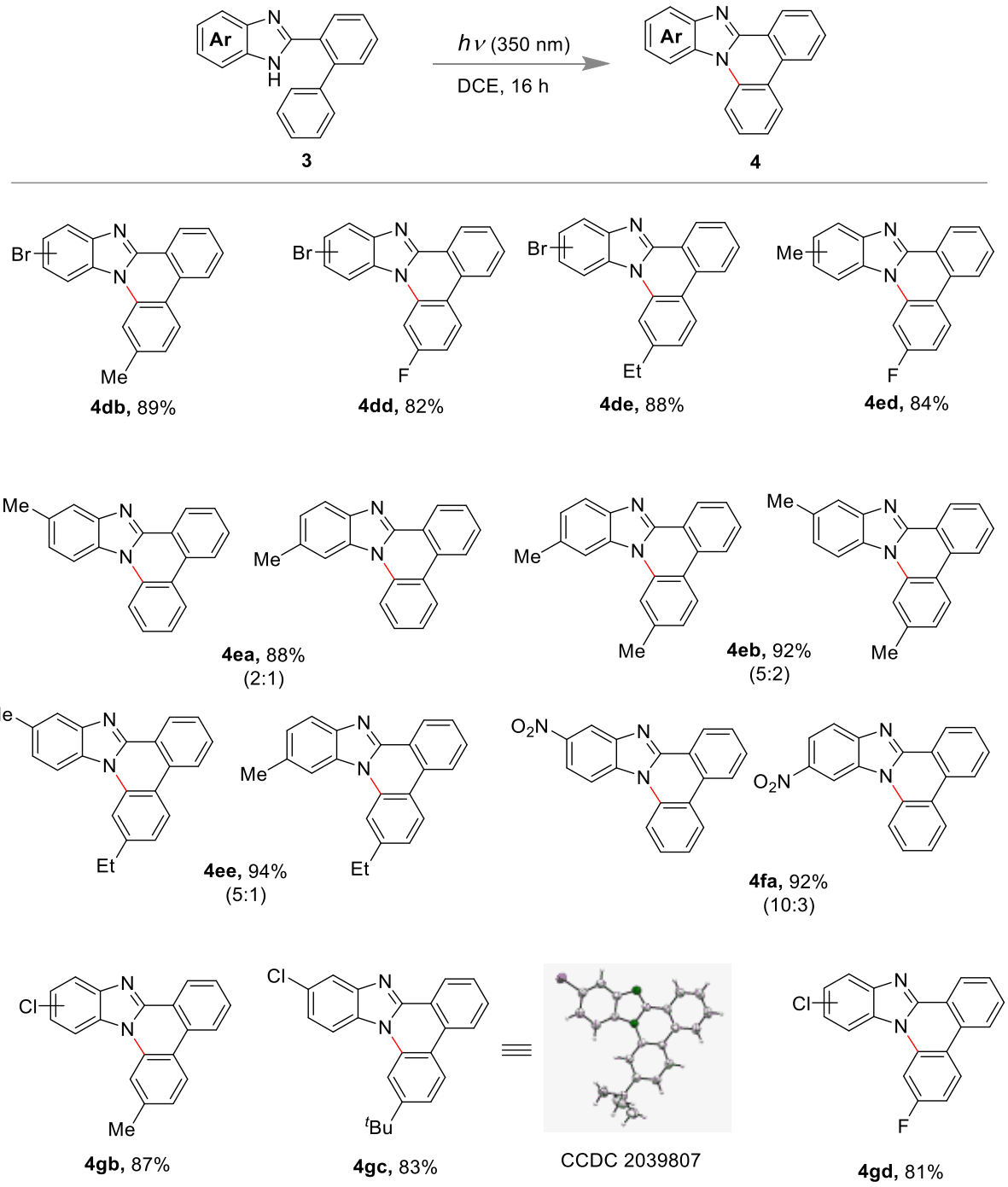

Figure 3.6. The cyclized products with the mono-substituted benzimidazole derivatives.

In Figure 3.6, the substrate scope is shown for the mono-substituted benzimidazole derivatives. Single regioisomers were obtained for the aryl moiety of 3-bromo-benzimidazoles with methyl, fluoro and ethyl substitutions (**4db**, **4dd, 4de**). Similarly, **4ed** was obtained with 84% yield as a major isomer. Regioisomeric mixture of products (**4eb, 4ee, 4ea** and **4fa**) were obtained for the unsymmetrical benzimidazole derivatives. On the other hand, 3-chloro benzimidazoles bearing methyl, *tert*-butyl and fluoro group also reacted smoothly to deliver corresponding products **4gb**, **4gc** and **4gd**. The structural assignments for the other compounds were done with the help of the X-ray crystal structure of **4gc** *i.e.*, 11-chloro-2-fluorobenzo[4,5]imidazo[1,2-f]phenanthridine (CCDC 2039807). The position of the -Cl group is identified at the carbon-11. The –Cl group shows –I effect, and we assumed that the –Me group which shows +I effect, is expected to be placed at the carbon-12.

The synthetic utility of this photochemical conversion was examined by scaling up the reaction up to 3.8 mmol of 2-([1,1'-biphenyl]-2-yl)-1H-benzo[d]imidazole (**1aa**) and expected product benzo[4,5]imidazo[1,2-f]phenanthridine (**2aa**) was isolated in 94% yield upon irradiation of ~350 nm light for 24 h in the solvent DCE (Figure 3.7).

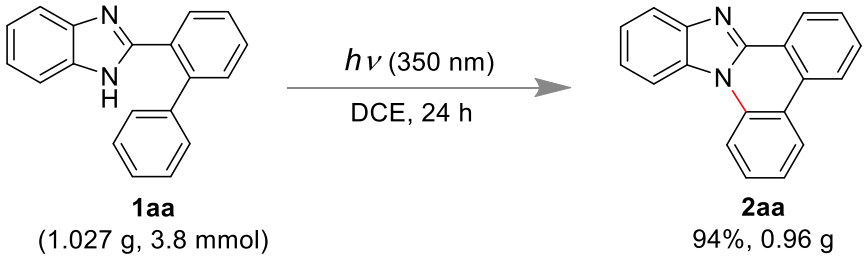

Figure 3.7. Gram scale synthesis.

Table 3.1. Photophysical data of benzimidazole-fused phenanthridine derivatives.

entry	compound	λ_{abs} (nm)[a]	λ_{em} (nm)[b]	φ_F[c]
1	2ac	346	374	0.61
2	2ad	331	369	0.94
3	2ae	346	373	0.90
4	2ba	354	401	0.67
5	2bb	330	383	0.73
6	2bc	347	381	0.66
7	2bd	338	394	0.96
8	2bf	359	384	0.84
9	2bi	354	386	0.94
10	2ca	351	374	0.18
11	2cb	341	401	0.58
12	2cc	344	379	0.64
13	2cd	351	373	0.72
14	2ce	357	378	0.39
15	2cg	354	399	0.37
16	2ci	357	379	0.31

[a]Absorption maxima in dichloromethane solution (3×10^{-6} M). [b]Emission maxima in dichloromethane solution (3×10^{-6} M). [c]Absolute fluorescence quantum yields were recorded using corresponding absorption and emission parameter in dichloromethane solution (3×10^{-6} M).

The absorption and emission spectra of benzimidazole-fused phenanthridine derivatives were recorded in dichloromethane solutions (3×10^{-6} M). The majority of the compounds exhibited high fluorescence quantum yields (φ_F, Table 1). For example, phenanthridine moiety with the fluoro group in phenyl ring (**2ad, 2bd**, **2bi**) showed φ_F in the range of 0.94-0.96. Contrastingly, the compound with dichloro substituents in the benzimidazole-fused phenanthridine rings (**2ca**) showed $\varphi_F \sim 0.18$.

3.4. CONCLUSION

In summary, we have demonstrated an unprecedented photochemical dehydrogenative C(sp^2)-H and N(sp^2)-H C-N coupling of non-prefunctionalized systems under direct irradiation (~350 nm). Neither any added reagents nor prefunctionalization of the substrates were needed for this transformation. The weak or noncovalent interaction like N-H…π interaction helped the molecules to absorb the light of lower energy than required. The benzimidazole ring of 2-([1,1′-biphenyl]-2-yl)-1H-benzo[d]imidazole led to the formation of imidazolyl-type radical which underwent ε-hydrogen abstraction to generate 1,6-diradical. Finally, the radical-radical coupling resulted in benzo[4,5]imidazo[1,2-f]phenanthridine. We anticipate that the photochemical reaction described here can lead to the initiation of a new research area under photochemistry.

3.5. EXPERIMENTAL SECTION

General Information. Commercially available reagents and solvents were used as received. UV-Visible spectra were recorded on a JASCO V-730 UV-Visible spectrometer and Emission spectral studies were measured using Perkin Elmer, LS-55 spectrophotometer with optical cell of 1 cm path length. Absolute fluorescence quantum yields in solution state were performed by integrating sphere method using Edinburgh FS30 Spectrofluorometer. Column chromatographic purifications of the compounds were performed using silica gel (mesh 230–400, 100-200) and hexane – ethyl acetate solvent mixtures. NMR spectra were recorded on 400 MHz or 700 MHz instruments at 25 °C. The chemical shift values are reported in parts per million (ppm) with respect to residual trichloromethane (7.26 ppm for ^{1}H and 77.16 ppm for ^{13}C). The peak patterns are designated as follows: s: singlet; d: doublet; t: triplet; q: quartet; m: multiplet; dd: doublet of doublets; td: triplet of doublets; brs: broad singlet. The

coupling constants (*J*) are reported in hertz (Hz). High-resolution mass spectra (HR-MS) were recorded on an ESI-TOF (time of flight) mass spectrometer. Infrared (IR) spectral data are reported in wave number (cm^{-1}). FT-IR spectra were recorded after making thin layer of the compounds on the surface of NaCl crystal using dichloromethane. Melting points of the compounds were determined using a digital melting point apparatus and uncorrected.

Representative procedure for the synthesis of 11,12-dichlorobenzo[4,5]imidazo[1,2-f]phenanthridine (2aa). 2-([1,1'-biphenyl]-2-yl)-1H-benzo[d]imidazole (60 mg) was dissolved in DCE (1.5 mL) and placed in a 10 mL screw capped quartz tube. The mixture was irradiated at ~350 nm for 16 h. The progress of the reaction was monitored by thin layer chromatography (TLC). After completion of the reaction the resulting solution was evaporated to dryness. The crude residue was purified on silica gel column chromatography (20% EtOAc in hexane) to get the pure product benzo[4,5]imidazo[1,2-f]phenanthridine (59 mg, yield 98%).

Gram scale synthesis. 2-([1,1'-biphenyl]-2-yl)-1H-benzo[d]imidazole (1.027 gm, 3.8 mmol) was dissolved in DCE (8.5 mL) and placed in a 10 mL screw capped quartz tube. Then the mixture was irradiated under ~350 nm for 20 h. After completion of reaction, the resulting solution was evaporated to dryness. The crude residue was purified on silica gel column chromatography (20% EtOAc in hexane). The isolated yield of cyclized product was found to be 94% (0.96 g).

Experiments to investigate the role of oxygen the transformation

Triplet oxygen. 2-([1,1'-Biphenyl]-2-yl)-1H-benzo[d]imidazole (60 mg) was dissolved in DCE (1.5 mL) and placed in a 10 mL screw capped quartz tube under the argon atmosphere.

Then mixture was irradiated under ~350 nm for 20 h. After the completion of reaction, the isolated yield of cyclized product was found to be 98%. Thus concluded that the triplet oxygen did not have effect in the photochemical transformation.

Singlet oxygen. Furthermore, to understand the role of singlet oxygen in this reaction, we have carried out the reaction in presence of excess amount (3 equiv) of 1,4-diazabicyclo[2.2.2]octane (DABCO, singlet oxygen scavenger) under aerobic atmosphere. Under this reaction condition, isolated yield of the expected product was found to be almost unchanged (96%).

Radical trapping experiments. The compound 2-([1,1'-biphenyl]-2-yl)-1H-benzo[d]imidazole **1aa** (0.12 mmol) was dissolved in DCE (1.5 mL) and TEMPO (1.2 equiv) was added in a 10 mL screw capped quartz tube. Then the reaction mixture was irradiated under ~350 nm at room temperature for 16 h. However, no product formation could be detected. Similar observation was also found using anther radical trapping reagent BHT (Butylated hydroxytoluene).

EPR Experiments. The compound 2-([1,1'-biphenyl]-2-yl)-1H-benzo[d]imidazole **1aa** (0.12 mmol) was dissolved in DCE (1.5 mL) and DMPO (20 μL) was added in a 10 mL quartz flask. Then the reaction mixture was irradiated under ~350 nm at room temperature for 3 h and the EPR experiment was performed.

2-(4'-Methyl-[1,1'-biphenyl]-2-yl)-1H-benzo[d]imidazole (1ab).[36] R_f = 0.50 (hexane/ethyl acetate 4:1); white solid; yield 94% (370 mg); mp 268−270 °C; ^{1}H NMR (400 MHz, DMSO-d_6) δ 12.08 (s, 1H), 7.71 – 7.67 (m, 1H), 7.61 – 7.56 (m, 1H), 7.52 –

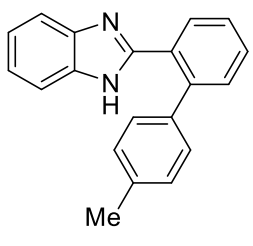

7.46 (m, 3H), 7.35 (s, 1H), 7.17 – 7.11 (m, 2H), 7.06 (q, *J* = 8.4 Hz, 4H), 2.23 (s, 3H); $^{13}C\{^{1}H\}$ NMR (100 MHz, DMSO-d_6) δ 152.4, 143.5, 141.0, 137.3, 136.4, 134.7, 131.2, 130.5, 130.1, 129.9, 128.9, 128.7, 127.3, 122.1, 121.4, 118.9, 111.4, 20.7; IR (KBr) $\tilde{\nu}$ = 3051, 3021, 2913, 2860, 1467, 1438, 1394, 1311, 1276, 1096, 968, 817, 764, 754 cm^{-1}; HR-MS (ESI-TOF) m/z calcd for $C_{20}H_{17}N_2$ $[M + H]^+$ 285.1386, found 285.1367.

2-(4'-(Tert-butyl)-[1,1'-biphenyl]-2-yl)-1H-benzo[d]imidazole (1ac). R_f = 0.50

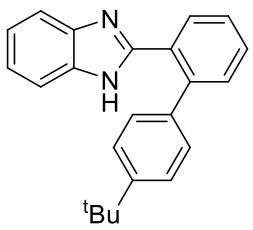

(hexane/ethyl acetate 4:1); white solid; yield 86% (387 mg); mp 242−244 °C; ^{1}H NMR [400 MHz, DMSO-d_6 : $CDCl_3$ (20:1)] δ 11.82 (s, 1H), 7.69 – 7.65 (m, 1H), 7.60 – 7.55 (m, 1H), 7.49 (d, *J* = 7.2 Hz, 2H), 7.45 (dd, *J* = 6.0, 3.6 Hz, 2H), 7.26 (d, *J* = 8.4 Hz. 2H), 7.15 – 7.12 (m, 3H), 7.12 (d, *J* = 2.0 Hz, 1H), 1.22 (s, 9H); $^{13}C\{^{1}H\}$ NMR [100 MHz, DMSO-d_6 : $CDCl_3$ (20:1)] δ 150.5, 147.7, 139.0, 137.3, 135.4, 129.4, 128.8, 128.2, 128.1, 126.7, 125.6, 125.4, 123.4, 123.2, 119.9, 113.5, 113.3, 32.4, 29.3; IR (KBr) $\tilde{\nu}$ = 3046, 2959, 2870, 1470, 1450, 1401, 1374, 1275, 1096, 1003, 837, 761, 742 cm^{-1}; HR-MS (ESI-TOF) m/z calcd for $C_{23}H_{23}N_2$ $[M + H]^+$ 327.1856, found 327.1848.

2-(4'-Methoxy-[1,1'-biphenyl]-2-yl)-1H-benzo[d]imidazole (1af). R_f = 0.60 (hexane/ethyl acetate 4:1); white solid; yield 93% (388 mg); mp 238−240 °C; ^{1}H NMR (400 MHz, DMSO-d_6) δ 12.07 (s, 1H), 7.72 – 7.64 (m, 1H), 7.60 – 7.55 (m, 2H), 7.51 – 7.45 (m, 2H), 7.35 (s, 1H), 7.16 – 7.11 (m, 3H), 7.10 – 7.09 (m, 1H), 6.83 – 6.81 (m, 1H), 6.80 – 6.78 (m, 1H). 3.69 (s, 3H); $^{13}C\{^{1}H\}$ NMR (100 MHz, DMSO-d_6) δ 158.6, 152.5, 140.7, 134.7, 132.5, 131.3, 130.5, 130.1, 130.0, 127.6, 127.1, 122.3, 121.5, 118.9, 113.9, 113.8, 111.5, 55.2; IR (KBr) $\tilde{\nu}$ =

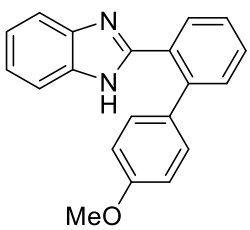

3053, 2969, 2935, 2841, 1608, 1509, 1464, 1449, 1388, 1296, 1250, 1173, 1036, 965, 765, 759, 745 cm^{-1}; HR-MS (ESI-TOF) m/z calcd for $C_{20}H_{17}N_2O$ $[M + H]^+$ 301.1335, found 301.1357.

2-(4'-(Trifluoromethyl)-[1,1'-biphenyl]-2-yl)-1H-benzo[d]imidazole (1ag). R_f = 0.40 (hexane/ethyl acetate 7:3); white solid; yield 90% (421 mg); mp 288−290 °C. ^1H NMR (700

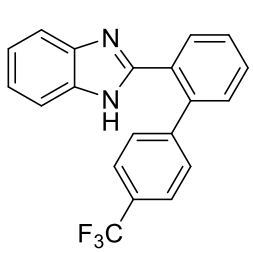

MHz, DMSO-d_6) δ 12.30 (s, 1H), 7.78 (d, *J* = 7.7 Hz, 1H), 7.65 (td, *J* = 7.7, 1.4 Hz, 1H), 7.62 (d, *J* = 8.4 Hz, 2H), 7.59 (dd, *J* = 7.7, 1.4 Hz, 1H), 7.57 – 7.52 (m, 2H), 7.38 (t, *J* = 8.4 Hz, 3H), 7.14 (s, 2H); $^{13}C\{^1H\}$ NMR (175 MHz, DMSO-d_6) δ 151.6, 144.6, 143.5, 139.6, 134.6, 131.2, 130.8, 130.2, 129.8, 128.4, 127.6 (q, $J_{C,F}$ = 32.0 Hz), 125.2 (q, $J_{C,F}$ = 272.2 Hz), 125.1, 125.0, 121.5, 119.0, 111.5; IR (KBr) $\tilde{\nu}$ = 3051, 2964, 2875, 1614, 1441, 1402, 1323, 1274, 1151, 1123, 1107, 1097, 1065, 1018, 841, 762, 747, 753 cm^{-1}; HR-MS (ESI-TOF) m/z calcd for $C_{20}H_{14}F_3N_2$ $[M + H]^+$ 339.1104, found 339.1098.

5,6-Dimethyl-2-(4'-methyl-[1,1'-biphenyl]-2-yl)-1H-benzo[d]imidazole (1bb). R_f = 0.40 (hexane/ethyl acetate 4:1); white solid; yield 88% (305 mg); mp 262−264 °C; ^1H NMR (700

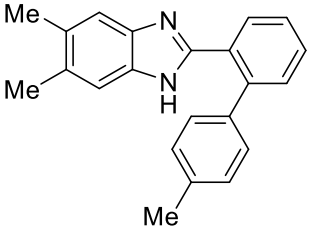

MHz, DMSO-d_6) δ 11.84 (s, 1H), 7.64 (d, *J* = 8.4 Hz, 1H), 7.57 (t, *J* = 7.7 Hz, 1H), 7.50-7.45 (m, 2H), 7.24 – 7.12 (brs, 2H), 7.07 – 7.01 (m, 4H), 2.26 (s, 6H), 2.23 (s, 3H); $^{13}C\{^1H\}$ NMR (100 MHz, DMSO-d_6) δ 151.4, 140.9, 140.6, 138.1, 137.4, 137.1, 136.3, 134.9, 131.1, 130.4, 129.8, 128.8, 128.7, 128.5, 127.2, 118.9, 111.5, 20.7,

20.0 (×2); IR (KBr) $\tilde{\nu}$ = 3019, 2914, 2856, 2688, 1455, 1444, 1427, 1395, 1311, 998, 971, 869, 851, 754 cm^{-1}; HR-MS (ESI-TOF) m/z calcd for $C_{22}H_{21}N_2$ $[M + H]^+$ 313.1699, found 313.1695.

2-(4'-Methoxy-[1,1'-biphenyl]-2-yl)-5,6-dimethyl-1H-benzo[d]imidazole (1bf). R_f = 0.40 (hexane/ethyl acetate 4:1); white solid; yield 96% (127 mg); mp 261−263 °C; ^{1}H NMR (700

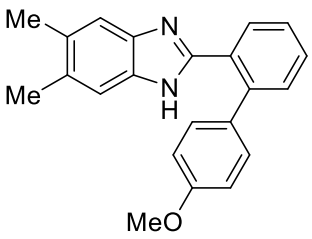

MHz, DMSO-d_6) δ 11.85 (s, 1H), 7.63 (d, *J* = 7.7 Hz, 1H), 7.55 (t, *J* = 7.7 Hz, 1H), 7.51 – 7.43 (m, 2H), 7.19 (s, 2H), 7.08 (d, *J* = 8.4 Hz, 2H), 6.79 (d, *J* = 8.4 Hz, 2H), 3.69 (s, 3H), 2.26 (s, 6H); $^{13}C\{^1H\}$ NMR (100 MHz, DMSO-d_6) δ 158.5, 151.3, 140.6, 137.5, 133.1, 132.4, 132.1, 131.2, 130.6, 130.4, 130.0, 129.9, 127.8, 127.0, 126.4, 115.1, 113.7, 55.1, 20.0 (×2); IR (KBr) $\tilde{\nu}$ = 3034, 2938, 2834, 1607, 1470, 1454, 1438, 1391, 1313, 1250, 1172, 1035, 871, 857, 758 cm^{-1}; HR-MS (ESI-TOF) m/z calcd for $C_{22}H_{21}N_2O$ $[M + H]^+$ 329.1648, found 329.1647.

5,6-Dimethyl-2-(4'-(trifluoromethyl)-[1,1'-biphenyl]-2-yl)-1H-benzo[d]imidazole (1bg). R_f = 0.45 (hexane/ethyl acetate 4:1); white solid; yield 97% (390 mg); mp 275−277 °C; ^{1}H

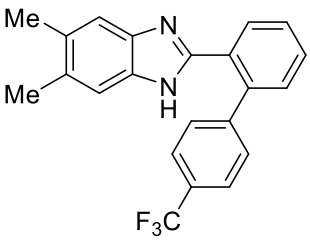

NMR (700 MHz, DMSO-d_6) δ 12.08 (s, 1H), 7.73 (d, *J* = 6.3 Hz, 1H), 7.63 – 7.57 (m, 3H), 7.58 – 7.51 (m, 2H), 7.36 (d, *J* = 6.3 Hz, 2H), 7.19 (s, 2H), 2.25 (s, 6H); $^{13}C\{^1H\}$ NMR (175 MHz, DMSO-d_6) δ 150.7, 144.7, 142.2, 141.3, 139.5, 133.2, 131.1, 130.7, 130.4, 129.9, 129.7, 128.3, 127.5 (q, $J_{C,F}$ = 32.4 Hz), 125.0, 124.4 (q, $J_{C,F}$ = 272.3 Hz), 119.1, 111.5, 20.1 (×2); IR (KBr) $\tilde{\nu}$ = 3065, 3020, 2985, 2855, 1614, 1443, 1394, 1321, 1152, 1125, 1104,

1065, 1046, 997, 856, 839, 766 cm^{-1}; HR-MS (ESI-TOF) m/z calcd for $C_{22}H_{18}F_3N_2$ $[M + H]^+$ 367.1417, found 367.1419.

5,6-Dichloro-2-(4'-methyl-[1,1'-biphenyl]-2-yl)-1H-benzo[d]imidazole (1cb). R_f = 0.40 (hexane/ethyl acetate 4:1); pale yellow solid; yield 95% (284 mg); mp 292−294 °C; ^1H NMR

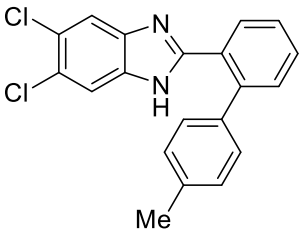

(700 MHz, DMSO-d_6) δ 7.73 (s, 2H), 7.70 – 7.68 (m, 1H), 7.62 (td, *J* = 7.7, 1.4 Hz, 1H), 7.53 – 7.49 (m, 2H), 7.06 – 7.03 (m, 4H), 2.24 (s, 3H); $^{13}C\{^1H\}$ NMR (100 MHz, DMSO-d_6) δ 155.1, 141.1, 137.0, 136.7, 131.2, 130.6, 130.5, 129.3, 129.1, 129.0, 128.7, 127.4, 126.9, 125.2, 124.7, 124.4, 116.7, 20.8; IR (KBr) $\tilde{\nu}$ = 3065, 3022, 2851, 2653, 1472, 1446, 1434, 1380, 1292, 1095, 968, 867, 851, 818, 754 cm^{-1}; HR-MS (ESI-TOF) m/z calcd for $C_{20}H_{15}Cl_2N_2$ $[M + H]^+$ 353.0607, found 353.0586.

2-([1,1'-Biphenyl]-2-yl)-5,6-difluoro-1H-benzo[d]imidazole (1da). R_f = 0.40 (hexane/ethyl acetate 4:1); pale yellow solid; yield 94% (399 mg); mp 228−230 °C; ^1H NMR (700 MHz,

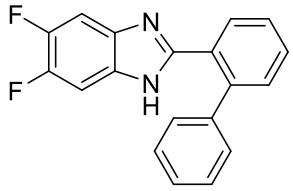

DMSO-d_6) δ 12.34 (s, 1H), 7.71 (d, *J* = 7.4 Hz, 1H), 7.62 (t, *J* = 7.3 Hz, 2H), 7.53 (t, *J* = 8.2 Hz, 2H), 7.38 (s, 1H), 7.26 (d, *J* = 6.3 Hz, 3H), 7.17 (d, *J* = 6.8 Hz, 2H); $^{13}C\{^1H\}$ (175 MHz, DMSO-d_6) δ 154.10 (s), 146.73 (d, *J* = 234.0 Hz), 146.44 (d, *J* = 240.2 Hz), 140.97 (s), 139.97 (s), 138.81 (s), 131.01 (s), 130.55 (s), 130.13 (s), 129.82 (s), 129.55 (s), 128.73 (s), 128.19 (s), 127.45 (s), 127.17 (s), 106.13 (d, *J* = 19.6 Hz), 99.23 (d, *J* = 22.5 Hz); IR (KBr) $\tilde{\nu}$ = 3058, 2929, 2860, 2768, 2693, 1599, 1476, 1456, 1431, 1398, 1296, 1154, 1135, 972, 874, 855, 779 cm^{-1}; HR-MS (ESI-TOF) m/z calcd for $C_{19}H_{13}F_2N_2$ $[M + H]^+$ 307.1041, found 307.1044.

2-(4'-Ethyl-[1,1'-biphenyl]-2-yl)-5,6-difluoro-1H-benzo[d]imidazole (1de). R_f = 0.40 (hexane/ethyl acetate 4:1); pale yellow solid; yield 82% (361 mg); mp 254−256 °C; ^{1}H NMR (700 MHz, DMSO-d_6) δ 12.34 (s, 1H), 7.68 (d, *J* = 7.0 Hz, 1H), 7.64 (dd, *J* = 10.5, 7.7 Hz, 1H), 7.60 (t, *J* = 7.7 Hz, 1H), 7.51 (s, 1H), 7.50 (d, *J* = 7.0 Hz, 1H), 7.38 (dd, *J* = 9.8, 7.7 Hz, 1H), 7.17 – 7.05 (m, 4H), 2.55 (q, *J* = 7.7 Hz, 2H), 1.14 (t, *J* = 7.7 Hz, 3H); ^{13}C{^{1}H} (175 MHz, DMSO-d_6) δ 154.3, 146.8 (d, *J* = 238.8 Hz), 146.7 (d, *J* = 238.8 Hz), 147.1 (d, *J* = 14.9 Hz), 145.7 (d, *J* = 14.7 Hz), 142.6, 140.9, 138.8 (d, *J* = 10.7 Hz), 137.3, 131.1, 130.5, 130.1, 129.8 (d, *J* = 11.4 Hz), 129.5, 128.6, 127.6, 127.2, 106.1 (d, *J* = 19.3 Hz), 99.2 (d, *J* = 22.2 Hz), 27.7, 15.3; IR (KBr) $\tilde{\nu}$ = 3075, 3023, 2979, 1597, 1475, 1457, 1437, 1391, 1276, 1152, 1133, 1045, 970, 854, 832, 753 cm^{-1}; HR-MS (ESI-TOF) m/z calcd for $C_{21}H_{17}F_2N_2$ [M + H]$^+$ 335.1354, found 335.1354.

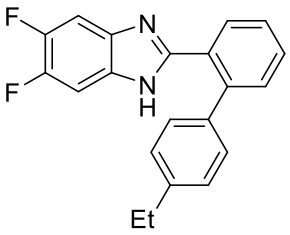

5-Bromo-2-(4'-methyl-[1,1'-biphenyl]-2-yl)-1H-benzo[d]imidazole OR 6-Bromo-2-(4'-methyl-[1,1'-biphenyl]-2-yl)-1H-benzo[d]imidazole (3db). R_f = 0.40 (hexane/ethyl acetate 4:1); white solid; yield 97% (284 mg); mp 274−276 °C; ^{1}H NMR (700 MHz, DMSO-d_6) δ 12.32 (s, 1H), 7.68 (d, *J* = 7.7 Hz, 1H), 7.63 – 7.58 (m, 1H), 7.50 (t, *J* = 7.7 Hz, 3H), 7.28 (dd, *J* = 8.4, 1.4 Hz, 1H), 7.05 (s, 5H), 2.23 (s, 3H); ^{13}C{^{1}H} NMR (100 MHz, DMSO-d_6) δ 153.7, 144.9, 141.0, 137.1, 136.5, 133.7, 131.2, 130.5, 130.3, 129.6, 128.9, 128.7, 127.3, 124.8, 121.2, 120.5, 114.1, 20.7; IR (KBr) $\tilde{\nu}$ = 3022, 2908, 2849, 1608, 1583, 1472, 1451, 1386, 1297, 1279, 1097, 1043, 915, 818, 798, 768, 754 cm^{-1}; HR-MS (ESI-TOF) m/z calcd for $C_{20}H_{16}BrN_2$ [M + H]$^+$ 363.0491, found 363.0474.

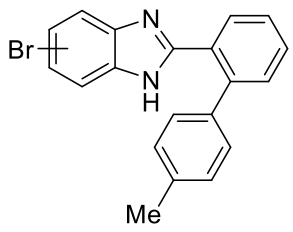

Mixer of 5-Bromo-2-(4'-fluoro-[1,1'-biphenyl]-2-yl)-1H-benzo[d]imidazole and 6-Bromo-2-(4'-fluoro-[1,1'-biphenyl]-2-yl)-1H-benzo[d]imidazole (3dd). R_f = 0.50 (hexane/ethyl acetate 4:1); Inseparable white solid (1:1); yield 74% (61 mg); mp 227−229 °C; ^{1}H NMR (400 MHz, DMSO-d$_6$) δ 12.41 (s, 1H), 12.33 (s, 1H), 7.78 – 7.70 (m, 3H), 7.62 (td, *J* = 7.6, 1.2 Hz, 2H), 7.56 – 7.49 (m, 6H), 7.34 (d, *J* = 8.4 Hz, 1H), 7.28 (d, *J* = 8.8 Hz, 2H), 7.21 – 7.15 (m, 4H),, 7.09 (t, *J* = 8.8 Hz, 4H); ^{13}C{^{1}H} NMR (100 MHz, DMSO-d$_6$) δ 161.62 (d, *J* = 243.9 Hz), 153.5, 153.1, 144.9, 142.6, 140.1, 136.4 (d, *J* = 2.9 Hz), 135.9, 133.7, 131.1, 130.9 (d, *J* = 8.2 Hz), 130.7, 130.4, 129.6, 127.8, 125.1, 124.5, 121.4, 120.8, 115.2 (d, *J* = 21.4 Hz), 114.1, 113.7, 113.3; IR (KBr) $\tilde{\nu}$ = 3065, 3031, 2851, 2769, 1604, 1508, 1476, 1437, 1384, 1278, 1236, 1092, 1044, 916, 834, 816, 806, 769, 756 cm^{-1}; HR-MS (ESI-TOF) m/z calcd for $C_{19}H_{13}BrFN_2$ $[M + H]^+$ 367.0241, found 367.0231.

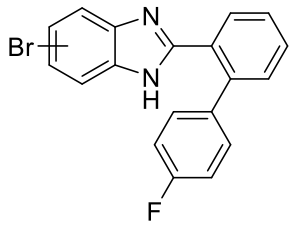

Mixer of 5-Bromo-2-(4'-ethyl-[1,1'-biphenyl]-2-yl)-1H-benzo[d]imidazole and 6-Bromo-2-(4'-ethyl-[1,1'-biphenyl]-2-yl)-1H-benzo[d]imidazole (3de). R_f = 0.50 (hexane/ethyl acetate 4:1); Inseparable white solid (2:1); yield 94% (285 mg); mp 237−238 °C; ^{1}H NMR (400 MHz, DMSO-d$_6$) δ 12.31 (s, 1H), 12.25 (s, 0.5H), 7.66 (d, *J* = 1.6 Hz, 0.5H), 7.64 (d, *J* = 1.4 Hz, 1H), 7.61 – 7.54 (m, 2H), 7.49 (d, *J* = 1.4 Hz, 2H), 7.47 (d, *J* = 1.4 Hz, 1.5H), 7.45 (d, *J* = 1.4 Hz, 0.5H), 7.26 (d, *J* = 2.0 Hz, 1H), 7.23 (d, *J* = 2.0 Hz, 0.5H), 7.05 (s, 7.5H), 2.53 (d, *J* = 7.6 Hz, 1H), 2.49 – 2.45 (m, 2H), 1.09 (t, *J* = 7.6 Hz, 4.5H). ^{13}C{^{1}H} NMR (100 MHz, DMSO-d$_6$) δ 153.8, 144.9, 142.7, 141.0, 137.3, 135.9, 135.8, 133.7, 131.2, 130.6, 130.3, 129.6, 128.7, 127.7, 127.3, 124.9, 124.5, 121.3, 120.7, 114.5, 114.0, 113.7,

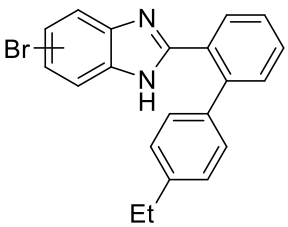

113.2, 27.8, 15.4; IR (KBr) $\tilde{\nu}$ = 3058, 3023, 2967, 1466, 1437, 1422, 1386, 1295, 1280, 1096, 1043, 914, 832, 806, 797, 768 cm^{-1}; HR-MS (ESI-TOF) m/z calcd for $C_{21}H_{18}BrN_2$ $[M + H]^+$ 377.0648, found 377.0649.

5-Methyl-2-(4'-methyl-[1,1'-biphenyl]-2-yl)-1H-benzo[d]imidazole OR 6-Methyl-2-(4'-methyl-[1,1'-biphenyl]-2-yl)-1H-benzo[d]imidazole (3eb). 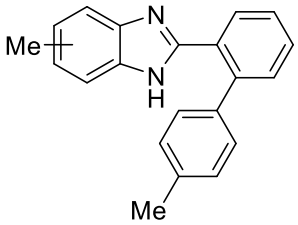

R_f = 0.45 (hexane/ethyl acetate 4:1); White solid; yield 94% (343 mg); mp 265−267 °C; ^{1}H NMR (400 MHz, DMSO-d_6) δ 11.96 (s, 1H), 7.65 (d, *J* = 7.2 Hz, 1H), 7.58 (t, *J* = 7.6 Hz, 1H), 7.48 (t, *J* = 6.0 Hz, 2H), 7.33 (s, 1H), 7.20 (s, 1H), 7.07 (s, 1H), 7.05 – 7.04 (m, 2H), 7.02 (s, 1H), 6.95 (d, J = 8.1 Hz, 1H), 2.36 (s, 3H), 2.23 (s, 3H); ^{13}C{^{1}H} NMR (100 MHz, DMSO-d_6) δ 152.0, 146.2, 140.9, 139.9, 137.3, 136.4, 131.2, 130.5, 130.3, 129.9, 128.9, 128.7, 127.3, 123.3, 123.2, 118.5, 111.1, 21.4, 20.7; IR (KBr) $\tilde{\nu}$ = 3019, 2916, 2858, 1460, 1444, 1393, 1305, 1284, 1096, 973, 817, 803, 797, 771, 753 cm^{-1}; HR-MS (ESI-TOF) m/z calcd for $C_{21}H_{19}N_2$ $[M + H]^+$ 299.1543, found 299.1528.

Mixer of 5-Chloro-2-(4'-methyl-[1,1'-biphenyl]-2-yl)-1H-benzo[d]imidazole and 6-Chloro-2-(4'-methyl-[1,1'-biphenyl]-2-yl)-1H-benzo[d]imidazole (3gb). R_f = 0.40 (hexane/ethyl acetate 4:1); Inseparable white solid (5:3); yield 97% (325 mg); mp 286−288 °C; ^{1}H NMR (400 MHz, DMSO-d_6) δ 12.33 (s, 1H), 12.27 (s, 0.6H), 7.68 (d, *J* = 7.2 Hz, 1.6H), 7.64 – 7.57 (m, 3.2H), 7.50 (t, *J* = 6.8 Hz, 3.2H), 7.37 (s, 1.6H), 7.16 (d, *J* = 8.4 Hz, 1.6H), 7.05 (s, 6.4H), 2.23 (s, 4.8H); ^{13}C{^{1}H} NMR (100 MHz, DMSO-d_6) δ 154.0, 153.6, 144.4, 142.3, 141.1, 137.1, 136.6, 135.3, 133.5, 131.1, 130.6, 130.3, 129.6, 128.9, 128.7,

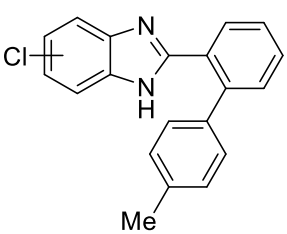

127.4, 126.7, 125.9, 122.4, 121.8, 120.2, 118.4, 112.8, 111.2, 20.8; IR (KBr) $\tilde{\nu}$ = 3051, 3022, 2911, 2858, 1615, 1538, 1470, 1455, 1424, 1388, 1296, 1096, 1058, 927, 818, 799, 768, 754 cm^{-1}; HR-MS (ESI-TOF) m/z calcd for $C_{20}H_{16}ClN_2$ $[M + H]^+$ 319.0997, found 319.0996.

2-(4'-(Tert-butyl)-[1,1'-biphenyl]-2-yl)-5-chloro-1H-benzo[d]imidazole OR 2-(4'-(Tert-butyl)-[1,1'-biphenyl]-2-yl)-6-chloro-1H-benzo[d]imidazole (3gc). R_f = 0.50 (hexane/ethyl acetate 4:1); Brownish Yellow solid; yield 95% (362 mg); mp 166−168 °C; ^{1}H NMR (400 MHz, DMSO-d_6) δ 12.32 (s, 1H), 7.67 (d, *J* = 7.6 Hz, 1H), 7.63 – 7.58 (m, 1H), 7.51 (d, *J* = 7.6 Hz, 3H), 7.48 (s, 1H), 7.27 (d, *J* = 8.4 Hz, 2H), 7.16 (dd, *J* = 8.4, 1.6 Hz, 1H), 7.11 (d, *J* = 8.4 Hz, 2H), 1.21 (s, 9H); ^{13}C{^{1}H} NMR (100 MHz, DMSO-d_6) δ 153.9, 149.6, 140.8, 137.1, 133.8, 131.3, 130.7, 130.3, 129.6, 128.5, 127.3, 126.1, 125.2, 122.1, 119.9, 118.5, 112.7, 34.3, 31.2; IR (KBr) $\tilde{\nu}$ = 3067, 3026, 2960, 2902, 2866, 1477, 1457, 1429, 1399, 1362, 1268, 1058, 923, 835, 763, 739 cm^{-1}; HR-MS (ESI-TOF) m/z calcd for $C_{23}H_{22}ClN_2$ $[M + H]^+$ 361.1466, found 361.1476.

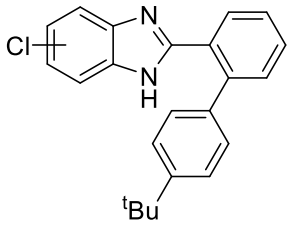

5-Chloro-2-(4'-fluoro-[1,1'-biphenyl]-2-yl)-1H-benzo[d]imidazole OR 6-Chloro-2-(4'-fluoro-[1,1'-biphenyl]-2-yl)-1H-benzo[d]imidazole (3gd). R_f = 0.40 (hexane/ethyl acetate 4:1); White solid; yield 92% (312 mg); mp 228−230 °C; ^{1}H NMR (700 MHz, DMSO-d_6) δ 12.38 (s, 1H), 7.73 (d, *J* = 7.7 Hz, 1H), 7.61 (t, *J* = 7.7 Hz, 1H), 7.57 – 7.50 (m, 3H), 7.40 (s, 1H), 7.19 – 7.15 (m, 3H), 7.08 (t, *J* = 8.4 Hz, 2H); ^{13}C{^{1}H} NMR (100 MHz, DMSO-d_6) δ 161.6 (d, *J* = 244.2 Hz), 153.5, 144.4, 140.1, 136.5, 131.1, 130.9 (d, *J* = 8.1 Hz), 130.7,

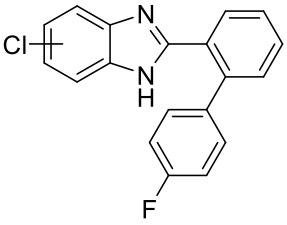

130.3, 129.6, 127.7, 122.4. 120.3, 118.4, 115.2 (d, J = 21.4 Hz), 112.9, 112.3; IR (KBr) $\tilde{\nu}$ = 3065, 2923, 2851, 1509, 1472, 1456, 1439, 1389, 1298, 1224, 1157, 1092, 1059, 923, 852, 834, 768, 755 cm^{-1}; HR-MS (ESI-TOF) m/z calcd for $C_{19}H_{13}ClFN_2$ $[M + H]^+$ 323.0746, found 323.0740.

Benzo[4,5]imidazo[1,2-f]phenanthridine (2aa).[37] R_f = 0.40 (hexane/ethyl acetate 9:1); pale yellow solid; yield 98% (58.4 mg); ^1H NMR (400 MHz, $CDCl_3$) δ 8.89 (d, J = 7.6 Hz, 1H),

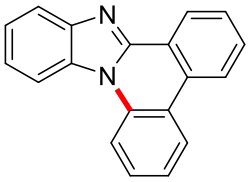

8.59 (d, J = 8.4 Hz, 1H), 8.51 (s, 1H), 8.40 (d, J = 8.0 Hz, 1H), 8.36 (d, J = 8.0 Hz, 1H), 8.06 (d, J = 7.6 Hz, 1H), 7.79 – 7.63 (m, 3H), 7.57 – 7.44 (m, 3H); $^{13}C\{^1H\}$ NMR (100 MHz, $CDCl_3$) δ 147.7, 144.7, 134.6, 132.1, 130.6, 129.7, 129.4, 128.8, 126.3, 124.7, 124.4, 124.3, 123.6, 123.1, 122.5, 121.9, 120.5, 116.2, 114.1.

2-Methylbenzo[4,5]imidazo[1,2-f]phenanthridine (2ab).[37] R_f = 0.60 (hexane/ethyl acetate 4:1); White solid; yield 93% (55.5 mg); mp 185−187 °C; ^1H NMR (400 MHz, $CDCl_3$) δ

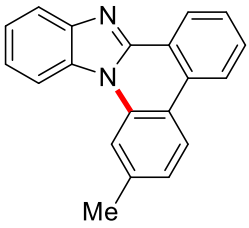

8.86 (dd, J = 8.0, 1.6 Hz, 1H), 8.37 – 8.33 (m, 3H), 8.32 (s, 1H), 8.08 – 8.00 (m, 1H), 7.75 – 7.69 (m, 1H), 7.68 – 7.62 (m, 1H), 7.55 – 7.50 (m, 1H), 7.50 – 7.44 (m, 1H), 7.31 (d, J = 8.0 Hz, 1H), 2.62 (s, 3H); $^{13}C\{^1H\}$ NMR (100 MHz, $CDCl_3$) δ 147.9, 144.7, 139.8, 134.7, 132.0, 130.5, 129.9, 128.3, 126.2, 125.8, 124.2, 124.2, 123.2, 122.9, 122.2, 120.5, 119.4, 116.5, 114.2, 22.1; IR (KBr) $\tilde{\nu}$ = 3060, 3029, 2920, 2851, 1613, 1536, 1447, 1363, 1347, 1282, 1256, 811, 764, 728, 713, 694 cm^{-1}; HR-MS (ESI-TOF) m/z calcd for $C_{20}H_{15}N_2$ $[M + H]^+$ 283.1230, found 283.1248.

2-(Tert-butyl)benzo[4,5]imidazo[1,2-f]phenanthridine (2ac). R_f = 0.45 (hexane/ethyl acetate 4:1); White solid; yield 88% (52.5 mg); mp 164−166 °C; ^{1}H NMR (700 MHz, $CDCl_3$) δ 8.89 (d, *J* = 7.7 Hz, 1H), 8.63 (d, *J* = 1.4 Hz, 1H), 8.44 (d, *J* = 8.4 Hz, 1H), 8.39 (d, *J* = 8.4 Hz, 1H), 8.36 (d, *J* = 7.7 Hz, 1H), 8.11 – 8.03 (m, 1H), 7.77 – 7.73 (m, 1H), 7.67 (t, *J* = 7.7 Hz, 1H), 7.59 (dd, *J* = 8.4, 1.4 Hz, 1H), 7.55 – 7.53 (m, 1H), 7.52 – 7.50 (m, 1H), 1.54 (s, 9H); ^{13}C{^{1}H} NMR (175 MHz, $CDCl_3$) δ 153.1, 148.0, 144.8, 134.6, 132.0, 130.6, 129.8, 128.4, 126.2, 124.2, 124.1, 123.4, 123.1, 122.3, 122.3, 120.6, 119.4, 114.0, 113.1, 35.6, 31.6; IR (KBr) $\tilde{\nu}$ = 3049, 2958, 2866, 1608, 1588, 1533, 1447, 1422, 1360, 1348, 1281, 1257, 1148, 1041, 864, 848, 767, 729, 694 cm^{-1}; HR-MS (ESI-TOF) m/z calcd for $C_{23}H_{21}N_2$ $[M + H]^+$ 325.1699, found 325.1683.

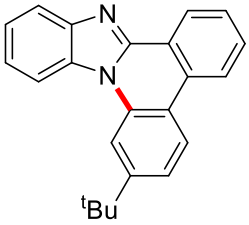

2-Fluorobenzo[4,5]imidazo[1,2-f]phenanthridine (2ad).[38] R_f = 0.40 (hexane/ethyl acetate 9:1); pale yellow solid; yield 84% (50 mg); ^{1}H NMR (400 MHz, $CDCl_3$) δ 8.82 – 8.70 (m, 1H), 8.35 (dd, *J* = 8.8, 6.0 Hz, 1H), 8.23 – 8.09 (m, 3H), 8.01 (t, *J* = 8.4 Hz, 1H), 7.71 – 7.58 (m, 2H), 7.56 – 7.41 (m, 2H), 7.21 – 7.07 (m, 1H); ^{13}C{^{1}H} NMR (100 MHz, $CDCl_3$) δ 162.9 (d, $J_{C,F}$ = 248.7 Hz), 147.7, 144.6, 135.3 (d, $J_{C,F}$ = 10.6 Hz), 131.7, 130.7, 129.1, 128.6, 127.9, 126.1 (d, $J_{C,F}$ = 12.5 Hz), 124.6, 123.3, 122.9, 122.1, 120.6, 118.2, 113.6, 112.1 (d, $J_{C,F}$ = 22.1 Hz), 103.3 (d, $J_{C,F}$ = 27.0 Hz).

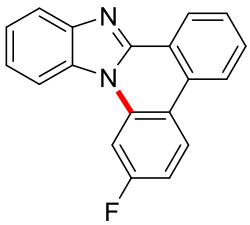

2-Ethylbenzo[4,5]imidazo[1,2-f]phenanthridine (2ae).[24] R_f = 0.60 (hexane/ethyl acetate 4:1); pale yellow solid; yield 87% (52 mg); ^{1}H NMR (400 MHz, $CDCl_3$) δ 8.86 (d, *J* = 7.6 Hz, 1H), 8.39 (s, 2H), 8.36 (dd, *J* = 7.6, 4.8 Hz, 2H), 8.06 (d, *J* = 7.6 Hz,

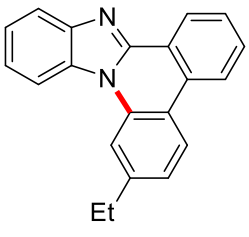

1H), 7.72 (t, *J* = 7.6 Hz, 1H), 7.65 (t, *J* = 7.6 Hz, 1H), 7.55 – 7.46 (m, 2H), 7.36 (d, *J* = 8.0 Hz, 1H), 2.93 (q, *J* = 7.6 Hz, 2H), 1.43 (t, *J* = 7.6 Hz, 3H); $^{13}C\{^{1}H\}$ NMR (100 MHz, $CDCl_3$) δ 147.9, 146.1, 144.7, 134.8, 132.1, 130.6, 129.9, 128.3, 126.2, 124.6, 124.4, 124.2, 123.2, 122.9, 122.2, 120.5, 119.6, 115.3, 114.1, 29.3, 15.7.

2-Methoxybenzo[4,5]imidazo[1,2-f]phenanthridine (2af).[39] R_f = 0.60 (hexane/ethyl acetate 4:1); White solid; yield 95% (56.5 mg); mp 218−220 °C; ^{1}H NMR (400 MHz, $CDCl_3$) δ

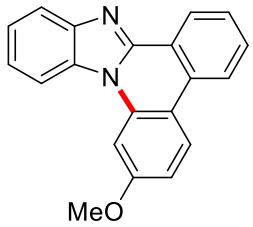

8.80 (d, *J* = 6.0 Hz, 1H), 8.18 (d, *J* = 6.4 Hz. 3H), 8.03 (d, *J* = 4.8 Hz, 1H), 7.87 (s, 1H), 7.63 (d, *J* = 8.8 Hz, 1H), 7.58 (d, *J* = 4.8 Hz, 1H), 7.50 (t, *J* = 8.8 Hz, 1H), 7.44 (d, *J* = 6.0 Hz, 1H), 7.01 – 6.88 (m, 1H), 3.95 (s, 3H); $^{13}C\{^{1}H\}$ NMR (100 MHz, $CDCl_3$) δ 160.3, 147.6, 144.1, 135.2, 131.6, 130.6, 129.7, 127.5, 126.1, 125.3, 124.3, 122.9, 121.8, 121.6, 120.1, 114.9, 113.8, 110.8, 101.2, 55.7; IR (KBr) $\tilde{\nu}$ = 3053, 2936, 2839, 1625, 1560, 1537, 1448, 1432, 1363, 1261, 1218, 1169, 1147, 1135, 1050, 1021, 816, 754, 720 cm^{-1}; HR-MS (ESI-TOF) m/z calcd for $C_{20}H_{15}N_2O$ $[M + H]^+$ 299.1179, found 299.1173.

2-(Trifluoromethyl)benzo[4,5]imidazo[1,2-f]phenanthridine (2ag).[39] R_f = 0.50 (hexane/ethyl acetate 4:1); White solid; yield 76% (45.4 mg); mp 207−209 °C; ^{1}H NMR

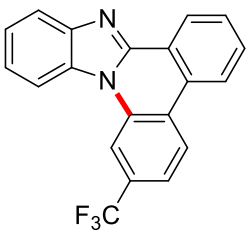

(400 MHz, $CDCl_3$) δ 8.84 – 8.77 (m, 1H), 8.71 (s, 1H), 8.49 (d, *J* = 8.4 Hz, 1H), 8.34 – 8.28 (m, 1H), 8.22 (dd, *J* = 6.8, 2.4 Hz, 1H), 8.02 (dd, *J* = 6.8, 2.4 Hz, 1H), 7.77 – 7.66 (m, 3H), 7.58 – 7.48 (m, 2H); $^{13}C\{^{1}H\}$ NMR (100 MHz, $CDCl_3$) δ 147.3, 144.7, 134.3, 131.7, 131.1 (q, $J_{C,F}$ = 33.3 Hz), 130.8, 129.9, 128.4, 126.3, 125.0, 124.8, 124.6, 124.2, 123.9 (q, $J_{C,F}$ = 272.8 Hz), 123.7, 122.8, 120.9, 113.7, 113.1; IR (KBr) $\tilde{\nu}$ = 3077, 3029, 1615, 1543, 1448, 1430, 1362,

1309, 1291, 1273, 1133, 1116, 1079, 989, 853, 823, 770, 733, 712 cm^{-1}; HR-MS (ESI-TOF) m/z calcd for $C_{20}H_{12}F_3N_2$ $[M + H]^+$ 337.0947, found 337.0941.

11,12-Dimethylbenzo[4,5]imidazo[1,2-f]phenanthridine) (2ba).[37] R_f = 0.60 (hexane/ethyl acetate 4:1); white solid; yield 94% (56 mg); ^1H NMR (400 MHz, $CDCl_3$) δ 8.83 (d, *J* = 7.6 Hz, 1H), 8.50 (dd, *J* = 8.4, 3.6 Hz, 1H), 8.45 (d, *J* = 8.0 Hz, 1H), 8.35 (d, *J* = 7.6 Hz, 1H), 8.05 (d, *J* = 2.8 Hz, 1H), 7.77 (s, 1H), 7.74 – 7.62 (m, 3H), 7.48 (dd, *J* = 10.4, 4.8 Hz, 1H), 2.52 (s, 3H), 2.46 (s, 3H); $^{13}C\{^1H\}$ NMR (100 MHz, $CDCl_3$) δ 147.0, 143.3, 134.7, 133.3, 132.2, 130.5, 130.2, 129.4, 129.2, 128.7, 126.0, 124.3 (×2), 123.9, 122.4, 121.8, 120.5, 116.1, 114.3, 21.2, 20.5.

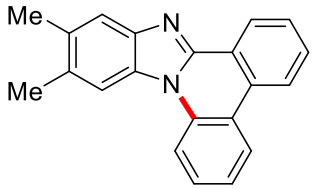

2,11,12-Trimethylbenzo[4,5]imidazo[1,2-f]phenanthridine (2bb). R_f = 0.50 (hexane/ethyl acetate 4:1); White solid; yield 91% (54 mg); mp 192−194 °C; ^1H NMR (700 MHz, $CDCl_3$) δ 8.80 (d, *J* = 7.7 Hz, 1H), 8.29 (d, *J* = 3.5 Hz, 1H), 8.28 (d, *J* = 3.5 Hz, 1H), 8.25 (s, 1H), 8.02 (s, 1H), 7.76 (s, 1H), 7.67 (t, *J* = 7.7 Hz, 1H), 7.62 (t, *J* = 7.7 Hz, 1H), 7.25 (s, 1H), 2.61 (s, 3H), 2.53 (s, 3H), 2.46 (s, 3H); $^{13}C\{^1H\}$ NMR (175 MHz, $CDCl_3$) δ 147.2, 143.3, 139.6, 134.7, 133.2, 132.0, 130.5, 130.1, 129.6, 128.2, 126.0, 125.4, 124.1, 123.4, 122.1, 120.4, 119.3, 116.3, 114.3, 22.1, 21.2, 20.5; IR (KBr) $\tilde{\nu}$ = 3077, 3024, 2917, 2853, 1615, 1590, 1537, 1461, 1425, 1362, 1346, 1324, 1272, 1141, 1091, 861, 840, 815, 765, 713 cm^{-1}; HR-MS (ESI-TOF) m/z calcd for $C_{22}H_{19}N_2$ $[M + H]^+$ 311.1543, found 311.1539.

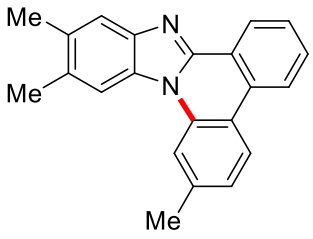

2-(Tert-butyl)-11,12-dimethylbenzo[4,5]imidazo[1,2-f]phenanthridine (2bc).[24] R_f = 0.65 (hexane/ethyl acetate 4:1); white solid; yield 86% (51 mg); ^{1}H NMR (400 MHz, $CDCl_3$) δ

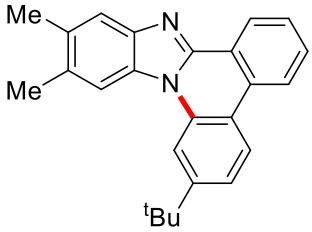

8.83 (dd, *J* = 8.0, 1.6 Hz, 1H), 8.58 (d, *J* = 1.6 Hz, 1H), 8.40 (d, *J* = 8.4 Hz, 1H), 8.35 (d, *J* = 8.0Hz, 1H), 8.09 (s, 1H), 7.80 (s, 1H), 7.72 – 7.67 (m, 1H), 7.66 – 7.60 (m, 1H), 7.56 (dd, *J* = 8.4, 1.6 Hz, 1H), 2.55 (s, 3H), 2.48 (s, 3H), 1.54 (s, 9H); ^{13}C{^{1}H} NMR (100 MHz, $CDCl_3$) δ 152.9, 147.3, 143.4, 134.6, 133.2, 132.0, 130.5, 130.2, 129.5, 128.3, 126.0, 124.0, 123.6, 122.2, 121.9, 120.5, 119.3, 114.4, 112.9, 35.5, 31.6, 21.5, 20.6.

2-Fluoro-11,12-dimethylbenzo[4,5]imidazo[1,2-f]phenanthridine (2bd).[24] R_f = 0.60 (hexane/ethyl acetate 4:1); white solid; yield 82% (49 mg); ^{1}H NMR (400 MHz, $CDCl_3$) δ

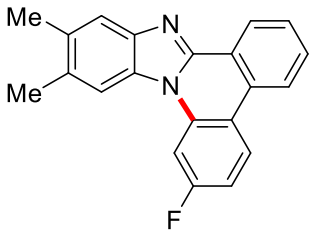

8.84 – 8.74 (m, 1H), 8.40 (dd, *J* = 8.8, 6.0 Hz, 1H), 8.26 (d, *J* = 8.1 Hz, 1H), 8.16 (dd, *J* = 10.4, 2.4 Hz, 1H), 7.94 (s, 1H), 7.78 (s, 1H), 7.66 – 7.72 (m, 1H), 7.64 (t, *J* = 7.2 Hz, 1H), 7.23 – 7.15 (m, 1H), 2.53 (s, 3H), 2.46 (s, 3H); ^{13}C{^{1}H} NMR (100 MHz, $CDCl_3$) δ 162.9 (d, $J_{C,F}$ = 248.1 Hz), 147.0, 143.2, 135.5 (d, $J_{C,F}$ = 10.2 Hz), 133.7, 132.6, 130.4, 130.2, 128.9, 128.5, 126.1, 126.1, 123.2, 122.2, 120.6, 118.2, 113.9, 111.8 (d, $J_{C,F}$ = 22.4 Hz), 103.3 (d, $J_{C,F}$ = 26.8 Hz), 21.2, 20.6.

2-Ethyl-11,12-dimethylbenzo[4,5]imidazo[1,2-f]phenanthridine (2be).[24] R_f = 0.60 (hexane/ethyl acetate 4:1); white solid; yield 88% (52.5 mg); ^{1}H NMR (400 MHz, $CDCl_3$) δ

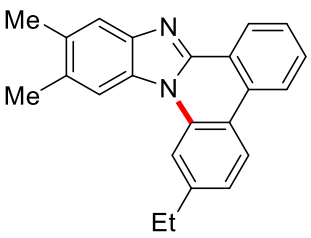

8.84 – 8.74 (m, 1H), 8.31 – 8.19 (m, 3H), 7.96 (s, 1H), 7.74 (s, 1H), 7.72 – 7.58 (m, 2H), 7.33 – 7.21 (m, 1H), 2.95 – 2.87 (m, 2H), 2.52 (s, 3H), 2.46 (s, 3H), 1.44 (s, 3H). ^{13}C{^{1}H} NMR (100 MHz,

$CDCl_3$) δ 146.9, 145.7, 143.1, 134.6, 133.1, 131.9, 130.4, 130.0, 129.5, 128.1, 125.9, 124.1, 124.0, 123.2, 122.0, 120.2, 119.3, 115.0, 114.2, 29.2, 21.3, 20.5, 15.5.

2-Methoxy-11,12-dimethylbenzo[4,5]imidazo[1,2-f]phenanthridine (2bf). R_f = 0.40 (hexane/ethyl acetate 4:1); white solid; yield 86% (51.5 mg); mp 180−181 °C; ^{1}H NMR (400 MHz, $CDCl_3$) δ 8.75 (s, 1H), 8.25 – 8.04 (m, 2H), 7.94 – 7.76 (m, 2H), 7.72 (d, *J* = 6.4 Hz, 1H), 7.65 – 7.51 (m, 2H), 6.90 (d, *J* = 8.4 Hz, 1H), 3.92 (s, 3H), 2.45 (s, 3H), 2.42 (s, 3H); ^{13}C{^{1}H} NMR (100 MHz, $CDCl_3$) δ 160.3, 147.1, 142.8, 135.5, 133.3, 132.0, 130.2, 130.1, 129.6, 127.5, 125.9, 125.3, 122.3, 121.7, 120.2, 114.9, 114.1, 110.2, 101.5, 55.7, 21.2, 20.5; IR (KBr) $\tilde{\nu}$ = 2966, 2920, 2839, 1614, 1591, 1536, 1460, 1433, 1347, 1317, 1220, 1177, 1088, 1045, 835, 816, 768, 762 cm^{-1}; HR-MS (ESI-TOF) m/z calcd for $C_{22}H_{19}N_2O$ $[M + H]^+$ 327.1492, found 327.1482.

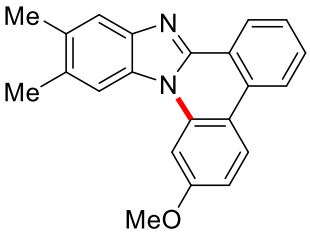

11,12-Dimethyl-2-(trifluoromethyl)benzo[4,5]imidazo[1,2-f]phenanthridine (2bg). R_f = 0.60 (hexane/ethyl acetate 4:1); White solid; yield 74% (44 mg); mp 252−254 °C; ^{1}H NMR (400 MHz, $CDCl_3$) δ 8.69 (d, *J* = 7.6 Hz, 1H), 8.54 (s, 1H), 8.42 (d, *J* = 8.4 Hz, 1H), 8.25 (d, *J* = 8.0 Hz, 1H), 7.78 (s, 1H), 7.75 – 7.70 (m, 2H), 7.66 (t, *J* = 8.0 Hz, 2H), 2.48 (s, 3H), 2.41 (s, 3H); ^{13}C{^{1}H} NMR (100 MHz, $CDCl_3$) δ 144.9, 139.0, 135.5, 134.3, 133.1, 131.6, 131.1 (q, $J_{C,F}$ = 33.3 Hz), 130.3, 128.9, 128.3, 126.5, 124.5, 123.7 (q, $J_{C,F}$ = 272.8 Hz), 122.8, 121.7, 121.5 (q, $J_{C,F}$ = 3.6 Hz), 119.3, 113.9, 113.3 (q, $J_{C,F}$ = 4.0 Hz), 21.3, 20.5; IR (KBr) $\tilde{\nu}$ = 3026, 2923, 2855, 1680, 1627, 1465, 1433, 1363, 1335, 1309, 1171,

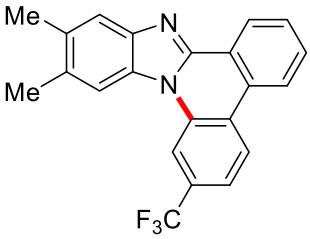

1119, 1081, 856, 768, 747, 734, 716 cm^{-1}; HR-MS (ESI-TOF) m/z calcd for $C_{22}H_{16}F_3N_2$ $[M + H]^+$ 365.1260, found 365.1266.

3-Chloro-11,12-dimethylbenzo[4,5]imidazo[1,2-f]phenanthridine (2bh).[24] R_f = 0.65 (hexane/ethyl acetate 4:1); white solid; yield 78% (31 mg); ^1H NMR (400 MHz, $CDCl_3$) δ 8.88 – 8.72 (m, 1H), 8.47 (d, *J* = 8.8 Hz, 1H), 8.43 (d, *J* = 2.4 Hz, 1H), 8.31 (d, *J* = 8.8 Hz, 1H), 8.02 (s, 1H), 7.79 (s, 1H), 7.76 – 7.69 (m, 2H), 7.69 – 7.62 (m, 1H), 2.54 (s, 3H), 2.49 (s, 3H).

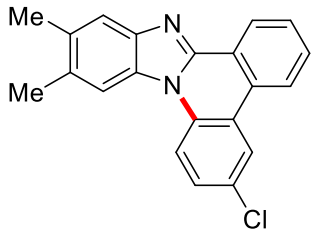

7-Fluoro-11,12-dimethylbenzo[4,5]imidazo[1,2-f]phenanthridine (2bi).[24] R_f = 0.70 (hexane/ethyl acetate 4:1); white solid; yield 93% (55.3 mg); ^1H NMR (400 MHz, $CDCl_3$) δ 8.64 (t, *J* = 7.6 Hz, 1H), 8.47 (dd, *J* = 8.4, 5.6 Hz, 3H), 8.19 (d, *J* = 4.8 Hz, 1H), 7.88 (dd, *J* = 8.4, 3.6 Hz, 1H), 7.74 (d, *J* = 5.6 Hz, 2H), 7.64 (s, 1H), 2.52 (s, 3H), 2.43 (s, 3H); $^{13}C\{^1H\}$ NMR (100 MHz, $CDCl_3$) δ 162.9 (d, $J_{C,F}$ = 255.3 Hz), 140.8, 139.3, 137.5, 131.2, 131.1, 131.1, 130.9, 130.6 (d, $J_{C,F}$ = 2.6 Hz), 128.0, 127.4 (d, $J_{C,F}$ = 12.3 Hz), 126.0 (d, $J_{C,F}$ = 8.6 Hz), 124.7, 123.1 (d, $J_{C,F}$ = 23.6 Hz), 121.7, 117.5, 115.5, 115.4, 112.0 (d, $J_{C,F}$ = 23.0 Hz), 21.2, 20.4.

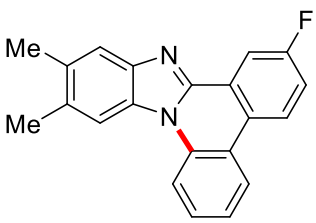

11,12-Dichlorobenzo[4,5]imidazo[1,2-f]phenanthridine (2ca).[37] R_f = 0.55 (hexane/ethyl acetate 4:1); white solid; yield 96% (57.3 mg); ^1H NMR (400 MHz, $CDCl_3$) δ 8.71 (d, *J* = 8.0 Hz, 1H), 8.41 (d, *J* = 8.0 Hz, 1H), 8.32 (s, 1H), 8.29 (d, *J* = 4.0 Hz, 1H), 8.22 (d, *J* = 8.4 Hz, 1H), 7.98 (s, 1H), 7.73 (t, *J* = 7.6 Hz,

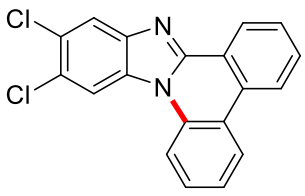

1H), 7.66 (td, *J* = 7.2, 4.0 Hz, 2H), 7.50 (t, *J* = 8.0 Hz, 1H); $^{13}C\{^{1}H\}$ NMR (175 MHz, $CDCl_3$) δ 149.2, 144.0, 133.7, 131.2, 130.8, 129.7, 129.5, 128.9, 128.3, 126.5, 126.3, 125.2, 124.5, 122.9, 122.4, 121.8, 121.1, 115.7, 115.2.

11,12-Dichloro-2-methylbenzo[4,5]imidazo[1,2-f]phenanthridine (2cb). R_f = 0.50 (hexane/ethyl acetate 4:1); White solid; yield 92% (55 mg); mp 235−237 °C; ^{1}H NMR (400

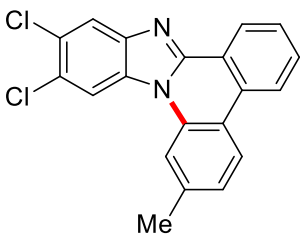

MHz, $CDCl_3$ + TFA-D) δ 8.72 (d, *J* = 8.0 Hz, 1H), 8.67 (s, 1H), 8.57 (dd, *J* = 8.4, 1.6 Hz, 2H), 8.33 (s, 1H), 8.16 (s. 1H), 8.07 (t, *J* = 7.6 Hz, 1H), 7.90 (t, *J* = 7.6 Hz, 1H), 7.68 (d, *J* = 8.4 Hz, 1H), 2.75 (s, 3H); $^{13}C\{^{1}H\}$ NMR (100 MHz, $CDCl_3$ + TFA-D) δ 144.6, 143.0, 135.7, 133.9, 131.9, 131.7, 131.1, 130.5, 130.1, 127.9, 126.5, 125.2, 123.2, 120.1, 117.2, 117.1, 116.6, 114.8, 113.6, 22.3; IR (KBr) $\tilde{\nu}$ = 3043, 2923, 2852 1616, 1533, 1462, 1442, 1357, 1316, 1290, 1270, 1142, 1109, 964, 883, 859, 835, 758, 711, 694 cm^{-1}; HR-MS (ESI-TOF) m/z calcd for $C_{20}H_{13}Cl_2N_2$ $[M + H]^+$ 351.0450, found 351.0460.

2-(Tert-butyl)-11,12-dichlorobenzo[4,5]imidazo[1,2-f]phenanthridine (2cc).[24] R_f = 0.60 (hexane/ethyl acetate 4:1); white solid; yield 89% (53 mg); ^{1}H NMR (400 MHz, $CDCl_3$) δ

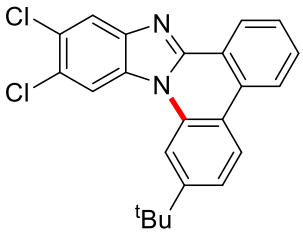

8.70 (d, *J* = 6.8 Hz, 1H), 8.42 – 8.33 (m, 1H), 8.28 (s, 3H), 7.98 (d, *J* = 2.4 Hz, 1H), 7.72 (s, 1H), 7.65 – 7.54 (m, 2H), 1.53 (s, 9H); $^{13}C\{^{1}H\}$ NMR (100 MHz, $CDCl_3$) δ 153.4, 149.4, 144.1, 133.7, 131.1, 130.8, 129.8, 128.5, 128.1, 126.3, 126.2, 124.2, 122.9, 122.6, 122.3, 121.1, 119.3, 115.2, 112.4, 35.5, 31.5.

11,12-Dichloro-2-fluorobenzo[4,5]imidazo[1,2-f]phenanthridine (2cd).[24] R_f = 0.60 (hexane/ethyl acetate 4:1); white solid; yield 85% (51 mg); ^{1}H NMR (400 MHz, $CDCl_3$ + TFA-D) δ 8.78 (dd, *J* = 9.2, 6.0 Hz, 1H), 8.67 (s, 1H), 8.62 (d, *J* = 8.4 Hz, 1H), 8.36 (d, *J* = 2.4 Hz, 1H), 8.34 (d, *J* = 2.4 Hz, 1H), 8.23 (s, 1H), 8.15 (t, *J* = 7.6 Hz, 1H), 7.98 (t, *J* = 7.6 Hz, 1H), 7.72 – 7.62 (m, 1H); ^{13}C{^{1}H} NMR (100 MHz, $CDCl_3$ + TFA-D) δ 163.7 (d, $J_{C,F}$ = 250.2 Hz), 145.0, 136.2, 134.4, 132.3, 131.9 (d, $J_{C,F}$ = 10.2 Hz), 131.4, 131.1, 131.0, 127.8 (d, $J_{C,F}$ = 9.2 Hz), 126.8, 123.4, 119.3 (d, $J_{C,F}$ = 2.8 Hz), 117.2, 116.9 (d, $J_{C,F}$ = 18.2 Hz), 116.2, 115.0, 113.3, 104.8 (d, $J_{C,F}$ = 27.7 Hz).

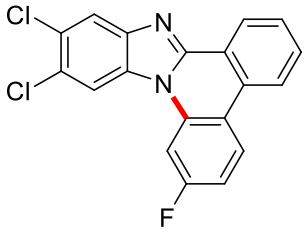

11,12-Dichloro-2-ethylbenzo[4,5]imidazo[1,2-f]phenanthridine (2ce).[24] R_f = 0.60 (hexane/ethyl acetate 4:1); white solid; yield 91% (54.3 mg); ^{1}H NMR (400 MHz, $CDCl_3$ + TFA-D) δ 8.61 (d, *J* = 8.0 Hz, 1H), 8.46 – 8.30 (m, 3H), 8.09 (s, 2H), 7.91 (t, *J* = 7.6 Hz, 1H), 7.73 (t, *J* = 7.6 Hz, 1H), 7.55 (d, *J* = 8.0 Hz, 1H), 2.96 (q, *J* = 7.6 Hz, 2H), 1.43 (t, *J* = 7.6 Hz, 3H); ^{13}C{^{1}H} NMR (100 MHz, $CDCl_3$ + TFA-D) δ 148.4, 145.2, 134.5, 133.8, 132.4, 131.3, 131.1, 130.3, 129.9, 128.0, 127.9, 126.8, 124.9, 122.8, 119.7, 117.7, 116.4, 116.2, 115.5, 29.2, 15.4.

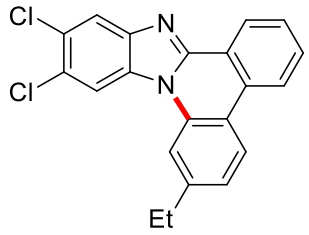

11,12-Dichloro-2-(trifluoromethyl)benzo[4,5]imidazo[1,2-f]phenanthridine (2cg).[24] R_f = 0.70 (hexane/ethyl acetate 4:1); white solid; yield 79% (47 mg); ^{1}H NMR (400 MHz, $CDCl_3$) δ 8.64 (d, *J* = 7.6 Hz, 1H), 8.50 (d, *J* = 8.0 Hz, 1H), 8.38 (s, 1H), 8.31 (d, *J* = 8.0 Hz, 1H), 8.13 (s, 1H), 7.91 (s, 1H), 7.83 – 7.66 (m, 3H); ^{13}C{^{1}H} NMR (100 MHz, $CDCl_3$) δ 148.9, 143.9, 133.5,

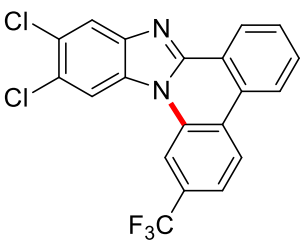

131.5, 131.1 (q, $J_{C,F}$ = 32.8 Hz), 130.2, 128.9, 128.5, 127.3, 126.7 (q, $J_{C,F}$ = 272 Hz), 126.5, 125.3, 124.8, 123.5, 122.9, 121.6 (q, $J_{C,F}$ = 3.2 Hz), 121.5, 114.8, 112.8 (q, $J_{C,F}$ = 3.8 Hz).

3,11,12-Trichlorobenzo[4,5]imidazo[1,2-f]phenanthridine (2ch).[24] R_f = 0.70 (hexane/ethyl acetate 4:1); white solid; yield 87% (52 mg); ^{1}H NMR (400 MHz, $CDCl_3$ + TFA-D) δ 8.66 (d, *J* = 8.0 Hz, 1H), 8.37 (s, 1H), 8.33 – 8.24 (m, 2H), 8.20 (d, *J* = 8.8 Hz, 1H), 8.11 (s, 1H), 7.90 (t, *J* = 7.6 Hz, 1H), 7.80 (t, *J* = 7.6 Hz, 1H), 7.66 (d, *J* = 8.8 Hz, 1H); ^{13}C{^{1}H} NMR (100 MHz, $CDCl_3$ + TFA-D) δ 146.2, 136.8, 133.7, 133.2, 131.7, 130.8, 130.5, 130.1, 129.8, 129.3, 128.5, 126.9, 124.6, 123.5, 122.9, 118.9, 118.8, 117.7, 115.7.

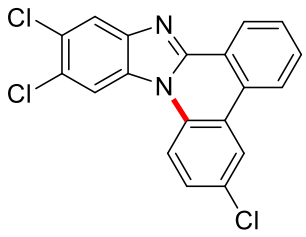

11,12-Dichloro-7-fluorobenzo[4,5]imidazo[1,2-f]phenanthridine (2ci).[24] R_f = 0.65 (hexane/ethyl acetate 4:1); White solid; yield 97% (58 mg); ^{1}H NMR (400 MHz, $CDCl_3$ + TFA-D) δ 8.71 (s, 1H), 8.68 – 8.62 (m, 2H), 8.62 (d, *J* = 8.4 Hz, 1H), 8.53 (d, *J* = 6.4 Hz, 1H), 8.22 (s, 1H), 8.01 (t, *J* = 8.0 Hz, 1H), 7.89 (t, *J* = 8.0 Hz, 1H), 7.81 (t, *J* = 7.6 Hz, 1H); ^{13}C{^{1}H} NMR (100 MHz, $CDCl_3$ + TFA-D) δ 163.1 (d, $J_{C,F}$ = 255.8 Hz), 143.8, 134.1, 131.9 (d, $J_{C,F}$ = 23.4 Hz), 131.4, 130.8, 128.8, 128.2 (d, $J_{C,F}$ = 24.0 Hz), 126.4 (d, $J_{C,F}$ = 8.5 Hz), 125.2, 124.33 (d, $J_{C,F}$ = 23.2 Hz), 122.1, 119.3, 117.2, 117.1, 116.5, 113.6, 112.42 (d, $J_{C,F}$ = 25.1 Hz), 110.8.

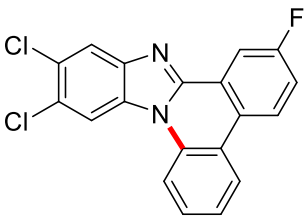

11,12-Difluorobenzo[4,5]imidazo[1,2-f]phenanthridine (2da). R_f = 0.60 (hexane/ethyl acetate 4:1); White solid; yield 90% (54 mg), mp 239−241 °C; ^{1}H NMR (700 MHz, $CDCl_3$) δ 8.81 (d, *J* = 7.6 Hz, 1H), 8.50 (d, *J* = 7.7 Hz, 1H), 8.39 (d, *J* = 7.9 Hz, 1H), 8.33 (d, *J* = 8.1 Hz, 1H), 8.14 (dd, *J* = 10.2, 7.1 Hz, 1H), 7.82 – 7.74 (m, 2H), 7.74 –

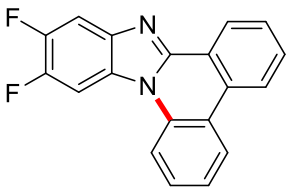

7.66 (m, 2H), 7.56 (t, *J* = 7.3 Hz, 1H); $^{13}C\{^{1}H\}$ NMR (175 MHz, $CDCl_3$) δ 148.9, 148.8 (d, *J* = 244.6 Hz), 148.7 (d, *J* = 244.5 Hz), 148.4 (d, *J* = 15.1 Hz), 147.1 (d, *J* = 15.0 Hz), 140.3 (d, *J* = 11.2 Hz), 133.8, 130.9, 129.6, 129.6, 129.0, 126.8 (d, *J* = 10.3 Hz), 126.1, 125.2, 124.6, 123.1, 122.5, 121.9, 115.5, 107.5 (d, *J* = 19.4 Hz), 102.5 (d, *J* = 24.7 Hz); IR (KBr) $\tilde{\nu}$ = 3036, 2921, 2852, 1591, 1542, 1477, 1463, 1452, 1348, 1230, 1147, 1126, 905, 830, 753, 709 cm^{-1}; HR-MS (ESI-TOF) m/z calcd for $C_{19}H_{11}F_2N_2$ $[M + H]^+$ 305.0885, found 305.0886.

2-Ethyl-11,12-difluorobenzo[4,5]imidazo[1,2-f]phenanthridine (2de). R_f = 0.60 (hexane/ethyl acetate 4:1); White solid; yield 92% (55 mg), mp 250−252 °C; ^{1}H NMR (700 MHz, $CDCl_3$+ TFA-D) δ 8.76 (d, *J* = 8.4 Hz, 1H), 8.64 (d, *J* = 8.4 Hz, 1H), 8.61 (d, *J* = 8.4 Hz, 1H), 8.47 (dd, *J* = 9.1, 6.3 Hz, 1H), 8.37 (s, 1H), 8.07 (t, *J* = 7.7 Hz, 1H), 7.98 (t, *J* = 7.7 Hz, 1H), 7.90 (t, *J* = 7.7 Hz, 1H), 7.74 (d, *J* = 8.4 Hz, 1H), 3.06 (q, *J* = 7.7 Hz, 2H), 1.48 (t, *J* = 7.7 Hz, 3H); $^{13}C\{^{1}H\}$ NMR (175 MHz, $CDCl_3$+ TFA-D) δ 151.0 (d, *J* = 255.6 Hz), 150.9 (d, *J* = 255.6 Hz), 150.4 (d, *J* = 14.8 Hz), 148.9, 144.7, 135.4, 131.5 (d, *J* = 61.6 Hz), 130.4, 128.8, 128.4 (d, *J* = 10.9 Hz), 126.2, 125.4, 124.4 (d, *J* = 9.4 Hz), 123.3, 120.4, 117.5, 115.9, 115.7, 115.2, 114.3, 112.6, 105.2 (d, *J* = 25.6 Hz), 104.1 (d, *J* = 23.1 Hz), 29.4, 15.5 (s); IR (KBr) $\tilde{\nu}$ = 3017, 2966, 2928, 1614, 1590, 1540, 1480, 1462, 1453, 1427, 1370, 1350, 1177, 1158, 1142, 900, 794, 762 cm^{-1}; HR-MS (ESI-TOF) m/z calcd for $C_{21}H_{15}F_2N_2$ $[M + H]^+$ 333.1198, found 333.1202.

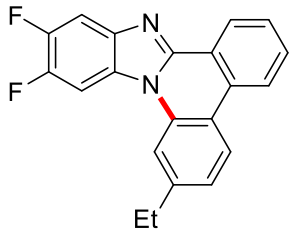

11-Bromo-2-methylbenzo[4,5]imidazo[1,2-f]phenanthridine or 12-Bromo-2-methylbenzo[4,5]imidazo[1,2-f]phenanthridine (4db). R_f = 0.55 (hexane/ethyl acetate 4:1); White solid; yield 89% (53 mg); mp 200−202 °C; ^{1}H NMR (700 MHz, $CDCl_3$) δ 8.73 (dd,

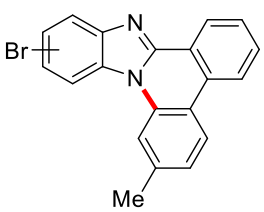

J = 7.7, 0.7 Hz, 1H), 8.23 (t, *J* = 8.4 Hz, 2H), 8.09 (d, *J* = 1.4 Hz, 1H), 8.06 (s, 1H), 8.05 (d, *J* = 8.4 Hz, 1H), 7.71 – 7.65 (m, 1H), 7.61 (t, *J* = 7.0 Hz, 1H), 7.48 (dd, *J* = 8.4, 1.4 Hz, 1H), 7.24 (d, *J* = 7.7 Hz, 1H), 2.55 (s, 3H); $^{13}C\{^{1}H\}$ NMR (175 MHz, $CDCl_3$) δ 148.6, 145.9, 139.9, 134.0, 130.8, 130.8, 129.9, 128.3, 126.2, 126.0, 125.6, 124.2, 123.0, 122.6, 122.1, 119.3, 117.3, 116.1, 115.1, 22.1; IR (KBr) $\tilde{\nu}$ = 3055, 2920, 2851, 1675, 1606, 1584, 1532, 1460, 1434, 1360, 1348, 1286, 1257, 1170, 1059, 919, 872, 812, 761, 733, 712, 696 cm^{-1}; HR-MS (ESI-TOF) m/z calcd for $C_{20}H_{14}BrN_2$ $[M + H]^+$ 361.0335, found 361.0333.

11-Bromo-2-fluorobenzo[4,5]imidazo[1,2-f]phenanthridine or 12-Bromo-2-fluorobenzo[4,5]imidazo[1,2-f]phenanthridine (4dd). R_f = 0.60 (hexane/ethyl acetate 4:1); White solid; yield 82% (49 mg); mp 234−235 °C; ^{1}H NMR (400 MHz, $CDCl_3$) δ 8.66 (dd, *J* = 8.0, 1.2 Hz, 1H), 8.31 (dd, *J* = 8.8, 6.0 Hz, 1H), 8.16 (d, *J* = 8.0 Hz, 1H), 8.04 (d, *J* = 2.0 Hz, 1H), 7.95 – 7.93 (m, 1H), 7.91 – 7.90 (m, 1H), 7.72 – 7.65 (m, 1H), 7.64 – 7.57 (m, 1H), 7.48 (dd, *J* = 8.8, 2.0 Hz, 1H), 7.19 – 7.13 (m, 1H); $^{13}C\{^{1}H\}$ NMR (100 MHz, $CDCl_3$) δ 162.9 (d, $J_{C,F}$ = 249.5 Hz), 148.5 146.0 134.8 (d, $J_{C,F}$ = 10.6 Hz), 131.1 130.6 129.2 128.7 126.3 126.2 126.1 123.4 122.5 122.2 118.3 117.7 114.5 112.5 (d, $J_{C,F}$ = 22.1 Hz), 103.3(d, $J_{C,F}$ = 27.0 Hz); IR (KBr) $\tilde{\nu}$ = 3077, 3046, 2922, 2852, 1619, 1567, 1537, 1461, 1436, 1361, 1349, 1288, 1274, 1171, 1058, 920, 881, 857, 825, 767, 756, 743, 733, 715 cm^{-1}; HR-MS (ESI-TOF) m/z calcd for $C_{19}H_{11}BrFN_2$ $[M + H]^+$ 365.0084, found 365.0056.

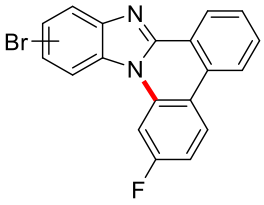

11-Bromo-2-ethylbenzo[4,5]imidazo[1,2-f]phenanthridine or 12-Bromo-2-ethylbenzo[4,5]imidazo[1,2-f]phenanthridine (4de). R_f = 0.70 (hexane/ethyl acetate 4:1); White solid; yield 88% (52.5 mg); mp 194−196 °C; ^{1}H NMR (700 MHz, $CDCl_3$) δ 8.79 (d, *J*

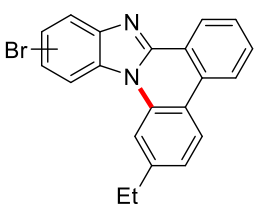

= 7.7 Hz, 1H), 8.35 (d, *J* = 8.4 Hz, 1H), 8.32 (d, *J* = 7.7 Hz, 1H), 8.22 (s, 1H), 8.17 – 8.12 (m, 2H), 7.72 (t, *J* = 7.0 Hz, 1H), 7.64 (t, *J* = 7.0 Hz, 1H), 7.53 (d, *J* = 8.4 Hz, 1H), 7.36 (d, *J* = 8.4 Hz, 1H), 2.91 (q, *J* = 7.7 Hz, 2H), 1.42 (t, *J* = 7.7 Hz, 3H); $^{13}C\{^{1}H\}$ NMR (175 MHz, $CDCl_3$) δ 148.8, 146.2, 146.1, 134.3, 130.9, 130.9, 129.9, 128.4, 126.3, 125.7, 124.9, 124.4, 123.2, 122.8, 122.2, 119.6, 117.3, 115.1, 115.1, 29.3, 15.6; IR (KBr) $\tilde{\nu}$ = 3048, 2959, 2921, 2855, 1730, 1608, 1529, 1450, 1432, 1361, 1348, 1257, 1053, 914, 867, 769, 758, 738, 730, 709, 693 cm^{-1}; HR-MS (ESI-TOF) m/z calcd for $C_{21}H_{16}BrN_2$ $[M + H]^+$ 375.0491, found 375.0488.

2-Fluoro-11-methylbenzo[4,5]imidazo[1,2-f]phenanthridine or 2-Fluoro-12-methylbenzo[4,5]imidazo[1,2-f]phenanthridine (4ed).[24] R_f = 0.50 (hexane/ethyl acetate 4:1); White solid; yield 84% (50 mg); ^{1}H NMR (400 MHz, $CDCl_3$) δ 8.82 (dd, *J* = 8.0, 1.2 Hz,

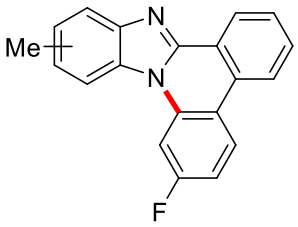

1H), 8.43 (dd, *J* = 8.8, 6.0 Hz, 1H), 8.28 (d, *J* = 8.0 Hz, 1H), 8.18 (dd, *J* = 10.4, 2.4 Hz, 1H), 8.09 (d, *J* = 8.4 Hz, 1H), 7.81 (s, 1H), 7.74 – 7.69 (m, 1H), 7.68 – 7.63 (m, 1H), 7.30 (d, *J* = 7.6 Hz, 1H), 7.25 – 7.19 (m, 1H), 2.58 (s, 3H); $^{13}C\{^{1}H\}$ NMR (100 MHz, $CDCl_3$) δ 162.9 (d, $J_{C,F}$ = 248.8 Hz), 147.7, 145.0, 135.4 (d, $J_{C,F}$ = 10.4 Hz), 134.5, 130.6, 129.8, 129.1, 128.6, 126.2, 126.1, 124.8, 123.1, 122.2, 120.4, 118.1 (d, $J_{C,F}$ = 2.7 Hz), 113.1, 112.0 (d, $J_{C,F}$ = 22.3 Hz), 103.3 (d, $J_{C,F}$ = 26.9 Hz), 21.8.

Mixer of 11-Methylbenzo[4,5]imidazo[1,2-f]phenanthridine and 12-Methylbenzo[4,5]imidazo[1,2-f]phenanthridine (4ea).[24] R_f = 0.60 (hexane/ethyl acetate

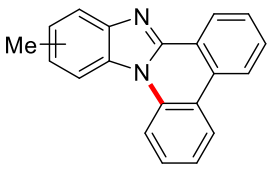

7:3); Inseparable white solid (2:1); yield 88% (35 mg); ^{1}H NMR (400 MHz, $CDCl_3$) δ 8.84 (d, *J* = 7.2 Hz, 1.5H), 8.54 – 8.40 (m, 3H), 8.34

(d, *J* = 7.2 Hz, 1.5H), 8.16 (d, *J* = 8.4 Hz, 1H), 8.10 (s, 0.5H), 7.91 (d, *J* = 8.4 Hz, 0.5H), 7.81 (s, 1H), 7.75 – 7.61 (m, 4.5H), 7.47 (t, J = 7.2 Hz, 1.5H), 7.33 (d, *J* = 8.4 Hz, 1H), 7.27 (d, *J* = 5.6 Hz, 1H), 2.64 (s, 1.5H), 2.58 (s, 3H).

Mixer of 2,11-Dimethylbenzo[4,5]imidazo[1,2-f]phenanthridine and 2,12-Dimethylbenzo[4,5]imidazo[1,2-f]phenanthridine (4eb) R_f = 0.45 (hexane/ethyl acetate 4:1); Inseparable white solid (5:2); yield 92% (55 mg); mp 185−186 °C; ^{1}H NMR (700 MHz, $CDCl_3$) δ 8.80 (d, *J* = 7.7 Hz, 1H), 8.78 (s, 0.4H), 8.26 – 8.20 (m, 3.2H), 8.18 (s, 1H), 8.10 (d, *J* = 8.4 Hz, 1H), 8.02 (s, 0.4H), 7.89 (d, *J* = 8.4 Hz, 0.4H), 7.79 (s, 1H), 7.67 – 7.63 (m, 1.4H), 7.62 – 7.58 (m, 1.4H), 7.31 (d, *J* = 8.4 Hz, 0.4H), 7.23 (d, *J* = 8.4 Hz, 1H), 7.20 (d, *J* = 8.4 Hz, 1.4H), 2.64 (s, 1.2H), 2.57 (s, 3H), 2.56 (s, 1.2H), 2.55 (s, 3H); ^{13}C{^{1}H} NMR (175 MHz, $CDCl_3$) δ 147.7, 147.4, 145.0, 142.7, 139.6, 139.6, 134.5, 133.9, 132.8, 132.2, 130.3, 130.2, 130.1, 129.7, 129.6, 128.2, 128.1, 126.0, 125.9, 125.7, 125.5, 125.5, 124.3, 124.0, 123.2, 122.1, 120.2, 119.8, 119.3, 119.2, 116.3, 116.2, 114.1, 113.6, 22.5, 22.1, 22.0, 21.8; IR (KBr) $\tilde{\nu}$ = 3029, 2914, 2853, 1613, 1591, 1537, 1433, 1359, 1347, 1273, 1176, 1155, 1122, 1038, 885, 838, 809, 765, 750, 727, 712, 694 cm^{-1}; HR-MS (ESI-TOF) m/z calcd for $C_{21}H_{17}N_2$ $[M + H]^+$ 297.1386, found 297.1386.

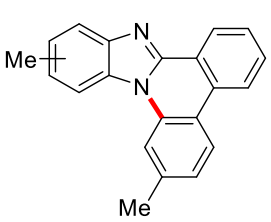

Mixer of 2-Ethyl-11-methylbenzo[4,5]imidazo[1,2-f]phenanthridine and 2-Ethyl-12-methylbenzo[4,5]imidazo[1,2-f]phenanthridine (4ee).[24] R_f = 0.60 (hexane/ethyl acetate 4:1); Inseparable pale yellow solid (5:1); yield 94% (37.5 mg); ^{1}H NMR (400 MHz, $CDCl_3$) δ 8.81 (d, *J* = 7.6 Hz, 1.2H), 8.34 – 8.23 (m, 4H), 8.15 (d, *J* = 8.4 Hz, 1H), 8.06 (s, 0.2H), 7.90 (d, *J* = 8.4 Hz, 0.2H), 7.80 (s, 1H),

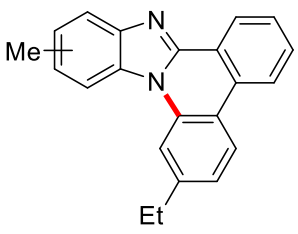

7.69 – 7.58 (m, 2.6H), 7.38 – 7.19 (m, 3H), 2.96 – 2.84 (m, 2.4H), 2.65 (s, 0.6H), 2.58 (s, 3H), 1.47 – 1.37 (m, 3.6H); $^{13}C\{^{1}H\}$ NMR (100 MHz, $CDCl_3$) δ 147.8, 145.9, 145.1, 142.8, 134.8, 134.7, 133.9, 132.8, 130.3, 130.1, 129.7, 128.2, 126.1, 125.9, 125.7, 124.4, 124.3, 124.2, 123.3, 122.1, 120.2, 119.9, 119.4, 115.2, 115.1, 114.1, 113.6, 29.3, 22.6, 21.8, 15.6.

Mixer of 11-Nitrobenzo[4,5]imidazo[1,2-f]phenanthridine and 12-Nitrobenzo[4,5]imidazo[1,2-f]phenanthridine (4fa).[24] R_f = 0.55 (hexane/ethyl acetate 4:1);

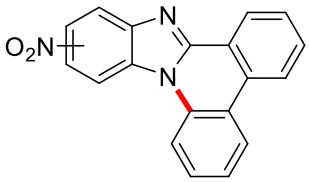

Inseparable pale yellow solid (10:3); yield 92% (36.6 mg); ^{1}H NMR (400 MHz, $CDCl_3$) δ 9.61 (d, *J* = 1.6 Hz, 0.3H), 8.98 (d, *J* = 1.6 Hz, 1H), 8.92 – 8.86 (m, 1.3H), 8.82 (q, *J* = 7.6 Hz, 3.6H), 8.74 – 8.69 (m, 1.3H), 8.64 (dd, *J* = 9.2, 1.6 Hz, 1H), 8.33 (d, *J* = 9.2 Hz, 0.3H), 8.22 – 8.11 (m, 1.6H), 8.10 – 7.90 (m, 3.9H).

11-Chloro-2-methylbenzo[4,5]imidazo[1,2-f]phenanthridine or 12-Chloro-2-methylbenzo[4,5]imidazo[1,2-f]phenanthridine (4gb). R_f = 0.40 (hexane/ethyl acetate 9:1); White solid; yield 87% (52 mg); mp 222−224 °C; ^{1}H NMR (400 MHz, $CDCl_3$) δ 8.68 (dd, *J* = 8.0, 1.2 Hz, 1H), 8.16 (d, *J* = 8.0 Hz, 1H), 8.13 (d, *J* = 8.4 Hz, 1H), 8.01 (d, *J* = 8.8 Hz, 1H), 7.96 (s, 1H), 7.89 (d, *J* = 2.0 Hz, 1H), 7.68 – 7.62 (m, 1H), 7.60 – 7.55 (m, 1H), 7.31 (dd, *J* = 8.8, 2.0 Hz, 1H), 7.16 (d, *J* = 8.0 Hz, 1H), 2.49 (s, 3H); $^{13}C\{^{1}H\}$ NMR (100 MHz, $CDCl_3$) δ 148.7, 145.6, 139.7, 133.9, 130.7, 130.4, 129.7, 129.6, 128.2, 126.1, 125.9, 124.1, 122.9, 122.7, 122.0, 119.9, 119.1, 115.9, 114.6, 22.0; IR (KBr) $\tilde{\nu}$ = 3024, 2923, 2855, 1614, 1586, 1532, 1453, 1434, 1359, 1347, 1170, 1066, 1041, 923, 877, 804, 763, 755, 738, 708,

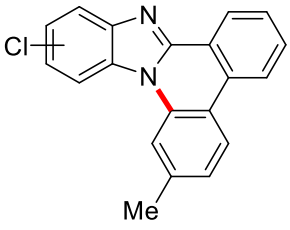

692 cm^{-1}; HR-MS (ESI-TOF) m/z calcd for $C_{20}H_{14}ClN_2$ $[M + H]^+$ 317.0840, found 317.0828.

2-(Tert-butyl)-11-chlorobenzo[4,5]imidazo[1,2-f]phenanthridine (4gc). R_f = 0.60 (hexane/ethyl acetate 4:1); White solid; yield 83% (49.5 mg); mp 199−201 °C; ^{1}H NMR (400 MHz, $CDCl_3$) δ 8.77 (d, *J* = 8.0 Hz, 1H), 8.44 (s, 1H), 8.38 (dd, *J* = 8.4, 3.6 Hz, 1H), 8.32 (d, *J* = 8.0 Hz, 1H), 8.16 (dd, *J* = 8.8, 3.6 Hz, 1H), 7.98 – 7.93 (m, 1H), 7.72 – 7.67 (m, 1H), 7.62 (t, *J* = 7.6 Hz, 1H), 7.59 – 7.56 (m, 1H), 7.40 (dd, *J* = 8.8, 2.0 Hz, 1H), 1.53 (s, 9H); ^{13}C{^{1}H} NMR (100 MHz, $CDCl_3$) δ 153.2, 148.9, 145.7, 134.0, 130.8, 130.5, 129.8, 129.7, 128.4, 126.2, 124.2, 123.1, 122.9, 122.6, 122.2, 120.1, 119.3, 114.5, 112.7, 35.5, 31.6; IR (KBr) $\tilde{\nu}$ = 3066, 2954, 2921, 2852, 1730, 1614, 1568, 1531, 1448, 1422, 1391, 1319, 1301, 1280, 1181, 1149, 1095, 934, 840, 822, 803, 765, 729, 713, 693 cm^{-1}; HR-MS (ESI-TOF) m/z calcd for $C_{23}H_{20}ClN_2$ $[M + H]^+$ 359.1310, found 359.1300.

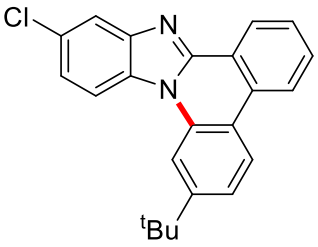

11-Chloro-2-fluorobenzo[4,5]imidazo[1,2-f]phenanthridine OR 12-Chloro-2-fluorobenzo[4,5]imidazo[1,2-f]phenanthridine (4gd). R_f = 0.50 (hexane/ethyl acetate 4:1); White solid; yield 81% (48.3 mg); mp 238−240 °C; ^{1}H NMR (700 MHz, $CDCl_3$) δ 8.79 (d, *J* = 8.4 Hz, 1H), 8.76 (dd, *J* = 9.1, 5.6 Hz, 1H), 8.60 (d, *J* = 8.4 Hz, 1H), 8.47 (d, *J* = 9.1 Hz, 1H), 8.41 (dd, *J* = 9.1, 2.1 Hz, 1H), 8.12 (t, *J* = 7.7 Hz, 1H), 8.08 (d, *J* = 2.1 Hz, 1H), 7.95 (t, *J* = 7.7 Hz, 1H), 7.76 (dd, *J* = 9.1, 1.4 Hz, 1H), 7.65 – 7.61 (m, 1H); ^{13}C{^{1}H} NMR (175 MHz, $CDCl_3$) δ 163.7 (d, $J_{C,F}$ = 255.3 Hz), 144.4, 135.8, 135.5, 132.8, 132.1 (d, $J_{C,F}$ = 10.7 Hz), 131.3, 130.8, 127.9, 127.7 (d, $J_{C,F}$ = 9.9 Hz), 127.5, 126.6, 123.3, 119.2, 116.9 (d,

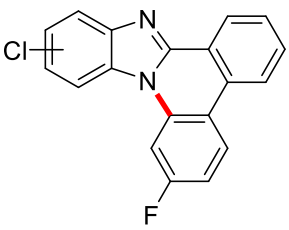

$J_{C,F}$ = 22.3 Hz), 116.3, 115.73 (d, $J_{C,F}$ = 27.1 Hz)., 114.2, 104.9 (d, $J_{C,F}$ = 27.5 Hz); IR (KBr) $\tilde{\nu}$ = 3154, 3072, 2957, 2923, 2853, 1617, 1590, 1535, 1459, 1436, 1346, 1309, 1252, 1165, 1144, 1067, 926, 883, 822, 776, 766, 759, 720, 693 cm^{-1}; HR-MS (ESI-TOF) m/z calcd for $C_{19}H_{11}ClFN_2$ $[M + H]^+$ 321.0589, found 321.0575.

3.6. REFERENCES

1. (a) Choudhuri, K.; Pramanik, M.; Mal, P., *J. Org. Chem.* **2020,** *85* (19), 11997-12011; (b) Pramanik, M.; Choudhuri, K.; Mal, P., *Org. Biomol. Chem.* **2020,** *18* (43), 8771-8792.

2. Gulías, M.; Mascareñas, J. L., *Angew. Chem. Int. Ed.* **2016,** *55* (37), 11000-11019.

3. Sun, C.-L.; Shi, Z.-J., *Chem. Rev.* **2014,** *114* (18), 9219-9280.

4. (a) He, G.; Lu, G.; Guo, Z.; Liu, P.; Chen, G., *Nat. Chem.* **2016,** *8* (Advanced Online Publications), 1131–1136; (b) Li, C.-J., *Acc. Chem. Res.* **2009,** *42* (2), 335-344; (c) Louillat, M.-L.; Patureau, F. W., *Chem. Soc. Rev.* **2014,** *43* (3), 901-910; (d) Narayan, R.; Manna, S.; Antonchick, A. P., *Synlett* **2015,** *26* (13), 1785-1803.

5. (a) Lian, F.; Sun, C.; Xu, K.; Zeng, C., *Org. Lett.* **2019,** *21* (1), 156-159; (b) Liu, K.; Tang, S.; Wu, T.; Wang, S.; Zou, M.; Cong, H.; Lei, A., *Nat. Commun.* **2019,** *10* (1), 639; (c) Yu, Y.; Yuan, Y.; Liu, H.; He, M.; Yang, M.; Liu, P.; Yu, B.; Dong, X.; Lei, A., *Chem. Commun.* **2019,** *55*, 1809-1812.

6. Bagdi, A. K.; Rahman, M.; Bhattacherjee, D.; Zyryanov, G. V.; Ghosh, S.; Chupakhin, O. N.; Hajra, A., *Green Chem.* **2020,** *22* (20), 6632-6681.

7. Kärkäs, M. D.; Porco, J. A.; Stephenson, C. R. J., *Chem. Rev.* **2016,** *116* (17), 9683-9747.

8. (a) Marzo, L.; Pagire, S. K.; Reiser, O.; König, B., *Angew. Chem. Int. Ed.* **2018,** *57* (32), 10034-10072; (b) Verschueren, R. H.; De Borggraeve, W. M., *Molecules* **2019,** *24* (11), 2122.

9. Guerra, W. D.; Rossi, R. A.; Pierini, A. B.; Barolo, S. M., *J. Org. Chem.* **2016,** *81* (12), 4965-4973.

10. (a) Mfuh, A. M.; Doyle, J. D.; Chhetri, B.; Arman, H. D.; Larionov, O. V., *J. Am. Chem. Soc.* **2016,** *138* (9), 2985-2988; (b) Mfuh, A. M.; Nguyen, V. T.; Chhetri, B.; Burch, J. E.; Doyle, J. D.; Nesterov, V. N.; Arman, H. D.; Larionov, O. V., *J. Am. Chem. Soc.* **2016,** *138* (27), 8408-8411.

11. Yuan, J.; To, W.-P.; Zhang, Z.-Y.; Yue, C.-D.; Meng, S.; Chen, J.; Liu, Y.; Yu, G.-A.; Che, C.-M., *Org. Lett.* **2018,** *20* (24), 7816-7820.

12. Camargo Solórzano, P.; Brigante, F.; Pierini, A. B.; Jimenez, L. B., *J. Org. Chem.* **2018,** *83* (15), 7867-7877.

13. Liu, B.; Lim, C. H.; Miyake, G. M., *J. Am. Chem. Soc.* **2017,** *139* (39), 13616-13619.

14. Zhou, J.; Li, L.; Wang, S.; Yan, M.; Wei, W., *Green Chem.* **2020,** *22* (11), 3421-3426.

15. Zhao, Y.; Huang, B.; Yang, C.; Xia, W., *Org. Lett.* **2016,** *18* (14), 3326-3329.

16. Fan, J.; Zhang, W.; Gao, W.; Wang, T.; Duan, W.-L.; Liang, Y.; Zhang, Z., *Org. Lett.* **2019,** *21* (22), 9183-9187.

17. S, U. D.; Julia, F.; Luridiana, A.; Douglas, J. J.; Leonori, D., *Nature* **2020,** *584* (7819), 75-81.

18. Skonieczny, K.; Gryko, D. T., *J. Org. Chem.* **2015,** *80* (11), 5753-5763.

19. Bartos, P.; Young, V. G.; Kaszyński, P., *Org. Lett.* **2020,** *22* (10), 3835-3840.

20. (a) Shi, J.; Li, J.; Zhao, W.; Cui, M.; Ni, W.; Li, L.; Liu, W.; Xu, K.; Zhang, S., *Org. Chem. Front.* **2021,** *8* (7), 1581-1586; (b) Zhang, S.; Li, L.; Xue, M.; Zhang, R.; Xu, K.; Zeng, C., *Org. Lett.* **2018,** *20* (12), 3443-3446.

21. Yamashita, H.; Ikezawa, T.; Kobayashi, Y.; Abe, J., *J. Am. Chem. Soc.* **2015,** *137* (15), 4952-4955.

22. Hamprecht, F. A.; Cohen, A. J.; Tozer, D. J.; Handy, N. C., *J. Chem. Phys.* **1998,** *109* (15), 6264-6271.

23. (a) Gill, P. M. W.; Johnson, B. G.; Pople, J. A.; Frisch, M. J., *Chem. Phys. Lett.* **1992,** *197* (4), 499-505; (b) Shavitt, I., *Isr. J. Chem.* **1993,** *33* (4), 357-367.

24. Bera, S. K.; Alam, M. T.; Mal, P., *J. Org. Chem.* **2019,** *84* (18), 12009-12020.

25. (a) Li, X.; Fang, X.; Zhuang, S.; Liu, P.; Sun, P., *Org. Lett.* **2017,** *19* (13), 3580-3583; (b) Yu, Y.; Yuan, W.; Huang, H.; Cai, Z.; Liu, P.; Sun, P., *J. Org. Chem.* **2018,** *83* (3), 1654-1660.

26. Wang, H.; Li, Y.; Tang, Z.; Wang, S.; Zhang, H.; Cong, H.; Lei, A., *ACS Catal.* **2018,** *8* (11), 10599-10605.

27. Schilling, W.; Riemer, D.; Zhang, Y.; Hatami, N.; Das, S., *ACS Catal.* **2018,** *8* (6), 5425-5430.

28. Ouannes, C.; Wilson, T., *J. Am. Chem. Soc.* **1968,** *90* (23), 6527-6528.

29. Ottiger, P.; Pfaffen, C.; Leist, R.; Leutwyler, S.; Bachorz, R. A.; Klopper, W., *J. Phys. Chem. B* **2009,** *113* (9), 2937-43.

30. Alonso, R.; Campos, P. J.; Rodríguez, M. A.; Sampedro, D., *J. Org. Chem.* **2008,** *73* (6), 2234-2239.

31. Frisch, M. J.; Trucks, G. W.; Schlegel, H. B.; Scuseria, G. E.; Robb, M. A.; Cheeseman, J. R.; Scalmani, G.; Barone, V.; Mennucci, B.; Petersson, G. A.; Nakatsuji, H.;

Caricato, M.; Li, X.; Dapprich, S.; Daniels, A. D.; Farkas; Foresman, J. B.; Ortiz, J. V.; Cioslowski, J.; Fox, D. J. *Gaussian 09, Revision B.01*, Wallingford CT, 2009.

32. Soberats, B.; Sanna, E.; Martorell, G.; Rotger, C.; Costa, A., *Org. Lett.* **2014,** *16* (3), 840-3.

33. Guo, W.; Zhao, M.; Tan, W.; Zheng, L.; Tao, K.; Fan, X., *Org. Chem. Front.* **2019,** *6* (13), 2120-2141.

34. Ranjan, N.; Story, S.; Fulcrand, G.; Leng, F.; Ahmad, M.; King, A.; Sur, S.; Wang, W.; Tse-Dinh, Y.-C.; Arya, D. P., *J. Med. Chem.* **2017,** *60* (12), 4904-4922.

35. Chen, Y.-H.; Chen, C.-H.; Chang, C.-M.; Fan, B.-A.; Chen, D.-G.; Lee, J.-H.; Chiu, T.-L.; Chou, P.-T.; Leung, M.-k., *J. Mater. Chem. C* **2020,** *8* (10), 3571-3579.

36. Wang, R.; Lu, X.-x.; Yu, X.-q.; Shi, L.; Sun, Y., *J. Mol. Catal. A: Chem.* **2007,** *266* (1), 198-201.

37. Chen, C.; Shang, G.; Zhou, J.; Yu, Y.; Li, B.; Peng, J., *Org. Lett.* **2014,** *16* (7), 1872-1875.

38. Zhao, G.; Chen, C.; Yue, Y.; Yu, Y.; Peng, J., *J. Org. Chem.* **2015,** *80* (5), 2827-2834.

39. Yan, L.; Zhao, D.; Lan, J.; Cheng, Y.; Guo, Q.; Li, X.; Wu, N.; You, J., *Org. Biomol. Chem.* **2013,** *11* (45), 7966-7977.

NMR Spectra

^{1}H NMR (700 MHz, DMSO-d_6)

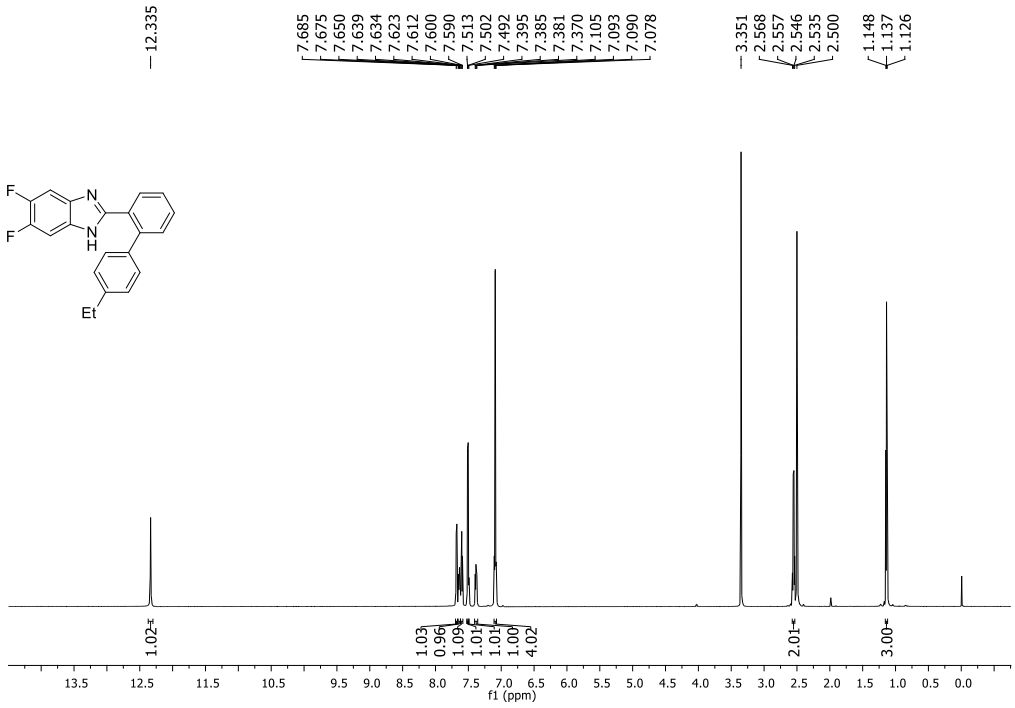

Figure 3.8. ^{1}H NMR spectrum of 2-(4'-Ethyl-[1,1'-biphenyl]-2-yl)-5,6-difluoro-1H-benzo[d]imidazole (**1de**).

^{13}C NMR (175 MHz, DMSO-d_6)

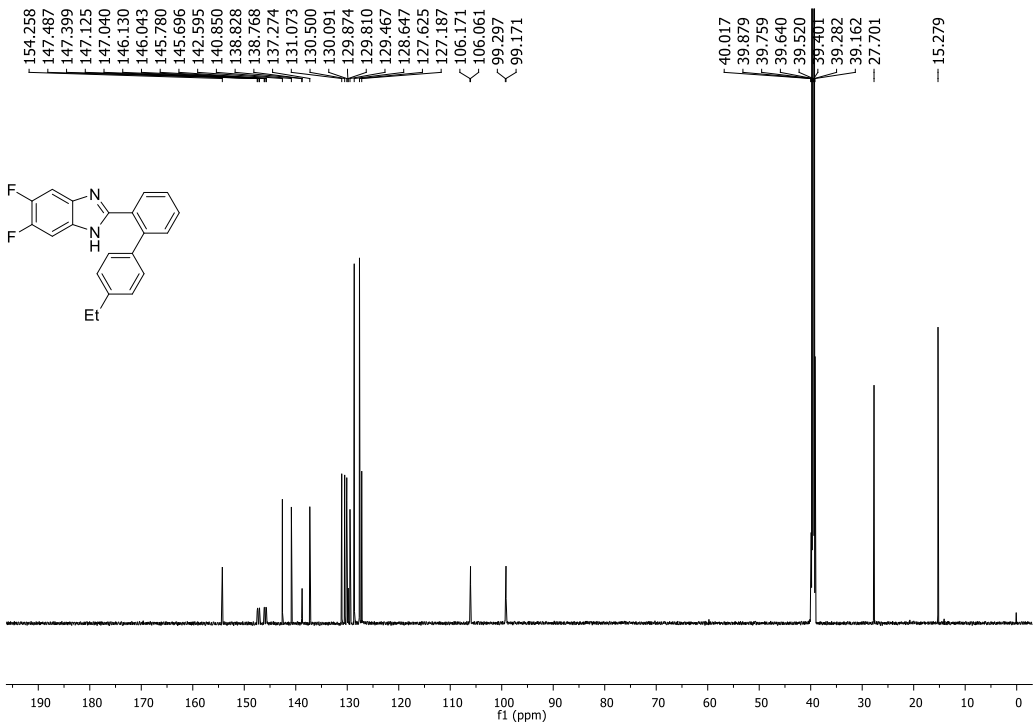

Figure 3.9. ^{13}C{^{1}H} NMR spectrum of2-(4'-Ethyl-[1,1'-biphenyl]-2-yl)-5,6-difluoro-1H-benzo[d]imidazole (**1de**).

^{1}H NMR (700 MHz, DMSO-d_6)

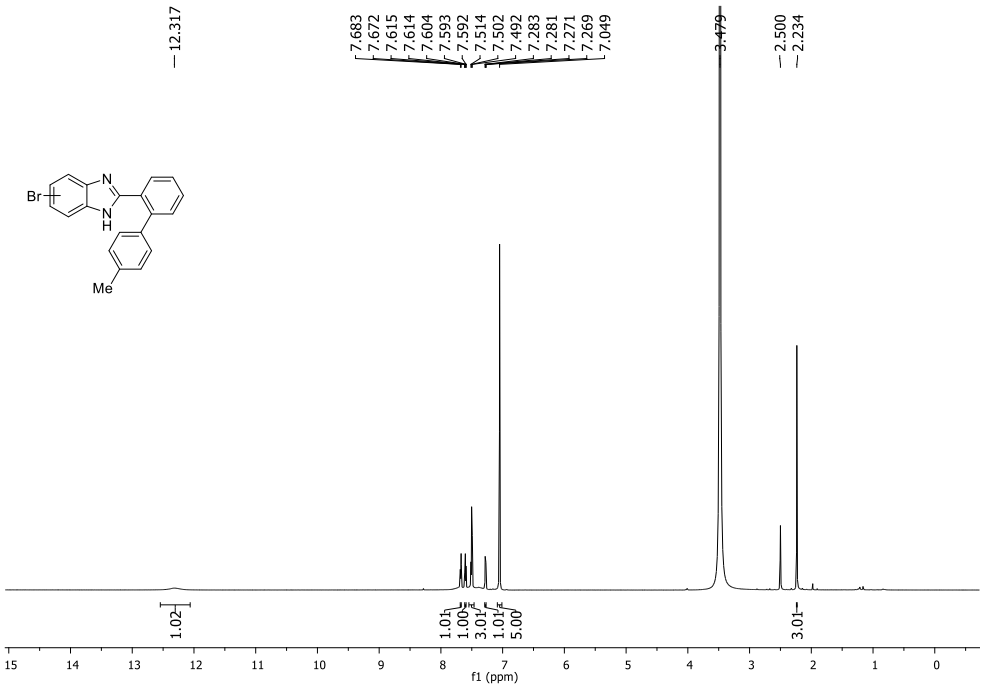

Figure 3.10. ^{1}H NMR spectrum of 5-Bromo-2-(4'-methyl-[1,1'-biphenyl]-2-yl)-1H-benzo[d]imidazole OR 6-Bromo-2-(4'-methyl-[1,1'-biphenyl]-2-yl)-1H-benzo[d]imidazole **(3db**).

^{13}C NMR (100 MHz, DMSO-d_6)

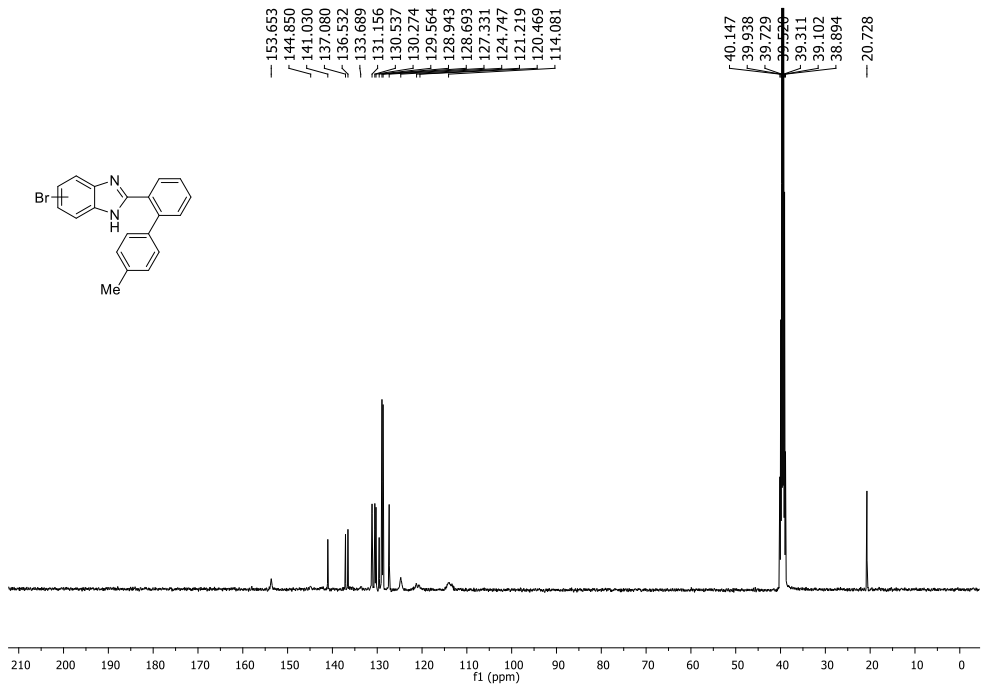

Figure 3.11. ^{13}C{^{1}H} NMR spectrum of 5-Bromo-2-(4'-methyl-[1,1'-biphenyl]-2-yl)-1H-benzo[d]imidazole OR 6-Bromo-2-(4'-methyl-[1,1'-biphenyl]-2-yl)-1H-benzo[d]imidazole **(3db).**

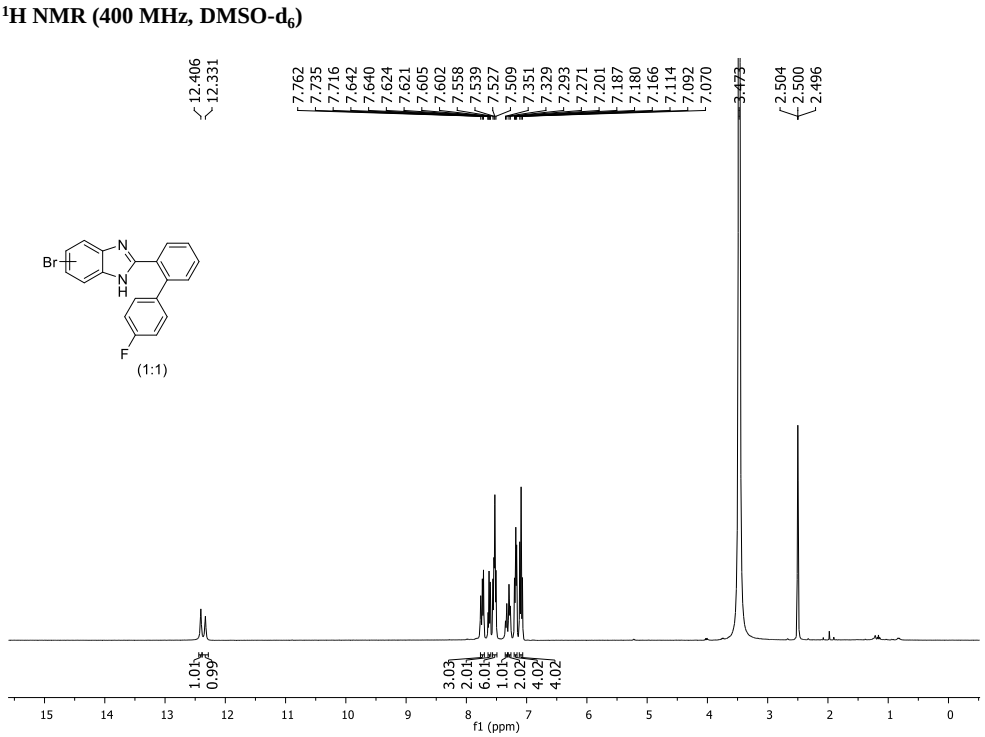

Figure 3.12. ^{1}H NMR spectrum of 5-Bromo-2-(4'-fluoro-[1,1'-biphenyl]-2-yl)-1H-benzo[d]imidazole and 6-Bromo-2-(4'-fluoro-[1,1'-biphenyl]-2-yl)-1H-benzo[d]imidazole **(3dd).**

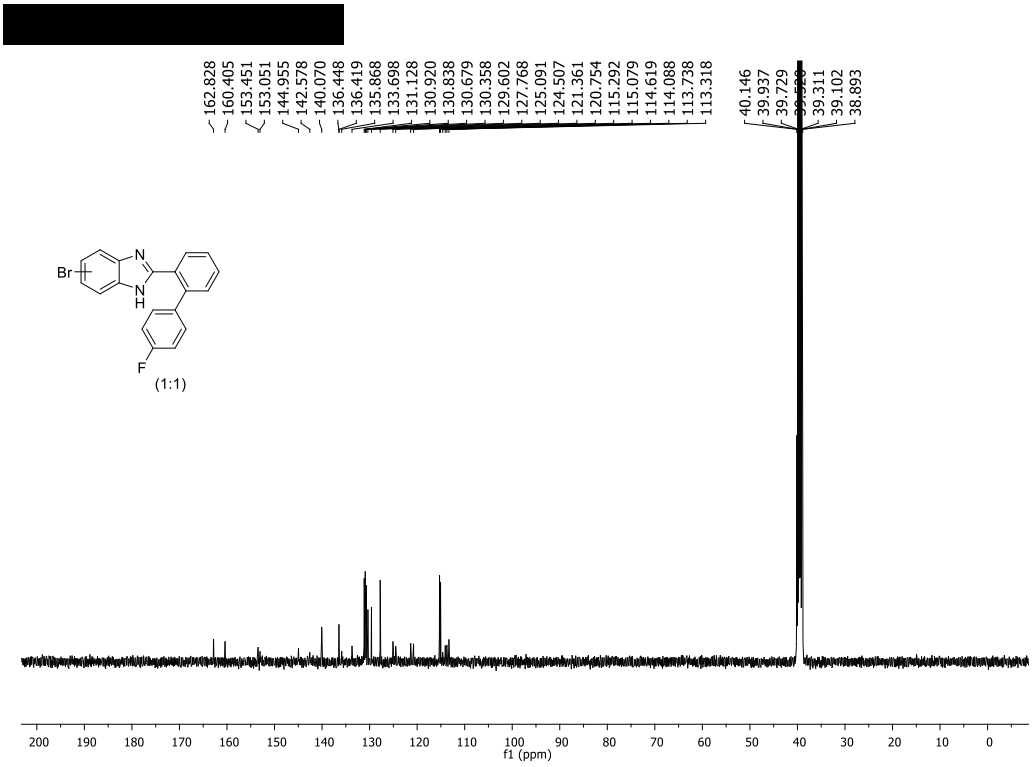

Figure 3.13. ^{13}C{^{1}H} NMR spectrum of 5-Bromo-2-(4'-fluoro-[1,1'-biphenyl]-2-yl)-1H-benzo[d]imidazole and 6-Bromo-2-(4'-fluoro-[1,1'-biphenyl]-2-yl)-1H-benzo[d]imidazole **(3dd).**

^{1}H NMR (700 MHz, $CDCl_3$)

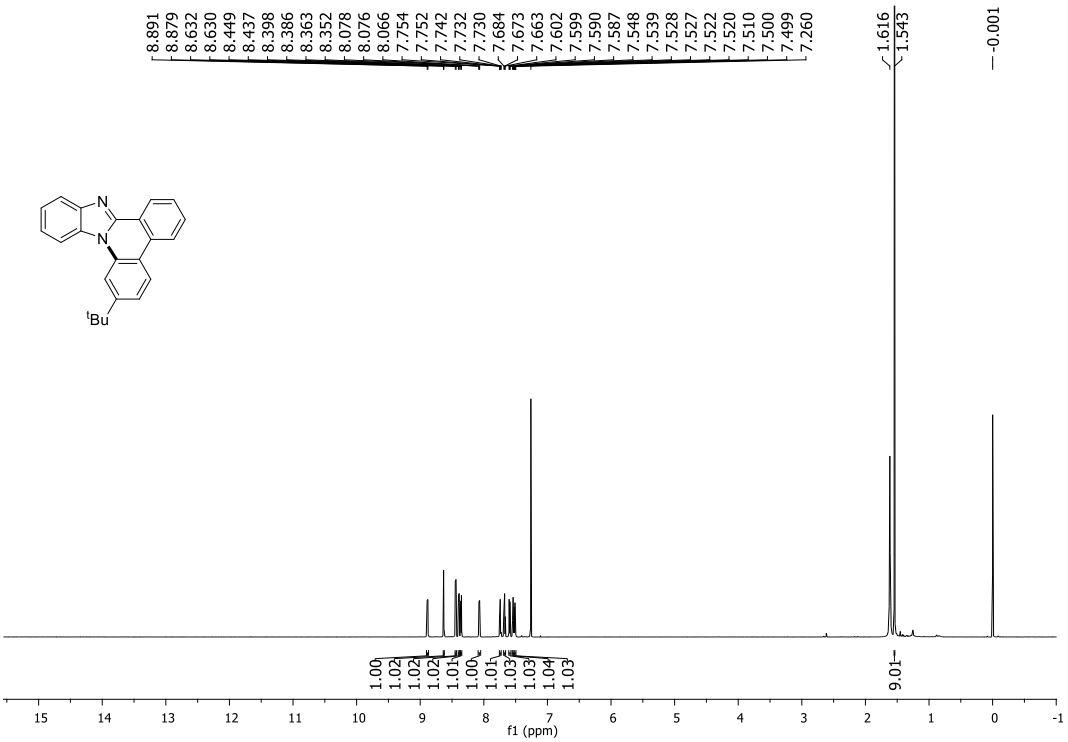

Figure 3.14. ^{1}H NMR spectrum of 2-(Tert-butyl)benzo[4,5]imidazo[1,2-f]phenanthridine **(2ac).**

^{13}C NMR (175 MHz, $CDCl_3$)

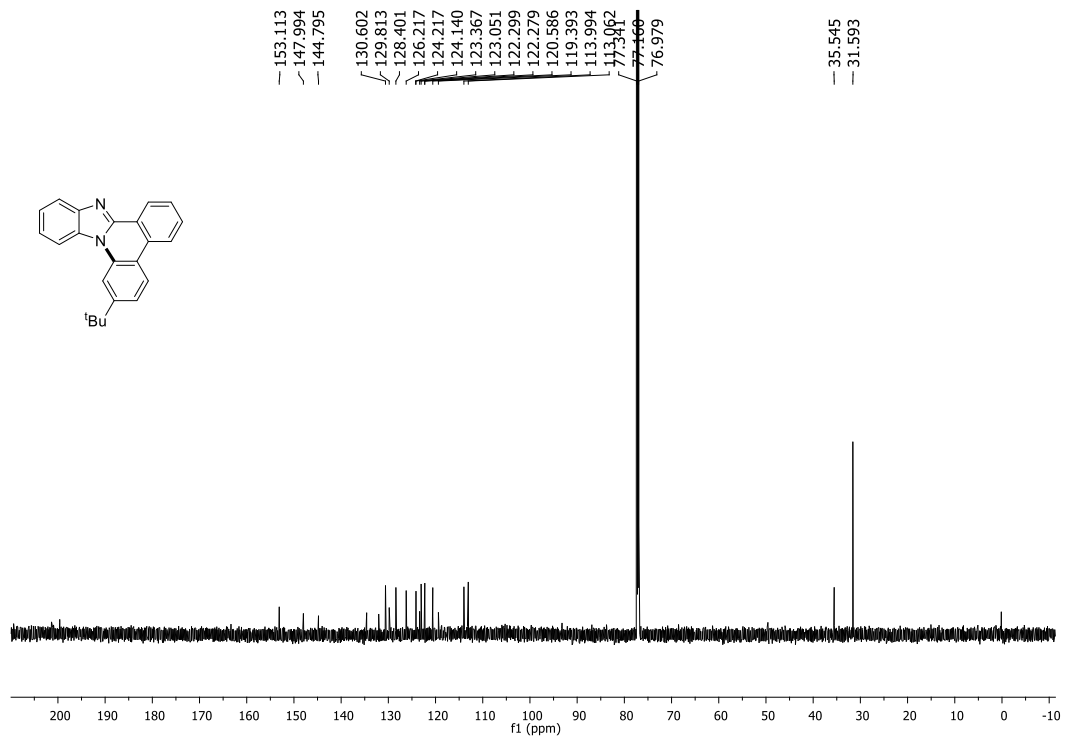

Figure 3.15. ^{13}C{^{1}H} NMR spectrum of 2-(Tert-butyl)benzo[4,5]imidazo[1,2-f]phenanthridine **(2ac).**

^{1}H NMR (400 MHz, $CDCl_3$)

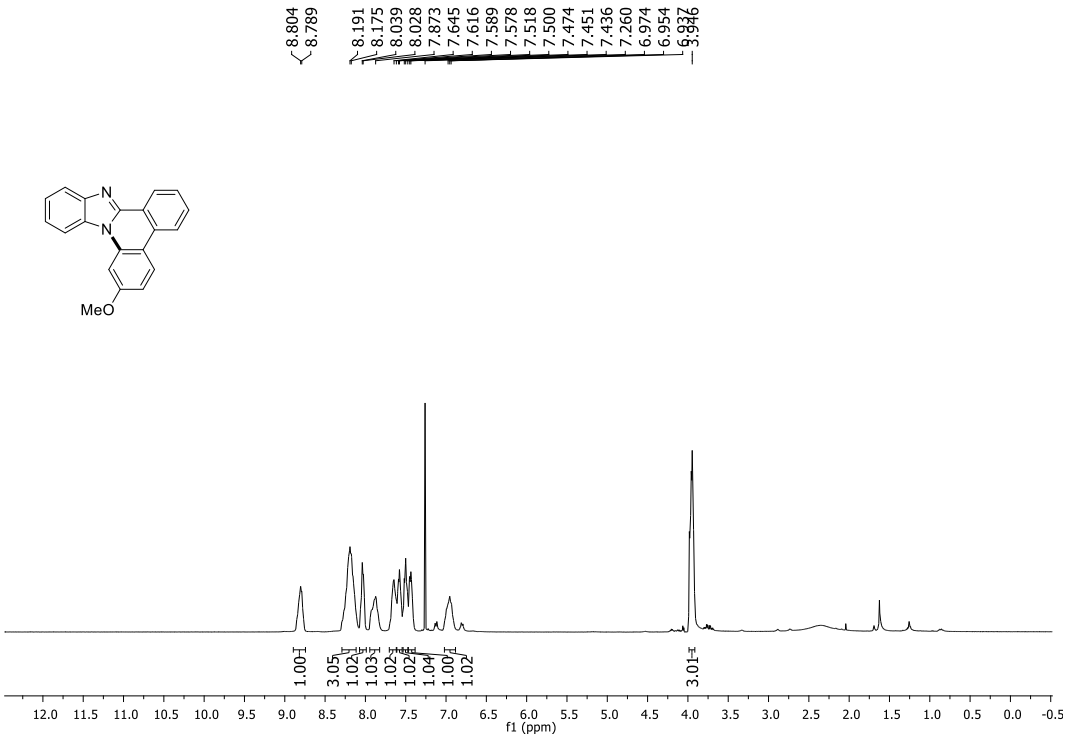

Figure 3.16. ^{1}H NMR spectrum of 2-Methoxybenzo[4,5]imidazo[1,2-f]phenanthridine **(2af).**

^{13}C NMR (100 MHz, $CDCl_3$)

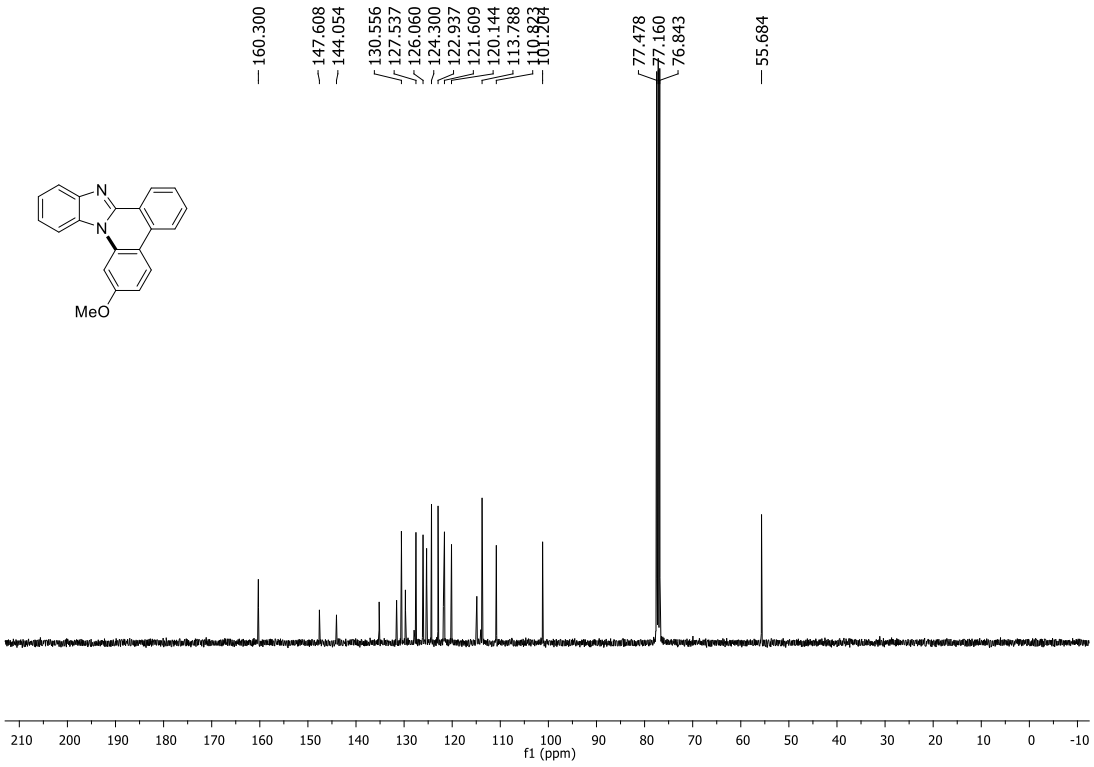

Figure 3.17. ^{13}C{^{1}H} NMR spectrum of 2-Methoxybenzo[4,5]imidazo[1,2-f]phenanthridine **(2af).**

^{1}H NMR (400 MHz, $CDCl_3$ + TFA-D)

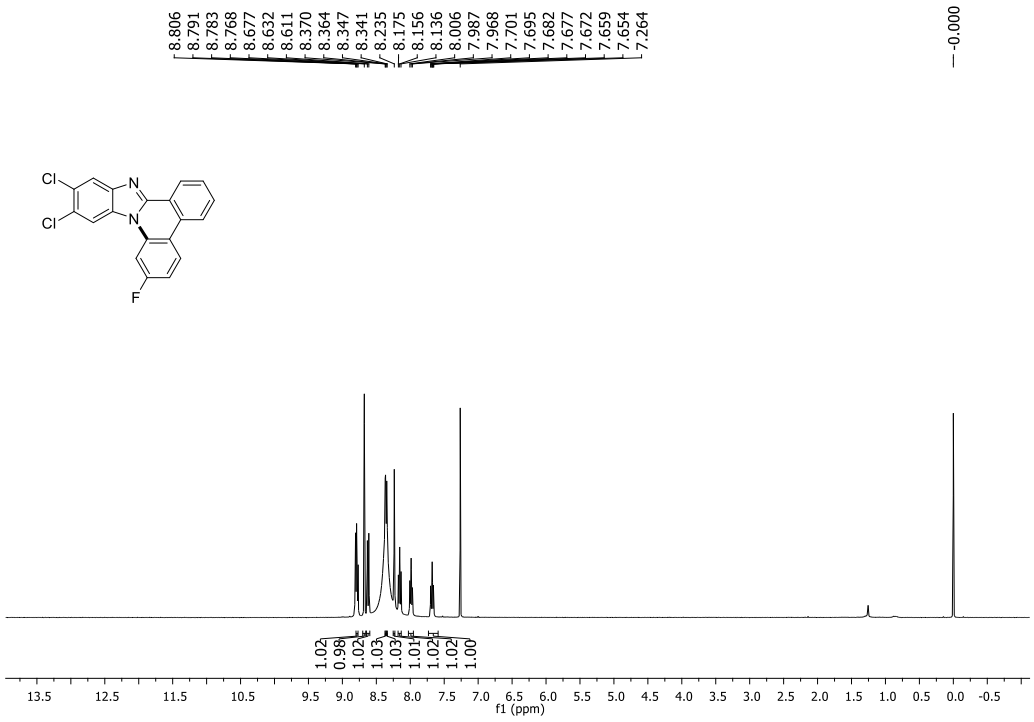

Figure 3.18. ^{1}H NMR spectrum of 11,12-Dichloro-2-fluorobenzo[4,5]imidazo[1,2-f]phenanthridine **(2cd**).

^{13}C NMR (100 MHz, $CDCl_3$ + TFA-D)

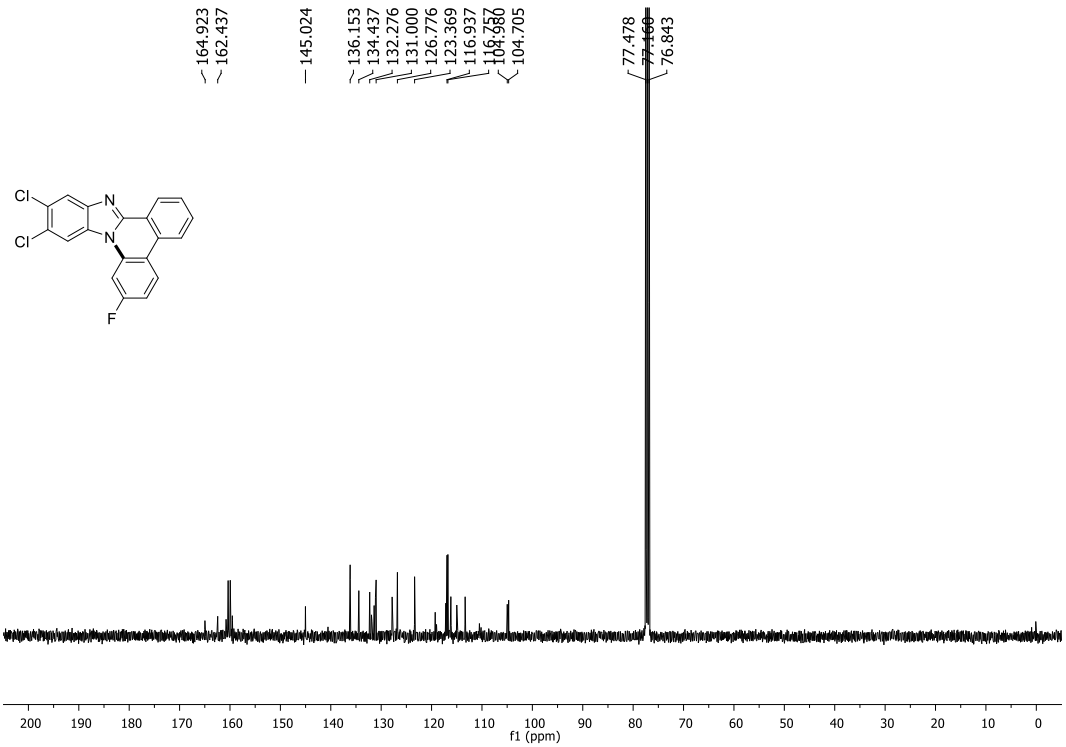

Figure 3.19. ^{13}C{^{1}H} NMR spectrum of 11,12-Dichloro-2-fluorobenzo[4,5]imidazo[1,2-f]phenanthridine **(2cd).**

^{1}H NMR (700 MHz, $CDCl_3$)

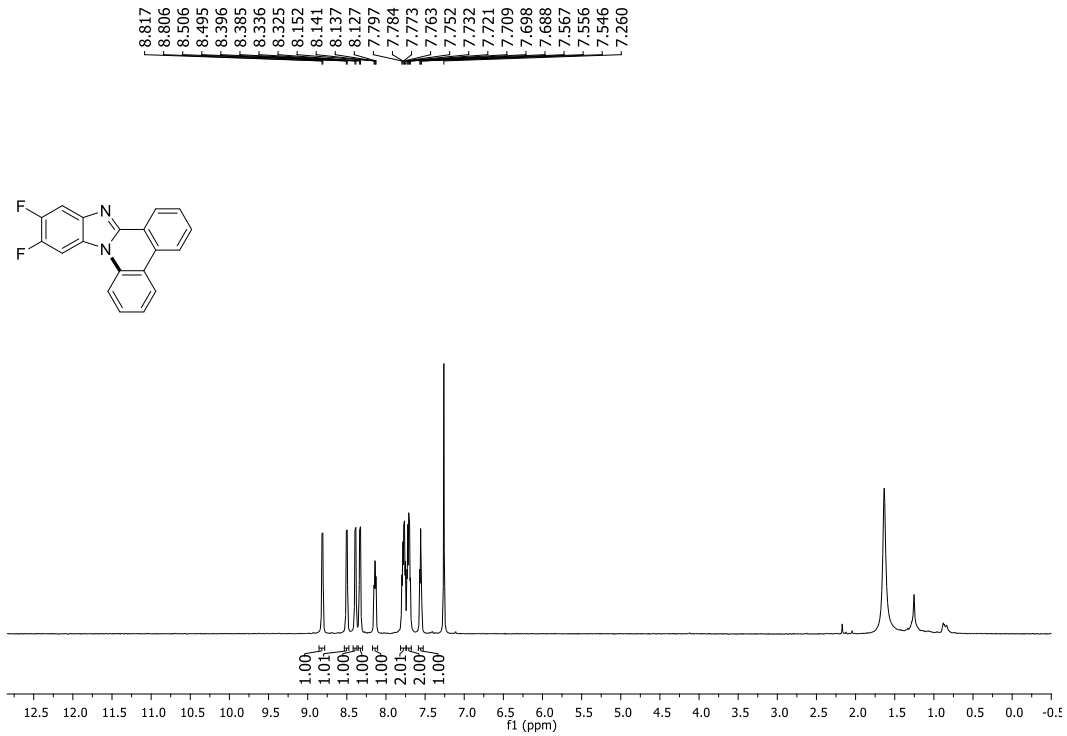

Figure 3.20. ^{1}H NMR spectrum of 11,12-Difluorobenzo[4,5]imidazo[1,2-f]phenanthridine **(2da).**

^{13}C NMR (175 MHz, $CDCl_3$)

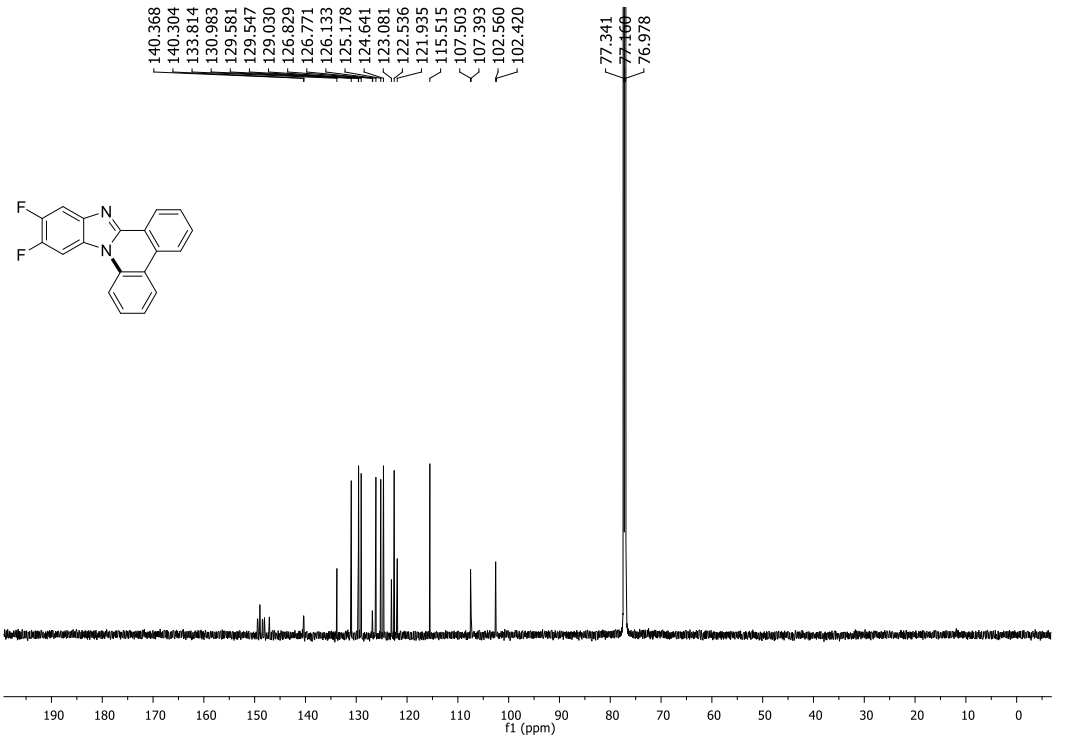

Figure 3.21. ^{13}C{^{1}H} NMR spectrum of 11,12-Difluorobenzo[4,5]imidazo[1,2-f]phenanthridine **(2da).**

^{1}H NMR (700 MHz, $CDCl_3$)

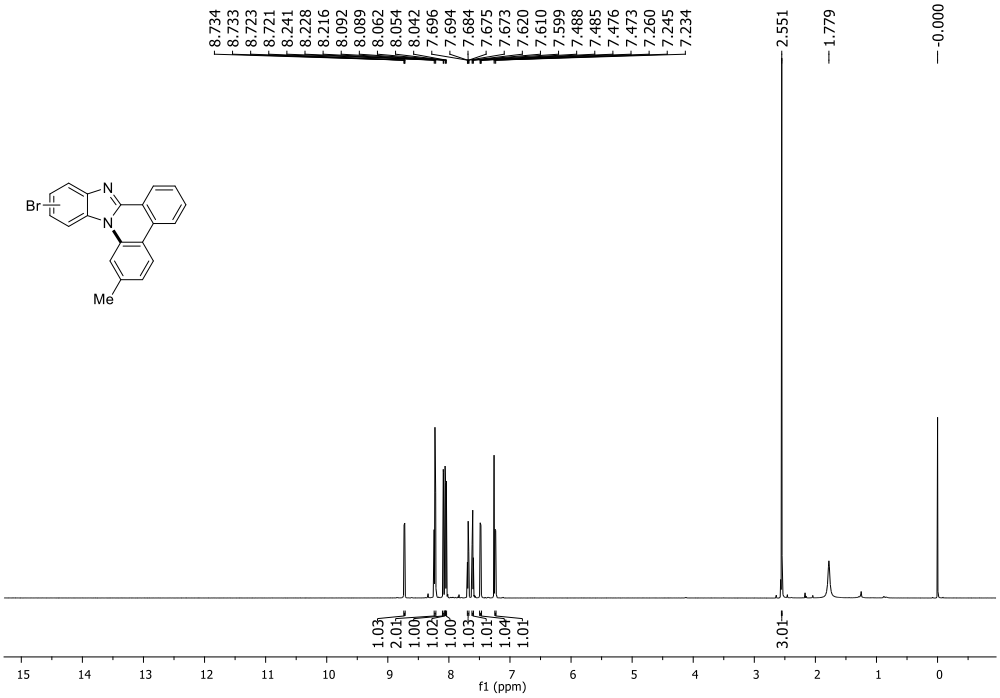

Figure 3.22. ^{1}H NMR spectrum of 11-Bromo-2-methylbenzo[4,5]imidazo[1,2-f]phenanthridine OR 12-Bromo-2-methylbenzo[4,5]imidazo[1,2-f]phenanthridine **(4db).**

^{13}C NMR (175 MHz, $CDCl_3$)

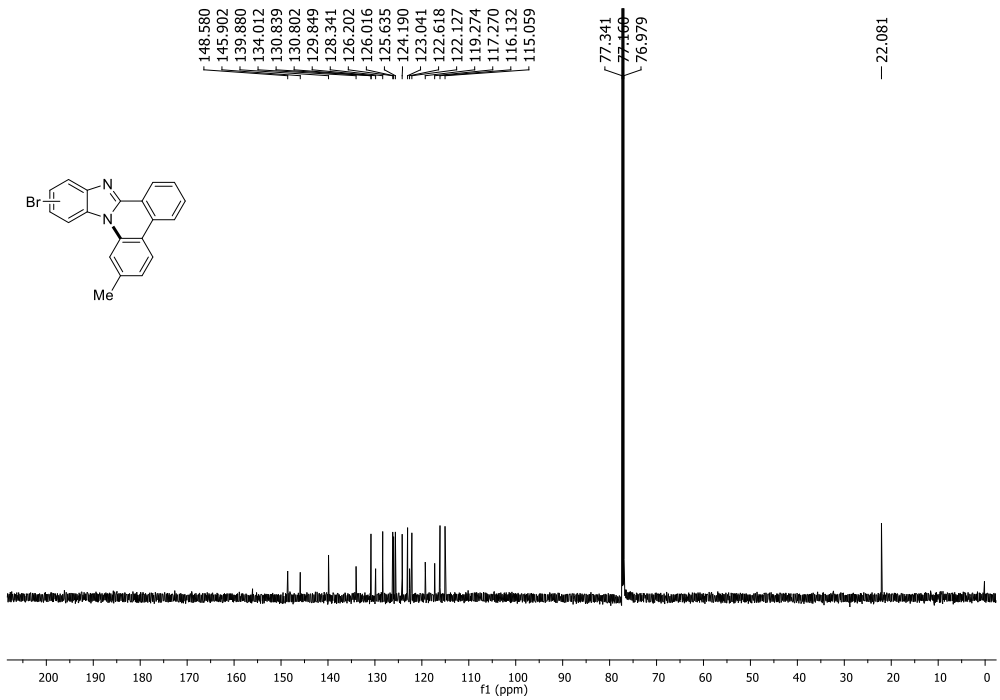

Figure 3.23. ^{13}C{^{1}H} NMR spectrum of 11-Bromo-2-methylbenzo[4,5]imidazo[1,2-f]phenanthridine OR 12-Bromo-2-methylbenzo[4,5]imidazo[1,2-f]phenanthridine **(4db).**

^{1}H NMR (400 MHz, $CDCl_3$)

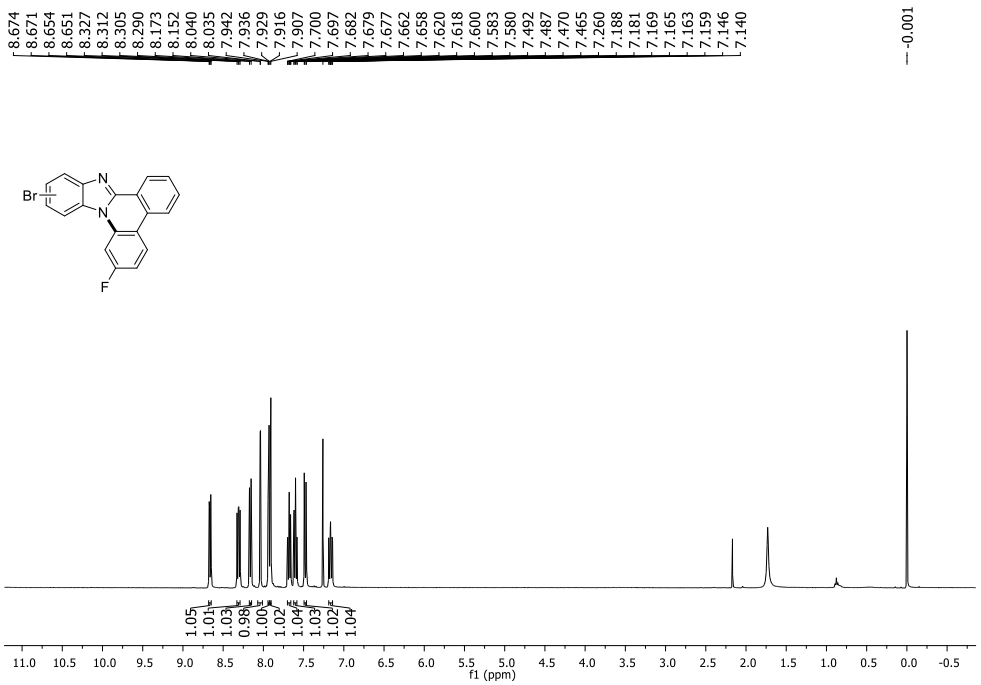

Figure 3.24. ^{1}H NMR spectrum of 11-Bromo-2-fluorobenzo[4,5]imidazo[1,2-f]phenanthridine OR 12-Bromo-2-fluorobenzo[4,5]imidazo[1,2-f]phenanthridine **(4dd).**

^{13}C NMR (100 MHz, $CDCl_3$)

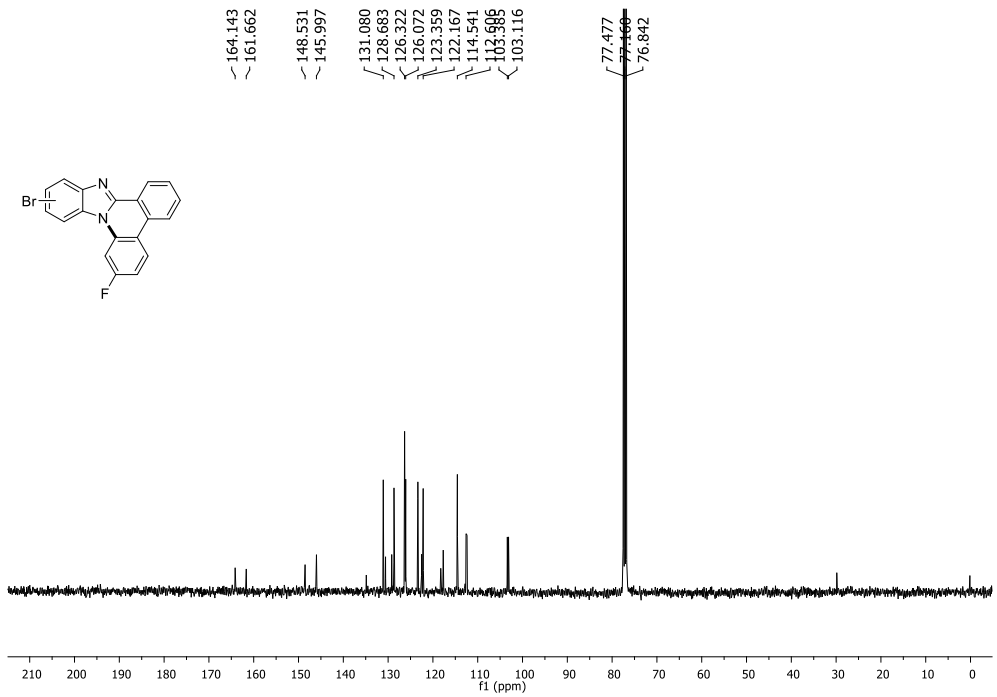

Figure 3.25. ^{13}C{^{1}H} NMR spectrum of 11-Bromo-2-fluorobenzo[4,5]imidazo[1,2-f]phenanthridine OR 12-Bromo-2-fluorobenzo[4,5]imidazo[1,2-f]phenanthridine **(4dd).**

^{1}H NMR (700 MHz, $CDCl_3$)

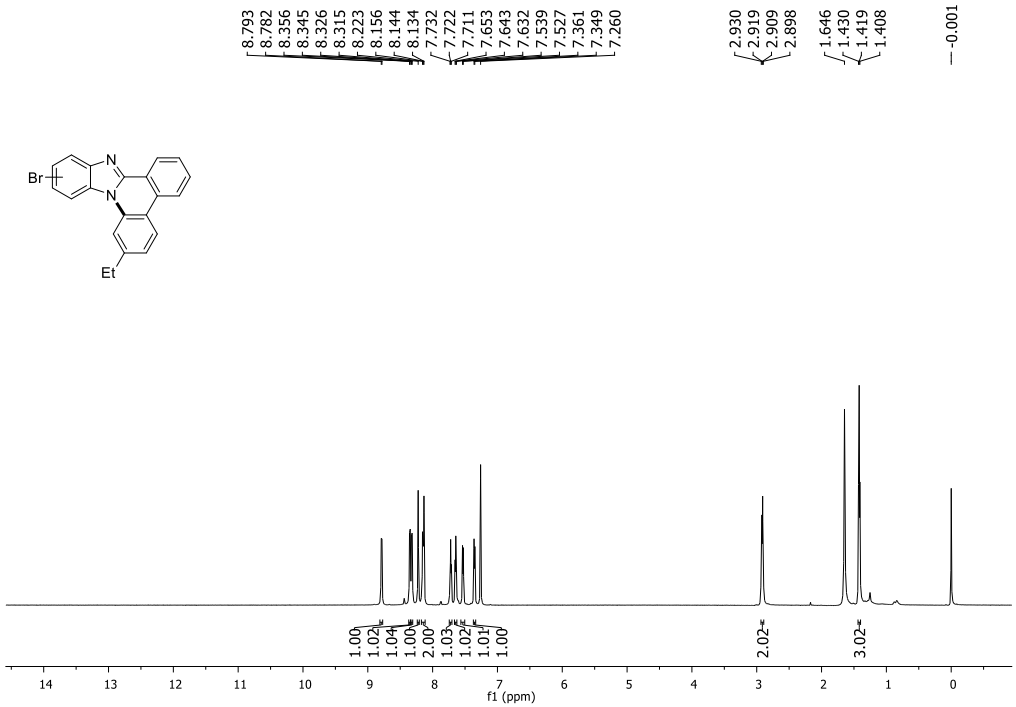

Figure 3.26. ^{1}H NMR spectrum of 11-Bromo-2-ethylbenzo[4,5]imidazo[1,2-f]phenanthridine OR 12-Bromo-2-ethylbenzo[4,5]imidazo[1,2-f]phenanthridine **(4de).**

^{13}C NMR (175 MHz, $CDCl_3$)

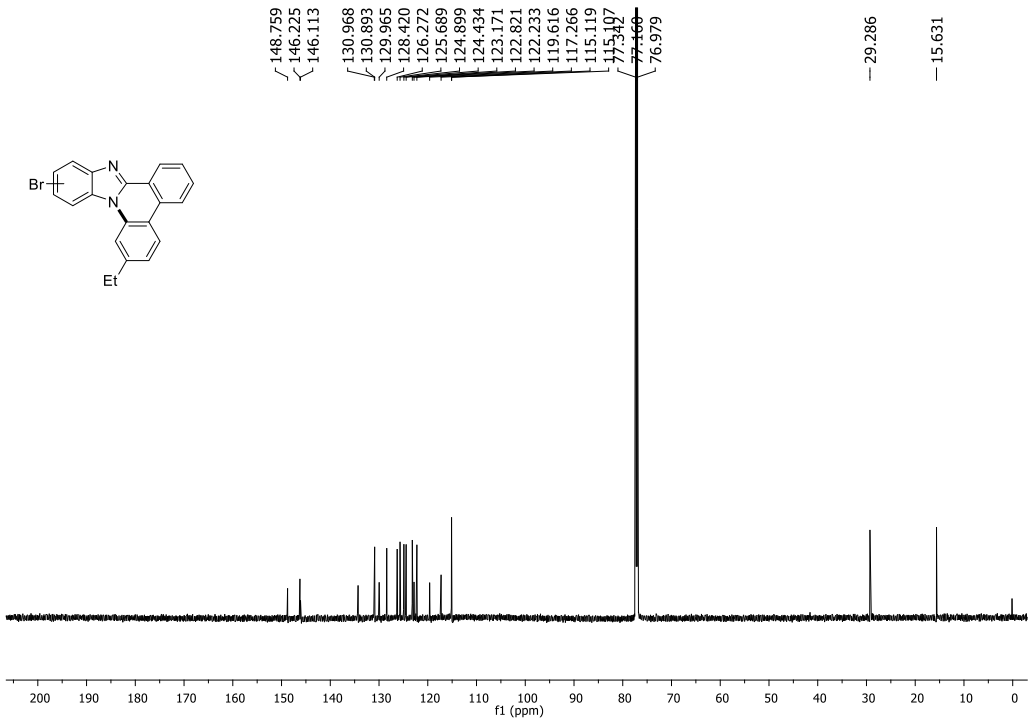

Figure 3.27. ^{13}C{^{1}H} NMR spectrum of 11-Bromo-2-ethylbenzo[4,5]imidazo[1,2-f]phenanthridine OR 12-Bromo-2-ethylbenzo[4,5]imidazo[1,2-f]phenanthridine **(4de).**

^{1}H NMR (400 MHz, $CDCl_3$)

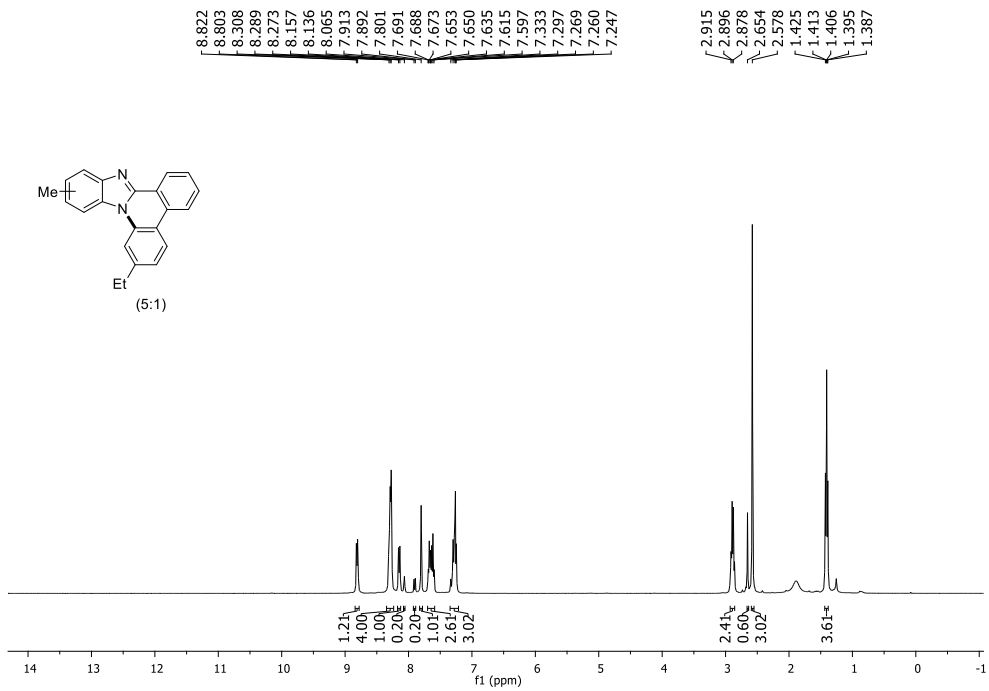

Figure 3.28. ^{1}H NMR spectrum of 2-Ethyl-11-methylbenzo[4,5]imidazo[1,2-f]phenanthridine and 2-Ethyl-12-methylbenzo[4,5]imidazo[1,2-f]phenanthridine **(4ee).**

^{13}C NMR (100 MHz, $CDCl_3$)

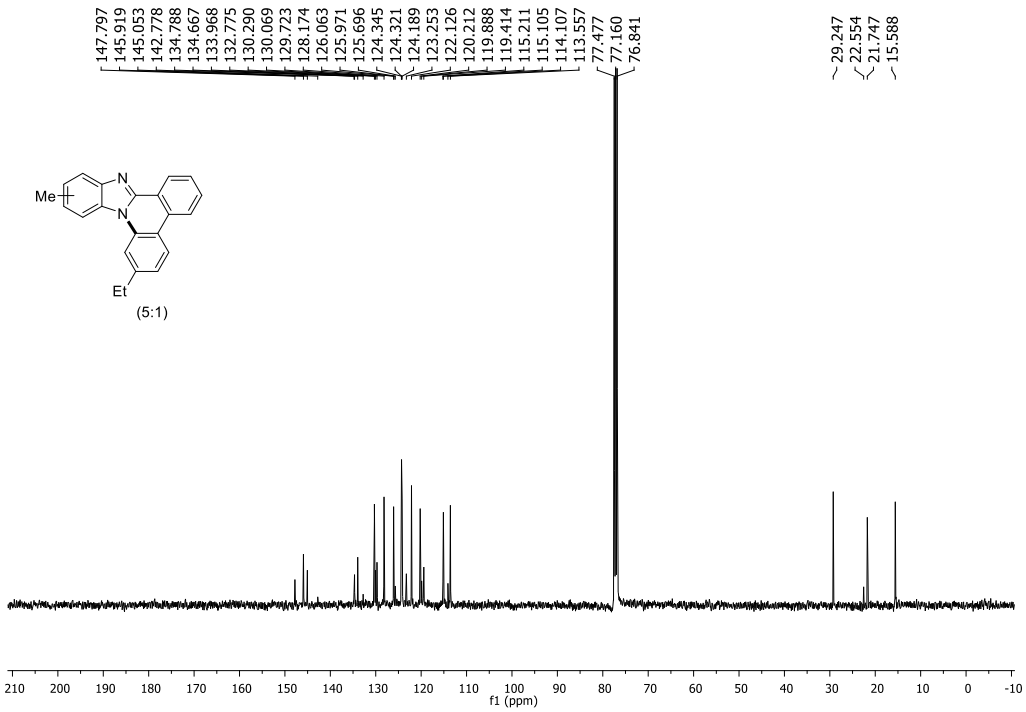

Figure 3.29. ^{13}C{^{1}H} NMR spectrum of 2-Ethyl-11-methylbenzo[4,5]imidazo[1,2-f]phenanthridine and 2-Ethyl-12-methylbenzo[4,5]imidazo[1,2-f]phenanthridine **(4ee).**

^{1}H NMR (400 MHz, $CDCl_3$)

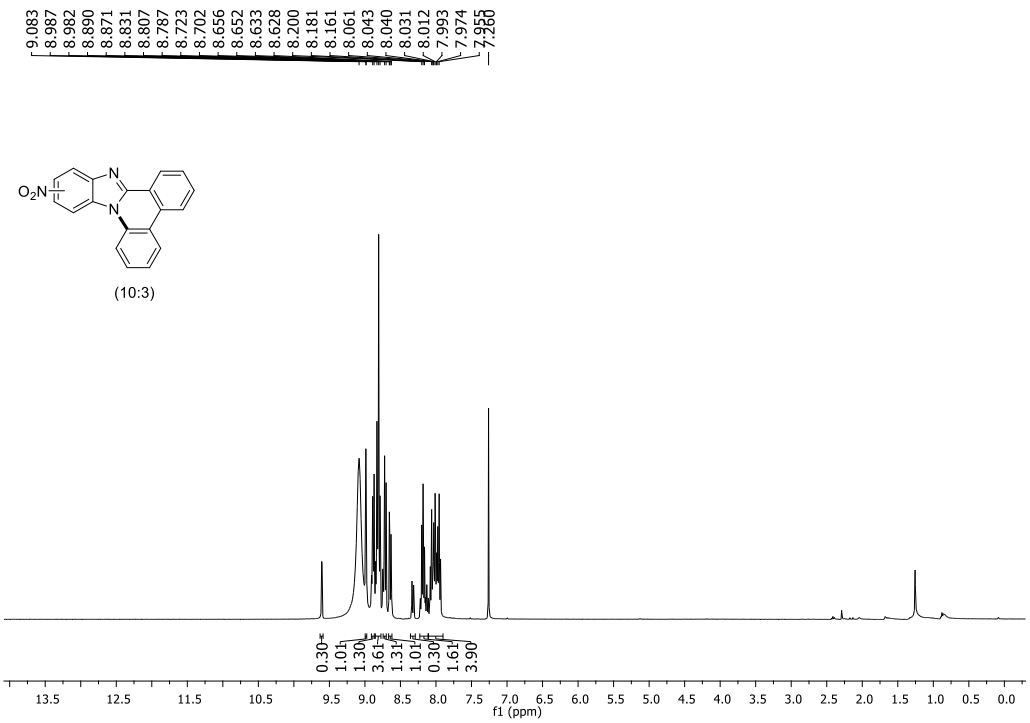

Figure 3.30. ^{1}H NMR spectrum of of 11-Nitrobenzo[4,5]imidazo[1,2-f]phenanthridine and 12-Nitrobenzo[4,5]imidazo[1,2-f]phenanthridine **(4fa).**

^{1}H NMR (400 MHz, $CDCl_3$)

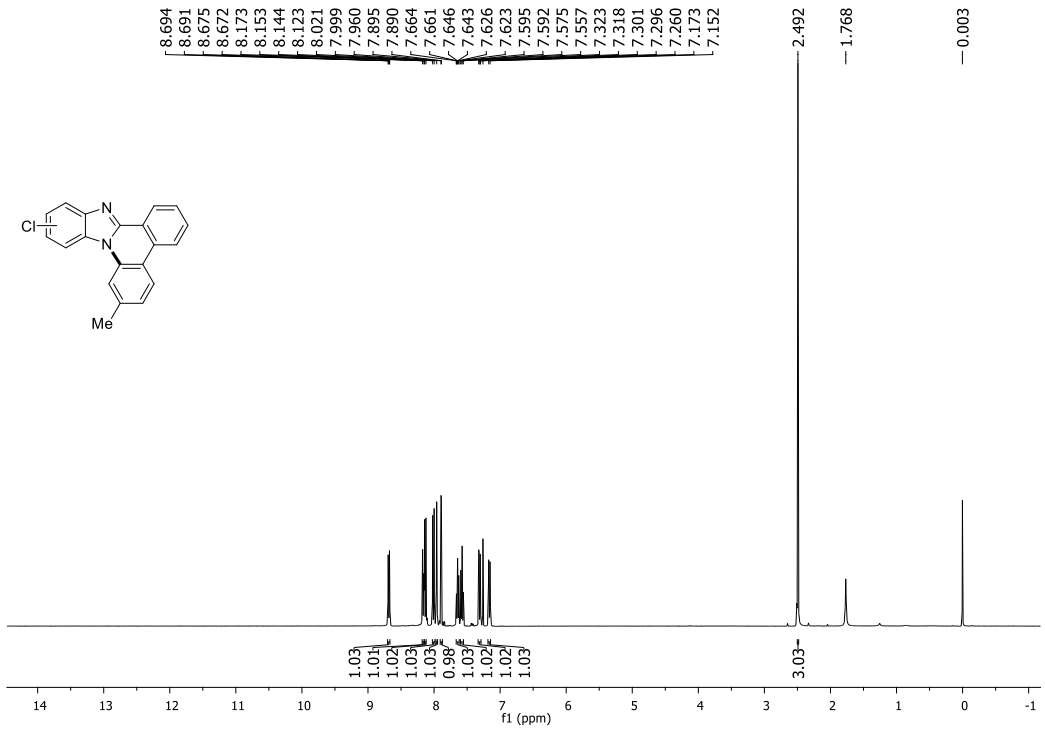

Figure 3.31. ^{1}H NMR spectrum of 11-Chloro-2-methylbenzo[4,5]imidazo[1,2-f]phenanthridine OR 12-Chloro-2-methylbenzo[4,5]imidazo[1,2-f]phenanthridine **(4gb).**

^{13}C NMR (100 MHz, $CDCl_3$)

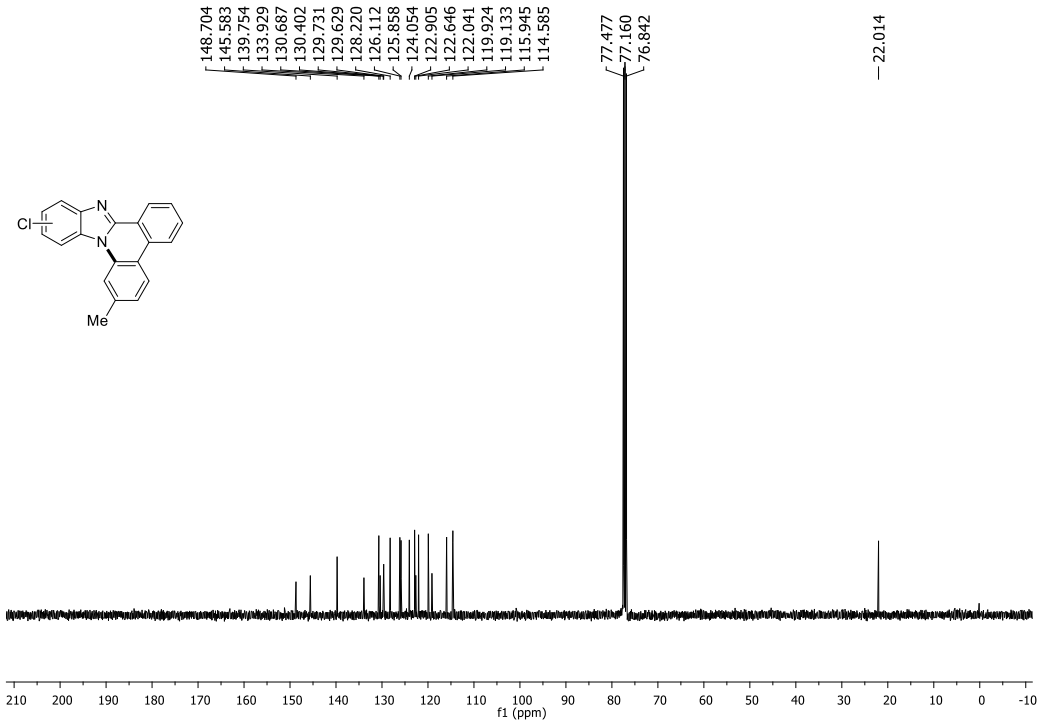

Figure 3.32. $^{13}C\{^1H\}$ NMR spectrum of 11-Chloro-2-methylbenzo[4,5]imidazo[1,2-f]phenanthridine OR 12-Chloro-2-methylbenzo[4,5]imidazo[1,2-f]phenanthridine **(4gb).**

^{1}H NMR (400 MHz, $CDCl_3$)

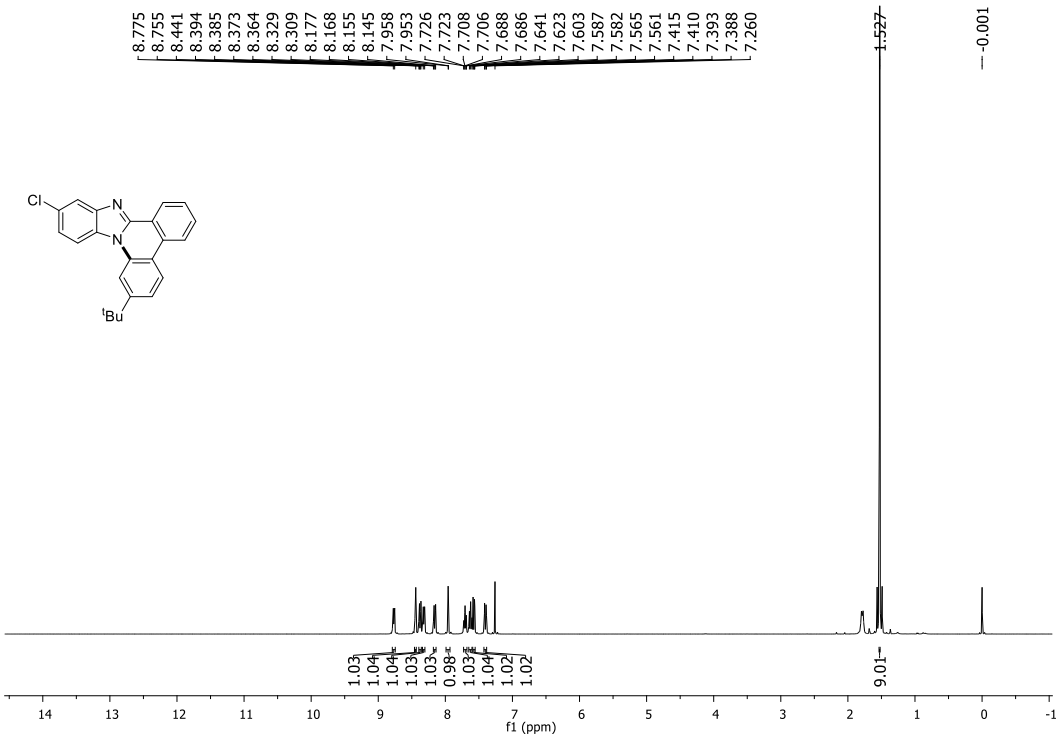

Figure 3.33. ^{1}H NMR spectrum of 2-(Tert-butyl)-11-chlorobenzo[4,5]imidazo[1,2-f]phenanthridine **(4gc).**

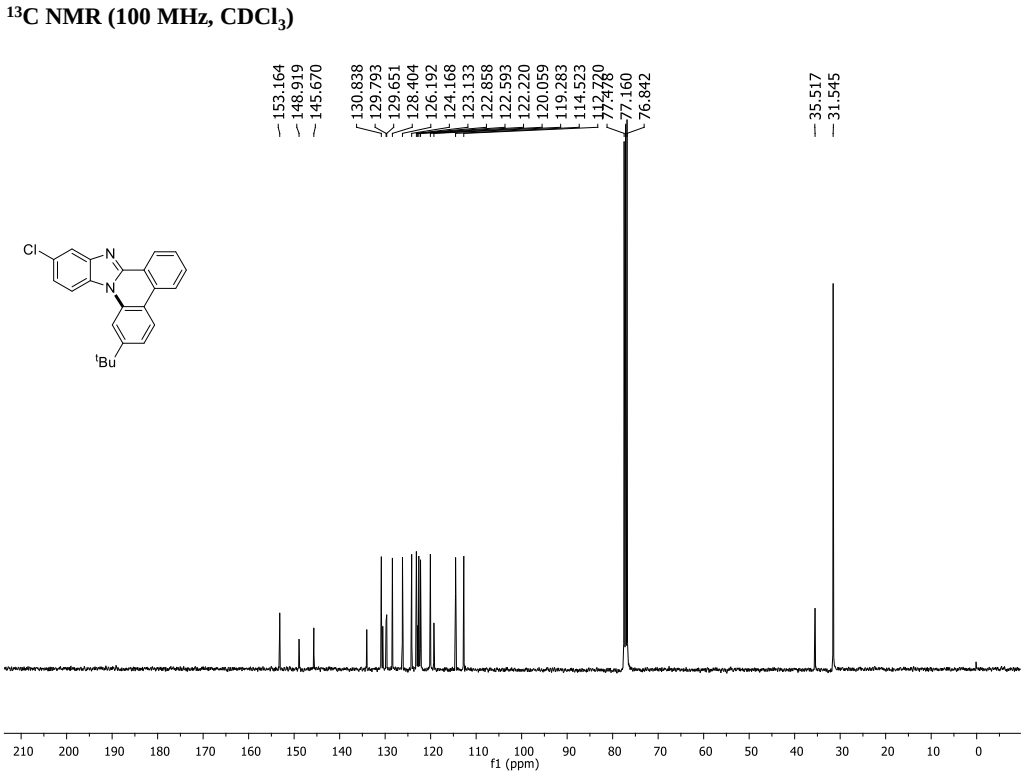

Figure 3.34. $^{13}C\{^{1}H\}$ NMR spectrum of 2-(Tert-butyl)-11-chlorobenzo[4,5]imidazo[1,2-f]phenanthridine **(4gc).**

CHAPTER 4

Regiodivergent C-N coupling of Quinazolinones Controlled by the Tautomers Dipole Moments

4.1 ABSTRACT

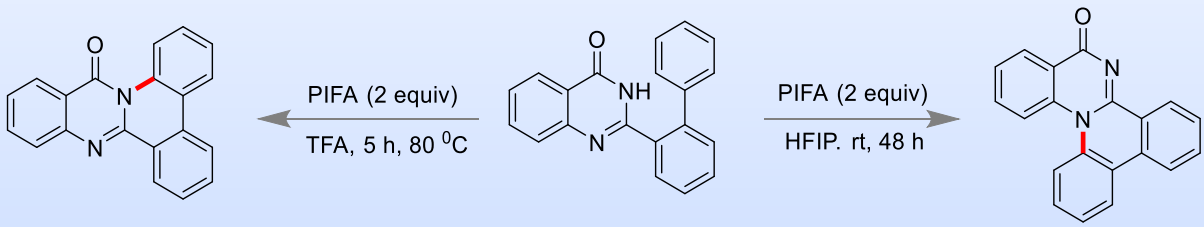

The dipole moments of tautomers can be the controlling factor for regiodivergent synthesis of either 14H-quinazolino[3,2-f]phenanthridin-14-ones or 6H-quinazolino[1,2-f]phenanthridin-6-ones, selectively, from unmasked 2-([1,1'-biphenyl]-2-yl)quinazolin-4(3H)-one. The combination of PIFA with N-H center of quinazoline moiety generates the nitrenium ion, and it delivers two types of cyclized products depending upon the reaction condition and solvent. This metal-free approach offers a wide range of substrates with good to excellent yield under mild reaction conditions.

4.2 INTRODUCTION

Recently regiodivergent strategies have attracted significant attention in synthetic organic chemistry due to its product selectivity, efficiency, and atom economy.[1] However, divergent synthesis was well documented toward the construction of structurally diverse molecular skeletons, which hold an essential role in synthesis.[2] In particular, regiodivergent C-H functionalization reactions is one of the popular techniques.[3] Various metal-catalyzed divergent reactions for the synthesis of heterocyclic scaffolds were well explored.[4] Similarly, Pd- and Cu- catalyzed annulative π-extension and *N*-arylation of unmasked 2-phenylquinazolin-4(3H)-ones were achieved in the presence of iodonium salts.[5] In this

context, Du and coworker reported the $PhI(OCOCF_3)_2$ or PIFA mediated divergent synthesis of spiro[4,5]trienones and iodinated quinilin-2-ones from *N*-arylpropynamides, where PIFA acted as an iodination reagent as well as oxidant.[6]Finding efficient methodologies for synthesizing complex molecular architecture is one of the popular research topics in chemistry.[7] Therefore, the synthesis of these complex-molecules by utilizing weak or noncovalent interactions can be the state of art practice in chemical science.[8]

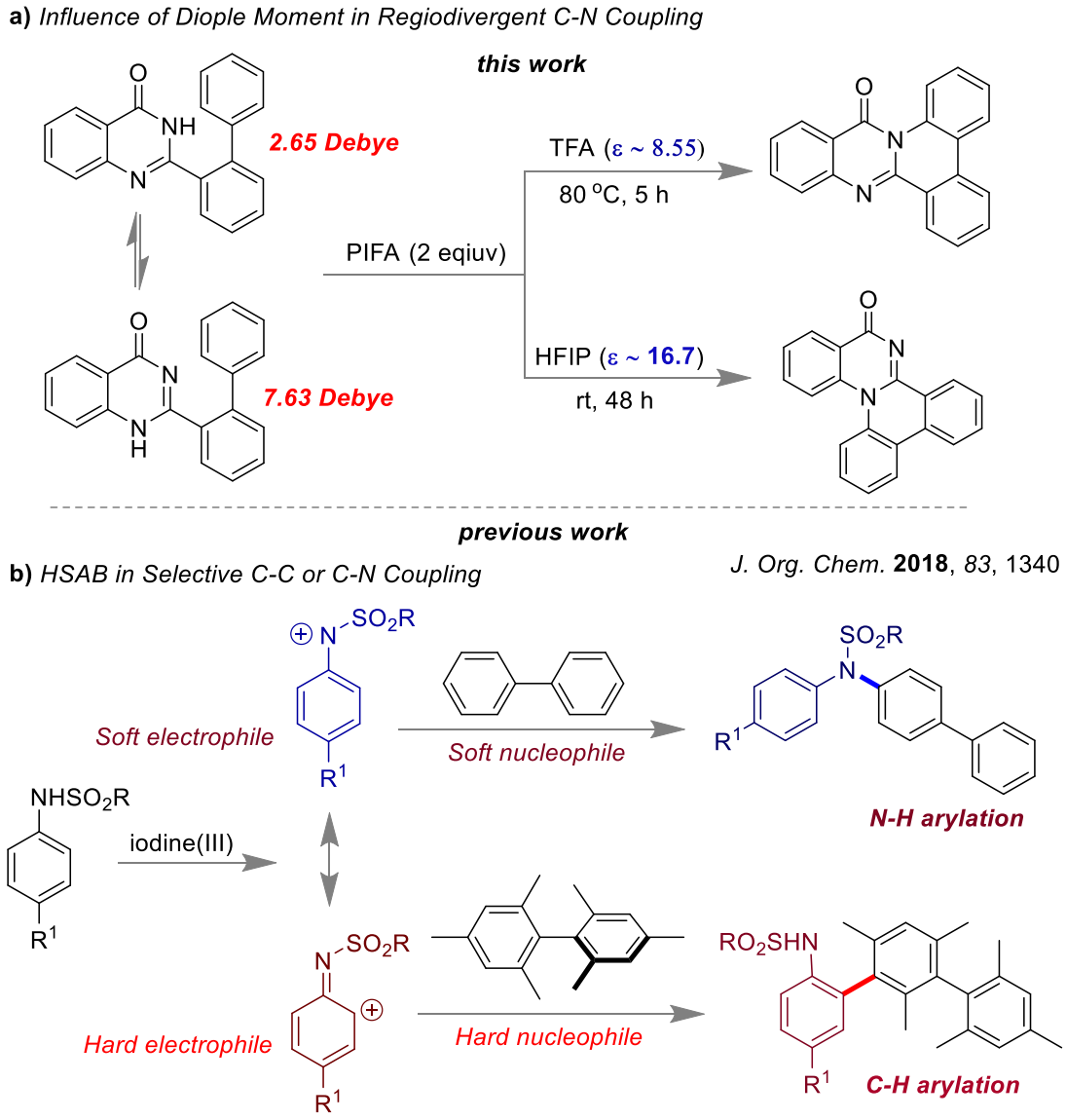

Scheme 4.1. a) This work: Based on regiodivergent C-N coupling controlled by tautomers dipole moment and solvent polarity. b) HSAB in the selective C-C or C-N bond formation reactions.[9]

The weak interactions[10] like cation-π,[11] anion-π,[12] hydrogen-bonding (H-bonding),[13] halogen-bonding (XB),[14] sulfur…oxygen,[15] hydrophobic effect,[16] etc., have been used regularly to control many chemical reactions.[8a] Due to the charge transfer complexation, amines or amine derivatives have high reactivity towards hypervalent iodine reagents.[17] This strategy is shown to be useful for various metal- free oxidative C-N coupling reactions.[18] In 2015, Hajela and coworkers reported palladium-catalyzed intramolecular C-H bond activation for the synthesis of phenanthridine-fused quinazolinones.[19] Additionally, Banerji's group demonstrated aerobic oxidative C-H amination towards synthesizing quinazolinone- and phenanthridine-fused pentacyclic heteropolycycles using palladium as a catalyst.[20] Herein, we have investigated the switchable and regiodivergent synthesis of 14H-quinazolino[3,2-f]phenanthridin-14-one and 6H-quinazolino[1,2-f]phenanthridin-6-one from 2-([1,1'-biphenyl]-2-yl)quinazolin-4(3H)-one (Scheme 4.1.a) using PIFA as the sole reagent in the hexafluoroisopropanol (HFIP) and trifluoroacetic acid (TFA) solvents. We anticipated that when the solvent polarity[21] and the dipole moment of the tautomers matched, a regiodivergent synthesis could be achieved. Therefore, this work can be categorized under the area of supramolecular catalysis. Next, it is shown in Scheme 4.1.b, that hard-soft acid base (HSAB) preferences from the selection of nucleophiles led to either C-C or C-N bond formation reactions selectively.[9]

4.3 RESULTS AND DISCUSSION

The reaction condition was optimized using 2-([1,1'-biphenyl]-2-yl)quinazolin-4(3H)-one (**1a**) as the model substrate (Table 4.1). The reaction of **1a** with 1.2 equiv of PIDA in TFE (trifluoroethanol) delivered the 6H-quinazolino[1,2-f]phenanthridin-6-one (**3a**) with 20% yield (entry 1, Table 1). Using PIDA (phenyl iodine diacetate) in HFIP, the yield of **3a** was also poor (entry 2).

Table 4.1. Optimization of reaction conditions.[a]

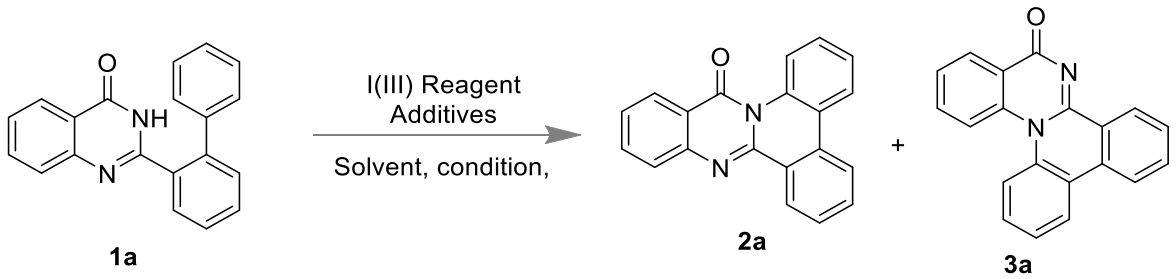

Entry	I(III) Reagent (equiv)	Additives (equiv)	Solvent	Yield % of 2a (Non-polar spot)	Yield % of 3a (polar spot)
1	PIDA (1.2)	-	TFE	00	20
2	PIDA (1.2)	-	HFIP	00	22
3	PIDA (1.5)	-	HFIP	00	25
4	PIFA (1.5)	-	HFIP	05	46
5	PIFA (2)	-	DCM	12	28
6	PIFA (2)	-	DCE	08	32
7	PIFA (2)	-	CH_3CN	07	27
8	PIFA (2)	-	EtOH	06	30
9	**PIFA (2)**	**-**	**HFIP**	**06**	**72**
10	PIFA (2)	-	DMSO	NR	NR
11	PIFA (2)	K_2CO_3 (2)	HFIP	00	25
12	PIFA (2)	$BF_3.OEt_2$ (2)	HFIP	21	00
13	$PhI(OCO^tBu)_2$ (2)	-	HFIP	NR	NR
14	PIFA (2)	-	HFIP, 0 ℃	05	40
15[b]	PIFA(2)		HFIP, 80 ℃	44	36
16	PIFA (2)	-	HFIP:TFA (1:1)	40	31
17[b]	PIFA (2)	-	HFIP:TFA (1:1), 80 ℃	47	50

18	PIFA (2)		TFA	42	14
19[b]	**PIFA (2)**	**-**	**TFA, 80 °C**	**84**	**08**
20[b]	PIFA (1.5)	-	TFA, 80 °C	61	16
21[b]	PIFA (2)	-	TFA:DCM (1:1), 80 °C	40	06
22[b]	PIFA (2)	-	TFA:CH_3CN (1:1), 80 °C	35	07
23[b]	PIFA (2)	-	TFA: DCE (1:1), 80 °C	44	11
24[b]	PIFA (2)	$BF_3.OEt_2$ (2)	DCM, 80 °C	56	13
25	PIFA (2)	-	Toluene	42	05

[a]Reaction conditions (isolated yields): 0.201 mmol (1 equiv) of **1a** and 0.402 mmol of PIFA (2 equiv) in 1.5 mL solvent at room temperature for 48 h; [b]reaction has stirred for 5 h at 80 °C.

However, the use of 1.5 equiv PIFA in HFIP led to **2a** and **3a** with 5% and 46% yields, respectively (entry 4). Interestingly, the maximum yield (72%) of **3a** was obtained with 2.0 equiv of PIFA in HFIP at room temperature (entry 9). The use of additives like K_2CO_3 and $BF_3.OEt_2$ did not lead to any improvement of the products yields (entry 11 and 12). The reaction failed when $PhI(OCO^tBu)_2$ was used as an oxidant (entry 13). It was observed that the effect of temperature did not show any encouraging result to obtain **2a** (entry 15). The mixture of solvent HFIP: TFA (1:1) at room temperature and 80 °C led to the mixture of products **2a** and **3a** (entries 16 and 17). A similar observation was made when TFA was used as solvent at room temperature (entry 18). Interestingly, when **1a** was treated with 2 equiv of PIFA in TFA solvent at 80 °C, **2a** was obtained as maximum yield (84%) with 8% of the product **3a** (entry 19).

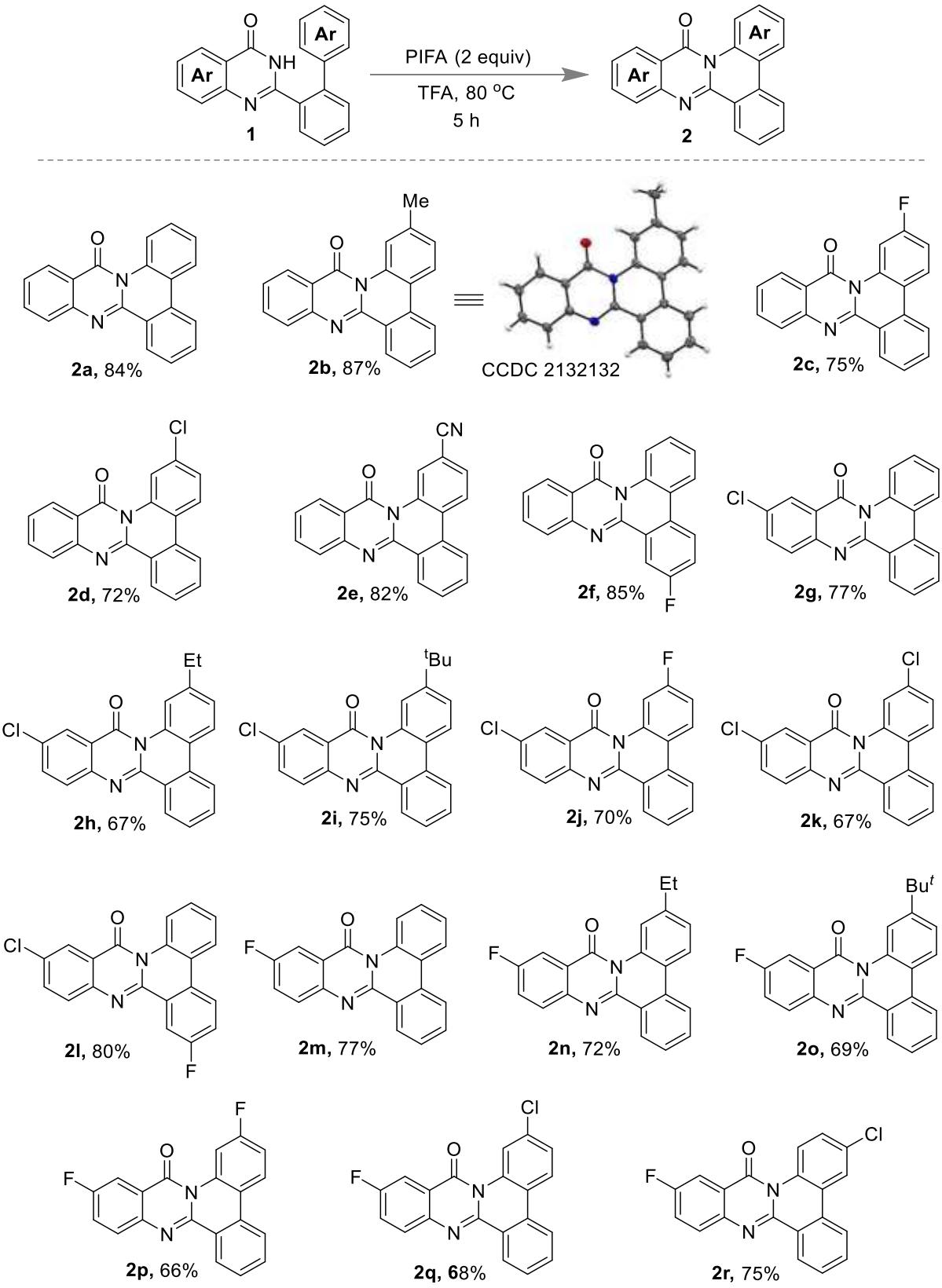

Figure 4.1. Synthesis of 14H-quinazolino[3,2-f]phenanthridin-14-ones in TFA.

Both quinazolinone and phenanthridine frameworks are important structural motifs in synthetic chemistry.[22] The substrate scope of the reaction is verified, which is shown in Figure 4.1 and Figure 4.2. The synthesis of 14H-quinazolino[3,2-f]phenanthridin-14-one derivatives (**2**) was achieved using PIFA (2.0 equiv) in 1.5 mL TFA solvent at 80 ℃ within 5 h. Various electron-donating and electron-withdrawing groups at biphenyl moiety of the 2-position of quinazolin-4(3H)-one were well tolerated. Initially, quinazolin-4(3H)-one ring having methyl, flouro, chloro and cyano at the biphenyl skeleton have delivered the corresponding cyclized product (**2b**-**2f**) with good yields. Next, chloro and fluoro groups in the quinazolin-4(3H)-one moiety was verified under the standard reaction condition. It was found that, biphenyl moiety at the 2-position of 6-chloroquinazolin-4(3H)-one produced **2g** with 77% yield. In contrast, different substitutions (like ethyl, *tert*-butyl, fluoro and chloro group) at biphenyl moiety were smoothly converted to the corresponding product (**2h**-**2l**) with good yields as well. Similarly, the substrate 2-([1,1'-biphenyl]-2-yl)-6-fluoroquinazolin-4(3H)-one (**1m**) also deliver the cyclized product (**2m**) with good yield. In addition, various electron-donating groups (ethyl and tert-butyl) as well as electron-withdrawing groups (fluoro and chloro) at the 2- position of 6-fluoroquinazolin-4(3H)-one moiety was explored and which afforded the respective products (**2n**-**2r**) with good yields.

The syntheses of 6H-quinazolino[1,2-f]phenanthridin-6-one derivatives (**3**) are shown In Figure 4.2, which were achieved as major products using 2.0 equiv of PIFA in 1.5 mL HFIP at room temperature for 48 h. The minor products could not be isolated. The substrate (**1a**) was efficiently converted to respective cyclized products **3a** with 72% yield. The incorporation of chloro and trifluoro substituent at biphenyl moiety of quinazolin-4(3H)-one ring was also well tolerated to afford the **3s** and **3t** with 87% and 76% yields, respectively. Similarly, 6-chloroquinazolin-4(3H)-one having trifluoro and chloro group at the biphenyl skeleton were smoothly converted to the respective product **3u** and **3v** with good yield.

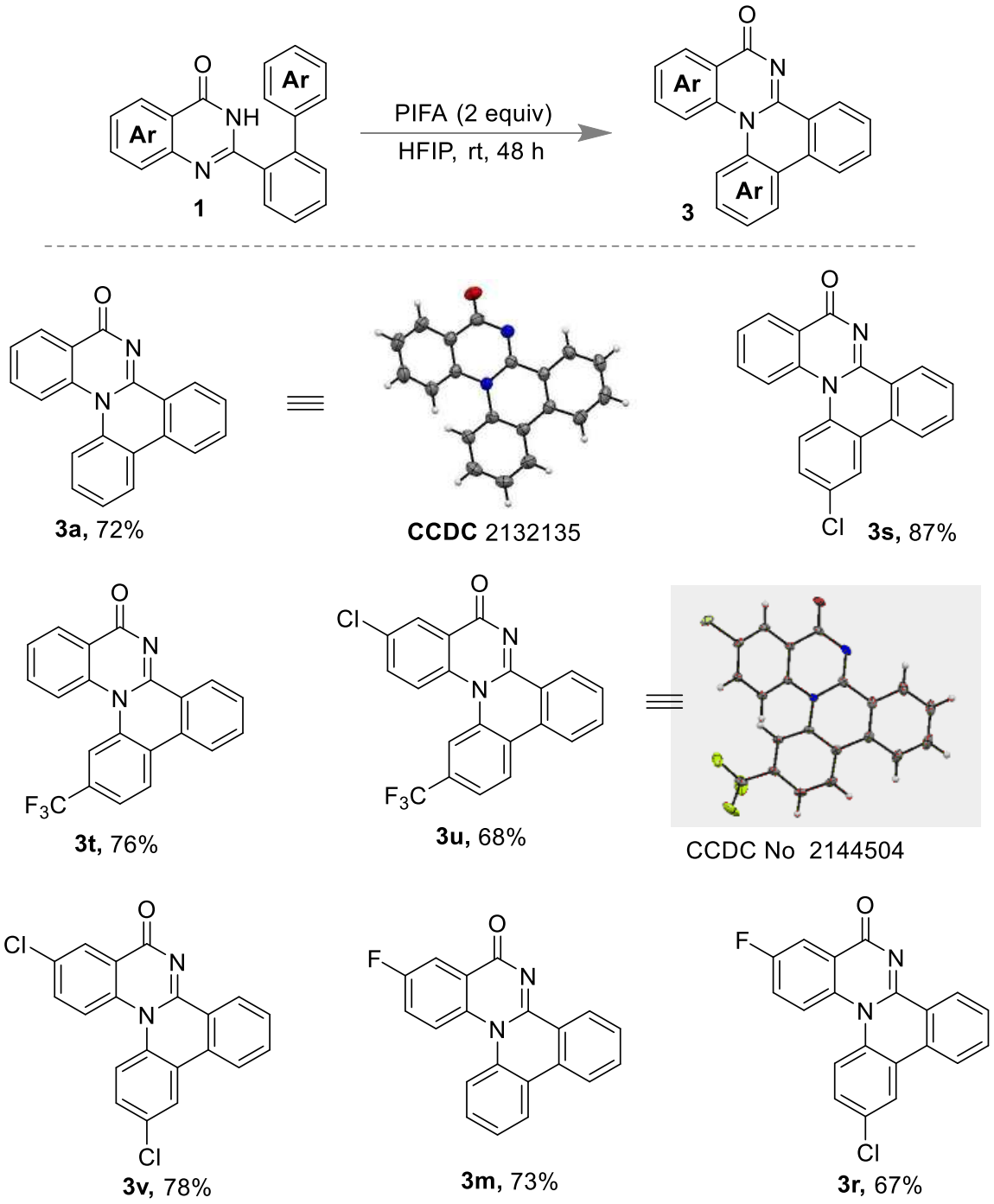

Figure 4.2. Synthesis of 6H-quinazolino[1,2-f]phenanthridin-6-ones in HFIP at room temperature.

The structures of **3a** and **3u** were also confirmed by single-crystal X-ray. Similarly, 6-fluoroquinazolin-4(3H)-one containing substrates were efficiently transformed to the corresponding products **3m** and **3r** with good yield.

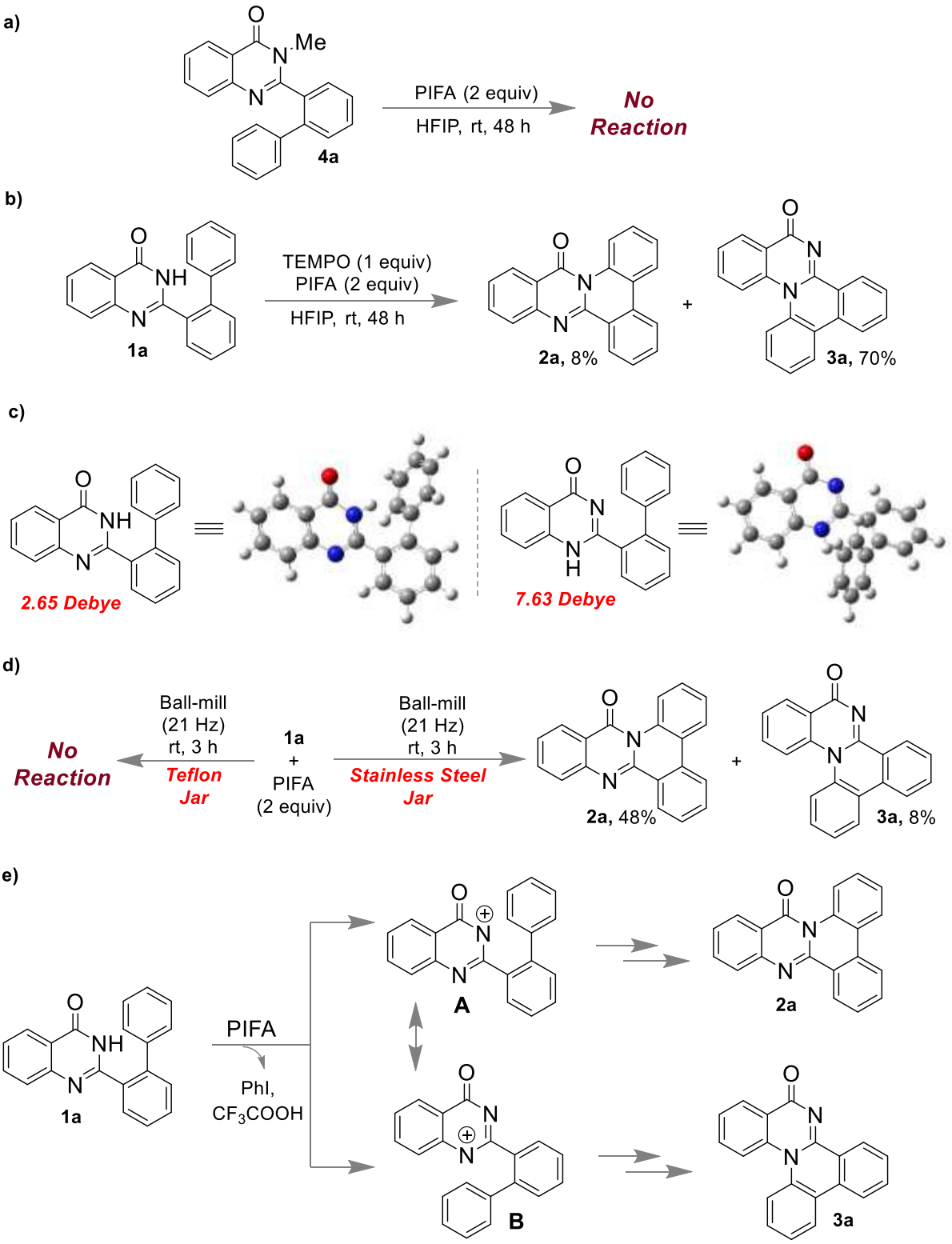

Figure 4.3. a) The *N*-methyl substituted derivative was found to be unreactive. b) TEMPO-radical experiment. c) The dipole moments of the tautomers. d) The ball-milling experiments. e) A plausible mechanism of the reaction.

The control experiments shown in Figure 4.3 helped to understand the mechanism of the reaction. The substrate 2-([1,1'-biphenyl]-2-yl)-3-methylquinazolin-4(3H)-one (**4a**) was unreacted under the standard reaction condition (Figure 4.3.a). This indicates that the presence of the N-H group is essential for the cyclization reaction. The involvement of the radical pathway could be ruled out because the radical scavenger TEMPO could not affect the progress of the reaction (Figure 4.3.b).

The DFT calculations using the B3LYP/6-311++G(d,p) basis set helped to estimate the dipole-moment of the tautomers of **1a**. The two tautomers shown to have the dipole moments for 2-([1,1'-biphenyl]-2-yl)quinazolin-4(3H)-one and 2-([1,1'-biphenyl]-2-yl)quinazolin-4(1H)-one are 2.65 and 7.63 Debye, respectively (Figure 4.3.c). Therefore, the tautomer with higher dipole moment (7.63 Debye) is expected to be more stable in HFIP, which has dielectric constant $\varepsilon \sim 16.7$.[23] However, the other tautomer having 2.65 Debye dipole moment should preferentially exist in TFA ($\varepsilon \sim 8.55$).

We have also carried out the experiments under solvent-free ball-milling (21 Hz, 3 h) conditions at room temperature using either teflon or stainless-steel jars (Figure 4.3.d). It was anticipated that due to Lewis acidic properties, a stainless-steel jar could influence the formation of one of the tautomers more efficiently and compound **2a** was isolated as the major product.[24] The C-N coupling could occur from the nitrogen center near the carbonyl group. However, in teflon jar the reaction was failed.

A plausible mechanism is proposed in Figure 4.3.e. Hypervalent iodine reagents are well known to form nitrenium ions (**A** or **B**)[25] with amine derivatives. The nitrenium ions are finally expected to result in the final products **2** or **3** from the intermediates **A** or **B**, respectively, *via* intramolecular aromatic electrophilic substitution reaction.[9] The oxygen is more electronegative than nitrogen, so, the protonation at carbonyl oxygen is more probable than the imine nitrogen center. So, we could rule out the possibilities for the regioselective

protonation of imine nitrogen under TFA and followed by a reaction of amide nitrogen with PIFA generating electrophilic nitrogen. Next, in the absence of TFA, the secondary amine of the other tautomer with a higher dipole moment could react with PIFA in HFIP generating the nitrenium ion **B** (Figure 4.3.e).

The products are expected to form efficiently *via* nitrenium ion intermediate (Figure 4.3.e) with hypervalent iodine reagents and mostly in fluorinated solvents.[9] However, the nonfluorinated solvents having a high dielectric constant DCE 10.36 (entry 6), CH_3CN 37.5 (entry 7), EtOH 24.5 (entry 8) delivered 6H-quinazolino[1,2-f]phenanthridin-6-one **3a** as a major product. However, toluene having a dielectric constant 2.38 (entry 25) produced the 14H-quinazolino[3,2-f]phenanthridin-14-one **2a** as a major product. The reaction was failed in the solvent DMSO (entry 10). The relative population of any of the tautomers can be controlled by the nature of the solvent. Therefore, the tautomers might have different dipole moments when the solvents were changed. Hence, we could establish that the dipole moment and solvent polarity could be a controlling factor of the reaction *via* the "Matched by Match" concept.

The large-scale synthesis for the compounds **2a** and **3a** is shown in Figures 4.5a and 4.5b, respectively. An organocatalytic version of the reaction is shown in Figure 4.5c where the hypervalent iodine reagent was generated *in situ* from phenyl iodide (PhI) and *m*-chloro perbenzoic acid (*m*CPBA).[26] The products **2a** and **3a** were isolated in 12% and 68 % within 5 days, respectively.

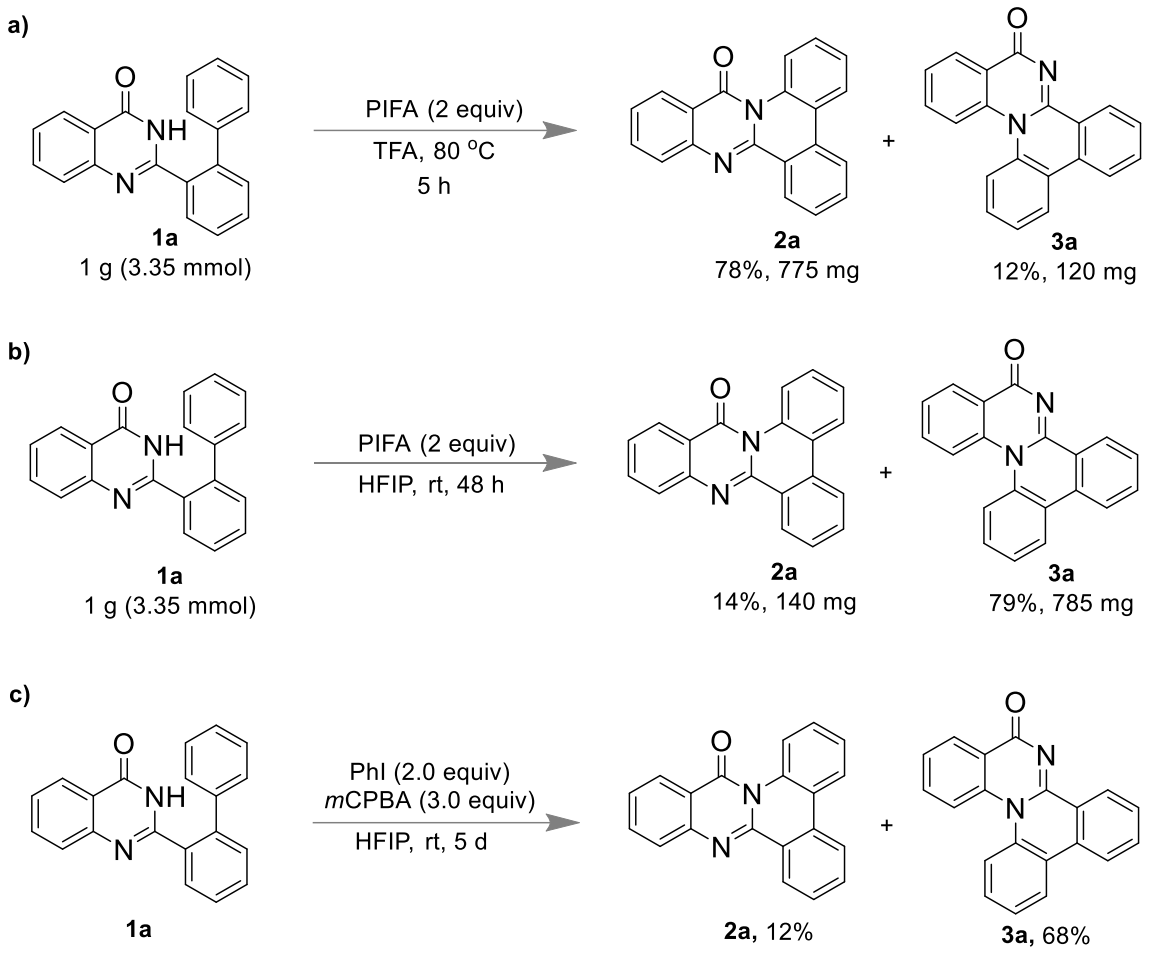

Figure 4.5. Gram-scale synthesis using the solvents a) TFA and b) HFIP. c) Organocatalytic version of the reaction.

The photophysical properties of the compounds similar to 14H-quinazolino[3,2-f]phenanthridin-14-ones **2** are reported in literature.[20] The UV/Vis and fluorescence spectra of selected 6H-quinazolino[1,2-f]phenanthridin-6-ones **3** are given in the Figure 4.6. The compounds show strong absorption in 320-400 nm region. In addition, strong emissions were observed (λ_{ex} ~ 254 nm) near 450 nm.

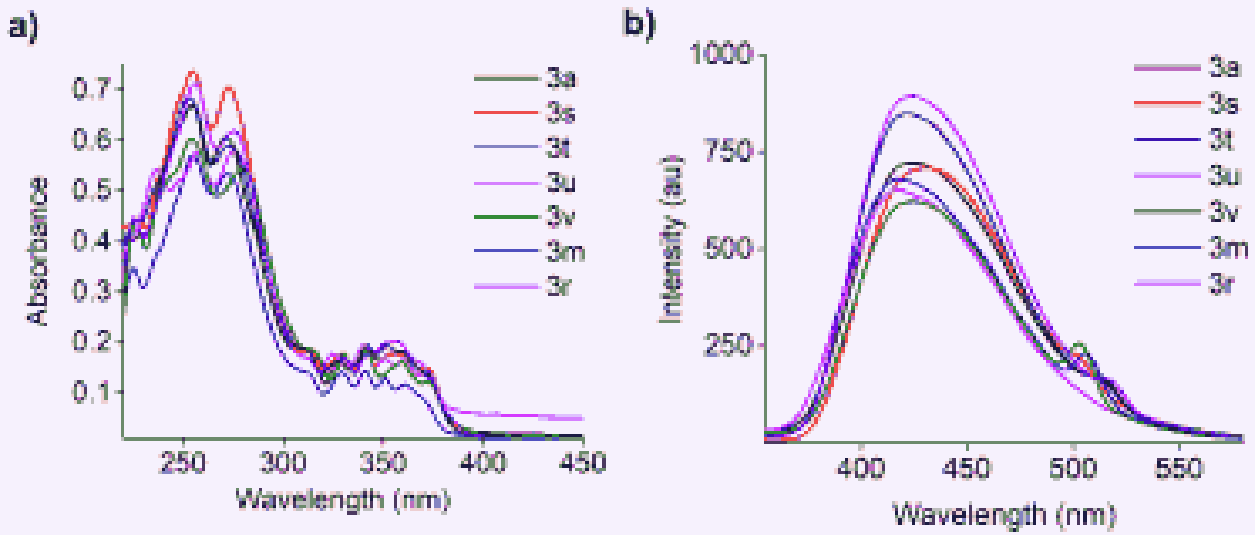

Figure 4.6. Photophysical studies. a) UV-visible (left) and b) fluorescence (right, λ_{ex} ~ 254 nm) spectra of selected 6H-quinazolino[1,2-f]phenanthridin-6-ones 3 (3×10^{-6} M in DCM).

4.4 CONCLUSION

In summary, we have established that the dipole moments of the tautomers can also be a controlling factor for regiodivergent synthesis of phenanthridine-fused quinazolinones *via* an intramolecular C-N coupling reaction initiated by PIFA. The tautomer having high dipole moment led to the corresponding regioisomers in a solvent having high dielectric constant. The reactions were controlled by cooperative weak or noncovalent interactions. Therefore, we anticipate that this work will be highly important to the chemistry community working on organic synthesis.

4.5 EXPERIMENTAL SECTION

General Information. Commercially available reagents and solvents were used as received. Column chromatographic purifications of the compounds were performed using silica gel (mesh 230–400, 100-200) and hexane – ethyl acetate solvent mixtures. NMR spectra were recorded on a 400 MHz or 700 MHz instruments at 25 °C. The chemical shift values are reported in parts per million (ppm) with respect to residual trichloromethane (7.26 ppm for ^{1}H and 77.16 ppm for ^{13}C). The peak patterns are designated as follows: s: singlet; d: doublet;

t: triplet; q: quartet; m: multiplet; dd: doublet of doublets; td: triplet of doublets; brs: broad singlet. The coupling constants (*J*) are reported in hertz (Hz). High-resolution mass spectra (HR-MS) were recorded on an ESI-TOF (time of flight) mass spectrometer. Infrared spectral data are reported in wavenumber (cm^{-1}). FT-IR spectra were recorded after making thin layer of the compounds on the surface of NaCl crystal using dichloromethane. Melting points of the compounds were determined using a digital melting point apparatus and are uncorrected.

General Procedure for preparation of 2-([1,1'-biphenyl]-2-yl)quinazolin-4(3H)-one

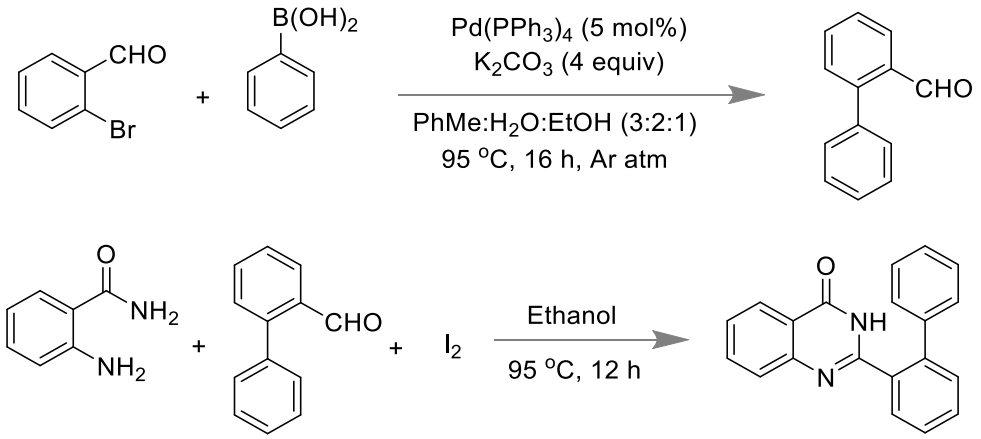

Synthesis of [1,1'-biphenyl]-2-carbaldehyde.[27] To a solution of 2-bromobenzaldehyde (5.4 mmol, 1 equiv), aryl boronic acid (5.94 mmol, 1.1 equiv), $Pd(PPh_3)_4$ (0.27 mmol, 0.05 equiv) and potassium carbonate (21.6 mmol, 4 equiv) in Toluene:H_2O:EtOH (9: 6 :3 mL) were stirred at 100 °C (in an oil bath) under an argon atmosphere until the starting material was completely consumed (typically 16 h). After cooling down to room temperature, the reaction mixture was concentrated and diluted with brine (25 mL). Then organic layer was extracted with EtOAc (25 mL × 2) and dried over Na_2SO_4. The concentrated crude product was purified by column chromatography to [1,1'-biphenyl]-2-carbaldehyde, which was used for the next step.

Synthesis of 2-([1,1'-biphenyl]-2-yl)quinazolin-4(3H)-one. A mixture of anthranilamide (1.10 mmol, 1.0 equiv), [1,1'-biphenyl]-2-carbaldehyde (1.21 mmol, 1.1 equiv) and iodine

(307 mg mmol, 1.1 equiv) were taken in ethanol solvent (5 mL). Then the reaction mixture was placed in a preheated oil bath (95 ºC) for 12 h. After cooling down to room temperature, the reaction mixture was concentrated under vacuum and appropriate amount aqueous of sodium thisulpahte solution was added to it. The mixture was extracted with EtOAc and the organic layer was dried over Na_2SO_4, filtered and concentrated in a vacuum. The residue was purified by column chromatography to give the product (94 % as a white solid).

Representative Procedure for Preparation of 14H-Quinazolino[3,2-f]phenanthridin-14-one (2a).

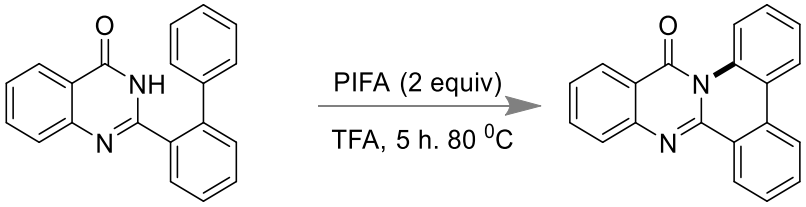

A solution of 2-([1,1'-biphenyl]-2-yl)quinazolin-4(3H)-one **1a** (60 mg, 0.201 mmol, 1.0 equiv), in trifluoroacetic acid (TFA) (2.0 mL), PIFA (173 mg, 0.40 mmol, 2.0 equiv) was added and the reaction mixture were stirred in a preheated oil bath (80 ºC) for 5 h. The reaction progress was monitored by TLC using ethyl acetate and hexane as eluent. After the completion, the reaction mixture was diluted with ethyl acetate and saturated solution of sodium hydrogen carbonate. Then organic layer was extracted with EtOAc (25 mL × 2) and dried over Na_2SO_4. Further the resulting solution was evaporated to dryness. The crude residue was purified on silica gel column chromatography (10% EtOAc in hexane) to get the pure product 14H-quinazolino[3,2-f]phenanthridin-14-one **2a** (50 mg, yield 84%).

.

Representative Procedure for Preparation of 6H-Quinazolino[1,2-f]phenanthridin-6-one (3a).

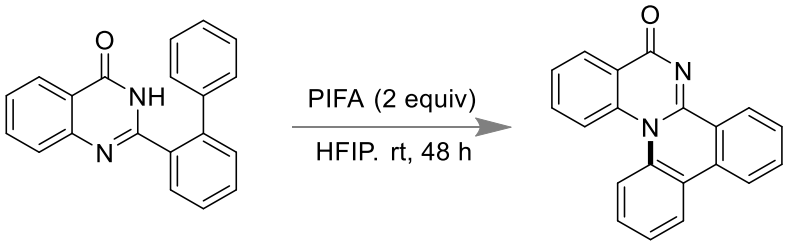

To a stirred solution of 2-([1,1'-biphenyl]-2-yl)quinazolin-4(3H)-one **1a** (60 mg, 0.201 mmol, 1.0 equiv), in 1,1,1,3,3,3-hexafluoro-2-propanol (HFIP) (2.0 mL), PIFA (173 mg, 0.40 mmol, 2.0 equiv) was added slowly at room temperature. The reaction mixture was allowed to stir until completion. The reaction progress was monitored by TLC using ethyl acetate and hexane as eluent. After the completion of reaction (48 h) resulting solution was evaporated to dryness. The crude residue was purified on silica gel column chromatography (50% EtOAc in hexane) to get the pure product 6H-quinazolino[1,2-f]phenanthridin-6-one **3a** (43 mg, yield 72%).

CHARACTERIZATION DATA

The product **2a** and **3a** was identified by using the ^{13}C NMR and TLC (SiO_2 plates) study. ^{13}C NMR of the carbonyl group of product **2a** was found in the 163.2 regions, whereas product **3a** shows the peak at 168.3 ppm. However, compound **2a** shows the R_f (in SiO_2 TLC plates) about 0.6 in hexane and ethyl acetate (9:1) mixture, whereas compound **3a** shows 0.3 in ethyl acetate and hexane (2:3) mixture. In addition to this, we have also shown the single crystallography data of the **3a** and **3u** (lower spot in SiO_2 TLC plates) as well as **2b** (upper spot in SiO_2 TLC plates) in our manuscript.

2-([1,1'-Biphenyl]-2-yl)quinazolin-4(3H)-one (1a):[20] R_f = 0.45 (hexane/ethyl acetate 7:3); white solid; yield 94% (119 mg); ^{1}H NMR (700 MHz, $CDCl_3$) δ 9.66 (s, 1H), 8.25 – 8.13 (m, 1H), 7.85 (t, *J* = 7.0 Hz, 1H), 7.80 – 7.75 (m, 2H), 7.59 – 7.55 (m, 1H), 7.52 – 7.45 (m, 3H), 7.31 (d, *J* = 7.0 Hz, 2H), 7.28 – 7.26 (m, 1H); 7.25 – 7.21 (m, 2H); ^{13}C NMR (175 MHz, $CDCl_3$) δ 162.1, 153.8, 149.2, 140.7, 139.3, 134.8, 132.8, 131.1, 130.9, 130.5, 129.1, 128.8, 128.1, 128.1, 127.9, 127.0, 126.5, 120.8.

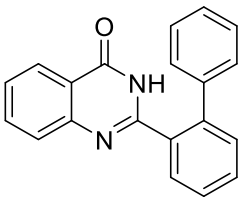

2-(4'-Methyl-[1,1'-biphenyl]-2-yl)quinazolin-4(3H)-one (1b):[20] R_f = 0.45 (hexane/ethyl acetate 7:3); white solid; yield 86% (197 mg); ^{1}H NMR (400 MHz, $CDCl_3$) δ 9.25 (s, 1H), 8.18 (d, *J* = 7.6 Hz, 1H), 7.86 (dd, *J* = 7.2, 6.0 Hz, 1H), 7.82 – 7.72 (m, 2H), 7.60 – 7.53 (m, 1H), 7.47 (tt, *J* = 10.4, 3.6 Hz, 3H), 7.21 (dd, *J* = 8.0, 2.4 Hz, 2H), 7.08 (t, *J* = 7.2 Hz, 2H), 2.30 (s, 3H); ^{13}C NMR (100 MHz, $CDCl_3$) δ 161.8, 153.8, 149.3, 140.5, 138.1, 136.2, 134.8, 132.6, 131.1, 131.0, 130.6, 129.7, 128.9, 127.9, 127.9, 127.0, 126.6, 120.9, 21.3; HR-MS (ESI-TOF) m/z calcd for $C_{21}H_{17}N_2O$ $[M + H]^+$ 313.1335, found 313.1339.

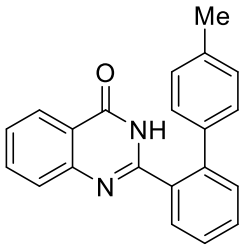

2-(4'-Fluoro-[1,1'-biphenyl]-2-yl)quinazolin-4(3H)-one (1c):[20] R_f = 0.45 (hexane/ethyl acetate 7:3); white solid; yield 82% (190 mg); ^{1}H NMR (400 MHz, $CDCl_3$) δ 10.14 (s, 1H), 8.16 (d, *J* = 7.6 Hz, 1H), 7.85 – 7.74 (m, 3H), 7.56 (d, *J* = 7.6 Hz, 1H), 7.52 – 7.41 (m, 3H), 7.26 (t, *J* = 6.8 Hz, 2H), 6.89 (t, *J* = 8.4 Hz, 2H); ^{13}C NMR (100 MHz, $CDCl_3$) δ ^{13}C NMR (100 MHz, $CDCl_3$) δ 162.6 (d, *J* = 248.0 Hz), 162.4, 153.7, 149.2, 139.7, 135.4 (d, *J* = 3.1 Hz), 134.9,

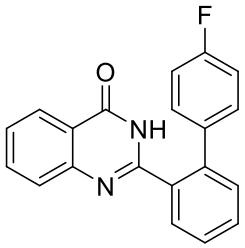

132.9, 131.1, 130.9, 130.8 (d, *J* = 8.1 Hz), 130.4, 128.2, 127.9, 127.2, 126.5, 120.7, 115.7 (d, *J* = 21.6 Hz); HR-MS (ESI-TOF) m/z calcd for $C_{20}H_{14}FN_2O$ $[M + H]^+$ 317.1085, found 317.1092.

2-(4'-Chloro-[1,1'-biphenyl]-2-yl)quinazolin-4(3H)-one (1d):[20] R_f = 0.45 (hexane/ethyl acetate 7:3); white solid; yield 92% (138 mg); ^{1}H NMR (400 MHz, $CDCl_3$) δ 10.08 (s, 1H), 8.17 (d, *J* = 7.6 Hz, 1H), 7.87 – 7.73 (m, 3H), 7.57 (d, *J* = 7.2 Hz, 1H), 7.53 – 7.43 (m, 3H), 7.30 – 7.13 (m, 4H); ^{13}C NMR (100 MHz, $CDCl_3$) δ 162.2, 153.5, 149.2, 139.5, 137.8, 135.0, 134.3, 132.8, 131.2, 130.9, 130.5, 130.4, 128.9, 128.4, 128.0, 127.3, 126.5, 120.7; HR-MS (ESI-TOF) m/z calcd for $C_{20}H_{14}ClN_2O$ $[M + H]^+$ 333.0789, found 333.0800.

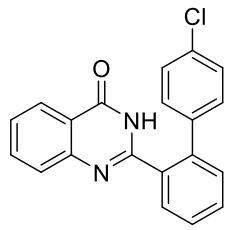

2'-(4-Oxo-3,4-dihydroquinazolin-2-yl)-[1,1'-biphenyl]-4-carbonitrile (1e): R_f = 0.45 (hexane/ethyl acetate 7:3); white solid; yield 84% (300 mg); mp 228-230 °C; ^{1}H NMR (400 MHz, $CDCl_3$) δ 11.08 (s, 1H), 8.14 (d, *J* = 8.0 Hz, 1H), 7.83 (d, *J* = 7.6 Hz, 1H), 7.79 (t, *J* = 7.6 Hz, 1H), 7.65 (d, *J* = 8.8 Hz, 1H), 7.63 (d, *J* = 9.2 Hz, 1H), 7.58 (t, *J* = 7.2 Hz, 1H), 7.54 – 7.48 (m, 2H), 7.47 (d, *J* = 7.2 Hz, 2H), 7.42 (s, 1H), 7.39 (s, 1H); ^{13}C NMR (100 MHz, $CDCl_3$) δ 163.2, 153.1, 149.1, 144.7, 139.3, 135.2, 132.9, 132.1, 131.3, 130.8, 130.4, 129.9, 129.1, 128.1, 127.4, 126.3, 120.5, 118.7, 111.4; IR (KBr) $\tilde{\nu}$ = 2921, 2223, 1666, 1602, 1336, cm^{-1}; HR-MS (ESI-TOF) m/z calcd for $C_{21}H_{13}N_3ONa$ $[M + Na]^+$ 346.0951, found 346.0922.

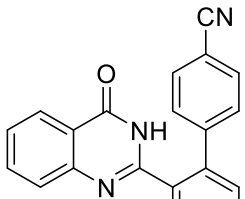

2-(4-Fluoro-[1,1'-biphenyl]-2-yl)quinazolin-4(3H)-one (1f):[20] R_f = 0.45 (hexane/ethyl acetate 7:3); white solid; yield 81% (189 mg); ^{1}H NMR (700 MHz, $CDCl_3$) δ 10.27 (s, 1H), 8.18 – 8.14 (m, 1H), 7.83 – 7.78 (m, 1H), 7.76 (d, *J* = 8.4 Hz, 1H), 7.55

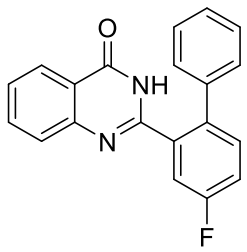

(dd, *J* = 8.4, 2.1 Hz, 1H), 7.52 – 7.48 (m, 1H), 7.45 (dd, *J* = 8.4, 5.6 Hz, 1H), 7.28 – 7.22 (m, 4H), 7.18 (t, *J* = 7.7 Hz, 2H); ^{13}C NMR (175 MHz, $CDCl_3$) δ 162.4, 162.1 (d, *J* = 248.8 Hz), 152.6, 149.1, 138.4, 136.9, 134.9, 134.3 (d, *J* = 7.8 Hz), 132.8 (d, *J* = 7.9 Hz), 129.2, 128.7, 128.1, 128.0, 127.3, 126.5, 120.8, 118.1 (d, *J* = 21.1 Hz), 117.4 (d, *J* = 23.5 Hz); HR-MS (ESI-TOF) m/z calcd for $C_{20}H_{14}FN_2O$ $[M + H]^+$ 317.1085, found 317.1101.

2-([1,1'-Biphenyl]-2-yl)-6-chloroquinazolin-4(3H)-one (1g): R_f = 0.45 (hexane/ethyl acetate 7:3); white solid; yield 94% (230 mg); mp 226-228 °C; ^{1}H NMR (400 MHz, $CDCl_3$) δ

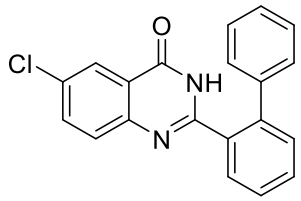

9.72 (s, 1H), 8.10 (s, 1H), 7.81 (t, *J* = 6.6 Hz, 1H), 7.69 (s, 2H), 7.58 (dd, *J* = 13.0, 6.1 Hz, 1H), 7.49 (s, 2H), 7.26 (s, 5H); ^{13}C NMR (100 MHz, $CDCl_3$) δ 161.1, 153.9, 147.7, 140.7, 139.2, 135.3, 132.9, 132.4, 131.3, 131.1, 130.4, 129.6, 129.1, 128.9, 128.2, 128.1, 125.9, 121.8; IR (KBr) $\tilde{\nu}$ = 3022, 1658, 1496, 1339 cm^{-1}; HR-MS (ESI-TOF) m/z calcd for $C_{20}H_{14}ClN_2O$ $[M + H]^+$ 333.0789, found 333.0775.

6-Chloro-2-(4'-ethyl-[1,1'-biphenyl]-2-yl)quinazolin-4(3H)-one (1h): R_f = 0.45 (hexane/ethyl acetate 7:3); white solid; yield 97% (205 mg); mp 197-199 °C; ^{1}H NMR (700

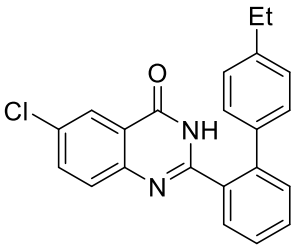

MHz, $CDCl_3$) δ 9.38 (s, 1H), 8.12 (d, *J* = 1.4 Hz, 1H), 7.82 (dd, *J* = 7.0, 3.5 Hz, 1H), 7.73 – 7.69 (m, 2H), 7.59 – 7.54 (m, 1H), 7.49 – 7.44 (m, 2H), 7.21 (d, *J* = 8.4 Hz, 2H), 7.14 – 7.08 (m, 2H), 2.60 (q, *J* = 7.7 Hz, 2H), 1.19 (t, *J* = 7.7 Hz, 3H); ^{13}C NMR (175 MHz, $CDCl_3$) δ 160.9, 154.1, 147.8, 144.5, 140.6, 136.3, 135.2, 132.8, 132.3, 131.3, 131.1, 130.5, 129.6, 128.9, 128.5, 127.9, 125.9, 121.9, 28.6, 15.4; IR (KBr) $\tilde{\nu}$ = 2921, 1666, 1492, 1478, 1336 cm^{-1}; HR-MS (ESI-TOF) m/z calcd for $C_{22}H_{18}ClN_2O$ $[M + H]^+$ 361.1102, found 361.1116.

2-(4'-(Tert-butyl)-[1,1'-biphenyl]-2-yl)-6-chloroquinazolin-4(3H)-one (1i): R_f = 0.45 (hexane/ethyl acetate 7:3); white solid; yield 89% (202 mg); mp 177-179 °C; ^{1}H NMR (400 MHz, $CDCl_3$) δ 9.06 (s, 1H), 8.15 (s, 1H), 7.89 (d, *J* = 7.6 Hz, 1H), 7.79 – 7.67 (m, 2H), 7.59 (t, *J* = 7.2 Hz, 1H), 7.49 (d, *J* = 7.2 Hz, 2H), 7.34 (t, *J* = 8.4 Hz, 2H), 7.26 (s, 2H), 1.29 (s, 9H); ^{13}C NMR (100 MHz, $CDCl_3$) δ 160.4, 153.9, 151.7, 147.8, 140.4, 135.9, 135.2, 132.9, 132.2, 131.4, 131.1, 130.7, 129.6, 128.7, 128.0, 126.2, 126.0, 121.9, 34.8, 31.3; IR (KBr) $\tilde{\nu}$ = 2962, 1664, 1475, 1309 cm^{-1}; HR-MS (ESI-TOF) m/z calcd for $C_{24}H_{22}ClN_2O$ $[M + H]^+$ 389.1415, found 389.1430.

6-Chloro-2-(4'-fluoro-[1,1'-biphenyl]-2-yl)quinazolin-4(3H)-one (1j): R_f = 0.45 (hexane/ethyl acetate 7:3); white solid; yield 94% (193 mg); mp 247-249 °C; ^{1}H NMR (700 MHz, $CDCl_3$) δ 10.16 (s, 1H), 8.10 (d, *J* = 2.1 Hz, 1H), 7.81 (d, *J* = 7.7 Hz, 1H), 7.73 (dd, *J* = 8.4, 2.1 Hz, 1H), 7.70 (d, *J* = 8.4 Hz, 1H), 7.62 (t, *J* = 7.0 Hz, 1H), 7.52 (t, *J* = 7.0 Hz, 1H), 7.49 (d, *J* = 7.7 Hz, 1H), 7.29 – 7.23 (m, 2H), 6.94 (t, *J* = 8.4 Hz, 2H); ^{13}C NMR (175 MHz, $CDCl_3$) δ 162.6 (d, *J* = 248.3 Hz), 161.5, 153.9, 147.7, 139.7, 135.4, 135.4 (d, *J* = 3.2 Hz), 133.0, 132.6, 131.3, 131.0, 130.8 (d, *J* = 8.1 Hz), 130.3, 129.6, 128.2, 125.8, 121.7, 115.8 (d, *J* = 21.6 Hz); IR (KBr) $\tilde{\nu}$ = 2864, 1661, 1514, 1490, 1239 cm^{-1}; HR-MS (ESI-TOF) m/z calcd for $C_{20}H_{13}ClFN_2O$ $[M + H]^+$ 351.0695, found 351.0701.

6-Chloro-2-(4'-chloro-[1,1'-biphenyl]-2-yl)quinazolin-4(3H)-one (1k): R_f = 0.45 (hexane/ethyl acetate 7:3); white solid; yield 88% (189 mg); mp 232-234 °C; ^{1}H NMR (700 MHz, $CDCl_3$) δ 10.37 (s, 1H), 8.09 (t, *J* = 2.8 Hz, 1H), 7.78 (dd, *J* =

7.0, 3.5 Hz, 1H), 7.72 (dd, *J* = 8.4, 2.1 Hz, 1H), 7.67 (d, *J* = 8.4 Hz, 1H), 7.60 (t, *J* = 7.7 Hz, 1H), 7.53 – 7.48 (m, 1H), 7.47 (d, *J* = 7.7 Hz, 1H), 7.24 – 7.16 (m, 4H); ^{13}C NMR (175 MHz, $CDCl_3$) δ 161.6, 153.8, 147.6, 139.6, 137.9, 135.4, 134.2, 133.1, 132.5, 131.4, 130.9, 130.4, 129.6, 128.9, 128.9, 128.4, 125.8, 121.7; IR (KBr) $\tilde{\nu}$ = 3044, 1664, 1468, 1121 cm^{-1}; HR-MS (ESI-TOF) m/z calcd for $C_{20}H_{13}Cl_2N_2O$ $[M + H]^+$ 367.0399, found 367.0405.

6-Chloro-2-(4-fluoro-[1,1'-biphenyl]-2-yl)quinazolin-4(3H)-one (1l): R_f = 0.45 (hexane/ethyl acetate 7:3); white solid; yield 86% (176 mg); mp 218-220 °C; ^{1}H NMR (400

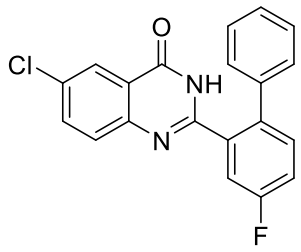

MHz, $CDCl_3$) δ 9.54 (s, 1H), 8.10 (d, *J* = 2.0 Hz, 1H), 7.73 (d, *J* = 9.2 Hz, 2H), 7.59 (dd, *J* = 7.6, 6.0 Hz, 1H), 7.49 – 7.44 (m, 1H), 7.30 (d, *J* = 2.4 Hz, 2H), 7.26 (s, 2H), 7.24 (d, *J* = 3.6 Hz, 2H); ^{13}C NMR (100 MHz, $CDCl_3$) δ 162.2 (d, *J* = 248.6 Hz), 152.6, 147.5, 138.3, 136.9, 135.4, 133.9 (d, *J* = 7.7 Hz), 133.3, 132.9 (d, *J* = 8.0 Hz), 129.7, 129.1, 129.0, 128.9, 128.3, 125.9, 121.8, 118.4 (d, *J* = 21.0 Hz), 117.4 (d, *J* = 23.4 Hz); IR (KBr) $\tilde{\nu}$ = 2868, 1670, 1598, 1307, 1292 cm^{-1}; HR-MS (ESI-TOF) m/z calcd for $C_{20}H_{13}ClFN_2O$ $[M + H]^+$ 351.0695, found 351.0705.

2-([1,1'-Biphenyl]-2-yl)-6-fluoroquinazolin-4(3H)-one (1m): R_f = 0.45 (hexane/ethyl acetate 7:3); white solid; yield 87% (178 mg); mp 215-217 °C; ^{1}H NMR (700 MHz, $CDCl_3$) δ 9.84 (s, 1H), 7.82 (t, *J* = 8.4 Hz, 1H), 7.79 – 7.74 (m, 2H), 7.61 – 7.55 (m, 1H), 7.52 – 7.44

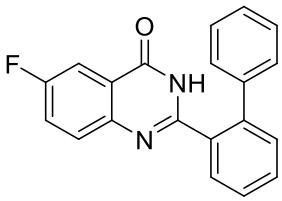

(m, 3H), 7.31 – 7.26 (m, 3H), 7.26 – 7.21 (m, 2H); ^{13}C NMR (175 MHz, $CDCl_3$) δ 161.6, 161.0 (d, *J* = 248.9 Hz), 153.1 (s), 145.9, 140.7, 139.3, 132.5, 131.2, 131.0, 130.4, 130.3, 129.1, 128.8, 128.1,

128.1. 123.4 (d, *J* = 24.1 Hz), 121.9 (d, *J* = 8.7 Hz), 111.4 (d, *J* = 23.5 Hz); IR (KBr) $\tilde{\nu}$ = 2947, 1660, 1599, 1351, 1339 cm^{-1}; HR-MS (ESI-TOF) m/z calcd for $C_{20}H_{14}FN_2O$ $[M + H]^+$ 317.1085, found 317.1091.

2-(4'-Ethyl-[1,1'-biphenyl]-2-yl)-6-fluoroquinazolin-4(3H)-one (1n): R_f = 0.45 (hexane/ethyl acetate 7:3); white solid; yield 95% (210 mg); mp 178-180 °C; ^{1}H NMR (400

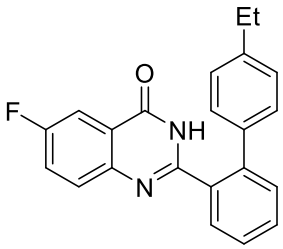

MHz, $CDCl_3$) δ 9.51 (s, 1H), 7.88 – 7.67 (m, 3H), 7.58 – 7.52 (m, 2H), 7.48 (t, *J* = 8.8 Hz, 2H), 7.25 – 7.18 (m, 2H), 7.10 (s, 2H), 2.79 – 2.46 (m, 2H), 1.18 (t, *J* = 7.6 Hz, 3H); ^{13}C NMR (175 MHz, $CDCl_3$) δ 161.1, 161.1 (d, *J* = 248.8 Hz), 153.1, 145.9, 144.5, 140.6, 136.3, 132.4, 131.2, 131.1, 130.5, 130.4 (d, *J* = 8.1 Hz), 129.0, 128.5, 127.9, 123.3 (d, *J* = 24.1 Hz), 122.1 (d, *J* = 8.6 Hz), 111.5 (d, *J* = 23.6 Hz), 28.6, 15.4; IR (KBr) $\tilde{\nu}$ = 2956, 1666, 1479, 1286 cm^{-1}; HR-MS (ESI-TOF) m/z calcd for $C_{22}H_{18}FN_2O$ $[M + H]^+$ 345.1389, found 345.1424.

2-(4'-(Tert-butyl)-[1,1'-biphenyl]-2-yl)-6-fluoroquinazolin-4(3H)-one (1o): R_f = 0.45 (hexane/ethyl acetate 7:3); white solid; yield 84% (203 mg); mp 172-174 °C; ^{1}H NMR (700 MHz, $CDCl_3$) δ 9.25 (s, 1H), 7.88 – 7.83 (m, 1H), 7.81 (dd, *J* = 8.4, 2.8 Hz, 1H), 7.79 (dd, *J*

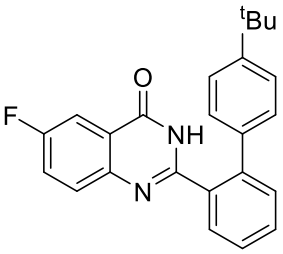

= 8.4, 4.2 Hz, 1H), 7.58 – 7.54 (m, 1H), 7.52 – 7.43 (m, 3H), 7.35 – 7.29 (m, 2H), 7.26 (d, *J* = 2.1 Hz, 1H), 7.25 (d, *J* = 2.1 Hz, 1H), 1.27 (s, 9H); ^{13}C NMR (175 MHz, $CDCl_3$) δ 160.9 (d, *J* = 248.8 Hz), 160.8, 153.0, 151.3, 145.8, 140.3, 135.9, 132.2, 131.1, 130.9, 130.5, 130.2 (d, *J* = 8.1 Hz), 128.6, 127.8, 125.9, 123.2 (d, *J* = 24.0 Hz), 122.0 (d, *J* = 8.6 Hz), 111.4 (d, *J* = 23.6 Hz), 34.6, 31.2; IR (KBr) $\tilde{\nu}$ = 2922, 1661, 1514, 1482, 1306 cm^{-1}; HR-MS (ESI-TOF) m/z calcd for $C_{24}H_{22}FN_2O$ $[M + H]^+$ 373.1711, found 373.1714.

6-Fluoro-2-(4'-fluoro-[1,1'-biphenyl]-2-yl)quinazolin-4(3H)-one (1p): R_f = 0.45 (hexane/ethyl acetate 7:3); white solid; yield 94% (202 mg); mp 210-212 °C; ^{1}H NMR (700 MHz, $CDCl_3$) δ 10.11 (s, 1H), 7.79 (dd, *J* = 7.7, 0.7 Hz, 1H), 7.76 (dd, *J* = 7.7, 2.1 Hz, 1H),

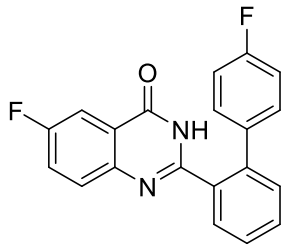

7.75 – 7.73 (m, 1H), 7.58 (td, *J* = 7.7, 1.4 Hz, 1H), 7.53 – 7.48 (m, 2H), 7.46 (d, *J* = 7.7 Hz, 1H), 7.25 (td, *J* = 4.9, 2.1 Hz, 2H), 6.91 (t, *J* = 8.4 Hz, 2H); ^{13}C NMR (175 MHz, $CDCl_3$) δ 162.6 (d, *J* = 248.2 Hz), 161.8, 161.1 (d, *J* = 249.1 Hz), 153.0, 145.9, 139.7, 135.4 (d, *J* = 3.3 Hz), 132.6, 131.2, 131.0, 130.8 (d, *J* = 8.1 Hz), 130.4 (d, *J* = 8.3 Hz), 130.4, 128.2, 123.6 (d, *J* = 24.1 Hz), 121.9 (d, *J* = 8.7 Hz), 115.8 (d, *J* = 21.6 Hz), 111.4 (d, *J* = 23.6 Hz); IR (KBr) $\tilde{\nu}$ = 2921, 2851, 1663, 1513, 1245 cm^{-1}; HR-MS (ESI-TOF) m/z calcd for $C_{20}H_{13}F_2N_2O$ $[M + H]^+$ 335.0990, found 335.1002.

2-(4'-Chloro-[1,1'-biphenyl]-2-yl)-6-fluoroquinazolin-4(3H)-one (1q): R_f = 0.45 (hexane/ethyl acetate 7:3); white solid; yield 94% (211 mg); mp 221-223 °C; ^{1}H NMR (400

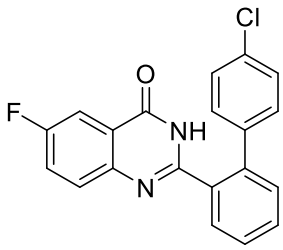

MHz, $CDCl_3$) δ 10.11 (s, 1H), 7.83 (t, *J* = 7.6 Hz, 2H), 7.80 – 7.76 (m, 1H), 7.64 (t, *J* = 7.6 Hz, 1H), 7.55 (t, *J* = 7.6 Hz, 2H), 7.51 (d, *J* = 7.6 Hz, 1H), 7.32 – 7.27 (m, 1H), 7.26 (s, 1H), 7.24 (d, *J* = 8.8 Hz, 2H); ^{13}C NMR (100 MHz, $CDCl_3$) δ 161.8, 161.1 (d, *J* = 249.1 Hz), 152.8, 145.9, 139.5, 137.9, 134.3, 132.6, 131.3, 130.9, 130.5, 130.4, 130.4, 128.9, 128.4, 123.6 (d, *J* = 24.2 Hz), 121.9 (d, *J* = 8.8 Hz), 111.4 (d, *J* = 23.5 Hz); IR (KBr) $\tilde{\nu}$ = 3104, 1669, 1508, 1137 cm^{-1}; HR-MS (ESI-TOF) m/z calcd for $C_{20}H_{13}ClFN_2O$ $[M + H]^+$ 351.0695, found 351.0696.

2-(3'-Chloro-[1,1'-biphenyl]-2-yl)-6-fluoroquinazolin-4(3H)-one (1r): R_f = 0.45 (hexane/ethyl acetate 7:3); white solid; yield 92% (260 mg); mp 222-223 °C; ^{1}H NMR (400

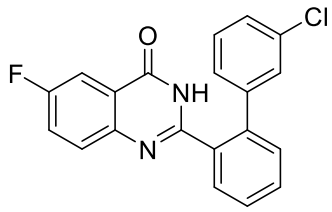

MHz, $CDCl_3$) δ 10.63 (s, 1H), 7.76 (d, *J* = 7.2 Hz, 3H), 7.57 (d, *J* = 7.2 Hz, 1H), 7.48 (t, *J* = 10.0 Hz, 3H), 7.36 (s, 1H), 7.20 (d, *J* = 6.0 Hz, 1H), 7.08 (d, *J* = 7.2 Hz, 2H); ^{13}C NMR (100 MHz, $CDCl_3$) δ 162.2, 161.1 (d, *J* = 249.0 Hz), 152.7, 145.9, 141.3, 139.5, 134.5, 132.6, 131.2, 130.9, 130.4, 130.3, 129.7, 129.3, 128.5, 127.9, 127.3, 123.6 (d, *J* = 24.1 Hz), 121.9 (d, *J* = 8.7 Hz), 111.4 (d, *J* = 23.5 Hz); IR (KBr) $\tilde{\nu}$ = 2883, 1672, 1481, 1441 cm^{-1}; HR-MS (ESI-TOF) m/z calcd for $C_{20}H_{13}ClFN_2O$ $[M + H]^+$ 351.0695, found 351.0675.

2-(3'-Chloro-[1,1'-biphenyl]-2-yl)quinazolin-4(3H)-one (1s):[20] R_f = 0.45 (hexane/ethyl

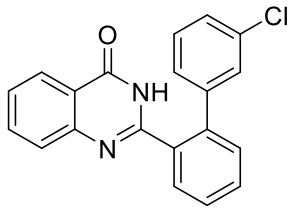

acetate 7:3); white solid; yield 89% (217 mg); mp 198-200 °C; ^{1}H NMR (400 MHz, $CDCl_3$) δ 10.49 (s, 1H), 8.17 (d, *J* = 8.0 Hz, 1H), 7.78 (d, *J* = 7.6 Hz, 2H), 7.74 (d, *J* = 8.0 Hz, 1H), 7.56 (t, *J* = 7.2 Hz, 1H), 7.53 – 7.42 (m, 3H), 7.38 (s, 1H), 7.23 – 7.17 (m, 1H), 7.09 (s, 2H); ^{13}C NMR (100 MHz, $CDCl_3$) δ 162.8, 153.4, 149.2, 141.3, 139.4, 134.9, 134.5 (×2), 132.9, 131.1, 130.9, 130.4, 129.7, 129.3, 128.5, 127.9, 127.3, 127.2, 126.5, 120.7; IR (KBr) $\tilde{\nu}$ = 2907, 1656, 1600, 1465 cm^{-1}; HR-MS (ESI-TOF) m/z calcd for $C_{20}H_{14}ClN_2O$ $[M + H]^+$ 333.0789, found 333.0775.

2-(4'-(Trifluoromethyl)-[1,1'-biphenyl]-2-yl)quinazolin-4(3H)-one (1t): R_f = 0.45 (hexane/ethyl acetate 7:3); white solid; yield 74% (180 mg); mp 199-201 °C; ^{1}H NMR (700

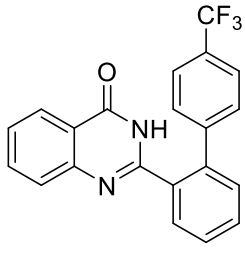

MHz, $CDCl_3$) δ 10.15 (s, 1H), 8.17 (d, *J* = 7.8 Hz, 1H), 7.81 (d, *J* = 8.0 Hz, 1H), 7.78 (d, *J* = 7.2 Hz, 1H), 7.70 (d, *J* = 8.0 Hz, 1H), 7.62 (t, *J* =

7.6 Hz, 1H), 7.55 (t, *J* = 7.6 Hz, 1H), 7.52 – 7.47 (m, 4H), 7.44 (d, *J* = 8.0 Hz, 2H); ^{13}C NMR (175 MHz, $CDCl_3$) δ 162.5, 153.2, 149.1, 143.3, 139.5, 135.1, 133.0, 131.2, 131.0, 130.5, 129.9 (q, *J* = 32.7 Hz), 129.5, 128.8, 128.0, 127.3, 126.5, 125.6 (q, *J* = 3.9 Hz), 124.1 (q, *J* = 272.3 Hz), 120.7; IR (KBr) $\tilde{\nu}$ = 2872, 1667, 1607, 1324, 1156 cm^{-1}; HR-MS (ESI-TOF) m/z calcd for $C_{21}H_{14}F_3N_2O$ $[M + H]^+$ 367.1053, found 367.1045.

6-Chloro-2-(4'-(trifluoromethyl)-[1,1'-biphenyl]-2-yl)quinazolin-4(3H)-one (1u): R_f = 0.45 (hexane/ethyl acetate 7:3); white solid; yield 94% (220 mg); mp 235-237 °C; ^{1}H NMR

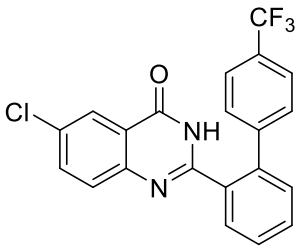

(400 MHz, $CDCl_3$) δ 10.23 (s, 1H), 8.10 (s, 1H), 7.80 (d, *J* = 7.6 Hz, 1H), 7.71 (d, *J* = 8.8 Hz, 1H), 7.67 – 7.61 (m, 2H), 7.57 (t, *J* = 7.6 Hz, 1H), 7.51 (d, *J* = 8.4 Hz, 3H), 7.42 (d, *J* = 8.0 Hz, 2H); ^{13}C NMR (100 MHz, $CDCl_3$) δ 161.5, 153.4, 147.5, 143.2, 139.5, 135.5, 133.2, 132.7, 131.5, 131.1, 130.4, 130.0 (q, *J* = 32.5 Hz), 129.6, 129.4, 128.9, 125.8, 125.6 (q, *J* = 3.2 Hz), 124.1, (q, *J* = 272.2 Hz), 121.7; IR (KBr) $\tilde{\nu}$ = 3095, 1668, 1605, 1330, 1101 cm^{-1}; HR-MS (ESI-TOF) m/z calcd for $C_{21}H_{13}ClF_3N_2O$ $[M + H]^+$ 401.0663, found 401.0674.

6-Chloro-2-(3'-chloro-[1,1'-biphenyl]-2-yl)quinazolin-4(3H)-one (1v): R_f = 0.45 (hexane/ethyl acetate 7:3); white solid; yield 93% (200 mg); mp 201-203 °C; ^{1}H NMR (400

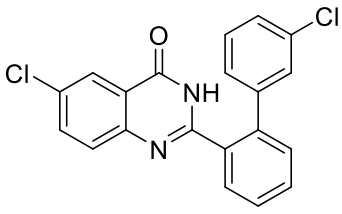

MHz, $CDCl_3$) δ 10.35 (s, 1H), 8.11 (s, 1H), 7.79 (d, *J* = 7.5 Hz, 1H), 7.72 (dd, *J* = 8.7, 1.7 Hz, 1H), 7.67 (d, *J* = 8.7 Hz, 1H), 7.60 (t, *J* = 7.4 Hz, 1H), 7.49 (dd, *J* = 13.5, 7.5 Hz, 2H), 7.37 (s, 1H), 7.22 (d, *J* = 7.7 Hz, 1H), 7.12 (t, *J* = 7.7 Hz, 1H), 7.07 (d, *J* = 7.5 Hz, 1H); ^{13}C NMR (100 MHz, $CDCl_3$) δ 161.6, 153.6, 147.7, 141.2, 139.4, 135.4, 134.7, 133.1, 132.6, 131.4, 130.9, 130.4, 129.8, 129.6, 129.3, 128.6, 128.1, 127.3, 125.8, 121.7; IR (KBr) $\tilde{\nu}$ = 2921,

1660, 1597, 1460, 1304 cm^{-1}; HR-MS (ESI-TOF) m/z calcd for $C_{20}H_{13}Cl_2N_2O$ $[M + H]^+$ 367.0399, found 367.0367.

14H-Quinazolino[3,2-f]phenanthridin-14-one (2a):[5] R_f = 0.60 (hexane/ethyl acetate 9:1); white solid; yield 84% (50 mg); ^1H NMR (400 MHz, $CDCl_3$) δ 9.11 (d, *J* = 8.4 Hz, 1H), 9.02 (d, *J* = 8.0 Hz, 1H), 8.43 (d, *J* = 8.0 Hz, 1H), 8.31 – 8.16 (m, 2H), 7.83 (s, 2H), 7.74 (t, *J* = 7.6 Hz, 1H), 7.61 (t, *J* = 7.6 Hz, 1H), 7.57 – 7.45 (m, 3H); ^{13}C NMR (175 MHz, $CDCl_3$) δ 163.1, 146.5, 146.2, 134.6, 133.2, 132.3, 131.4, 128.6, 128.3, 128.2, 127.5, 127.3, 127.1, 126.6, 126.3, 123.2, 122.3, 121.9, 120.9; HR-MS (ESI-TOF) m/z calcd for $C_{20}H_{13}N_2O$ $[M + H]^+$ 297.1022, found 297.1025.

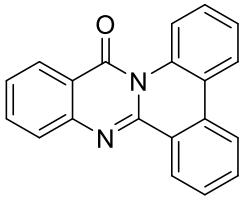

2-Methyl-14H-quinazolino[3,2-f]phenanthridin-14-one (2b):[5] R_f = 0.60 (hexane/ethyl acetate 9:1); white solid; yield 87% (52 mg); ^1H NMR (400 MHz, $CDCl_3$) δ 8.99 (d, *J* = 8.0 Hz, 1H), 8.92 (s, 1H), 8.42 (d, *J* = 8.0 Hz, 1H), 8.18 (d, *J* = 8.0 Hz, 1H), 8.12 (d, *J* = 8.0 Hz, 1H), 7.82 (d, *J* = 3.6 Hz, 2H), 7.70 (t, *J* = 7.6 Hz, 1H), 7.57 (t, *J* = 7.6 Hz, 1H), 7.51 (dd, *J* = 7.6, 3.6 Hz, 1H), 7.29 (d, *J* = 8.0 Hz, 1H), 2.51 (s, 3H); ^{13}C NMR (100 MHz, $CDCl_3$) δ 163.2, 146.8, 146.3, 138.6, 134.7, 133.2, 132.3, 131.7, 128.4, 128.3, 127.8, 127.5, 127.1, 126.9, 126.3, 123.1, 122.5, 121.7, 120.9, 120.8, 22.1; HR-MS (ESI-TOF) m/z calcd for $C_{21}H_{15}N_2O$ $[M + H]^+$ 311.1179, found 311.1172.

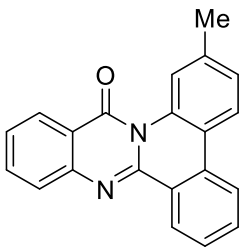

2-Fluoro-14H-quinazolino[3,2-f]phenanthridin-14-one (2c):[5] R_f = 0.60 (hexane/ethyl acetate 9:1); white solid; yield 75% (45 mg); ^1H NMR (400 MHz, $CDCl_3$) δ 8.97 (d, *J* = 8.0 Hz, 1H), 8.39 (d, *J* = 8.0 Hz, 1H), 8.25 (d, *J* = 2.0 Hz, 1H), 8.21 (d, *J* =

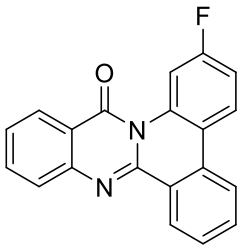

8.0 Hz, 1H), 7.99 (dd, *J* = 12.0, 8.8 Hz, 2H), 7.84 (d, *J* = 7.6 Hz, 1H), 7.68 (t, *J* = 7.6 Hz, 2H), 7.59 (d, *J* = 7.6 Hz, 1H), 7.48 (dd, *J* = 8.8, 2.0 Hz, 1H); ^{13}C NMR (100 MHz, $CDCl_3$) δ 163.1, 161.8 (d, *J* = 239.2 Hz), 146.3, 145.9, 135.3, 134.8, 132.4, 130.8, 128.4 (d, *J* = 4.7 Hz), 127.5, 127.0, 126.7, 126.5, 124.6 (d, *J* = 9.4 Hz), 121.6, 120.6, 119.6, 119.5, 114.2 (d, *J* = 22.6 Hz), 109.7 (d, *J* = 29.8 Hz); HR-MS (ESI-TOF) m/z calcd for $C_{20}H_{12}FN_2O$ $[M + H]^+$ 315.0928, found 315.0917.

2-Chloro-14H-quinazolino[3,2-f]phenanthridin-14-one (2d):[20] R_f = 0.60 (hexane/ethyl acetate 9:1); white solid; yield 72% (43 mg); ^{1}H NMR (700 MHz, $CDCl_3$) δ 9.23 (s, 1H),

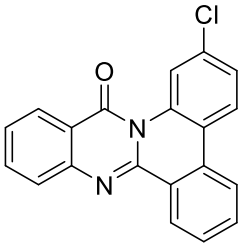

8.99 (d, *J* = 8.4 Hz, 1H), 8.42 (d, *J* = 7.7 Hz, 1H), 8.19 – 8.14 (m, 2H), 7.85 – 7.80 (m, 2H), 7.73 (s, 1H), 7.61 (t, *J* = 7.7 Hz, 1H), 7.53 (s, 1H), 7.46 (d, *J* = 8.4 Hz, 1H); ^{13}C NMR (175 MHz, $CDCl_3$) δ 163.0, 146.2, 146.1, 136.4, 134.9, 134.2, 133.9, 132.5, 130.7, 129.0, 128.5, 127.6, 127.2, 126.9, 126.7, 124.3, 122.4, 121.9, 121.8, 120.8; HR-MS (ESI-TOF) m/z calcd for $C_{20}H_{12}ClN_2O$ $[M + H]^+$ 331.0633, found 331.0610.

14-Oxo-14H-quinazolino[3,2-f]phenanthridine-2-carbonitrile (2e): R_f = 0.65 (hexane/ethyl acetate 9:1); white solid; yield 82% (81.5 mg); mp 274-276 °C; ^{1}H NMR (400 MHz, $CDCl_3$) δ 9.59 (s, 1H), 9.04 (d, *J* = 8.0 Hz, 1H), 8.44 (d, *J* = 8.0 Hz, 1H), 8.34 (d, *J* =

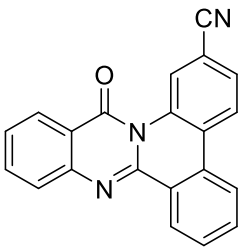

8.4 Hz, 1H), 8.23 (d, *J* = 8.0 Hz, 1H), 7.86 (d, *J* = 6.0 Hz, 2H), 7.79 (t, *J* = 7.2 Hz, 1H), 7.75 – 7.66 (m, 2H), 7.61 – 7.52 (m, 1H); ^{13}C NMR (175 MHz, $CDCl_3$) δ 162.9, 145.9, 145.7, 135.3, 133.4, 132.8, 130.4, 129.8, 129.3, 128.7, 128.3, 127.8, 127.3, 127.1, 127.1, 126.5, 124.1, 122.6, 120.7, 118.5, 111.8; IR (KBr) $\tilde{\nu}$ = 2919, 2227, 1681, 1594, 1553, 1154 cm^{-1}; HR-MS (ESI-TOF) m/z calcd for $C_{21}H_{12}N_3O$ $[M + H]^+$ 322.0975, found 322.0965.

7-Fluoro-14H-quinazolino[3,2-f]phenanthridin-14-one (2f):[20] R_f = 0.65 (hexane/ethyl acetate 9:1); white solid; yield 85% (50.5 mg); ^{1}H NMR (700 MHz, $CDCl_3$) δ 9.11 (d, *J* = 8.4 Hz, 1H), 8.67 (dd, *J* = 9.8, 2.1 Hz, 1H), 8.42 (d, *J* = 8.4 Hz, 1H), 8.21 (dd, *J* = 8.4, 5.6 Hz, 1H), 8.18 (d, *J* = 7.7 Hz, 1H), 7.83 (d, *J* = 5.6 Hz, 2H), 7.55 – 7.50 (m, 2H), 7.48 (t, *J* = 7.7 Hz, 1H), 7.45 – 7.41 (m, 1H); ^{13}C NMR (175 MHz, $CDCl_3$) δ 163.0, 162.8 (d, *J* = 248.5 Hz), 146.0, 145.6 (d, *J* = 3.7 Hz), 134.8, 132.9, 129.5 (d, *J* = 8.7 Hz), 128.2, 128.0, 127.9, 127.6, 127.2, 126.8, 124.4 (d, *J* = 8.4 Hz), 123.1, 122.6, 122.4, 121.1, 120.5 (d, *J* = 23.0 Hz), 114.1 (d, *J* = 24.4 Hz); HR-MS (ESI-TOF) m/z calcd for $C_{20}H_{12}FN_2O$ $[M + H]^+$ 315.0928, found 315.0938.

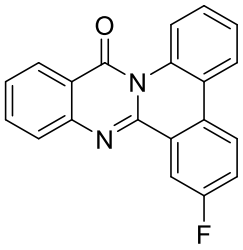

12-Chloro-14H-quinazolino[3,2-f]phenanthridin-14-one (2g):[28] R_f = 0.60 (hexane/ethyl acetate 9:1); white solid; yield 77% (46 mg); mp 250-252 °C; ^{1}H NMR (400 MHz, $CDCl_3$) δ 9.12 – 9.06 (m, 1H), 8.99 (d, *J* = 8.0 Hz, 1H), 8.39 (d, *J* = 2.0 Hz, 1H), 8.29 – 8.21 (m, 2H), 7.80 – 7.70 (m, 3H), 7.62 (t, *J* = 7.6 Hz, 1H), 7.52 (dq, *J* = 7.2, 5.6 Hz, 2H); ^{13}C NMR (100 MHz, $CDCl_3$) δ 162.2, 146.8, 144.8, 135.2, 133.1, 132.6, 132.0, 131.6, 131.3, 128.8, 128.8, 128.4, 128.1, 127.2, 126.9, 126.9, 123.3, 122.3, 122.1, 121.9; HR-MS (ESI-TOF) m/z calcd for $C_{20}H_{12}ClN_2O$ $[M + H]^+$ 331.0633, found 331.0633.

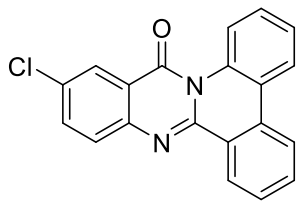

12-Chloro-2-ethyl-14H-quinazolino[3,2-f]phenanthridin-14-one (2h): R_f = 0.65 (hexane/ethyl acetate 9:1); white solid; yield 67% (41 mg); mp 188-190 °C; ^{1}H NMR (400 MHz, $CDCl_3$) δ 8.98 (d, *J* = 8.0 Hz, 1H), 8.95 (s, 1H), 8.39 (d, *J* = 2.0 Hz, 1H), 8.21 (d, *J* = 8.0 Hz, 1H), 8.18 (d, *J* = 8.0 Hz, 1H), 7.82

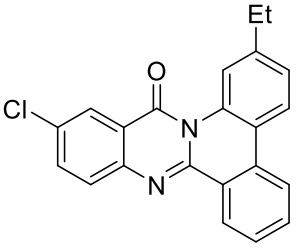

– 7.68 (m, 3H), 7.58 (t, *J* = 7.6 Hz, 1H), 7.36 (d, *J* = 8.0 Hz, 1H), 2.82 (q, *J* = 7.6 Hz, 2H), 1.34 (t, *J* = 7.6 Hz, 3H); ^{13}C NMR (100 MHz, $CDCl_3$) δ 162.3, 147.1, 145.0, 144.8, 135.1, 133.1, 132.6, 131.9, 131.8, 128.8, 128.4 (×2), 126.9, 126.8, 126.8, 123.3, 121.8, 121.6, 121.1, 29.4, 15.6; IR (KBr) $\tilde{\nu}$ = 2964, 1681, 1550, 1485, 1152 cm^{-1}; HR-MS (ESI-TOF) m/z calcd for $C_{22}H_{16}ClN_2O$ $[M + H]^+$ 359.0946, found 359.0947.

2-(Tert-butyl)-12-chloro-14H-quinazolino[3,2-f]phenanthridin-14-one (2i): R_f = 0.65 (hexane/ethyl acetate 9:1); white solid; yield 75% (45 mg); mp 180-182 °C; ^{1}H NMR (700 MHz, $CDCl_3$) δ 9.17 (d, *J* = 1.4 Hz, 1H), 9.01 (d, *J* = 8.4 Hz, 1H), 8.42 (d, *J* = 2.1 Hz, 1H),

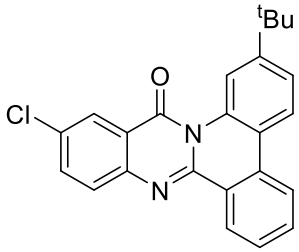

8.22 (d, *J* = 8.4 Hz, 1H), 8.20 (d, *J* = 8.4 Hz, 1H), 7.81 (d, *J* = 8.4 Hz, 1H), 7.77 – 7.71 (m, 2H), 7.60 (d, *J* = 7.0 Hz, 1H), 7.56 (dd, *J* = 8.4, 1.4 Hz, 1H), 1.44 (s, 9H); ^{13}C NMR (175 MHz, $CDCl_3$) δ 162.2, 151.8, 147.2, 144.6, 135.2, 132.9, 132.7, 131.9, 131.7, 128.6, 128.5, 128.4, 126.9, 126.6, 124.4, 122.9, 121.9, 121.8, 120.8, 119.5, 35.5, 31.4; IR (KBr) $\tilde{\nu}$ = 2951, 1680, 1547, 1358 cm^{-1}; HR-MS (ESI-TOF) m/z calcd for $C_{24}H_{20}ClN_2O$ $[M + H]^+$ 387.1259, found 387.1268.

12-Chloro-2-fluoro-14H-quinazolino[3,2-f]phenanthridin-14-one (2j): R_f = 0.60 (hexane/ethyl acetate 9:1); white solid; yield 70% (35 mg); mp 240-242 °C; ^{1}H NMR (700

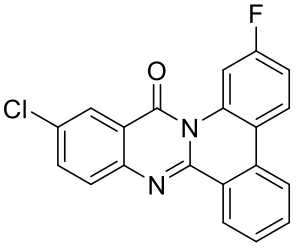

MHz, $CDCl_3$) δ 9.04 – 9.00 (m, 1H), 8.98 (d, *J* = 8.4 Hz, 1H), 8.38 (s, 1H), 8.28 – 8.22 (m, 1H), 8.16 (d, *J* = 8.4 Hz, 1H), 7.82 – 7.71 (m, 4H), 7.61 (t, *J* = 7.7 Hz, 1H); ^{13}C NMR (175 MHz, $CDCl_3$) δ 162.1, 161.9 (d, *J* = 247.6 Hz), 146.7, 144.6, 135.4, 134.2 (d, *J* = 11.4 Hz), 132.8, 132.3, 131.0, 128.9, 128.6 (d, *J* = 22.8 Hz), 126.9, 126.6, 124.9, 124.8, 121.9, 121.6, 119.7 (d, *J* = 2.5 Hz), 114.7 (d, *J* = 22.5 Hz), 109.8 (d, *J* = 29.5 Hz); IR (KBr)

$\tilde{\nu}$ = 2922, 1681, 1552, 1487, 1334 cm^{-1}; HR-MS (ESI-TOF) m/z calcd for $C_{20}H_{11}ClFN_2O$ $[M + H]^+$ 349.0538, found 349.0516.

2,12-Dichloro-14H-quinazolino[3,2-f]phenanthridin-14-one (2k): R_f = 0.60 (hexane/ethyl acetate 9:1); white solid; yield 67% (40 mg); mp 264-266 °C; ^{1}H NMR (400 MHz, $CDCl_3$ + TFA-D) δ 9.01 (dd, *J* = 4.4, 2.8 Hz, 2H), 8.44 (dd, *J* = 9.2, 5.2 Hz, 2H), 8.39 (d, *J* = 8.8 Hz, 1H), 8.08 (dd, *J* = 8.0, 4.4 Hz, 2H), 7.97 (dd, *J* = 8.8, 2.0 Hz, 1H), 7.88 (t, *J* = 7.6 Hz, 1H), 7.71 (dd, *J* = 8.8, 2.0 Hz, 1H); ^{13}C NMR (100 MHz, $CDCl_3$ +TFA-D) δ 159.1, 149.0, 137.9, 137.0, 136.8, 136.3, 135.3, 132.9, 131.3, 130.7, 129.4, 128.8, 127.9, 127.9, 124.9, 123.2, 122.3, 121.6, 119.6, 119.4; IR (KBr) $\tilde{\nu}$ = 2920, 1680, 1594, 1542, 1328 cm^{-1}; HR-MS (ESI-TOF) m/z calcd for $C_{20}H_{11}Cl_2N_2O$ $[M + H]^+$ 365.0243, found 365.0221.

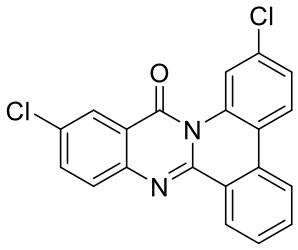

12-Chloro-7-fluoro-14H-quinazolino[3,2-f]phenanthridin-14-one (2l): R_f = 0.60 (hexane/ethyl acetate 9:1); white solid; yield 80% (48 mg); mp 232-234 °C; ^{1}H NMR (400 MHz, $CDCl_3$) δ 9.12 – 9.07 (m, 1H), 8.64 (dd, *J* = 9.6, 2.8 Hz, 1H), 8.38 (s, 1H), 8.26 – 8.17 (m, 2H), 7.76 (s, 2H), 7.57 – 7.49 (m, 2H), 7.49 – 7.42 (m, 1H); ^{13}C NMR (175 MHz, $CDCl_3$) δ 162.8 (d, *J* = 249.1 Hz), 162.0, 145.9 (d, *J* = 3.4 Hz), 144.5, 135.3, 132.7, 132.4, 129.3 (d, *J* = 8.7 Hz), 128.9, 128.3, 128.0, 127.1, 126.9, 124.5 (d, *J* = 8.1 Hz), 123.1, 122.6, 122.3, 121.9, 120.8 (d, *J* = 23.0 Hz), 114.1 (d, *J* = 24.7 Hz); IR (KBr) $\tilde{\nu}$ = 2921, 1697, 1677, 1568, 1485 cm^{-1}; HR-MS (ESI-TOF) m/z calcd for $C_{20}H_{11}ClFN_2O$ $[M + H]^+$ 349.0538, found 349.0518.

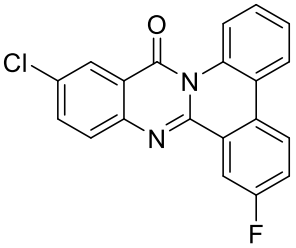

12-Fluoro-14H-quinazolino[3,2-f]phenanthridin-14-one (2m):[5] R_f = 0.60 (hexane/ethyl acetate 9:1); white solid; yield 77% (46 mg); ^{1}H NMR (400 MHz, $CDCl_3$) δ 9.10 (d, *J* = 8.0 Hz, 1H), 8.96 (d, *J* = 8.0 Hz, 1H), 8.25 (d, *J* = 8.0 Hz, 1H), 8.22 (d, *J* = 8.0 Hz, 1H), 8.04 (dd, *J* = 8.4, 2.8 Hz, 1H), 7.84 – 7.78 (m, 1H), 7.72 (s, 1H), 7.60 (d, *J* = 7.6 Hz, 1H), 7.52 (dd, *J* = 13.2, 5.6 Hz, 3H); ^{13}C NMR (100 MHz, $CDCl_3$) δ 162.4, 160.7 (d, *J* = 247.7 Hz), 146.0, 142.9, 133.0, 132.4, 131.4, 129.5 (d, *J* = 8.2 Hz), 128.8, 128.3 (d, *J* = 8.4 Hz), 127.2, 126.9, 123.6, 123.4, 123.3, 123.2, 122.3, 121.9, 121.9, 112.2 (d, *J* = 23.9 Hz); HR-MS (ESI-TOF) m/z calcd for $C_{20}H_{12}FN_2O$ $[M + H]^+$ 315.0928, found 315.0943.

2-Ethyl-12-fluoro-14H-quinazolino[3,2-f]phenanthridin-14-one (2n): R_f = 0.65 (hexane/ethyl acetate 9:1); white solid; yield 72% (36 mg); mp 192-194 °C; ^{1}H NMR (400 MHz, $CDCl_3$) δ 8.97 (s, 1H), 8.94 (s, 1H), 8.17 (t, *J* = 9.2 Hz, 2H), 8.05 (dd, *J* = 8.4, 2.4 Hz, 1H), 7.82 (dd, *J* = 8.8, 4.8 Hz, 1H), 7.71 (t, *J* = 7.6 Hz, 1H), 7.58 – 7.50 (m, 2H), 7.35 (d, *J* = 8.0 Hz, 1H), 2.81 (q, *J* = 7.6 Hz, 2H), 1.34 (t, *J* = 7.6 Hz, 3H); ^{13}C NMR (100 MHz, $CDCl_3$) δ 162.5, 160.7 (d, *J* = 247.5 Hz), 146.3, 144.9, 143.0, 133.1, 132.4, 131.6, 129.5 (d, *J* = 8.1 Hz), 128.3, 128.2, 126.9, 126.8, 123.4 (d, *J* = 24.6 Hz), 123.2, 121.9 (d, *J* = 8.7 Hz), 121.8, 121.6, 121.1, 112.2 (d, *J* = 23.9 Hz), 29.4, 15.7; IR (KBr) $\tilde{\nu}$ = 2920, 1671, 1599, 1489, 1335 cm^{-1}; HR-MS (ESI-TOF) m/z calcd for $C_{22}H_{16}FN_2O$ $[M + H]^+$ 343.1241, found 343.1235.

2-(Tert-butyl)-12-fluoro-14H-quinazolino[3,2-f]phenanthridin-14-one (2o): R_f = 0.65 (hexane/ethyl acetate 9:1); white solid; yield 69% (41 mg); mp 158-160 °C; ^{1}H NMR (700 MHz, $CDCl_3$) δ 9.21 (d, *J* = 1.4 Hz, 1H), 8.95 (t, *J* = 7.0 Hz, 1H),

8.20 – 8.15 (m, 2H), 8.08 (dd, *J* = 8.4, 2.8 Hz, 1H), 7.82 (dt, *J* = 10.5, 4.9 Hz, 1H), 7.73 – 7.68 (m, 1H), 7.60 – 7.50 (m, 3H), 1.44 (s, 9H); ^{13}C NMR (175 MHz, $CDCl_3$) δ 162.6, 160.7 (d, *J* = 247.5 Hz), 151.8, 146.3 (d, *J* = 1.8 Hz), 142.9, 132.9, 132.4, 131.5 (d, *J* = 11.0 Hz), 129.4, 128.3, 128.3, 126.9, 124.3, 123.4 (d, *J* = 24.4 Hz), 122.9, 122.5, 121.8, 120.8, 119.5, 112.3 (d, *J* = 23.9 Hz), 35.5, 31.4; IR (KBr) $\tilde{\nu}$ = 2961, 1679, 1555, 1488, 1354 cm^{-1}; HR-MS (ESI-TOF) m/z calcd for $C_{24}H_{20}FN_2O$ $[M + H]^+$ 371.1554, found 371.1526.

2,12-Difluoro-14H-quinazolino[3,2-f]phenanthridin-14-one (2p): R_f = 0.60 (hexane/ethyl acetate 9:1); white solid; yield 66% (33 mg); mp 240-242 °C; ^{1}H NMR (400 MHz, $CDCl_3$) δ 9.05 (dd, *J* = 12.4, 2.4 Hz, 1H), 8.98 (d, *J* = 8.0 Hz, 1H), 8.25 (dd, *J* = 8.8, 6.4 Hz, 1H), 8.16 (d, *J* = 8.0 Hz, 1H), 8.06 (dd, *J* = 8.4, 2.8 Hz, 1H), 7.84 (dd, *J* = 8.8, 4.8 Hz, 1H), 7.74 (t, *J* = 7.6 Hz, 1H), 7.61 (d, *J* = 7.6 Hz, 1H), 7.58 (d, *J* = 8.4 Hz, 1H), 7.54 (dd, *J* = 9.2, 6.4 Hz, 1H); ^{13}C NMR (175 MHz, $CDCl_3$) δ 162.4, 161.9 (d, *J* = 247.0 Hz), 160.9 (d, *J* = 248.4 Hz), 145.9, 142.8, 134.2 (d, *J* = 11.4 Hz), 132.6, 130.9, 129.6 (d, *J* = 8.2 Hz), 128.7, 128.4, 126.7, 124.8 (d, *J* = 9.4 Hz), 123.8 (d, *J* = 24.3 Hz), 121.9, 121.8 (d, *J* = 8.7 Hz), 119.8 (d, *J* = 2.9 Hz), 114.6 (d, *J* = 22.5 Hz), 112.4 (d, *J* = 23.9 Hz), 109.9 (d, *J* = 29.8 Hz); IR (KBr) $\tilde{\nu}$ = 2852, 1677, 1514, 1492, 1262 cm^{-1}; HR-MS (ESI-TOF) m/z calcd for $C_{20}H_{11}F_2N_2O$ $[M + H]^+$ 333.0834, found 333.0808.

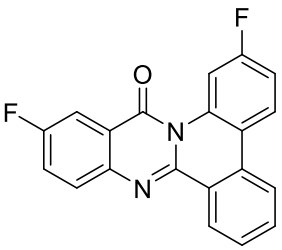

2-Chloro-12-fluoro-14H-quinazolino[3,2-f]phenanthridin-14-one (2q): R_f = 0.60 (hexane/ethyl acetate 9:1); white solid; yield 68% (34 mg); mp 248-250 °C; ^{1}H NMR (700 MHz, $CDCl_3$) δ 9.26 (s, 1H), 8.98 (d, *J* = 7.9 Hz, 1H), 8.18 (t, *J* = 8.3 Hz, 2H), 8.05 (d, *J* = 6.1 Hz, 1H), 7.84 (dd, *J* = 8.6, 4.7 Hz, 1H), 7.74 (t, *J* = 7.6 Hz, 1H), 7.62 (t, *J* = 7.5 Hz, 1H), 7.56 (t, *J* = 7.1 Hz, 1H),

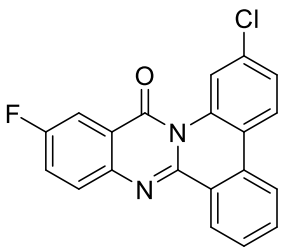

7.48 (d, *J* = 8.3 Hz, 1H); ^{13}C NMR (175 MHz, $CDCl_3$) δ 162.3, 160.9 (d, *J* = 248.4 Hz), 145.7, 142.8, 134.4, 133.7, 132.6, 130.6, 129.6 (d, *J* = 8.2 Hz), 129.1, 128.4, 127.2, 127.1, 124.3, 123.8 (d, *J* = 24.3 Hz), 122.4, 121.9, 121.9, 121.8 (d, *J* = 8.5 Hz), 112.4 (d, *J* = 23.9 Hz); IR (KBr) $\tilde{\nu}$ = 2954, 2919, 1682, 1490, 1276 cm^{-1}; HR-MS (ESI-TOF) m/z calcd for $C_{20}H_{11}ClFN_2O$ $[M + H]^+$ 349.0538, found 349.0518.

3-Chloro-12-fluoro-14H-quinazolino[3,2-f]phenanthridin-14-one (2r): R_f = 0.60 (hexane/ethyl acetate 9:1); white solid; yield 75% (45 mg); mp 210-212 °C; ^{1}H NMR (700 MHz, $CDCl_3$ + DMSO-d_6) δ 8.89 (d, *J* = 9.1 Hz, 1H), 8.77 (d, *J* = 7.7 Hz, 1H), 8.03 (s, 1H),

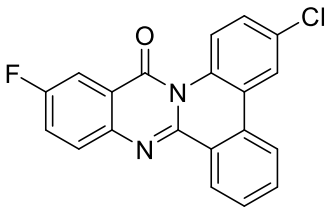

7.99 (d, *J* = 7.7 Hz, 1H), 7.78 (s, 1H), 7.63 (d, *J* = 4.9 Hz, 1H), 7.56 (d, *J* = 7.0 Hz, 1H), 7.43 (dd, *J* = 19.6, 12.6 Hz, 1H), 7.36 (s, 1H), 7.25 (s, 1H); ^{13}C NMR (175 MHz, $CDCl_3$ + DMSO-d_6) δ 161.9, 160.5 (d, *J* = 248.1 Hz), 145.2, 142.6, 132.5, 132.2, 131.2, 129.8, 129.5 (d, *J* = 7.8 Hz), 129.3, 128.1, 127.8, 127.1, 124.9, 123.6, 123.5 (d, *J* = 24.3 Hz), 122.8, 121.9, 121.5 (d, *J* = 8.7 Hz), 111.8 (d, *J* = 24.1 Hz); IR (KBr) $\tilde{\nu}$ = 2955, 2920, 1677, 1482, 1463, 1185 cm^{-1}; HR-MS (ESI-TOF) m/z calcd for $C_{20}H_{11}ClFN_2O$ $[M + H]^+$ 349.0538, found 349.0569.

6H-Quinazolino[1,2-f]phenanthridin-6-one (3a): R_f = 0.30 (hexane/ethyl acetate 2:3); white solid; yield 72% (43 mg); mp 294-296 °C; ^{1}H NMR (400 MHz,

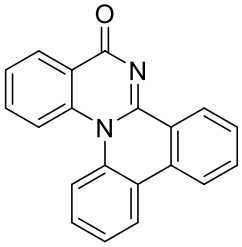

$CDCl_3$) δ 8.96 (dd, *J* = 8.0, 1.2 Hz, 1H), 8.39 (dd, *J* = 8.0, 1.6 Hz, 1H), 8.30 (dd, *J* = 6.0, 3.6 Hz, 1H), 8.26 (d, *J* = 8.0 Hz, 1H), 8.03 (dd, *J* = 7.2, 2.4 Hz, 2H), 7.84 – 7.78 (m, 1H), 7.69 – 7.65 (m, 1H), 7.65 – 7.60 (m, 1H), 7.58 – 7.53 (m, 1H), 7.53 – 7.48 (m, 2H); ^{13}C NMR (100 MHz, $CDCl_3$) δ 168.3, 152.5, 138.6, 133.6, 132.9, 131.9, 129.0(×2), 128.8(×2), 128.4, 128.2, 127.4, 126.4, 124.6, 123.8,

123.2, 121.9, 120.6, 119.6; IR (KBr) $\tilde{\nu}$ = 2920, 1647, 1607, 1518, 1149, cm^{-1}; HR-MS (ESI-TOF) m/z calcd for $C_{20}H_{13}N_2O$ $[M + H]^+$ 297.1022, found 297.1035.

14-Chloro-6H-quinazolino[1,2-f]phenanthridin-6-one (3s): R_f = 0.30 (hexane/ethyl acetate 2:3); white solid; yield 87% (52 mg); mp 279-281 °C; ^1H NMR (700 MHz, $CDCl_3$) δ

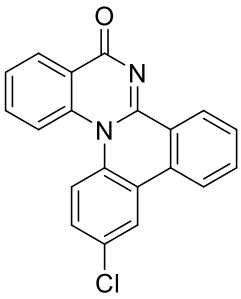

8.99 (d, *J* = 8.4 Hz, 1H), 8.41 (d, *J* = 7.7 Hz, 1H), 8.28 (s, 1H), 8.23 (d, *J* = 7.7 Hz, 1H), 8.02 (d, *J* = 8.4 Hz, 1H), 7.99 (d, *J* = 8.4 Hz, 1H), 7.86 (t, *J* = 7.7 Hz, 1H), 7.70 (dd, *J* = 13.3, 7.0 Hz, 2H), 7.59 (t, *J* = 7.7 Hz, 1H), 7.49 (dd, *J* = 8.7, 2.1 Hz, 1H); ^{13}C NMR (175 MHz, $CDCl_3$) δ 168.1, 152.3, 138.5, 133.8, 132.2, 132.1, 131.5, 130.9, 129.8, 128.9, 128.5, 128.4, 127.6, 126.7, 125.4, 124.4, 123.3, 122.1, 122.0, 119.3; IR (KBr) $\tilde{\nu}$ = 2922, 1651, 1516, 1321, 1146 cm^{-1}; HR-MS (ESI-TOF) m/z calcd for $C_{20}H_{12}ClN_2O$ $[M + H]^+$ 331.0633, found 331.0610.

13-(Trifluoromethyl)-6H-quinazolino[1,2-f]phenanthridin-6-one (3t): R_f = 0.30 (hexane/ethyl acetate 2:3); white solid; yield 76% (45.5 mg); mp 258-260 °C; ^1H NMR (700

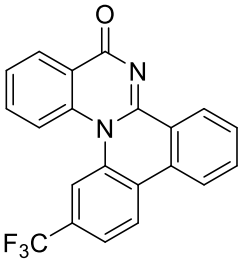

MHz, $CDCl_3$) δ 9.00 (d, *J* = 8.4 Hz, 1H), 8.46 (d, *J* = 8.4 Hz, 1H), 8.43 (d, *J* = 7.7 Hz, 1H), 8.33 (d, *J* = 8.4 Hz, 2H), 7.96 (d, *J* = 8.4 Hz, 1H), 7.89 (t, *J* = 7.7 Hz, 1H), 7.80 – 7.68 (m, 3H), 7.63 (t, *J* = 7.7 Hz, 1H); ^{13}C NMR (175 MHz, $CDCl_3$) δ 167.9, 152.3, 138.4, 133.9, 133.0, 132.5, 130.8, 130.4 (q, *J* = 33.4 Hz), 130.3, 129.0, 128.6, 127.9, 127.1, 125.6, 123.5 (q, *J* = 272.2 Hz), 123.4, 122.7 (q, *J* = 3.6 Hz), 122.5, 118.9, 117.8 (q, *J* = 8.2 Hz); IR (KBr) $\tilde{\nu}$ = 2918,

1654, 1596, 1525, 1360 cm^{-1}; HR-MS (ESI-TOF) m/z calcd for $C_{21}H_{12}F_3N_2O$ $[M + H]^+$ 365.0896, found 365.0900.

8-Chloro-13-(trifluoromethyl)-6H-quinazolino[1,2-f]phenanthridin-6-one (3u): R_f = 0.30 (hexane/ethyl acetate 2:3); white solid; yield 68% (68 mg); mp 292-294 °C; ^1H NMR (400

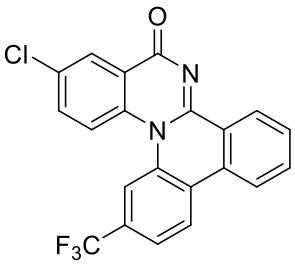

MHz, $CDCl_3$) δ 8.98 (d, *J* = 8.0 Hz, 1H), 8.47 (d, *J* = 8.4 Hz, 1H), 8.38 (s, 1H), 8.34 (d, *J* = 8.0 Hz, 1H), 8.26 (s, 1H), 7.91 (t, *J* = 8.8 Hz, 2H), 7.78 (d, *J* = 8.4 Hz, 1H), 7.74 (t, *J* = 7.6 Hz, 1H), 7.70 (dd, *J* = 8.8, 2.4 Hz, 1H); ^{13}C NMR (100 MHz, $CDCl_3$) δ 166.7, 152.5, 136.8, 134.2, 133.8, 132.8, 132.8, 130.8, 130.4, 129.1, 128.0, 126.9, 126.8, 125.7, 124.6, 123.5 (q, *J* = 272.8 Hz), 122.9 (q, *J* = 3.4 Hz), 122.5, 120.7, 117.6 (q, *J* = 4.1 Hz); IR (KBr) $\tilde{\nu}$ = 2918, 1648, 1509, 1358, 1330, 1164 cm^{-1}; HR-MS (ESI-TOF) m/z calcd for $C_{21}H_{11}ClF_3N_2O$ $[M + H]^+$ 399.0507, found 399.0519.

8,14-Dichloro-6H-quinazolino[1,2-f]phenanthridin-6-one (3v): R_f = 0.30 (hexane/ethyl acetate 2:3); white solid; yield 78% (78 mg); mp 294-296 °C; ^1H NMR (700 MHz, $CDCl_3$) δ

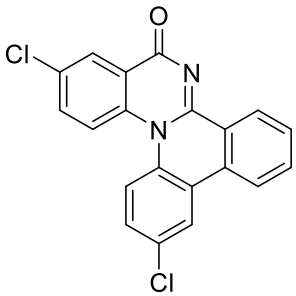

8.99 (d, *J* = 7.7 Hz, 1H), 8.38 (s, 1H), 8.31 (s, 1H), 8.25 (d, *J* = 8.4 Hz, 1H), 7.95 (dd, *J* = 8.4, 3.5 Hz, 2H), 7.88 (t, *J* = 7.7 Hz, 1H), 7.71 (dd, *J* = 16.8, 9.1 Hz, 1H), 7.65 (d, *J* = 8.4 Hz, 1H), 7.51 (d, *J* = 9.1 Hz, 1H); ^{13}C NMR (175 MHz, $CDCl_3$) δ 166.9, 152.4, 136.9, 134.1, 133.5, 132.5, 132.4, 131.3, 130.9, 129.9, 129.1, 128.7, 127.9, 126.5, 125.5, 124.6, 124.5, 122.2, 121.8, 121.1; IR (KBr) $\tilde{\nu}$ = 2920, 2850, 1654, 1557, 1523 cm^{-1}; HR-MS (ESI-TOF) m/z calcd for $C_{20}H_{11}Cl_2N_2O$ $[M + H]^+$ 365.0243, found 365.0250.

8-Fluoro-6H-quinazolino[1,2-f]phenanthridin-6-one (3m) R_f = 0.35 (hexane/ethyl acetate 2:3); white solid; yield 73% (43.5 mg); mp 276-278 °C; ^{1}H NMR (700 MHz, $CDCl_3$) δ 8.98 (d, *J* = 8.4 Hz, 1H), 8.39 – 8.34 (m, 1H), 8.30 (d, *J* = 8.4 Hz, 1H), 8.07 (dd, *J* = 9.1, 3.5 Hz, 1H), 8.05 (dd, *J* = 7.7, 2.8 Hz, 1H), 8.03 – 7.99 (m, 1H), 7.84 (t, *J* = 7.7 Hz, 1H), 7.66 (t, *J* = 7.7 Hz, 1H), 7.55 (dd, *J* = 5.6, 3.5 Hz, 2H), 7.41 (dd, *J* = 11.9, 4.9 Hz, 1H); ^{13}C NMR (175 MHz, $CDCl_3$) δ 167.4, 161.0 (d, *J* = 250.7 Hz), 152.5, 135.1, 133.8, 132.9, 131.9, 129.2, 128.9, 128.6, 126.6, 126.3, 125.2 (d, *J* = 7.2 Hz), 124.7, 123.9, 122.1 (d, *J* = 7.7 Hz), 121.9, 120.4, 120.2 (d, *J* = 24.5 Hz), 113.4 (d, *J* = 22.9 Hz); IR (KBr) $\tilde{\nu}$ = 2918, 2849, 1660, 1512, 1484, 1292 cm^{-1}; HR-MS (ESI-TOF) m/z calcd for $C_{20}H_{12}FN_2O$ $[M + H]^+$ 315.0928, found 315.0945.

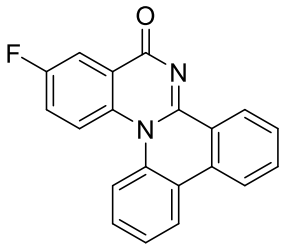

14-Chloro-8-fluoro-6H-quinazolino[1,2-f]phenanthridin-6-one (3r): R_f = 0.30 (hexane/ethyl acetate 2:3); white solid; yield 67% (40 mg); mp 297-299 °C; ^{1}H NMR (400 MHz, $CDCl_3$) δ 8.99 (d, *J* = 8.4 Hz, 1H), 8.30 (d, *J* = 2.4 Hz, 1H), 8.24 (d, *J* = 8.0 Hz, 1H), 8.05 (dd, *J* = 8.0, 2.8 Hz, 1H), 8.03 – 7.99 (m, 1H), 7.97 (d, *J* = 9.2 Hz, 1H), 7.87 (t, *J* = 7.6 Hz, 1H), 7.71 (t, *J* = 7.6 Hz, 1H), 7.51 (dd, *J* = 9.2, 2.4 Hz, 1H), 7.46 – 7.40 (m, 1H); ^{13}C NMR (100 MHz, $CDCl_3$) δ 167.2, 161.1 (d, *J* = 251.1 Hz), 152.3, 134.9, 133.9, 132.3, 131.4, 130.8, 129.9, 129.0, 128.6, 126.6, 125.4, 125.3 (d, *J* = 7.2 Hz), 124.5, 122.1, 121.9, 121.8, 120.5 (d, *J* = 24.6 Hz), 113.6 (d, *J* = 22.8 Hz); IR (KBr) $\tilde{\nu}$ = 2855, 1653, 1528, 1316, 1172 cm^{-1}; HR-MS (ESI-TOF) m/z calcd for $C_{20}H_{11}ClFN_2O$ $[M + H]^+$ 349.0538, found 349.0561.

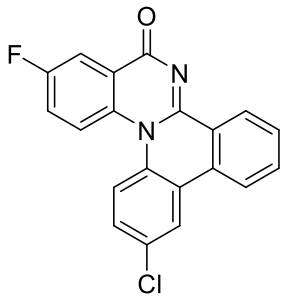

4.6. REFERENCES

1. (a) Alam, M. N.; K. M, L.; Maity, P., *Org. Biomol. Chem.* **2018,** *16* (46), 8922-8926; (b) Nájera, C.; Beletskaya, I. P.; Yus, M., *Chem. Soc. Rev.* **2019,** *48* (16), 4515-4618.

2. Sakakibara, Y.; Murakami, K., *ACS Catal.* **2022,** *12*, 1857-1878.

3. (a) Huang, T.; Wang, T.; Shi, Y.; Chen, J.; Guo, X.; Lai, R.; Liu, X.; Wu, Z.; Peng, D.; Wang, L.; Li, H.; Hai, L.; Wu, Y., *Org. Lett.* **2021,** *23* (5), 1548-1553; (b) Jeong, S.; Joo, J. M., *Acc. Chem. Res.* **2021,** *54* (24), 4518-4529; (c) Zhang, C.; Cheng, Y.; Li, F.; Luan, Y.; Li, P.; Li, W., *Adv. Synth. Catal.* **2020,** *362* (6), 1286-1291; (d) Zhao, K.; Du, Y.; Peng, Q.; Yu, W.-H.; Wang, B.-Q.; Feng, C.; Xiang, S.-K., *J. Org. Chem.* **2021,** *86* (3), 2986-2997.

4. (a) Luo, H.; Li, Y.; Du, L.; Xin, X.; Wang, T.; Han, J.; Tian, Y.; Li, B., *Org. Lett.* **2021,** *23* (20), 7883-7887; (b) Zhu, Y. M.; Fang, Y.; Li, H.; Xu, X. P.; Ji, S. J., *Org. Lett.* **2021,** *23* (19), 7342-7347.

5. Lee, J. B.; Kang, M. E.; Kim, J.; Lee, C. Y.; Kee, J. M.; Myung, K.; Park, J. U.; Hong, S. Y., *Chem. Commun.* **2017,** *53* (75), 10394-10397.

6. Zhou, Y.; Zhang, X.; Zhang, Y.; Ruan, L.; Zhang, J.; Zhang-Negrerie, D.; Du, Y., *Org. Lett.* **2017,** *19* (1), 150-153.

7. (a) Aubert, S.; Bezagu, M.; Spivey, A. C.; Arseniyadis, S., *Nat. Rev. Chem.* **2019,** *3* (12), 706-722; (b) Caprice, K.; Pál, D.; Besnard, C.; Galmés, B.; Frontera, A.; Cougnon, F. B. L., *J. Am. Chem. Soc.* **2021,** *143* (31), 11957-11962; (c) Yamashina, M.; Tanaka, Y.; Lavendomme, R.; Ronson, T. K.; Pittelkow, M.; Nitschke, J. R., *Nature* **2019,** *574* (7779), 511-515.

8. (a) Choudhuri, K.; Pramanik, M.; Mal, P., *J. Org. Chem.* **2020,** *85* (19), 11997-12011; (b) Soberats, B.; Sanna, E.; Martorell, G.; Rotger, C.; Costa, A., *Org. Lett.* **2014,** *16* (3), 840-3; (c) Tang, B.; Zhao, J.; Xu, J.-F.; Zhang, X., *Chem. Eur. J.* **2020,** *26* (67), 15446-15460.

9. Maiti, S.; Mal, P., *J. Org. Chem.* **2018,** *83* (3), 1340-1347.

10. Maharramov, A. M.; Mahmudov, K. T.; Kopylovich, M. N.; Aliyeva, R. A.; Pombeiro, A. J. L., Cooperation of Non-covalent Interactions and Coordination in Catalysis. In *Non-covalent Interactions in the Synthesis and Design of New Compounds*, John Wiley & Sons, Inc: 2016; pp 327-344.

11. Kennedy, C. R.; Lin, S.; Jacobsen, E. N., *Angew. Chem. Int. Ed.* **2016,** *55* (41), 12596–12624.

12. Giese, M.; Albrecht, M.; Rissanen, K., *Chem. Rev.* **2015,** *115* (16), 8867-8895.

13. Smith, D. K., *Chem. Rec.* **2021,** *21* (9), 2488-2501.

14. Nandy, A.; Kazi, I.; Guha, S.; Sekar, G., *J. Org. Chem.* **2021,** *86* (3), 2570-2581.

15. Murai, T.; Lu, W.; Kuribayashi, T.; Morisaki, K.; Ueda, Y.; Hamada, S.; Kobayashi, Y.; Sasamori, T.; Tokitoh, N.; Kawabata, T.; Furuta, T., *ACS Catal.* **2021,** *11*, 568-578.

16. Li, C.-J., *Chem. Rev.* **2005,** *105* (8), 3095-3166.

17. Tornieporth-Oetting, I.; Klapötke, T., *Angew. Chem. Int. Ed. Engl.* **1990,** *29* (6), 677-679.

18. (a) Bosnidou, A. E.; Muñiz, K., *Angew. Chem. Int. Ed.* **2019,** *58* (22), 7485-7489; (b) Maertens, G.; Deruer, E.; Denis, M.; Canesi, S., *J. Org. Chem.* **2020,** *85* (9), 6098-6108; (c) Maiti, S.; Achar, T. K.; Mal, P., *Org. Lett.* **2017,** *19* (8), 2006-2009; (d) Reitti, M.; Villo, P.; Olofsson, B., *Angew. Chem. Int. Ed.* **2016,** *55* (31), 8928-8932; (e) Yoshimura, A.; Zhdankin, V. V., *Chem. Rev.* **2016,** *116* (5), 3328-3435.

19. Gupta, P. K.; Yadav, N.; Jaiswal, S.; Asad, M.; Kant, R.; Hajela, K., *Chem. Eur. J.* **2015,** *21* (38), 13210-13215.

20. Banerji, B.; Bera, S.; Chatterjee, S.; Killi, S. K.; Adhikary, S., *Chem. Eur. J.* **2016,** *22* (10), 3506-3512.

21. Payra, S.; Yadav, N.; Moorthy, J. N., *New J. Chem.* **2022,** *46* (2), 582-591.

22. (a) Horton, D. A.; Bourne, G. T.; Smythe, M. L., *Chem. Rev.* **2003,** *103* (3), 893-930; (b) Laha, J. K.; Patel, K. V.; Tummalapalli, K. S.; Dayal, N., *Chem. Commun.* **2016,** *52* (67), 10245-8.

23. Ramos-Villaseñor, J. M.; Rodríguez-Cárdenas, E.; Barrera Díaz, C. E.; Frontana-Uribe, B. A., *J. Electrochem. Soc.* **2020,** *167* (15).

24. Pickhardt, W.; Grätz, S.; Borchardt, L., *Chem. Eur. J.* **2020,** *26* (57), 12903-12911.

25. Maiti, S.; Alam, M. T.; Bal, A.; Mal, P., *Adv. Synth. Catal.* **2019,** *361* (19), 4401-4425.

26. Dohi, T.; Kita, Y., *Chem. Commun.* **2009,** (16), 2073-2085.

27. Bera, S. K.; Alam, M. T.; Mal, P., *J. Org. Chem.* **2019,** *84* (18), 12009-12020.

28. Peng, J.; Yu, Y.; Yue, Y.; Wang, D.; Li, X.; Chen, C., *Synthesis* **2016,** *48* (22), 3941-3950.

NMR Spectrum of Selected Compounds

^{1}H NMR (700 MHz, $CDCl_3$)

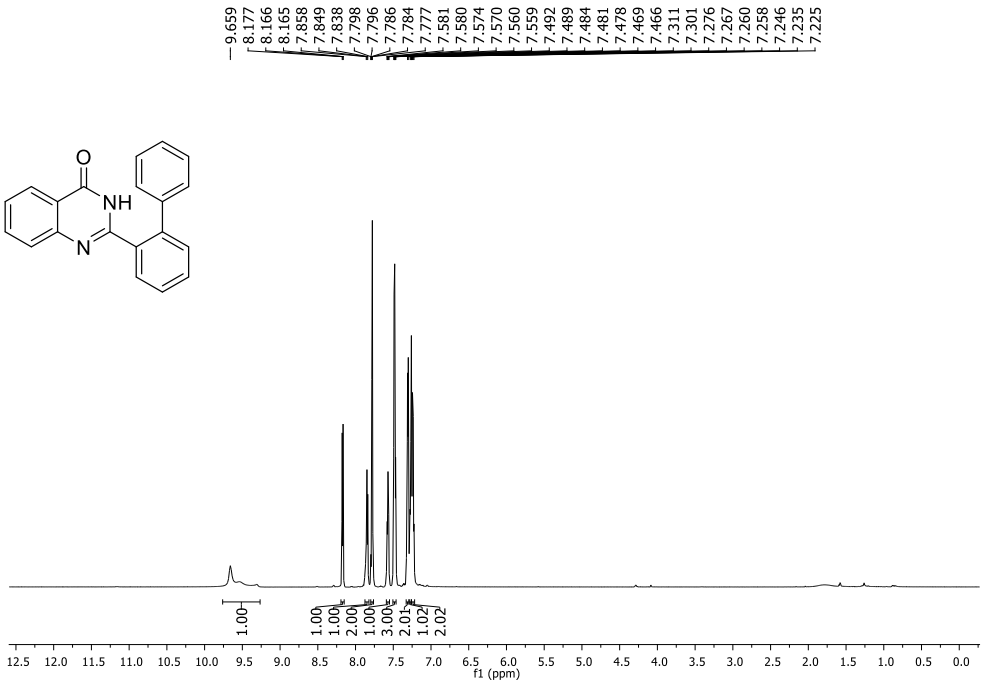

Figure 4.7. ^{1}H NMR spectrum of 2-([1,1'-biphenyl]-2-yl)quinazolin-4(3H)-one **(1a)**

^{13}C NMR (175 MHz, $CDCl_3$)

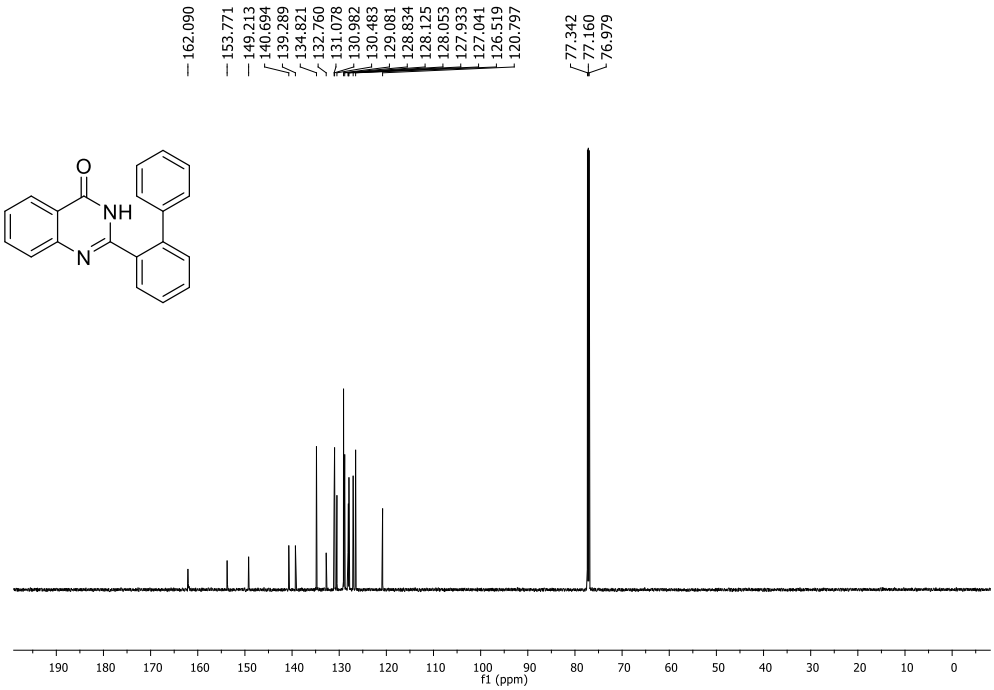

Figure 4.8. ^{13}C NMR spectrum of 2-([1,1'-biphenyl]-2-yl)quinazolin-4(3H)-one **(1a)**

^{1}H NMR (400 MHz, $CDCl_3$)

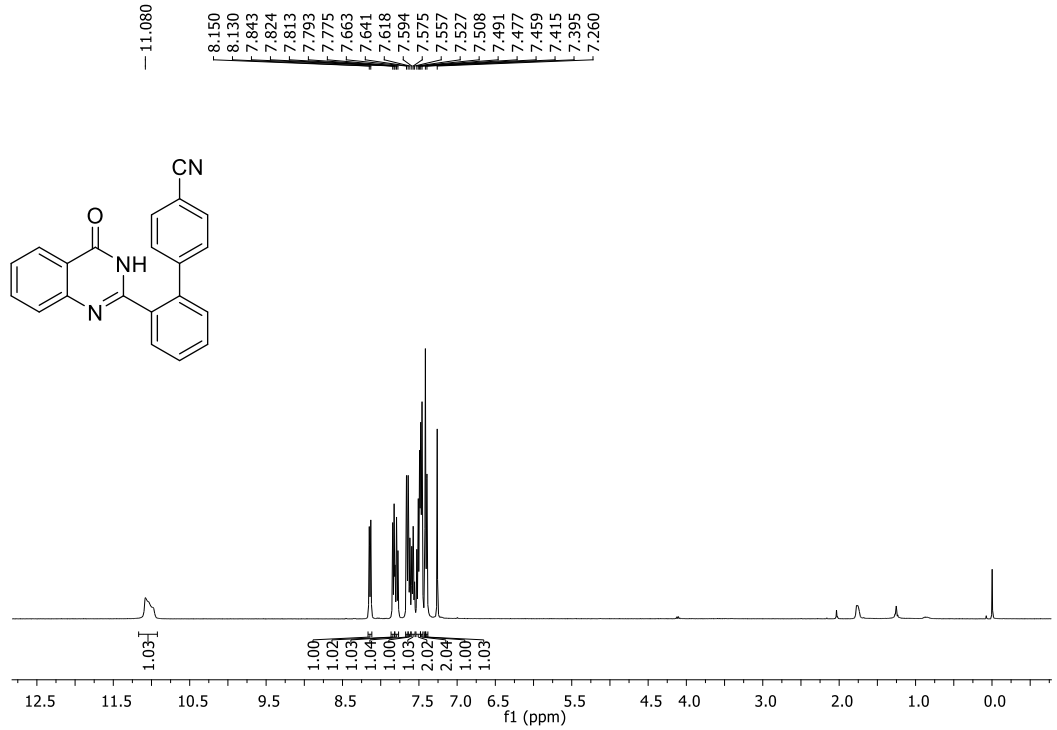

Figure 4.9. ^{1}H NMR spectrum of 2'-(4-Oxo-3,4-dihydroquinazolin-2-yl)-[1,1'-biphenyl]-4-carbonitrile **(1e)**

^{13}C NMR (100 MHz, $CDCl_3$)

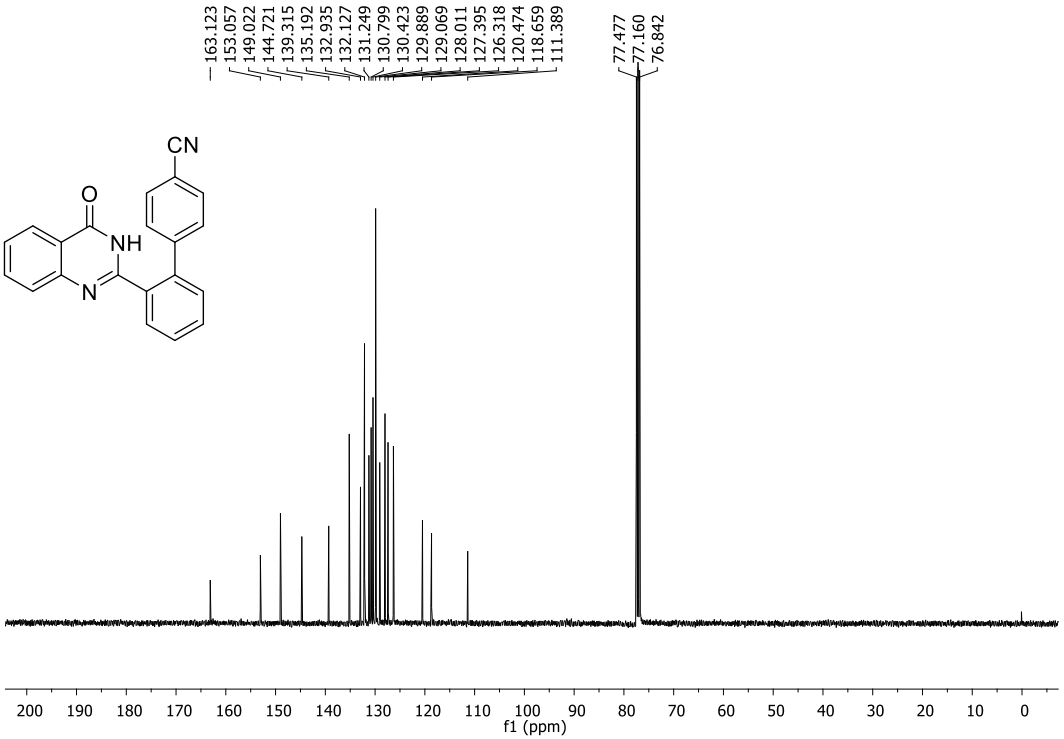

Figure 4.10. ^{13}C NMR spectrum of 2'-(4-Oxo-3,4-dihydroquinazolin-2-yl)-[1,1'-biphenyl]-4-carbonitrile **(1e)**

^{1}H NMR (700 MHz, $CDCl_3$)

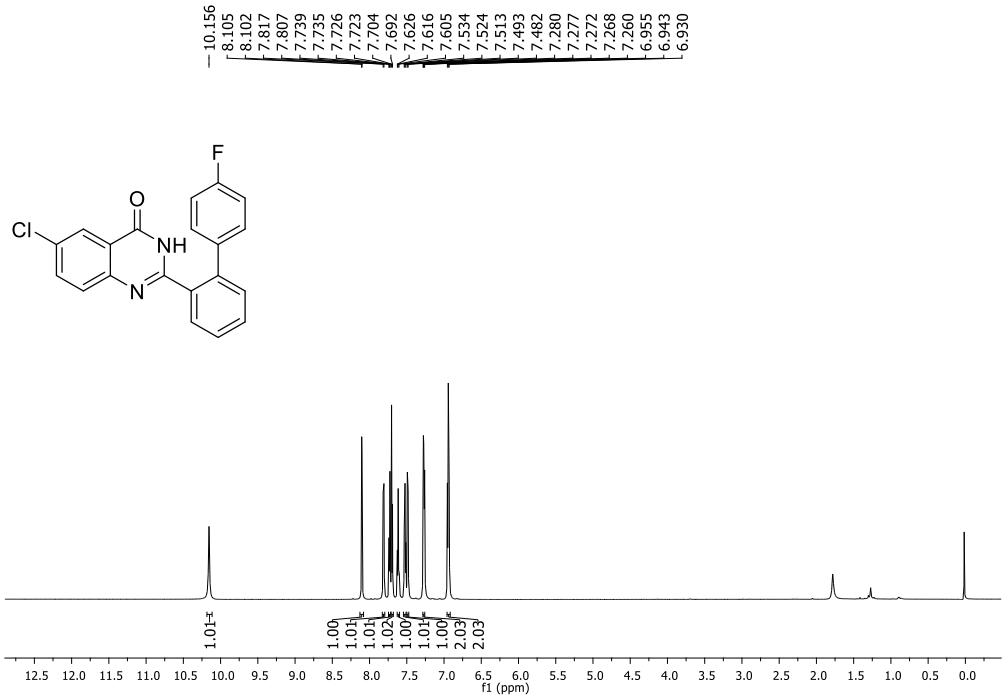

Figure 4.11. ^{1}H NMR spectrum of 6-Chloro-2-(4'-fluoro-[1,1'-biphenyl]-2-yl)quinazolin-4(3H)-one **(1j)**

^{13}C NMR (175 MHz, $CDCl_3$)

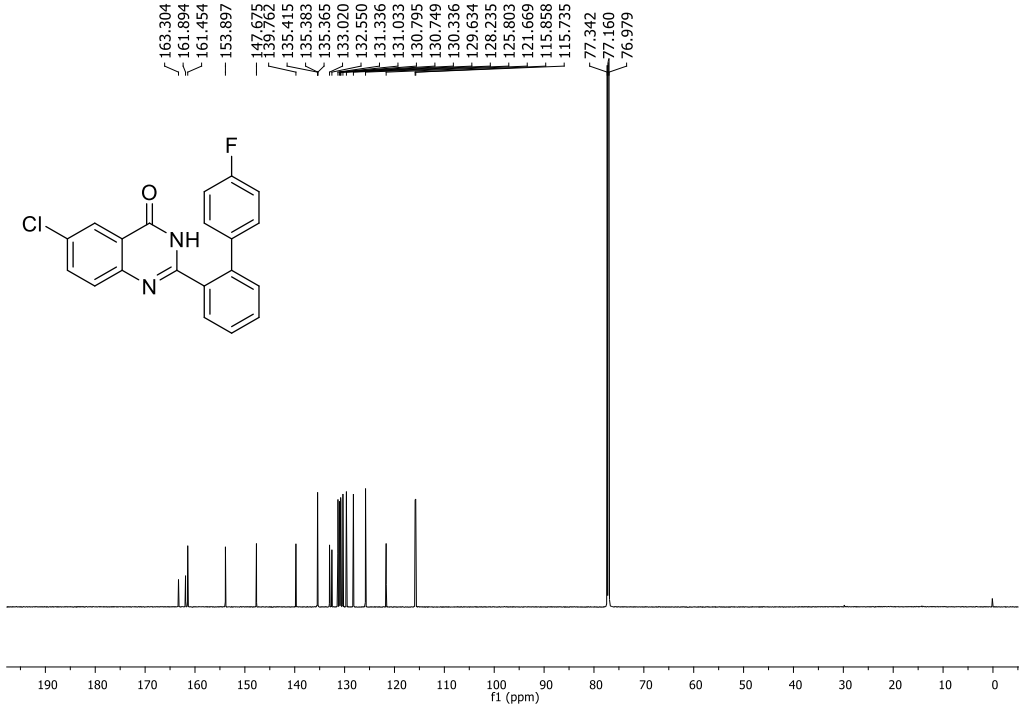

Figure 4.12. ^{13}C NMR spectrum of 6-Chloro-2-(4'-fluoro-[1,1'-biphenyl]-2-yl)quinazolin-4(3H)-one **(1j)**

^{1}H NMR (400 MHz, $CDCl_3$)

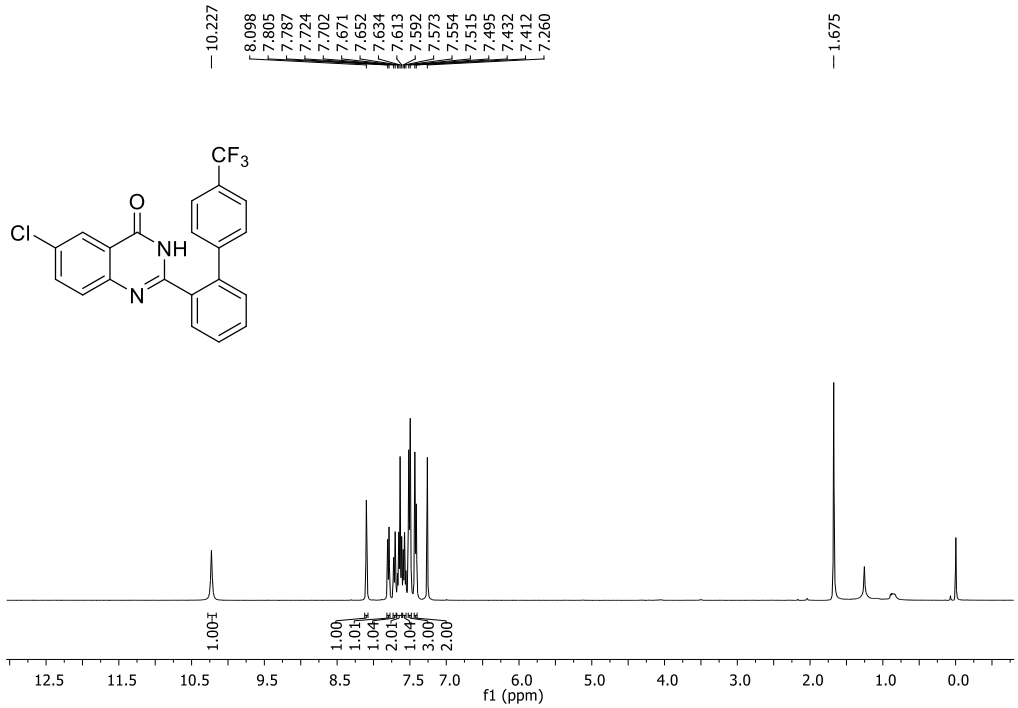

Figure 4.13. ^{1}H NMR spectrum of 6-Chloro-2-(4'-(trifluoromethyl)-[1,1'-biphenyl]-2-yl)quinazolin-4(3H)-one **(1u)**

^{13}C NMR (100 MHz, $CDCl_3$)

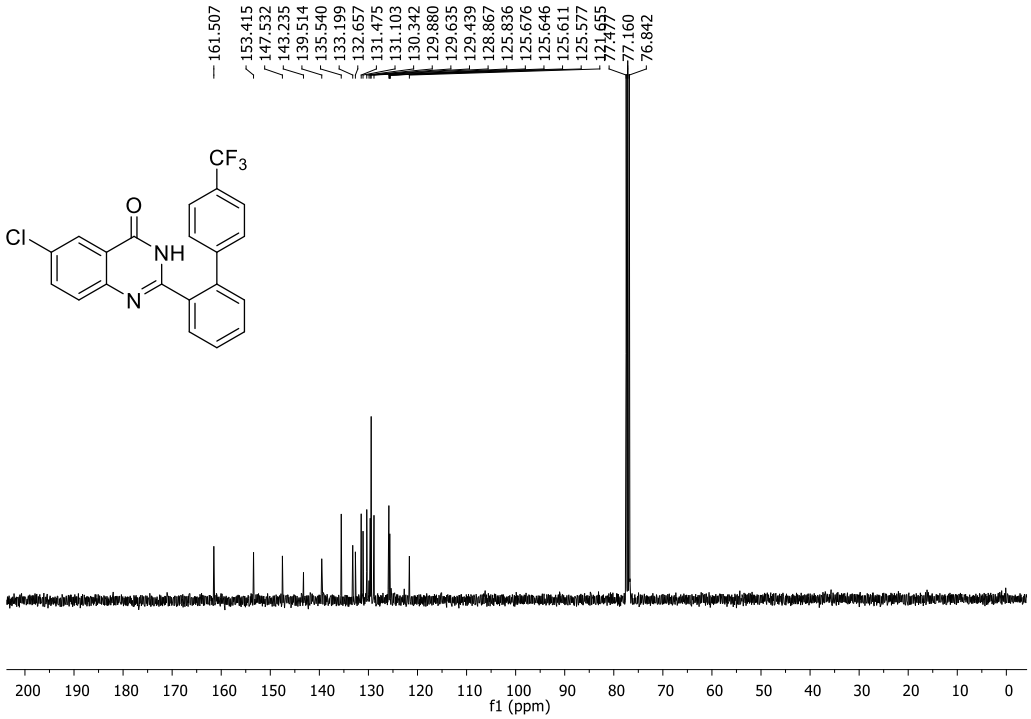

Figure 4.14. ^{13}C NMR spectrum of 6-Chloro-2-(4'-(trifluoromethyl)-[1,1'-biphenyl]-2-yl)quinazolin-4(3H)-one **(1u)**

^{1}H NMR (400 MHz, $CDCl_3$)

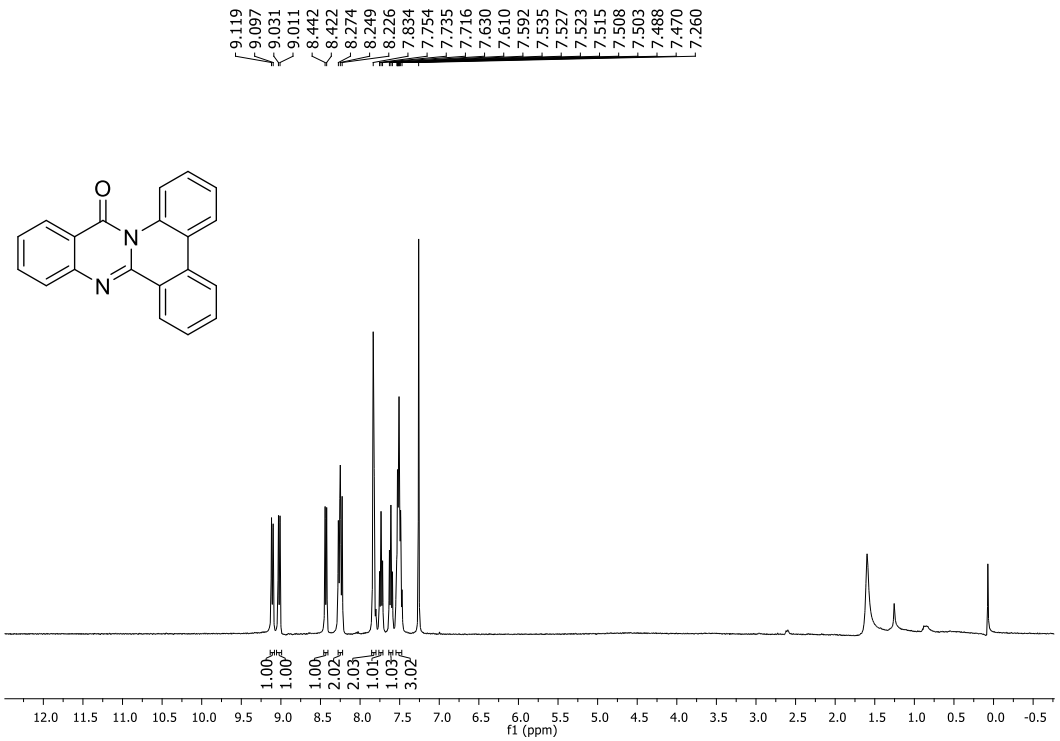

Figure 4.15. ^{1}H NMR spectrum of 14H-Quinazolino[3,2-f]phenanthridin-14-one (**2a**)

^{13}C NMR (175 MHz, $CDCl_3$)

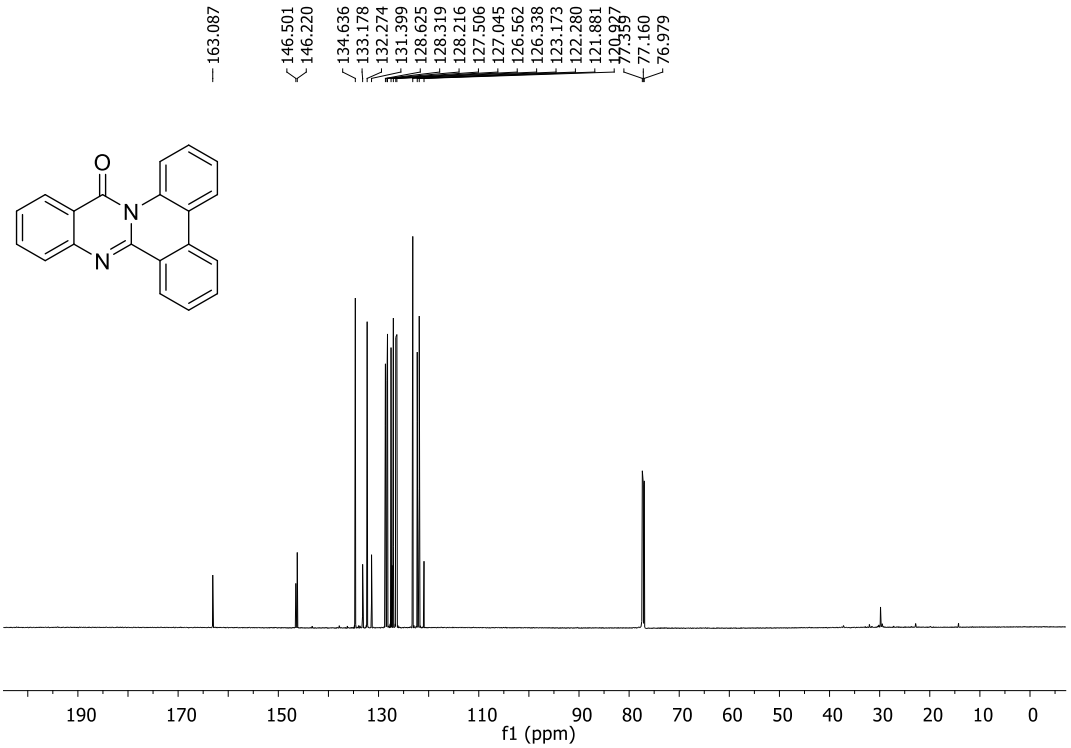

Figure 4.16. ^{13}C NMR spectrum of 14H-Quinazolino[3,2-f]phenanthridin-14-one (**2a**)

^{1}H NMR (400 MHz, $CDCl_3$)

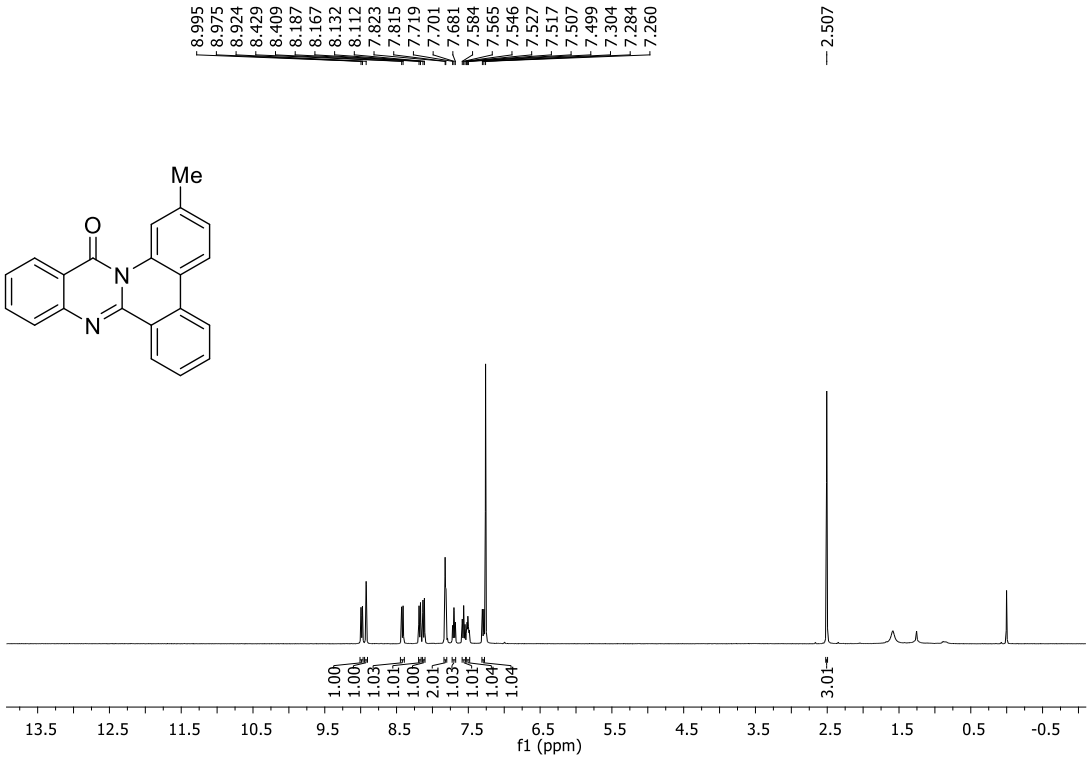

Figure 4.17. ^{1}H NMR spectrum of 2-Methyl-14H-quinazolino[3,2-f]phenanthridin-14-one **(2b)**

^{13}C NMR (100 MHz, $CDCl_3$)

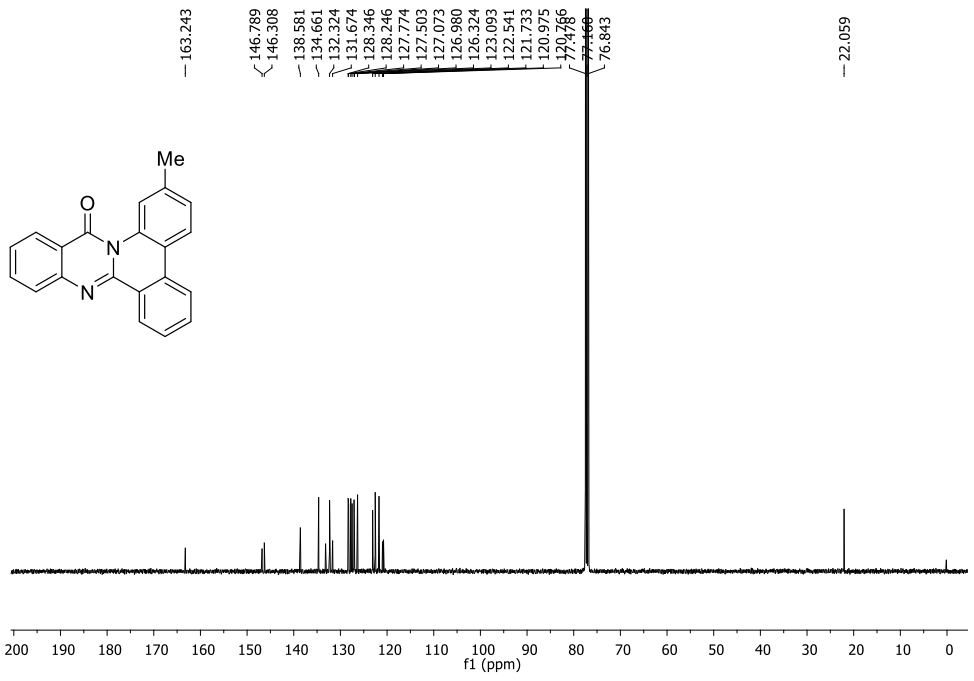

Figure 4.18. ^{13}C NMR spectrum of 2-Methyl-14H-quinazolino[3,2-f]phenanthridin-14-one **(2b)**

^{1}H NMR (400 MHz, $CDCl_3$)

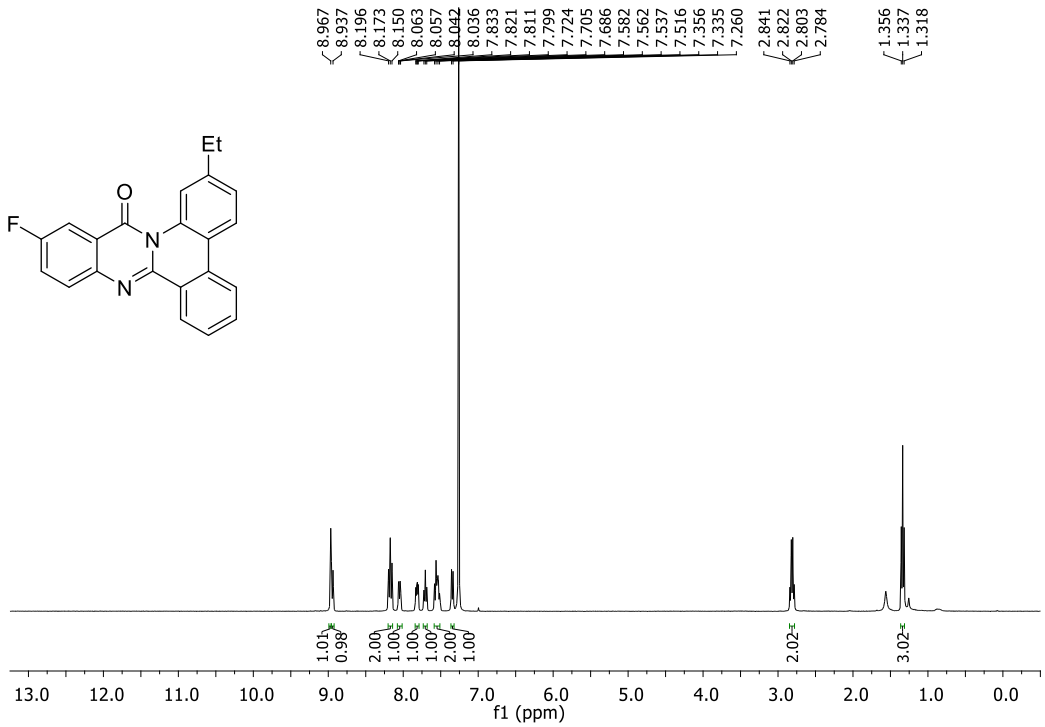

Figure 4.19. ^{1}H NMR spectrum of 2-Ethyl-12-fluoro-14H-quinazolino[3,2-f]phenanthridin-14-one **(2n)**

^{13}C NMR (175 MHz, $CDCl_3$)

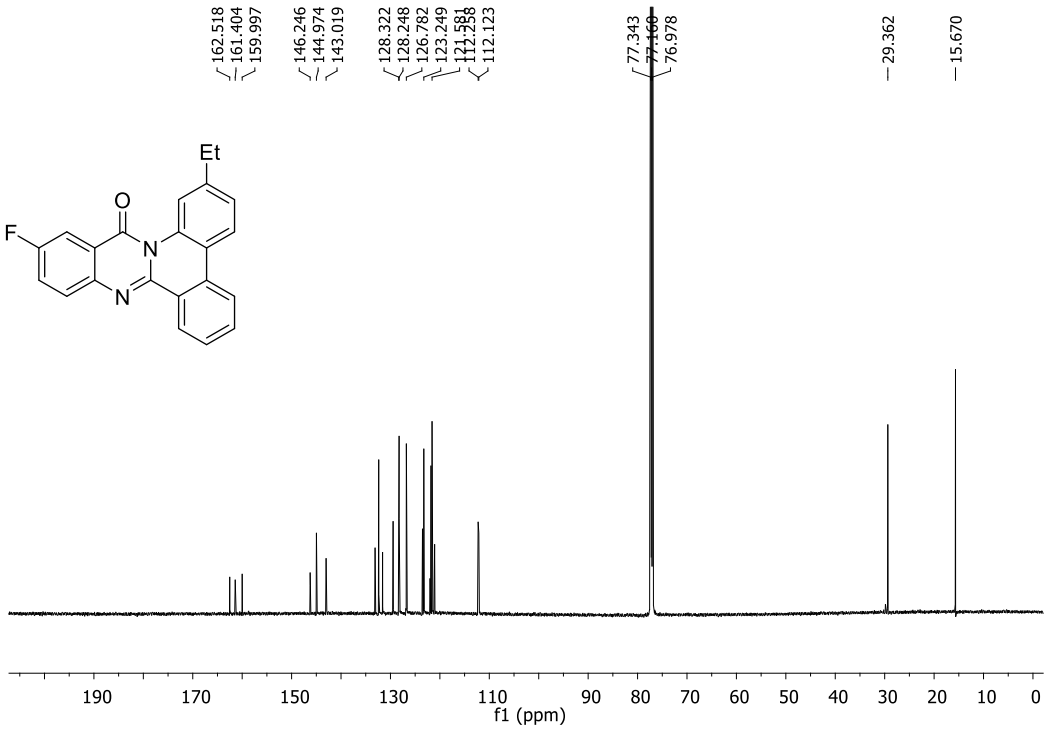

Figure 4.20. ^{13}C NMR spectrum of 2-Ethyl-12-fluoro-14H-quinazolino[3,2-f]phenanthridin-14-one **(2n)**

^{1}H NMR (400 MHz, $CDCl_3$)

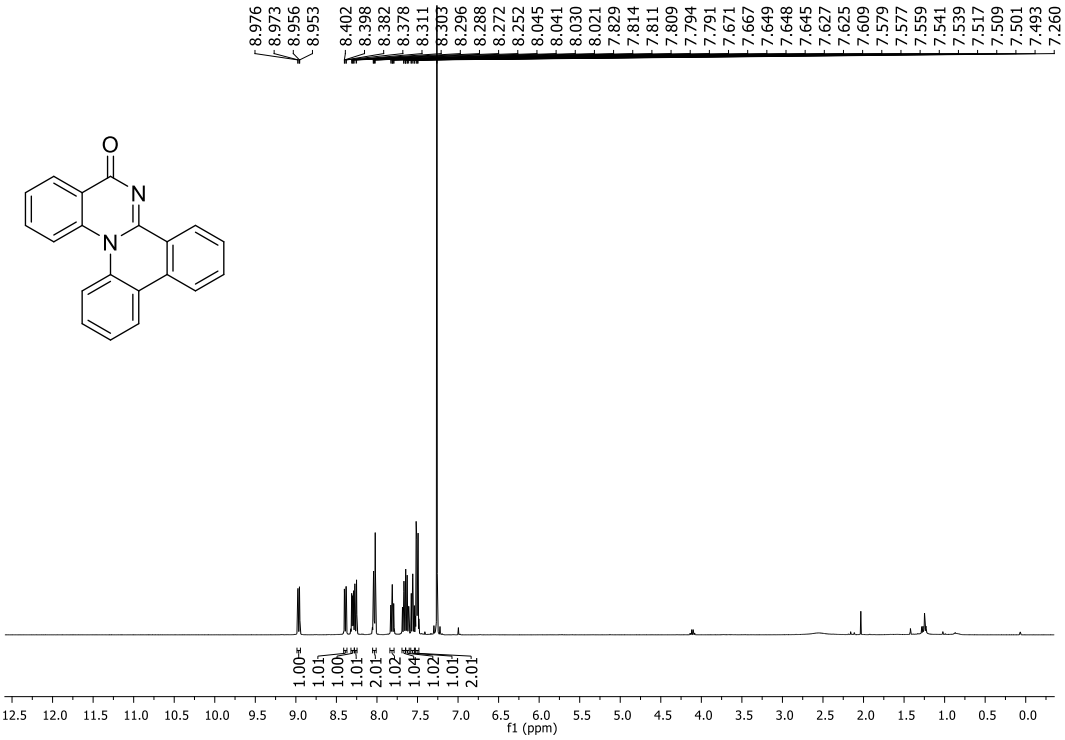

Figure 4.21. ^{1}H NMR spectrum of 6H-Quinazolino[1,2-f]phenanthridin-6-one **(3a)**

^{13}C NMR (100 MHz, $CDCl_3$)

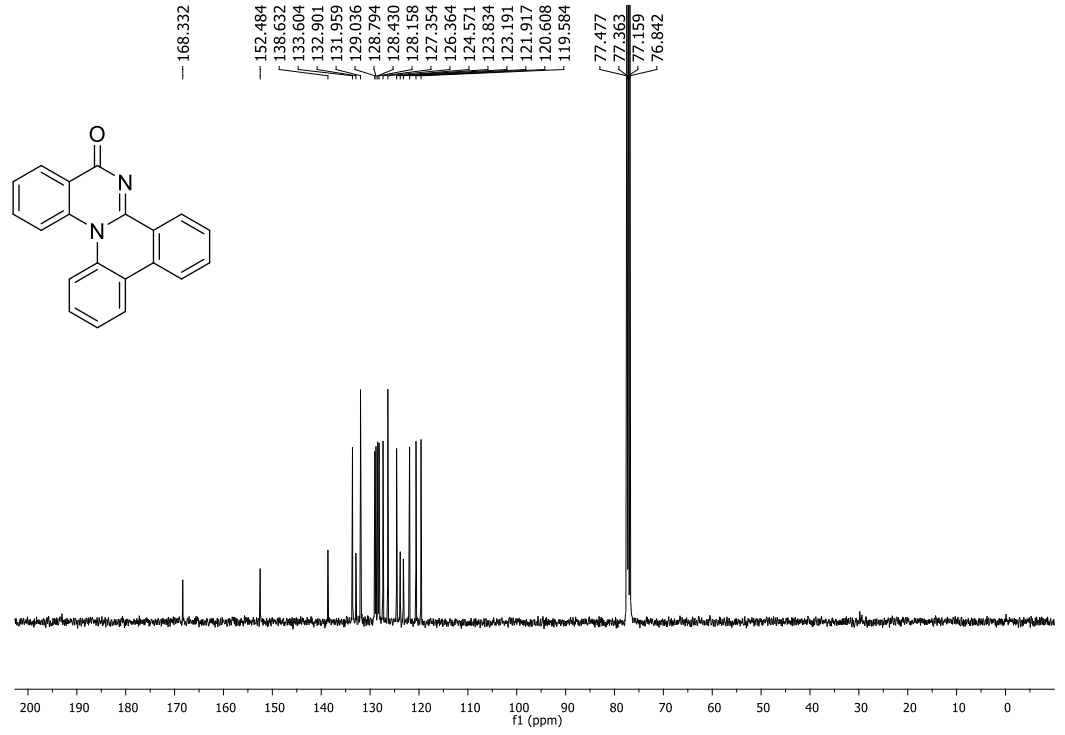

Figure 4.22. ^{13}C NMR spectrum of 6H-Quinazolino[1,2-f]phenanthridin-6-one **(3a)**

^{1}H NMR (700 MHz, $CDCl_3$)

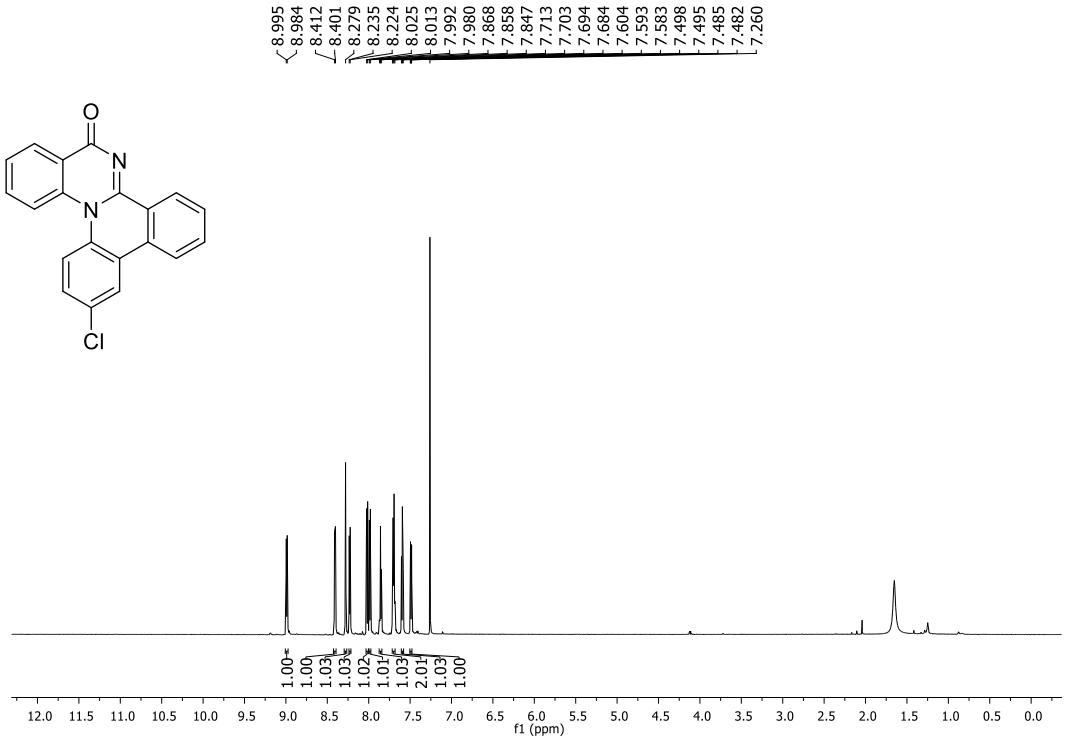

Figure 4.23. ^{1}H NMR spectrum of 3-Chloro-14H-quinazolino[3,2-f]phenanthridin-14-one **(3s)**

^{13}C NMR (175 MHz, $CDCl_3$)

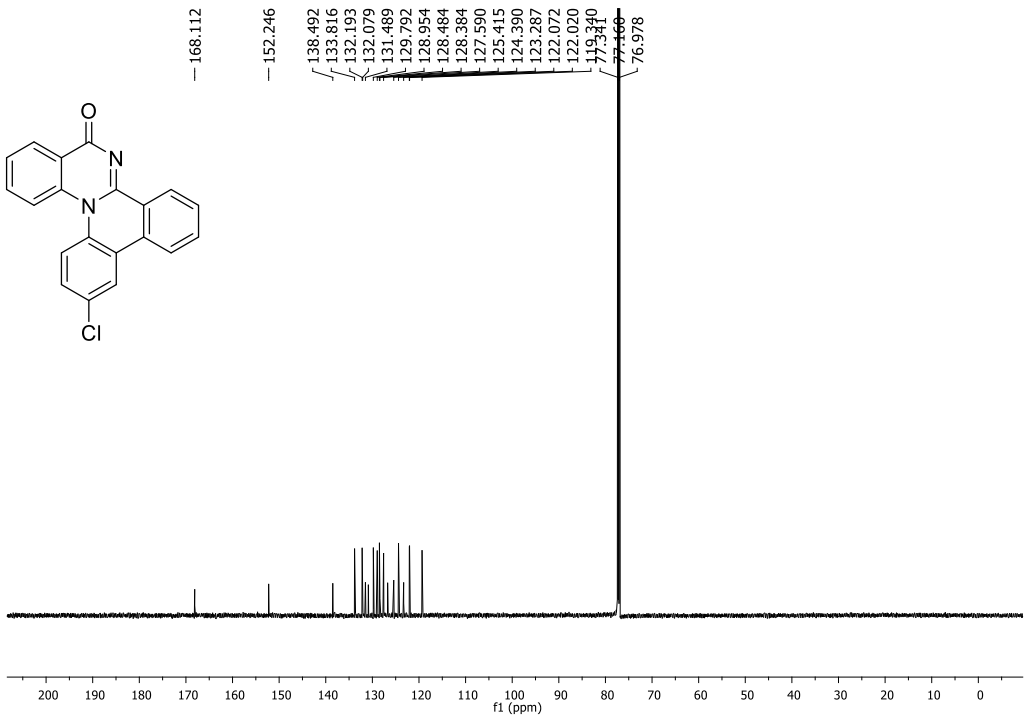

Figure 4.24. ^{13}C NMR spectrum of 3-Chloro-14H-quinazolino[3,2-f]phenanthridin-14-one **(3s)**

^{1}H NMR (400 MHz, $CDCl_3$)

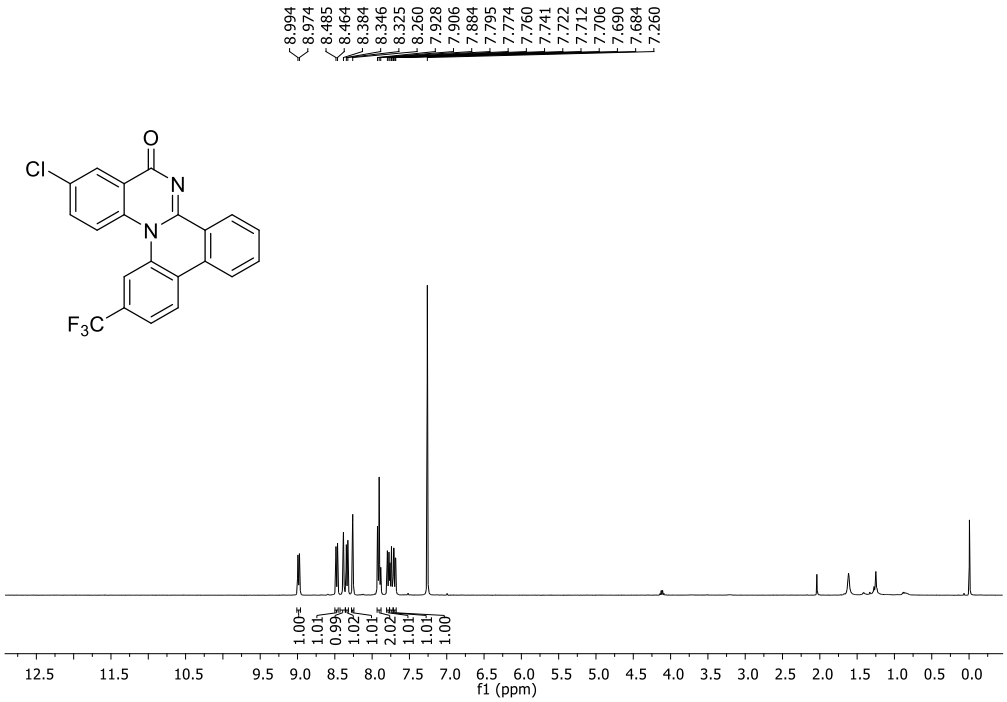

Figure 4.25. ^{1}H NMR spectrum of 12-Chloro-2-(trifluoromethyl)-14H-quinazolino[3,2-f]phenanthridin-14-one **(3u)**

^{13}C NMR (100 MHz, $CDCl_3$)

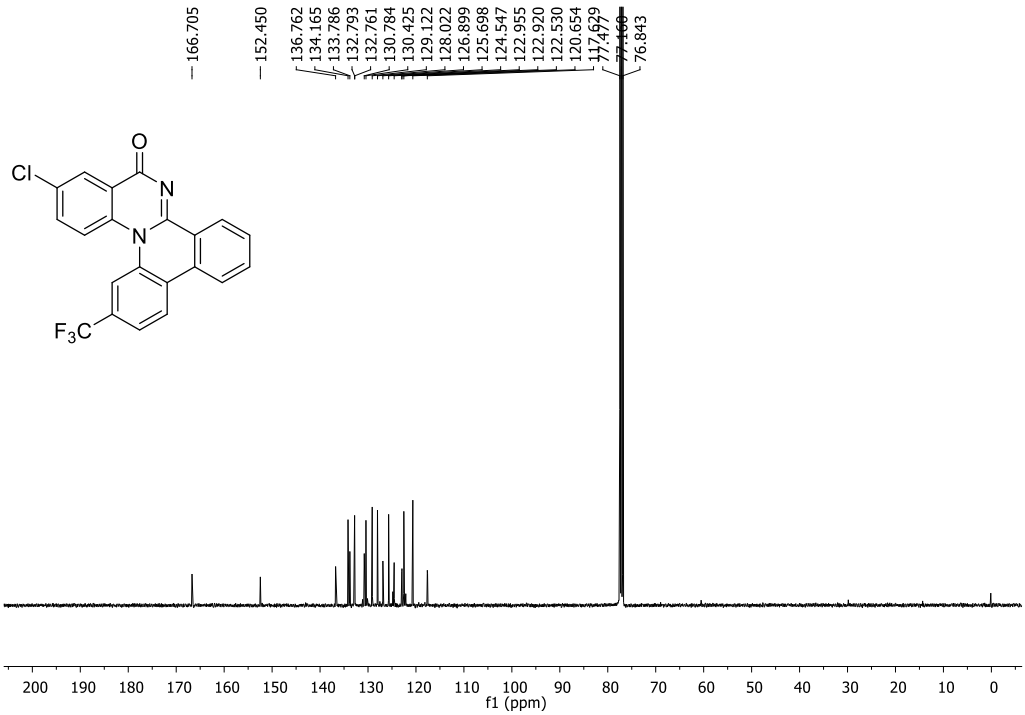

Figure 4.26. ^{13}C NMR spectrum of 12-Chloro-2-(trifluoromethyl)-14H-quinazolino[3,2-f]phenanthridin-14-one **(3u)**

^{1}H NMR (400 MHz, $CDCl_3$)

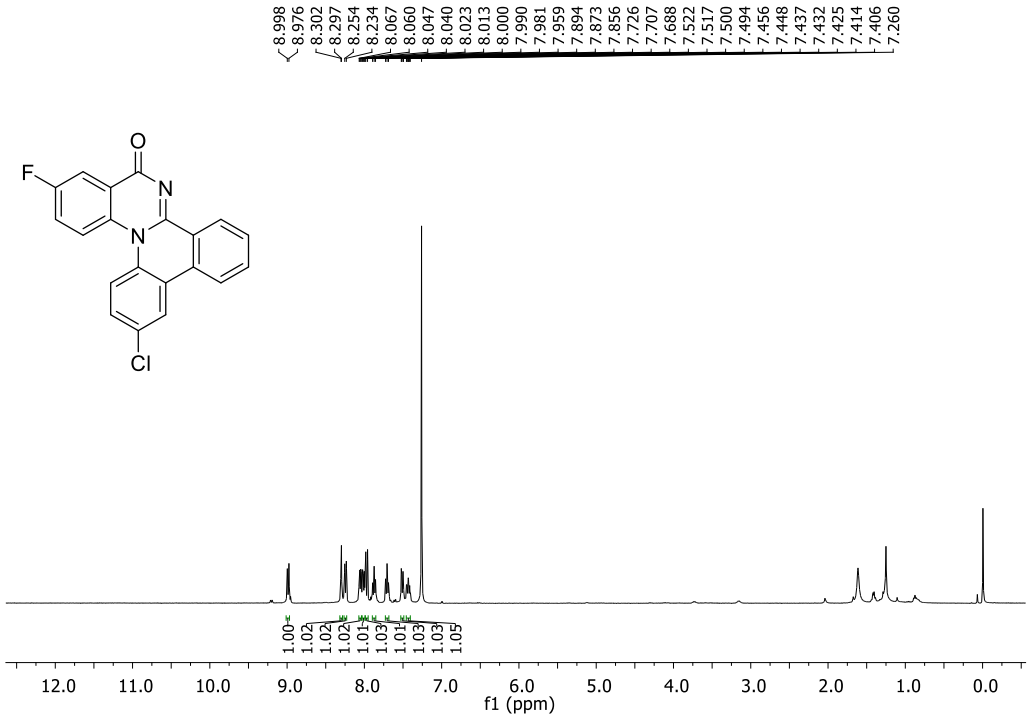

Figure 4.27. ^{1}H NMR spectrum of 14-Chloro-8-fluoro-6H-quinazolino[1,2-f]phenanthridin-6-one **(3r)**

^{13}C NMR (175 MHz, $CDCl_3$)

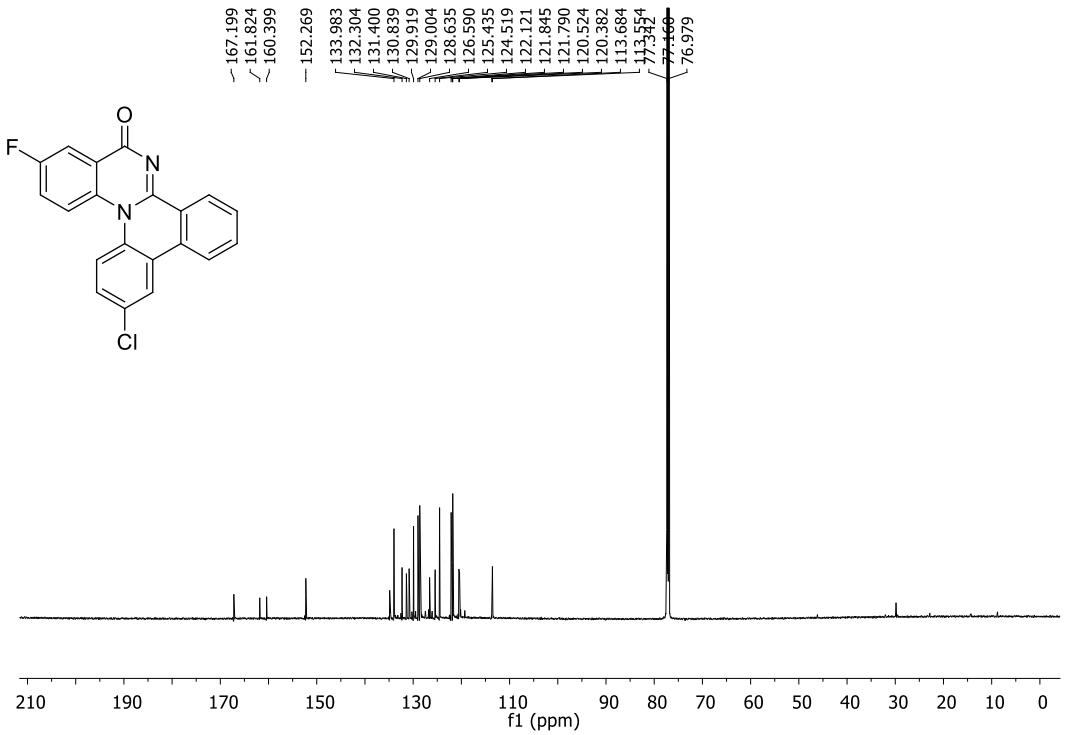

Figure 4.28. ^{13}C NMR spectrum of 14-Chloro-8-fluoro-6H-quinazolino[1,2-f]phenanthridin-6-one **(3r**

CHAPTER 5

Mechanochemical Synthesis of Phenanthridinones using N-Halosuccinamides

5.1 ABSTRACT

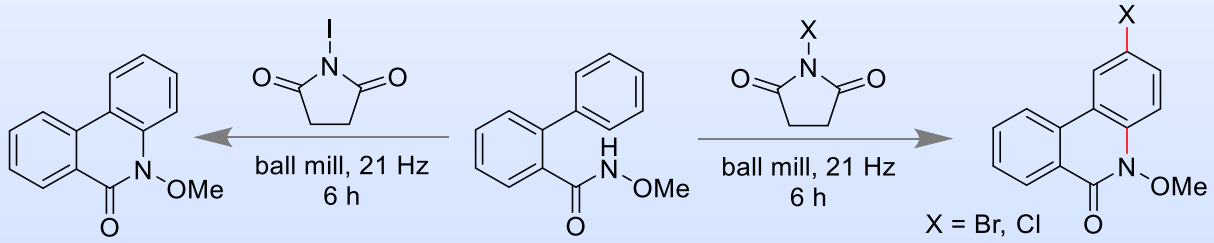

The development of alternative energy sources for chemical transformations has gained significant interest to chemists. Herein we report the use of *N*-bromosuccinimides (NBS) and *N*-chlorosuccinimides (NCS) as bifunctional reagents for a cascaded C-N bond formation and subsequent halogenation reactions. Under the solvent-free mechanochemical (ball-milling) condition, the synthesis of a wide range of phenanthridinone derivatives from *N*-methoxy-[1,1'-biphenyl]-2-carboxamides is accomplished. During the reactions, NBS and NCS first assisted for the oxidative C-N coupling reaction and subsequently promoted a halogenation reaction. Thus the role of NBS and NCS established to be bifunctional. Overall, a mild, solvent-free, convenient, one-pot, and direct synthesis of various -bromo and -chloro substituted phenanthridinone derivatives was achieved.

5.2 INTRODUCTION

The utilization of readily accessible chemicals for the convenient and economical synthesis of functional materials and bioactive molecules is the state of art practice in synthetic organic chemistry. Recently, nontraditional energy sources like microwave,[1] visible light,[2] electrochemical,[3] mechanochemical,[4] and ultrasonication,[5] become popular. The mechanochemical approach also offers a robust and sustainable strategy in organic synthesis.[6] The primary advantages of mechanochemical synthesis is the solvent-free condition,[7] which

can avoid the issues like high reaction temperature and solubility.[8] Towards, quantitative conversion, minimum purification process, and less undesired side-products carry extra significance to this practice.[9] In addition, the mechanochemical reactions expected to follow the "Twelve Principles of Green Chemistry".[10] IUPAC recognizes that out of ten innovative technologies, mechanochemistry is one of them.[11] The mechanochemical approaches are widely used in the research areas like the synthesis of heterocyclic compounds,[12] synthesis of metal complexes,[13] molecular syntheses,[6a, 14] supramolecular chemistry,[15] asymmetric organic synthesis,[16] etc. Also, solid-state transformations such as C-H Borylation,[17] C-H bond amidation,[18] C-C[19] and C-N[20] bond formations have been well explored in mechanochemistry.[20]

Recently, the bifunctional reagents[21] are gaining popularity because multistep reactions can be done in minimum steps and cost-effective ways.[22] The bifunctional systems are well-known in supramolecular chemistry,[23] material science,[24] organic synthesis,[22b] catalysis,[25] anion-relay chemistry,[26] etc. Wu and coworkers reported an oxidative aminohalogenation of maleimides using haloamines as bifunctional reagent.[27] Also, tandem electrochemical cyclization, trifluoromethylation, and SO_2 insertion of *N*-cyanamide alkenes were achieved using CF_3SO_2Na as a bifunctional reagent in which CF_3SO_2Na acted as both CF_3 and SO_2 sources.[28] However, the use of *N*-bromosuccinimide (NBS) and *N*-chlorosuccinimide (NCS) as bifunctional reagents in organic synthesis is relatively unknown, if any. Recently, we reported the utilization of *N*-iodosuccinimide (NIS) as a bifunctional reagent in (*E*)-selective sulfonylation reaction of styrenes.[29] We have shown herein the use of NBS and NCS as bifunctional reagents for one-pot synthesis of phenanthridinones *via* a cascaded intramolecular oxidative C-N coupling and subsequent halogenation reaction under solvent-free ball milling mechanochemical condition.

Phenanthridinones are important *N*-containing heterocycles omnipresent in many natural products and pharmacologically active compounds (Figure 5.1). The molecules *N*-methylcrinasiadine and phenaglydon[30] are potent HIV-1 integrase inhibitors.[31] Oxynitidine derivatives have shown the TOP1 and TDP1 inhibitor activity.[32] Amaryllidaceae alkaloids[33] like Narciclasine[34] exhibits antimitotic activity, antitumor effects[35] and inhibit angiogenic process.[36]

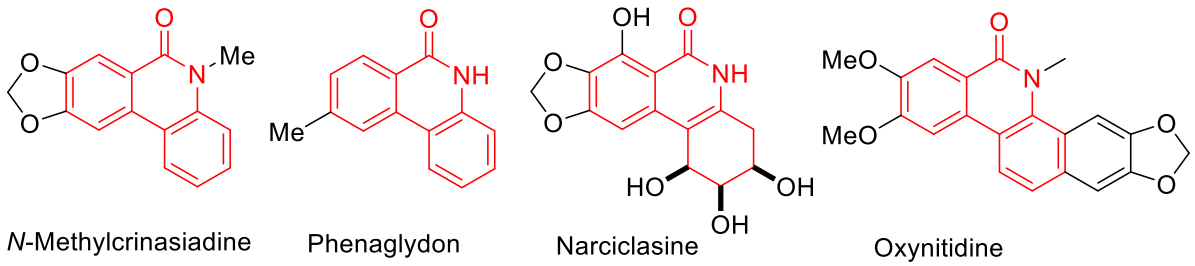

Figure 5.1. Phenanthridinones containing biologically active drug molecules.

In the synthesis of phenanthridinones, the notable examples are palladium-catalyzed oxidative annulation of *N*-methoxy benzamide with arynes,[30, 37] Pd-nanoparticles catalyzed C-H activation reaction,[38] deaminative synthesis from aniline *via* activation of C-H bonds,[39] oxidative insertion of CO to *o*-arylanilines[40] and *N*-sulfonyl-2-aminobiaryls,[41] Pd-Catalyzed aryne multicomponent reaction,[42] etc. Xue and coworkers reported the synthesis of 2-substituted-phenanthridinones from *N*-methoxybenzamides *via* a sequential one-pot synthesis using tetrabutylammonium bromide and PhI-peracid combination (Scheme 5.1.a).[43] Again, Xue and coworkers reported phenanthridinone synthesis using PhI-*m*CPBA mediated an oxidative C-N coupling (Scheme 5.1.a).[44] The mechanochemical synthesis of phenanthridinone or their halogenated derivatives is shown in Scheme 5.1.b (this work). During the reactions, NBS and NCS initially helped an oxidative C-N coupling reaction followed by a halogenation reaction. Therefore, the bifunctionality of the reagents NBS and

NCS was established. However, NIS led to the oxidative C-N coupling reaction,[45] and no halogenation was observed (Scheme 5.1.b).

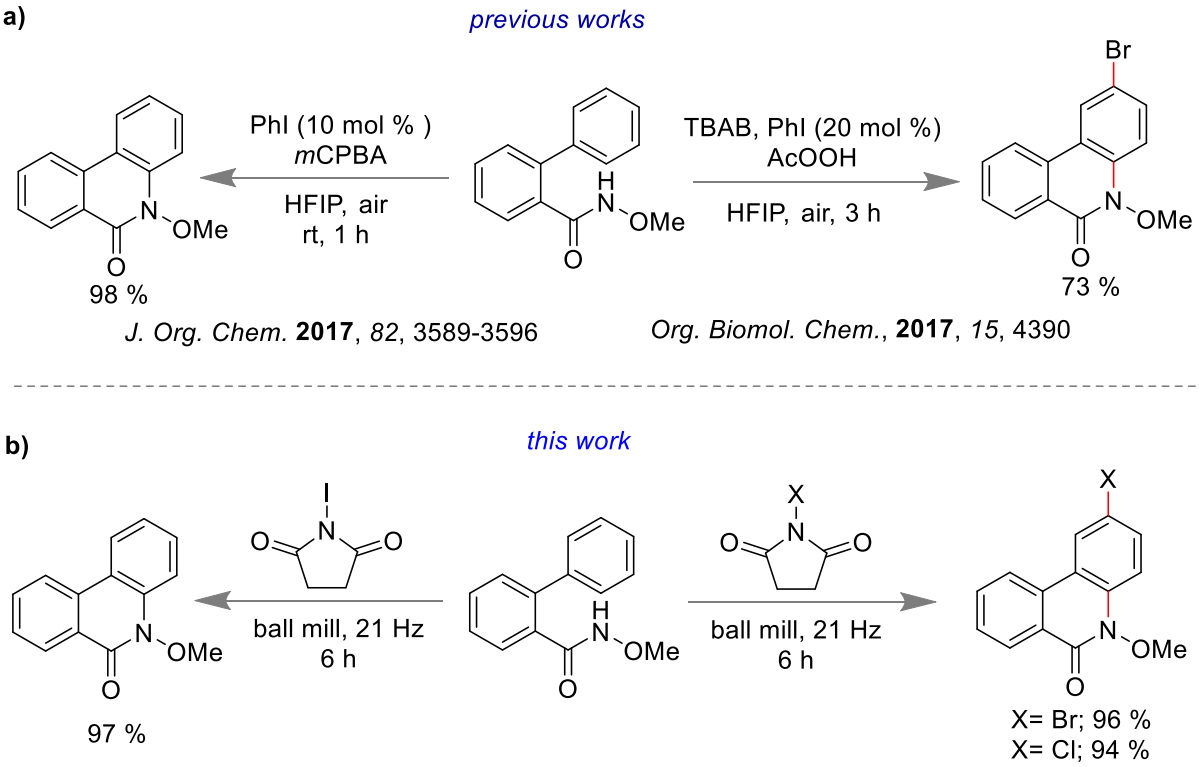

Scheme 5. 1. a) Sequential one-pot synthesis of bromo-phenanthridinones using tetrabutylammonium bromide and PhI-peracetic acid (right-hand side), and the use of PhI-*m*CPBA combination for oxidative C-N coupling (left-hand side).[44] b) Our work is based on the mechanochemical synthesis of phenanthridinones or their halogenated derivatives using *N*-halosuccinimides.

5.3. RESULTS AND DISCUSSION

During optimization of the reaction condition (Table 1), *N*-methoxy-[1,1'-biphenyl]-2-carboxamide (**1a**) was used as the model substrate under mechanochemical ball-milling conditions (21 Hz) for 6 h to monitor the formation of unsubstituted (**2a**), bromo- (**3a**), or chloro- (**4a**) phenanthridinones. The ratios of the products were determined using ^{1}H NMR

spectroscopy. Using 1.0 equiv of NBS, an inseparable mixture of the non-brominated (**2a**) and brominated (**3a**) phenanthridinones in a ratio of 1:3 was obtained with 53 % overall yield (entry 1). However, the ratio was changed to 1:10 with 1.5 equiv of NBS, and the overall yield was increased to 73 % (entry 2). Compound **3a** obtained with 96% yield when 2.0 equiv of the NBS was used (entry 3). A similar trend was observed using NCS (entries 4-5) and the corresponding products obtained with 51% and 94% overall yields. On the other hand, NIS led to 5-methoxyphenanthridin-6(5H)-one (**2a**) up to 97% yields (entries 6-8). The iodine(III) reagents PIDA and PIFA led to **2a** with 60 % and 54 % yield, respectively (entries 9 and 10). No product was detected when oxidants like $NH_4S_2O_8$-TBAI (entry 11), $K_2S_2O_8$-TBAI (entry 12), and molecular iodine (entry 13) were used. The yield of product **2a** was not encouraging using oxone (entry 14). Interestingly, selective bromination or chlorination took place at the 2-position of the 5-methoxyphenanthridin-6(5H)-one. Furthermore, the yield of expected product (**2a**) decreased with the lowering of operating frequency from 21 to 16 Hz (entry 15). On the other hand, the desired product (**2a**) yield was unaltered with increasing the operating frequency from 21 Hz to 25 Hz (entry 16). Interestingly, the selective bromination and chlorination took place at the *p*-position with respect to the newly formed C-N bond. The halogenation reaction was inhibited when the 3'-position of the starting compounds (i.e., the *p*-position with respect to the newly formed C-N bond) had a substituent, only cyclization reactions were preferable. In this context, substitutions at the *m*-position of phenyl ring linked with *N*-methoxybenzamide were unable to deliver the halogenated-phenanthridinones.

Table 5. 1 Optimization of reaction conditions.[a]

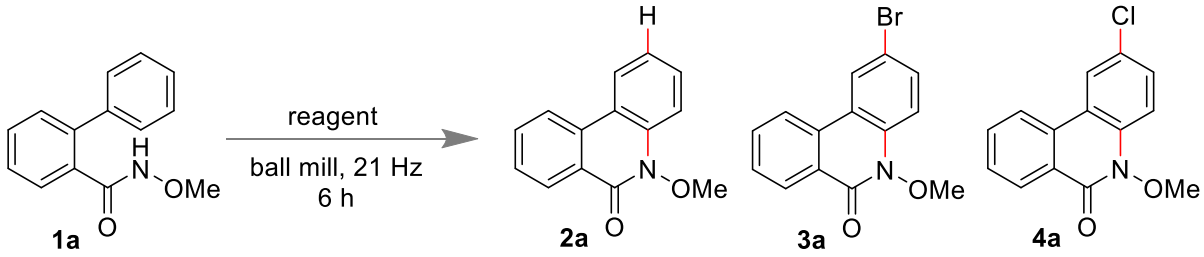

entry	reagent (equiv)	Product (yield in %)[d]
1	NBS (1.0)	**2a:3a** (53)
2	NBS (1.5)	**2a:3a** (73)
3	NBS (2)	**3a** (96)
4	NCS (1)	**2a:4a** (51)
5	NCS (2)	**4a** (94)
6	NIS (1)	**2a** (69)
7	NIS (1.5)	**2a** (84)
8	NIS (2)	**2a** (97)
9	PIDA (2)	**2a** (60)
10	PIFA (2)	**2a** (54)
11	TBAI, $K_2S_2O_8$ (2)	**2a** (0)
12	TBAI, $(NH_4)_2S_2O_8$ (2)	**2a** (0)
13	I_2 (2)	**2a** (0)
14	Oxone (2)	**2a** (52)
15[b]	NIS (2)	**2a** (91)
16[c]	NIS (2)	**2a** (97)

[a]All reactions are carried out on 0.18 mmol scale of **1a** for 6 h. [b]Reaction was carried out at 16 Hz for 6 h. [c]Reaction was carried out at 25 Hz for 6 h. [d] = Overall isoalated yield.

The substrate scope for the NBS mediated cyclization followed by bromination reaction is shown in Figure 5.2. When *N*-methoxy-[1,1'-biphenyl]-2-carboxamide (**1a**) was treated with 2.0 equiv of NBS, 2-bromo-5-methoxyphenanthridin-6(5H)-one (**3a**), the yield was 96%.

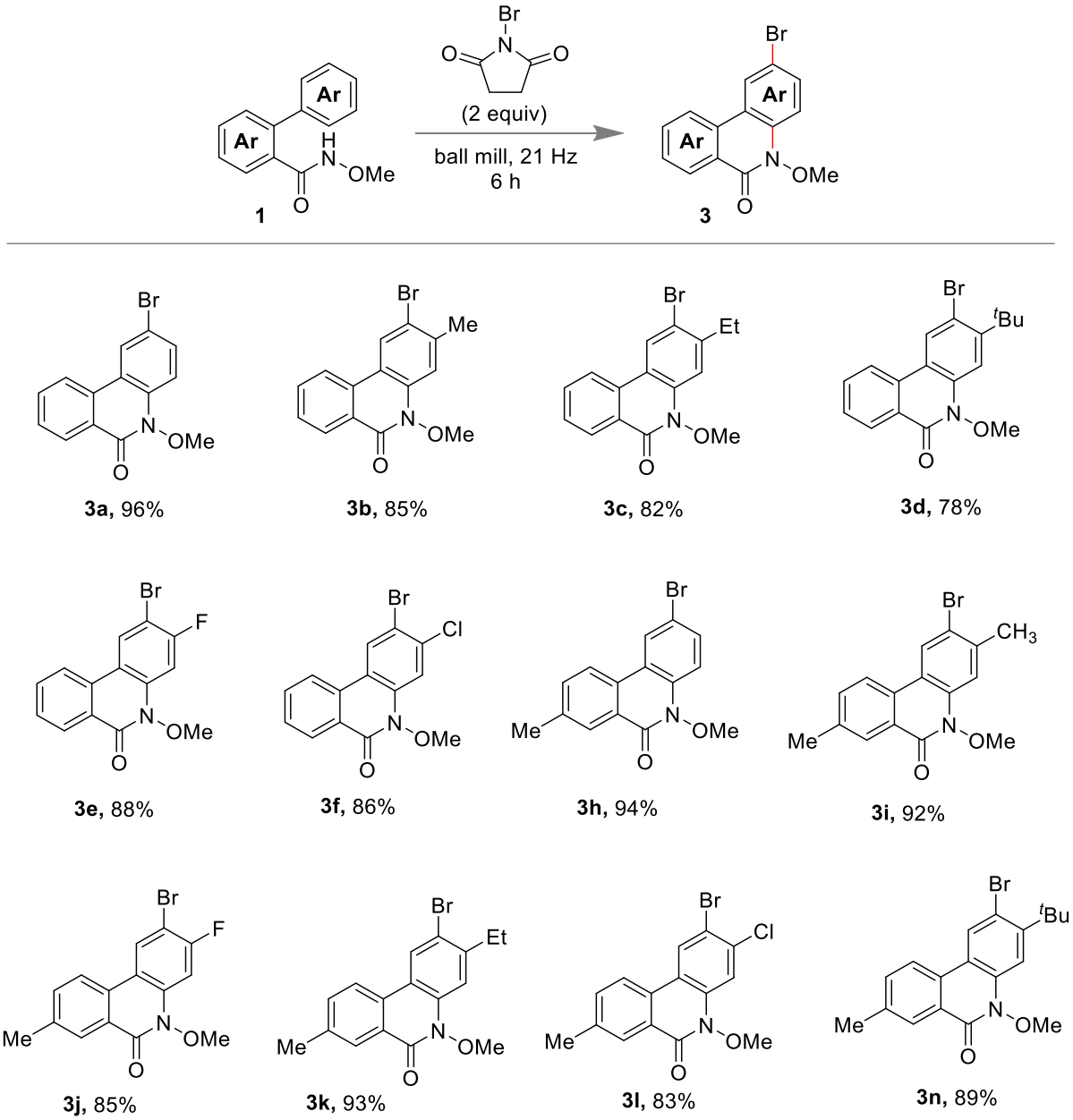

Figure 5.2 The substrate scope for the NBS mediated cascaded cyclization and bromination reaction.

The methyl, ethyl, and *tert*-butyl substituted phenyl ring attached to *N*-methoxybenzamide groups led to the **3b**, **3c** and **3d**, respectively, in good yields. The structure of **3c** (CCDC 2074176) was confirmed by the X-Ray crystallography. Similarly, fluoro and chloro

substituted derivatives resulted in **3e** and **3f** with 88% and 86% yields, respectively. The alkyl substitution at the *N*-methoxybenzamide also resulted in good yields of the products (up to 94%). The phenyl ring containing fluoro and chloro group led to the corresponding phenanthridinones in good yields. Similarly, various alkyl substitutions at phenyl rings of methyl-substituted *N*-methoxybenzamide yielded the corresponding products in high yields.

The NCS mediated cascaded cyclization and chlorination reactions were done using 2.0 equiv of NCS (Figure 5.3). Compound **4a** was obtained with 94% yield and the structure was confirmed by X-ray crystallography (CCDC 2074177). The substrate **1b** and **1i** could be transformed into the expected products **4b** and **4i**, with 91% and 87% yields, respectively. However, the phenyl ring containing fluoro group of methyl-substituted *N*-methoxybenzamide (**1j**) afforded the desire phenanthridinones (**4j**) with 85% yields. Similarly, various alkyl substitutions at phenyl rings of methyl-substituted *N*-methoxybenzamide yielded the corresponding products in high yields.

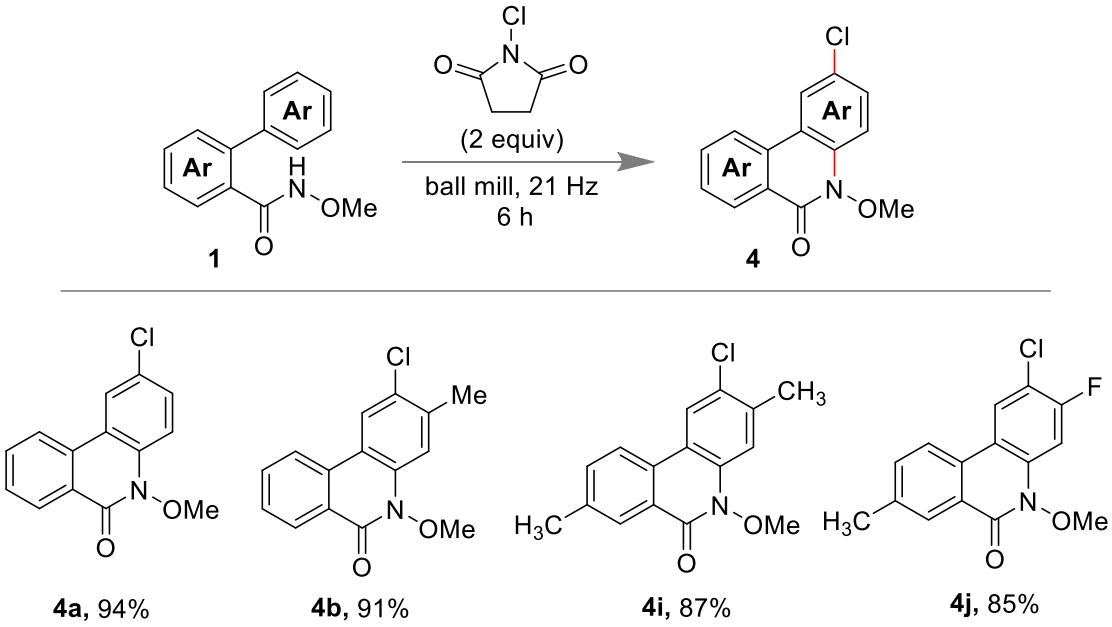

Figure 5.3 The substrate scope for the NCS mediated reaction.

The substrate scope for the synthesis of phenanthridinones **2** using NIS is shown in Figure 5.4. For example, 5-methoxyphenanthridin-6(5H)-one (**2a**) was obtained with 97% yield. Different substitutions at the phenyl ring linked with *N*-methoxybenzamide played a crucial role in the reaction yields. Methyl and *tert*-butyl substituted derivatives **2b** and **2d** the yields were 94% and 87% yields, respectively. The structure of **2b** was confirmed by X-ray crystallography (CCDC 2074179). An identical structure to compound **2b** has also been reported previously.[38] Similarly, electron-withdrawing substitutions such as fluoro, chloro, and trifluoromethyl also resulted in the corresponding compounds **2e**, **2f** and **2g** with good yields. Again, the methyl-substituted *N*-methoxybenzamide derivatives also led to the corresponding cyclized products (**2h**) with 88% yield. Likewise, the phenyl group having methyl, fluoro, ethyl and chloro substitution afforded the corresponding products **2i**, **2j, 2k** and **2l** in moderate yields (up to 86%). Notably, the incorporation of -chloro group at the - *meta* position of phenyl ring linked with methyl-substituted *N*-methoxybenzamide was converted to the desired product **2m** with a 78% yield. Similarly, a -nitro group at the - *meta* position of phenyl ring linked with *N*-methoxybenzamide led to cyclized product **2o** with 88% yield. Again, having electron-withdrawing -COMe group at the aromatic ring (**1p**) was successfully converted to **2p** with 91% yield. The replacement of the methoxy group to thephenyl group of biphenyl benzamide (**1q**) also afforded the corresponding product (**2q**) with 94% yield. Unfortunately, methoxy (-OMe) substituted phenyl rings attached to *N*-methoxybenzamide group and (C=O)NH-Me group on the aromatic rings failed to provide the desired products.

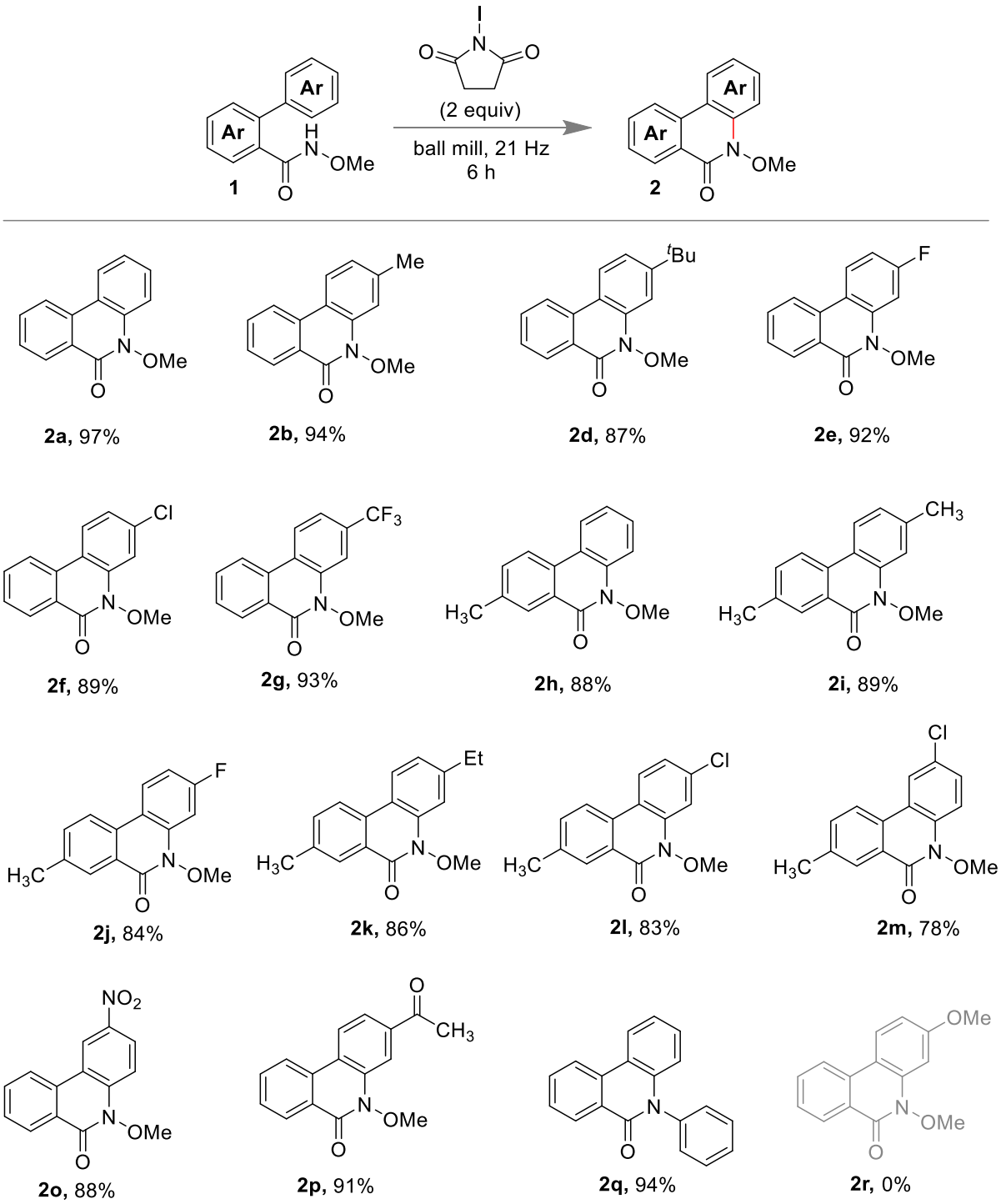

Figure 5.4. The substrate scope for the cyclization reaction using NIS.

.

Control experiments shown in Figure 5.5, helped to understand the mechanism of the reaction. The radical trapping experiment using BHT (butylated hydroxytoluene) and TEMPO (2,2,6,6-tetramethylpiperidine-1-oxyl) supported a radical-induced mechanism

(Figure 5.5a). The EPR experiments also endorsed for the radical-based mechanism since an EPR signal was observed when a free-radical spin trapping reagent DMPO (5,5-dimethyl-1-pyrroline-*N*-oxide)[46] was used under the optimized reaction condition (Figure 5.5b). The DMPO-adduct was also identified by ESI-MS study.

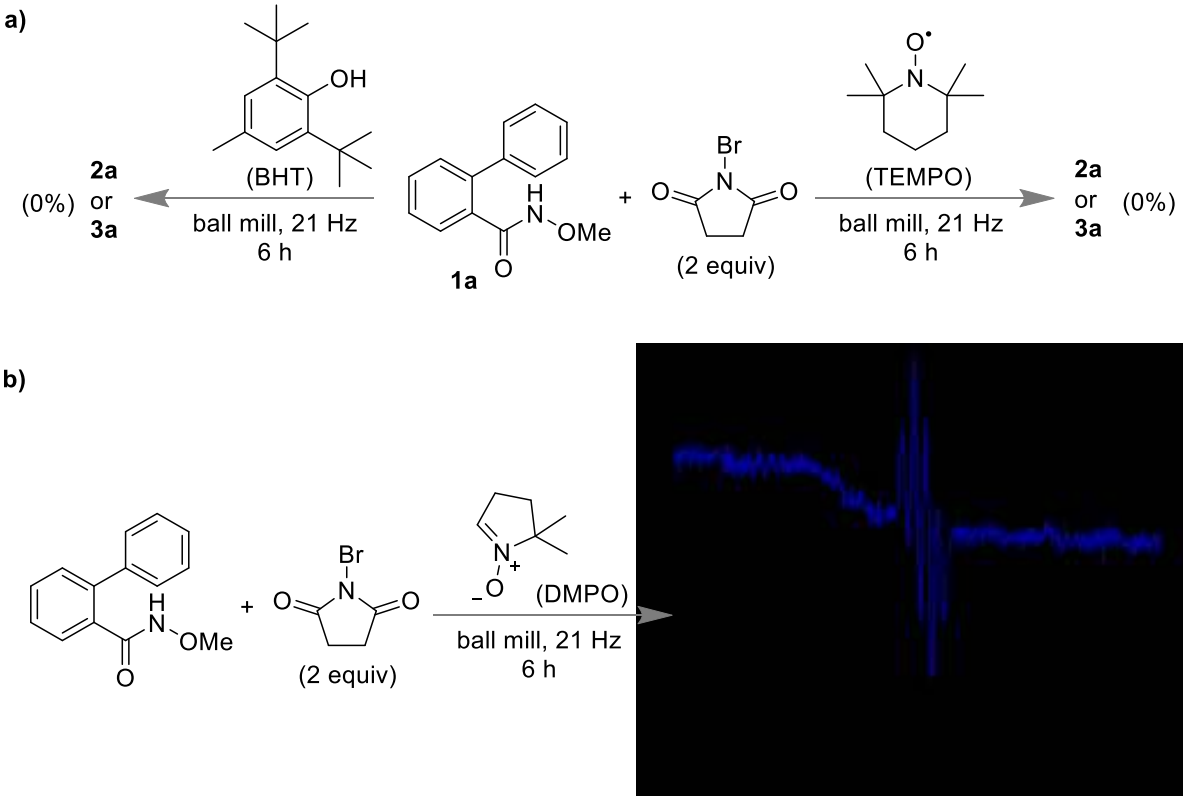

Figure 5.5. Control experiments. a) The experiments with BHT and TEMPO. b) EPR experiment using DMPO under standard conditions and the corresponding spectrum.

Based on the control experiments and literature report,[47] a plausible mechanism of the NBS-mediated reaction is proposed in Figure 5.6. It was expected that NCS also followed a similar pathway for the formation of **4a** *via* **2a**. First, *N*-bromosuccinimide underwent a homolytic cleavage to form succinimide and bromine radical. Next, **1a** reacted with succinimide to produce the intermediate **A** which underwent an intramolecular cyclization to form another intermediate **B**. The intermediate **B** was aromatized by the bromine radical to form the cyclized product **2a** (confirmed by HRMS). The compound **2a** was further brominated to **3a**

in presence of bromine radical *via* the intermediate **C**. Using NIS, the cyclized product **2a** was obtained as the final product because, under mechanochemical condition, halogenation using NIS could be possible only for the electron-rich substrates.[48]

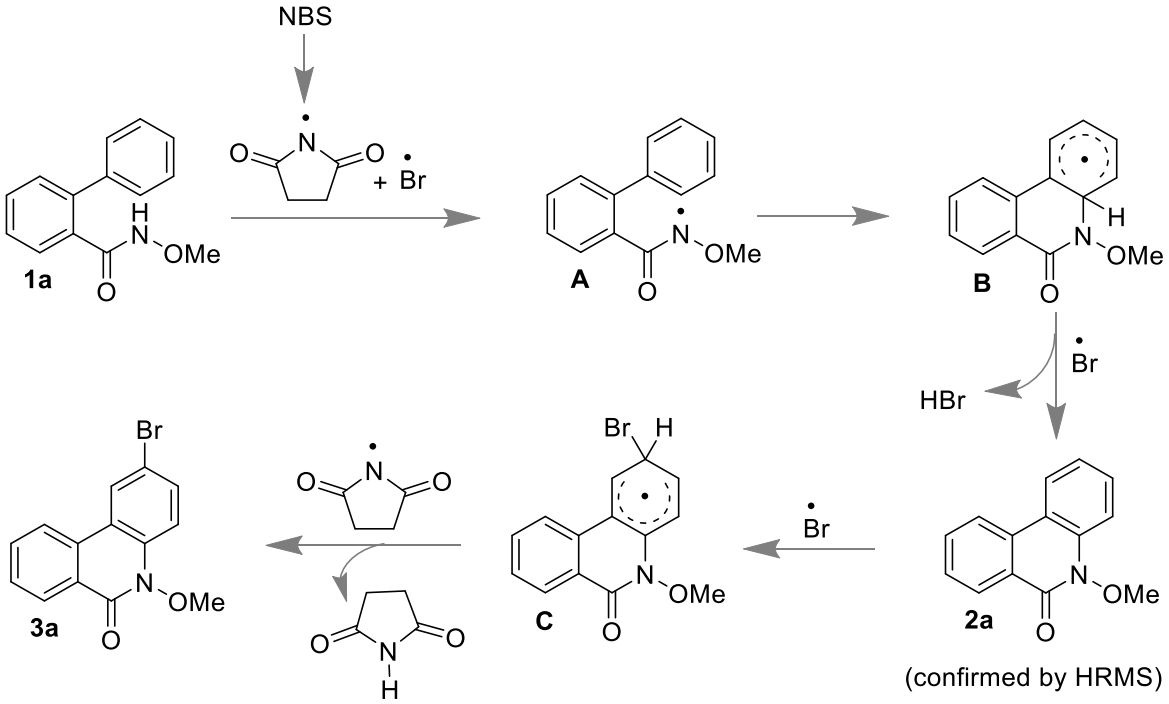

Figure 5.6. A plausible mechanism of the NBS-mediated reaction.

The synthetic utility of the methodology is shown in Figure 5.7 using 2-bromo-5-methoxy-8-methylphenanthridin-6(5H)-one (**3h**). The Suzuki coupling reaction between **3h** and phenyl

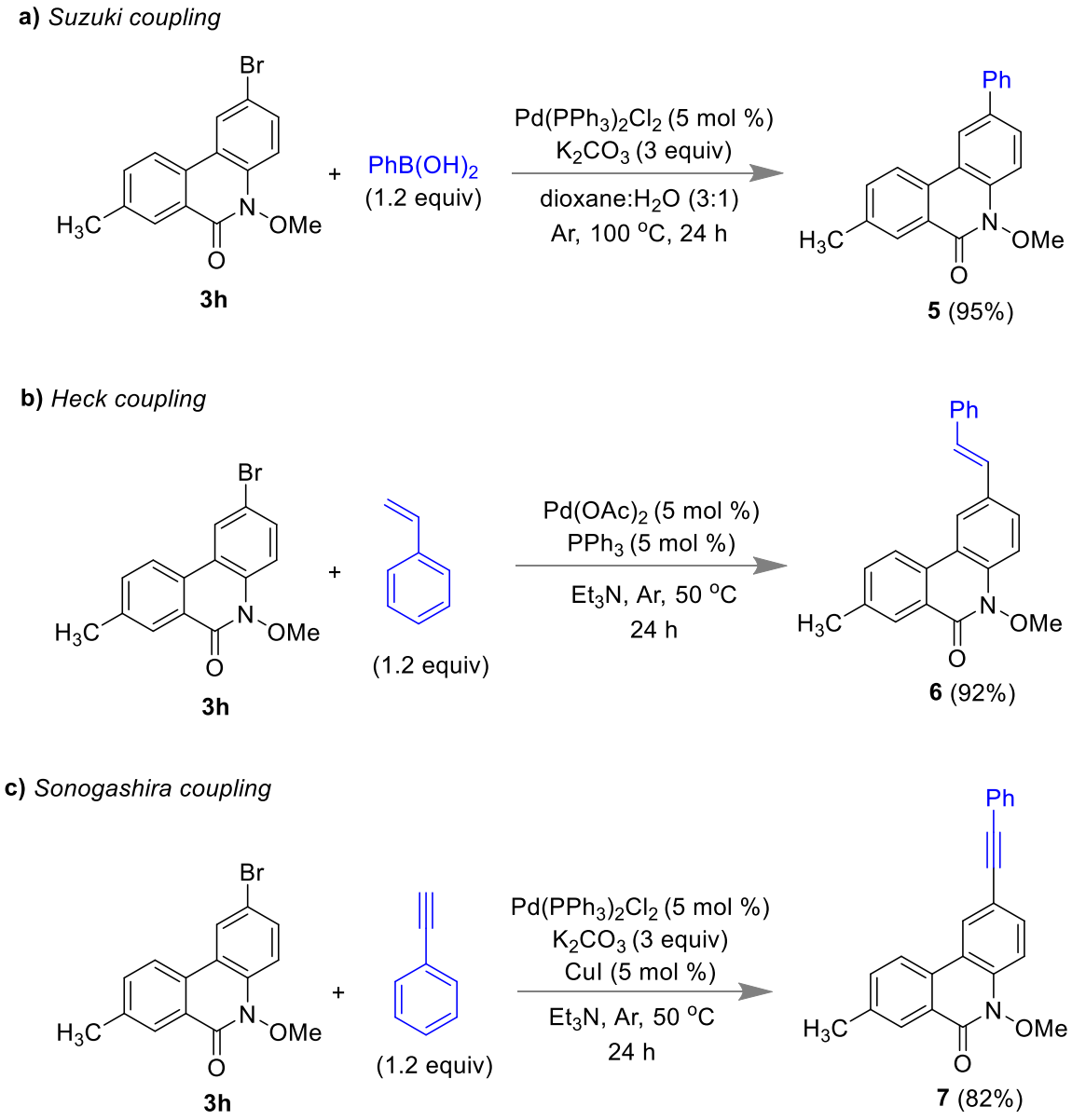

Figure 5.7. Synthetic applications of **3h**.

boronic acid led to **5** with 95% yields (Figure 5.7a). The treatment of **3h** with styrene afforded compound **6** in 92 % yields *via* Heck coupling (Figure 5.7b). In addition, the Sonogashira coupling of 2-bromo-5-methoxy-8-methylphenanthridin-6(5H)-one **3h** and phenylacetylene in presence of $Pd(PPh_3)_2Cl_2$ using CuI gave 5-methoxy-8-methyl-2-(phenylethynyl)phenanthridin-6(5H)-one **7** in 82% yield (Figure 5.7c).

Furthermore, we have performed a gram-scale synthesis using *N*-methoxy-[1,1'-biphenyl]-2-carboxamide (**1a)** as the starting materials (Figure 5.8). Under the standard reaction condition, when *N*-methoxy-[1,1'-biphenyl]-2-carboxamide (**1a)** was treated with appropriate proportions of NBS (for **3a**, Figure 5.8a) and NIS (for **2a**, Figure 5.8b), corresponding phenanthridinones **3a** and **2a** were isolated with 94% and 96% yields, respectively.

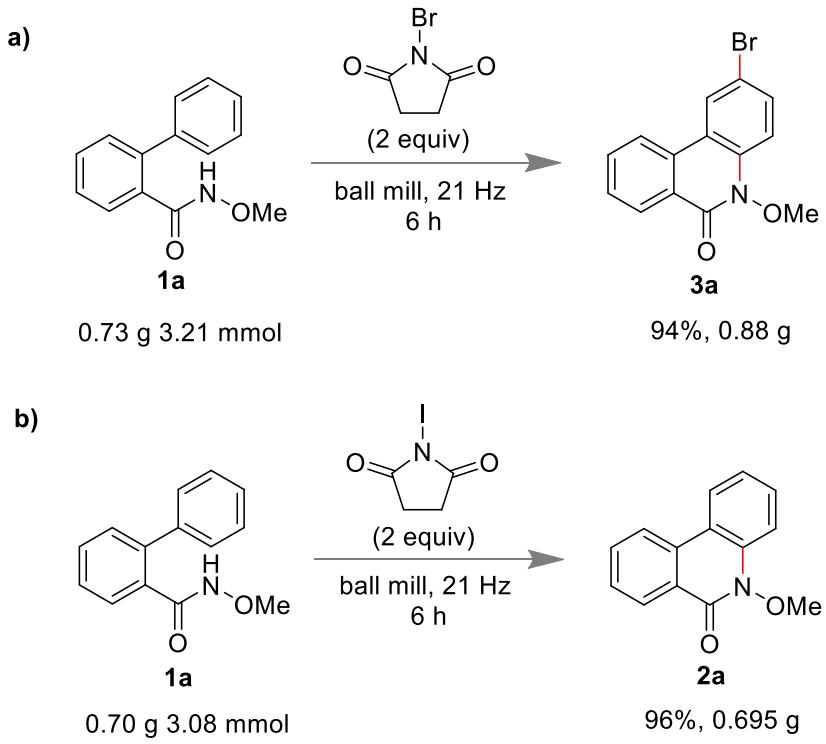

Figure 5.8. Gram-scale synthesis of a) **3a** and b) **2a**.

Nitrogen-based heterocyclic compounds containing carbonyl groups in their molecular skeleton show *n*-π^* and π-π^* electronic transitions. We have also examined the photophysical behavior[49] of the phenanthridinone derivatives. The UV-Visible and fluorescence spectra of the phenanthridinone derivatives were recorded in dichloromethane solvent at λ_{ex} ~ 240 nm (Figure 5.9). Interestingly, the second λ_{em} of the selected phenanthridinones have appeared ~500 nm. We anticipate that these dual emission properties of the phenanthridinone derivatives might be useful in materials chemistry.[49a, 50]

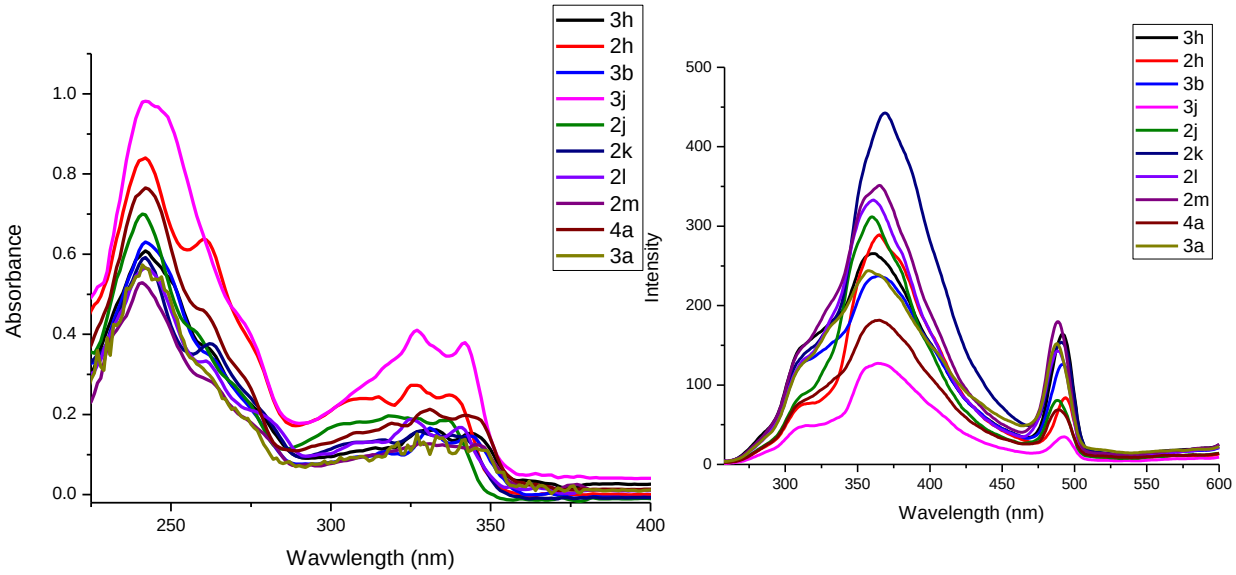

Figure 5.9 UV-Visible (left) and fluorescence (right, λ_{ex} ~ 240 nm) spectra of selected phenanthridinone derivatives (3×10^{-6} M in DCM).

5.4. CONCLUSION

In summary, we have developed a solvent-free mechanochemical method for a cascaded oxidative C-N bond coupling and followed by a halogenation reaction using *N*-bromosuccinimides (NBS) and *N*-chlorosuccinimide (NCS) as bifunctional reagents for the synthesis of phenanthridinones. The NBS and NCS first helped for an oxidative C-N coupling and subsequent halogenation reactions. However, only oxidative intramolecular C-N coupling was observed for the reactions using *N*-iodosuccinimide (NIS). All the reactions were highly efficient worked under metal-free and mild conditions. The results from radical trapping experiments with BHT and TEMPO and the EPR experiment using DMPO helped mechanistically establish that the reaction proceeded *via* a radical pathway. In addition, the calculation of the environmental impact factor (E-factor) also helped to rationalize that the current approach is superior to the existing methods. Again, the dual emissive nature of the

phenanthridinone derivatives reveal that these synthesized compounds might be useful for materials applications.

5.5. EXPERIMENTAL SECTION

General Information. Commercially available reagents and solvents were used as received. Column chromatographic purifications of the compounds were performed using silica gel (mesh 230–400, 100-200) and hexane-ethyl acetate solvent mixtures. NMR spectra were recorded on 400 MHz or 700 MHz instruments at 25 °C. The chemical shift values are reported in parts per million (ppm) concerning residual trichloromethane (7.26 ppm for ^{1}H and 77.16 ppm for ^{13}C). The peak patterns are designated as follows: s: singlet; d: doublet; t: triplet; q: quartet; m: multiplet; dd: doublet of doublets; td: triplet of doublets; brs: broad singlet. The coupling constants (*J*) are reported in hertz (Hz). High-resolution mass spectra (HR-MS) were recorded on an ESI-TOF (time of flight) mass spectrometer. Infrared (IR) spectral data are reported in wavenumber (cm^{-1}). The mechanochemical experiments were performed in a Mixer Mill MM 200, which has a maximum operating frequency of up to 25 Hz. For the optimization of the reaction condition and substrates scope, 10 mL milling jar with one grinding ball (15 mm diameter, stainless steel) were used. However, for the large-scale synthesis, 25 mL milling jar with one grinding ball (15 mm diameter, stainless steel) were used. For every milling procedure after 90 minutes the instrument was stopped and waited for 15 min. The resting time is not included during the calculation of the reaction time. The reactions were performed in a well-ventilated fume hood to avoid excessive heating of the jars during the milling process. The software used for NMR analyasis was MestreNova, and for UV-Vis, and fluorescence it was origin pro-2015. UV-Visible spectra were recorded on a JASCO V-730 UV-Visible spectrometer and Emission spectral studies were measured using Perkin Elmer, LS 55spectrophotometer with an optical cell of 1 cm path lengthFT-IR

spectra were recorded after making a thin layer of the compounds on the surface of the NaCl crystal using dichloromethane. Melting points of the compounds were determined using a digital melting point apparatus and uncorrected.

General procedure for the preparation of *N*-methoxy-[1,1'-biphenyl]-2-carboxamide (1a)[44] and followed by 2, 3 and 4 (Figure 5.10).

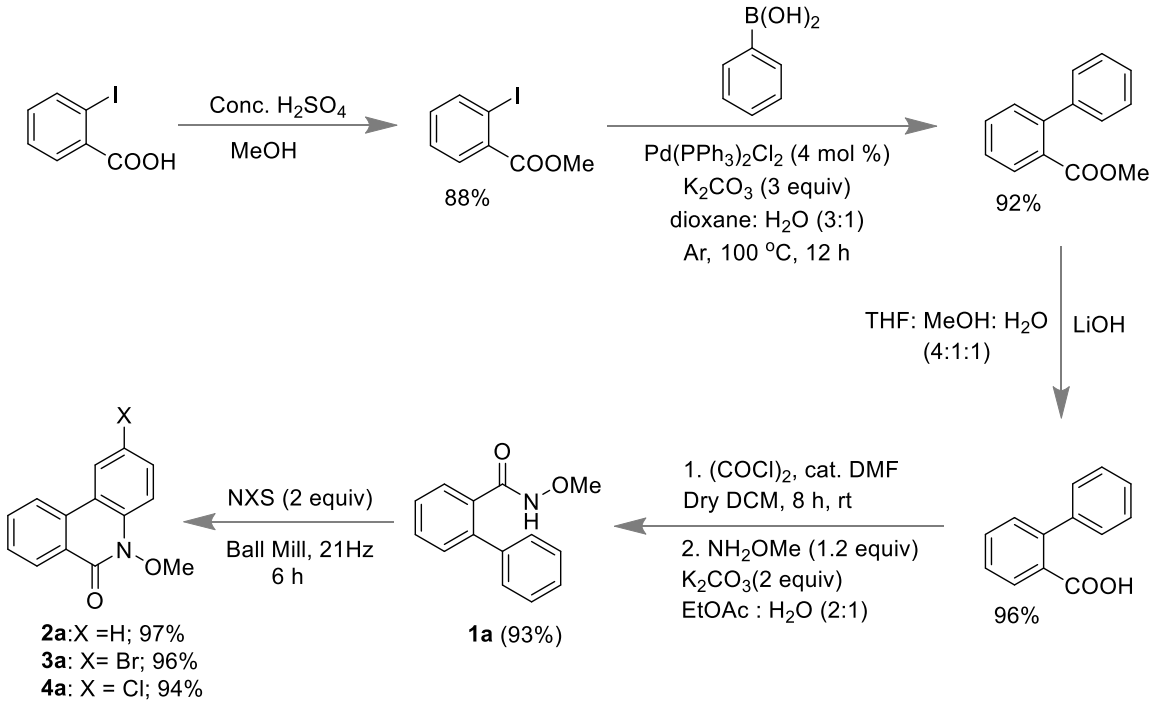

Figure 5.10. Synthesis of *N*-methoxy-[1,1'-biphenyl]-2-carboxamide (**1a**) and followed by **2a, 3a** and **4a**.

Synthesis of methyl 2-iodobenzoate. In an oven-dried 100 mL round bottom flask equipped with a stir-bar, 2-iodobenzoic acid (10 mmol, 2.5 g) and 30 mL MeOH were taken. Concentrated sulfuric acid (2 mL) was added slowly to the reaction mixture and refluxed at 80 ºC for 8 h. After completion of the reaction, the round bottom flask was cooled to room temperature and excess MeOH was evaporated. Then the reaction mixture was washed with

saturated $NaHCO_3$ (aq) solution and ethyl acetate (2 × 25 mL). The organic layer was collected and concentrated under a vacuum to give a colorless liquid, which was directly used in the next step.

Synthesis of methyl [1,1'-biphenyl]-2-carboxylate. To a solution of substituted 2-halogenated methyl benzoate (2 mmol), aryl boronic acid (3 mmol, 1.5 equiv), $Pd(PPh_3)_2Cl_2$ (0.08 mmol, 0.04 equiv) and potassium carbonate (6 mmol, 3 equiv) in dioxane/H_2O (6 mL/2 mL) were stirred at 100 °C under an argon atmosphere until the starting material was completely consumed (typically 12 h). The reaction mixture was diluted with brine (25 mL) and extracted with EtOAc (25 mL × 2). Then, the combined organic layers were dried over Na_2SO_4 and the concentrated crude product was purified by column chromatography to afford substituted methyl [1,1′-biphenyl]-2-carboxylate, which was used directly in the next step.

Synthesis of [1,1'-Biphenyl]-2-carboxylic acid. A mixture of methyl [1,1'-biphenyl]-2-carboxylate (3.95 mmol, 1.0 equiv) and LiOH (11.8 mmol, 3.0 equiv) were taken in a mixed solvent of THF: MeOH: H_2O in a 4:1:1 ratio. Then the reaction mixture was heated at 70 ºC for 8 h. After cooling down to room temperature, the reaction mixture was concentrated under vacuum and adjusted to pH~1 by using 1N HCl. The mixture was extracted with EtOAc and the organic layer was dried over Na_2SO_4, filtered and concentrated in a vacuum. The residue was purified by column chromatography to give the product (96 % as a white solid).

Synthesis of *N*-methoxy-[1,1'-biphenyl]-2-carboxamide 1. To a solution of [1,1'-biphenyl]-2-carboxylic acid (3.0 mmol, 1.0 equiv) in dry CH_2Cl_2 (10 mL) at 0 ºC under Argon (Ar) was

added dropwise oxalyl chloride (0.34 mL, 3.6 mmol, 1.2 equiv) followed by a catalytic amount of dry DMF (2 drops). The reaction mixture was allowed to stir at room temperature until completion (typically 8 h). The solvent was then removed under reduced pressure to afford the corresponding crude acyl chloride and proceeded to the next step without any further purification.

Methoxyamine hydrochloride (3.6 mmol, 1.2 equiv) and K_2CO_3 (6.00 mmol, 2.0 equiv) were added to a biphasic mixture of EtOAc and H_2O in a ratio of 2:1. The resulting solution was cooled to 0 °C followed by dropwise addition of the unpurified acid chloride which was dissolved in a minimum amount of EtOAc. The reaction was allowed to stir at room temperature for 8 h. After that, the organic phases were extracted with EtOAc (3 × 30 mL) and dried over $MgSO_4$. The solvent was concentrated under vacuum and the crude product was purified by column chromatography to afford *N*-methoxy-[1,1'-biphenyl]-2-carboxamide (93%).

General procedure for the synthesis of 5-methoxyphenanthridin-6(5H)-ones 2. In a 10 mL stainless steel milling jar, *N*-methoxy-[1,1'-biphenyl]-2-carboxamide (60 mg, 0.264 mmol), *N*-halosuccinimide (0.528 mmol, 2 equiv), and one grinding ball (15 mm diameter, stainless steel) was added. Then the reaction was carried out for 6 h at 21 Hz and the progress of the reaction was monitored by TLC (thin layer chromatography). After completion of the reaction, the mixture was dissolved in 15 mL (3 × 5 mL) of dichloromethane (DCM) and the resulting solution was evaporated to dryness. The crude residue was purified on silica gel column chromatography (20% EtOAc in hexane) to get the products.

Procedure for large scale synthesis. *N*-methoxy-[1,1'-biphenyl]-2-carboxamide (**1a**) (3 mmol) and appropriate proportions of NBS (for **3a**) and NIS (for **2a**) were taken in a 25 mL stainless steel milling jar containing one grinding ball (15 mm diameter, stainless steel). The reaction mixer was milled for 6 h for complete conversion. Then the reaction mixture was extracted with dichloromethane (DCM) and the crude product was purified by flash chromatography to obtain **3a** and **2a,** with 94% and 96% yield, respectively.

Synthesis of 5-methoxy-8-methyl-2-phenylphenanthridin-6(5H)-one (5). A 15 mL sealed tube containing a magnetic bar was charged with 2-bromo-5-methoxy-8-methylphenanthridin-6(5H)-one (0.25 mmol, 1.0 equiv), phenyl boronic acid (0.32 mmol, 1.3 equiv), K_2CO_3 (0.75 mmol, 3.0 equiv), and $Pd(PPh_3)_2Cl_2$ (0.01 mmol, 9 mg) in dioxane/H_2O (6 mL/2 mL) under an argon atmosphere. Then reaction mixture was placed into a preheated oil bath at 100 °C for 24 h. The reaction mixture was cooled to room temperature, diluted with brine (25 mL) and extracted with EtOAc (25 mL × 2). The layers were separated, and the aqueous layer was extracted with 2 × 8 mL of ethyl acetate. The combined organic extracts were dried over anhydrous sodium sulphate, filtered, and concentrated in vacuum. Crude product was purified by column chromatography to afford 5-methoxy-8-methyl-2-phenylphenanthridin-6(5H)-one (**5**) with 95% yield.

Synthesis of (*E*)-5-methoxy-8-methyl-2-styrylphenanthridin-6(5H)-one (6). 2-Bromo-5-methoxy-8-methylphenanthridin-6(5H)-one (0.18 mmol, 1.0 equiv), styrene (0.22 mmol, 1.2 equiv), PPh_3 (0.013 mmol, 4 mg), and $Pd(OAc)_2$ (5 mol%, 23 mg) in triethyl amine (6 mL) was placed in a 15 mL sealed tube under an argon atmosphere. Then reaction mixture was stirred into a preheated oil bath at 100 °C for 12 h. After cooling down to room temperature, solvent was evaporated to dryness. Then brine water and ethyl acetate were added to the

reaction mixture. The combined organic extracts were dried over anhydrous Na_2SO_4 and the solvent was evaporated. The resulting residue was purified by column chromatography to produce (*E*)-5-methoxy-8-methyl-2-styrylphenanthridin-6(5H)-one (6) with 92% yield.

Synthesis of 5-Methoxy-8-methyl-2-(phenylethynyl)phenanthridin-6(5H)-one (7). A 15 mL sealed tube equipped with a magnetic stirring bar was charged with 2-bromo-5-methoxy-8-methylphenanthridin-6(5H)-one (0.18 mmol, 1.0 equiv), phenyl acetelene (0.20 mmol, 1.1 equiv), CuI (5 mol%, 2 mg), and $Pd(PPh_3)_2Cl_2$ (5 mol%, 7 mg) in triethyl amine (6 mL) under an argon atmosphere. Then reaction mixture was stirred into a preheated oil bath at 50 °C for 24 h. The mixture was cooled to room temperature and solvent was evaporated to dryness. Then reaction mixture was diluted with brine solution and ethyl acetate (15 mL × 2). Then the organic layer was dried over anhydrous sodium sulphate, filtered, and concentrated in vacuum. The crude product was then purified by flash chromatography to afford 5-Methoxy-8-methyl-2-(phenylethynyl)phenanthridin-6(5H)-one (7) with 82 % yield.

Compound characterization data

***N*-Methoxy-[1,1'-biphenyl]-2-carboxamide (1a).**[43] R_f = 0.50 (hexane/ethyl acetate 7:3); white solid; yield 93% (533 mg); ^{1}H NMR (400 MHz, $CDCl_3$) δ 7.90 (s, 1H), 7.64 (d, *J* = 6.8 Hz, 1H), 7.51 (t, *J* = 7.6 Hz, 1H), 7.44 – 7.40 (m, 5H), 7.40 - 7.36 (m, 2H), 3.51 (s, 3H); ^{13}C{^{1}H} NMR (100 MHz, $CDCl_3$) δ 167.5, 140.0, 139.7, 132.3, 130.9, 130.2, 129.3, 128.9, 128.8, 128.2, 127.8, 64.1; HR-MS (ESI-TOF) m/z calcd for $C_{14}H_{14}NO_2$ $[M + H]^+$ 228.1019, found 228.1023.

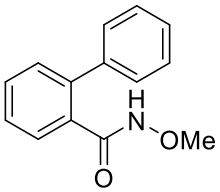

***N*-Methoxy-4'-methyl-[1,1'-biphenyl]-2-carboxamide (1b).**[44] R_f = 0.45 (hexane/ethyl acetate 7:3); white solid; yield 97% (576 mg); ^{1}H NMR (400 MHz,

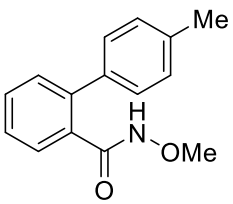

$CDCl_3$) δ 7.93 (s, 1H), 7.66 (s, 1H), 7.51 (t, *J* = 7.2 Hz, 1H), 7.44 – 7.36 (m, 2H), 7.33 (d, *J* = 7.6 Hz, 2H), 7.26 (t, *J* = 7.2 Hz, 2H), 3.58 (s, 3H), 2.41 (s, 3H); $^{13}C\{^1H\}$ NMR (100 MHz, $CDCl_3$) δ 167.7, 139.9, 138.1, 136.7, 132.2, 130.9, 130.2, 129.6, 129.4, 128.7, 127.6, 64.1, 21.3; HR-MS (ESI-TOF) m/z calcd for $C_{15}H_{16}NO_2$ $[M + H]^+$ 242.1176, found 242.1179.

4'-Ethyl-*N*-methoxy-[1,1'-biphenyl]-2-carboxamide (1c). R_f = 0.50 (hexane/ethyl acetate 7:3); white solid; yield 91% (453 mg); mp 103−105 °C; ^1H NMR (400 MHz, $CDCl_3$) δ 7.83

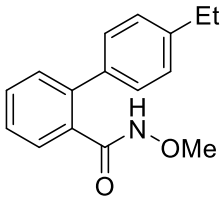

(s, 1H), 7.66 (d, *J* = 7.6 Hz, 1H), 7.50 (td, *J* = 7.6, 1.2 Hz, 1H), 7.39 (dd, *J* = 6.4, 1.2 Hz, 2H), 7.37 – 7.33 (m, 2H), 7.30 – 7.25 (m, 2H), 3.55 (s, 3H), 2.71 (q, *J* = 7.6 Hz, 2H), 1.28 (t, *J* = 7.6 Hz, 3H); $^{13}C\{^1H\}$ NMR (100 MHz, $CDCl_3$) δ 167.7, 144.5, 140.1, 137.1, 132.4, 130.8, 130.2, 129.4, 128.8, 128.4, 127.6, 64.0, 28.7, 15.6; IR (KBr) $\tilde{\nu}$ = 3169, 2964, 2917, 2848, 1651, 1537, 1492, 1456, 1438, 1301, 1158, 1041, 1029, 839 cm^{-1}; HR-MS (ESI-TOF) m/z calcd for $C_{16}H_{17}NO_2Na$ $[M + Na]^+$ 278.1151, found 278.1150.

4'-(tert-Butyl)-*N*-methoxy-[1,1'-biphenyl]-2-carboxamide (1d). R_f = 0.50 (hexane/ethyl

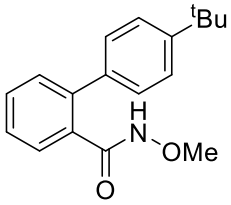

acetate 7:3); white solid; yield 94% (670 mg); mp 128−130 °C; ^1H NMR (400 MHz, $CDCl_3$) δ 7.85 (s, 1H), 7.65 (d, *J* = 6.8 Hz, 1H), 7.52 – 7.42 (m, 3H), 7.42 – 7.30 (m, 4H), 3.50 (s, 3H), 1.34 (s, 9H); $^{13}C\{^1H\}$ NMR (100 MHz, $CDCl_3$) δ 167.6, 151.3, 139.9, 136.7, 132.3, 130.9, 130.2, 129.3, 128.5, 127.6, 125.8, 63.9, 34.7, 31.4; IR (KBr) $\tilde{\nu}$ = 3157, 2959, 2900, 2862, 1659, 1638, 1513, 1477, 1458, 1439, 1307, 1268, 1029, 886 cm^{-1}; HR-MS (ESI-TOF) m/z calcd for $C_{18}H_{21}NO_2Na$ $[M + Na]^+$ 306.1465, found 306.1459.

4'-Fluoro-*N*-methoxy-[1,1'-biphenyl]-2-carboxamide (1e).[44] R_f = 0.45 (hexane/ethyl acetate 4:1); white solid; yield 87% (585 mg); ^{1}H NMR (400 MHz, $CDCl_3$) δ 7.97 (s, 1H), 7.59 (d, *J* = 5.2 Hz, 1H), 7.50 (tt, *J* = 7.6, 1.6 Hz, 1H), 7.45 – 7.37 (m, 3H), 7.37 – 7.33 (m, 1H), 7.15 – 7.07 (m, 2H), 3.58 (s, 3H); ^{13}C{^{1}H} NMR (100 MHz, $CDCl_3$) δ 167.5, 162.8 (d, *J* = 247.9 Hz), 139.1, 135.7, 132.4, 130.9, 130.5 (d, *J* = 8.1 Hz), 130.2, 129.2, 127.9, 115.8 (d, *J* = 21.5 Hz), 64.2; HR-MS (ESI-TOF) m/z calcd for $C_{14}H_{12}FNO_2Na$ $[M + Na]^+$ 268.0744, found 268.0735.

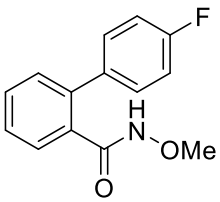

4'-Chloro-*N*-methoxy-[1,1'-biphenyl]-2-carboxamide (1f).[44] R_f = 0.50 (hexane/ethyl acetate 7:3); white solid; yield 90% (580 mg); ^{1}H NMR (400 MHz, $CDCl_3$) δ 8.14 (s, 1H), 7.57 (d, *J* = 6.8 Hz, 1H), 7.50 (t, *J* = 7.2 Hz, 1H), 7.45 – 7.37 (m, 3H), 7.37 – 7.29 (m, 3H), 3.57 (s, 3H); ^{13}C{^{1}H} NMR (100 MHz, $CDCl_3$) δ 167.4, 138.9, 138.2, 134.3, 132.4, 130.9, 130.2, 130.1, 129.1, 128.9, 128.0, 64.1; HR-MS (ESI-TOF) m/z calcd for $C_{14}H_{12}ClNO_2Na$ $[M + Na]^+$ 284.0449, found 284.0440.

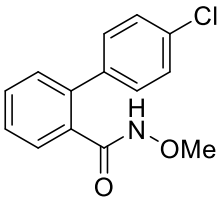

***N*-Methoxy-4'-(trifluoromethyl)-[1,1'-biphenyl]-2-carboxamide (1g).**[44] R_f = 0.45 (hexane/ethyl acetate 7:3); white solid; yield 94% (557 mg); ^{1}H NMR (700 MHz, $CDCl_3$) δ 8.51 (s, 1H), 7.69 – 7.62 (m, 2H), 7.58 – 7.47 (m, 4H), 7.46 – 7.32 (m, 2H), 3.51 (s, 3H); ^{13}C{^{1}H} NMR (175 MHz, $CDCl_3$) δ 167.1, 143.5, 139.0, 132.5, 131.0, 130.3, 129.2, 128.9, 128.4, 125.6, 124.2 (q, *J* = 272.2 Hz), 64.0; HR-MS (ESI-TOF) m/z calcd for $C_{15}H_{12}F_3NO_2Na$ $[M + Na]^+$ 318.0712, found 318.0726.

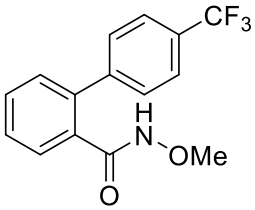

***N*-Methoxy-4-methyl-[1,1'-biphenyl]-2-carboxamide (1h).**[43] R_f = 0.50 (hexane/ethyl acetate 7:3); white solid; yield 90% (404 mg); ^{1}H NMR (400 MHz, $CDCl_3$) δ 7.75 (s, 1H), 7.49 (s, 1H), 7.44 – 7.40 (m, 4H), 7.40 – 7.36 (m, 1H), 7.31 – 7.27 (m, 2H), 3.53 (s, 3H), 2.41 (s, 3H); ^{13}C{^{1}H} NMR (100 MHz, $CDCl_3$) 167.7, 139.7, 137.9, 137.2, 132.1, 131.7, 130.1, 129.9, 128.9, 128.9, 128.0, 64.1, 21.1; HR-MS (ESI-TOF) m/z calcd for $C_{15}H_{15}NO_2Na$ $[M + Na]^+$ 264.0995, found 264.0990.

***N*-Methoxy-4,4'-dimethyl-[1,1'-biphenyl]-2-carboxamide (1i).** R_f = 0.50 (hexane/ethyl acetate 7:3); white solid; yield 88% (415 mg); mp 135−137 °C; ^{1}H NMR (400 MHz, $CDCl_3$) δ 7.79 (s, 1H), 7.48 (s, 1H), 7.29 (d, *J* = 7.2 Hz, 3H), 7.26 – 7.19 (m, 3H), 3.57 (s, 3H), 2.39 (s, 3H), 2.38 (s, 3H); ^{13}C{^{1}H} NMR (100 MHz, $CDCl_3$) δ 168.0, 137.9, 137.6, 137.1, 136.7, 131.9, 131.7, 130.2, 129.9, 129.6, 128.7, 64.1, 21.3, 21.0; IR (KBr) $\tilde{\nu}$ = 3155, 3021, 2918, 2851, 1659, 1606, 1466, 1439, 1416, 1294, 1036, 943 cm^{-1}; HR-MS (ESI-TOF) m/z calcd for $C_{16}H_{18}NO_2$ $[M + H]^+$ 256.1332, found 256.1331.

4'-Fluoro-*N*-methoxy-4-methyl-[1,1'-biphenyl]-2-carboxamide (1j). R_f = 0.50 (hexane/ethyl acetate 7:3); white solid; yield 97% (475 mg); mp 154−156 °C; ^{1}H NMR (400 MHz, $CDCl_3$) δ 7.95 (s, 1H), 7.41 (s, 1H), 7.36 (dd, *J* = 8.0, 5.6 Hz, 2H), 7.30 (d, *J* = 8.0 Hz, 1H), 7.24 (t, *J* = 7.2 Hz, 1H), 7.09 (t, *J* = 8.4 Hz, 2H), 3.57 (s, 3H), 2.39 (s, 3H); ^{13}C{^{1}H} NMR (100 MHz, $CDCl_3$) δ 167.6, 162.7 (d, *J* = 247.5 Hz), 137.9, 136.1, 135.7, 132.1, 131.7, 130.4 (d, *J* = 8.1 Hz), 130.1, 129.7, 115.8 (d, *J* = 21.5 Hz), 64.1, 21.0; IR (KBr)

$\tilde{\nu}$ = 3112, 2917, 2820, 1641, 1601, 1510, 1488, 1442, 1313, 1219, 1158, 1036, 948, 849 cm^{-1}; HR-MS (ESI-TOF) m/z calcd for $C_{15}H_{15}FNO_2$ $[M + H]^+$ 260.1081, found 260.1085.

4'-Ethyl-*N*-methoxy-4-methyl-[1,1'-biphenyl]-2-carboxamide (1k). R_f = 0.50

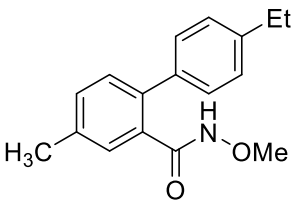

(hexane/ethyl acetate 7:3); white solid; yield 98% (474 mg); mp 128−130 °C; ^{1}H NMR (400 MHz, $CDCl_3$) δ 7.83 (s, 1H), 7.51 (s, 1H), 7.36 - 7.31 (m, 3H), 7.30 – 7.26 (m, 3H), 3.57 (s, 3H), 2.70 (q, *J* = 7.6 Hz, 2H), 2.42 (s, 3H), 1.28 (t, *J* = 7.6 Hz, 3H); ^{13}C{^{1}H} NMR (100 MHz, $CDCl_3$) δ 168.0, 144.3, 137.6, 137.1, 136.9, 131.8, 131.8, 130.1, 129.9, 128.8, 128.4, 28.7, 21.1, 15.7; IR (KBr) $\tilde{\nu}$ = 3130, 2959, 2929, 2865, 1659, 1637, 1507, 1481, 1436, 1316, 1147, 1040, 945, 846 cm^{-1}; HR-MS (ESI-TOF) m/z calcd for $C_{17}H_{19}NO_2Na$ $[M + Na]^+$ 292.1308, found 292.1321.

4'-Chloro-*N*-methoxy-4-methyl-[1,1'-biphenyl]-2-carboxamide (1l). R_f = 0.50

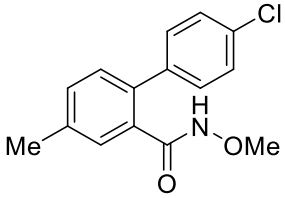

(hexane/ethyl acetate 7:3); white solid; yield 94% (329 mg); mp 151−153 °C; ^{1}H NMR (400 MHz, $CDCl_3$) δ 7.98 (s, 1H), 7.47 – 7.40 (m, 2H), 7.40 – 7.35 (m, 3H), 7.33 (s, 1H), 7.28 (t, *J* = 6.4 Hz, 1H), 3.62 (s, 3H), 2.43 (s, 3H); ^{13}C{^{1}H} NMR (100 MHz, $CDCl_3$) δ 167.5, 138.2, 138.1, 136.1, 134.1, 132.1, 131.8, 130.1 (×2), 129.7, 128.9, 64.2, 21.1; IR (KBr) $\tilde{\nu}$ = 3204, 2921, 2852, 1648, 1509, 1473, 1312, 1121, 1093, 1050, 1016, 838, 810 cm^{-1}; HR-MS (ESI-TOF) m/z calcd for $C_{15}H_{14}ClNO_2Na$ $[M + Na]^+$ 298.0605, found 298.0614.

3'-Chloro-*N*-methoxy-4-methyl-[1,1'-biphenyl]-2-carboxamide (1m). R_f = 0.50

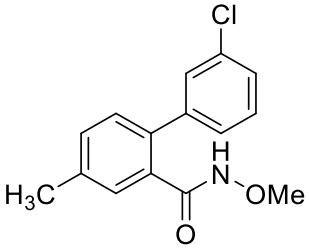

(hexane/ethyl acetate 7:3); white solid; yield 98% (478 mg); mp 126−128 °C; ^{1}H NMR (400 MHz, $CDCl_3$) δ 8.05 (s, 1H), 7.42 (s,

2H), 7.36 – 7.34 (m, 2H), 7.34 – 7.30 (m, 2H), 7.27 (d, *J* = 8.0 Hz, 1H), 3.59 (s, 3H), 2.42 (s, 3H); $^{13}C\{^{1}H\}$ NMR (100 MHz, $CDCl_3$) δ 167.2, 141.5, 138.4, 135.8, 134.6, 132.2, 131.7, 130.0, 129.7, 128.8, 127.9, 127.1, 64.1, 21.1; IR (KBr) $\tilde{\nu}$ = 3127, 2970, 2923, 1629, 1595, 1523, 1465, 1436, 1318, 1120, 1046, 930, 820 cm^{-1};HR-MS (ESI-TOF) m/z calcd for $C_{15}H_{14}ClNO_2Na$ $[M + Na]^+$ 298.0605, found 298.0621.

4'-(*Tert*-Butyl)-*N*-methoxy-4-methyl-[1,1'-biphenyl]-2-carboxamide (1n). R_f = 0.50 (hexane/ethyl acetate 7:3); white solid; yield 96% (530 mg); mp 112−114 °C; ^{1}H NMR (700 MHz, $CDCl_3$) δ 7.83 (s, 1H), 7.57 (s, 1H), 7.52 (s, 1H), 7.51 (s, 1H), 7.42 (s, 1H), 7.41 (s, 1H), 7.38 (d, *J* = 7.7 Hz, 1H), 7.35 (d, *J* = 8.4 Hz, 1H), 3.59 (s, 3H), 2.48 (s, 3H), 1.42 (s, 9H); $^{13}C\{^{1}H\}$ NMR (175 MHz, $CDCl_3$) δ 167.8, 151.1, 137.6, 137.1, 136.7, 132.1, 131.7, 130.1, 129.9, 128.5, 125.8, 63.9, 34.7, 31.5, 21.1; IR (KBr) $\tilde{\nu}$ = 3215, 2960, 1654, 1478, 1393, 1297, 1203, 1034, 928, 814 cm^{-1}; HR-MS (ESI-TOF) m/z calcd for $C_{19}H_{23}NO_2Na$ $[M + Na]^+$ 320.1621, found 320.1638.

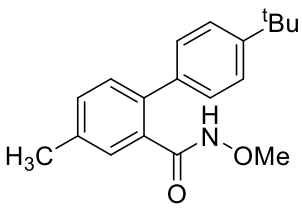

N-Methoxy-3'-nitro-[1,1'-biphenyl]-2-carboxamide (1o). R_f = 0.45 (hexane/ethyl acetate 7:3); white solid; yield 93% (257 mg); mp 176−177 °C; ^{1}H NMR (400 MHz, $CDCl_3$ + TFA-D) δ 8.20 (d, *J* = 7.2 Hz, 2H), 7.70 (s, 1H), 7.59 (t, *J* = 7.2 Hz, 2H), 7.52 (s, 1H), 7.49 – 7.40 (m, 2H), 3.58 (s, 3H); $^{13}C\{^{1}H\}$ NMR (100 MHz, $CDCl_3$ + TFA-D) δ 168.7, 148.3, 140.9, 138.4, 135.1, 132.2, 130.7, 130.4, 130.0, 128.9, 128.8, 123.5, 123.1, 64.5; IR (KBr) $\tilde{\nu}$ = 3134, 2933, 2846, 1654, 1632, 1526, 1497, 1350, 1313, 1036, 939, 762 cm^{-1}; HR-MS (ESI-TOF) m/z calcd for $C_{14}H_{12}N_2O_4Na$ $[M + Na]^+$ 295.0689, found 295.0678.

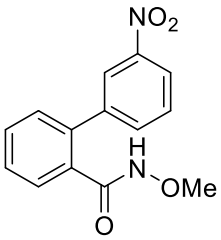

4'-Acetyl-N-methoxy-[1,1'-biphenyl]-2-carboxamide (1p). R_f = 0.45 (hexane/ethyl acetate 7:3); white solid; yield 78% (380 mg); mp 153−155 °C; ^{1}H NMR (400 MHz, $CDCl_3$) δ 8.51 – 8.22 (brs, 1H), 8.11 – 7.85 (m, 2H), 7.64 – 7.47 (m, 4H), 7.45 – 7.34 (m, 2H), 3.57 (s, 3H), 2.59 (s, 3H); ^{13}C{^{1}H} (100 MHz, $CDCl_3$) δ 197.8, 167.2, 144.5, 139.1, 136.4, 136.3, 132.5, 130.9, 130.1, 129.0, 128.7, 128.4, 64.1, 26.8; IR (KBr) $\tilde{\nu}$ = 3153, 2974, 1678, 1634, 1576, 1440, 1267, 1032, 1003, 887, 762 cm^{-1}; HR-MS (ESI-TOF) m/z calcd for $C_{16}H_{16}NO_3$ $[M + H]^+$ 270.1125, found 270.1124.

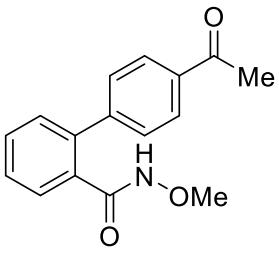

N-Phenyl-[1,1'-biphenyl]-2-carboxamide (1q).[51] R_f = 0.50 (hexane/ethyl acetate 4:1); reddish yellow solid; yield 80% (410 mg); mp 103−105 °C; ^{1}H NMR (400 MHz, $CDCl_3$) δ 7.88 (d, *J* = 7.2 Hz, 1H), 7.55 (t, *J* = 7.2 Hz, 1H), 7.51 – 7.37 (m, 7H), 7.24 (dd, *J* = 14.0, 6.4 Hz, 2H), 7.15 – 7.03 (m, 3H), 6.98 (s, 1H); ^{13}C{^{1}H} NMR (100 MHz, $CDCl_3$) δ 167.3, 140.1, 139.7, 137.7, 135.4, 130.8, 130.5, 129.7, 129.1, 128.9 (×2), 128.2, 128.0, 124.5, 120.1; IR (KBr) $\tilde{\nu}$ = 3331, 2922, 1713, 1662, 1515, 1450, 1131, 1093, 948, 752 cm^{-1}; HR-MS (ESI-TOF) m/z calcd for $C_{19}H_{16}NO$ $[M + H]^+$ 274.1226, found 274.1251.

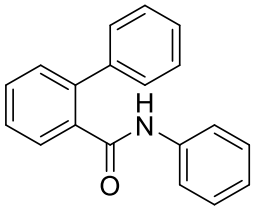

2-Bromo-5-methoxyphenanthridin-6(5H)-one (3a).[43] R_f = 0.50 (hexane/ethyl acetate 4:1); white solid; yield 96% (74 mg); ^{1}H NMR (400 MHz, DMSO-d_6) δ 8.71 (s, 1H), 8.61 (d, *J* = 8.0 Hz, 1H), 8.34 (d, *J* = 8.0 Hz, 1H), 7.87 (d, *J* = 7.6 Hz, 1H), 7.80 (d, *J* = 8.8 Hz, 1H), 7.71 (t, *J* = 7.6 Hz, 1H), 7.59 (d, *J* = 8.8 Hz, 1H), 4.02 (s, 3H); ^{13}C{^{1}H} NMR (100 MHz, DMSO-d_6) δ 155.9, 134.7, 133.3, 132.9, 131.6, 129.1, 127.7, 126.4, 126.0, 123.4, 120.0, 115.9, 114.7, 62.8; HR-

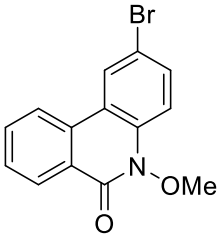

MS (ESI-TOF) m/z calcd for $C_{14}H_{10}{}^{79}BrNO_2Na$ $[M + Na]^+$ 325.9787, found 325.9789, $C_{14}H_{10}{}^{81}BrNO_2Na$ $[M + Na]^+$ 327.9767, found 327.9776.

2-Bromo-5-methoxy-3-methylphenanthridin-6(5H)-one (3b).[43] R_f = 0.50 (hexane/ethyl acetate 4:1); white solid; yield 85% (112 mg); ^1H NMR (400 MHz, $CDCl_3$) δ 8.51 (d, *J* = 8.0 Hz, 1H), 8.35 (s, 1H), 8.14 (d, *J* = 8.0 Hz, 1H), 7.76 (t, *J* = 7.6 Hz, 1H), 7.59 (t, *J* = 7.6 Hz, 1H), 7.52 (s, 1H), 4.12 (s, 3H), 2.55 (s, 3H); $^{13}C\{^1H\}$ NMR (100 MHz, $CDCl_3$) δ 157.2, 140.1, 135.0, 132.9, 131.9, 128.7, 128.4, 126.9, 126.3, 121.9, 119.4, 118.2, 114.5, 62.9, 23.6; HR-MS (ESI-TOF) m/z calcd for $C_{15}H_{13}{}^{79}BrNO_2$ $[M + H]^+$ 318.0124, found 318.0133, $C_{15}H_{13}{}^{81}BrNO_2$ $[M + H]^+$ 320.0104, found 320.0125.

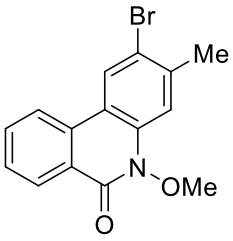

2-Bromo-3-ethyl-5-methoxyphenanthridin-6(5H)-one (3c). R_f = 0.45 (hexane/ethyl acetate 4:1); white solid; yield 82% (106 mg); mp 130−132 °C; ^1H NMR (400 MHz, $CDCl_3$) δ 8.51 (d, *J* = 8.0 Hz, 1H), 8.34 (s, 1H), 8.14 (d, *J* = 8.0 Hz, 1H), 7.75 (t, *J* = 7.6 Hz, 1H), 7.58 (t, *J* = 7.6 Hz, 1H), 7.50 (s, 1H), 4.13 (s, 3H), 2.89 (q, *J* = 7.6 Hz, 2H), 1.32 (t, *J* = 7.6 Hz, 3H); $^{13}C\{^1H\}$ NMR (100 MHz, $CDCl_3$) δ 157.2, 145.5, 135.3, 132.9, 131.9, 128.7, 128.4, 127.3, 126.3, 121.9, 118.7, 118.2, 113.2, 62.9, 29.9, 14.4; IR (KBr) $\tilde{\nu}$ = 2957, 2922, 2851, 1661, 1605, 1495, 1446, 1402, 1326, 1174, 1074, 1051, 1035, 908 cm^{-1};HR-MS (ESI-TOF) m/z calcd for $C_{16}H_{15}{}^{79}BrNO_2$ $[M + H]^+$ 332.0281, found 332.0262, $C_{16}H_{15}{}^{81}BrNO_2$ $[M + H]^+$ 334.0261, found 320.0246.

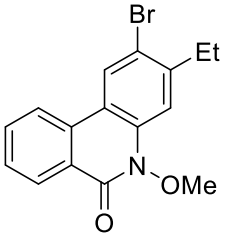

2-Bromo-3-(tert-butyl)-5-methoxyphenanthridin-6(5H)-one (3d). R_f = 0.50 (hexane/ethyl acetate 4:1); white solid; yield 78% (99 mg); mp 135−137 °C; ^1H NMR (400 MHz, $CDCl_3$) δ 8.53 (d, *J* = 8.0 Hz, 1H), 8.42 (s, 1H), 8.17 (d, *J* =

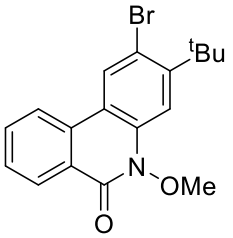

8.0 Hz, 1H), 7.77 (t, *J* = 7.6 Hz, 1H), 7.74 (s, 1H), 7.60 (t, *J* = 7.6 Hz, 1H), 4.14 (s, 3H), 1.61 (s, 9H); $^{13}C\{^{1}H\}$ NMR (100 MHz, $CDCl_3$) δ 157.4, 150.1, 134.8, 132.9, 131.7, 130.3, 128.8, 128.5, 126.6, 121.9, 117.9, 116.7, 112.1, 62.9, 37.3, 29.8; IR (KBr) $\tilde{\nu}$ = 2954, 2922, 2852, 1668, 1601, 1465, 1396, 1382, 1315, 1294, 1170, 1048, 1012, 913, 809 cm^{-1}; HR-MS (ESI-TOF) m/z calcd for $C_{18}H_{19}{}^{79}BrNO_2$ $[M + H]^+$ 360.0594, found 360.0592, $C_{18}H_{19}{}^{81}BrNO_2$ $[M + H]^+$ 362.0574, found 362.0575.

2-Bromo-3-fluoro-5-methoxyphenanthridin-6(5H)-one (3e). R_f = 0.45 (hexane/ethyl acetate 4:1); white solid; yield 88% (92 mg); mp 210−212 °C; ^{1}H NMR (400 MHz, DMSO-d_6) δ 8.80 (d, *J* = 7.2 Hz, 1H), 8.53 (d, *J* = 8.0 Hz, 1H), 8.30 (d, *J* = 8.0 Hz, 1H), 7.85 (t, *J* = 7.6 Hz, 1H), 7.67 (t, *J* = 7.6 Hz, 1H), 7.60 (d, *J* = 10.2 Hz, 1H), 4.03 (s, 3H); $^{13}C\{^{1}H\}$ NMR (100 MHz, DMSO-d_6) δ 158.9 (d, *J* = 246.3 Hz), 156.1, 136.4 (d, *J* = 10.2 Hz), 133.3, 131.2, 128.9, 128.7, 127.6, 125.3, 123.3, 116.1, 102.6 (d, *J* = 22.0 Hz), 100.9 (d, *J* = 28.8 Hz), 62.9; IR (KBr) $\tilde{\nu}$ = 2915, 2848, 1668, 1644, 1584, 1480, 1447, 1308, 1297, 1277, 1189, 1171, 1057, 1038, 890 cm^{-1};HR-MS (ESI-TOF) m/z calcd for $C_{14}H_{10}{}^{79}BrFNO_2$ $[M + H]^+$ 321.9873, found 321.9868, $C_{14}H_{10}{}^{81}BrFNO_2$ $[M + H]^+$ 323.9854, found 323.9849.

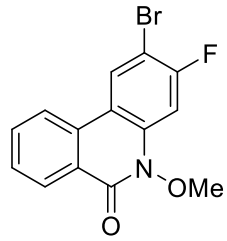

2-Bromo-3-chloro-5-methoxyphenanthridin-6(5H)-one (3f).[43] R_f = 0.40 (hexane/ethyl acetate 4:1); white solid; yield 86% (89 mg); ^{1}H NMR (400 MHz, DMSO-d_6) δ 8.90 (s, 1H), 8.62 (d, *J* = 8.0 Hz, 1H), 8.34 (d, *J* = 8.0 Hz, 1H), 7.89 (t, *J* = 7.6 Hz, 1H), 7.83 (s, 1H), 7.72 (t, *J* = 7.6 Hz, 1H), 4.04 (s, 3H); $^{13}C\{^{1}H\}$ NMR (100 MHz, DMSO- d_6) δ 156.0, 135.7, 134.7, 133.4,

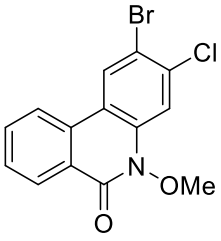

131.0, 129.3, 128.9, 127.7, 125.9, 123.6, 118.7, 115.6, 113.9, 63.0; HR-MS (ESI-TOF) m/z calcd for $C_{14}H_{10}{}^{79}BrClNO_2$ $[M + H]^+$ 337.9578, found 337.9560, $C_{14}H_{10}{}^{81}BrClNO_2$ $[M + H]^+$ 339.9557, found 339.9542.

2-Bromo-5-methoxy-8-methylphenanthridin-6(5H)-one (3h).[43] R_f = 0.45 (hexane/ethyl acetate 4:1); white solid; yield 94% (62 mg); ^1H NMR (400 MHz, DMSO-d_6) δ 8.61 (d, *J* = 2.0 Hz, 1H), 8.44 (d, *J* = 8.4 Hz, 1H), 8.13 (s, 1H), 7.75 (dd, *J* = 8.8, 2.0 Hz, 1H), 7.67 (dd, *J* = 8.4, 1.6 Hz, 1H), 7.56 (d, *J* = 8.8 Hz, 1H), 4.02 (s, 3H), 2.48 (s, 3H); $^{13}C\{^1H\}$ NMR (100 MHz, DMSO-d_6) δ 155.8, 138.9, 134.3, 134.2, 132.3, 128.9, 127.3, 125.9, 125.8, 123.3, 119.9, 115.7, 114.5, 62.7; HR-MS (ESI-TOF) m/z calcd for $C_{15}H_{13}{}^{79}BrNO_2$ $[M + H]^+$ 318.0124, found 318.0123, $C_{15}H_{13}{}^{81}BrNO_2$ $[M + H]^+$ 320.0104, found 320.0106.

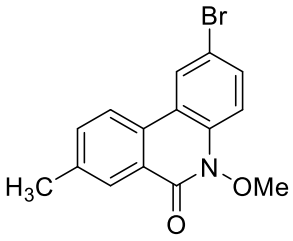

2-Bromo-5-methoxy-3,8-dimethylphenanthridin-6(5H)-one (3i). R_f = 0.45 (hexane/ethyl acetate 4:1); white solid; yield 92% (65 mg); mp 168−170 °C; ^1H NMR (400 MHz, $CDCl_3$ + DMSO-d_6) δ 8.27 (d, *J* = 5.6 Hz, 2H), 8.00 (d, *J* = 8.0 Hz, 1H), 7.54 (d, *J* = 8.0 Hz, 1H), 7.46 (s, 1H), 4.07 (s, 3H), 2.50 (s, 3H), 2.47 (s, 3H); $^{13}C\{^1H\}$ NMR (100 MHz, $CDCl_3$ + DMSO-d_6) δ 157.2, 139.4, 138.7, 134.5, 134.2, 129.4, 128.3, 126.6, 126.0, 121.9, 119.2, 118.3, 114.3, 62.8, 23.5, 21.4; IR (KBr) $\tilde{\nu}$ = 2954, 2917, 2849, 1729, 1608, 1537, 1492, 1462, 1397, 1207, 1184, 1161, 1079, 1056, 966, 812 cm^{-1}; HR-MS (ESI-TOF) m/z calcd for $C_{16}H_{15}{}^{79}BrNO_2$ $[M + H]^+$ 332.0281, found 332.0265, $C_{16}H_{15}{}^{81}BrNO_2$ $[M + H]^+$ 334.0261, found 334.0246.

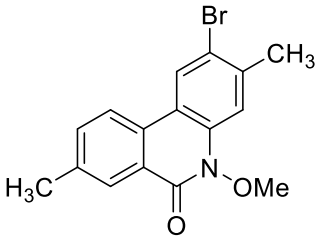

2-Bromo-3-fluoro-5-methoxy-8-methylphenanthridin-6(5H)-one (3j). R_f = 0.50 (hexane/ethyl acetate 4:1); white solid; yield 85% (88 mg); mp 206−208 °C; ^{1}H NMR (400

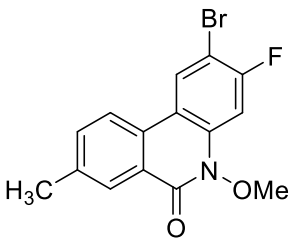

MHz, $CDCl_3$ + DMSO-d_6) δ 8.22 (d, *J* = 6.8 Hz, 1H), 8.18 (d, *J* = 0.4 Hz, 1H), 7.88 (d, *J* = 8.4 Hz, 1H), 7.49 (dd, *J* = 8.4, 1.6 Hz, 1H), 7.29 (d, *J* = 9.6 Hz, 1H), 4.04 (s, 3H), 2.43 (s, 3H); ^{13}C{^{1}H} NMR (100 MHz, $CDCl_3$ + DMSO-d_6) δ 159.3 (d, *J* = 248.7 Hz), 157.0, 138.9, 135.9 (d, *J* = 9.7 Hz), 134.3, 128.7, 128.2, 127.9, 125.6, 121.8, 116.2 (d, *J* = 2.5 Hz), 103.3 (d, *J* = 22.2 Hz), 100.7 (d, *J* = 28.7 Hz), 62.9, 21.3; IR (KBr) $\tilde{\nu}$ = 3011, 2948, 2931, 1669, 1607, 1584, 1421, 1397, 1239, 1230, 1187, 1056, 1009, 886, 851 cm^{-1}; HR-MS (ESI-TOF) m/z calcd for $C_{15}H_{12}{}^{79}BrFNO_2$ $[M + H]^+$ 336.0030, found 336.0033, $C_{15}H_{12}{}^{81}BrFNO_2$ $[M + H]^+$ 338.0010, found 338.0013.

2-Bromo-3-ethyl-5-methoxy-8-methylphenanthridin-6(5H)-one (3k). R_f = 0.50 (hexane/ethyl acetate 4:1); white solid; yield 93% (95 mg); mp 141−143 °C; ^{1}H NMR (400

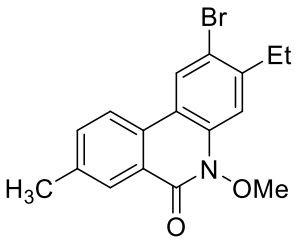

MHz, DMSO-d_6) δ 8.59 (s, 1H), 8.40 (d, *J* = 8.4 Hz, 1H), 8.10 (s, 1H), 7.65 (d, *J* = 8.4 Hz, 1H), 7.54 (s, 1H), 4.02 (s, 3H), 2.83 (d, *J* = 7.6 Hz, 2H), 2.47 (s, 3H), 1.25 (t, *J* = 7.6 Hz, 3H); ^{13}C{^{1}H} NMR (100 MHz, DMSO-d_6) δ 155.9, 144.3, 138.5, 134.6, 134.2, 128.9, 127.3, 127.0, 125.5, 123.0, 117.8, 117.8, 113.0, 62.6, 29.1, 20.9, 14.2; IR (KBr) $\tilde{\nu}$ = 2920, 2851, 1729, 1645, 1605, 1462, 1422, 1399, 1336, 1290, 1157, 1049, 1016, 940, 868 cm^{-1}; HR-MS (ESI-TOF) m/z calcd for $C_{17}H_{17}{}^{79}BrNO_2$ $[M + H]^+$ 346.0437, found 346.0436, $C_{17}H_{17}{}^{81}BrNO_2$ $[M + H]^+$ 348.0417, found 348.0419.

2-Bromo-3-chloro-5-methoxy-8-methylphenanthridin-6(5H)-one (3l). R_f = 0.50 (hexane/ethyl acetate 4:1); white solid; yield 83% (85 mg); mp

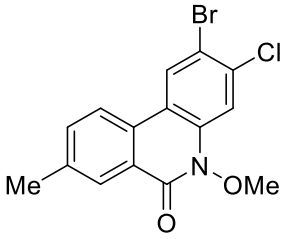

216−218 °C; ^{1}H NMR (400 MHz, $CDCl_3$) δ 8.34 (s, 1H), 8.24 (s, 1H), 7.97 (d, *J* = 8.0 Hz, 1H), 7.66 (s, 1H), 7.55 (d, *J* = 8.0 Hz, 1H), 4.06 (s, 3H), 2.46 (s, 3H); ^{13}C{^{1}H} NMR (100 MHz, $CDCl_3$ + DMSO-d_6) δ 156.9, 139.5, 135.3, 135.2, 134.4, 128.6, 128.4, 127.8, 126.2, 122.1, 118.8, 116.3, 114.0, 40.6, 21.4; IR (KBr) $\tilde{\nu}$ = 2920, 2851, 1711, 1672, 1617, 1459, 1389, 1321, 1233, 1221, 1211, 1040, 939, 875 cm^{-1}; HR-MS (ESI-TOF) m/z calcd for $C_{15}H_{12}{}^{79}BrClNO_2$ $[M + H]^+$ 351.9734, found 351.9738, $C_{15}H_{12}{}^{81}BrClNO_2$ $[M + H]^+$ 353.9714, found 353.9719.

2-Bromo-3-(tert-butyl)-5-methoxy-8-methylphenanthridin-6(5H)-one (3n). R_f = 0.50 (hexane/ethyl acetate 4:1); white solid; yield 89% (89 mg); mp 153−155 °C; ^{1}H NMR (700 MHz, $CDCl_3$) δ 8.38 (s, 1H), 8.32 (s, 1H), 8.05 (d, *J* = 8.4 Hz, 1H), 7.72 (s, 1H), 7.58 (d, *J* = 8.4 Hz, 1H), 4.13 (s, 3H), 2.52 (s, 3H), 1.60 (s, 9H); ^{13}C{^{1}H} NMR (175 MHz, $CDCl_3$) δ 157.5, 149.5, 138.9, 134.3, 134.3, 130.1, 129.2, 128.5, 126.4, 121.9, 118.1, 116.7, 112.1, 62.8, 37.3, 29.8, 21.5; IR (KBr) $\tilde{\nu}$ = 2956, 2920, 2851, 1667, 1614, 1465, 1398, 1383, 1288, 1259, 1046, 1025, 876 cm^{-1}; HR-MS (ESI-TOF) m/z calcd for $C_{19}H_{20}{}^{79}BrNO_2$ $[M + H]^+$ 374.0750, found 374.0750, $C_{19}H_{20}{}^{81}BrNO_2$ $[M + H]^+$ 376.0731, found 376.0732.

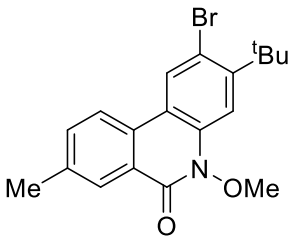

2-Chloro-5-methoxyphenanthridin-6(5H)-one (4a).[37] R_f = 0.55 (hexane/ethyl acetate 4:1); white solid; yield 94% (70 mg); ^{1}H NMR (400 MHz, $CDCl_3$ + DMSO-d_6) δ 8.46 (d, *J* = 8.0 Hz, 1H), 8.14 (d, *J* = 7.2 Hz, 2H), 7.74 (t, *J* = 7.6 Hz, 1H), 7.63 – 7.51 (m, 2H), 7.51 – 7.43 (m, 1H), 4.05 (s, 3H); ^{13}C{^{1}H} NMR (100 MHz, $CDCl_3$ + DMSO-d_6) δ 156.9, 134.3, 132.9, 131.8, 129.9, 128.9, 128.7, 128.5, 126.5, 123.0, 122.1, 119.8, 114.1, 62.8; HR-MS (ESI-TOF) m/z calcd for $C_{14}H_{11}ClNO_2$ $[M + H]^+$ 260.0473, found 260.0468.

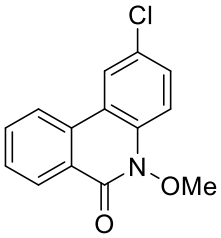

2-Chloro-5-methoxy-3-methylphenanthridin-6(5H)-one (4b).[43] R_f = 0.45 (hexane/ethyl acetate 4:1); white solid; yield 91% (103 mg); ^{1}H NMR (400 MHz, $CDCl_3$) δ 8.54 (d, *J* = 8.0 Hz, 1H), 8.21 (s, 1H), 8.17 (d, *J* = 8.0 Hz, 1H), 7.78 (t, *J* = 7.2 Hz, 1H), 7.61 (t, *J* = 7.6 Hz, 1H), 7.54 (s, 1H), 4.14 (s, 3H), 2.55 (s, 3H); ^{13}C{^{1}H} NMR (100 MHz, $CDCl_3$ + DMSO-d_6) δ 156.9, 138.2, 134.2, 132.8, 131.9, 129.4, 128.4, 128.2, 126.1, 123.4, 121.8, 117.7, 114.5, 62.7, 20.6; HR-MS (ESI-TOF) m/z calcd for $C_{15}H_{13}ClNO_2$ $[M + H]^+$ 274.0629, found 274.0644.

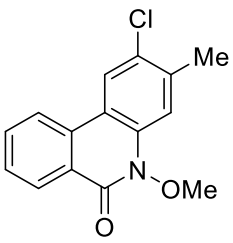

2-Chloro-5-methoxy-3,8-dimethylphenanthridin-6(5H)-one (4i). R_f = 0.45 (hexane/ethyl acetate 4:1); white solid; yield 87% (98 mg); mp 268−270 °C; ^{1}H NMR (400 MHz, $CDCl_3$ + DMSO-d_6) δ 8.08 (s, 1H), 7.95 (s, 1H), 7.90 – 7.78 (m, 1H), 7.40 (d, *J* = 8.0 Hz, 1H), 7.31 (s, 1H), 3.92 (s, 3H), 2.33 (s, 6H); ^{13}C{^{1}H} NMR (100 MHz, $CDCl_3$ + DMSO-d_6) δ 156.7, 138.2, 137.3, 133.8, 133.5, 129.1, 128.9, 127.8, 125.6, 122.8, 121.6, 117.5, 114.1, 62.4, 21.0, 20.3; IR (KBr) $\tilde{\nu}$ = 3080, 2950, 2922, 1627, 1607, 1577, 1472, 1401, 1379, 1349, 1257, 1062, 1036, 939, 810 cm^{-1}; HR-MS (ESI-TOF) m/z calcd for $C_{16}H_{14}ClNaNO_2$ $[M + Na]^+$ 310.0605, found 310.0600.

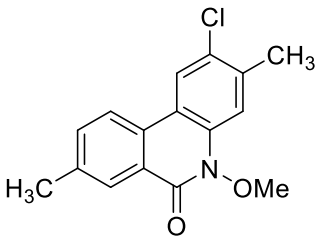

2-Chloro-3-fluoro-5-methoxy-8-methylphenanthridin-6(5H)-one (4j). R_f = 0.50 (hexane/ethyl acetate 4:1); white solid; yield 85% (76 mg); mp 187−188 °C; ^{1}H NMR (400 MHz, $CDCl_3$) δ 8.30 (s, 1H), 8.18 (d, *J* = 7.2 Hz, 1H), 7.98 (d, *J* = 8.4 Hz, 1H), 7.59 (d, *J* = 8.0 Hz, 1H), 7.42 (d, *J* = 10.0 Hz, 1H), 4.12 (s, 3H), 2.51 (s, 3H); ^{13}C{^{1}H} NMR (100 MHz, $CDCl_3$) δ 158.6 (d, *J*

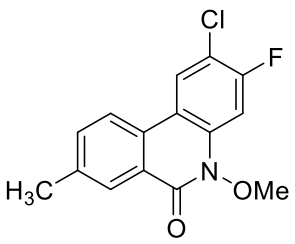

= 250.7 Hz), 157.3, 139.1, 135.5 (d, *J* = 9.7 Hz), 134.5, 129.1, 128.6, 125.9, 125.2, 121.9, 116.2 (d, *J* = 19.0 Hz), 115.9 (d, *J* = 3.2 Hz), 101.2 (d, *J* = 27.4 Hz), 63.1, 21.5; IR (KBr) $\tilde{\nu}$ = 2951, 2921, 2852, 1663, 1617, 1588, 1480, 1427, 1326, 1281, 1241, 1186, 840 cm^{-1}; HR-MS (ESI-TOF) m/z calcd for $C_{15}H_{12}ClFNO_2$ $[M + H]^+$ 292.0535, found 292.0539.

5-Methoxyphenanthridin-6(5H)-one (2a).[44] R_f = 0.55 (hexane/ethyl acetate 4:1); white solid; yield 97% (57.5 mg); ^1H NMR (400 MHz, $CDCl_3$ + DMSO-d_6) δ 8.21 (d, *J* = 8.0 Hz, 1H), 7.97 (dd, *J* = 7.6, 5.2 Hz, 2H), 7.48 (t, *J* = 7.6 Hz, 1H), 7.36 (d, *J* = 8.4 Hz, 1H), 7.32 – 7.24 (m, 2H), 7.10 – 7.00 (m, 1H), 3.82 (s, 3H); $^{13}C\{^1H\}$ NMR (100 MHz, $CDCl_3$ + DMSO-d_6) δ 157.2, 135.6, 132.9, 132.6, 129.9, 128.3, 128.0, 126.1, 123.2, 123.2, 121.9, 118.4, 112.5, 62.6; HR-MS (ESI-TOF) m/z calcd for $C_{14}H_{12}NO_2$ $[M + H]^+$ 226.0863, found 226.0865.

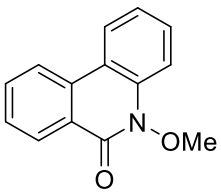

5-Methoxy-3-methylphenanthridin-6(5H)-one (2b).[39] R_f = 0.50 (hexane/ethyl acetate 4:1); white solid; yield 94% (93 mg); ^1H NMR (400 MHz, $CDCl_3$) δ 8.53 (d, *J* = 8.0 Hz, 1H), 8.21 (d, *J* = 8.0 Hz, 1H), 8.12 (d, *J* = 8.0 Hz, 1H), 7.74 (t, *J* = 7.2 Hz, 1H), 7.55 (t, *J* = 7.6 Hz, 1H), 7.47 (s, 1H), 7.15 (d, *J* = 8.0 Hz, 1H), 4.13 (s, 3H), 2.52 (s, 3H); $^{13}C\{^1H\}$ NMR (100 MHz, $CDCl_3$) δ 157.5, 140.7, 135.9, 133.2, 132.7, 128.6, 127.7, 126.0, 124.5, 123.2, 121.8, 116.8, 112.8, 62.8, 22.0, HR-MS (ESI-TOF) m/z calcd for $C_{15}H_{13}NaNO_2$ $[M + Na]^+$ 262.0838, found 262.0825.

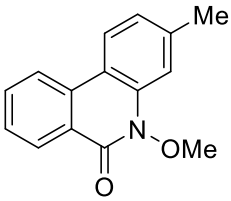

3-(Tert-butyl)-5-methoxyphenanthridin-6(5H)-one (2d). R_f = 0.50 (hexane/ethyl acetate 4:1); white solid; yield 87% (88 mg); mp 122−124 °C; ^1H NMR (400 MHz, $CDCl_3$) δ 8.55 (d, *J* = 8.0 Hz, 1H), 8.25 (d, *J* = 8.0 Hz, 1H), 8.20 (d, *J* = 8.4 Hz, 1H), 7.76

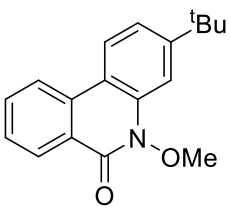

(t, *J* = 7.6 Hz, 1H), 7.68 (s, 1H), 7.57 (t, *J* = 7.6 Hz, 1H), 7.41 (d, *J* = 8.0 Hz, 1H), 4.15 (s, 3H), 1.43 (s, 9H); $^{13}C\{^{1}H\}$ NMR (100 MHz, $CDCl_3$) δ 157.7, 153.9, 135.8, 133.2, 132.7, 128.7, 127.8, 126.2, 123.2, 121.9, 120.9, 116.3, 109.3, 62.7, 35.4, 31.4; IR (KBr) $\tilde{\nu}$ = 2962, 2919, 2851, 1659, 1606, 1574, 1475, 1413, 1320, 1250, 1175, 1045, 1004, 908, 807 cm^{-1}; HR-MS (ESI-TOF) m/z calcd for $C_{18}H_{20}NO_2$ $[M + H]^+$ 282.1489, found 282.1512.

3-Fluoro-5-methoxyphenanthridin-6(5H)-one (2e).[44] R_f = 0.50 (hexane/ethyl acetate 4:1); white solid; yield 92% (73 mg); ^{1}H NMR (400 MHz, $CDCl_3$) δ 8.52 (dd, *J* = 8.0, 1.2 Hz, 1H), 8.25 – 8.20 (m, 1H), 8.20 – 8.15 (m, 1H), 7.80 – 7.74 (m, 1H), 7.58 (dd, *J* = 11.2, 4.0 Hz, 1H), 7.36 (dd, *J* = 10.2, 2.8 Hz, 1H), 7.09 – 7.02 (m, 1H), 4.14 (s, 3H); $^{13}C\{^{1}H\}$ NMR (100 MHz, $CDCl_3$) δ 163.9 (d, *J* = 249.0 Hz), 157.6, 137.5 (d, *J* = 11.0 Hz), 133.0, 132.7, 128.8, 128.0, 125.8, 125.5 (d, *J* = 9.8 Hz), 121.9, 115.0 (d, *J* = 2.7 Hz), 111.1 (d, *J* = 22.8 Hz), 99.9 (d, *J* = 27.9 Hz), 63.0; HR-MS (ESI-TOF) m/z calcd for $C_{14}H_{11}FNO_2$ $[M + H]^+$ 244.0768, found 244.0771.

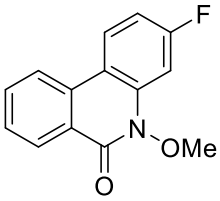

3-Chloro-5-methoxyphenanthridin-6(5H)-one (2f).[39] R_f = 0.45 (hexane/ethyl acetate 4:1); white solid; yield 89% (71 mg); ^{1}H NMR (400 MHz, $CDCl_3$ + DMSO-d_6) δ 8.63 (dd, *J* = 8.0, 1.2 Hz, 1H), 8.32 (d, *J* = 8.0 Hz, 1H), 8.29 (d, *J* = 8.4 Hz, 1H), 7.93 – 7.87 (m, 1H), 7.77 (d, *J* = 2.0 Hz. 1H), 7.75 – 7.69 (m, 1H), 7.44 – 7.39 (m, 1H), 4.25 (s, 3H); $^{13}C\{^{1}H\}$ NMR (100 MHz, $CDCl_3$ + DMSO-d_6) δ 157.3, 136.7, 136.1, 132.9, 132.3, 128.6, 128.4, 126.1, 124.6, 123.5, 122.0, 117.1, 112.6, 62.9; HR-MS (ESI-TOF) m/z calcd for $C_{14}H_{11}ClNO_2$ $[M + H]^+$ 260.0473, found 260.0474.

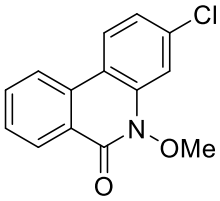

5-Methoxy-3-(trifluoromethyl)phenanthridin-6(5H)-one (2g).[44] R_f = 0.50 (hexane/ethyl acetate 4:1); white solid; yield 93% (55.5 mg); ^{1}H NMR (700 MHz, $CDCl_3$) δ 8.59 (dd, *J* = 8.4, 0.7 Hz, 1H), 8.38 (d, *J* = 8.4 Hz, 1H), 8.31 (d, *J* = 8.4 Hz, 1H), 7.93 (s, 1H), 7.87 – 7.82 (m, 1H), 7.69 (dd, *J* = 11.2, 3.5 Hz, 1H), 7.59 (d, *J* = 8.4 Hz, 1H), 4.18 (s, 3H); ^{13}C{^{1}H} NMR (175 MHz, $CDCl_3$) δ 157.3, 136.1, 133.2, 131.9, 131.9 (q, *J* = 33.0 Hz), 129.4, 128.9, 127.1, 124.2, 123.9 (q, *J* = 272.5 Hz), 122.6, 121.4, 119.8 (q, *J* = 3.3 Hz), 63.2; HR-MS (ESI-TOF) m/z calcd for $C_{15}H_{11}F_3NO_2$ $[M + H]^+$ 294.0736, found 294.0727.

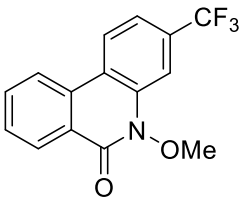

5-Methoxy-8-methylphenanthridin-6(5H)-one (2h).[44] R_f = 0.50 (hexane/ethyl acetate 4:1); white solid; yield 88% (87 mg); ^{1}H NMR (400 MHz, DMSO-d_6) δ 8.47 (d, *J* = 8.0 Hz, 1H), 8.43 (d, *J* = 8.4 Hz, 1H), 8.16 (s, 1H), 7.69 (dd, *J* = 8.4, 1.6 Hz, 1H), 7.64 (d, *J* = 4.0 Hz, 2H), 7.42 – 7.30 (m, 1H), 4.02 (s, 3H), 2.49 (s, 3H); ^{13}C{^{1}H} NMR (100 MHz, DMSO-d_6) δ 156.1, 138.2, 135.1, 134.2, 130.2, 129.9, 127.3, 125.6, 123.6, 123.3, 122.8, 117.9, 112.2, 62.5, 20.9; HR-MS (ESI-TOF) m/z calcd for $C_{15}H_{14}NO_2$ $[M + H]^+$ 240.1019, found 240.1028.

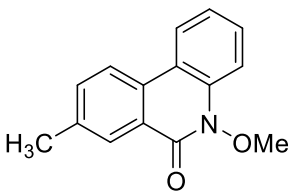

5-Methoxy-3,8-dimethylphenanthridin-6(5H)-one (2i).[39] R_f = 0.50 (hexane/ethyl acetate 4:1); white solid; yield 89% (88 mg); ^{1}H NMR (400 MHz, $CDCl_3$) δ 8.33 (s, 1H), 8.09 (dd, *J* = 8.0, 5.2 Hz, 2H), 7.56 (d, *J* = 8.0 Hz, 1H), 7.45 (s, 1H), 7.15 (d, *J* = 8.0 Hz, 1H), 4.14 (s, 3H), 2.51 (s, 3H), 2.49 (s, 3H); ^{13}C{^{1}H} NMR (100 MHz, $CDCl_3$) δ 157.7, 140.1, 137.9, 135.4, 134.1, 130.8, 128.3, 1258, 124.5, 123.0, 121.8, 116.4, 112.8, 62.8, 21.9, 21.4; HR-MS (ESI-TOF) m/z calcd for $C_{16}H_{15}NaNO_2$ $[M + Na]^+$ 276.0995, found 276.1008.

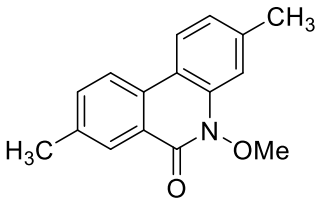

3-Fluoro-5-methoxy-8-methylphenanthridin-6(5H)-one (2j). R_f = 0.45 (hexane/ethyl acetate 4:1); white solid; yield 84% (67 mg); mp 190−192 °C; ^{1}H NMR (400 MHz, DMSO-d_6) δ 8.48 (dd, *J* = 8.4, 6.0 Hz, 1H), 8.34 (d, *J* = 8.4 Hz, 1H), 8.10 (s, 1H), 7.66 (d, *J* = 8.0 Hz, 1H), 7.42 (dd, *J* = 10.2, 1.6 Hz, 1H), 7.21 (dd, *J* = 12.0, 5.2 Hz, 1H), 4.03 (s, 3H), 2.46 (s, 3H); ^{13}C{^{1}H} NMR (100 MHz, DMSO-d_6) δ 163.4 (d, *J* = 245.6 Hz), 156.8, 138.5, 137.1 (d, *J* = 11.0 Hz), 134.8, 130.2, 127.8, 126.7 (d, *J* = 9.3 Hz), 125.4, 123.3, 115.1, 111.1 (d, *J* = 22.3 Hz), 99.8 (d, *J* = 27.9 Hz), 63.2, 21.3; IR (KBr) $\tilde{\nu}$ = 2954, 2916, 2848, 1660, 1617, 1593, 1482, 1426, 1328, 1266, 1171, 1037, 1010, 941, 836 cm^{-1}; HR-MS (ESI-TOF) m/z calcd for $C_{15}H_{13}FNO_2$ [M + H]$^+$ 258.0925, found 258.0936.

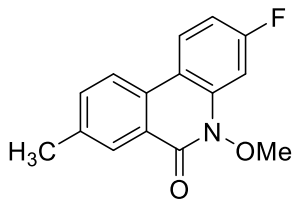

3-Ethyl-5-methoxy-8-methylphenanthridin-6(5H)-one (2k). R_f = 0.45 (hexane/ethyl acetate 4:1); white solid; yield 86% (68 mg); mp 116−118 °C; ^{1}H NMR (400 MHz, $CDCl_3$) δ 8.34 (s, 1H), 8.13 (d, *J* = 3.6 Hz, 1H), 8.11 (d, *J* = 3.6 Hz, 1H), 7.56 (dd, *J* = 8.4, 1.6 Hz, 1H), 7.48 (s, 1H), 7.18 (dd, *J* = 8.4, 1.2 Hz, 1H), 4.13 (d, *J* = 4.4 Hz, 3H), 2.81 (q, *J* = 7.6 Hz, 2H), 2.51 (s, 3H), 1.33 (t, *J* = 7.6 Hz, 3H); ^{13}C{^{1}H} NMR (100 MHz, $CDCl_3$) δ 157.7, 146.5, 137.9, 135.6, 134.0, 130.8, 128.3, 125.9, 123.3, 123.1, 121.9, 116.7, 111.7, 62.7, 29.3, 21.4, 15.7; IR (KBr) $\tilde{\nu}$ = 2922, 2852, 1707, 1646, 1613, 1482, 1458, 1327, 1284, 1159, 1097, 1065, 984, 862 cm^{-1}; HR-MS (ESI-TOF) m/z calcd for $C_{17}H_{18}NO_2$ [M + H]$^+$ 268.1332, found 268.1334.

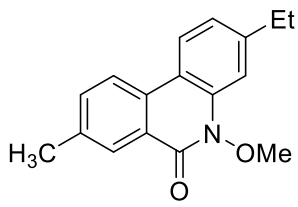

3-Chloro-5-methoxy-8-methylphenanthridin-6(5H)-one (2l). R_f = 0.50 (hexane/ethyl acetate 4:1); white solid; yield 83% (66 mg); mp 191−193 °C; ^{1}H NMR (400 MHz, $CDCl_3$ + DMSO-d_6) δ 8.17 (s, 1H), 8.02 (d, *J* = 8.4 Hz, 1H), 7.98 (d, *J* = 8.4 Hz, 1H), 7.51 (d, *J* = 2.0 Hz, 1H), 7.48 (d, *J*

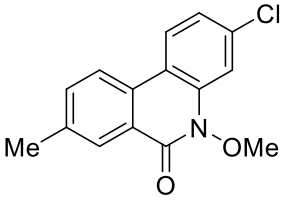

= 8.4 Hz, 1H), 7.17 (dt, *J* = 8.4, 2.0 Hz, 1H), 4.01 (s, 3H), 2.40 (s, 3H); $^{13}C\{^{1}H\}$ NMR (100 MHz, $CDCl_3$ + DMSO-d_6) δ 157.1, 138.6, 136.0, 135.2, 134.1, 129.6, 128.0, 125.6, 124.2, 123.3, 121.9, 116.9, 112.3, 62.7, 21.2; IR (KBr) $\tilde{\nu}$ = 2915, 2847, 1659, 1618, 1537, 1425, 1312, 1137, 1091, 1039, 827 cm^{-1}; HR-MS (ESI-TOF) m/z calcd for $C_{15}H_{13}ClNO_2$ $[M + H]^+$ 274.0629, found 274.0629.

2-Chloro-5-methoxy-8-methylphenanthridin-6(5H)-one (2m): R_f = 0.50 (hexane/ethyl acetate 4:1); white solid; yield 78% (62 mg); mp 182−184 °C; ^{1}H NMR (400 MHz, DMSO-d_6) δ 8.49 (s, 1H), 8.43 (d, *J* = 8.4 Hz, 1H), 8.13 (s, 1H), 7.67 (dd, *J* = 8.4, 1.6 Hz, 1H), 7.62 (s, 2H), 4.02 (s, 3H), 2.48 (s, 3H); $^{13}C\{^{1}H\}$ NMR (100 MHz, DMSO-d_6) δ 156.3, 139.4, 134.7, 134.4, 129.9, 129.6, 128.3, 127.8, 126.4, 123.7, 123.6, 120.1, 114.7, 63.2, 21.3; IR (KBr) $\tilde{\nu}$ = 2975, 2927, 1663, 1613, 1583, 1477, 1404, 1332, 1227, 1132, 1038, 848 cm^{-1}; HR-MS (ESI-TOF) m/z calcd for $C_{15}H_{12}ClNaNO_2$ $[M + Na]^+$ 296.0449, found 296.0478.

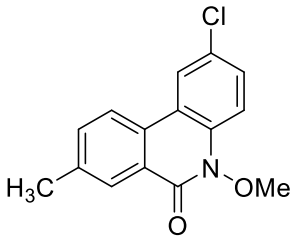

5-Methoxy-2-nitrophenanthridin-6(5H)-one (2o). R_f = 0.50 (hexane/ethyl acetate 4:1); white solid; yield 88% (70 mg); mp 246−247 °C; ^{1}H NMR (400 MHz, $CDCl_3$) δ 9.18 (s, 1H), 8.58 (d, *J* = 8.0 Hz, 1H), 8.44 (d, *J* = 9.2 Hz, 1H), 8.37 (d, *J* = 8.0 Hz, 1H), 7.89 (d, *J* = 8.0 Hz, 1H), 7.79 (d, *J* = 9.2 Hz, 1H), 7.73 (d, *J* = 7.6 Hz, 1H), 4.18 (s, 3H); $^{13}C\{^{1}H\}$ NMR (100 MHz, $CDCl_3$) δ 157.3, 143.3, 140.1, 133.6, 131.8, 129.6, 128.9, 126.5, 124.9, 122.5, 119.6, 118.7, 113.4, 63.3; IR (KBr) $\tilde{\nu}$ = 3072, 2946, 1658, 1517, 1488, 1332, 1299, 1284, 1136, 1033, 912 cm^{-1}; HR-MS (ESI-TOF) m/z calcd for $C_{14}H_{11}N_2O_4$ $[M + H]^+$ 271.0713, found 271.0711.

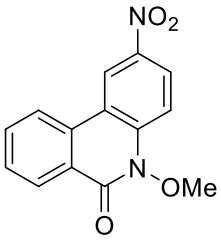

Methyl 5-methoxy-6-oxo-5,6-dihydrophenanthridine-3-carboxylate (2p). R_f = 0.45 (hexane/ethyl acetate 4:1); white solid; yield 91% (54 mg); mp 162−164 °C; ^{1}H NMR (400

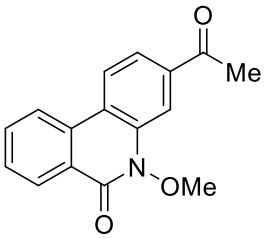

MHz, $CDCl_3$) δ 8.56 (d, *J* = 8.0 Hz, 1H), 8.31 (dd, *J* = 11.2, 8.4 Hz, 2H), 8.20 (s, 1H), 7.89 (d, *J* = 8.4 Hz, 1H), 7.81 (t, *J* = 7.6 Hz, 1H), 7.66 (t, *J* = 7.6 Hz, 1H), 4.17 (s, 3H), 2.72 (s, 3H); ^{13}C{^{1}H} NMR (100 MHz, $CDCl_3$) δ 197.3, 157.3, 137.9, 136.0, 133.1, 132.1, 129.4, 128.8, 127.2, 123.8, 122.9, 122.8, 122.4, 112.7, 63.1, 27.1; IR (KBr) $\tilde{\nu}$ = 3071, 2939, 1680, 1657, 1605, 1509, 1412, 1316, 1278, 1246, 1175, 983 cm^{-1}; HR-MS (ESI-TOF) m/z calcd for $C_{16}H_{14}NO_3$ $[M + H]^+$ 268.0968, found 268.0989.

5-Phenylphenanthridin-6(5H)-one (2q).[51] R_f = 0.50 (hexane/ethyl acetate 4:1); white solid;

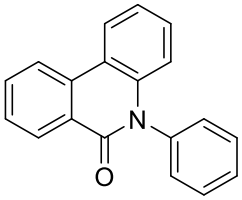

yield 94% (37.4 mg); mp 220−222 °C; ^{1}H NMR (400 MHz, $CDCl_3$) δ 8.57 (d, *J* = 8.0 Hz, 1H), 8.42 – 8.26 (m, 2H), 7.83 (t, *J* = 7.6 Hz, 1H), 7.63 (t, *J* = 7.6 Hz, 3H), 7.58 – 7.51 (m, 1H), 7.34 (d, *J* = 8.0 Hz, 2H), 7.33 – 7.28 (m, 2H), 6.76 – 6.66 (m, 1H); ^{13}C{^{1}H} NMR (100 MHz, $CDCl_3$) δ 161.9, 139.3, 138.4, 134.2, 133.0, 130.4, 129.3, 129.2, 129.2, 128.9, 128.3, 125.9, 123.1, 122.8, 121.9, 119.2, 117.2; IR (KBr) $\tilde{\nu}$ = 3056, 1651, 1602, 1502, 1484, 1332, 1317, 1174, 1160, 1075, 756 cm^{-1}; HR-MS (ESI-TOF) m/z calcd for $C_{19}H_{14}NO$ $[M + H]^+$ 272.1070, found 272.1077.

5-Methoxy-8-methyl-2-phenylphenanthridin-6(5H)-one (5). R_f = 0.50 (hexane/ethyl acetate 4:1); white solid; yield 95% (75 mg); mp 162−164 °C; ^{1}H NMR (700 MHz, $CDCl_3$) δ

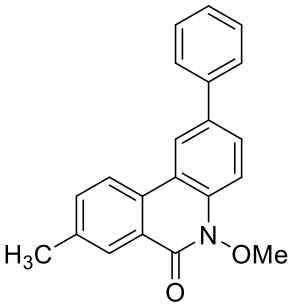

8.41 (s, 1H), 8.38 (s, 1H) 8.24 (d, *J* = 8.4 Hz, 1H), 7.78 (d, *J* = 8.4 Hz, 1H), 7.72 (d, *J* = 8.4 Hz, 1H), 7.68 (d, *J* = 7.0 Hz, 2H), 7.61 (d, *J* = 7.7 Hz, 1H), 7.50 (t, *J* = 7.0 Hz, 2H), 7.40 (t, *J* = 7.0 Hz, 1H), 4.17

(s, 3H), 2.53 (s, 3H); $^{13}C\{^{1}H\}$ NMR (175 MHz, $CDCl_3$) δ 157.5, 140.5, 138.7, 136.6, 134.8, 134.2, 130.6, 129.1, 128., 128.5, 127.6, 127.3, 126.4, 122.1, 121.6, 119.2, 113.3, 62.9, 21.5; IR (KBr) $\tilde{\nu}$ = 3131, 2962, 2926, 2848, 1637, 1615, 1538, 1323, 1158, 1320, 1068, 1038, 1019, 947, 854 cm^{-1}; HR-MS (ESI-TOF) m/z calcd for $C_{21}H_{18}NO_2$ $[M + H]^+$ 316.1332, found 316.1336.

(*E*)-5-Methoxy-8-methyl-2-styrylphenanthridin-6(5H)-one (6). R_f = 0.50 (hexane/ethyl acetate 4:1); white solid; yield 92% (59 mg); mp 132−134 °C; ^{1}H NMR (700 MHz, $CDCl_3$) δ 8.36 (s, 1H), 8.30 (s, 1H), 8.23 (d, *J* = 8.4 Hz, 1H), 7.74 (d, *J* = 8.4 Hz, 1H), 7.65 (d, *J* = 8.4 Hz, 1H), 7.62 (d, *J* = 8.4 Hz, 1H), 7.56 (d, *J* = 7.7 Hz, 2H), 7.39 (t, *J* = 7.7 Hz, 2H), 7.29 (t, *J* = 7.0 Hz, 1H), 7.20 (q, *J* = 16.1 Hz, 2H), 4.15 (s, 3H), 2.54 (s, 3H); $^{13}C\{^{1}H\}$ NMR (175 MHz, $CDCl_3$) δ 157.3, 138.7, 137.3, 134.9, 134.2, 132.7, 130.5, 128.9, 128.8, 128.5, 127.9, 127.8, 127.5, 126.6, 126.5, 122.1, 121.3, 119.0, 113.2, 62.9, 21.5; IR (KBr) $\tilde{\nu}$ = 3057, 3022, 2946, 2920, 2849, 1668, 1633, 1614, 1594, 1495, 1435, 1326, 1289, 1231, 1143, 1041, 963, 814 cm^{-1}; HR-MS (ESI-TOF) m/z calcd for $C_{23}H_{20}NO_2$ $[M + H]^+$ 342.1489, found 342.1489.

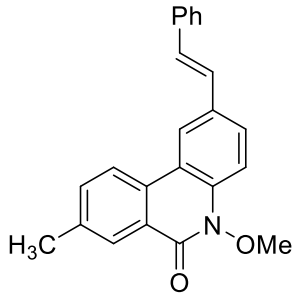

5-Methoxy-8-methyl-2-(phenylethynyl)phenanthridin-6(5H)-one (7). R_f = 0.45 (hexane/ethyl acetate 4:1); white solid; yield 82% (52.5 mg); mp 180−182 °C; ^{1}H NMR (700 MHz, $CDCl_3$) δ 8.34 (s, 1H), 8.32 (d, *J* = 1.4 Hz, 1H), 8.08 (d, *J* = 8.4 Hz, 1H), 7.63 (dd, *J* = 8.4, 1.4 Hz, 1H), 7.60 (d, *J* = 8.4 Hz, 1H), 7.55 (s, 1H), 7.53 (d, *J* = 8.4 Hz, 2H), 7.37 (d, *J* = 7.0 Hz, 1H), 7.29 (t, *J* = 7.0 Hz, 2H), 4.12 (s, 3H), 2.53 (s, 3H); $^{13}C\{^{1}H\}$ NMR (175 MHz, $CDCl_3$) δ 157.2, 139.4, 134.6, 134.4, 134.4, 134.3, 132.3,

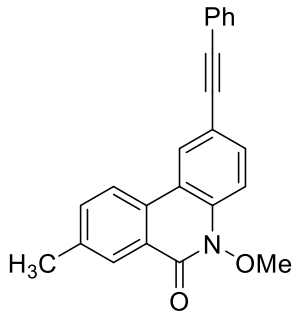

131.7, 129.7, 129.4, 128.6, 128.5, 128.5, 126.6, 125.9, 122.2, 120.6, 116.4, 114.5, 62.9, 21.5; IR (KBr) $\widetilde{\nu}$ = 3053, 2941, 2917, 2818, 1664, 1615, 1584, 1477, 1432, 1329, 1299, 1225, 1035, 959, 841 cm^{-1}; HR-MS (ESI-TOF) m/z calcd for $C_{23}H_{18}NO_2$ $[M + H]^+$ 340.1332, found 340.1333.

5.6. REFERENCES

1. (a) de la Hoz, A.; Díaz-Ortiz, Á.; Moreno, A., *Chem. Soc. Rev.* **2005,** *34* (2), 164-178; (b) Sharma, N.; Sharma, U. K.; Van der Eycken, E. V., Microwave-Assisted Organic Synthesis: Overview of Recent Applications. In *Green Techniques for Organic Synthesis and Medicinal Chemistry*, Zhang, W.; Cue, B. W., Eds. John Wiley & Sons, Ltd.: 2018; pp 441-468.

2. Marzo, L.; Pagire, S. K.; Reiser, O.; König, B., *Angew. Chem. Int. Ed.* **2018,** *57* (32), 10034-10072.

3. Verschueren, R. H.; De Borggraeve, W. M., *Molecules* **2019,** *24* (11), 2122.

4. (a) Toda, F., *Acc. Chem. Res.* **1995,** *28* (12), 480-486; (b) Toda, F.; Tanaka, K.; Iwata, S., *J. Org. Chem.* **1989,** *54* (13), 3007-3009.

5. (a) Baig, R. B. N.; Varma, R. S., *Chem. Soc. Rev.* **2012,** *41* (Copyright (C) 2012 American Chemical Society (ACS). All Rights Reserved.), 1559-1584; (b) Kimura, T., Chapter 7 - Application of Ultrasound to Organic Synthesis. In *Sonochemistry and the Acoustic Bubble*, Grieser, F.; Choi, P.-K.; Enomoto, N.; Harada, H.; Okitsu, K.; Yasui, K., Eds. Elsevier: Amsterdam, 2015; pp 171-186.

6. (a) Achar, T. K.; Bose, A.; Mal, P., *Beilstein J. Org. Chem.* **2017,** *13*, 1907-1931; (b) James, S. L.; Adams, C. J.; Bolm, C.; Braga, D.; Collier, P.; Friščić, T.; Grepioni, F.; Harris, K. D. M.; Hyett, G.; Jones, W.; Krebs, A.; Mack, J.; Maini, L.; Orpen, A. G.; Parkin, I. P.;

Shearouse, W. C.; Steed, J. W.; Waddell, D. C., *Chem. Soc. Rev.* **2012,** *41* (1), 413-447; (c) Sharma, H.; Singh, N.; Jang, D. O., *Green Chem.* **2014,** *16* (12), 4922-4930.

7. Constable, D. J. C.; Jimenez-Gonzalez, C.; Henderson, R. K., *Org. Proc. Res. Dev.* **2007,** *11* (1), 133-137.

8. Walsh, P. J.; Li, H.; de Parrodi, C. A., *Chem. Rev.* **2007,** *107* (6), 2503-2545.

9. Do, J.-L.; Friščić, T., *ACS Cent. Sci.* **2017,** *3* (1), 13-19.

10. Ardila-Fierro, K. J.; Hernández, J. G., *ChemSusChem* **2021,** *14* (10), 2145-2162.

11. Gomollón-Bel, F., *Chem. Int.* **2019,** *41* (2), 12-17.

12. (a) Howard, J. L.; Nicholson, W.; Sagatov, Y.; Browne, D. L., *Beilstein J. Org. Chem.* **2017,** *13*, 1950-1956; (b) Ranu, B. C.; Chatterjee, T.; Mukherjee, N., CHAPTER 1 Carbon-Heteroatom Bond Forming Reactions and Heterocycle Synthesis under Ball Milling. In *Ball Milling Towards Green Synthesis: Applications, Projects, Challenges*, The Royal Society of Chemistry: 2015; pp 1-33.

13. Garay, A. L.; Pichon, A.; James, S. L., *Chem. Soc. Rev.* **2007,** *36* (6), 846-855.

14. Howard, Joseph L.; Cao, Q.; Browne, D. L., *Chem. Sci.* **2018,** *9* (12), 3080-3094.

15. (a) Bose, A.; Mal, P., *Beilstein J. Org. Chem.* **2019,** *15*, 881-900; (b) Giri, C.; Sahoo, P. K.; Puttreddy, R.; Rissanen, K.; Mal, P., *Chem. Eur. J.* **2015,** *21* (17), 6390–6393.

16. (a) Egorov, I. N.; Santra, S.; Kopchuk, D. S.; Kovalev, I. S.; Zyryanov, G. V.; Majee, A.; Ranu, B. C.; Rusinov, V. L.; Chupakhin, O. N., *Green Chem.* **2020,** *22* (2), 302-315; (b) Hernández, J. G.; Juaristi, E., *J. Org. Chem.* **2011,** *76* (5), 1464-1467; (c) Rodríguez, B.; Bruckmann, A.; Bolm, C., *Chem. Eur. J.* **2007,** *13* (17), 4710-4722.

17. Pang, Y.; Ishiyama, T.; Kubota, K.; Ito, H., *Chem. Eur. J.* **2019,** *25* (18), 4654-4659.

18. Hermann, G. N.; Bolm, C., *ACS Catal.* **2017,** *7* (7), 4592-4596.

19. (a) Seo, T.; Ishiyama, T.; Kubota, K.; Ito, H., *Chem. Sci.* **2019,** *10* (35), 8202-8210; (b) Yu, J.; Shou, H.; Yu, W.; Chen, H.; Su, W., *Adv. Synth. Catal.* **2019,** *361* (22), 5133-5139.

20. Kubota, K.; Seo, T.; Koide, K.; Hasegawa, Y.; Ito, H., *Nat. Commun.* **2019,** *10* (1), 111.

21. Huang, H.-M.; Bellotti, P.; Ma, J.; Dalton, T.; Glorius, F., *Nat. Rev. Chem.* **2021,** *5* (5), 301-321.

22. (a) Fier, P. S., *J. Am. Chem. Soc.* **2017,** *139* (28), 9499-9502; (b) Liu, Y.-L.; Zhou, J., *Synthesis* **2015,** *47* (9), 1210-1226; (c) Zhang, Z.; Tanaka, K.; Yu, J.-Q., *Nature* **2017,** *543* (7646), 538-542.

23. (a) Friščić, T., *Chem. Soc. Rev.* **2012,** *41* (Copyright (C) 2012 American Chemical Society (ACS). All Rights Reserved.), 3493-3510; (b) Ghosh, B. N.; Lahtinen, M.; Kalenius, E.; Mal, P.; Rissanen, K., *Cryst. Growth Des.* **2016,** *16* (5), 2527-2534; (c) Zeng, Y.; Liao, S.; Dai, J.; Fu, Z., *Chem. Commun.* **2012,** *48* (Copyright (C) 2013 American Chemical Society (ACS). All Rights Reserved.), 11641-11643.

24. Huang, W.-T.; Shi, Y.; Xie, W.-Y.; Luo, H.-Q.; Li, N.-B., *Chem. Commun.* **2011,** *47* (Copyright (C) 2012 American Chemical Society (ACS). All Rights Reserved.), 7800-7802.

25. Li, H.; Neumann, H.; Beller, M.; Wu, X.-F., *Angew. Chem., Int. Ed.* **2014,** *53* (12), 3183-3186.

26. Chen, M. Z.; Gutierrez, O.; Smith, A. B., 3rd, *Angew. Chem. Int. Ed. Engl.* **2014,** *53* (5), 1279-82.

27. Zhou, X.; Yao, Y.; Wang, C.; Xu, Y.; Zhang, W.; Ma, Y.; Wu, G., *Org. Lett.* **2021,** *23* (9), 3669-3673.

28. Li, Z.; Jiao, L.; Sun, Y.; He, Z.; Wei, Z.; Liao, W.-W., *Angew. Chem. Int. Ed.* **2020,** *59* (18), 7266-7270.

29. Pramanik, M.; Choudhuri, K.; Mal, P., *Asian J. Org. Chem.* **2019,** *8* (1), 144-150.

30. Pimparkar, S.; Jeganmohan, M., *Chem. Commun.* **2014,** *50* (81), 12116-12119.

31. Patil, S.; Kamath, S.; Sanchez, T.; Neamati, N.; Schinazi, R. F.; Buolamwini, J. K., *Biorg. Med. Chem.* **2007,** *15* (3), 1212-1228.

32. Zhang, X.-R.; Wang, H.-W.; Tang, W.-L.; Zhang, Y.; Yang, H.; Hu, D.-X.; Ravji, A.; Marchand, C.; Kiselev, E.; Ofori-Atta, K.; Agama, K.; Pommier, Y.; An, L.-K., *J. Med. Chem.* **2018,** *61* (22), 9908-9930.

33. Jin, Z., *Nat. Prod. Rep.* **2009,** *26* (3), 363-381.

34. Piozzi, F.; Fuganti, C.; Mondelli, R.; Ceriotti, G., *Tetrahedron* **1968,** *24* (3), 1119-1131.

35. Lefranc, F.; Sauvage, S.; Van Goietsenoven, G.; Mégalizzi, V.; Lamoral-Theys, D.; Debeir, O.; Spiegl-Kreinecker, S.; Berger, W.; Mathieu, V.; Decaestecker, C.; Kiss, R., *Mol. Cancer Ther.* **2009,** *8* (7), 1739-50.

36. Bräutigam, J.; Bischoff, I.; Schürmann, C.; Buchmann, G.; Epah, J.; Fuchs, S.; Heiss, E.; Brandes, R. P.; Fürst, R., *J Mol Cell Cardiol* **2019,** *135*, 97-108.

37. Zhao, J.; Li, H.; Li, P.; Wang, L., *J. Org. Chem.* **2019,** *84* (14), 9007-9016.

38. Saha, R.; Sekar, G., *J. Catal.* **2018,** *366*, 176-188.

39. Yedage, S. L.; Bhanage, B. M., *J. Org. Chem.* **2016,** *81* (10), 4103-4111.

40. Liang, D.; Hu, Z.; Peng, J.; Huang, J.; Zhu, Q., *Chem. Commun.* **2013,** *49* (2), 173-175.

41. Rajeshkumar, V.; Lee, T.-H.; Chuang, S.-C., *Org. Lett.* **2013,** *15* (7), 1468-1471.

42. Feng, M.; Tang, B.; Xu, H.-X.; Jiang, X., *Org. Lett.* **2016,** *18* (17), 4352-4355.

43. Liang, D.; Sersen, D.; Yang, C.; Deschamps, J. R.; Imler, G. H.; Jiang, C.; Xue, F., *Org. Biomol. Chem.* **2017,** *15* (20), 4390-4398.

44. Liang, D.; Yu, W.; Nguyen, N.; Deschamps, J. R.; Imler, G. H.; Li, Y.; MacKerell, A. D., Jr.; Jiang, C.; Xue, F., *J. Org. Chem.* **2017,** *82* (7), 3589-3596.

45. Wu, L.; Hao, Y.; Liu, Y.; Wang, Q., *Org. Biomol. Chem.* **2019,** *17* (28), 6762-6770.

46. Wang, H.; Li, Y.; Tang, Z.; Wang, S.; Zhang, H.; Cong, H.; Lei, A., *ACS Catal.* **2018,** *8* (11), 10599-10605.

47. Zhang, N.; Yang, R.; Zhang-Negrerie, D.; Du, Y.; Zhao, K., *J. Org. Chem.* **2013,** *78* (17), 8705-8711.

48. Bose, A.; Mal, P., *Tetrahedron Lett.* **2014,** *55* (13), 2154-2156.

49. (a) Demeter, A.; Bérces, T.; Hinderberger, J.; Timári, G., *Photochem Photobiol Sci* **2003,** *2* (3), 273-81; (b) Gentili, P. L.; Ortica, F.; Romani, A.; Favaro, G., *J. Phys. Chem. A* **2007,** *111* (2), 193-200.

50. Demeter, A.; Bérces, T.; Zachariasse, K. A., *J. Phys. Chem. A* **2001,** *105* (19), 4611-4621.

51. Moon, Y.; Jang, E.; Choi, S.; Hong, S., *Org. Lett.* **2018,** *20* (1), 240-243.

NMR Spectra

^{1}H NMR (400 MHz, $CDCl_3$)

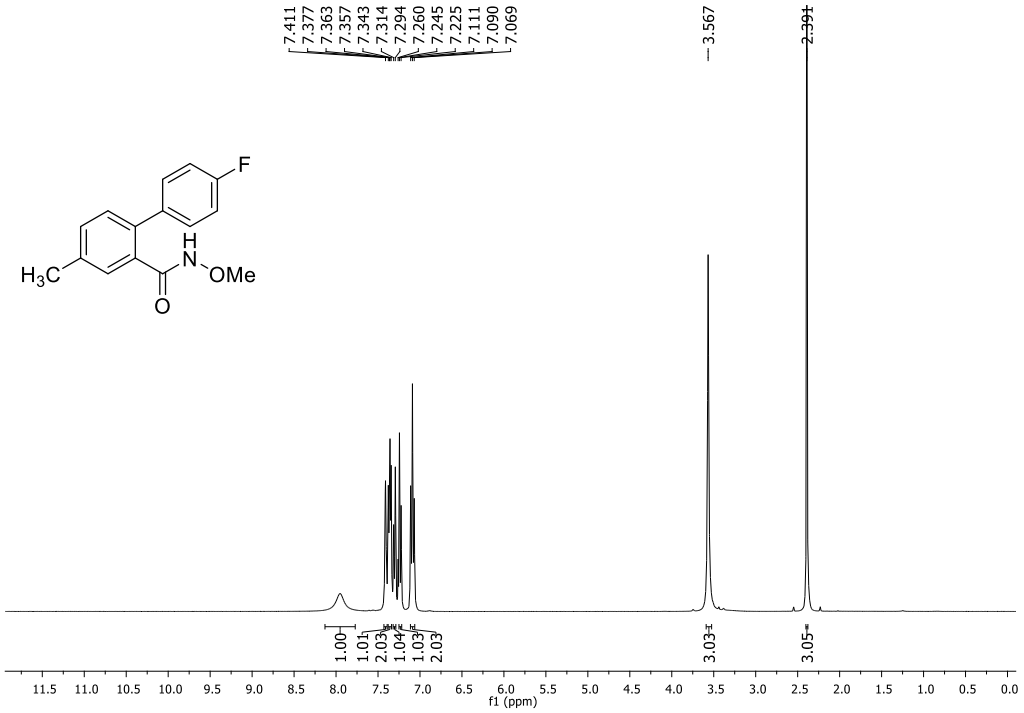

Figure 5.11. ^{1}H NMR spectrum of 4'-Fluoro-N-methoxy-4-methyl-[1,1'-biphenyl]-2-carboxamide (**1j**)

^{13}C{^{1}H} NMR (100 MHz, $CDCl_3$)

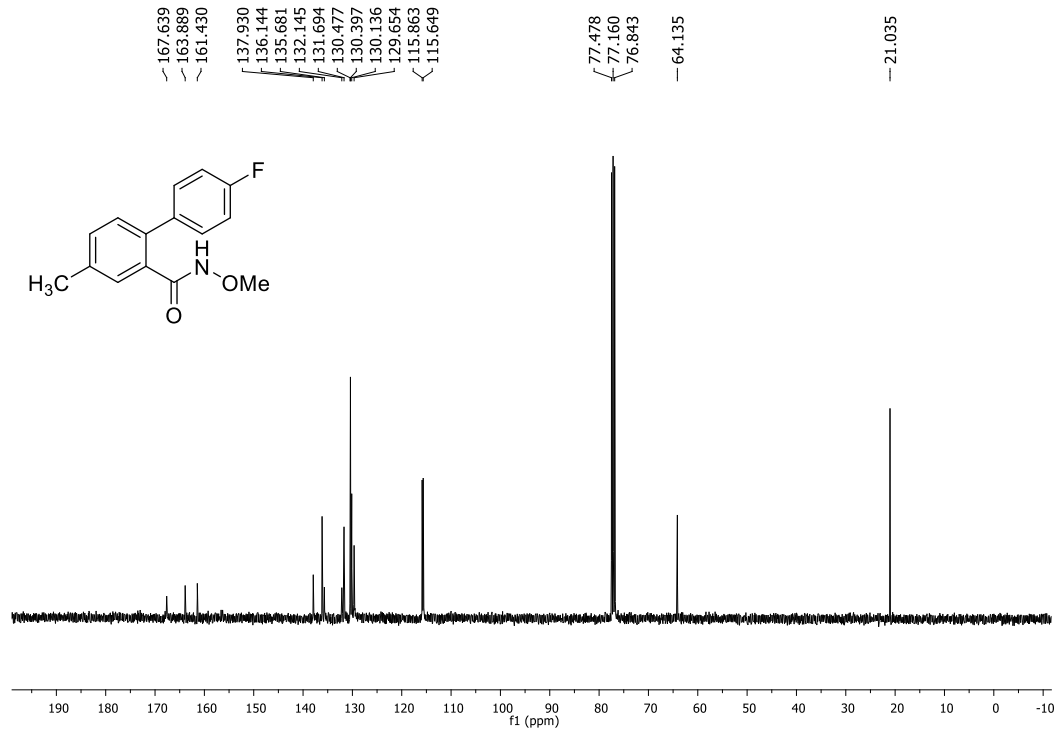

Figure 5.12. ^{13}C{^{1}H}NMR spectrum of 4'-Fluoro-N-methoxy-4-methyl-[1,1'-biphenyl]-2-carboxamide (**1j**)

^{1}H NMR (400 MHz, DMSO-d_6)

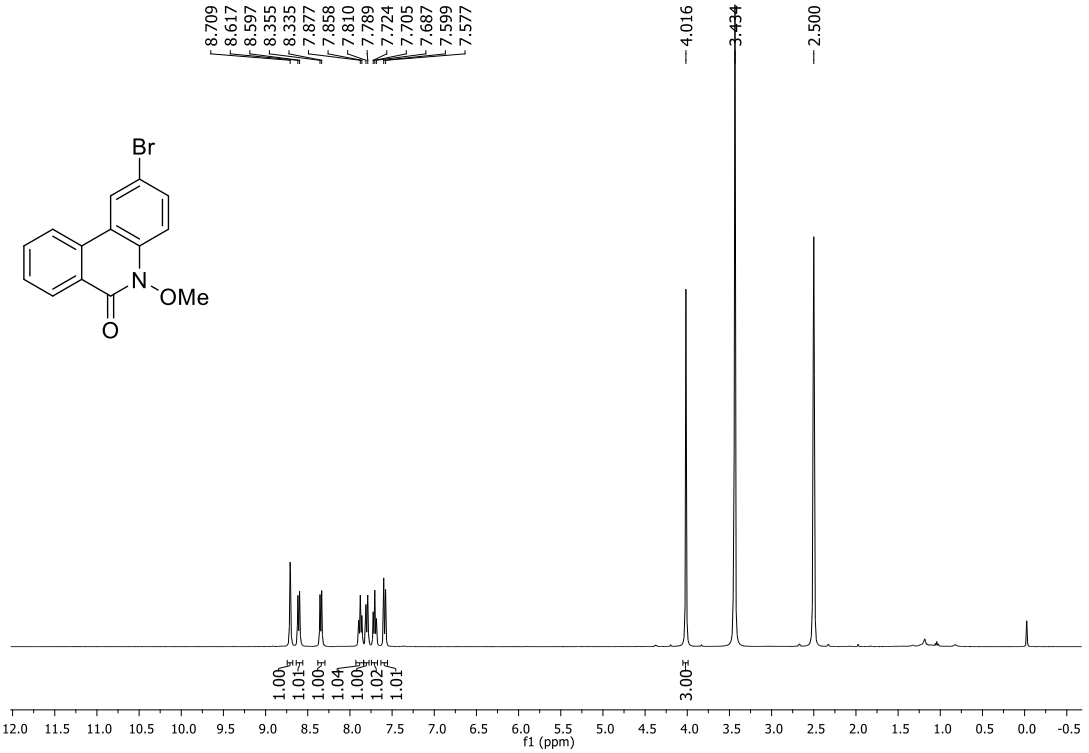

Figure 5.13. ^{1}H NMR spectrum of 2-Bromo-5-methoxyphenanthridin-6(5H)-one (**3a**)

^{13}C{^{1}H} NMR (100 MHz, DMSO-d_6)

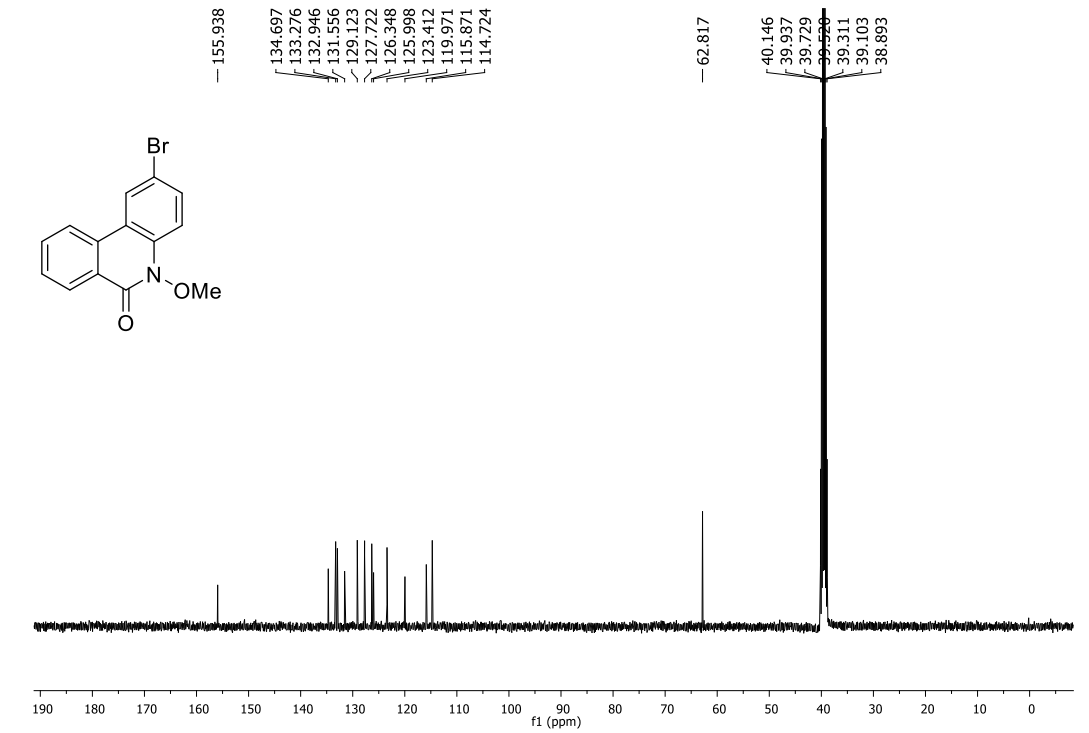

Figure 5.14. ^{13}C{^{1}H} NMR spectrum of 2-Bromo-5-methoxyphenanthridin-6(5H)-one (**3a**)

^{1}H NMR (400 MHz, DMSO-d_6)

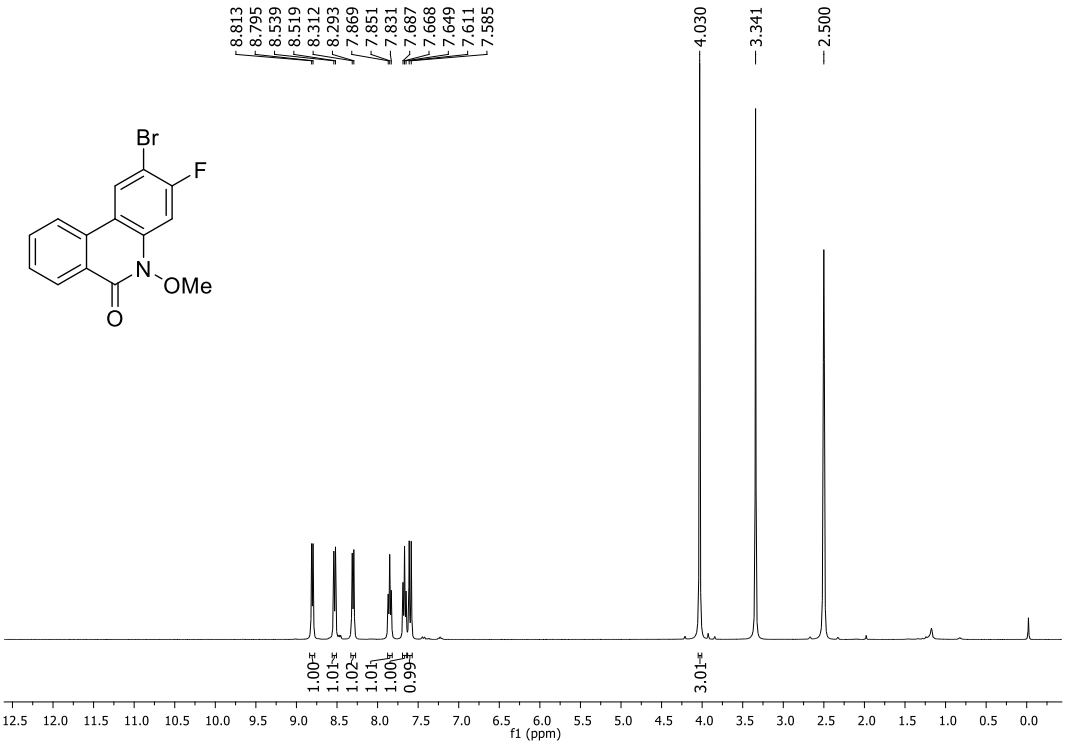

Figure 5.15. ^{1}H NMR spectrum of 2-Bromo-3-fluoro-5-methoxyphenanthridin-6(5H)-one (**3e**)

^{13}C{^{1}H} NMR (100 MHz, DMSO-d_6)

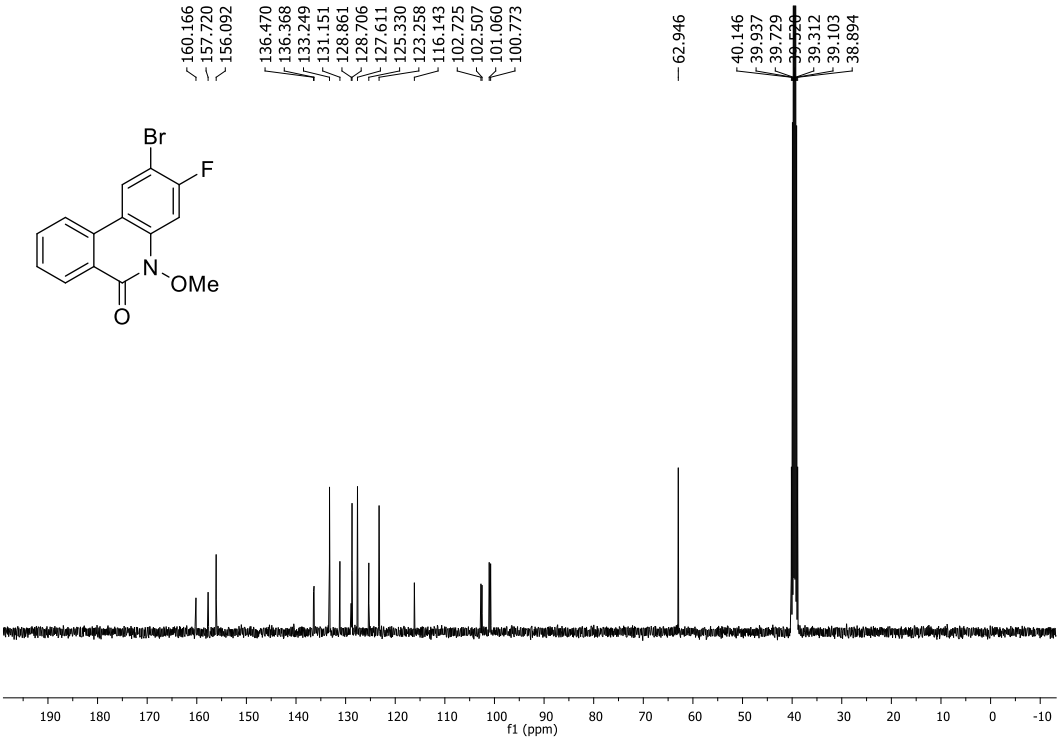

Figure 5.16. ^{13}C{^{1}H} NMR spectrum of 2-Bromo-3-fluoro-5-methoxyphenanthridin-6(5H)-one (**3e**)

^{1}H NMR (400 MHz, $CDCl_3$)

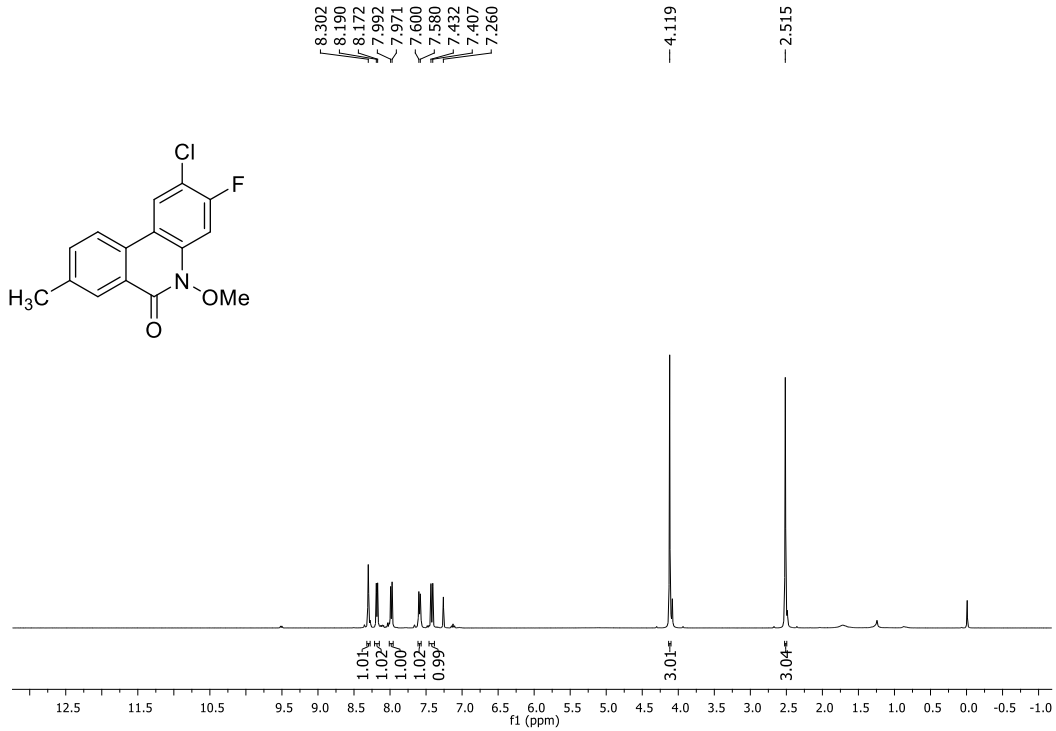

Figure 5.17. ^{1}H NMR spectrum of 2-Chloro-3-fluoro-5-methoxy-8-methylphenanthridin-6(5H)-one **(4j)**

^{13}C{^{1}H} NMR(100 MHz, $CDCl_3$)

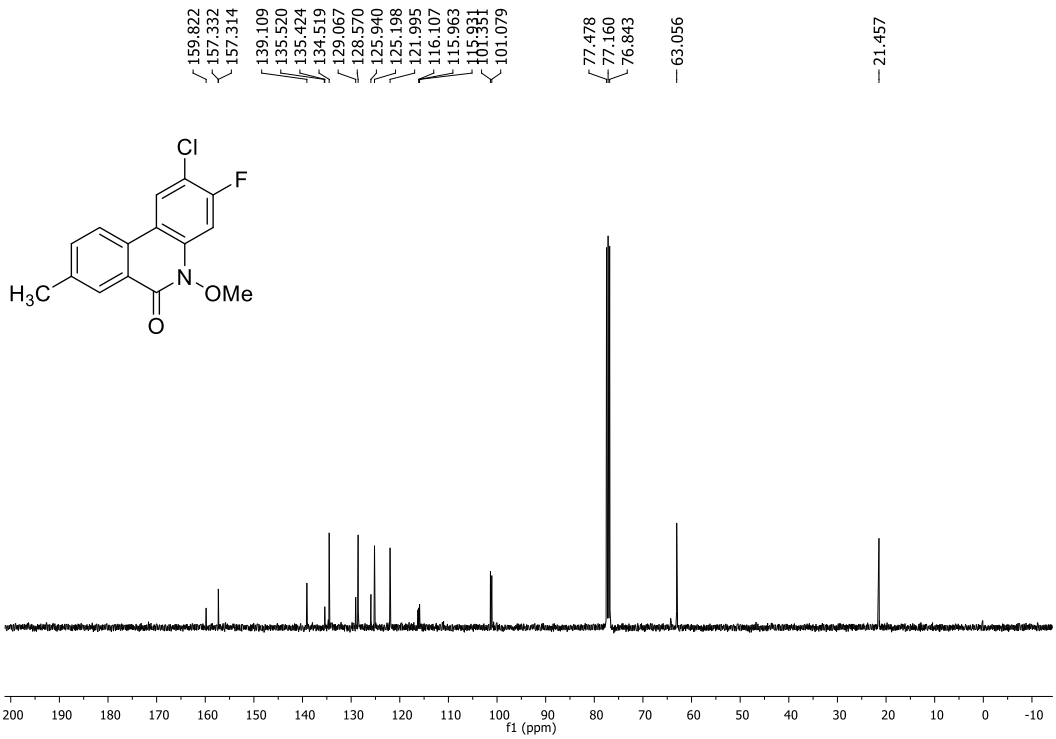

Figure 5.18. ^{13}C{^{1}H} NMR spectrum of 2-Chloro-3-fluoro-5-methoxy-8-methylphenanthridin-6(5H)-one **(4j)**

^{1}H NMR (400 MHz, $CDCl_3$)

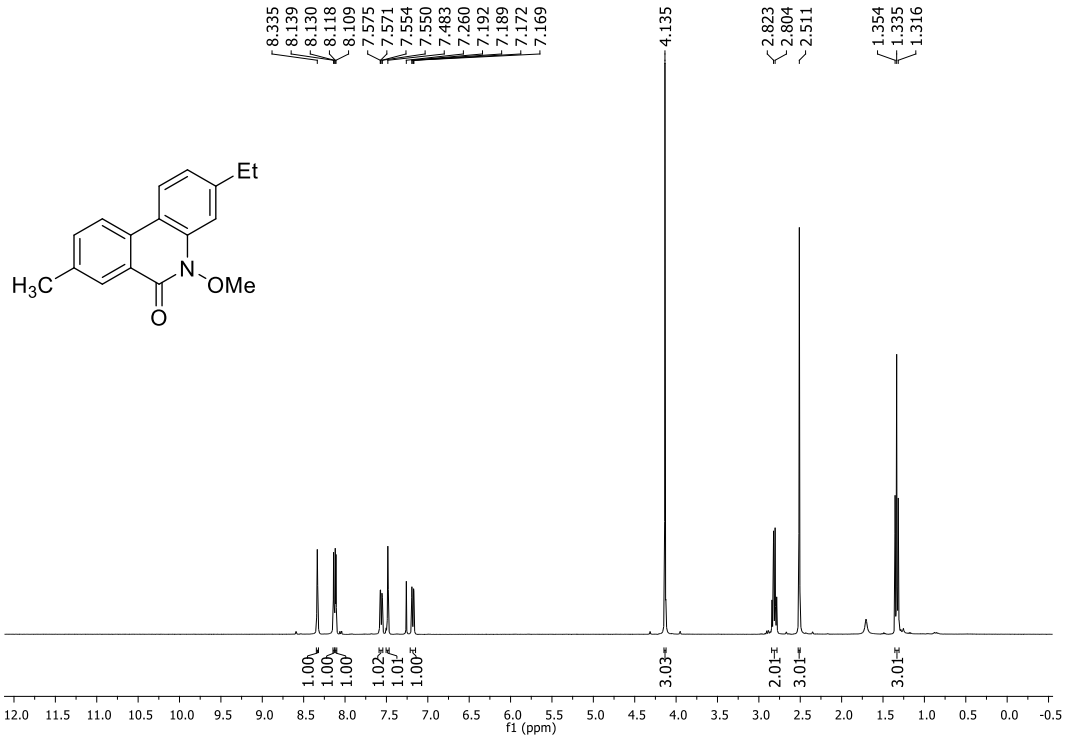

Figure 5.19. ^{1}H NMR spectrum of 3-Ethyl-5-methoxy-8-methylphenanthridin-6(5H)-one (**2k**)

^{13}C{^{1}H} NMR (100 MHz, $CDCl_3$)

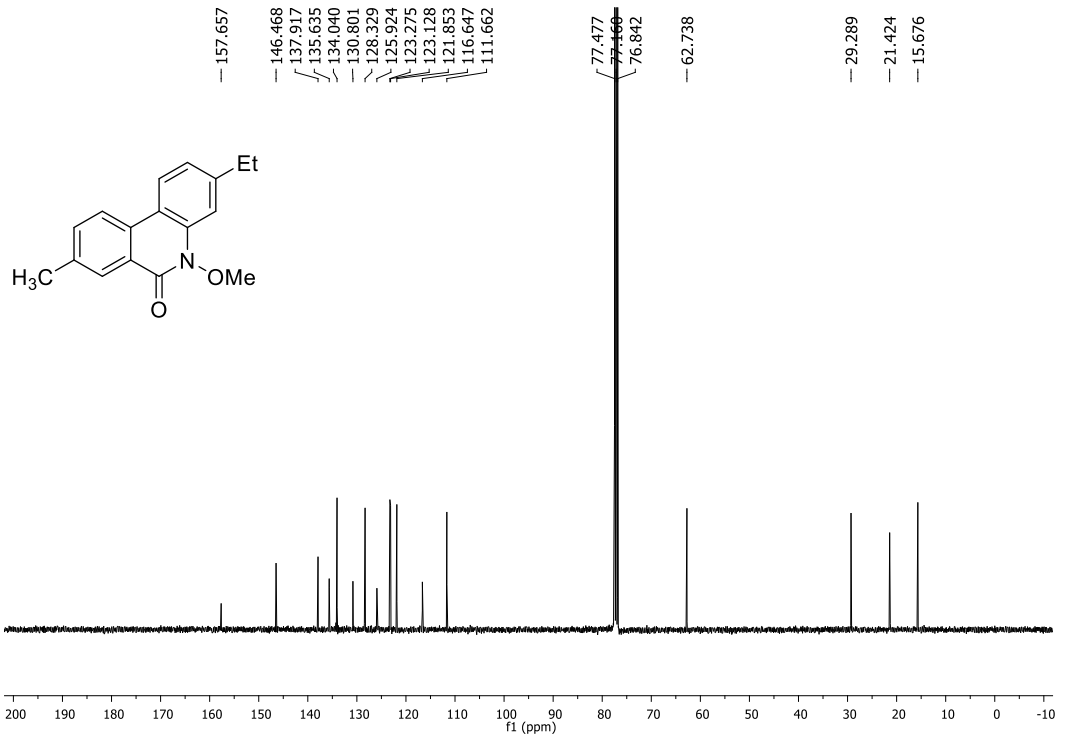

Figure 5.20. ^{13}C{^{1}H} NMR spectrum of 3-Ethyl-5-methoxy-8-methylphenanthridin-6(5H)-one (**2k**)

^{1}H NMR (700 MHz, $CDCl_3$)

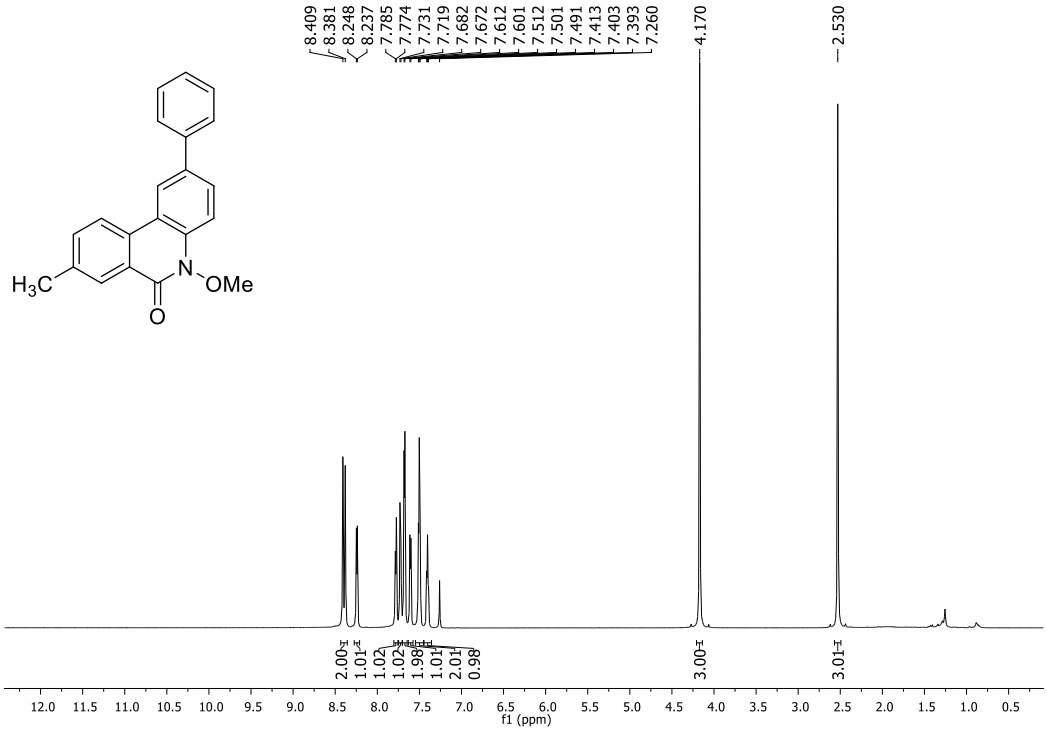

Figure 5.21. ^{1}H NMR spectrum of 5-Methoxy-8-methyl-2-phenylphenanthridin-6(5H)-one (**5**)

^{13}C{^{1}H} NMR (175 MHz, $CDCl_3$)

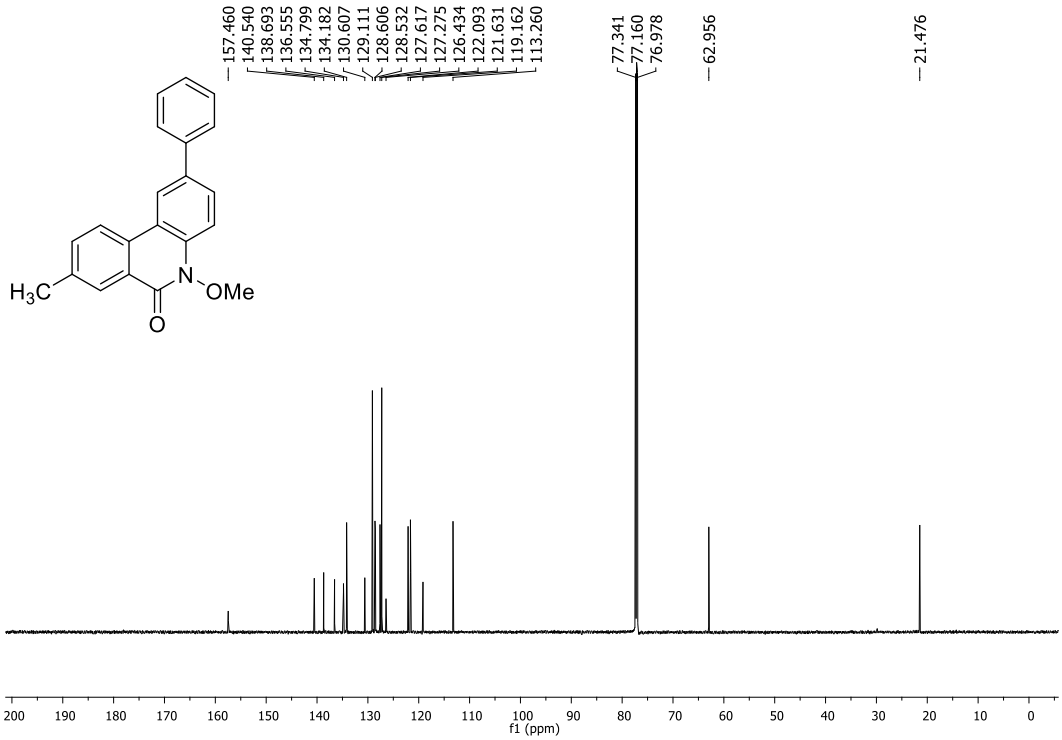

Figure 5.22. ^{13}C{^{1}H} NMR spectrum of 5-Methoxy-8-methyl-2-phenylphenanthridin-6(5H)-one (**5**)

^{1}H NMR (700 MHz, $CDCl_3$)

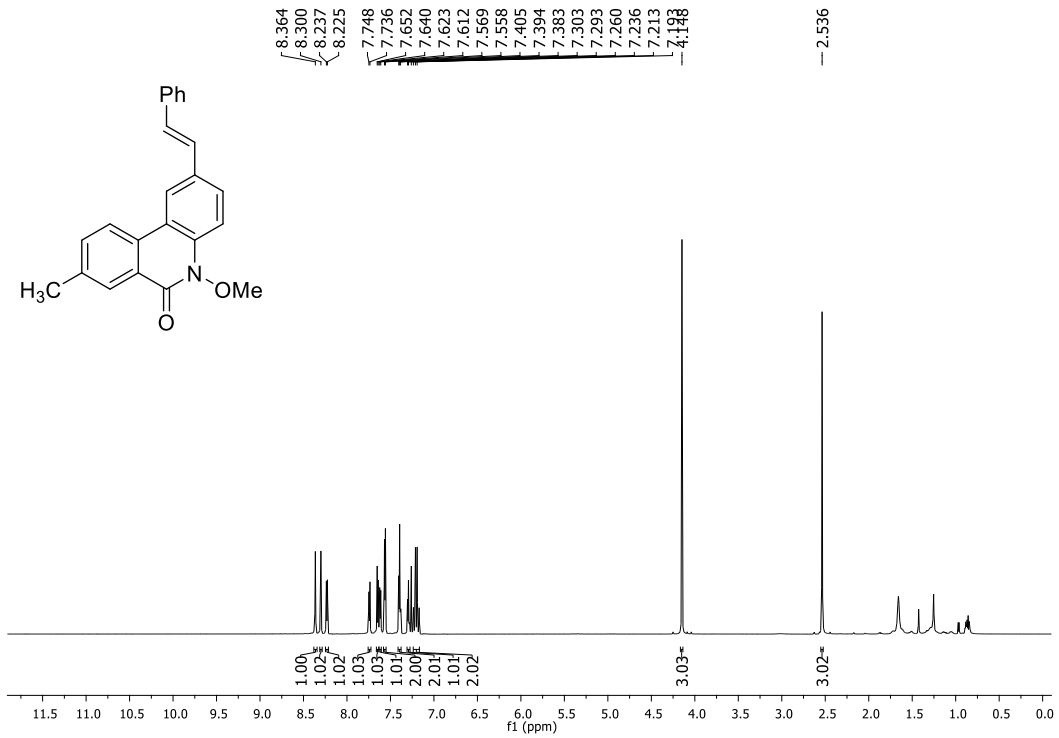

Figure 5.23. ^{1}H NMR spectrum of (E)-5-Methoxy-8-methyl-2-styrylphenanthridin-6(5H)-one (**6**)

^{13}C{^{1}H} NMR (175 MHz, $CDCl_3$)

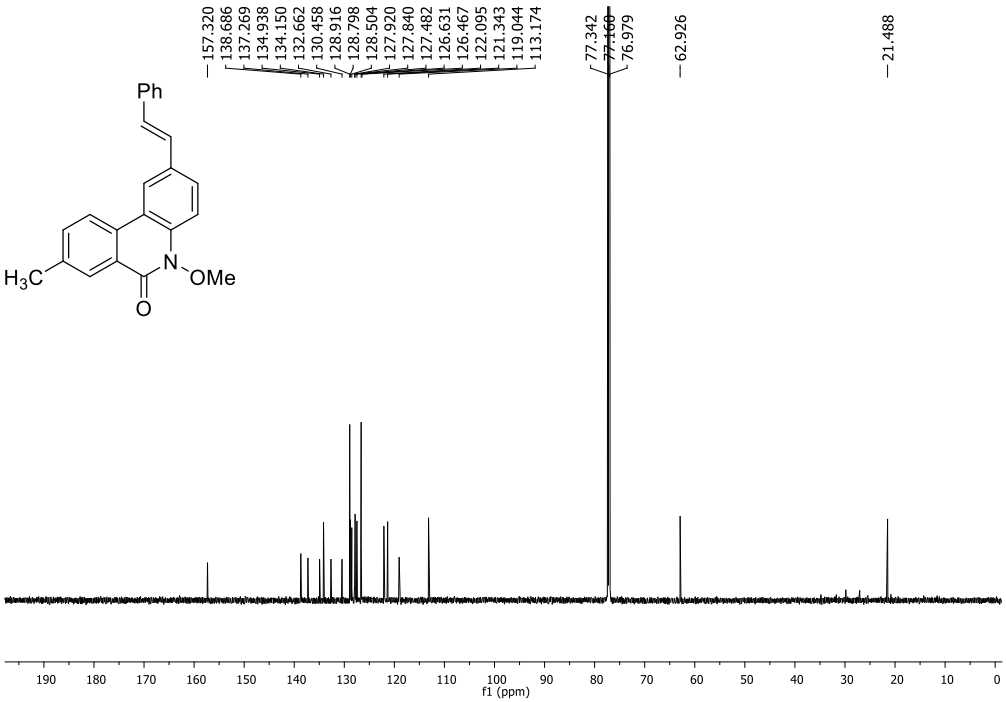

Figure 5.24. ^{13}C{^{1}H} NMR spectrum of (E)-5-Methoxy-8-methyl-2-styrylphenanthridin-6(5H)-one (**6**)

^{1}H NMR (700 MHz, $CDCl_3$)

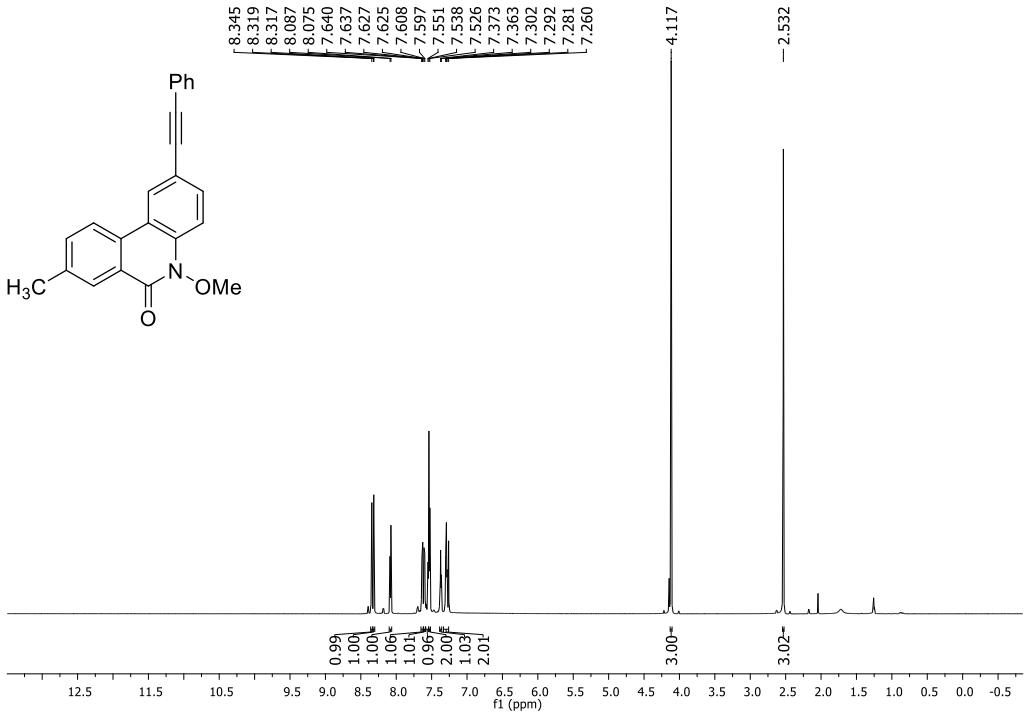

Figure 5.25. ^{1}H NMR spectrum of 5-Methoxy-8-methyl-2-(phenylethynyl)phenanthridin-6(5H)-one (**7**)

^{13}C{^{1}H} NMR (175 MHz, $CDCl_3$)

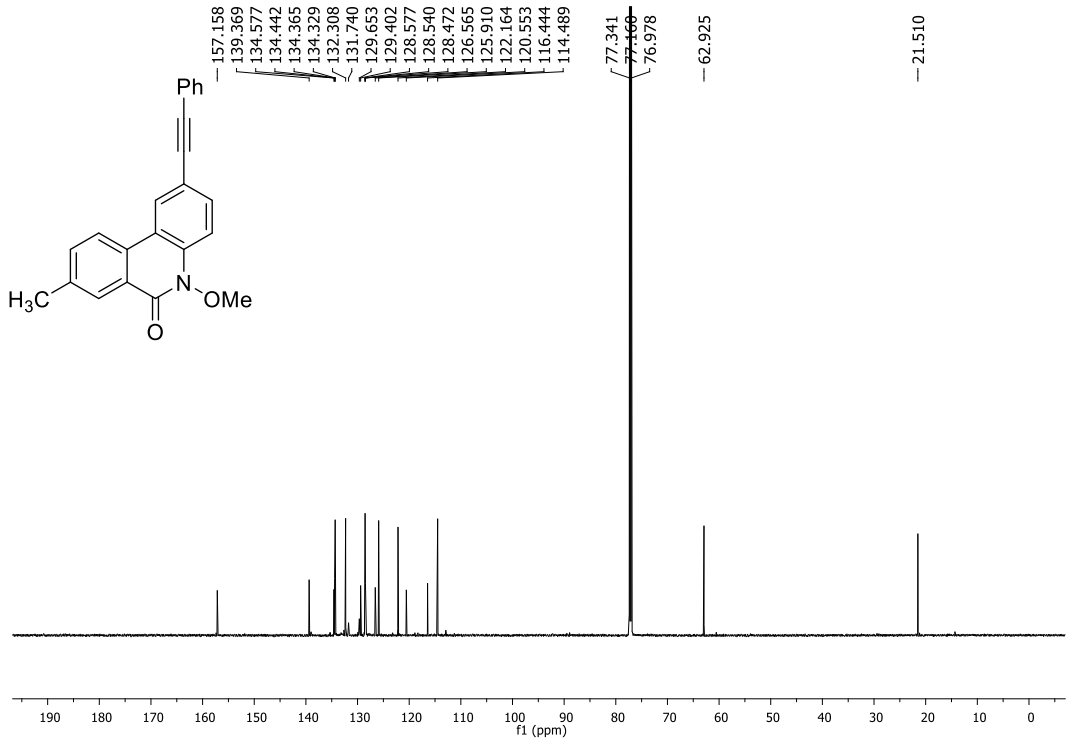

Figure 5.26. ^{13}C{^{1}H} NMR spectrum of 5-Methoxy-8-methyl-2-(phenylethynyl)phenanthridin-6(5H)-one (**7**).

CHAPTER 6

CBr_4 as Halogen Bond Donor Catalyst in Activation of α,β-Unsaturated Ketones

6.1 ABSTRACT

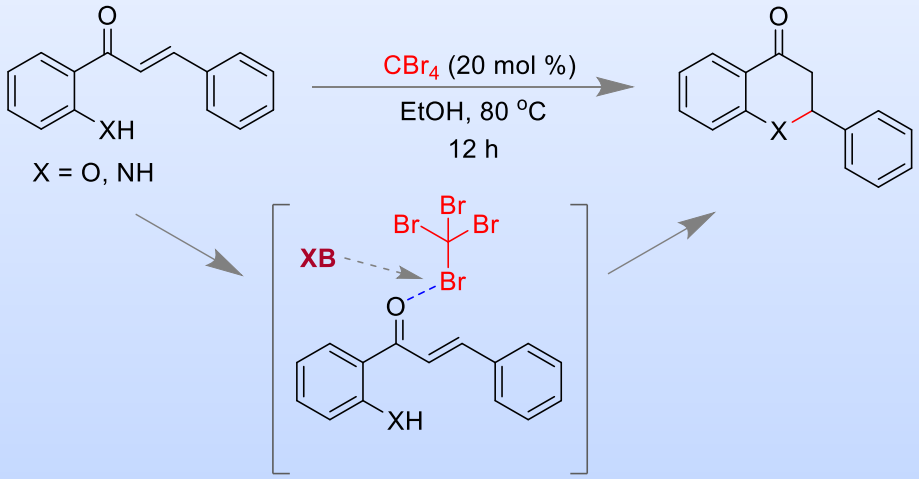

Herein we demonstrated the synthesis of flavanones and aza-flavanones from the 2′-hydroxy and 2′-amino chalcones using CBr_4 as the halogen bond donor catalyst. The catalytic activity of the halogen bond donor catalyst (CBr_4) for this cyclization reaction was supported by the DFT calculations. This metal-free approach offers a wide range of substrates with good to excellent yield under the mild reaction conditions.

6.2 INTRODUCTION

Noncovalent or weak interactions, e.g., halogen-bonding (XB),[1] chalcogen bonding,[2] cation-π bonding,[3] anion-π bonding,[4] hydrogen bonding (H-bonding),[5] have been used extensively in organic synthesis. These interactions were found to assist many chemical reactions either by stabilizing the reaction intermediates or activating the functional groups.[6] Catalysis through XB as an alternative to transition-metal catalysts has recently garnered considerable attention. The XB has its origin in the noncovalent interaction between the nonbonding electrons of the

nucleophilic partner and the antibonding orbital of the halogen atoms.[7] XB has relatively higher strength and directionality, than a typical H-bond.[8] The electron density in the halogen atom in XB is anisotropically distributed leading to the directional nature of the bond parters.[9] The strength of XB lies in the range of 10 - 200 $kJmol^{-1}$,[8] whereas the H-bond is about 1-40 $kJmol^{-1}$.[10] The strength of XB can be tuned by choosing an appropriate XB accepter atom (oxygen, sulfur, etc.) of different polarizability.[1] The XB interaction has widely been exploited in organic synthesis,[11] catalysis,[12, 1] supramolecular chemistry,[13] anion recognition,[14] medicinal chemistry, and chemical biology.[15] Various C-H functionalization reactions in the synthesis of thioethers,[16] 2H-indazoles,[17] α-hydroxy ketones,[18] iodinations of heterocyclic[19] have been well documented in the literature. Additionally, XB-assisted halide-abstraction reactions,[20] Friedel–Crafts reaction,[21] bromocarbocyclization,[22] asymmetric Mannich reactions,[23] and enantioselective Michael addition reaction[24] were also achieved under milder reaction conditions.

The XB-assisted activation of different functional groups is also well-known in organic synthesis.[25] Activation of carbonyl compounds by using chalcogen-bonding,[26] iodoalkyne,[27] and imidazolinium-based XB donor organocatalyst[28] have already been documented. As shown in Scheme 6.1.a, the α,β-unsaturated ketones, or chalcones were synthesized using the CBr_4 as an XB donor organocatalyst.[29] In addition, XB interactions were employed to activate the thioamide group toward the construction of benzoxazoles[30] and benzothiazole derivatives.[31]

The activation of α,β-unsaturated ketones was explored earlier using a chiral amine catalyst to construct an enantioselective carbon-carbon bond.[32] The catalytic activity of molecular iodine was well documented in various organic reactions.[33] The XB catalyzed Friedel-Crafts reactions of furan using a 2,2'-bipyridine-based catalyst is also known.[34] The XB promoted Michael addition reaction using the 2-iodoimidazolinium triflate salt,[35] and

(benz)imidazolium-based XB donors catalysts[36] have been developed to afford the 1,4-addition products.

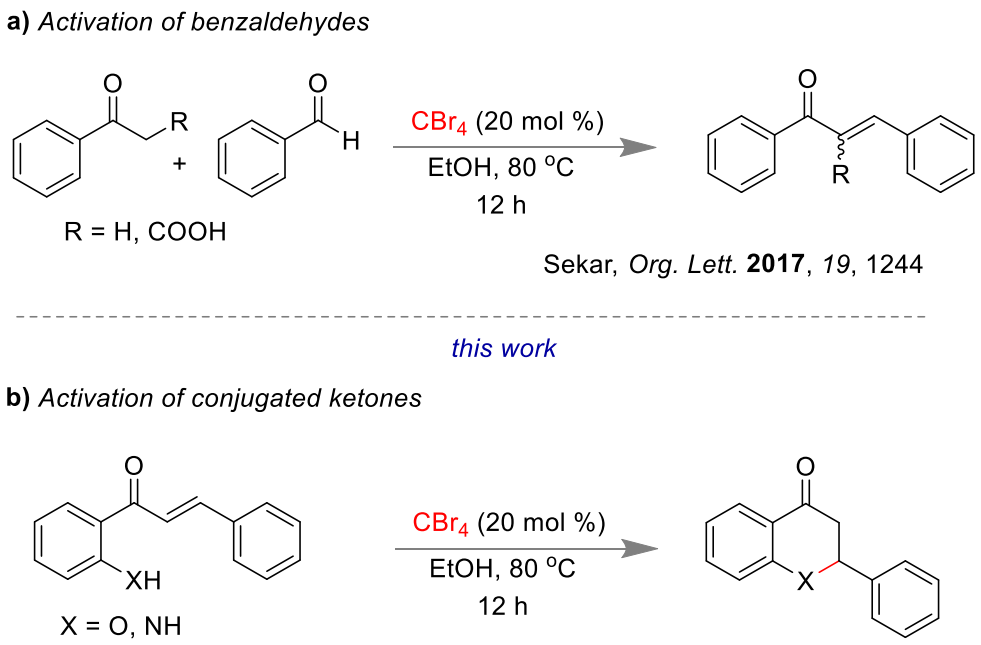

Scheme 6.1. The XB catalysis. a) Activation of benzaldehyde (previous work).[29] b) Activation of α,β-unsaturated ketones.

However, the use of CBr_4 as XB donor catalysts in organic synthesis is still in its infancy. The examples of catalytic CBr_4 mediated reactions are acylation,[37] syntheses of α-amino phosphonates *via* three-component solvent-free strategy,[38] etc. Herein, we report the use of CBr_4 as an XB donor catalyst for an intramolecular -oxa and aza-Michael reactions toward the synthesis of flavanones and aza-flavanones from the corresponding 2′-hydroxy and 2′-amino chalcones (Scheme 6.1.b). It was anticipated that the reaction proceeded through the activation of α,β-unsaturated ketones *via* XB and followed by 6-*endo-trig* cyclization. The participation of halogen bonding is supported by the electronic structure calculations based on the density functional theory (DFT).

6.3 RESULTS AND DISCUSSION

To optimize the reaction condition (Table 1), (*E*)-1-(2-hydroxyphenyl)-3-phenylprop-2-en-1-one (**1a**) was used as the model substrate. When **1a** was treated with 20 mol % of CBr_4 at 80 °C under the neat condition, 2-phenylchroman-4-one (**2a**) was obtained in 79% yield (entry 1). Under the neat reaction condition, the starting compounds were not completely consumed. It was reported that the formation of halogen bonded co-crystals is favored in more polar solvents.[39] We have examined the reactions using polar protic and polar aprotic solvents as well. The desired cyclized product (**2a**) was isolated in 81% yield when 20 mol% of CBr_4 and methanol solvent were used at 80 °C (entry 2). However, the maximum yield of **2a** was observed when 20 mol % of CBr_4 in ethanol at 80 °C was used (entry 3). The yield of **2a** was drastically reduced when polar aprotic solvents such as DMSO and DMF were used (entries 4 and 5). The reaction in THF gave rise the **2a** with 67% yield (entry 6). Moreover, no satisfactory result was observed when the reaction was carried out in acetone (entry 7). The reaction was unsuccessful in the non-polar solvents namely benzene and toluene (entries 8 and 9). Upon varying the catalyst loading from 20 mol % to 10 mol % and 5 mol %, the yield of **2a** was reduced (entries 10 and 11). When the reaction was performed in the absence of CBr_4 in ethanol at 80 °C, a trace amount of the expected product was obtained (entry 12). Therefore 20 mol % of CBr_4 in ethanol at 80 °C was found to be the optimum condition for the reaction (entry 3).

Table 6.1. Optimization of reaction conditions.[a]

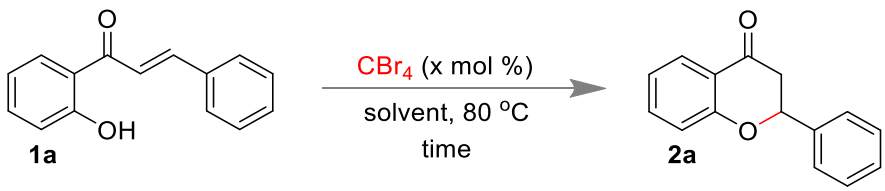

Entry	Catalyst (mol %)	Solvent	Yield (%)[b]
1[c]	CBr_4 (20)	-	79

2	CBr_4 (20)	MeOH	81
3	CBr_4 (20)	EtOH	92
4	CBr_4 (20)	DMSO	45
5	CBr_4 (20)	DMF	32
6	CBr_4 (20)	THF	67
7	CBr_4 (20)	Acetone	38
8	CBr_4 (20)	C_6H_6	--
9	CBr_4 (20)	Toluene	--
10	CBr_4 (10)	EtOH	80
11	CBr_4 (5)	EtOH	76
12	-	EtOH	8

[a]Reaction conditions: 0.44 mmol of **1a** and 0.08 mmol of CBr_4 in 2.0 mL of ethanol solvent at 80 °C for 12 h. [b]Isolated yields. [c] Under neat condition.

Flavanones and their derivatives are important building blocks in many natural products, with significant applications in medicinal chemistry.[40] Some of the flavanones possess anticonvulsant properties.[41] Nitrogen-containing flavonoid derivatives are commonly known as aza-flavanones, famous as selective microRNA inhibitors.[42] Towards the synthesis of flavanones[43] and aza-flavanones[44] many reports are available in the literature. Herein, we have explored the synthesis of flavanones and aza-flavanones using CBr_4 as an XB donor catalyst. Under standard reaction conditions, a series of 2′ -hydroxy chalcones (Figure 6.1) and 2′-amino chalcone (Figure 6.2) derivatives were examined. Compound (*E*)-1-(2-hydroxyphenyl)-3-phenylprop-2-en-1-one (**1a**) led to 2-phenylchroman-4-one (**2a**) with 92% yield.

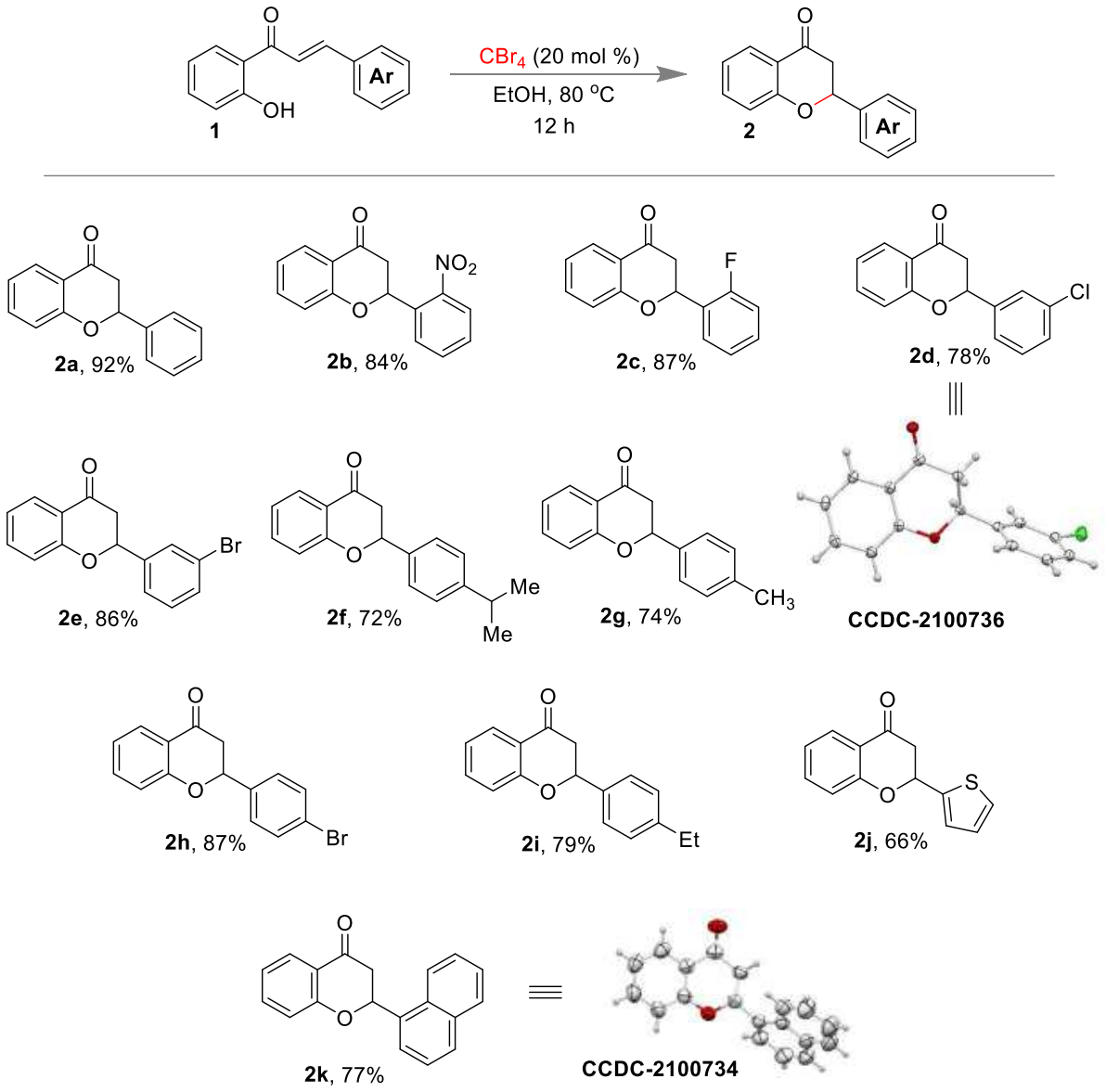

Figure 6.1. The substrate scopes for the synthesis of flavanones.

The substrates with the electron-withdrawing groups such as nitro and fluoro (**1b** and **1c**) at the *ortho*-substituted arene moiety were efficiently converted to corresponding products **2b** and **2c** with 84 and 87% yield, respectively. Similarly, the *meta*-substituted arenes with chloro and bromo groups were also well-tolerated to produce **2d** and **2e** with good yield. On the other hand, isopropyl, methyl, bromo and ethyl substitution at the *p*-position of arene moiety could be transformed into the corresponding products **2f** - **2i** with good yields. Arene moiety containing thiophenyl and naphthyl groups resulted in the **2j** and **2k** with 66 and 77% yield, respectively.

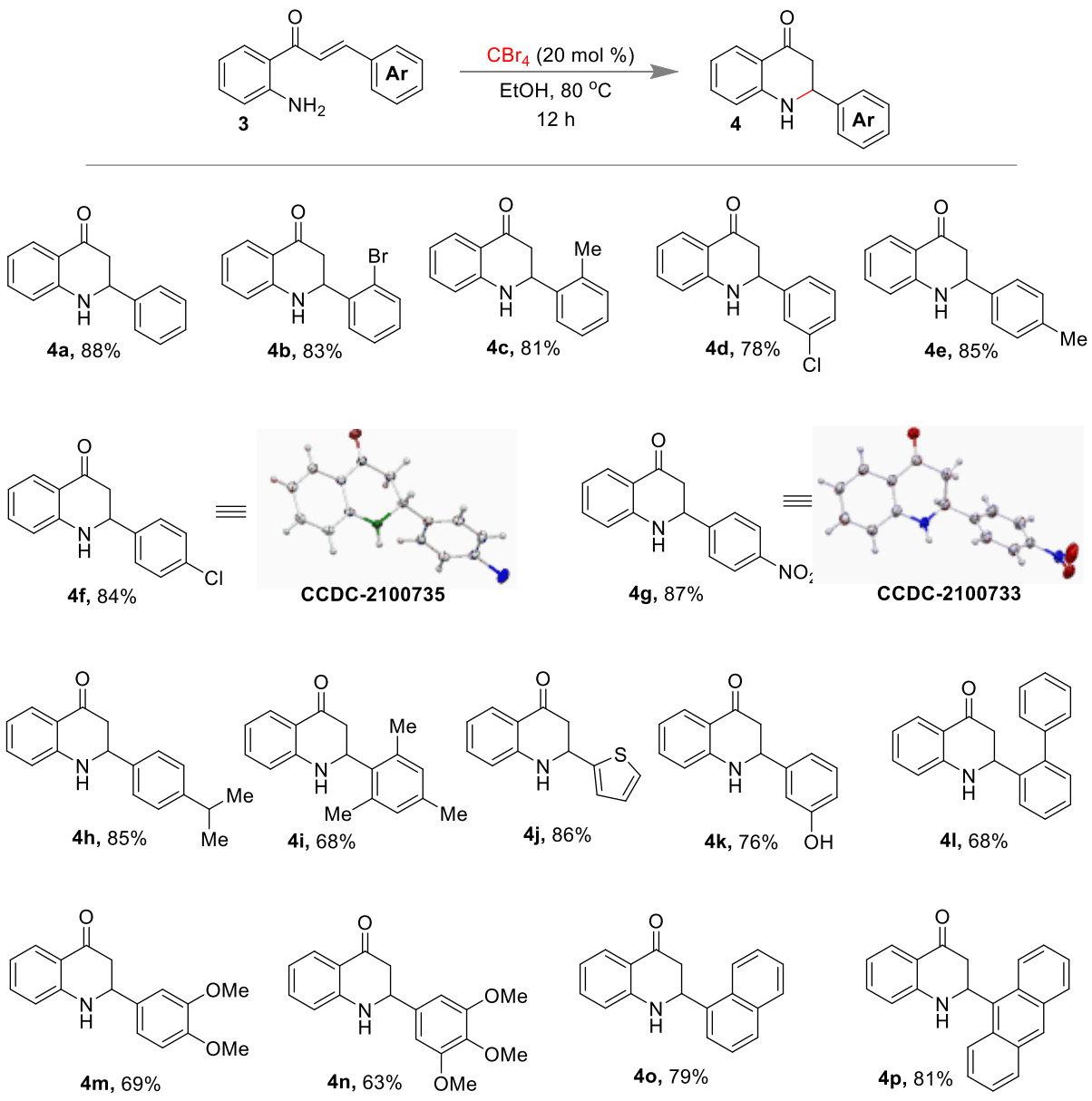

Figure 6.2. The substrate scopes for the synthesis of aza-flavanones.

The synthesis of aza-flavanones from the corresponding 2′-amino chalcones using CBr_4 catalyst (20 mol %) is shown in Figure 6.2. (*E*)-1-(2-aminophenyl)-3-phenylprop-2-en-1-one (**3a**) led to 2-phenyl-2,3-dihydroquinolin-4(1H)-one (**4a**) with 88% yield. Bromo and methyl substitutions at the arene moiety could be transformed into corresponding cyclized products **4b** and **4c** with 83 and 81% yield, respectively. Similarly, the *meta*-chloro- and hydroxy-substituted substrates **3d** and **3k** reacted smoothly to produce **4d** and **4k** with 78% and 76% yields, respectively. On the other hand, *p*-substitution of arene moiety by methyl, chloro,

nitro and isopropyl also led to the product **4e**-**4h** with fair yields. Again, 2-mesityl (**3i**), 2-thienyl (**3j**), and 2-biphenyl (**3l**) substituted derivatives afforded the respective products **4i**, **4j** and **4l** with reasonable yields. Arene moieties with di-methoxy and the tri-methoxy substitution also resulted in the products **4m** and **4n** with 69 and 63% yield, respectively. Similarly, 2-naphthyl and 2-anthracenyl group substituted substrates (**3o** and **3p**) also transformed to the corresponding products (**4o** and **4p**) with 79 and 81% yield, respectively.

We carried out density functional theory (DFT) calculations at the level of M06-2X/ 6-311+G(d,p) using Gaussian 16 software suite[45] to determine the most stable structures of the relevant reactants (2′-aminochalcone or 2′-hydroxychalcone), products (aza-flavanone or flavanone) and corresponding transition states in the presence and absence of CBr_4. The M06-2X functional[33a] implemented in Gaussian 16 incorporates Grimme's D3 empirical dispersion corrections.[46] M06-2X in combination with 6-311+G(d,p) basis set was used in earlier studies as well.[33a] A tolerance of 10^{-10} hartree for the energy change was enforced during all the optimizations. The harmonic frequencies of the optimized structures were analyzed to ascertain the minimum/ saddle-point behavior. The weakly bound complex of 2′-aminochalcone (2′-hydroxychalcone) and CBr_4 was found to be stabilized by 20.20 kJ/mol (22.07 kJ/mol) in comparison to the monomers. These binding energies (D_0) include zero-point energy corrections. These D_0 values are higher than the D_0 for the N...Cl XB interaction (10 kJ/mol) reported by Cavallo et al.[7] This weak interaction between CBr_4 and the carbonyl O of the chalcones is also reflected in the electrostatic potentials (ESP) (Figure 6.3.a) as well as the frontier molecular orbitals (Figure 6.3.b). A significant electron density appears between Br atom of CBr_4 and the carbonyl O atom. The occupied molecular orbital, namely HOMO-2, of the complex between CBr_4 and 2′-aminochalcone is indicative of bonding overlap between -Br and the carbonyl -O.

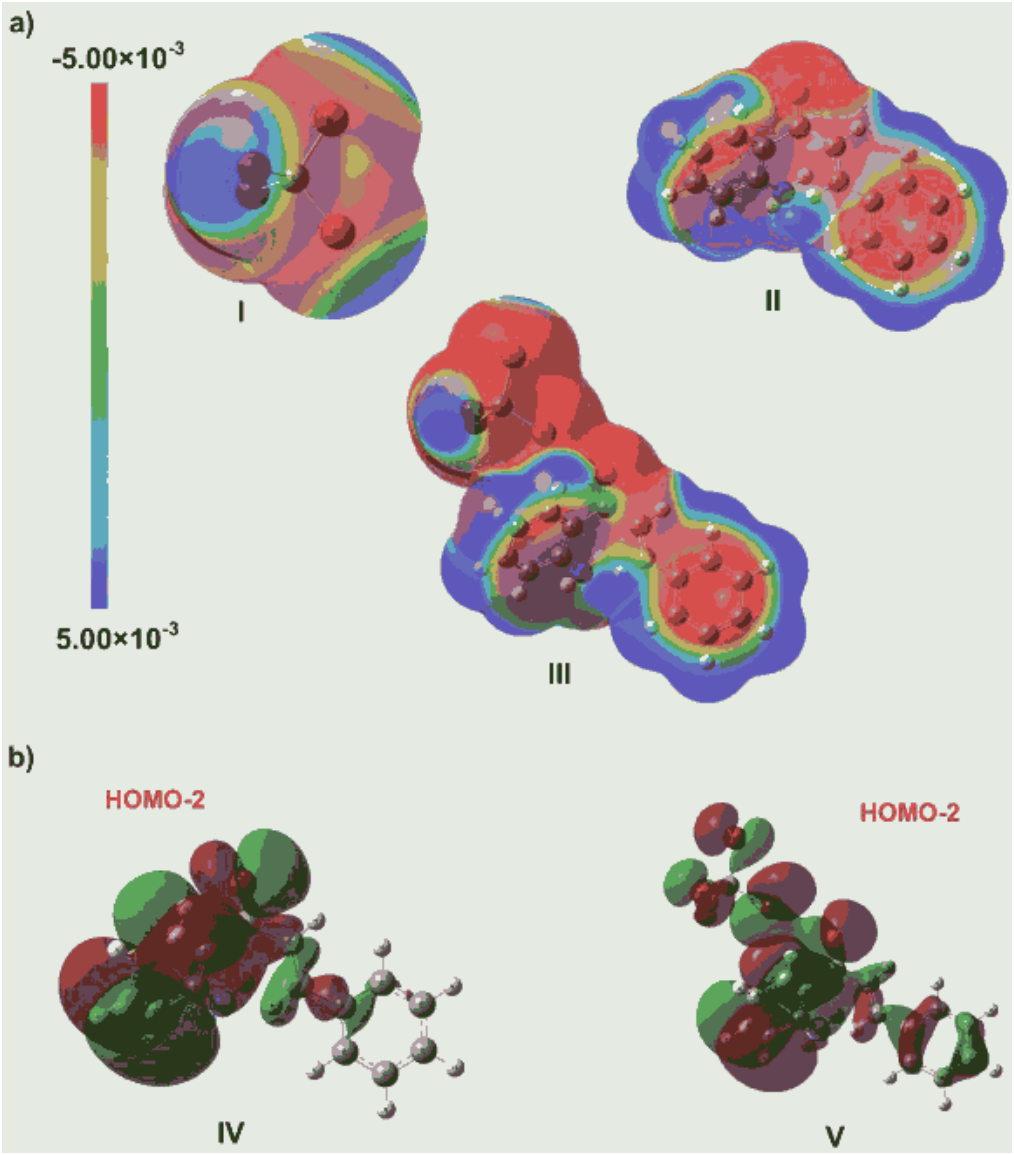

Figure 6.3. a) I, II and III are plots of the electrostatic potential of CBr_4, 2′-aminochalcone, and the complex of 2′-aminochalcone with CBr_4, respectively. b) IV and V are HOMO-2 orbitals of 2′-aminochalcone and 2′-aminochalcone and its complex with CBr_4, respectively.

This is also supported by the natural bond order (NBO) analysis. Mulliken charges on the carbonyl -O in the aminochalcone moiety and the nearest -Br change from -0.23 to -0.24 and 0.07 to 0.04, respectively, upon complexation. The distance (2.86 Å) between the carbonyl -O of 2′-aminochalcone and the -Br atom of CBr_4 in the complex is lower than the sum of the van der Waals radii of -O and -Br (3.35 Å), but higher than the sum of the covalent radii of -O and -Br (2.71 Å). Similarly, the distance (3.10 Å) of carbonyl -O and -Br in the complex of

2′-hydroxychalcone with CBr_4 is higher than the sum of the covalent radii of -O and -Br (2.71 Å), but lower than the sum of the van der Waals radii of -O and -Br (3.35 Å). Moreover, the change in enthalpy (ΔH) upon complexation between 2′-aminochalcone (2′-hydroxychalcone) and CBr_4 was found to be -16.29 kJ/mol (-16.31 kJ/mol). These are comparable to the ΔH value (-18.82 kJ/mol) reported for the XB interaction between I_2 and nitrostyrene.[33a] All these findings point to the XB interaction between the CBr_4 and the chalcones.

In order to understand the catalytic effect of XB between the chalcones and CBr_4 on the intramolecular nucleophilic substitution reactions of the chalcones, we also investigated the transition state (TS) of the reaction in the presence of CBr_4 and without CBr_4 at the same level of theory (Figure 6.4). Each optimized structure of the TSs was found to have a single imaginary frequency. A visual inspection revealed that the normal mode vibration of the TSs corresponding to the imaginary frequency leads to the product. The activation energy was found to be lowered by 6.75 kJ/mol in presence of CBr_4. This lowering of activation barrier is likely to facilitate the reaction.

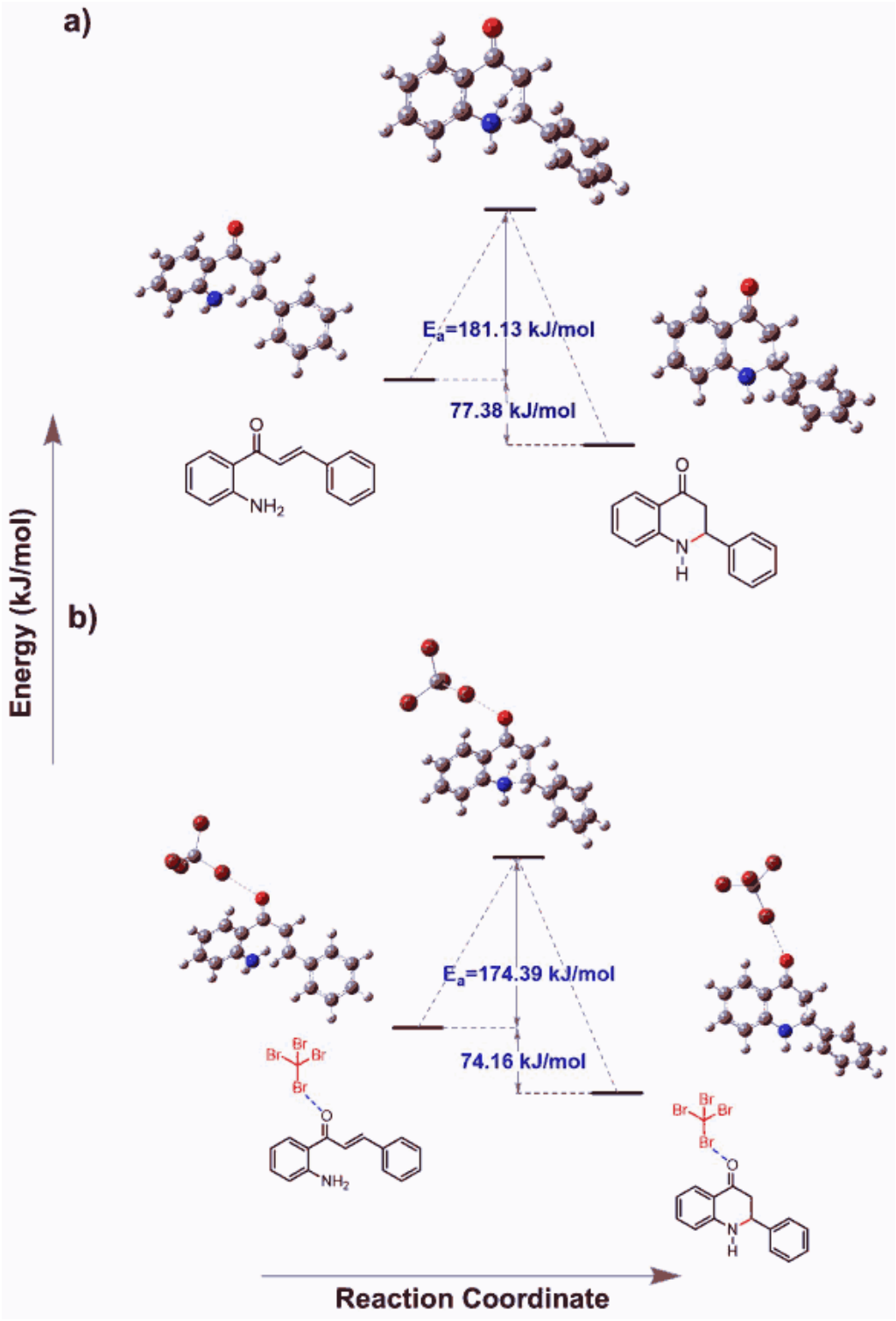

Figure 6.4. a) Schematic diagram for the formation of aza-flavanone in absence of CBr_4. b) Schematic diagram for the formation of aza-flavanone presence of CBr_4.

Under standard conditions, the radical trapping experiment of **1a** with TEMPO failed, and **2a** was obtained in 91% yield (Figure 6.5.a). This indicates that the reaction did not proceed *via*

a radical pathway. Based on the literature report[29, 31] as well as evidences from the experimental and computational observations, a plausible mechanism is proposed in Figure 6.5.b. Initially, the interaction between the oxygen atom of the carbonyl with the bromine atom of CBr_4 (XB donor) leads to the activation of carbonyl oxygen to form the intermediate **A**. Further, the nucleophilic attack of the amine or hydroxyl group results in the formation of cyclized products **B** *via* a 6-*endo-trig* mode of cyclization. Next the enol intermediate **B** was tautomerized to the corresponding flavanones (**2**) or aza-flavanones (**3**).

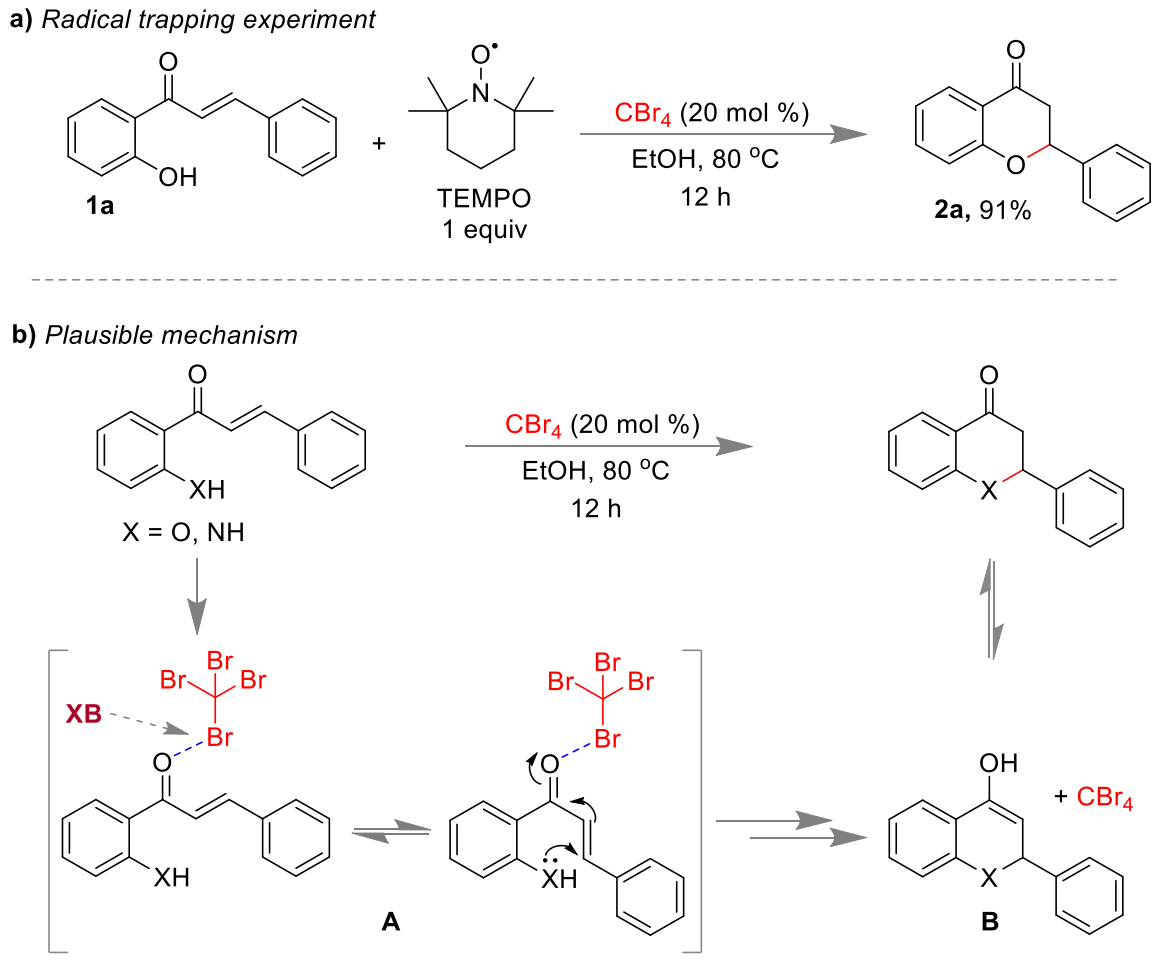

Figure 6.5. a) Radical trapping (control) experiment and b) a plausible mechanism of the reaction.

When the reaction was performed in the absence of CBr_4 in ethanol at 80 °C, a trace amount of the expected product was obtained (entry 12, Table 6.1). Therefore, it is anticipated that the CBr_4 might have played a certain role during the reactions. Next, the reaction was also successful under neat conditions (entry 1, Table 6.1), which indicates that the solvent may not be essential for the reactions. Furthermore, Sekar and co-workers have also shown that the halogen bond donor catalyst (CBr_4) is stable under heating (60 °C) conditions.[29] The literature report also suggests that the formation of halogen bonded co-crystals was one of the favorable processes in more polar solvents than less polar solvents.[39] Contrastingly, relatively poor yields of the products were obtained in the solvents DMSO (entry 4, Table 1) and DMF (entry 5, Table 6.1), which might be due to the formation of strong H-bond by the -OH or -NH_2 groups of the starting compounds and the respective solvents.

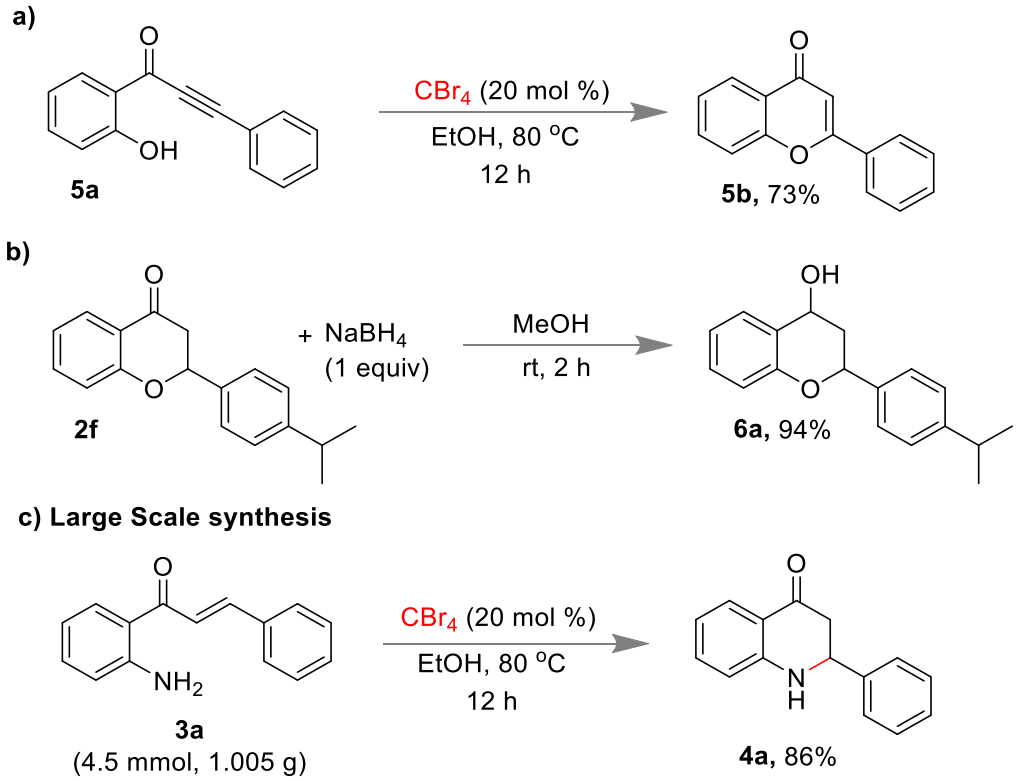

Figure 6.6. Synthetic application.

The methodology was also explored with 1-(2-hydroxyphenyl)-3-phenylprop-2-yn-1-one (**5a**) to synthesize 2-phenyl-4H-chromen-4-one (**5b**) with 73% under standard reaction condition (Figure 6.6.a). In addition, the compound 2-(4-isopropylphenyl)chroman-4-one (**2f**) was reduced with $NaBH_4$ in methanol to deliver the 2-(4-isopropylphenyl)chroman-4-ol (**6a**) with 94% yield (Figure 6.6.b). To extend the synthetic utility of the methodology, a large-scale synthesis by using 4.5 mmol of (*E*)-1-(2-aminophenyl)-3-phenylprop-2-en-1-one (**3a**) was performed. Under the standard reaction condition, the expected cyclized product (**4a**) was obtained in 86% yield (Figure 6.6.c).

6.4. CONCLUSION

In summary, we have demonstrated a simple and efficient strategy toward synthesizing flavanones and aza-flavanones from the corresponding 2′-hydroxy- and 2′-amino-chalcones, respectively. This methodology can offer an excellent guideline for constructing various heterocyclic motifs *via* mild and metal-free reaction conditions. The reaction was catalyzed by XB donor CBr_4 *via* noncovalent interaction. DFT studies also supported the catalytic action of XB. This work provides a link between organic synthesis and supramolecular chemistry. We anticipate that the work presented herein will substantially impact on the research in organic chemistry.

6.5. EXPERIMENTAL SECTION

General Information. Commercially available reagents and solvents were used as received. Column chromatographic purifications of the compounds were performed using silica gel (mesh 230–400, 100-200) and hexane – ethyl acetate solvent mixtures. NMR spectra were recorded on a 400 MHz or 700 MHz instrument at 25 °C. The chemical shift values are reported in parts per million (ppm) with respect to residual trichloromethane (7.26 ppm for ^{1}H and 77.16 ppm for ^{13}C). The peak patterns are designated as follows: s: singlet; d: doublet;

t: triplet; q: quartet; m: multiplet; dd: doublet of doublets; td: triplet of doublets; brs: broad singlet. The coupling constants (*J*) are reported in hertz (Hz). High-resolution mass spectra (HR-MS) were recorded on an ESI-TOF (time of flight) mass spectrometer. Infrared spectral data are reported in wave number (cm^{-1}). FT-IR spectra were recorded after making thin layer of the compounds on the surface of NaCl crystal using dichloromethane. Melting points of the compounds were determined using a digital melting point apparatus and are uncorrected.

General Procedure for the Preparation of 2′-amino or 2′-hydroxy Chalcones.[47]

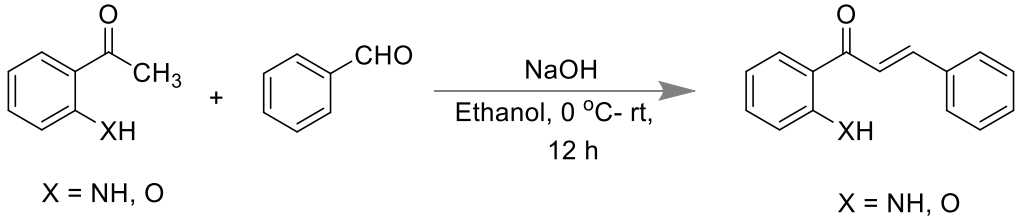

2-Amino and 2-hydroxy chalcone derivatives were synthesized with the help of advanced literature procedure.[47] A round bottom flask containing a magnetic stirring bar was charged with acetophenone derivatives (1 equiv) in ethanol and 50% w/v NaOH (5 mL). Then mixture was kept in 0 °C and corresponding benzaldehyde (1.1 equiv) was added. Then reaction mixture was stirred for 12 h and organic layer was separated by using ethyl acetate. Crude reaction mixture was purified by column chromatography to afford the chalcone derivative as a yellow solid.

Representative Procedure for Synthesis of 2-phenylchroman-4-one

A sealed tube equipped with (*E*)-1-(2-hydroxyphenyl)-3-phenylprop-2-en-1-one (**1a**) (0.44 mmol, 100 mg) and CBr_4 (30 mg, 0.08 mmol) was taken 2 mL ethanol. Then the reaction mixture was placed in preheated oil bath (80 °C) for 12h and reaction was monitored by TLC. After completion of reaction, the crude residue was dried over vacuum and purified by column chromatography to produces the cyclized products.

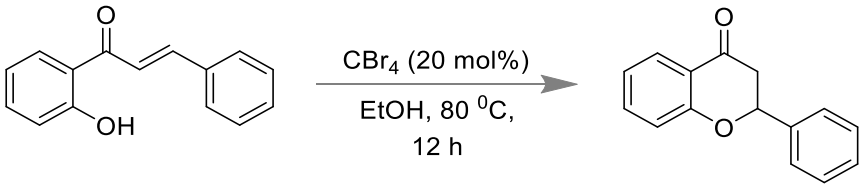

Preparation of 1-(2-hydroxyphenyl)-3-phenylprop-2-yn-1-one (5a).[48]

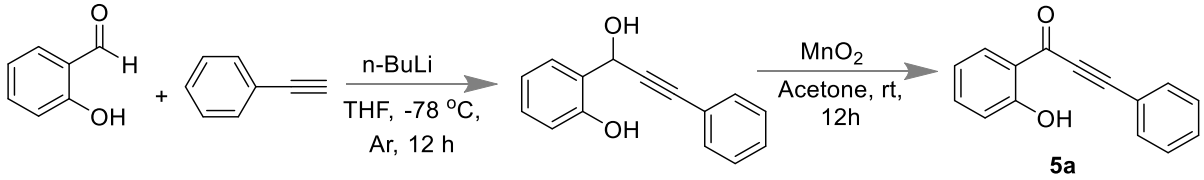

5a

Phenylacetylene (621 µl, 5.65 mmol) was taken in a 15mL dry THF solvent, and then n-butyl lithium (5.65 mmol, 2.3 equiv) was added dropwise at -78 ^oC under Ar atmosphere. The solution was stirred for 1 h at the same temperature. Then the 2-hydroxybenzaldehyde (2.45 mmol, 1 equiv) was added dropwise with continuous stirring at -78 ^oC under Ar atmosphere. The reaction mixture was allowed to stirrer for 2 h at -78 ^oC and followed by 30 min at 0 ^oC. Upon completion of the reactions, the reaction mixture was quenched with saturated aqueous NH_4Cl at 0 °C. The organic layer was extracted with 30 mL (2×15 mL) ethyl acetate and dried over anhydrous Na_2SO_4, and the resulting solution was evaporated to dryness. The crude product was purified by silica gel column chromatography with n-Hexane-EtOAc, to afford the product 2-(1-hydroxy-3-phenylprop-2-yn-1-yl)phenol with 69% yield. Then this product was used for the next step.

In an oven-dried round-bottom flask compound 2-(1-hydroxy-3-phenylprop-2-yn-1-yl)phenol (360 mg, 1.6 mmol, 1.0 equiv) was dissolved in acetone (10 mL) at room temperature and MnO_2 (699 mg, 8.03 mmol, 5 equiv) were added on the reaction vessel. The reaction mixture was stirred for 12h at the same temperature. Upon completion of the reactions (TLC showed complete consumption of starting material), the reaction mixture was filtered using Buchner funnel and washed with dichloromethane. The filtrate was concentrated in vacuo, and the crude product was purified by flash column chromatography with n-Hexane- EtOAc to obtain the 1-(2-hydroxyphenyl)-3-phenylprop-2-yn-1-one (**5a**) with 82% yield.

Preparation of 2-phenyl-4H-chromen-4-one (5b)

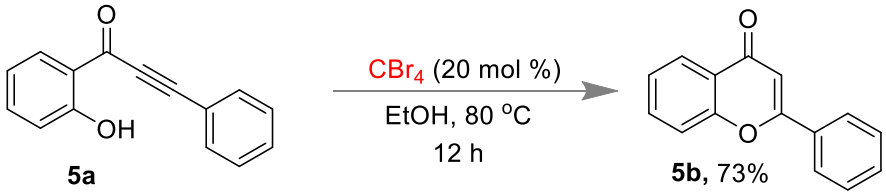

In an oven-dried sealed tube, 1-(2-hydroxyphenyl)-3-phenylprop-2-yn-1-one (**5a**) (0.36 mmol, 80 mg) and CBr_4 (24 mg, 0.07 mmol) was taken 2 mL ethanol. Then the reaction mixture was placed in a preheated oil bath (80 ^oC) for 12h and the reaction was monitored by TLC. After completion of the reaction, the crude residue was dried over vacuum and purified by column chromatography to produce 2-phenyl-4H-chromen-4-one (**5b**) with 73% yield.

Preparation of 2-(4-isopropylphenyl)chroman-4-ol (6a).[49]

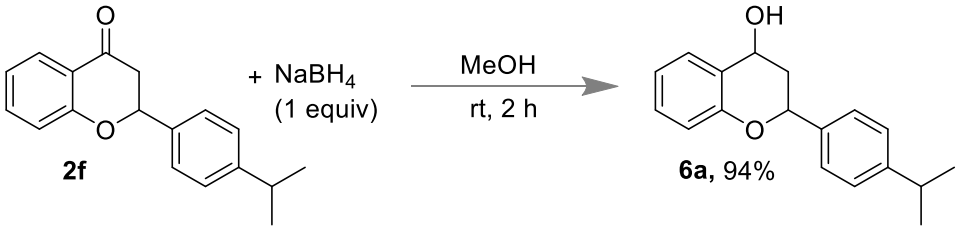

In an oven-dried round bottom flask, sodium borohydride (0.375 mmol, 14 mg) in methanol was charged with a stirred solution of 2-(4-isopropylphenyl)chroman-4-one (**2f**) (100 mg, 0.375 mmol) at 0 ^oC. Then the reaction mixture was stirred at room temperature, typically~ 2h. The progress of the reaction was monitored by thin-layer chromatography (TLC) using ethyl acetate and hexane as eluent. After completion of the reaction, the mixture was concentrated under a vacuum. The crude residue was quenched with 15 ml saturated solution of $NaHCO_3$ and ethyl acetate was added to extract the organic layer. Then the organic layer was dried over anhydrous Na_2SO_4 and the resulting solution was evaporated to dryness. The crude product was purified by silica gel column chromatography with n-Hexane-EtOAc, to afford the product 2-(4-isopropylphenyl)chroman-4-ol (**6a**) with 94% yield.

(*E*)-1-(2-Hydroxyphenyl)-3-phenylprop-2-en-1-one (1a):[50] R_f = 0.50 (hexane/ethyl acetate 19:1); yellow solid; yield 85% (139 mg). ^{1}H NMR (400 MHz, $CDCl_3$) δ 12.82 (s, 1H), 7.95 (d, *J* = 3.2 Hz, 1H), 7.92 (d, *J* = 3.6 Hz, 1H), 7.72 – 7.62 (m, 3H), 7.51 (dd, *J* = 8.0, 7.2 Hz, 1H), 7.46 – 7.42 (m, 3H), 7.04 (d, *J* = 8.4 Hz, 1H), 6.96 (t, *J* = 7.6 Hz, 1H); ^{13}C{^{1}H} NMR (100 MHz, $CDCl_3$) δ 193.9, 163.8, 145.6, 136.5, 134.7, 131.1, 129.8, 129.2, 128.8, 120.3, 120.2, 118.9, 118.8.

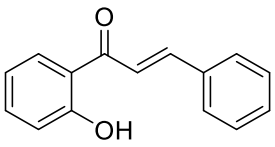

(*E*)-1-(2-Hydroxyphenyl)-3-(2-nitrophenyl)prop-2-en-1-one (1b):[41] R_f = 0.30 (hexane/ethyl acetate 9:1); yellow solid; yield 76% (150 mg). ^{1}H NMR (400 MHz, $CDCl_3$) δ 12.55 (s, 1H), 8.28 (d, *J* = 15.2 Hz, 1H), 8.09 (dd, *J* = 8.0, 0.8 Hz, 1H), 7.89 (dd, *J* = 8.0, 1.2 Hz, 1H), 7.77 – 7.74 (m, 1H), 7.71 (t, J = 7.2 Hz, 1H), 7.62 – 7.56 (m, 1H), 7.55 – 7.52 (m, 1H), 7.51 – 7.47 (m, 1H), 7.04 (dd, *J* = 8.0, 0.8 Hz, 1H), 6.99 – 6.91 (m, 1H); ^{13}C{^{1}H} NMR (100 MHz, $CDCl_3$) δ 193.3, 163.8, 148.8, 140.8, 136.9, 133.7, 131.2, 130.8, 130.0, 129.4, 125.3, 125.2, 119.8, 119.2, 118.9.

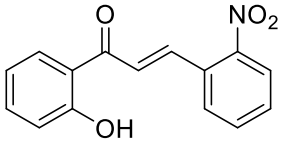

(*E*)-3-(2-Fluorophenyl)-1-(2-hydroxyphenyl)prop-2-en-1-one (1c):[47] R_f = 0.35 (pure hexane); yellow solid; yield 90% (160 mg); ^{1}H NMR (400 MHz, $CDCl_3$) δ 12.76 (s, 1H), 8.00 (d, *J* = 15.6 Hz, 1H), 7.92 (dd, *J* = 8.0, 1.2 Hz, 1H), 7.79 (d, *J* = 15.6 Hz, 1H), 7.66 (td, *J* = 7.6, 1.6 Hz, 1H), 7.55 – 7.47 (m, 1H), 7.44 – 7.38 (m, 1H), 7.22 (t, *J* = 7.6 Hz, 1H), 7.18 – 7.13 (m, 1H), 7.04 (d, *J* = 8.4 Hz, 1H), 6.96 (t, J = 7.6 Hz, 1H); ^{13}C{^{1}H} NMR (100 MHz, $CDCl_3$) δ 193.9, 163.8, 162.1 (d, *J* = 254.9 Hz), 138.4, 136.7, 132.4 (d, *J* = 8.8 Hz), 130.4, 129.9, 124.8, 124.7, 123.1 (d, *J* = 8.1 Hz), 122.9, 120.1, 118.9 (d, *J* = 26.7 Hz), 116.6 (d, *J* = 21.9 Hz).

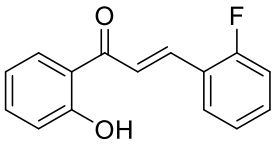

(*E*)-3-(3-Chlorophenyl)-1-(2-hydroxyphenyl)prop-2-en-1-one (1d):[47] R_f = 0.35 (pure hexane); yellow solid; yield 92% (174 mg). ^{1}H NMR (400 MHz, $CDCl_3$) δ 12.71 (s, 1H), 7.90 (dd, *J* = 8.0, 1.2 Hz, 1H), 7.82 (d, *J* = 15.6 Hz, 1H), 7.66 – 7.60 (m, 2H), 7.53 – 7.47 (m, 2H), 7.42 – 7.37 (m, 1H), 7.35 (d, *J* = 8.0 Hz, 1H), 7.05 – 7.00 (m, 1H), 6.98 – 6.92 (m, 1H); ^{13}C{^{1}H} NMR (100 MHz, $CDCl_3$) δ 193.5, 163.8, 143.8, 136.8, 136.5, 135.2, 130.8, 130.4, 129.8, 128.2, 127.1, 121.6, 120.0, 119.1, 118.8.

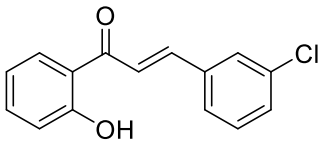

(*E*)-3-(3-Bromophenyl)-1-(2-hydroxyphenyl)prop-2-en-1-one (1e):[50] R_f = 0.50 (hexane/ethyl acetate 19:1); yellow solid; yield 70% (158 mg). ^{1}H NMR (400 MHz, $CDCl_3$) δ 12.70 (s, 1H), 7.91 (dd, *J* = 8.0, 1.6 Hz, 1H), 7.84 – 7.78 (m, 2H), 7.62 (d, *J* = 15.6 Hz, 1H), 7.57 – 7.53 (m, 2H), 7.53 – 7.48 (m, 1H), 7.30 (t, *J* = 8.0 Hz, 1H), 7.03 (dd, *J* = 8.4, 1.2 Hz, 1H), 6.97 – 6.93 (m, 1H); ^{13}C{^{1}H} NMR (100 MHz, $CDCl_3$) δ 193.5, 163.8, 143.7, 136.8, 136.8, 133.7, 131.1, 130.7, 129.8, 127.6, 123.3, 121.6, 120.0, 119.1, 118.8.

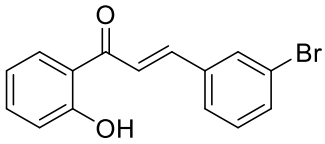

(*E*)-1-(2-Hydroxyphenyl)-3-(4-isopropylphenyl)prop-2-en-1-one (1f):[51] R_f = 0.45 (pure hexane); yellow solid; yield 75% (146 mg). ^{1}H NMR (400 MHz, $CDCl_3$) δ 12.88 (s, 1H), 7.95 – 7.90 (m, 2H), 7.65 – 7.62 (m, 1H), 7.61 – 7.59 (m, 2H), 7.52 – 7.47 (m, 1H), 7.30 (d, *J* = 8.4 Hz, 2H), 7.03 (dd, *J* = 8.4, 1.2 Hz, 1H), 6.98 – 6.91 (m, 1H), 3.00 – 2.92 (m, 1H), 1.29 (s, 3H), 1.28 (s, 3H); ^{13}C{^{1}H} NMR (100 MHz, $CDCl_3$) δ 193.9, 163.7, 152.6, 145.7, 136.4, 132.4, 129.8, 129.0, 127.3, 120.2, 119.3, 118.9, 118.8, 34.3, 23.9 (×2).

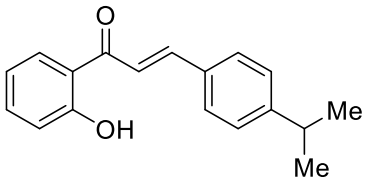

(*E*)-1-(2-Hydroxyphenyl)-3-(p-tolyl)prop-2-en-1-one (1g):[50] R_f = 0.45 (pure hexane); yellow solid; yield 88% (154 mg). ^{1}H NMR (400 MHz, $CDCl_3$) δ 12.87 (s, 1H), 7.92 – 7.90 (m, 1H), 7.88 (d, *J* = 8.4 Hz, 1H), 7.60 (d, *J* = 15.2 Hz, 1H), 7.55 (d, *J* = 8.0 Hz, 2H), 7.50 – 7.45 (m, 1H), 7.25 – 7.20 (m, 2H), 7.03 – 7.00 (m, 1H), 6.96 – 6.89 (m, 1H), 2.39 (s, 3H); ^{13}C{^{1}H} NMR (100 MHz, $CDCl_3$) δ 193.9, 163.7, 145.7, 141.7, 136.4, 132.0, 129.9, 129.7, 128.8, 120.2, 119.1, 118.9, 118.7, 21.7.

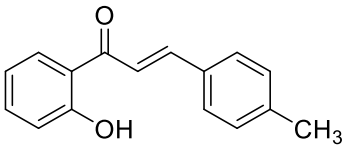

(*E*)-3-(4-Bromophenyl)-1-(2-hydroxyphenyl)prop-2-en-1-one (1h):[50] R_f = 0.25 (pure hexane); yellow solid; yield 92% (205 mg). ^{1}H NMR (400 MHz, $CDCl_3$) δ 12.76 (s, 1H), 7.91 (d, *J* = 8.0 Hz, 1H), 7.85 (d, *J* = 15.6 Hz, 1H), 7.64 (d, *J* = 15.6 Hz, 1H), 7.57 (d, *J* = 8.4 Hz, 2H), 7.53 (s, 1H), 7.50 (d, *J* = 8.0 Hz, 2H), 7.04 (d, *J* = 8.4 Hz, 1H), 6.95 (t, *J* = 7.6 Hz, 1H); ^{13}C{^{1}H} NMR (100 MHz, $CDCl_3$) δ 193.6, 163.8, 144.1, 136.7, 133.6, 132.4, 130.1, 129.8, 125.4, 120.8, 120.0, 119.1, 118.8.

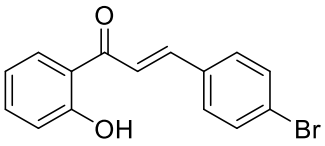

(*E*)-3-(4-Ethylphenyl)-1-(2-hydroxyphenyl)prop-2-en-1-one (1i):[52] R_f = 0.45 (hexane/ethyl acetate 19:1); yellow solid; yield 86% (159 mg). ^{1}H NMR (400 MHz, $CDCl_3$) δ 12.89 (s, 1H), 7.93 – 7.89 (m, 1H), 7.90 – 7.87 (m, 1H), 7.61 (d, *J* = 15.6 Hz, 1H), 7.59 – 7.56 (m, 2H), 7.49 – 7.44 (m, 1H), 7.26 (s, 1H), 7.24 (s, 1H), 7.02 (dd, *J* = 8.4, 1.2 Hz, 1H), 6.95 – 6.89 (m, 1H), 2.68 (q, *J* = 7.6 Hz, 2H), 1.25 (t, *J* = 7.6 Hz, 3H); ^{13}C{^{1}H} NMR (100 MHz, $CDCl_3$) δ 193.9, 163.7, 147.9, 145.7, 136.4, 132.2, 129.7, 128.9, 128.7, 120.2, 119.2, 118.9, 118.7, 28.9, 15.4.

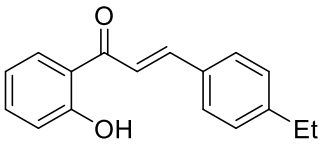

(*E*)-1-(2-Hydroxyphenyl)-3-(thiophen-2-yl)prop-2-en-1-one (1j):[50] R_f = 0.60 (hexane/ethyl acetate 19:1); yellow solid; yield 88% (149 mg); ^{1}H NMR (400 MHz, $CDCl_3$) δ 12.85 (s, 1H), 8.05 (d, *J* = 15.2 Hz, 1H), 7.88 (dd, *J* = 8.0, 1.2 Hz, 1H), 7.52 – 7.46 (m, 2H), 7.44 (d, *J* = 15.2 Hz, 1H), 7.40 (d, *J* = 3.6 Hz, 1H), 7.13 – 7.09 (m, 1H), 7.06 – 6.99 (m, 1H), 6.99 – 6.92 (m, 1H); ^{13}C{^{1}H} NMR (100 MHz, $CDCl_3$) δ 193.3, 163.7, 140.3, 137.9, 136.5, 132.9, 129.7, 128.7, 120.1, 118.9, 118.8.

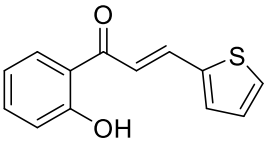

(*E*)-1-(2-Hydroxyphenyl)-3-(naphthalen-1-yl)prop-2-en-1-one (1k):[50] R_f = 0.40 (pure hexane); white solid; yield 89% (178 mg). ^{1}H NMR (400 MHz, $CDCl_3$) δ 12.87 (s, 1H), 8.79 (d, *J* = 15.2 Hz, 1H), 8.28 (d, *J* = 8.4 Hz, 1H), 7.99 – 7.94 (m, 2H), 7.93 – 7.89 (m, 2H), 7.75 (d, *J* = 15.2 Hz, 1H), 7.64 – 7.59 (m, 1H), 7.58 – 7.54 (m, 2H), 7.54 – 7.49 (m, 1H), 7.07 (dd, *J* = 8.4, 1.2 Hz, 1H), 7.00 – 6.92 (m,1H); ^{13}C{^{1}H} NMR (100 MHz, $CDCl_3$) δ 193.7, 163.9, 142.5, 136.6, 133.9, 132.2, 131.9, 131.4, 129.9, 128.9, 127.3, 126.6, 125.6, 125.5, 123.6, 122.9, 120.2, 119.1, 118.8.

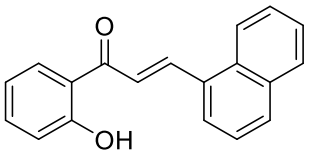

(*E*)-1-(2-Aminophenyl)-3-phenylprop-2-en-1-one (3a):[53] R_f = 0.45 (hexane/ethyl acetate 9:1); yellow solid; yield 93% (154 mg). ^{1}H NMR (400 MHz, $CDCl_3$) δ 7.87 (dd, *J* = 8.4, 1.2 Hz, 1H), 7.75 (d, *J* = 15.6 Hz, 1H), 7.67 – 7.63 (m, 2H), 7.60 (s, 1H), 7.45 – 7.38 (m, 3H), 7.32 – 7.27 (m, 1H), 6.73 – 6.67 (m, 2H), 6.34 (s, 2H); ^{13}C{^{1}H} NMR (100 MHz, $CDCl_3$) δ 191.8, 151.1, 143.1, 135.4, 134.4, 131.2, 130.2, 129.0, 128.4, 123.3, 119.2, 117.4, 116.0.

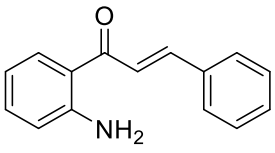

(*E*)-1-(2-Aminophenyl)-3-(2-bromophenyl)prop-2-en-1-one (3b):[44] R_f = 0.50 (hexane/ethyl acetate 4:1); yellow solid; yield 86% (192 mg); ^{1}H NMR (400 MHz, $CDCl_3$) δ

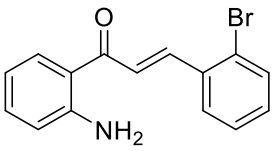

8.07 (d, *J* = 15.6 Hz, 1H), 7.85 (d, *J* = 8.0 Hz, 1H), 7.72 (dd, *J* = 8.0, 1.2 Hz, 1H), 7.64 (d, *J* = 8.0 Hz, 1H), 7.53 (d, *J* = 15.6 Hz, 1H), 7.35 (t, *J* = 7.6 Hz, 1H), 7.32 – 7.27 (m, 1H), 7.26 – 7.20 (m, 1H), 6.69 (t, *J* = 8.0 Hz, 2H), 6.37 (s, 2H); ^{13}C{^{1}H} NMR (100 MHz, $CDCl_3$) δ 191.5, 151.3, 141.4, 135.6, 134.6, 133.6, 131.3, 131.1, 127.9, 127.8, 126.2, 125.8, 118.9, 117.5, 116.0.

(*E*)-1-(2-Aminophenyl)-3-(o-tolyl)prop-2-en-1-one (3c):[44] R_f = 0.50 (hexane/ethyl acetate 9:1); yellow solid; yield 81% (142 mg). ^{1}H NMR (400 MHz, $CDCl_3$) δ 8.04 (d, *J* = 15.6 Hz,

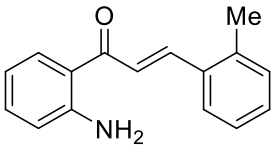

1H), 7.87 (dd, *J* = 8.4, 1.2 Hz, 1H), 7.68 (d, *J* = 8.0 Hz, 1H), 7.54 (d, *J* = 15.6 Hz, 1H), 7.32 – 7.27 (m, 2H), 7.26 – 7.20 (m, 2H), 6.73 – 6.66 (m, 2H), 6.35 (s, 2H), 2.49 (s, 3H); ^{13}C{^{1}H} NMR (100 MHz, $CDCl_3$) δ 191.8, 151.2, 140.7, 138.1, 134.4, 131.2, 130.9, 129.9, 126.5, 126.4, 124.4, 119.2, 117.4, 116.0, 20.0.

(*E*)-1-(2-Aminophenyl)-3-(3-chlorophenyl)prop-2-en-1-one (3d):[54] R_f = 0.50 (hexane/ethyl acetate 9:1); yellow solid; yield 73% (140 mg)); ^{1}H NMR (400 MHz, $CDCl_3$) δ

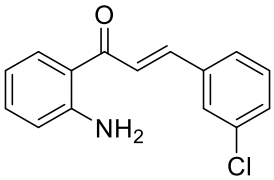

7.85 (d, *J* = 8.0 Hz, 1H), 7.61 (t, *J* = 11.2 Hz, 3H), 7.48 (d, *J* = 5.6 Hz, 1H), 7.39 – 7.27 (m, 3H), 6.70 (d, *J* = 7.6 Hz, 2H), 6.37 (s, 2H); ^{13}C{^{1}H} NMR (100 MHz, $CDCl_3$) δ 191.3, 151.3, 141.3, 137.3, 135.0, 134.7, 131.1, 130.3, 130.0, 127.8, 126.7, 124.5, 118.9, 117.5, 116.1; IR (KBr) $\tilde{\nu}$ = 3384, 3287, 1646, 1575, 1481, 1314, 1202, 1155, 1009, 994, 854, 762 cm^{-1}; HR-MS (ESI-TOF) m/z calcd for $C_{15}H_{12}ClNONa$ $[M + Na]^+$ 280.0500, found 280.0484.

(*E*)-1-(2-Aminophenyl)-3-(p-tolyl)prop-2-en-1-one (3e):[44] R_f = 0.50 (hexane/ethyl acetate 9:1); yellow solid; yield 90% (159 mg). ^{1}H NMR (400 MHz, $CDCl_3$) δ 7.87 (dd, *J* = 8.4, 1.6 Hz, 1H), 7.73 (d, *J* = 15.6 Hz, 1H), 7.60 (s, 1H), 7.58 – 7.50 (m, 2H), 7.32 – 7.26 (m, 1H), 7.22 (d, *J* = 8.0 Hz, 2H), 6.72 – 6.68 (m, 2H), 6.32 (s, 2H), 2.39 (s, 3H); ^{13}C{^{1}H} NMR (100 MHz, $CDCl_3$) δ 191.9, 151.1, 143.2, 140.7, 134.3, 132.7, 131.1, 129.8, 128.4, 122.3, 119.3, 117.4, 115.9, 21.6.

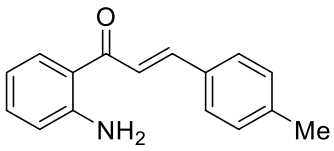

(*E*)-1-(2-Aminophenyl)-3-(4-chlorophenyl)prop-2-en-1-one (3f):[44] R_f = 0.50 (hexane/ethyl acetate 4:1); yellow solid; yield 85% (162 mg). ^{1}H NMR (400 MHz, $CDCl_3$) δ 7.84 (d, *J* = 8.0 Hz, 1H), 7.68 (d, *J* = 15.6 Hz, 1H), 7.61 – 7.50 (m, 3H), 7.38 (d, *J* = 8.0 Hz, 2H), 7.29 (dd, *J* = 14.8, 7.2 Hz, 1H), 6.70 (d, *J* = 6.0 Hz, 2H), 6.36 (s, 2H); ^{13}C{^{1}H} NMR (100 MHz, $CDCl_3$) δ 191.4, 151.2, 141.5, 136.0, 134.6, 133.9, 131.1, 129.5, 129.3, 123.6, 118.9, 117.6, 116.0; IR (KBr) $\tilde{\nu}$ = 3470, 3323, 2923, 1641, 1566, 1490, 1310, 1208, 1155, 1027, 980, 862, 778 cm^{-1}; HR-MS (ESI-TOF) m/z calcd for $C_{15}H_{12}ClNONa$ $[M + Na]^+$ 280.0500, found 280.0498.

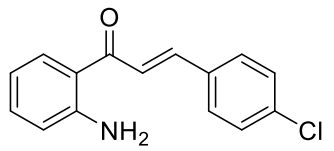

(*E*)-1-(2-Aminophenyl)-3-(4-nitrophenyl)prop-2-en-1-one (3g):[55] R_f = 0.45 (hexane/ethyl acetate 9:1); yellow solid; yield 82% (176 mg). ^{1}H NMR (400 MHz, $CDCl_3$) δ 8.26 (d, *J* = 8.4 Hz, 2H), 7.86 – 7.81 (m, 1H), 7.75 (d, *J* = 8.4 Hz, 2H), 7.72 (s. 2H), 7.36 – 7.28 (m, 1H), 6.73 – 6.67 (m, 2H), 6.41 (s, 2H); ^{13}C{^{1}H} NMR (100 MHz, $CDCl_3$) δ 190.7, 151.5, 148.4, 141.7, 139.8, 135.0, 131.1, 128.8, 127.2, 124.3, 118.6, 117.6, 116.1.

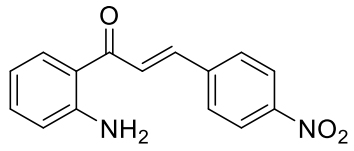

(*E*)-1-(2-Aminophenyl)-3-(4-isopropylphenyl)prop-2-en-1-one (3h):[54] R_f = 0.50 (hexane/ethyl acetate 19:1); yellow solid; yield 68% (114 mg). ^{1}H NMR (400 MHz, $CDCl_3$) δ

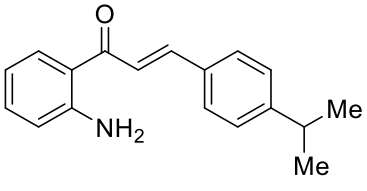

7.84 (dd, *J* = 8.4, 1.2 Hz, 1H), 7.72 (d, *J* = 15.6 Hz, 1H), 7.58 (s, 1H), 7.56 – 7.52 (m, 2H), 7.29 – 7.26 (m, 1H), 7.25 – 7.21 (m, 2H), 6.71 – 6.65 (m, 2H), 6.31 (s, 2H), 2.97 – 2.86 (m, 1H), 1.26 (s, 3H), 1.24 (s, 3H); $^{13}C\{^1H\}$ NMR (100 MHz, $CDCl_3$) δ 191.9, 151.5, 151.1, 143.1, 134.3, 133.0, 131.1, 128.5, 127.1, 122.3, 119.3, 117.4, 115.9, 34.2, 23.9 (×2).

(*E*)-1-(2-Aminophenyl)-3-mesitylprop-2-en-1-one (3i): R_f = 0.50 (hexane/ethyl acetate 9:1); yellow solid; yield 87% (170 mg). mp 118−120 °C; ^1H NMR (400 MHz, $CDCl_3$) δ 7.88 (d, *J* = 16.0 Hz, 1H), 7.77 (d, *J* = 8.0 Hz, 1H), 7.32 – 7.27 (m, 1H), 7.23 (d, *J* = 16.0 Hz, 1H), 6.94 (s, 2H), 6.72 – 6.65 (m, 2H), 6.37 (s, 2H), 2.40 (s, 6H), 2.31 (s, 3H); $^{13}C\{^1H\}$ NMR (100 MHz, $CDCl_3$) δ 191.9, 151.2, 141.5, 138.3, 137.1, 134.4, 132.2, 131.2, 129.3, 128.6, 119.1, 117.4, 116.0, 21.3 (×2), 21.2; IR (KBr) $\tilde{\nu}$ = 3427, 3316, 2966, 2916, 1639, 1612, 1573, 1539, 1479, 1330, 1206, 1161, 1009, 980, 848, 761 cm^{-1}; HR-MS (ESI-TOF) m/z calcd for $C_{18}H_{20}NO$ $[M + H]^+$ 266.1539, found 266.1517.

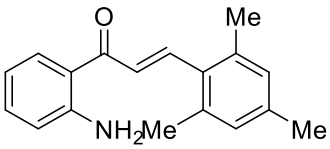

(*E*)-1-(2-Aminophenyl)-3-(thiophen-2-yl)prop-2-en-1-one (3j):[44] R_f = 0.50 (hexane/ethyl acetate 9:1); yellow solid; yield 71% (120 mg). ^1H NMR (400 MHz, $CDCl_3$) δ 7.88 (d, *J* = 15.2 Hz, 1H), 7.83 (d, *J* = 8.0 Hz, 1H), 7.44 (s, 1H), 7.41 – 7.36 (m, 1H), 7.32 (d, *J* = 3.6 Hz, 1H), 7.31 – 7.26 (m, 1H), 7.09 – 7.05 (m, 1H), 6.72 – 6.67 (m, 2H), 6.34 (s, 2H); $^{13}C\{^1H\}$ NMR (100 MHz, $CDCl_3$) δ 191.1, 151.1, 140.8, 135.6, 134.4, 131.5, 130.9, 128.3, 128.3, 121.9, 119.1, 117.4, 116.0.

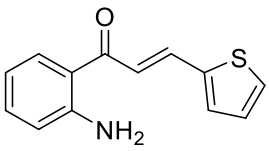

(*E*)-1-(2-Aminophenyl)-3-(3-hydroxyphenyl)prop-2-en-1-one (3k):[56] R_f = 0.45 (hexane/ethyl acetate 4:1); yellow solid; yield 85% (151 mg). ^1H NMR (400 MHz, $CDCl_3$ +

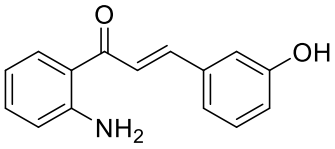

DMSO-d_6) δ 8.87 (s, 1H), 7.73 (d, *J* = 8.0 Hz, 1H), 7.49 (q, *J* = 15.6 Hz, 2H), 7.19 – 7.13 (m, 1H), 7.10 (d, *J* = 7.6 Hz, 1H), 7.05 – 6.94 (m, 2H), 6.82 – 6.75 (m, 1H), 6.61 (d, *J* = 8.4 Hz, 1H), 6.56 (t, *J* = 7.6 Hz, 1H), 6.38 (s, 2H); $^{13}C\{^1H\}$ NMR (100 MHz, $CDCl_3$ + DMSO-d_6) δ 191.6, 157.5, 151.0, 142.9, 136.3, 134.1, 130.9, 129.7, 122.9, 119.6, 118.7, 117.5, 117.2, 115.5, 114.7.

(*E*)-3-([1,1'-Biphenyl]-2-yl)-1-(2-aminophenyl)prop-2-en-1-one (3l): R_f = 0.45 (hexane/ethyl acetate 19:1); yellow solid; yield 78% (173 mg). mp 90−92 °C; ^1H NMR (400

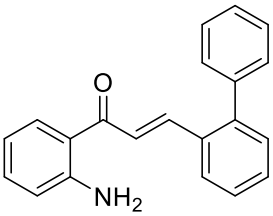

MHz, $CDCl_3$) δ 7.83 – 7.78 (m, 2H), 7.77 (d, *J* = 15.6 Hz, 1H), 7.52 (d, *J* = 15.6 Hz, 1H), 7.48 – 7.43 (m, 4H), 7.41 – 7.38 (m, 2H), 7.38 – 7.34 (m, 2H), 7.30 – 7.27 (m, 1H), 6.72 – 6.62 (m, 2H), 6.28 (s, 2H); $^{13}C\{^1H\}$ NMR (100 MHz, $CDCl_3$) δ 191.8, 151.1, 143.3, 142.2, 140.3, 134.4, 133.7, 131.2, 130.8, 129.9, 129.8, 128.5, 127.7, 127.7, 127.2, 124.7, 119.1, 117.4, 115.9; IR (KBr) $\tilde{\nu}$ = 3433, 3320, 2919, 2849, 1636, 1614, 1570, 1540, 1480, 1324, 1202, 1158, 1052, 1004, 978, 860, 788 cm^{-1}; HR-MS (ESI-TOF) m/z calcd for $C_{21}H_{18}NO$ $[M + H]^+$ 300.1383, found 300.1396.

(*E*)-1-(2-Aminophenyl)-3-(3,4-dimethoxyphenyl)prop-2-en-1-one (3m):[56] R_f = 0.40 (hexane/ethyl acetate 4:1); yellow solid; yield 81% (170 mg). ^1H NMR (400 MHz, $CDCl_3$) δ

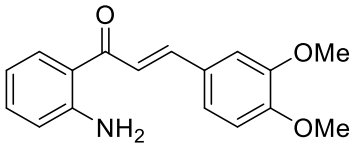

7.86 (dd, *J* = 8.4, 1.6 Hz, 1H), 7.70 (d, *J* = 15.6 Hz, 1H), 7.47 (d, *J* = 15.5 Hz, 1H), 7.31 – 7.26 (m, 1H), 7.22 (dd, *J* = 8.4, 2.0 Hz, 1H), 7.15 (d, *J* = 2.0 Hz, 1H), 6.89 (d, *J* = 8.4 Hz, 1H), 6.77 – 6.63 (m, 2H), 6.31 (s, 2H), 3.95 (s, 3H), 3.92 (s, 3H); $^{13}C\{^1H\}$ NMR (100 MHz, $CDCl_3$) δ 191.9, 151.2, 151.0, 149.4, 143.3, 134.2, 131.0, 128.4, 122.9, 121.2, 119.4, 117.4, 115.9, 111.3, 110.2, 56.1 (×2).

(*E*)-1-(2-Aminophenyl)-3-(3,4,5-trimethoxyphenyl)prop-2-en-1-one (3n):[44] R_f = 0.40 (hexane/ethyl acetate 4:1); yellow solid; yield 82% (190 mg). ^{1}H NMR (400 MHz, $CDCl_3$) δ

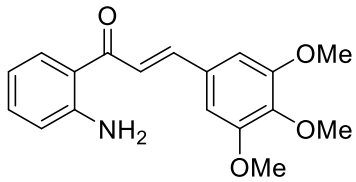

7.86 (dd, *J* = 8.4, 1.2 Hz, 1H), 7.65 (d, *J* = 15.6 Hz, 1H), 7.48 (d, *J* = 15.6 Hz, 1H), 7.36 – 7.26 (m, 1H), 6.85 (s, 2H), 6.73 – 6.70 (m, 1H), 6.70 – 6.67 (m, 1H), 6.32 (s, 2H), 3.92 (s, 6H), 3.90 (s, 3H); ^{13}C{^{1}H} NMR (100 MHz, $CDCl_3$) δ 191.7, 153.6, 151.1, 143.2, 140.2, 134.4, 131.1, 130.9, 122.6, 119.2, 117.5, 115.9, 105.6, 61.1, 56.4.

(*E*)-1-(2-Aminophenyl)-3-(naphthalen-1-yl)prop-2-en-1-one (3o):[44] R_f = 0.45 (hexane/ethyl acetate 9:1); yellow solid; yield 79% (160 mg). ^{1}H NMR (400 MHz, $CDCl_3$) δ

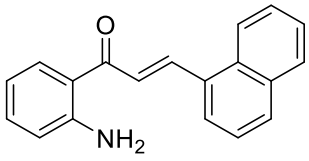

8.60 (d, *J* = 15.2 Hz, 1H), 8.29 (d, *J* = 8.4 Hz, 1H), 7.92 (d, *J* = 8.4 Hz, 2H), 7.88 (d, *J* = 7.6 Hz, 2H), 7.71 (d, *J* = 15.2 Hz, 1H), 7.63 – 7.57 (m, 1H), 7.56 – 7.50 (m, 2H), 7.35 – 7.29 (m, 1H), 6.74 – 6.69 (m, 2H), 6.41 (s, 2H); ^{13}C{^{1}H} NMR (100 MHz, $CDCl_3$) δ 191.7, 151.3, 140.1, 134.5, 133.8, 132.9, 131.9, 131.2, 130.5, 128.8, 126.9, 126.4, 126.0, 125.6, 125.0, 123.8, 119.1, 117.5, 116.0.

(*E*)-1-(2-Aminophenyl)-3-(anthracen-9-yl)prop-2-en-1-one (3p): R_f = 0.45 (hexane/ethyl acetate 4:1); yellow solid; yield 87% (208 mg). mp 151−153 °C; ^{1}H NMR (400 MHz, $CDCl_3$) δ 8.70 (d, *J* = 15.6 Hz, 1H), 8.46 (s, 1H), 8.36 – 8.26 (m, 2H), 8.05 – 8.01 (m, 2H), 7.82 (dd, *J* = 8.0, 1.2 Hz, 1H), 7.62 (d, *J* = 15.6 Hz, 1H), 7.55 – 7.47 (m, 4H), 7.35 – 7.27 (m, 1H), 6.75 (d, *J* = 8.0 Hz, 1H), 6.70 – 6.62 (m, 1H), 6.51 (s, 2H); ^{13}C{^{1}H} NMR (100 MHz, $CDCl_3$) δ 191.1, 151.5, 140.1, 134.7, 132.4, 131.5, 131.3, 130.9, 129.7, 128.9, 128.1, 126.4,

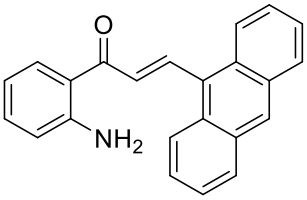

125.6, 125.5, 118.9, 117.5, 116.1; IR (KBr) $\tilde{\nu}$ = 3471, 3329, 3048, 1633, 1621, 1573, 1537, 1478, 1354, 1275, 1251, 1157, 1017, 982, 971, 756 cm^{-1}; HR-MS (ESI-TOF) m/z calcd for $C_{23}H_{18}NO$ $[M + H]^+$ 324.1383, found 324.1392.

2-Phenylchroman-4-one (2a):[49] R_f = 0.45 (hexane/ethyl acetate 9:1); white solid; yield 92% (92 mg). ^1H NMR (400 MHz, $CDCl_3$) δ 7.94 (dd, *J* = 8.0, 1.6 Hz, 1H), 7.55 – 7.51 (m, 1H),

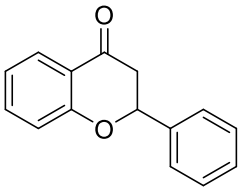

7.51 – 7.45 (m, 3H), 7.44 – 7.37 (m, 2H), 7.08 – 7.06 (m, 1H), 7.06 – 7.04 (m, 1H), 5.49 (dd, *J* = 13.2, 2.8 Hz, 1H), 3.10 (dd, *J* = 16.8, 13.2 Hz, 1H), 2.90 (dd, *J* = 16.8, 2.8 Hz, 1H); $^{13}C\{^1H\}$ NMR (100 MHz, $CDCl_3$) δ 192.1, 161.7, 138.9, 136.4, 129.0, 128.9, 127.2, 126.3, 121.8, 121.1, 118.8, 79.8, 44.8; HR-MS (ESI-TOF) m/z calcd for $C_{15}H_{13}O_2$ $[M + H]^+$ 225.0910, found 225.0926.

2-(2-Nitrophenyl)chroman-4-one (2b):[57] R_f = 0.45 (hexane/ethyl acetate 4:1); yellow solid; yield 84% (84 mg); ^1H NMR (400 MHz, $CDCl_3$) δ 8.06 (dd, *J* = 8.0, 1.2 Hz, 1H), 8.01 (dd, *J*

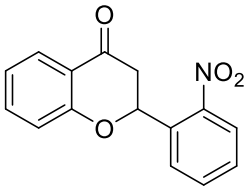

= 8.0, 1.2 Hz, 1H), 7.97 (dd, *J* = 8.0, 1.6 Hz, 1H), 7.77 (td, *J* = 8.0, 1.2 Hz, 1H), 7.59 – 7.54 (m, 1H), 7.54 – 7.50 (m, 1H), 7.13 – 7.07 (m, 1H), 7.04 (d, *J* = 8.4 Hz, 1H), 6.11 (dd, *J* = 13.2, 2.8 Hz, 1H), 3.22 (dd, *J* = 16.8, 2.8 Hz, 1H), 2.95 (dd, *J* = 16.8, 13.2 Hz, 1H); $^{13}C\{^1H\}$ NMR (100 MHz, $CDCl_3$) δ 190.9, 161.3, 147.5, 136.4, 134.9, 134.2, 129.5, 128.3, 127.4, 125.0, 122.3, 121.2, 118.1, 75.8, 44.6; IR (KBr) $\tilde{\nu}$ = 2920, 2850, 1686, 1645, 1602, 1579, 1519, 1474, 1462, 1357, 1303, 1221, 1117, 1063, 989, 879, 789 cm^{-1}; HR-MS (ESI-TOF) m/z calcd for $C_{15}H_{12}NO_4$ $[M + H]^+$ 270.0761, found 270.0763.

2-(2-Fluorophenyl)chroman-4-one (2c):[58] R_f = 0.50 (hexane/ethyl acetate 19:1); yield 87% (87 mg); ^1H NMR (400 MHz, $CDCl_3$) δ 7.97 – 7.93 (m, 1H), 7.65 (td, *J* = 7.6, 1.6 Hz, 1H),

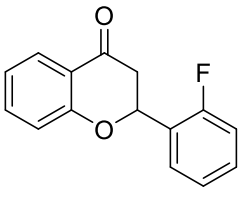

7.54 – 7.48 (m, 1H), 7.40 – 7.33 (m, 1H), 7.27 – 7.21 (m, 1H), 7.14 – 7.09 (m, 1H), 7.06 (d, *J* = 7.6 Hz, 2H), 5.78 (dd, *J* = 13.2, 3.2 Hz, 1H), 3.06 (dd, *J* = 16.8, 13.2 Hz, 1H), 2.93 (dd, *J* = 16.8, 3.2 Hz, 1H); $^{13}C\{^1H\}$ NMR (100 MHz, $CDCl_3$) δ 191.7, 161.6, 159.7 (d, *J* = 247.9 Hz), 136.3, 130.4 (d, *J* = 8.3 Hz), 127.6 (d, *J* = 3.2 Hz), 127.3, 126.3 (d, *J* = 12.9 Hz), 124.7 (d, *J* = 3.1 Hz), 121.9, 121.0, 118.2, 115.9 (d, *J* = 21.3 Hz), 73.9, 43.8; IR (KBr) $\tilde{\nu}$ = 3065, 2921, 2850, 1689, 1605, 1588, 1576, 1491, 1471, 1461, 1302, 1256, 1114, 1067, 1026, 989, 802, 757 cm^{-1}; HR-MS (ESI-TOF) m/z calcd for $C_{15}H_{12}FO_2$ $[M + H]^+$ 243.0816, found 243.0804.

2-(3-Chlorophenyl)chroman-4-one (2d):[49] R_f = 0.45 (hexane/ethyl acetate 19:1); brownish yellow solid; yield 78% (78 mg); ^1H NMR (400 MHz, $CDCl_3$) δ 7.93 (dd, *J* = 8.0, 1.6 Hz, 1H), 7.57 – 7.50 (m, 2H), 7.39 – 7.31 (m, 3H), 7.10 – 7.05 (m, 2H), 5.46 (dd, *J* = 13.2, 3.2 Hz, 1H), 3.04 (dd, *J* = 16.8, 13.2 Hz, 1H), 2.89 (dd, *J* = 16.8, 3.2 Hz, 1H); $^{13}C\{^1H\}$ NMR (100 MHz, $CDCl_3$) δ 191.5, 161.4, 140.9, 136.5, 134.9, 130.3, 129.0, 127.2, 126.5, 124.3, 122.0, 121.0, 118.2, 78.9, 44.8; IR (KBr) $\tilde{\nu}$ = 3360, 2916, 2848, 1693, 1601, 1573, 1469, 1459, 1316, 1230, 1220, 1098, 1076, 920, 808, 788 cm^{-1}; HR-MS (ESI-TOF) m/z calcd for $C_{15}H_{12}ClO_2$ $[M + H]^+$ 259.0520, found 259.0496.

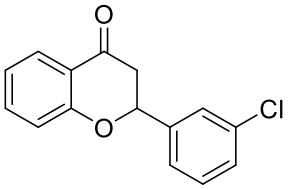

2-(3-Bromophenyl)chroman-4-one (2e):[59] R_f = 0.45 (hexane/ethyl acetate 19:1); brownish yellow solid; yield 86% (86 mg); ^1H NMR (400 MHz, $CDCl_3$) δ 7.96 – 7.90 (m, 1H), 7.68 (s, 1H), 7.57 – 7.49 (m, 2H), 7.39 (d, *J* = 8.0 Hz, 1H), 7.31 (t, *J* = 8.0 Hz, 1H), 7.08 (td, *J* = 7.2, 0.8 Hz, 2H), 5.45 (dd, *J* = 13.2, 2.0 Hz, 1H), 3.08 – 2.98 (m, 1H), 2.89 – 2.86 (m, 1H); $^{13}C\{^1H\}$ NMR (100 MHz, $CDCl_3$) δ 191.49, 161.38, 141.18, 136.48, 131.97, 130.57, 129.40, 127.26, 124.77,

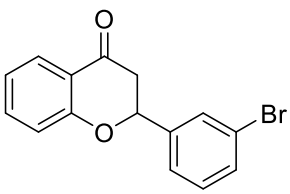

123.10, 122.04, 121.04, 118.25, 78.85, 44.81; IR (KBr) $\tilde{\nu}$ = 3360, 3065, 2916, 2848, 1680, 1600, 1572, 1469, 1458, 1316, 1297, 1220, 1111, 1065, 915, 806, 786 cm^{-1}; HR-MS (ESI-TOF) m/z calcd for $C_{15}H_{12}{}^{81}BrO_2$ $[M + H]^+$ 304.9995, found 304.9983.

2-(4-Isopropylphenyl)chroman-4-one (2f):[57] R_f = 0.50 (hexane/ethyl acetate 19:1); yellow solid; yield 72% (72 mg); ^1H NMR (400 MHz, $CDCl_3$) δ 7.94 (dd, *J* = 8.0, 1.6 Hz, 1H), 7.53 – 7.48 (m, 1H), 7.42 (d, *J* = 8.0 Hz, 2H), 7.31 (d, *J* = 8.0 Hz, 2H), 7.07 – 7.03 (m, 2H), 5.46 (dd, *J* = 13.2, 2.8 Hz, 1H), 3.12 (dd, *J* = 16.8, 13.2 Hz, 1H), 2.96 (dd, *J* = 13.6, 6.8 Hz, 1H), 2.89 (dd, *J* = 16.8, 2.8 Hz, 1H), 1.29 (s, 3H), 1.27 (s, 3H); $^{13}C\{^1H\}$ NMR (100 MHz, $CDCl_3$) δ 192.3, 161.8, 149.8, 136.3, 136.2, 127.2, 127.1, 126.4, 121.7, 121.1, 118.3, 79.7, 44.6, 34.1, 24.1; IR (KBr) $\tilde{\nu}$ = 2958, 2869, 1687, 1646, 1603, 1514, 1462, 1420, 1338, 1301, 1223, 1113, 1066, 1053, 906, 860, 761 cm^{-1}; HR-MS (ESI-TOF) m/z calcd for $C_{18}H_{19}O_2$ $[M + H]^+$ 267.1380, found 267.1374.

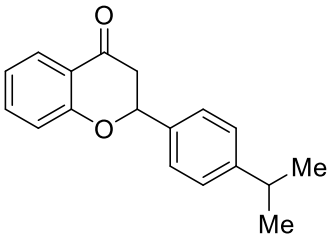

2-(p-Tolyl)chroman-4-one (2g):[49] R_f = 0.450 (hexane/ethyl acetate 19:1); yellow solid; yield 74% (74 mg); ^1H NMR (400 MHz, $CDCl_3$) δ 7.94 (dd, *J* = 8.0, 1.6 Hz, 1H), 7.54 – 7.47 (m, 1H), 7.38 (d, *J* = 8.0 Hz, 2H), 7.26 (s, 1H), 7.24 (s, 1H), 7.07 – 7.03 (m, 2H), 5.45 (dd, *J* = 13.2, 2.8 Hz, 1H), 3.10 (dd, *J* = 16.8, 13.2 Hz, 1H), 2.88 (dd, *J* = 16.8, 2.8 Hz, 1H), 2.39 (s, 3H); $^{13}C\{^1H\}$ NMR (100 MHz, $CDCl_3$) δ 192.3, 161.8, 138.9, 136.3, 135.9, 129.6, 127.2, 126.3, 121.7, 121.1, 118.3, 79.7, 44.7, 21.3; IR (KBr) $\tilde{\nu}$ = 3034, 2918, 2851, 1603, 1566, 1463, 1412, 1369, 1311, 1280, 1226, 1122, 1041, 905, 815, 769 cm^{-1}; HR-MS (ESI-TOF) m/z calcd for $C_{16}H_{15}O_2$ $[M + H]^+$ 239.1067, found 239.1053.

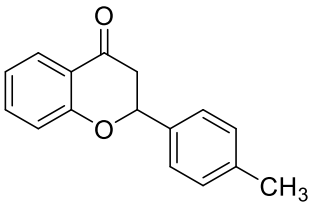

2-(4-Bromophenyl)chroman-4-one (2h):[49] R_f = 0.50 (hexane/ethyl acetate 19:1); yellow solid; yield 87% (87 mg); ^{1}H NMR (400 MHz, $CDCl_3$) δ 7.93 (dd, *J* = 8.0, 1.6 Hz, 1H), 7.59 – 7.51 (m, 3H), 7.37 (d, *J* = 8.4 Hz, 2H), 7.09 – 7.03 (m, 2H), 5.46 (dd, *J* = 13.2, 2.8 Hz, 1H), 3.04 (dd, *J* = 16.8, 13.2 Hz, 1H), 2.88 (dd, *J* = 16.8, 3.2 Hz, 1H); ^{13}C{^{1}H} NMR (100 MHz, $CDCl_3$) δ 191.7, 161.4, 137.9, 136.5, 132.2, 127.9, 127.2, 122.9, 121.9, 121.0, 118.2, 78.9, 44.7; IR (KBr) $\tilde{\nu}$ = 3357, 2916, 2847, 1686, 1596, 1488, 1460, 1320, 1298, 1221, 1111, 1065, 1025, 941, 870, 860 cm^{-1}; HR-MS (ESI-TOF) m/z calcd for $C_{15}H_{12}{}^{81}BrO_2$ $[M + H]^+$ 304.9995, found 304.9981

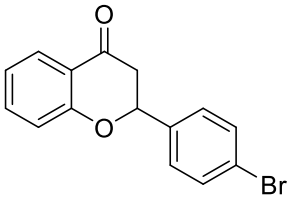

2-(4-Ethylphenyl)chroman-4-one (2i):[49] R_f = 0.60 (hexane/ethyl acetate 9:1); yellow solid; yield 79% (79 mg). ^{1}H NMR (400 MHz, $CDCl_3$) 7.94 (dd, *J* = 8.0, 1.6 Hz, 1H), 7.53 – 7.48 (m, 1H), 7.41 (d, *J* = 8.0 Hz, 2H), 7.33 – 7.24 (m, 2H), 7.08 – 7.06 (m, 2H), 5.46 (dd, *J* = 13.2, 2.8 Hz, 1H), 3.11 (dd, *J* = 16.8, 13.2 Hz, 1H), 2.89 (dd, *J* = 16.8, 2.8 Hz, 1H), 2.69 (q, *J* = 7.6 Hz, 2H), 1.26 (t, *J* = 7.6 Hz, 3H); ^{13}C{^{1}H} NMR (100 MHz, $CDCl_3$) δ 192.3, 161.8, 145.2, 136.3, 136.1, 128.5, 127.2, 126.4, 121.7, 121.1, 118.3, 79.7, 44.7, 28.8, 15.7; HR-MS (ESI-TOF) m/z calcd for $C_{17}H_{17}O_2$ $[M + H]^+$ 253.1223, found 253.1217.

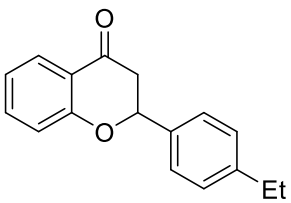

2-(Thiophen-2-yl)chroman-4-one (2j):[60] R_f = 0.45 (hexane/ethyl acetate 9:1); yellow solid; yield 66% (66 mg). ^{1}H NMR (400 MHz, $CDCl_3$) δ 7.92 (dd, *J* = 8.0, 1.6 Hz, 1H), 7.53 – 7.48 (m, 1H), 7.39 – 7.35 (m, 1H), 7.15 – 7.12 (m, 1H), 7.08 – 7.05 (m, 1H), 7.05 – 7.01 (m, 2H), 5.80 – 5.74 (m, 1H), 3.20 (dd, *J* = 16.8, 11.6 Hz, 1H), 3.07 (dd, *J* = 16.8, 3.6 Hz, 1H); ^{13}C{^{1}H} NMR (100 MHz, $CDCl_3$)

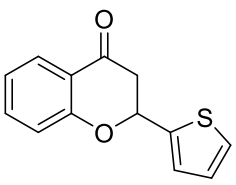

δ 191.4, 161.0, 141.6, 136.4, 127.2, 127.0, 126.5, 126.1, 121.9, 121.1, 118.4, 75.3, 44.5; HR-MS (ESI-TOF) m/z calcd for $C_{13}H_9O_2S$ $[M - H]^+$ 229.0318, found 229.0298.

2-(Naphthalen-1-yl)chroman-4-one (2k):[60] R_f = 0.45 (hexane/ethyl acetate 19:1); white solid; yield 77% (77 mg). ^1H NMR (400 MHz, $CDCl_3$) δ 8.08 – 8.04 (m, 1H), 8.02 (dd, *J* = 8.0, 1.6 Hz, 1H), 7.93 (dd, *J* = 6.8, 3.2 Hz, 1H), 7.90 (d, *J* = 8.4 Hz, 1H), 7.79 (d, *J* = 7.2 Hz, 1H), 7.61 – 7.50 (m, 4H), 7.13 – 7.08 (m, 2H), 6.23 (dd, *J* = 13.2, 2.8 Hz, 1H), 3.27 (dd, *J* = 16.8, 13.2 Hz, 1H), 3.11 (dd, *J* = 16.8, 2.8 Hz, 1H)); $^{13}C\{^1H\}$ NMR (100 MHz, $CDCl_3$) δ 192.4, 161.9, 136.4, 134.3, 134.0, 130.3, 129.5, 129.2, 127.3, 126.8, 126.1, 125.5, 124.0, 122.9, 121.9, 121.2, 118.4, 76.8, 44.1; HR-MS (ESI-TOF) m/z calcd for $C_{19}H_{15}O_2$ $[M + H]^+$ 275.1067, found 275.1058.

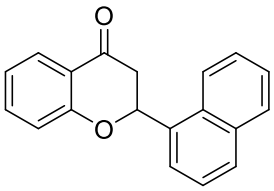

2-Phenyl-2,3-dihydroquinolin-4(1H)-one (4a):[44] R_f = 0.55 (hexane/ethyl acetate 4:1); Pale yellow solid; yield 88% (88 mg). ^1H NMR (400 MHz, $CDCl_3$) δ 7.88 (d, *J* = 8.0 Hz, 1H), 7.46 (d, *J* = 7.2 Hz, 2H), 7.41 (t, *J* = 7.2 Hz, 2H), 7.38 – 7.30 (m, 2H), 6.80 (t, *J* = 7.6 Hz, 1H), 6.71 (d, *J* = 8.0 Hz, 1H), 4.78 – 4.72 (m, 1H), 4.52 (s, 1H), 2.93 – 2.84 (m, 1H), 2.81 – 2.74 (m, 1H); $^{13}C\{^1H\}$ NMR (100 MHz, $CDCl_3$) δ 193.4, 151.7, 141.2, 135.5, 129.1, 128.6, 127.8, 126.8, 119.2, 118.6, 116.1, 58.7, 46.6; HR-MS (ESI-TOF) m/z calcd for $C_{15}H_{14}NO$ $[M + H]^+$ 224.1070, found 224.1077.

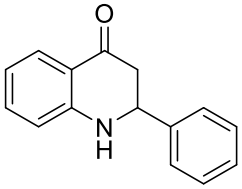

2-(2-Bromophenyl)-2,3-dihydroquinolin-4(1H)-one (4b):[44] R_f = 0.45 (hexane/ethyl acetate 4:1); Pale yellow solid; yield 83% (83 mg). ^1H NMR (400 MHz, $CDCl_3$) δ 7.88 (dd, *J* = 8.0, 1.6 Hz, 1H), 7.68 (dd, *J* = 8.0, 1.6 Hz, 1H), 7.59 (dd, *J* = 8.0, 1.2 Hz, 1H), 7.39 – 7.32 (m,

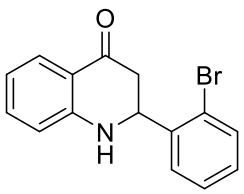

2H), 7.24 – 7.16 (m, 1H), 6.83 – 6.78 (m, 1H), 6.74 (d, *J* = 8.4 Hz, 1H), 5.22 (dd, *J* = 12.4, 4.0 Hz, 1H), 4.56 (s, 1H), 2.98 – 2.91 (m, 1H), 2.80 – 2.71 (m, 1H); $^{13}C\{^1H\}$ NMR (100 MHz, $CDCl_3$) δ 192.9, 151.6, 140.0, 135.6, 133.5, 129.8, 128.3, 127.8, 127.8, 123.1, 119.3, 118.8, 116.2, 56.9, 44.3; HR-MS (ESI-TOF) m/z calcd for $C_{15}H_{13}{}^{79}BrNO$ $[M + H]^+$ 302.0175, found 302.0162, $C_{15}H_{13}{}^{81}BrNO$ $[M + H]^+$ 304.0155, found 304.0153.

2-(o-Tolyl)-2,3-dihydroquinolin-4(1H)-one (4c):[44] R_f = 0.45 (hexane/ethyl acetate 9:1); yellow solid; yield 81% (81 mg). ^1H NMR (400 MHz, $CDCl_3$) δ 7.87 (d, *J* = 8.0 Hz, 1H),

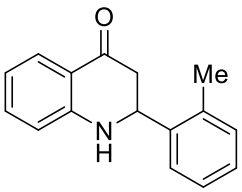

7.65 (d, *J* = 7.2 Hz, 1H), 7.36 – 7.30 (m, 1H), 7.25 (dd, *J* = 14.8, 7.2 Hz, 2H), 7.19 (t, *J* = 6.8 Hz, 1H), 6.78 (t, *J* = 7.6 Hz, 1H), 6.72 (d, *J* = 8.2 Hz, 1H), 5.00 (dd, *J* = 13.2, 4.0 Hz, 1H), 4.48 (d, *J* = 12.0 Hz, 1H), 2.84 – 2.63 (m, 2H), 2.35 (s, 3H); $^{13}C\{^1H\}$ NMR (100 MHz, $CDCl_3$) δ 193.5, 152.1, 139.1, 135.5, 135.1, 131.0, 128.1, 127.8, 126.9, 125.9, 119.0, 118.5, 116.1, 54.6, 45.3, 19.2; HR-MS (ESI-TOF) m/z calcd for $C_{16}H_{16}NO$ $[M + H]^+$ 238.1226, found 238.1222.

2-(3-Chlorophenyl)-2,3-dihydroquinolin-4(1H)-one (4d):[61] R_f = 0.65 (hexane/ethyl acetate 4:1); yellow solid; yield 78% (78 mg). ^1H NMR (400 MHz, $CDCl_3$) δ 7.86 (d, *J* = 8.0 Hz,

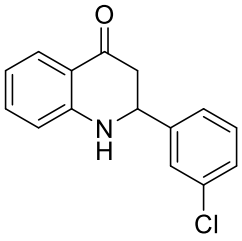

1H), 7.48 (s, 1H), 7.38 – 7.30 (m, 4H), 6.81 (t, *J* = 7.6 Hz, 1H), 6.74 (d, *J* = 8.0 Hz, 1H), 4.72 (dd, *J* = 13.2, 2.8 Hz, 1H), 4.56 (s, 1H), 2.88 – 2.79 (m, 1H), 2.79 – 2.71 (m, 1H); $^{13}C\{^1H\}$ NMR (100 MHz, $CDCl_3$) δ 192.9, 151.4, 143.2, 135.7, 134.9, 130.5, 128.8, 127.7, 126.9, 124.9, 119.2, 118.9, 116.1, 58.2, 46.5; HR-MS (ESI-TOF) m/z calcd for $C_{15}H_{11}ClNO$ $[M - H]^+$ 256.0524, found 256.0502.

2-(p-Tolyl)-2,3-dihydroquinolin-4(1H)-one (4e):[44] R_f = 0.45 (hexane/ethyl acetate 9:1); yellow solid; yield 85% (85 mg). ^{1}H NMR (400 MHz, $CDCl_3$) δ 7.87 (d, *J* = 8.0 Hz, 1H), 7.39 – 7.30 (m, 3H), 7.21 (d, *J* = 8.0 Hz, 2H), 6.78 (t, *J* = 7.6 Hz, 1H), 6.71 (d, *J* = 8.0 Hz, 1H), 4.70 (d, *J* = 13.6 Hz, 1H), 4.54 (s, 1H), 2.91 – 2.80 (m, 1H), 2.77 – 2.70 (m, 1H), 2.37 (s, 3H); ^{13}C{^{1}H} NMR (100 MHz, $CDCl_3$) δ 193.6, 151.8, 138.4, 138.2, 135.5, 129.7, 127.7, 126.7, 119.1, 118.5, 116.0, 58.3, 46.6, 21.3; HR-MS (ESI-TOF) m/z calcd for $C_{16}H_{15}NONa$ $[M + Na]^+$ 260.1046, found 260.1047.

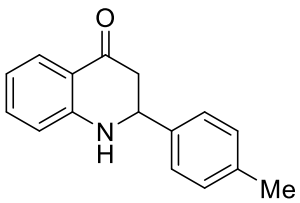

2-(4-Chlorophenyl)-2,3-dihydroquinolin-4(1H)-one (4f):[44] R_f = 0.45 (hexane/ethyl acetate 9:1); yellow solid; yield 84% (84 mg). ^{1}H NMR (400 MHz, $CDCl_3$) δ 7.86 (d, *J* = 8.0 Hz, 1H), 7.43 – 7.37 (m, 3H), 7.37 – 7.30 (m, 2H), 6.80 (t, *J* = 7.6 Hz, 1H), 6.73 (d, *J* = 8.0 Hz, 1H), 4.73 (dd, *J* = 13.2, 4.0 Hz, 1H), 4.52 (s, 1H), 2.86 – 2.78 (m, 1H), 2.77 – 2.70 (m, 1H); ^{13}C{^{1}H} NMR (100 MHz, $CDCl_3$) δ 193.0, 151.5, 139.7, 135.7, 134.3, 129.3, 128.1, 127.7, 119.2, 118.8, 116.1, 58.0, 46.5; HR-MS (ESI-TOF) m/z calcd for $C_{15}H_{13}ClNO$ $[M + H]^+$ 258.0680, found 258.0660.

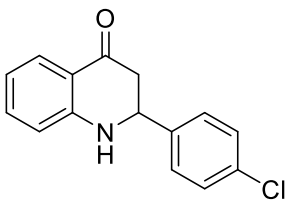

2-(4-Nitrophenyl)-2,3-dihydroquinolin-4(1H)-one (4g):[62] R_f = 0.45 (hexane/ethyl acetate 4:1); yellow solid; yield 87% (87 mg). ^{1}H NMR (400 MHz, $CDCl_3$) δ 8.25 (d, *J* = 8.8 Hz, 2H), 7.87 (dd, *J* = 8.0, 1.2 Hz, 1H), 7.65 (d, *J* = 8.8 Hz, 2H), 7.41 – 7.35 (m, 1H), 6.87 – 6.82 (m, 1H), 6.77 (d, *J* = 8.0 Hz, 1H), 4.93 – 4.86 (m, 1H), 4.58 (s, 1H), 2.86 – 2.83 (m, 1H), 2.82 (s, 1H);

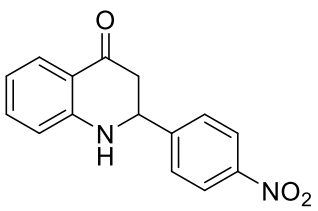

$^{13}C\{^1H\}$ NMR (100 MHz, $CDCl_3$) δ 192.1, 151.1, 148.4, 148.0, 136.1, 135.9, 127.8, 127.7, 124.5, 119.3, 116.2, 58.0, 46.3; HR-MS (ESI-TOF) m/z calcd for $C_{15}H_{12}N_2O_3Na$ $[M + Na]^+$ 291.0740, found 291.0738.

2-(4-Isopropylphenyl)-2,3-dihydroquinolin-4(1H)-one (4h):[62] R_f = 0.50 (hexane/ethyl acetate 19:1); yellow solid; yield 85% (85 mg). ^1H NMR (400 MHz, $CDCl_3$) δ 7.90 – 7.81 (m, 1H), 7.37 (d, *J* = 8.0 Hz, 2H), 7.34 – 7.29 (m, 1H), 7.26 (s, 1H), 7.25 – 7.23 (m, 1H), 6.81 – 6.74 (m, 1H), 6.68 (d, *J* = 8.0 Hz, 1H), 4.71 (dd, *J* = 13.6, 3.6 Hz, 1H), 4.51 (s, 1H), 2.97 – 2.83 (m, 2H), 2.78 – 2.72 (m, 1H), 1.27 (s, 3H), 1.25 (s, 3H); $^{13}C\{^1H\}$ NMR (100 MHz, $CDCl_3$) δ 193.6, 151.8, 149.4, 138.5, 135.5, 127.7, 127.1, 126.8, 119.1, 118.5, 116.0, 58.3, 46.5, 34.0, 24.1 (×2) ; HR-MS (ESI-TOF) m/z calcd for $C_{18}H_{20}NO$ $[M + H]^+$ 266.1539, found 266.1535.

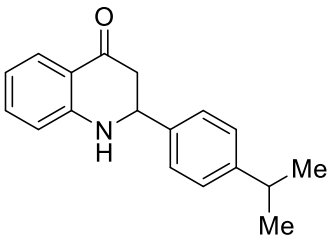

2-Mesityl-2,3-dihydroquinolin-4(1H)-one (4i):[42] R_f = 0.50 (hexane/ethyl acetate 9:1); yellow solid; yield 68% (68 mg). ^1H NMR (400 MHz, $CDCl_3$) δ 7.90 (dd, *J* = 8.0, 1.2 Hz, 1H), 7.35 – 7.30 (m, 1H), 6.89 (s, 2H), 6.80 – 6.74 (m, 1H), 6.67 (d, *J* = 8.0 Hz, 1H), 5.29 – 5.21 (m, 1H), 4.37 (s, 1H), 3.31 – 3.18 (m, 1H), 2.60 – 2.54 (m, 1H), 2.48 (s, 6H), 2.28 (s, 3H); $^{13}C\{^1H\}$ NMR (100 MHz, $CDCl_3$) δ 194.1, 152.1, 137.8, 137.1, 135.4, 132.5, 130.8, 128.0, 118.8, 118.1, 116.0, 54.1, 41.7, 21.4, 20.9 (×2) ; HR-MS (ESI-TOF) m/z calcd for $C_{18}H_{20}NO$ $[M + H]^+$ 266.1539, found 266.1535.

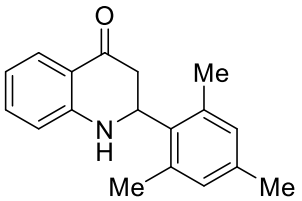

2-(Thiophen-2-yl)-2,3-dihydroquinolin-4(1H)-one (4j):[44] R_f = 0.50 (hexane/ethyl acetate 9:1); yellow solid; yield 86% (86 mg). ^1H NMR (400 MHz, $CDCl_3$) δ 7.87 (dd, *J* = 8.0, 1.2

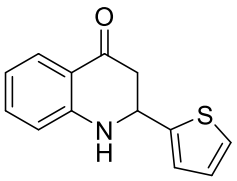

Hz, 1H), 7.38 – 7.31 (m, 1H), 7.30 – 7.26 (m, 1H), 7.07 (d, *J* = 3.2 Hz. 1H), 7.01 – 6.97 (m, 1H), 6.81 (t, *J* = 7.2 Hz, 1H), 6.72 (d, *J* = 8.0 Hz, 1H), 5.05 (dd, *J* = 10.8, 5.6 Hz, 1H), 4.66 (s, 1H), 2.99 – 2.93 (m, 1H), 2.92 – 2.87 (m, 1H); $^{13}C\{^1H\}$ NMR (100 MHz, $CDCl_3$) δ 192.8, 150.9, 144.7, 135.6, 127.7, 127.0, 125.3, 125.1, 119.4, 118.9, 116.1, 53.9, 47.2; HR-MS (ESI-TOF) m/z calcd for $C_{13}H_{12}NOS$ $[M + H]^+$ 230.0634, found 230.0617.

2-(3-Hydroxyphenyl)-2,3-dihydroquinolin-4(1H)-one (4k): R_f = 0.45 (hexane/ethyl acetate 4:1); yellow solid; yield 76% (76 mg); mp 108−110 °C. ^1H NMR (400 MHz, $CDCl_3$ + DMSO-d_6) δ 8.49 (s, 1H), 7.35 (t, *J* = 8.0 Hz, 1H), 6.90 – 6.79 (m, 1H), 6.78 – 6.68 (m, 1H), 6.54 – 6.40 (m, 2H), 6.40 – 6.30 (m, 2H), 6.31 – 6.20 (m, 1H), 4.98 – 4.77 (m, 1H), 4.23 – 4.13 (m, 1H), 2.44 – 2.18 (m, 2H); $^{13}C\{^1H\}$ NMR (100 MHz, $CDCl_3$ + DMSO-d_6) δ 193.6, 157.4, 151.9, 142.5, 135.2, 129.7, 127.0, 118.3, 117.5, 117.4, 116.0, 115.3, 113.5, 57.7, 45.9; IR (KBr) $\tilde{\nu}$ = 3387, 3132, 2922, 2901, 2850, 1636, 1580, 1473, 1409, 1360, 1339, 1276, 1233, 1151, 1084, 994, 808, 778 cm^{-1}; HR-MS (ESI-TOF) m/z calcd for $C_{15}H_{14}NO_2$ $[M + H]^+$ 240.1019, found 240.1020.

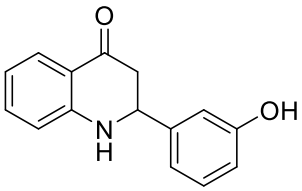

2-([1,1'-Biphenyl]-2-yl)-2,3-dihydroquinolin-4(1H)-one (4l): R_f = 0.60 (hexane/ethyl acetate 4:1); white solid; yield 68% (68 mg); mp 142−143 °C. ^1H NMR (400 MHz, $CDCl_3$) δ 7.84 (d, *J* = 8.0 Hz, 1H), 7.81 (d, *J* = 7.9 Hz, 1H), 7.49 – 7.42 (m, 1H), 7.42 – 7.34 (m, 4H), 7.31 – 7.26 (m, 3H), 7.25 (s, 1H), 6.73 (t, *J* = 7.6 Hz, 1H), 6.62 (d, *J* = 8.0 Hz, 1H), 4.89 (dd, *J* = 14.0, 3.6 Hz, 1H), 4.36 (s, 1H), 2.94 – 2.85 (m, 1H), 2.76 – 2.65 (m, 1H); $^{13}C\{^1H\}$ NMR (100 MHz, $CDCl_3$) δ 193.17, 151.77, 141.74, 140.35, 138.53, 135.44, 130.63, 129.08, 128.62, 128.28, 128.07, 127.71, 127.68, 126.79, 118.93, 118.40, 115.97, 54.32, 46.20; IR (KBr) $\tilde{\nu}$ = 3315, 3057,

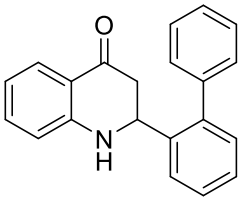

1656, 1606, 1479, 1355, 1330, 1256, 1153, 1024, 997, 757 cm^{-1}; HR-MS (ESI-TOF) m/z calcd for $C_{21}H_{17}NONa$ $[M + Na]^+$ 322.1202, found 322.1192.

2-(3,4-Dimethoxyphenyl)-2,3-dihydroquinolin-4(1H)-one (4m):[61] R_f = 0.40 (hexane/ethyl acetate 4:1); yellow solid; yield 69% (69 mg). ^1H NMR (400 MHz, $CDCl_3$) δ 7.87 (dd, *J* = 8.0, 1.2 Hz, 1H), 7.36 – 7.31 (m, 1H), 7.00 (s, 1H), 6.98 – 6.95(m, 1H), 6.87 (d, *J* = 8..0 Hz, 1H), 6.82 – 6.76 (m, 1H), 6.71 (d, *J* = 8.0 Hz, 1H), 4.69 (dd, *J* = 14.0, 3.6 Hz, 1H), 4.49 (s, 1H), 3.90 (s, 3H), 3.89 (s, 3H), 2.92 – 2.83 (m, 1H), 2.78 – 2.72 (m, 1H); $^{13}C\{^1H\}$ NMR (100 MHz, $CDCl_3$) δ 193.6, 151.7, 149.5, 149.2, 138.0, 135.5, 133.7, 127.8, 119.1, 118.6, 116.1, 111.5, 109.6, 58.5, 58.3, 56.1, 46.8; HR-MS (ESI-TOF) m/z calcd for $C_{17}H_{16}NO_3$ $[M - H]^+$ 282.1125, found 282.1120.

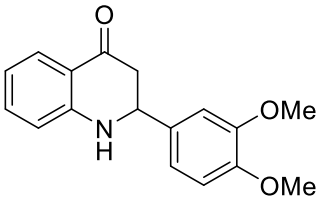

2-(3,4,5-Trimethoxyphenyl)-2,3-dihydroquinolin-4(1H)-one (4n):[44] R_f = 0.40 (hexane/ethyl acetate 4:1); yellow solid; yield 63% (63 mg). ^1H NMR (400 MHz, $CDCl_3$) δ 7.84 (d, *J* = 8.0 Hz, 1H), 7.36 – 7.31 (m, 1H), 6.77 (dd, *J* = 15.6, 8.0 Hz, 2H), 6.65 (s, 2H), 4.67 (d, *J* = 14.0 Hz, 1H), 4.62 (s, 1H), 3.85 (s, 3H), 3.84 (s, 3H), 3.83 (s, 3H), 2.88 – 2.78 (m, 1H), 2.76 – 2.67 (m, 1H); $^{13}C\{^1H\}$ NMR (100 MHz, $CDCl_3$) δ 193.4, 153.6, 151.7, 137.8, 136.9, 135.5, 127.6, 119.1, 118.6, 116.1, 103.5, 60.9, 58.9, 56.2 (×2), 46.8; HR-MS (ESI-TOF) m/z calcd for $C_{18}H_{20}NO_4$ $[M + H]^+$ 314.1387, found 314.1389.

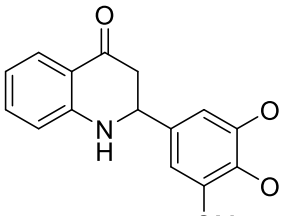

2-(Naphthalen-1-yl)-2,3-dihydroquinolin-4(1H)-one (4o):[63] R_f = 0.45 (hexane/ethyl acetate 9:1); yellow solid; yield 79% (79 mg). ^1H NMR (400 MHz, $CDCl_3$) δ 8.14 – 8.11 (m, 1H), 7.95 – 7.90 (m, 2H), 7.86 (d, *J* = 8.0 Hz, 1H), 7.80 (d, *J* = 7.2 Hz, 1H), 7.57 – 7.49 (m, 3H), 7.41 –7.34 (m, 1H), 6.86 – 6.81 (m, 1H), 6.77 (d, *J* = 8.0 Hz, 1H), 5.58 – 5.52 (m, 1H), 4.63 (s, 1H), 3.08 –

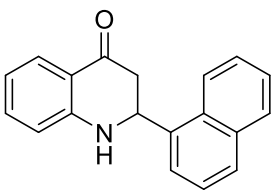

2.93 (m, 2H); $^{13}C\{^1H\}$ NMR (100 MHz, $CDCl_3$) δ 193.6, 152.0, 136.6, 135.6, 134.2, 130.5, 129.4, 129.0, 127.9, 126.8, 126.2, 125.7, 123.9, 122.5, 119.3, 118.7, 116.2, 54.6, 45.5; HR-MS (ESI-TOF) m/z calcd for $C_{19}H_{16}NO$ $[M + H]^+$ 274.1226, found 274.1231.

2-(Anthracen-9-yl)-2,3-dihydroquinolin-4(1H)-one (4p): R_f = 0.60 (hexane/ethyl acetate 9:1); yellow solid; yield 81% (81 mg); mp 212−214 °C. ^1H NMR (400 MHz, $CDCl_3$) δ 9.23

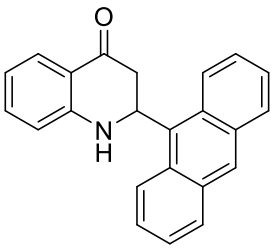

(s, 1H), 8.43 (s, 1H), 8.27 (s, 1H), 8.01 (d, *J* = 8.0 Hz, 3H), 7.54 – 7.43 (m, 4H), 7.40 – 7.33 (m, 1H), 6.85 (t, *J* = 7.6 Hz, 1H), 6.72 (d, *J* = 8.0 Hz, 1H), 6.35 (dd, *J* = 15.6, 3.6 Hz, 1H), 4.80 (s, 1H), 3.80 – 3.53 (m, 1H), 2.82 – 2.71 (m, 1H); $^{13}C\{^1H\}$ NMR (100 MHz, $CDCl_3$) δ 193.8, 151.9, 135.5, 132.1, 129.8, 129.7, 129.7, 129.3, 128.2, 126.9, 125.1, 122.5, 119.1, 118.5, 116.2, 53.6, 43.3; IR (KBr) $\tilde{\nu}$ = 3374, 3296, 3049, 2920, 2852, 1655, 1623, 1523, 1487, 1329, 1257, 1182, 1170, 998, 790 cm^{-1}; HR-MS (ESI-TOF) m/z calcd for $C_{23}H_{17}NONa$ $[M + Na]^+$ 346.1202, found 346.1194.

1-(2-Hydroxyphenyl)-3-phenylprop-2-yn-1-one (5a):[48] R_f = 0.60 (hexane/ethyl acetate

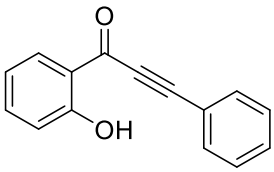

4:1); yellowish solid; yield 82% (97 mg); ^1H NMR (400 MHz, $CDCl_3$) δ 11.74 (s, 1H), 8.13 (dd, *J* = 8.0, 1.6 Hz, 1H), 7.73 – 7.66 (m, 2H), 7.58 – 7.48 (m, 2H), 7.48 – 7.41 (m, 2H), 6.99 (dd, *J* = 12.0, 4.4 Hz, 2H); $^{13}C\{^1H\}$ NMR (100 MHz, $CDCl_3$) δ 182.4, 162.9, 137.3, 133.3, 133.2, 131.3, 128.9, 120.9, 119.8, 119.6, 118.3, 96.2, 85.9; HR-MS (ESI-TOF) m/z calcd for $C_{15}H_{11}O_2$ $[M + H]^+$ 223.0754, found 223.0750.

2-Phenyl-4H-chromen-4-one (5b):[64] R_f = 0.55 (hexane/ethyl acetate 4:1); white solid; yield

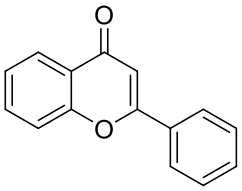

73% (58 mg). ^1H NMR (400 MHz, $CDCl_3$ + DMSO-d_6) δ 8.10 (d, *J* = 8.0 Hz, 1H), 7.84 (dd, *J* = 5.2, 2.4 Hz, 2H), 7.63 (t, *J* = 7.6 Hz, 1H), 7.50 (d, *J* = 8.4 Hz, 1H), 7.44 (d, *J* = 5.2 Hz, 3H), 7.33 (t, *J* = 7.6 Hz, 1H), 6.73 (s, 1H); $^{13}C\{^1H\}$ NMR (100 MHz, $CDCl_3$ + DMSO-d_6) δ 178.3,

163.3, 156.0, 133.7, 131.5, 131.4, 128.9, 126.1, 125.3, 125.1, 123.6, 118.0, 107.2; HR-MS (ESI-TOF) m/z calcd for $C_{15}H_{11}O_2$ $[M + H]^+$ 223.0754, found 223.0743.

2-(4-Isopropylphenyl)chroman-4-ol (6a): R_f = 0.45 (hexane/ethyl acetate 9:1); white solid; yield 94% (95 mg); mp 151−153 °C. ^{1}H NMR (400 MHz, $CDCl_3$) δ 7.49 (d, *J* = 7.6 Hz, 1H), 7.36 (d, *J* = 8.0 Hz, 2H), 7.26 – 7.23 (m, 2H), 7.20 – 7.15 (m, 1H), 6.96 (td, *J* = 7.6, 1.0 Hz, 1H), 6.89 – 6.84 (m, 1H), 5.13 (dd, *J* = 11.6, 1.6 Hz, 1H), 5.09 – 5.03 (m, 1H), 2.96 – 2.86 (m, 1H), 2.52 – 2.45 (m, 1H), 2.19 – 2.09 (m, 1H), 1.26 (s, 3H), 1.24 (s, 3H); $^{13}C\{^1H\}$ NMR (100 MHz, $CDCl_3$) δ 154.7, 149.2, 137.9, 129.3, 127.1, 126.9, 126.3, 125.9, 121.0, 116.9, 76.9, 66.0, 39.9, 34.0, 24.1 (×2); IR (KBr) $\tilde{\nu}$ = 3219, 2958, 1607, 1509, 1483, 1338, 1300, 1228, 1182, 1066, 1055, 1035, 904, 864 cm^{-1}; HR-MS (ESI-TOF) m/z calcd for $C_{18}H_{20}O_2Na$ $[M + Na]^+$ 291.1356, found 291.1327.

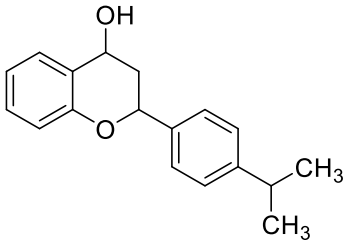

6.6. REFERENCES

1. Sutar, R. L.; Huber, S. M., *ACS Catal.* **2019,** *9* (10), 9622-9639.

2. (a) Mahmudov, K. T.; Kopylovich, M. N.; Guedes da Silva, M. F. C.; Pombeiro, A. J. L., *Dalton Trans.* **2017,** *46* (31), 10121-10138; (b) Vogel, L.; Wonner, P.; Huber, S. M., *Angew. Chem., Int. Ed.* **2019,** *58* (7), 1880-1891.

3. Kennedy, C. R.; Lin, S.; Jacobsen, E. N., *Angew. Chem. Int. Ed.* **2016,** *55* (41), 12596–12624.

4. Breugst, M.; von der Heiden, D.; Schmauck, J., *Synthesis* **2017,** *49* (15), 3224-3236.

5. (a) Auria-Luna, F.; Mohammadi, S.; Divar, M.; Gimeno, M. C.; Herrera, R. P., *Adv. Synth. Catal.* **2020,** *362* (23), 5275-5300; (b) Jeffrey, J. L.; Terrett, J. A.; MacMillan, D. W. C., *Science* **2015,** *349* (6255), 1532-1536.

6. Choudhuri, K.; Pramanik, M.; Mal, P., *J. Org. Chem.* **2020,** *85* (19), 11997-12011.

7. Cavallo, G.; Metrangolo, P.; Milani, R.; Pilati, T.; Priimagi, A.; Resnati, G.; Terraneo, G., *Chem. Rev.* **2016,** *116* (4), 2478-2601.

8. Metrangolo, P.; Meyer, F.; Pilati, T.; Resnati, G.; Terraneo, G., *Angew. Chem. Int. Ed. Engl.* **2008,** *47* (33), 6114-27.

9. Lommerse, J. P. M.; Stone, A. J.; Taylor, R.; Allen, F. H., *J. Am. Chem. Soc.* **1996,** *118* (13), 3108-3116.

10. Afonin, A. V.; Vashchenko, A. V.; Sigalov, M. V., *Org. Biomol. Chem.* **2016,** *14* (47), 11199-11211.

11. (a) Dreger, A.; Wonner, P.; Engelage, E.; Walter, S. M.; Stoll, R.; Huber, S. M., *Chem. Commun.* **2019,** *55* (57), 8262-8265; (b) Sun, X.; Wang, W.; Li, Y.; Ma, J.; Yu, S., *Org. Lett.* **2016,** *18* (18), 4638-41.

12. Bulfield, D.; Huber, S. M., *Chem. Eur. J.* **2016,** *22* (41), 14434-14450.

13. Gilday, L. C.; Robinson, S. W.; Barendt, T. A.; Langton, M. J.; Mullaney, B. R.; Beer, P. D., *Chem. Rev.* **2015,** *115* (15), 7118-7195.

14. Brown, A.; Beer, P. D., *Chem. Commun.* **2016,** *52* (56), 8645-8658.

15. Wilcken, R.; Zimmermann, M. O.; Lange, A.; Joerger, A. C.; Boeckler, F. M., *J. Med. Chem.* **2013,** *56* (4), 1363-1388.

16. Nandy, A.; Kazi, I.; Guha, S.; Sekar, G., *J. Org. Chem.* **2021,** *86* (3), 2570-2581.

17. Yi, X.; Jiao, L.; Xi, C., *Org. Biomol. Chem.* **2016,** *14* (41), 9912-9918.

18. Guha, S.; Kazi, I.; Mukherjee, P.; Sekar, G., *Chem. Commun.* **2017,** *53* (79), 10942-10945.

19. Kazi, I.; Guha, S.; Sekar, G., *J. Org. Chem.* **2019,** *84* (11), 6642-6654.

20. (a) Dreger, A.; Engelage, E.; Mallick, B.; Beer, P. D.; Huber, S. M., *Chem. Commun.* **2018,** *54* (32), 4013-4016; (b) Jungbauer, S. H.; Huber, S. M., *J. Am. Chem. Soc.* **2015,** *137* (37), 12110-20.

21. Liu, X.; Ma, S.; Toy, P. H., *Org. Lett.* **2019,** *21* (22), 9212-9216.

22. Chan, Y. C.; Yeung, Y. Y., *Angew. Chem. Int. Ed.* **2018,** *57* (13), 3483-3487.

23. Kuwano, S.; Suzuki, T.; Hosaka, Y.; Arai, T., *Chem. Commun.* **2018,** *54* (31), 3847-3850.

24. Kaasik, M.; Martõnova, J.; Erkman, K.; Metsala, A.; Järving, I.; Kanger, T., *Chem. Sci.* **2021,** *12* (21), 7561-7568.

25. Saito, M.; Tsuji, N.; Kobayashi, Y.; Takemoto, Y., *Org. Lett.* **2015,** *17* (12), 3000-3.

26. Wonner, P.; Steinke, T.; Vogel, L.; Huber, S. M., *Chem. Eur. J.* **2020,** *26* (6), 1258-1262.

27. Alegre-Requena, J. V.; Valero-Tena, A.; Sonsona, I. G.; Uriel, S.; Herrera, R. P., *Org. Biomol. Chem.* **2020,** *18* (8), 1594-1601.

28. (a) Jungbauer, S. H.; Walter, S. M.; Schindler, S.; Rout, L.; Kniep, F.; Huber, S. M., *Chem. Commun.* **2014,** *50* (47), 6281-4; (b) Saito, M.; Kobayashi, Y.; Tsuzuki, S.; Takemoto, Y., *Angew. Chem. Int. Ed.* **2017,** *56* (26), 7653-7657.

29. Kazi, I.; Guha, S.; Sekar, G., *Org. Lett.* **2017,** *19* (5), 1244-1247.

30. Matsuzawa, A.; Takeuchi, S.; Sugita, K., *Chem. Asian J.* **2016,** *11* (20), 2863-2866.

31. Kazi, I.; Sekar, G., *Org. Biomol. Chem.* **2019,** *17* (45), 9743-9756.

32. Northrup, A. B.; MacMillan, D. W. C., *J. Am. Chem. Soc.* **2002,** *124* (11), 2458-2460.

33. (a) Breugst, M.; Detmar, E.; von der Heiden, D., *ACS Catal.* **2016,** *6* (5), 3203-3212; (b) Wu, L.; Niu, B.; Li, W.; Yan, F., *Bull. Korean Chem. Soc.* **2009,** *30* (11), 2777-2778.

34. Zhang, H.; Toy, P. H., *Adv. Synth. Catal.* **2021,** *363* (1), 215-221.

35. Ge, Y. C.; Yang, H.; Heusler, A.; Chua, Z.; Wong, M. W.; Tan, C. H., *Chem. Asian J.* **2019,** *14* (15), 2656-2661.

36. (a) Breugst, M.; von der Heiden, D.; Detmar, E.; Kuchta, R., *Synlett* **2017,** *29* (10), 1307-1313; (b) Gliese, J.-P.; Jungbauer, S. H.; Huber, S. M., *Chem. Commun.* **2017,** *53* (88), 12052-12055.

37. Zhang, L.; Luo, Y.; Fan, R.; Wu, J., *Green Chem.* **2007,** *9* (9).

38. Wu, J.; Sun, W.; Sun, X.; Xia, H.-G., *Green Chem.* **2006,** *8* (4).

39. Robertson, C. C.; Wright, J. S.; Carrington, E. J.; Perutz, R. N.; Hunter, C. A.; Brammer, L., *Chem. Sci.* **2017,** *8* (8), 5392-5398.

40. Nijveldt, R. J.; van Nood, E.; van Hoorn, D. E. C.; Boelens, P. G.; van Norren, K.; van Leeuwen, P. A. M., *The American Journal of Clinical Nutrition* **2001,** *74* (4), 418-425.

41. Sharma, C. S.; Verma, T.; Singh, H. P.; Kumar, N., *Med. Chem. Res.* **2014,** *23* (11), 4814-4824.

42. Chandrasekhar, S.; Pushpavalli, S. N. C. V. L.; Chatla, S.; Mukhopadhyay, D.; Ganganna, B.; Vijeender, K.; Srihari, P.; Reddy, C. R.; Janaki Ramaiah, M.; Bhadra, U., *Bioorg. Med. Chem. Lett.* **2012,** *22* (1), 645-648.

43. (a) Matsui, J. K.; Molander, G. A., *Org. Lett.* **2017,** *19* (4), 950-953; (b) Shaikh, M.; Atyam, K. K.; Sahu, M.; Ranganath, K. V. S., *Chem. Commun.* **2017,** *53* (44), 6029-6032.

44. Saito, K.; Moriya, Y.; Akiyama, T., *Org. Lett.* **2015,** *17* (13), 3202-3205.

45. Frisch, M. J.; Foresman, J. B.; Fox, D. J. *Gaussian 16 Rev. C.01*, Wallingford, CT, 2016.

46. Grimme, S.; Antony, J.; Ehrlich, S.; Krieg, H., *J. Chem. Phys.* **2010,** *132* (15), 154104.

47. Zeng, B.-S.; Yu, X.; Siu, P. W.; Scheidt, K. A., *Chem. Sci.* **2014,** *5* (6), 2277-2281.

48. Yoshida, M.; Fujino, Y.; Doi, T., *Org. Lett.* **2011,** *13* (17), 4526-4529.

49. He, X.; Xie, M.; Li, R.; Choy, P. Y.; Tang, Q.; Shang, Y.; Kwong, F. Y., *Org. Lett.* **2020,** *22* (11), 4306-4310.

50. Chai, G.-L.; Qiao, Y.; Zhang, P.; Guo, R.; Wang, J.; Chang, J., *Org. Lett.* **2020,** *22* (20), 8023-8027.

51. Du, Z.; Ng, H.; Zhang, K.; Zeng, H.; Wang, J., *Org. Biomol. Chem.* **2011,** *9* (20), 6930-6933.

52. Vimal, M.; Pathak, U.; Halve, A. K., *Synth. Commun.* **2019,** *49* (21), 2805-2814.

53. Climent, M. J.; Corma, A.; Iborra, S.; Martí, L., *ACS Catal.* **2015,** *5* (1), 157-166.

54. Arunprasath, D.; Sekar, G., *Org. Lett.* **2019,** *21* (4), 867-871.

55. Mai, C. W.; Yaeghoobi, M.; Abd-Rahman, N.; Kang, Y. B.; Pichika, M. R., *Eur. J. Med. Chem.* **2014,** *77*, 378-387.

56. Ullah, A.; Ansari, F. L.; Ihsan ul, H.; Nazir, S.; Mirza, B., *Chem. Biodivers.* **2007,** *4* (2), 203-214.

57. Rajesh, U. C.; Manohar, S.; Rawat, D. S., *Adv. Synth. Catal.* **2013,** *355* (16), 3170-3178.

58. Bakthadoss, M.; Kumar, P. V.; Reddy, T. S., *Eur. J. Org. Chem.* **2017,** (30), 4439-4444.

59. Zhou, Z.; Zhao, P.; Huang, W.; Yang, G., *Adv. Synth. Catal.* **2006,** *348* (1-2), 63-67.

60. Muller, B. M.; Litberg, T. J.; Yocum, R. A.; Pniewski, C. A.; Adler, M. J., *J. Org. Chem.* **2016,** *81* (13), 5775-5781.

61. Mondal, B.; Pan, S. C., *Org. Biomol. Chem.* **2014,** *12* (48), 9789-9792.

62. Kanagaraj, K.; Pitchumani, K., *J. Org. Chem.* **2013,** *78* (2), 744-751.

63. Pan, G.-F.; Su, L.; Zhang, Y.-L.; Guo, S.-H.; Wang, Y.-Q., *RSC Adv.* **2016,** *6* (30), 25375-25378.

64. Zhang, X.-W.; Jiang, G.-Q.; Lei, S.-H.; Shan, X.-H.; Qu, J.-P.; Kang, Y.-B., *Org. Lett.* **2021,** *23* (5), 1611-1615.

NMR Spectra

^{1}H NMR (400 MHz, $CDCl_3$)

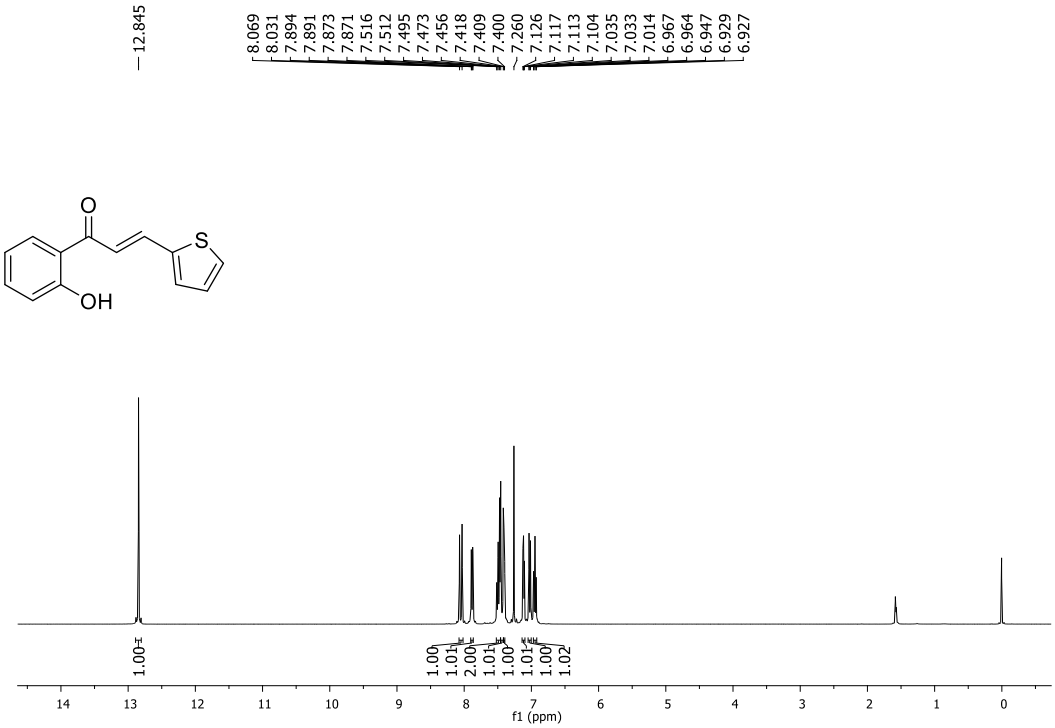

Figure 6.7. ^{1}H NMR spectrum of (*E*)-1-(2-Hydroxyphenyl)-3-(thiophen-2-yl)prop-2-en-1-one **(1j)**

^{13}C{^{1}H} NMR (100 MHz, $CDCl_3$)

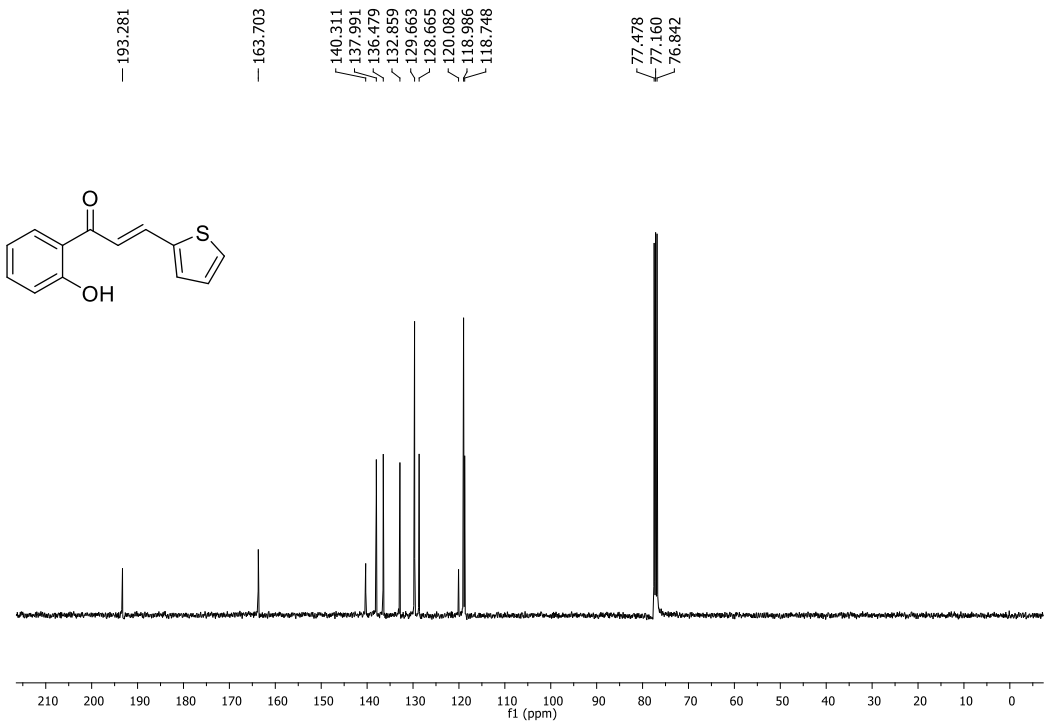

Figure 6.8. ^{13}C{^{1}H} NMR spectrum of (*E*)-1-(2-Hydroxyphenyl)-3-(thiophen-2-yl)prop-2-en-1-one **(1j)**

^{1}H NMR (400 MHz, $CDCl_3$)

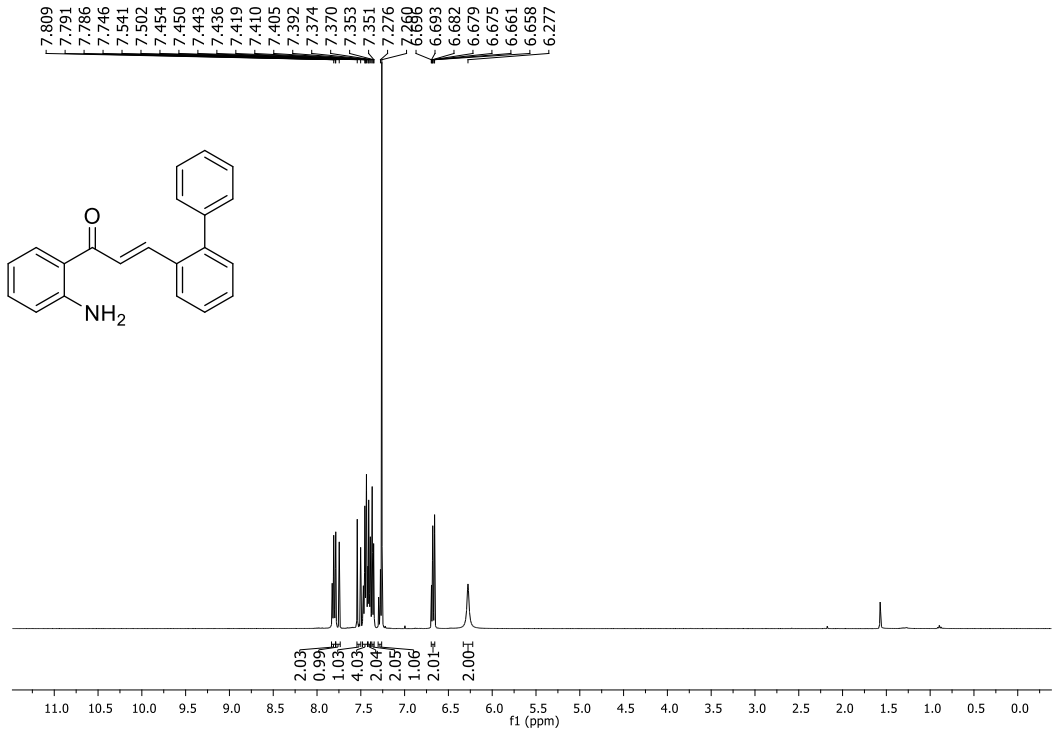

Figure 6.9. ^{1}H NMR spectrum of (*E*)-3-([1,1'-Biphenyl]-2-yl)-1-(2-aminophenyl)prop-2-en-1-one **(3l)**

^{13}C{^{1}H} NMR (100 MHz, $CDCl_3$)

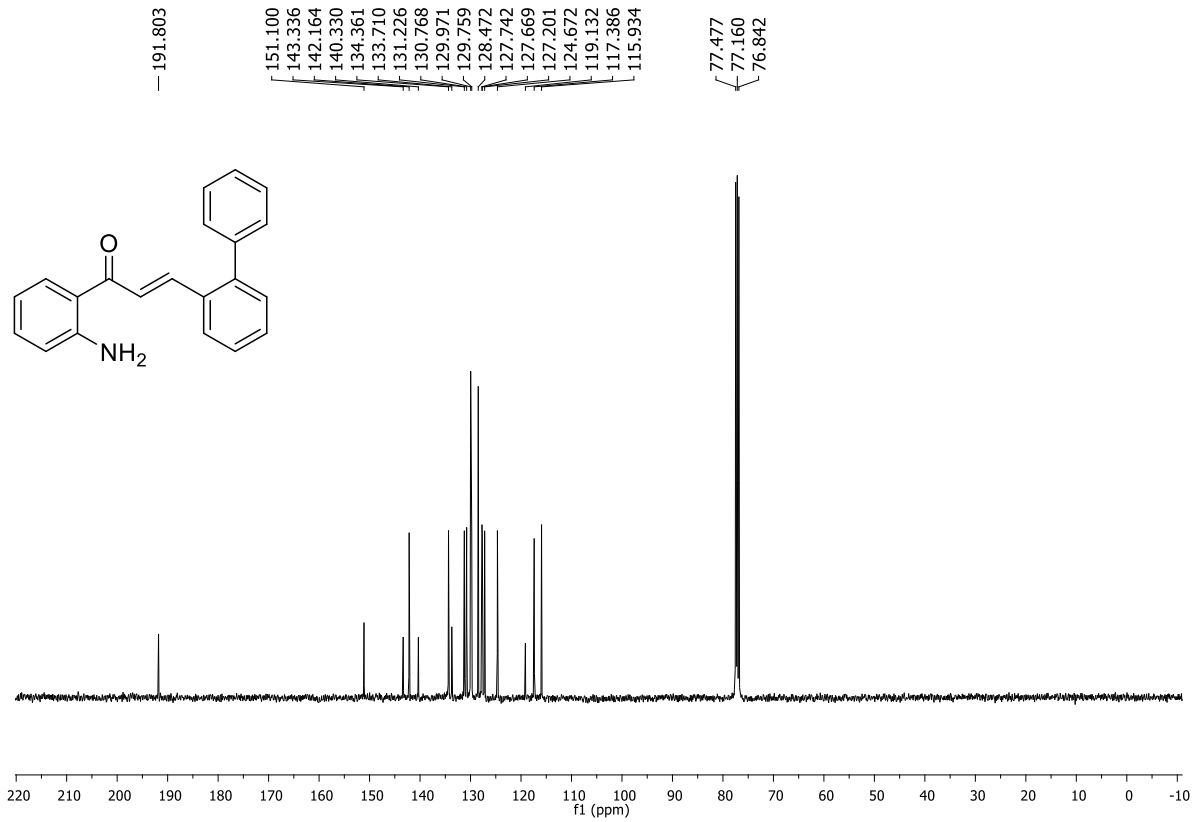

Figure 6.10. ^{13}C{^{1}H} NMR spectrum of (*E*)-3-([1,1'-Biphenyl]-2-yl)-1-(2-aminophenyl)prop-2-en-1-one **(3l)**

^{1}H NMR (400 MHz, $CDCl_3$)

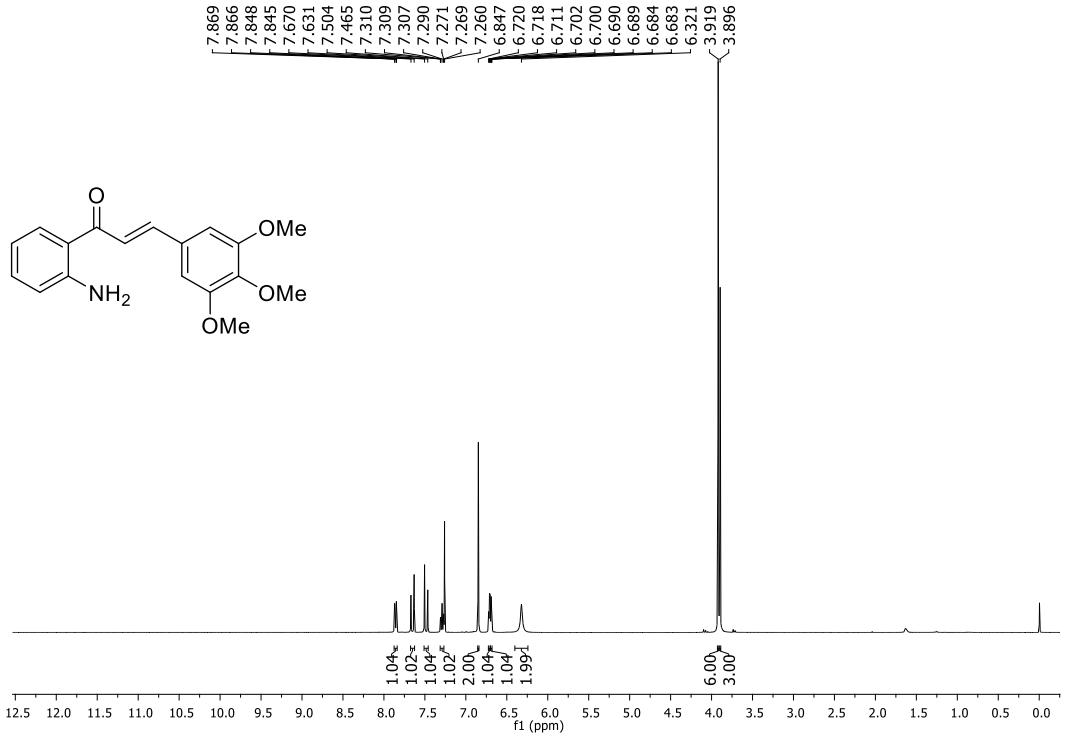

Figure 6.11. ^{1}H NMR spectrum of (*E*)-1-(2-Aminophenyl)-3-(3,4,5-trimethoxyphenyl)prop-2-en-1-one **(3n)**

^{13}C{^{1}H} NMR (100 MHz, $CDCl_3$)

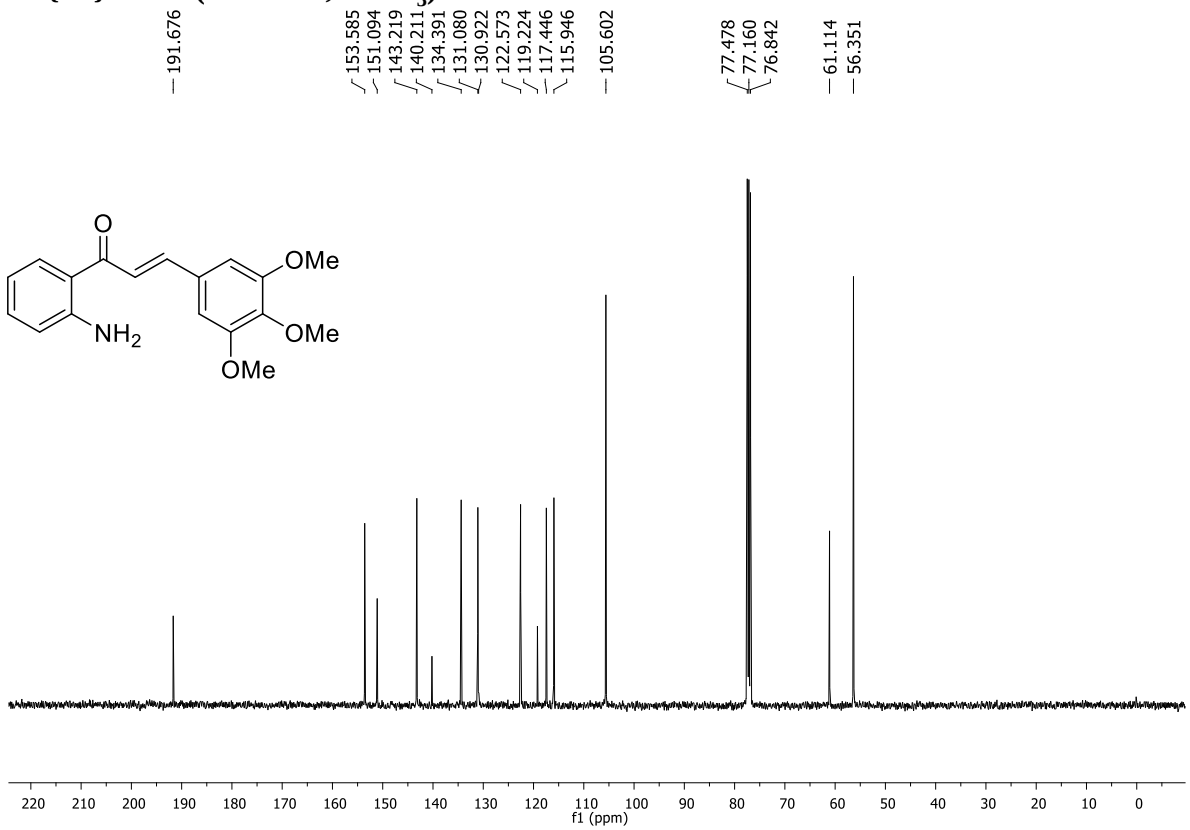

Figure 6.12. ^{13}C{^{1}H} NMR spectrum of (*E*)-1-(2-Aminophenyl)-3-(3,4,5-trimethoxyphenyl)prop-2-en-1-one **(3n)**

^{1}H NMR (400 MHz, $CDCl_3$)

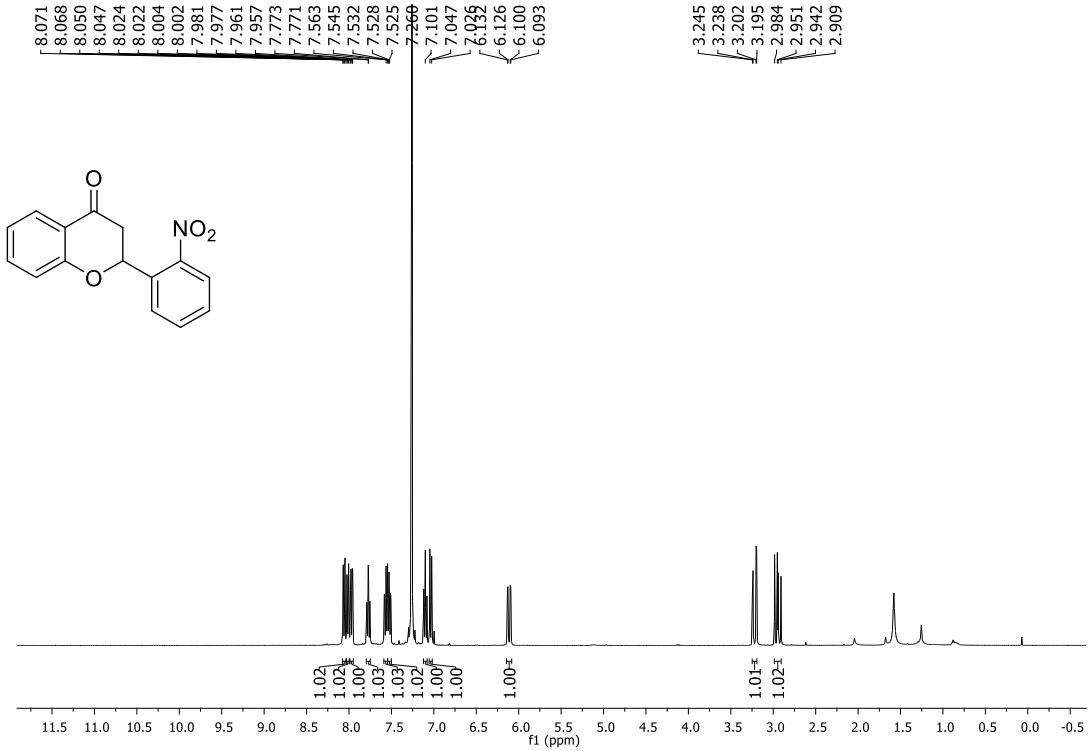

Figure 6.13. ^{1}H NMR spectrum of 2-(2-Nitrophenyl)chroman-4-one **(2b)**

^{13}C{^{1}H} NMR (100 MHz, $CDCl_3$)

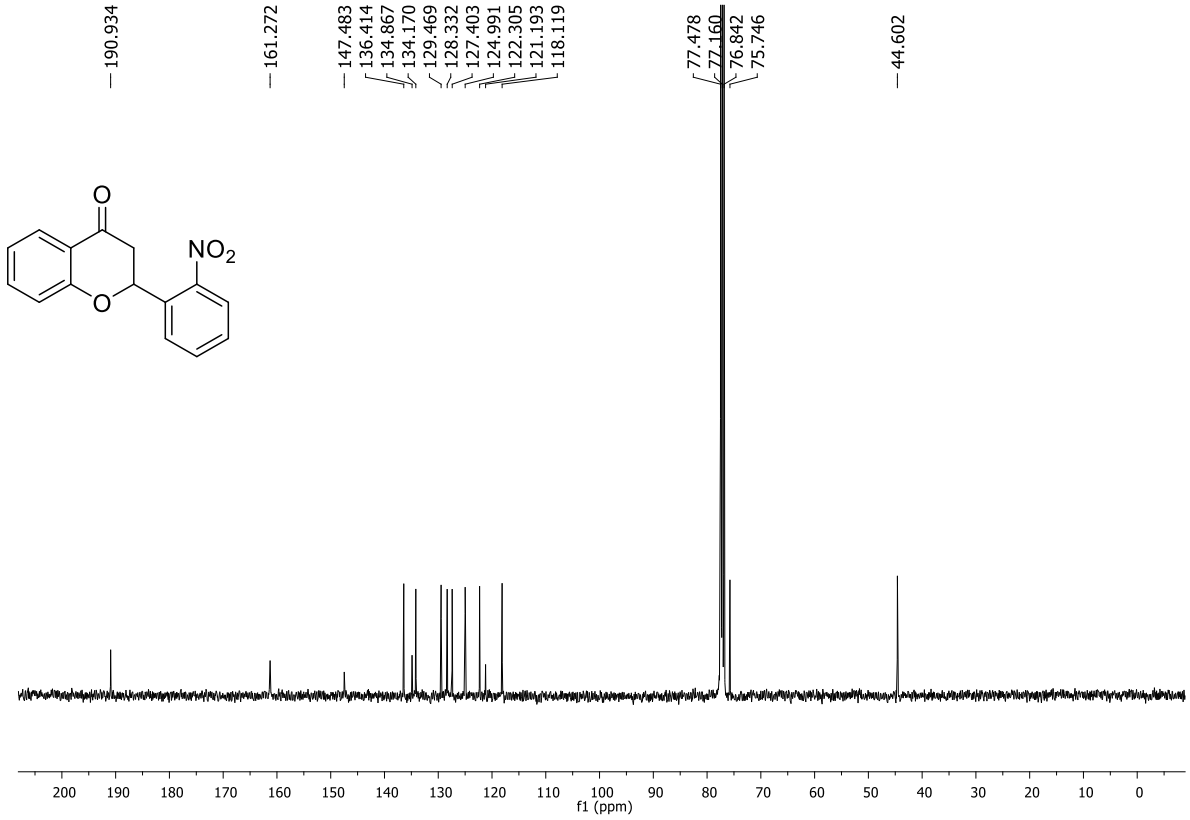

Figure 6.14. ^{13}C{^{1}H} NMR spectrum of 2-(2-Nitrophenyl)chroman-4-one **(2b)**

^{1}H NMR (400 MHz, $CDCl_3$)

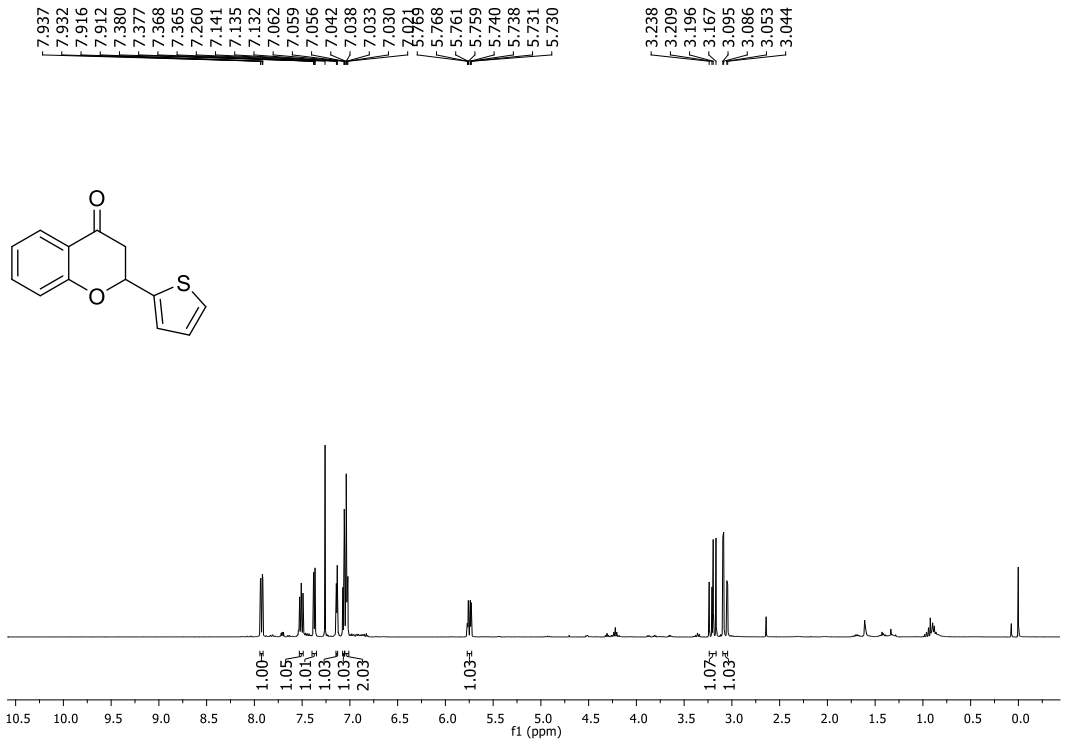

Figure 6.15. ^{1}H NMR spectrum of 2-(Thiophen-2-yl)chroman-4-one **(2j)**

^{13}C{^{1}H} NMR (100 MHz, $CDCl_3$)

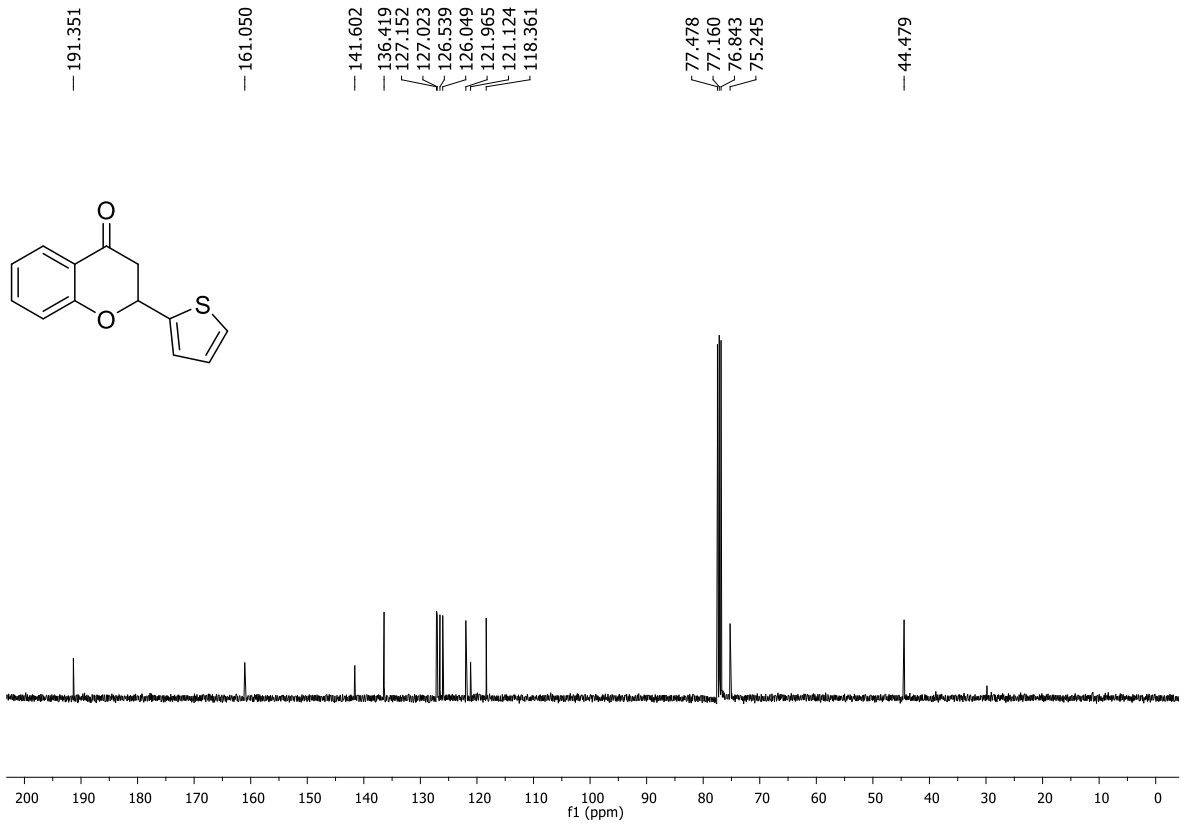

Figure 6.16. ^{13}C{^{1}H} NMR spectrum of 2-(Thiophen-2-yl)chroman-4-one **(2j)**

^{1}H NMR (400 MHz, $CDCl_3$)

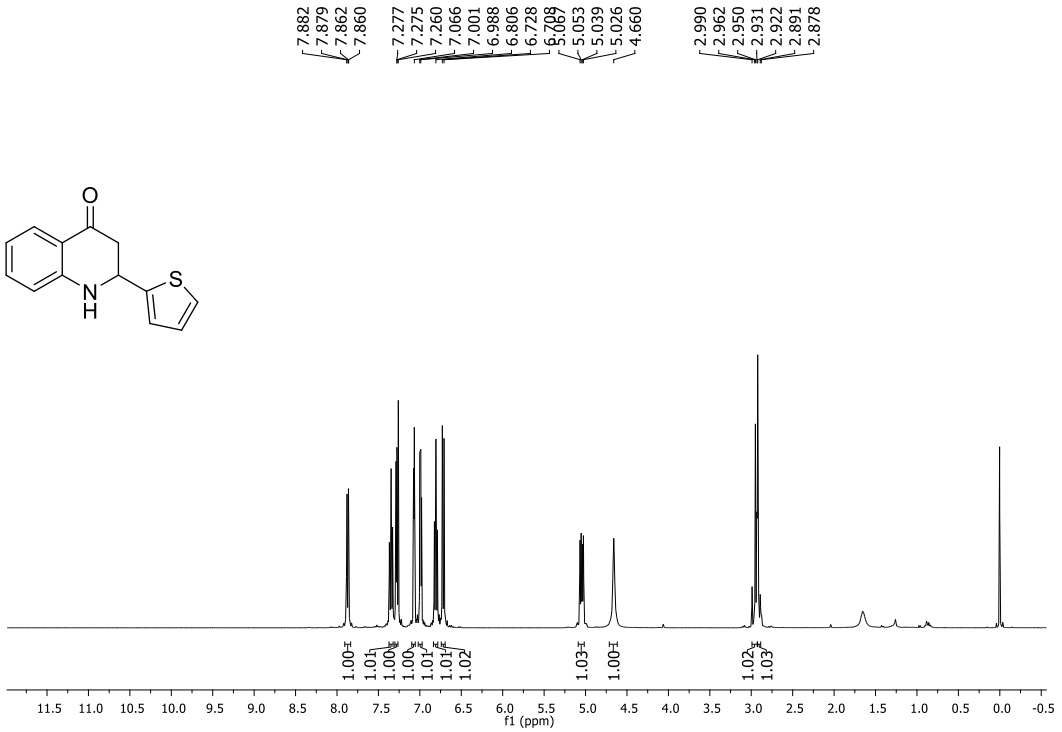

Figure 6.17. ^{1}H NMR spectrum of 2-(Thiophen-2-yl)-2,3-dihydroquinolin-4(1H)-one **(4j)**

^{13}C{^{1}H} NMR (100 MHz, $CDCl_3$)

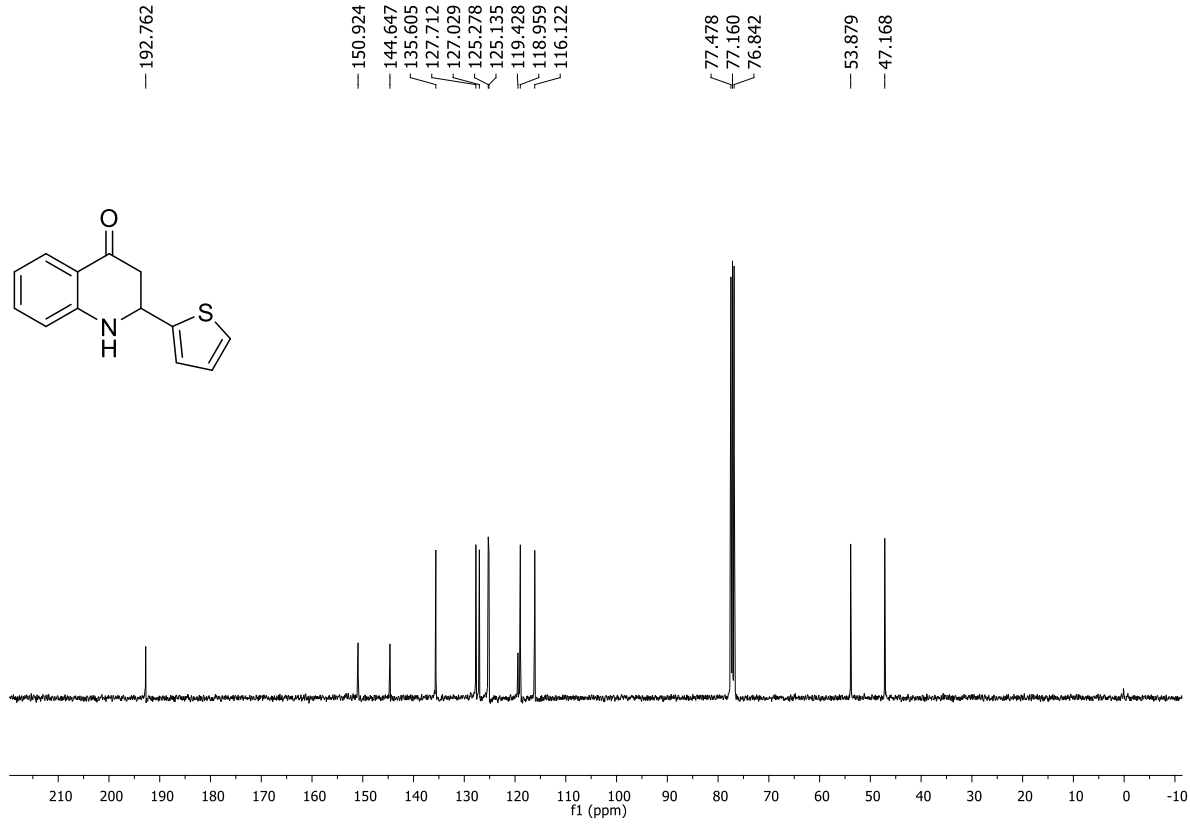

Figure 6.18. ^{13}C{^{1}H} NMR spectrum of 2-(Thiophen-2-yl)-2,3-dihydroquinolin-4(1H)-one **(4j)**

^{1}H NMR (400 MHz, $CDCl_3$ + DMSO-d_6)

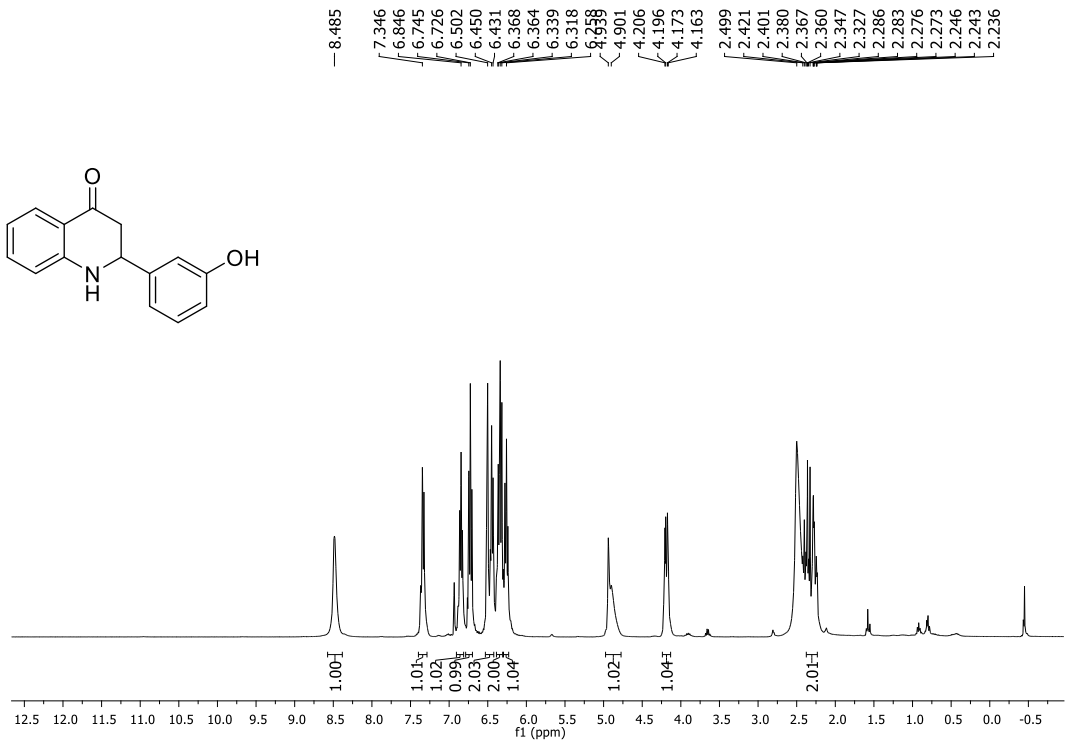

Figure 6.19. ^{1}H NMR spectrum of 2-(3-Hydroxyphenyl)-2,3-dihydroquinolin-4(1H)-one **(4k)**

^{13}C{^{1}H} NMR (100 MHz, $CDCl_3$ + DMSO-d_6)

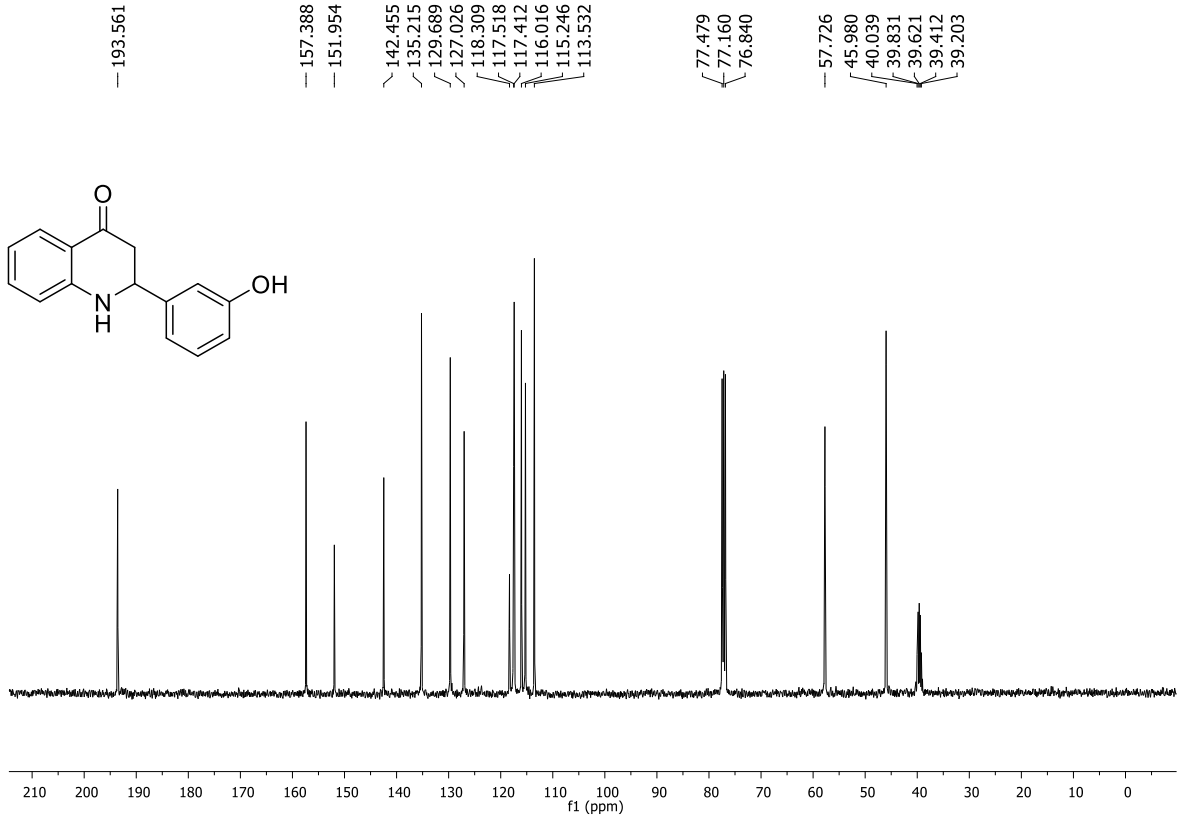

Figure 6.20. ^{13}C{^{1}H} NMR spectrum of 2-(3-Hydroxyphenyl)-2,3-dihydroquinolin-4(1H)-one **(4k)**

^{1}H NMR (400 MHz, $CDCl_3$)

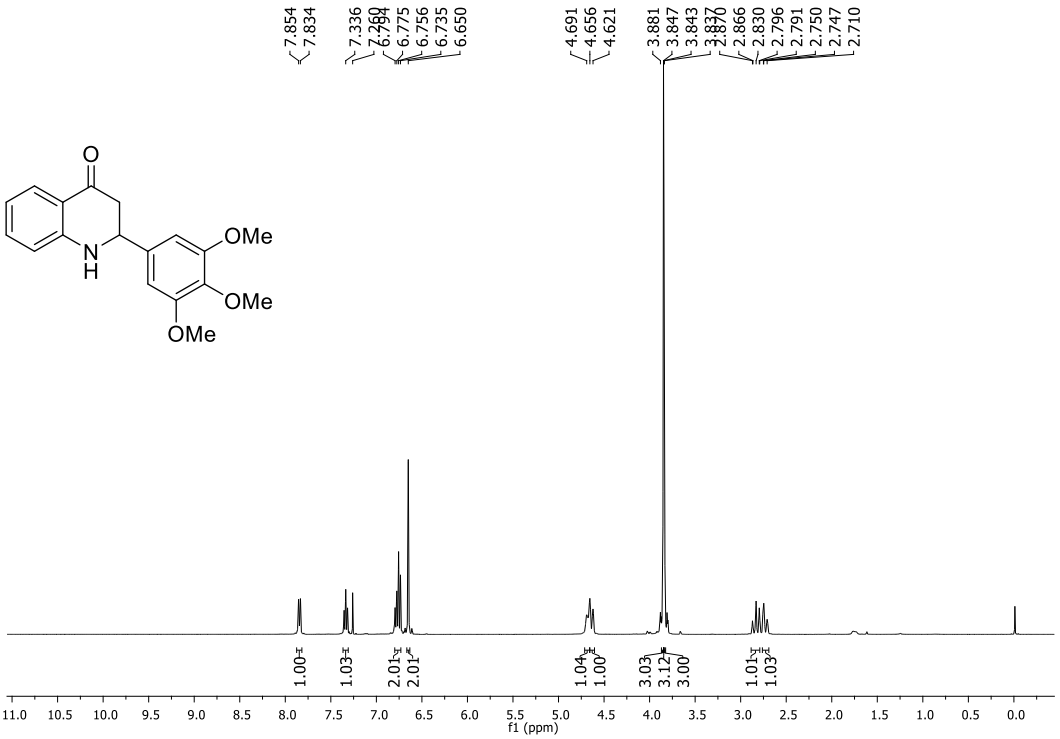

Figure 6.21. ^{1}H NMR spectrum of 2-(3,4,5-Trimethoxyphenyl)-2,3-dihydroquinolin-4(1H)-one **(4n)**

^{13}C{^{1}H} NMR (100 MHz, $CDCl_3$)

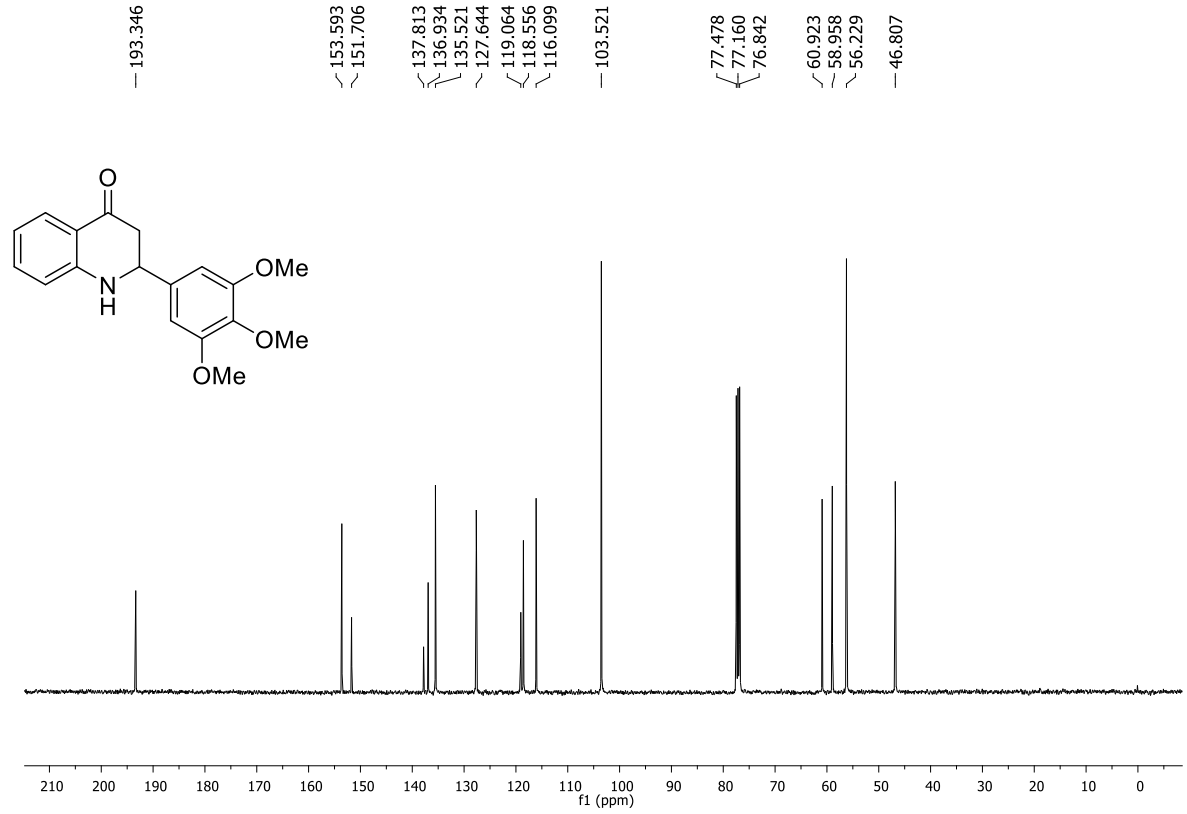

Figure 6.22. ^{13}C{^{1}H} NMR spectrum of 2-(3,4,5-Trimethoxyphenyl)-2,3-dihydroquinolin-4(1H)-one **(4n)**

^{1}H NMR (400 MHz, $CDCl_3$)

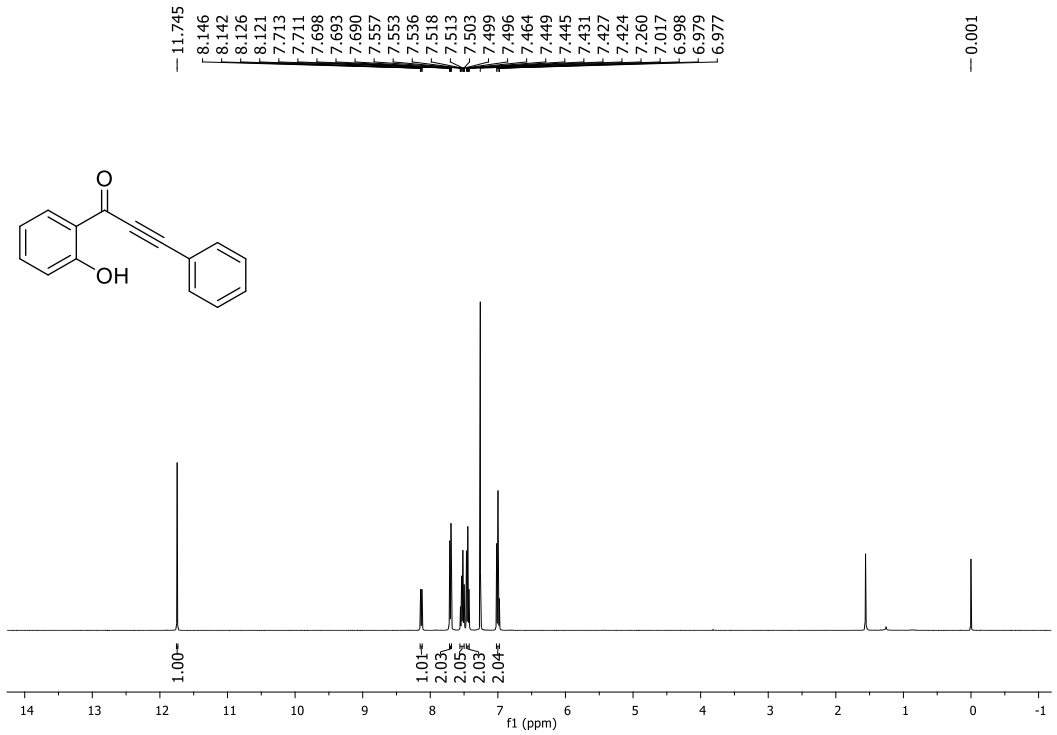

Figure 6.23. ^{1}H NMR spectrum of 1-(2-Hydroxyphenyl)-3-phenylprop-2-yn-1-one **(5a)**

^{13}C{^{1}H} NMR (100 MHz, $CDCl_3$)

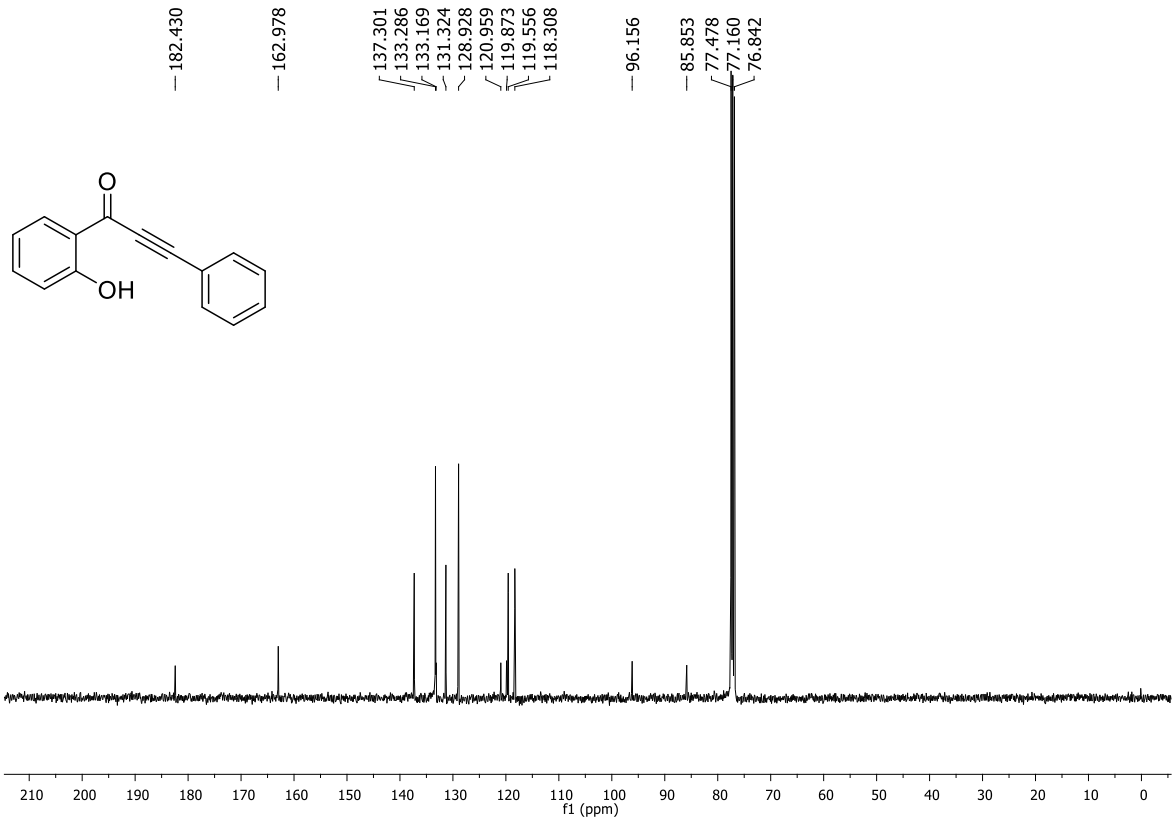

Figure 6.24. ^{13}C{^{1}H} NMR spectrum of1-(2-Hydroxyphenyl)-3-phenylprop-2-yn-1-one **(5a)**

^{1}H NMR (400 MHz, $CDCl_3$ + DMSO-d_6)

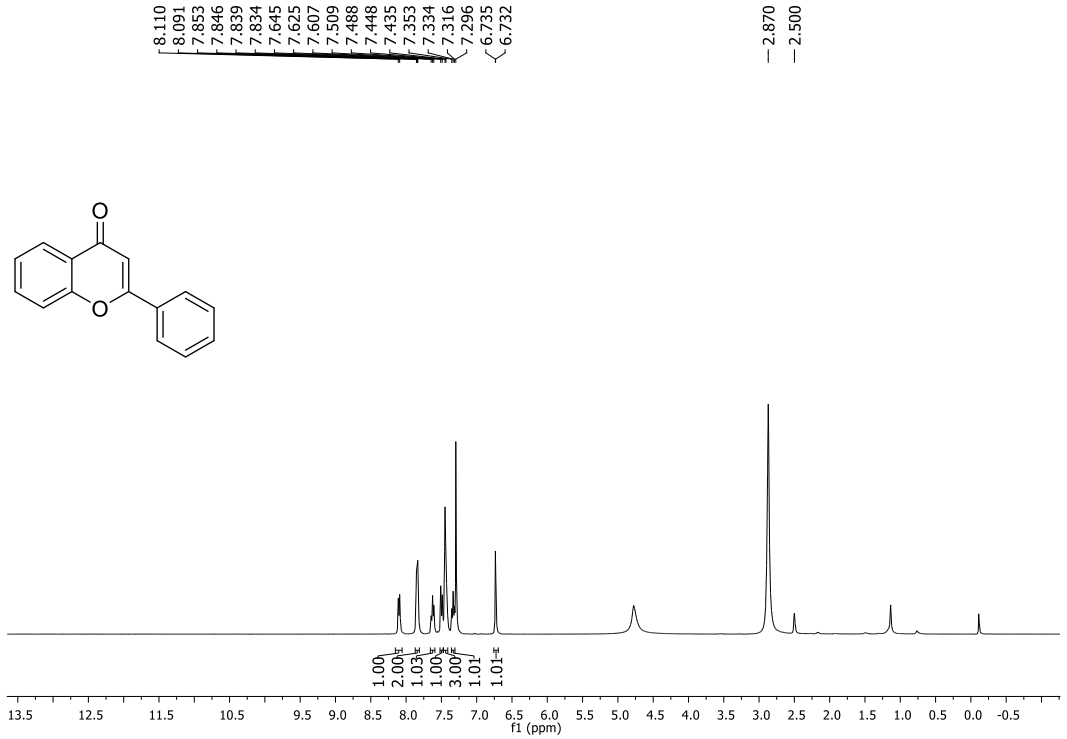

Figure 6.25. ^{1}H NMR spectrum of 2-Phenyl-4H-chromen-4-one **(5b)**

^{13}C{^{1}H} NMR (100 MHz, $CDCl_3$ + DMSO-d_6)

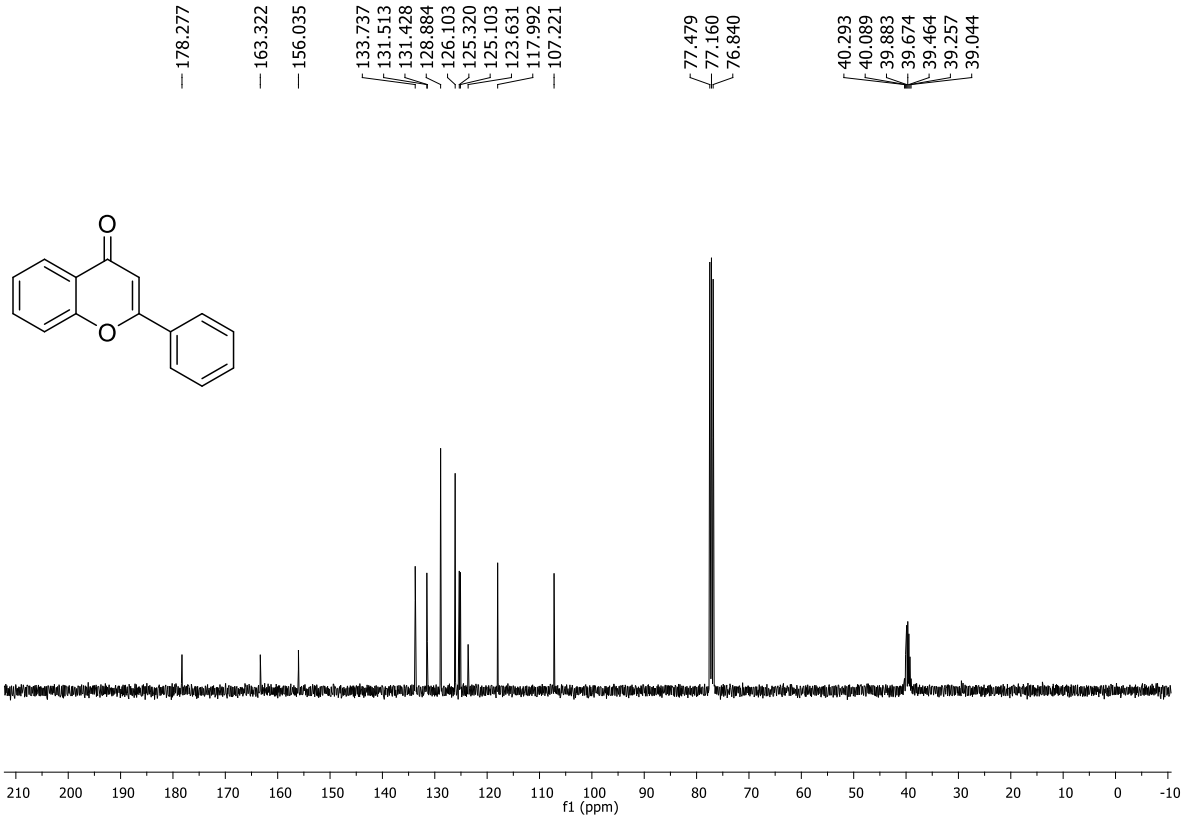

Figure 6.26. ^{13}C{^{1}H} NMR spectrum of 2-Phenyl-4H-chromen-4-one **(5b)**

^{1}H NMR (400 MHz, $CDCl_3$)

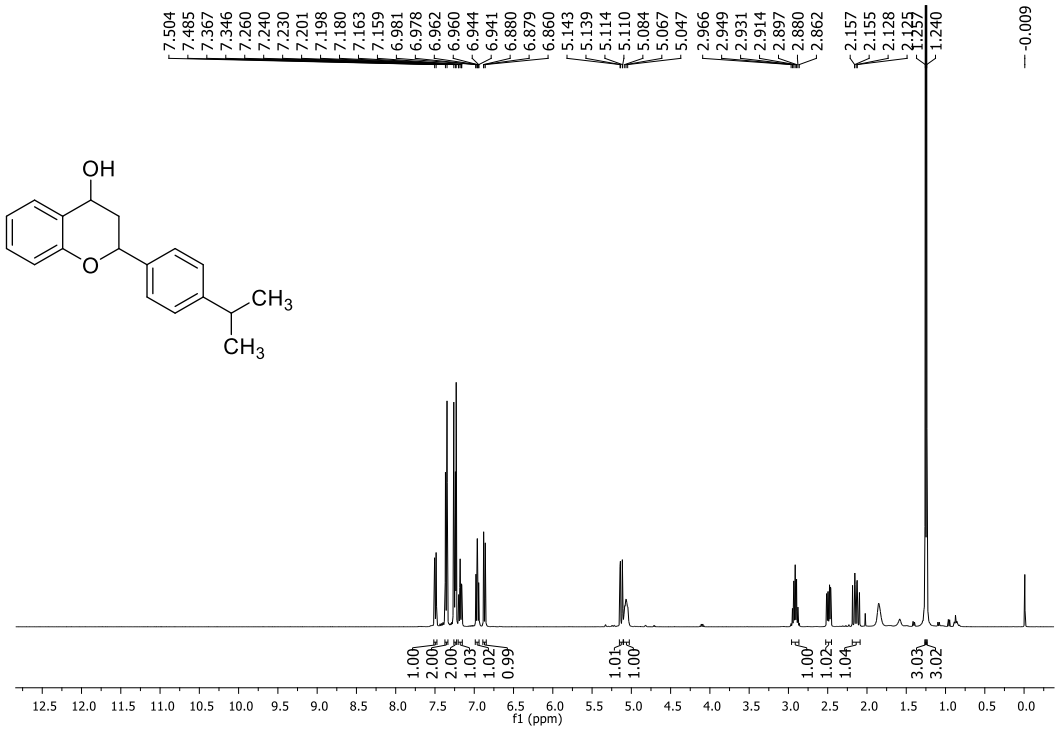

Figure 6.27. ^{1}H NMR spectrum of 2-(4-Isopropylphenyl)chroman-4-ol **(6a)**

^{13}C{^{1}H} NMR (100 MHz, $CDCl_3$)

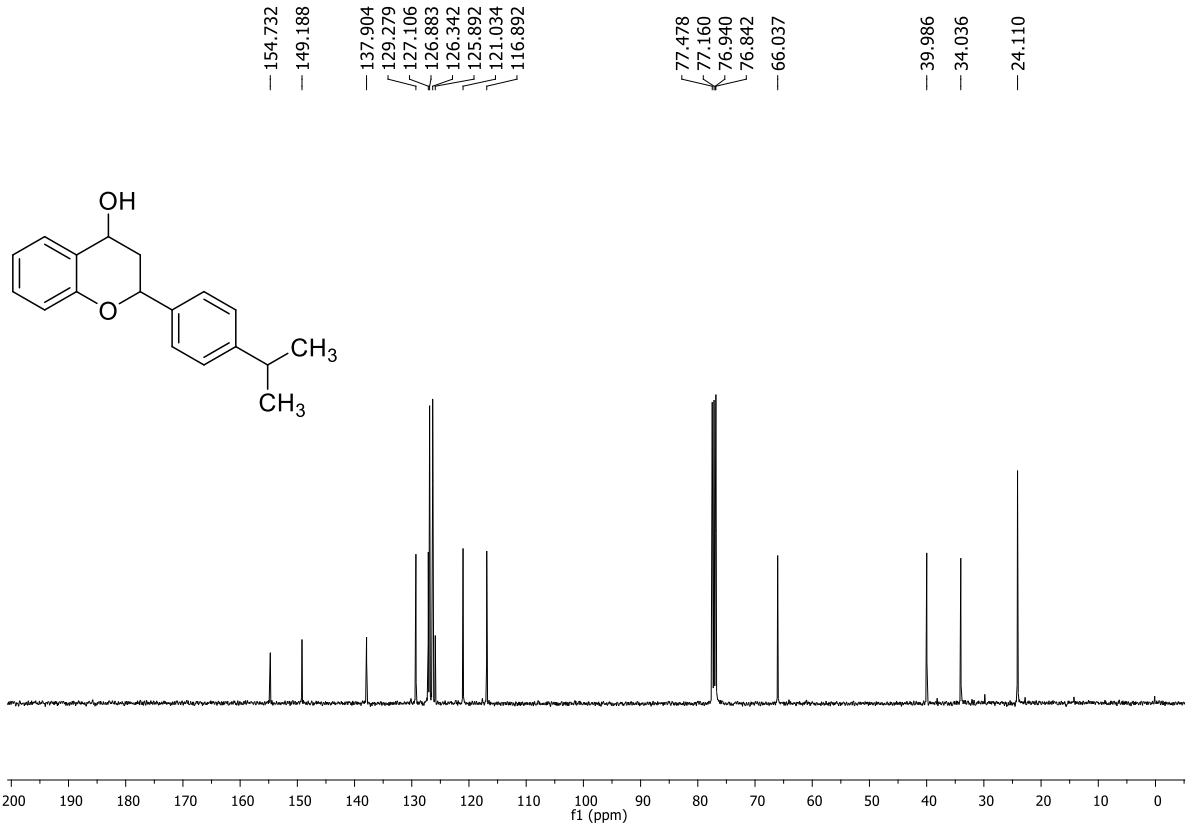

Figure 6.28. ^{13}C{^{1}H} NMR spectrum of 2-(4-Isopropylphenyl)chroman-4-ol **(6a)**

Chapter 2 and 3
Synthesis of Benzimid-azole-Fused Phenanthri-dines

J. Org. Chem. **2019,** *84*, 12009-12020.
J. Org. Chem. **2021,** *86*, 9587-9602.

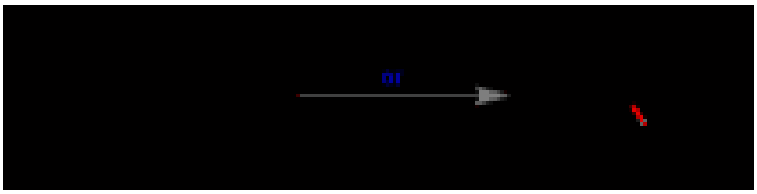

Chapter 4
Synthesis of Phe-nanthridine-fused quinazoli-nones

Org. Lett. **2022,** *24*, 3144-3148.

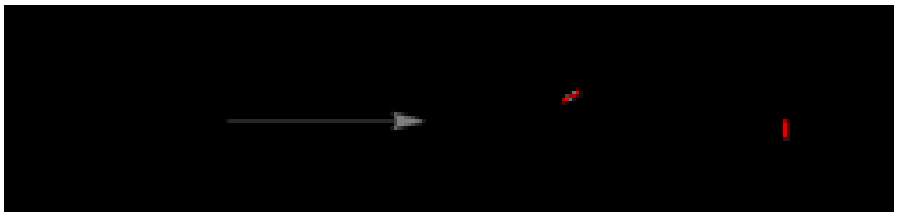

Chapter 5
Synthesis of Phe-nanthridinones

J. Org. Chem. **2021,** *86*, 14144-14159.

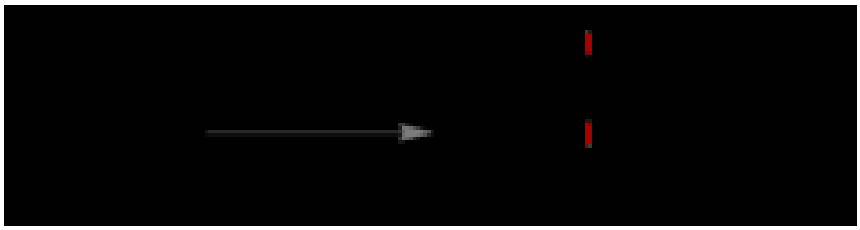

Chapter 6
Synthesis of Flavanones and Aza-flavanones

Org. Biomol. Chem. **2022,** *20* (35), 7085-7091

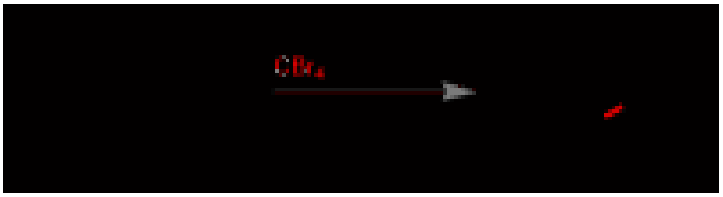

Outlook for Future Research

In this thesis, various sustainable approaches have been used for synthesizing various heterocycles under the metal-free (using CBr_4 and iodine reagents) and photocatalyst-free (without any reagent except the light) reaction conditions. The scope of the reaction, mechanistic studies, and the synthetic application of our synthesized heterocyclic compounds are presented in every chapter. In this regard, these efficient and cost-effective methods will substantially impact the field of organic synthesis, which will be highly important to the chemistry community working on organic synthesis. We anticipate that these sustainable approaches can offer an excellent guideline for constructing complex heterocyclic motifs and helpful for scientists working in a similar research area. Mainly, we have synthesized the nitrogen-containing fused heteroaromatic compounds such as benzimidazole-fused phenanthridines, phenanthridine-fused quinazolinones, phenanthridinone derivatives, flavanones, and aza-flavanones via the C-N and C-O bond formation reactions. The nitrogen-containing fused heteroaromatic compounds having phenanthridine moiety are ubiquitous in many pharmaceuticals and natural products. Phenanthridinone derivatives such as N-methylcrinasiadine and phenaglydon are potent HIV-1 integrase inhibitors, and Oxynitidine derivatives have shown TOP1 and TDP1 inhibitor activity. Whereas maryllidaceae alkaloids like narciclasine exhibit antimitotic activity and antitumor effects and inhibit angiogenic processes. So, we assumed that our synthesized compounds might have lots of applications in medicinal chemistry. We have also shown how various non-covalent interactions like N-H…π interaction and halogen-bonding interaction could play a role in C-N and C-O bond formations. Therefore, our work provides a link between organic synthesis and supramolecular chemistry. We anticipate that the work presented herein will substantially impact the research in organic chemistry. This research work may also find commercial value in the near future.